SUBCOOLING EFFECTS FOR FLOODING EXPERIMENTS WITH STEAM AND WATER IN A LARGE DIAMETER VERTICAL TUBE

A Thesis

by

WES LEE CULLUM

Submitted to the Office of Graduate Studies of
Texas A&M University
in partial fulfillment of the requirements for the degree of

MASTER OF SCIENCE

August 2012

Major Subject: Nuclear Engineering

SUBCOOLING EFFECTS FOR FLOODING EXPERIMENTS WITH STEAM AND WATER IN A LARGE DIAMETER VERTICAL TUBE

A Thesis

by

WES LEE CULLUM

Submitted to the Office of Graduate Studies of
Texas A&M University
in partial fulfillment of the requirements for the degree of

MASTER OF SCIENCE

Approved by:

Chair of Committee,	Karen Vierow
Committee Members,	Gerald Morrison
	Yassin Hassan
Head of Department,	Yassin Hassan

August 2012

Major Subject: Nuclear Engineering

ABSTRACT

Subcooling Effects for Flooding Experiments with Steam and Water in a Large Diameter Vertical Tube. (August 2012)

Wes Lee Cullum, B.S., Texas A&M University

Chair of Advisory Committee: Dr. Karen Vierow

A counter current annular flow experiment was performed to determine flooding conditions for varying degrees of subcooling using steam and water. The findings can be used in reactor safety codes to provide an improved model of flooding during accident analysis. The test section is a stainless steel tube which is approximately a 5/16 scale version of a pressurized water reactor (PWR) surge line. The water flows in an annular film down the inside of the tube and steam flows upward through the annulus. Flooding is the point at which the water film reverses direction and begins to travel upward. Flooding tests were conducted at atmospheric pressure for water flow rates between 3.5 gallons per minute (GPM) and 11 GPM and water inlet temperatures between 35°C and 97°C. The data obtained at high water subcooling indicate a significant departure from accepted flooding correlations developed for air-water systems which is expected because vapor condensation alters the steam inlet flow rate needed to induce flooding. The data more closely follow air-water data at low subcooling. Such data has not been seen in the literature for steam-water flooding experiments in a large diameter vertical tube and will serve as an important benchmark.

To my wife Leanna

and my parents

Jim and Debbie Cullum

ACKNOWLEDGMENTS

First, I would like to acknowledge my advisor Dr. Karen Vierow. Thank you for giving me a chance in graduate school at Texas A&M University. I appreciate your guidance through my research and your assistance through the problems that I have encountered along the way. I also sincerely appreciate the support of my graduate committee members Dr. Yassin Hassan and Dr. Gerald Morrison.

Next, I would like to express my gratitude to my wife for dealing with me through this difficult time in my career. Thank you for always taking care of things for me and relieving the stress of everyday tasks so I can focus on my research. I love you very much. I would also like to thank my parents for always supporting me and giving me the tools to accomplish difficult tasks in life. I know that I can always count on you for advice if I have a problem.

I would like to thank Dr. Reece and the Texas A&M Nuclear Science Center, the Montgomery G.I. Bill, and the state of Texas for providing the financial funding for my education.

Finally, I would like to thank all of the professors that have helped me along the way, Matt Solom for all of your assistance in the lab, and Jack Reid for helping me obtain the data for this research.

NOMENCLATURE

ABBREVIATIONS

PWR	pressurized water reactor
CCFL	counter-current flow limitation
ID	inner diameter
OD	outer diameter
SS	stainless steel
ASME	American Society of Mechanical Engineers
NPT	national pipe thread
PWR	pressurized water reactor
GPM	gallons per minute

SYMBOLS

C	Wallis correlation constant
c_p	specific heat capacity
D	diameter
f	fraction of condensed steam
g	acceleration due to gravity
h	enthalpy
j	superficial velocity
m	Wallis and Kutateladze correlation constant
K	Kutateladze number
$\dot{m}$	mass flow rate
R_T	thermodynamic ratio
T	temperature

Greek symbols:

ρ	density
ω	surface tension

Subscripts:

f	liquid
g	gas
ge	effective gas
f,d	liquid flow downward during flooding
in	in
st	steam
sub	subcooled

TABLE OF CONTENTS

Page

LIST OF TABLES

LIST OF FIGURES

FIGURE Page

1. INTRODUCTION

In reactor accident analysis, flooding is an important phenomenon which can preclude accident mitigation and, in certain circumstances, compound the accident. Flooding occurs in two-phase annular flow regimes where the liquid is in an annular film inside a pipe and a gas is traveling through the center of the annulus. Flooding is defined as the partial or complete reversal of the liquid film flow direction. Another term for flooding is called the counter-current flow limitation (CCFL) or the transition from counter-current flow to co-current flow. This phenomenon is not specific to nuclear power plants and can be found in many engineering applications. Due to it's broad existence, flooding has been studied for many decades in different forms.

1.1 Problem Statement and Motivation for this Research

This research pertains to a specific type of flooding which occurs in nuclear power plants. In a pressurized water reactor (PWR), the reactor coolant system pressure is maintained by a component called the pressurizer. The pressurizer is connected to the hot leg of the main coolant system via the pressurizer surge line. A simplified diagram of this system is shown in Figure 1.1.

In certain reactor accidents such as a station blackout, the ability to remove heat from the reactor core is lost. This results in the generation of steam within the reactor coolant piping. As the pressure within the main coolant piping increases due to the formation of steam, the chance of flooding in the pressurizer surge line intensifies. If flooding occurs in the pressurizer surge line, the surface temperature of the pressurizer surge line can increase sharply to the steam temperature flowing through the center of the annulus. This is due to a breakdown of the annular film which

This thesis follows the style of the International Journal of Heat and Mass Transfer.

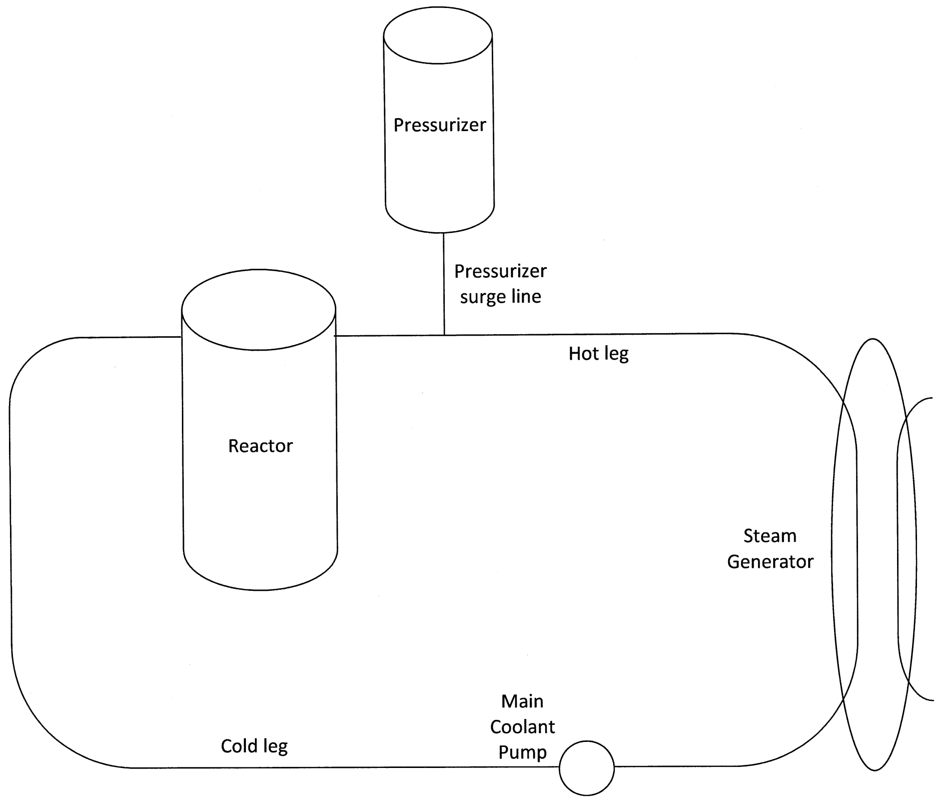

Fig. 1.1.: A simplified diagram of the main coolant system of a PWR. Other primary loops without the pressurizer are not shown

causes local dryout conditions within the pipe. If flooding occurs for an extended period of time, the pressurizer surge line could rupture due to plastic deformation caused by high temperature creep.

One of the functions of the pressurizer is to serve as an expansion volume to keep the core covered with water in the event of a loss of coolant accident. Flooding in the pressurizer surge line can cause the water to remain in the pressurizer during a loss of coolant accident. During normal operation, the main coolant piping is filled with water. Since the pressurizer is directly connected to the main coolant system, water flows in and out of the pressurizer as needed to accommodate thermal expansion and contraction of the coolant inventory and changes in the gas space volume. If flooding occurs in the pressurizer surge line during hypothetical accident conditions, the makeup water will stay in the pressurizer and the reactor core could become partially voided with steam. Since the operators rely on pressurizer level indication to indicate the water inventory of the main coolant system, flooding may lead the operators astray by indicating a high pressurizer level while the main coolant system is largely voided with steam.

In previous flooding experiments with steam and water, a comprehensive analysis of the water subcooling effects has not been available. In order to develop a better flooding model, research must be performed over a range of water inlet temperatures to determine the effects on flooding. This new model can be used to determine if the pressurizer surge line can rupture due to high temperature creep.

1.2 Research Objectives

The objective of the research is to study the effects on flooding produced by varying the subcooling of inlet water. In order to produce the necessary data, numerous flooding tests will be conducted at differing degrees of water subcooling. First, the maximum level of subcooling achievable while still allowing the flooding phenomenon will be identified. Then, flooding tests will be performed in increments of 5°C until the water inlet temperature reaches the saturation temperature or until a limitation of the experimental facility is reached. After all of the flooding tests have been performed, the data will be compared to previous data obtained at similar conditions to validate the current data. The data will then be plotted and analyzed for consistency using correlations already developed for flooding. If existing correlations do not agree with the current data, then a new correlation will be produced to account for the water subcooling effects in flooding.

At the conclusion of this research, several outcomes should be produced. Primarily, a correlation should be developed or verified to account for the water subcooling effects on flooding using steam and water. This correlation can be used in reactor accident computer codes to better predict conditions within the pressurizer surge line in severe accidents such as a station blackout or loss of coolant accident. Additionally, more data will be added to the flooding database to step towards a more complete model of flooding instead of individualized correlations. As researchers continue to analyze the counter-current flow limitation, aspects of flooding can be generalized to form one complete model. Lastly, an important benchmark should be achieved by comparing low subcooling steam-water flooding data to air-water data. This comparison has not been performed in previous research and will provide a basis for validation of the current research.

1.3 Thesis Organization

This thesis contains 6 main sections to detail the extent of research performed. The first section is an introductory section which explains the problem statement and objectives for the research. The second section consists of a literature survey of previous work and events leading up to the current research. Section 3 describes the experimental facility in detail including dimensions of the test section and important flow paths through the facility. The fourth section details the experiment facility procedures used to obtain the data and ensure the safety of the equipment and experimentalists. Section 5 provides the results of the data analysis along with methodology used in analyzing the data. A discussion of the various results obtained from the experiments is also given in this section. Finally, section 6 delivers the conclusions from the experiment and future work needed in this research field. Appendices A through D are provided after the conclusions with graphs and tables of experimental parameters for the readers convenience.

2. LITERATURE SURVEY

Counter-current flow limitation is a phenomenon which has been studied in various forms for many years. Numerous fluids and gases have been studied along with various inlet and outlet geometries. For the purpose of this research, many of these experiments can be disregarded as they do not pertain to the direct concentration of this experiment. However, some important past work influential to this endeavor will be examined to provide the essential framework. This previous work does not necessarily deal solely with steam/water flooding, nonetheless each provide significant insight into the phenomenon.

2.1 Origin of Flooding and the Wallis Correlation

Flooding was first investigated in the use of packed towers to separate waste products from gases. In packed towers, scrubbing liquor flows down through the packed tower as gas flows upward. As the gas passes through the liquor, the waste products are stripped out of the gas leaving clean gas at the outlet of the tower. The limiting velocity of the gas is the point at which flooding occurs and the liquor reverses direction which was studied by Sherwood and Lobo [1,2]. Some of the initial studies were performed by G. B. Wallis who researched and developed correlations primarily for air and water experiments although he performed some studies with steam and water as well. Wallis first performed experiments using air and water in which he developed the correlation known as the Wallis correlation [3–5].

$$j_g^{*\frac{1}{2}} + m j_{f,d}^{*\frac{1}{2}} = c \tag{2.1}$$

The dimensionless volumetric fluxes for the gas and fluid, j_g^* and j_f^* respectively, are described mathematically by relating the momentum of the fluid to the viscous dissipation.

$$j_f^* = \frac{\rho_f{}^{\frac{1}{2}} j_f}{[gD(\rho_f - \rho_g)]^{\frac{1}{2}}} \tag{2.2}$$

$$j_g^* = \frac{\rho_g{}^{\frac{1}{2}} j_g}{[gD(\rho_f - \rho_g)]^{\frac{1}{2}}} \tag{2.3}$$

The constants, m and c, in Equation 2.1 are constants determined by the geometry of the experimental setup. The constants are influenced by the test section diameter as well as the entrance and exit arrangements of the test section. Small changes in the design of the experiment can generate substantial differences in these constants. Wallis considered the entrance and exit of different facilities to either be sharp or smooth. The parameter $j_{f,d}$ in Equation 2.1 is the liquid superficial velocity that flows in the downward direction during flooding.

The Wallis correlation has provided a baseline for flooding experimentation, yet it has limitations. Specifically, it is only valid for small diameter tubes and experiments using air and water since he developed the correlation with data solely from experiments using air and water. The experimental data obtained from the packed tower research correlates well with the Wallis correlation as shown in Figure 2.1.

2.2 The Kutateladze Correlation

After the initial development of the Wallis correlation, Pushinka and Sorokin studied the occurrence of film breakdown, or a complete reversal of the liquid film, in vertical tubes of varying sizes [6]. In the performance of this experiment they used the dimensionless number developed by Kutateladze to compare to the Wallis correlation. The Kutateladze number was developed during a hydrodynamic study to determine if bubble formation during boiling and bubbling were similar [7]. As such, the Kutateladze number includes the same buoyancy and fluid friction forces as the volumetric flux used in the Wallis correlation while also taking into account the surface tension effects produced by the bubble [8, 9].

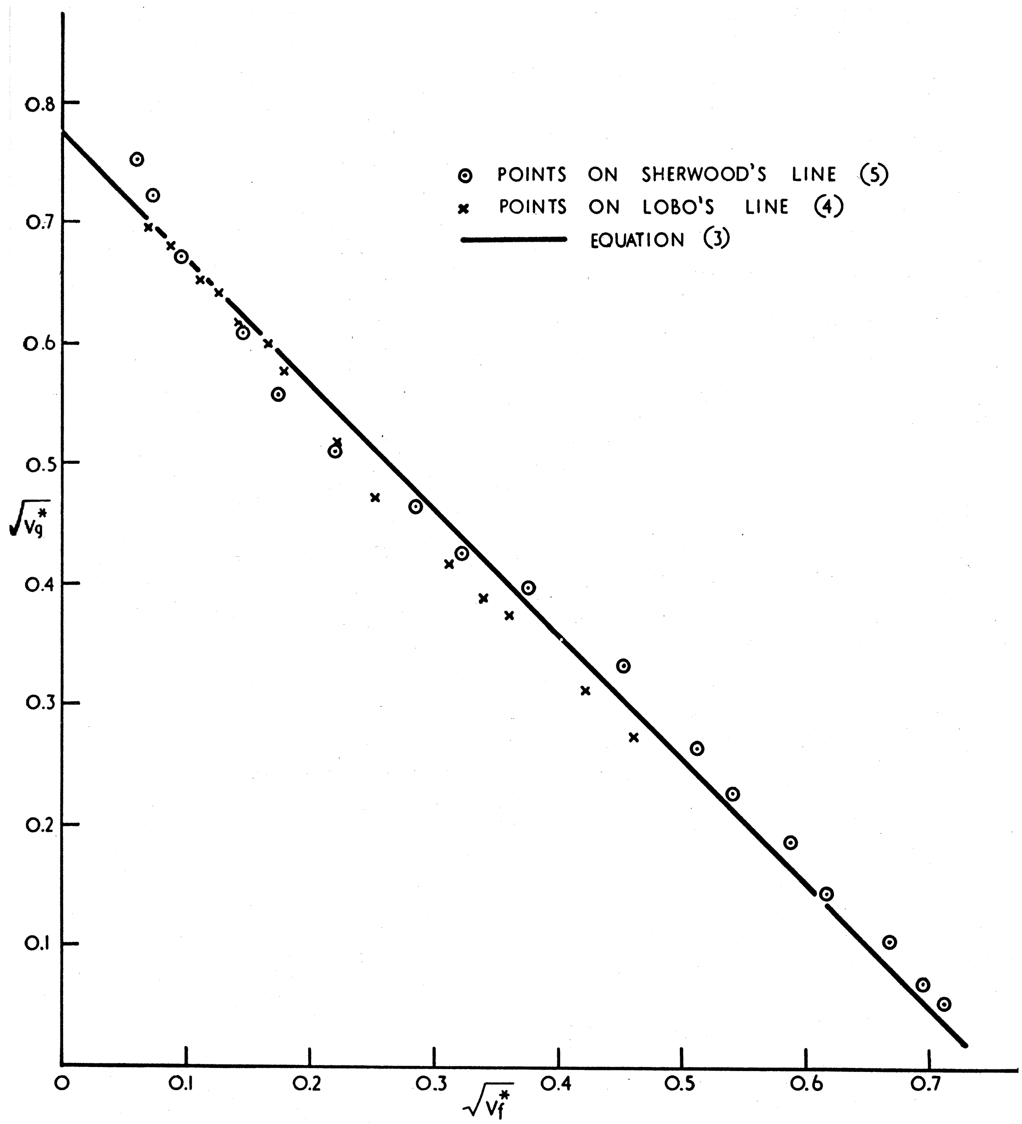

Fig. 2.1.: Data obtained by Sherwood and Lobo plotted with the Wallis correlation [5].

$$K_g = \frac{\rho_g^{\frac{1}{2}} j_g}{[g\sigma(\rho_f - \rho_g)]^{\frac{1}{4}}} \tag{2.4}$$

$$K_f = \frac{\rho_f^{\frac{1}{2}} j_f}{[g\sigma(\rho_f - \rho_g)]^{\frac{1}{4}}} \tag{2.5}$$

Pushinka and Sorokin observed that for the large diameter tubes used in the experiment, the tube diameter does not have an impact on the magnitude of air velocity required to breakdown the film. Therefore, the data they obtained by using the Kutateladze number did not agree with the Wallis correlation since the Wallis correlation predicts that the tube diameter has a significant impact on the air velocity required to induce flooding.

The threshold for declaring a tube large or small has also been studied by several researchers. The most widely accepted method for determining this threshold is to use the critical Kutateladze value of 3.2. This also correlates the better known bond number of 30 or greater [10]. The Bond number equation is shown in Equation 2.6 and is a ratio of the gravitational forces to surface tension forces. Vijayan et al performed research to determine the diameter effects of tubes of differing sizes on flooding. Upon the conclusion of his experiment, he found that tubes greater than 67 mm in diameter can be consider large and the Kutateladze number can be used to accurately quantify results [11]. Other dependencies for the tube diameter threshold include the film thickness relative to the tube diameter, the tube wall thickness and the type of fluid used in the experiment.

$$D^* = D[\frac{g(\rho_f - \rho_g)}{\sigma}]^{\frac{1}{2}} \tag{2.6}$$

Using the Wallis correlation as a basis, an analogous correlation was developed using the Kutateladze numbers to describe flooding in large diameter tubes.

$$[K_g]^{\frac{1}{2}} + [K_f]^{\frac{1}{2}} = c_k \tag{2.7}$$

This version of the Wallis correlation using the Kutateladze numbers was first proposed by Tien although Pushinka and Sorokin previously plotted data in terms of the Kutateladze numbers [12].

2.3 Steam and Water Flooding Tests

There have only been a few experimenters who have performed flooding tests using steam and water. Wallis performed steam and water experiments using multiple facilities. The majority of the steam and water experiments have arisen from studies of the emergency core cooling (ECC) injection into the reactor core following a loss of coolant accident (LOCA). One notable study [12] was conducted on this topic in the 1970's. The experimental setup for this research consisted of flow along flat plates with counter-current steam flow between the plates. The experiment was conducted on a 1/15 scale model of actual PWR piping. Flooding tests were conducted at several values of liquid subcooling to attempt to determine a correction to the Wallis correlation to account for subcooling [13]. An analytic solution was proposed by using an energy balance to determine the amount of energy required to heat the water film to the saturation temperature.

$$J_g^* - J_g = fJ_{f,in}^* \frac{c_p \Delta T_{sub}}{h_{fg}} (\frac{\rho_f}{\rho_g})^{\frac{1}{2}} \tag{2.8}$$

The parameter, f, in Equation 2.8 represents the fraction of steam condensed in the test section and depends on the injection flow rate as well as the amount of liquid that penetrates the injection port denoted by the parameter N [13, 14]. The parameter N is an empirical constant which varies between 0.2 and 0.8 according to the amount of ECC penetration.

$$f = e^{-N\sqrt{J_{f,in}^*}} \tag{2.9}$$

Again, an analogy can be deduced from the Wallis parameters to the Kutateladze parameters to illustrate the dependence of flooding on the amount of water subcooling [12].

$$[K_g - f(\frac{c_p}{h_{fg}})(\frac{\rho_f}{\rho_g})^{\frac{1}{2}} \Delta T_{sub} K_f]^{\frac{1}{2}} + [K_f]^{\frac{1}{2}} = c_k \tag{2.10}$$

Investigation into the heat transfer effects of flooding suggest that critical heat flux (CHF) may be reached during a flooding event due to the limitation of the heat transfer rate imposed by the flow reversal [15]. This reduction in the heat transfer rate combined with possibly crossing the CHF threshold could lead to a failure of the pressurizer surge line.

In 1980, Wallis performed tests using air and water first and then steam and water to compare the results. The trends observed from these experiments are described in Figure 2.2.

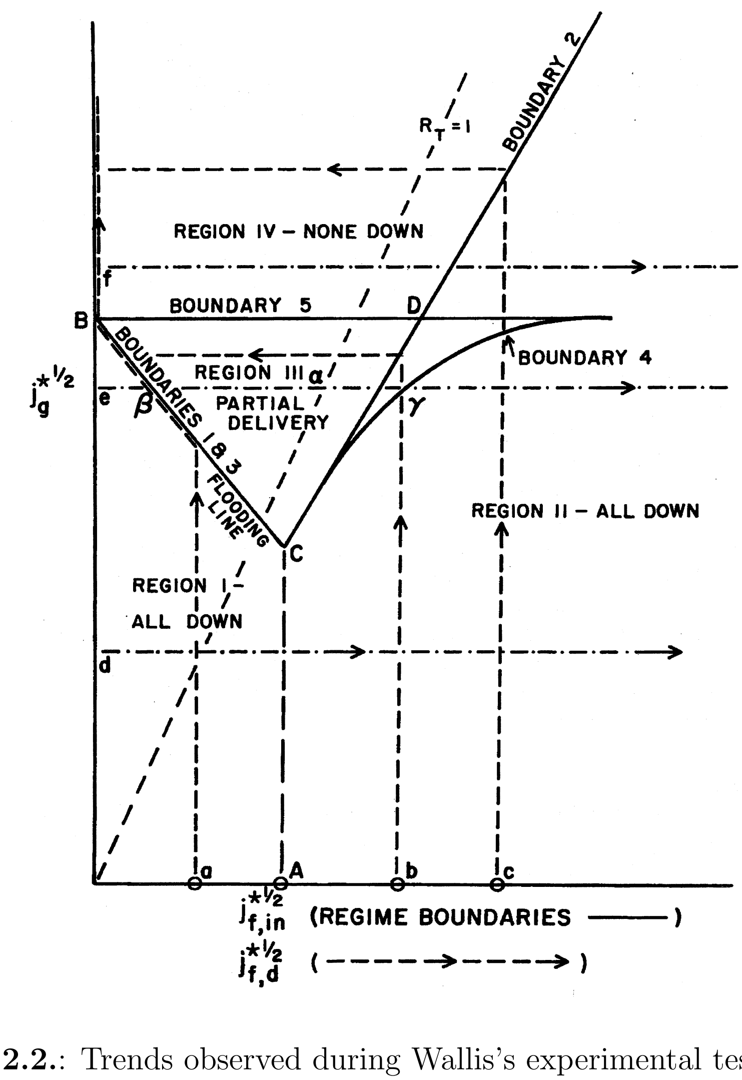

Fig. 2.2.: Trends observed during Wallis's experimental testing [3].

Wallis performed water first flooding tests as well as steam first flooding tests. Only water first tests are performed throughout the current research and therefore only these tests will be considered. In Figure 2.2, the boundaries 1 and 2 govern the trend for water first tests. For water flow rates below point A, three scenarios can occur. First, if the steam flow rate is below boundary 1, all of the water travels to the outlet of the test section because all of the steam is condensed in the test section. If the steam flow rate is greater than boundary 1, some of the steam passes completely through the test section and upholds a portion of the water in the test section. Therefore, some of the water that enters the test section does not exit through the bottom. In the event that the steam flow rate exceeds boundary 5, all of the water is suspended and no water exits the test section.

If the water flow rate is greater than point A, the same conditions are true. If boundary 4 is exceed, only a portion of the water makes it to the outlet of the test section. The transition point C shifts from left to right on the graph for increasing water temperatures. This is an important fact for the current research. The transition point marks the change in condensation of the steam from the lower region of the test section to the upper region of the test section.

In 2009, a test facility was constructed at Texas A&M University to conduct steam/water flooding experiments using a test section modeled as a scaled down PWR pressurizer surge line. This research was performed to provide a better flooding correlation for reactor accident analysis codes. The test section tube meets the large tube criterion of Vijayan and Equation 6 with a 76.2 mm diameter [10,11]. Tests were conducted with varying water flow rates to determine specifically when flooding will occur in a vertical straight tube or inclined tube. The collected data was collapsed and plotted using the Wallis and Kutateladze correlations from Equations 1, 7, and 10. None of these correlations projected the correct data for flooding conditions. A new correlation was developed using an energy balance from the fact that the energy released from steam condensing is equal to the energy gained by the water in the annular film. From this relationship and the temperature on the surface of the water film, the fraction of steam condensed can be determined.

$$f = \frac{\dot{m}_f c_p (T_s - T_{wall})}{\dot{m}_{st}(h_{st} - h_f)} \tag{2.11}$$

This development led to the correlation used to fit the flooding test data from the pressurizer surge line experiments [16].

$$[K_g(1-f)]^{\frac{1}{2}} + [K_f]^{\frac{1}{2}} = c_k \tag{2.12}$$

The data Williams obtained was at a constant water inlet temperature of 70°C. While this data was useful to develop a correlation for a large diameter pipe similar to a PWR pressurizer surge line, it was not tested for varying degrees of steam condensation on the annular film. Draznin performed flooding tests at varying degrees of subcooling on the same test facility that Williams constructed. During these tests, the inlet water temperature was varied between 50°C and 80°C. For each temperature, a range of water flow rates between 3.5 and 12 gpm were used to obtain a range of data for flooding conditions [17]. Draznin's data showed similar trends to those observed by Wallis in Figure 2.2. This data was not analyzed using Equations 2.11 and 2.12 developed by Williams. Due to the limited range of subcooling collected by Draznin, more testing is necessary to understand how subcooling effects flooding.

Although numerous studies have been conducted on flooding in vertical tubes, data has been broadly distributed with correlations pertaining only to specific experiment geometry and conditions. McQuillan and Whalley summarized and compared all flooding points and correlations to date in 1985 to show the different trends among the data [18]. Figure 2.3 shows the large distribution in flooding points for the data up to the point that their compilation was performed.

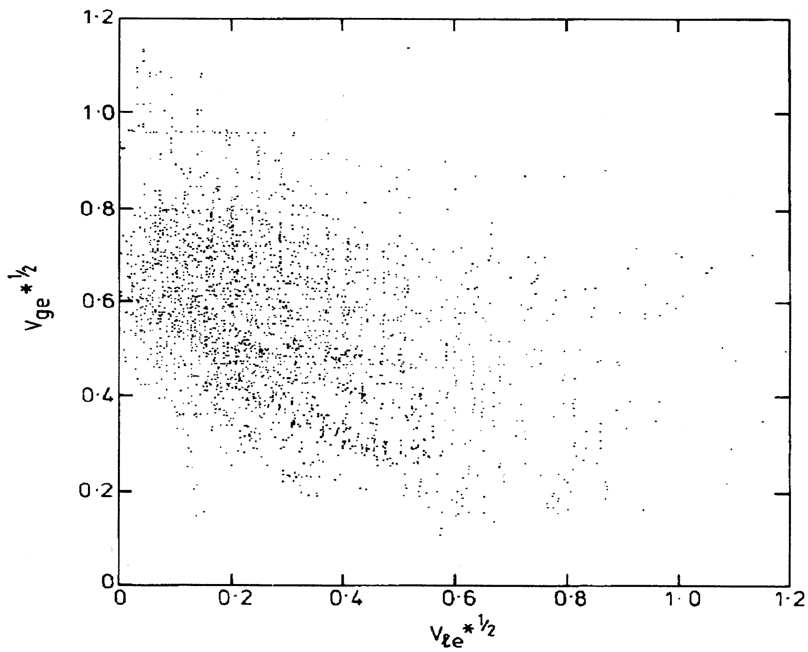

Fig. 2.3.: A plot of the collection of flooding data points compiled by McQuillan. [18].

2.4 Flooding Mechanisms

Qualitatively, flooding can be described in three different regimes [19]. The initial regime is described by a smooth annular film falling with a small steam flow rate through the center of the annulus. In this condition, the shear stress at the steam-water interface is negligible in comparison to the friction shear at the interface between the tube wall and water. As the steam flow rate is increased, the film becomes wavy in regions with larger waves appearing as the steam flow rate rises. The condition of wave formation on the film is the second regime in flooding. Finally, as the flooding point is reached, the annular film becomes rough and chaotic. In this final regime, some of the water in the film reverses direction while a portion of the film still travels in the downward direction. Any further increase in the steam flow rate will begin to strip the water from the film causing a transition from annular to slug flow and potentially even tube dryout.

McQuillian et al conducted visualization experiments with air and water in a transparent tube to characterize the mechanism of flooding. They found that small disturbances form on the film and travel downward to approximately the water inlet location. The disturbances collect at the water inlet forming a standing wave which grows as the air flow rate is increased. Eventually, the wave begins to travel upward initiating the flooding event. Droplets of water break off from the wave and become entrained in the air stream. These droplets travel ahead of the wave and impinge on the annular film [20].

2.5 Flooding Models in Reactor Analysis Computer Codes

Some effort has been made to validate the Wallis and other flooding correlations in reactor analysis computer codes. The validation of flooding correlations developed through experimentation is an important step in this research. It allows for data comparison between the experiment and computer code and verification of the applicable ranges of the correlation within the code.

The Wallis, Kutateladze, and Bankoff correlations were investigated in version 5.0 of the TRACE code used by the Nuclear Regulatory Commission [21]. The geometric simulation used in the TRACE code was based on a flooding experimental test facility. The testing was conducted using a variety of pipe diameters for varying steam and water flow rates. The TRACE results for small diameter pipes fit the Wallis correlation while larger diameter pipes fit the Kutateladze correlation better. This methodology validated the computer code because the results agreed with actual experimental data. Although these results were not compared to any other reactor analysis code results, the data seemed to be a good prediction of flooding.

3. FACILITY DESCRIPTION

The flooding test facility at Texas A&M University was originally designed and built by Nicole Williams in 2009. Some modifications were made to the facility to enable high temperature testing to study the subcooling effects of the inlet water on flooding. The experiment consists of two main flow paths; one for water and one for steam. These flow paths and the main components in each will be discussed in this section. Additionally, the instrumentation used to collect data in the facility will be discussed along with the data acquisition system.

3.1 Test Section

The test section is a 72-inch tall 3-inch ID pipe made out of stainless steel (SS) 304. The tube thickness is 1/4-inches which makes the tube OD 3 1/2 inches. The top of the test section is encapsulated by a 6-inch diameter, 7 3/8-inch long pipe which serves to direct the inlet water. This pipe serves as an inlet plenum and is attached to the test section using flanges on either end. The 6-inch pipe has four equally spaced 3/4-inch NPT fittings welded to the outside as water injection ports. Only two of these ports are currently connected for water injection. A 2 3/4-inch OD tube is located in the top of the test section providing a 1/8-inch gap between the test section and the inner tube. The top of the test section has twelve holes drilled circumferentially around to allow uniform flow into the pipe in all directions. As water enters through the inlet plenum, it passes through the twelve holes in the top of the test section. The water then impinges on the smaller pipe in the test section where it is forced downward in a 1/8-inch thick annular film. A diagram of the water injection is shown in Figure 3.1. The lower end of the test section serves as the water outlet path while also allowing for a steam entrance path. Similarly, it has a 6-inch pipe which is attached to the bottom through the use of flanges. The underside of the bottom flange has four ports for water to exit the test section.

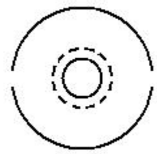

Fig. 3.1.: A diagram of the top view of the water inlet to the test section.

In addition to water flow path accommodations, the test section also serves to transport steam. The steam enters the test section from the bottom through a hole in the center of the bottom flange which is connected to the 1 1/2-inch steam line. The top side of the bottom flange also has a 1 1/2-inch steam pipe surrounded by a 2-inch pipe which is welded on to the flange so that air provides insulation to minimize steam condensation as steam enters the test section. The end of the 2-inch pipe is reduced to 1 1/2 inches as the pipe meets the top flange to direct steam into the center of the test section. The steam exits the top of the test section where a high temperature hose directs it to a blowdown tank.

3.2 Steam Flow Path

A simplified diagram of the experimental flow path can be seen in Figure 3.2. This figure aids in the description of the flow paths for the water and steam.

The steam generator provides the saturated steam supply to the test section. A picture of the steam generator and its control panel is shown in Figure 3.3. The steam generator is typically operated at a pressure of about 50 psig. The steam generator is a Schedule 10 stainless steel 304 pressure vessel manufactured by Kennedy Tank and Manufacturing Co., Incorporated. The vessel is a 24-inch diameter pipe which is 60 inches tall with two caps welded on the top and bottom. The steam generator has a working pressure of 135 psig at a temperature of 350°C. The water in the steam generator is heated primarily by three 8-inch flanged immersion heaters produced by

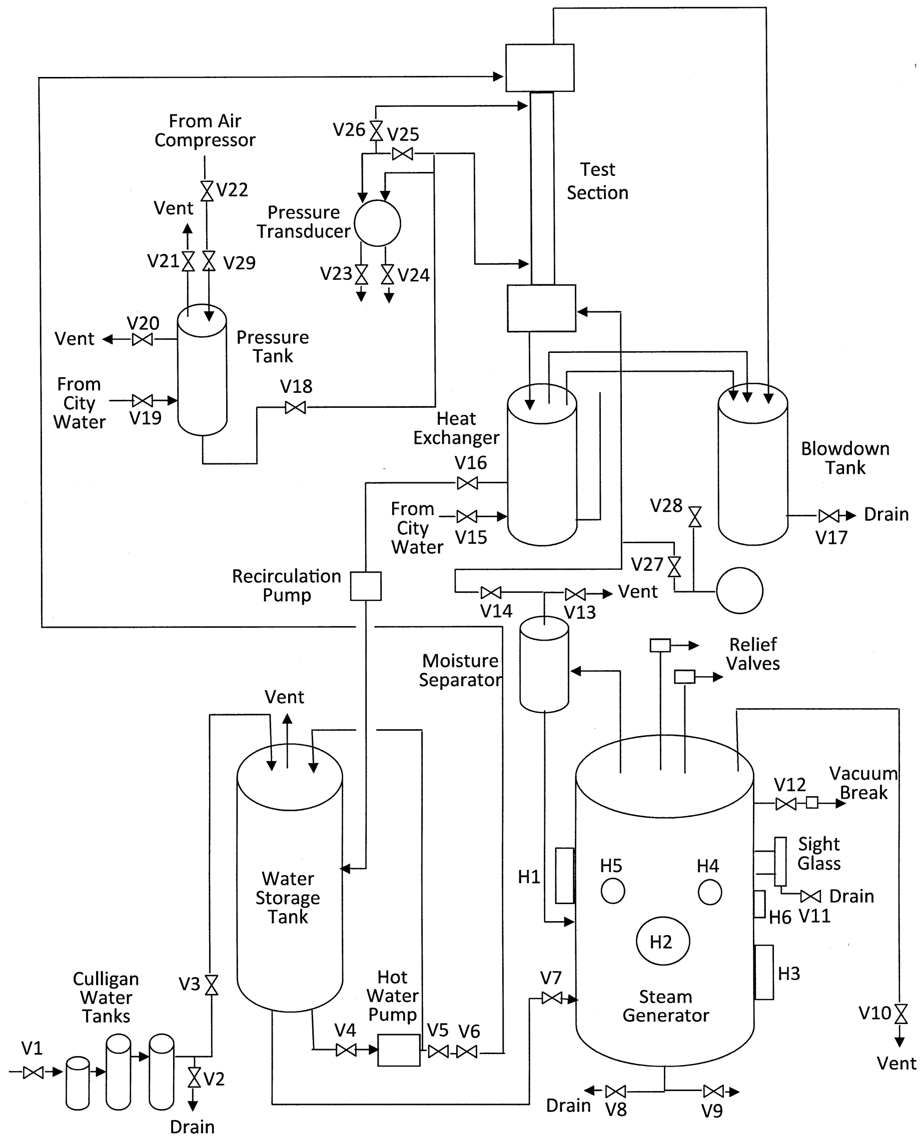

Fig. 3.2.: A diagram of the Texas A&M University flooding test facility.

Watlow Process Systems. The heaters are controlled from a custom control panel also developed by Watlow. Two of the Watlow heaters are divided into two 25 kW

Fig. 3.3.: The steam generator and associated components.

circuits controlled individually by switches on the control panel. The third Watlow heater is divided into eight 6.25 kW circuits. This arrangement of the heater control circuit allows the experimenter the ability to vary heater power for a wide range of steam demand requirements. There are also 3 smaller heaters which provide for fine tuning needed in the calibration of the vortex flow meter and heat loss determination. The steam generator has a vacuum break which is designed to prevent pressure from falling below atmospheric pressure. The vacuum break is equipped with a small filter to prevent dust from entering the vessel. Vent piping used to depressurize the steam generator is directed outside the lab where it is dissipated into the environment. Overpressure protection for the steam generator is provided by two 1/2-inch Kunkle relief valves which both lift at a pressure of 105 psig. Water level indication is provided by a magnetic float in a standpipe connected to the steam generator. A magnetic reed switch manufactured by Orion provides a safety feature which turns off all heaters if float level indicator drops below 35 inches.

Steam flows from the steam generator into a moisture separator unit supplied by Clark Reliance Corporation through a 1-inch steam pipe. This moisture separator is an ASME certified pressure vessel which removes water droplets from the steam before it enters the main steam piping. The steam exits the moisture separator through a 1-inch steam pipe where it quickly transitions to a 1 1/2-inch steam pipe which travels to the test section. The steam travels through the test section as described in Section 1 and exits through a 2 3/4-inch high temperature silicone hose. The hose is rated to a temperature of 250 °C to ensure that it withstands any flooding test performed at this facility. The end of the silicone hose is connected to a 55 gallon drum which serves as a blowdown tank to condense the steam. The blowdown tank is kept partially filled with water to help condense the steam. Additionally, cooling water is directed through the tank perpendicular to the steam entrance to aid in steam condensation.

3.3 Water Flow Path

The main source of water for recirculation through the test section is the water storage tank. The water storage tank is filled through a series of Culligan deionized water tanks which remove impurities from the water to minimize corrosion and scale buildup within the facility piping and the steam generator. The hot water pump takes a suction from the water storage tank and pumps water to the test section. The hot water pump is a Deanline vertical inline pump (Model 185012) with a maximum working pressure of 100 psig and temperature of 250°F. Water enters the top of the test section and exits through the bottom as described in Section 1. Upon exiting the test section, the water is carried through hoses to a 55 gallon drum located directly below the test section. This drum serves as a heat exchanger to cool the water exiting the test section. From the heat exchanger, the recirculation pump propels the water back to the water storage tank.

3.4 Facility Modifications

The major change to the facility from the original design was a change in the water flow path. The changes made to the facility can be observed in the before and after pictures in Figures 3.4 and 3.5 respectively. The old design consisted of a small steel tank to collect the water at the base of the test section. Then, the water flowed into an aluminum tank with copper coils inside which served as a heat exchanger. City water flowed through the copper coils to cool the hot water from the test section flowing around the outside of the coils. The recirculation pump took a suction on the aluminum tank to pump water back to the test section. This design was not conducive to high temperature testing because the aluminum tank was prone to overflowing which rendered it unable to be insulated. Insulating the aluminum tank was desired to reduce heat loss and provide better temperature control during flooding experiments. The water flow path was modified by removing the water collection tank and the aluminum heat exchanger and replacing them with a 55 gallon drum located beneath the test section. The 55 gallon drum combines the functions of the steel tank and the aluminum tank into one unit and for clarity is referred to as the heat exchanger. The heat exchanger was modified by cutting three holes in the bottom portion of the side of the drum located approximately 90 degrees apart from one another. A tank fitting was inserted into each one of these holes to provide the following functions; a tank level indication, an inlet for cooling water flow and an outlet for water collected from the test section. Additionally, five holes were cut in the lid of the barrel and each was equipped with a tank fitting. Four of these fittings were used to collect water from the test section while the last fitting serves as an outlet for the cooling water. A high temperature plastic lining was placed inside the heat exchanger to minimize corrosion within the barrel from exposure to high temperature water and steam. The same copper coils that were used in the aluminum tank in the original facility design are used in the heat exchanger. Short

Fig. 3.4.: The outlet of the test section prior to the facility modification.

sections of flexible hose connect the copper coils inside the heat exchanger to the tank fittings to provide a closed path for cooling water within the copper coils.

This change to the water flow path improved the facility for several reasons. The larger volume of the heat exchanger compared with that of the aluminum tank allowed the water level in the heat exchanger to be controlled such that the risk of overflow was minimized. This allowed the heat exchanger to be insulated which minimized the heat loss in the system. Furthermore, the larger volume in the heat exchanger provides more net positive suction head for the recirculation pump to prevent cavitation during high temperature flooding tests. Lastly, the flow path was simplified which eliminated some hosing leading to a reduction in heat loss.

A modification was also made to the wiring throughout the facility. Some of the pumps were powered by extension cords which were plugged into outlets due to the few number of power outlets in the facility. More outlets were hardwired into the electrical distribution system at the lab to eliminate these extension cords and

Fig. 3.5.: The outlet of the test section after the facility modification.

provide safe wiring to major components. The wiring was also enclosed in liquid-tight conduit as a safety measure in the event of water spraying or dripping in the experiment.

For low subcooling flooding tests, heat tape was installed on portions of the water piping between the water storage tank and the test section to heat the water as close to saturation as possible. Two Omegalux heat tapes were used on the water piping to raise the temperature. One heat tape was installed between the outlet of the hot water pump and the magnetic flow meter. This heat tape was 2 inches wide by 72 inches long and rated to a power of 864 Watts. The other heater tape was installed between the magnetic flow meter and the water inlet to the test section. This heat tape was 2 inches wide by 120 inches long and rated to a power of 1440 Watts. To install the heat tapes, a portion of insulation was removed from the water pipe. No insulation was installed over the heat tape.

Preliminary testing was performed to ensure that all instruments were performing as expected. During this preliminary testing, it was observed that the fourth surface thermocouple from the top on the test section was not indicating consistently with the other test section thermocouples. This thermocouple was removed and replaced with a new thermocouple of the same specifications. Further testing proved that the new thermocouple was responding properly.

3.5 Instrumentation

The experiment is equipped with an array of instrumentation to provide the user with essential data during flooding tests. The instrumentation consists of thermocouples, pressure transducers, a vortex flow meter, and a magnetic flow meter. A general layout of the facility instrumentation is shown in Figure 3.6. All instruments with the exception of the thermocouples rely on a power source in order to perform their intended functions. The power source used for these instruments is a DC power supply which is set to a constant output of 24 VDC.

3.5.1 Thermocouples

All temperature measurements in the facility are made with type T copper-constantan thermocouples manufactured by Omega. There are 8 thin film thermocouples which are bonded to the outer test section surface using a high temperature, thermally conductive epoxy. These thermocouples are approximately equally spaced axially on the test section surface from top to bottom. A probe type thermocouple is inserted into a 1/8-inch NPT threaded half coupling port which is welded to the test section to provide temperature indication inside the test section. There are also thermocouple probes inserted into the facility piping to measure the water storage tank outlet temperature, test section water inlet temperature, heat exchanger outlet

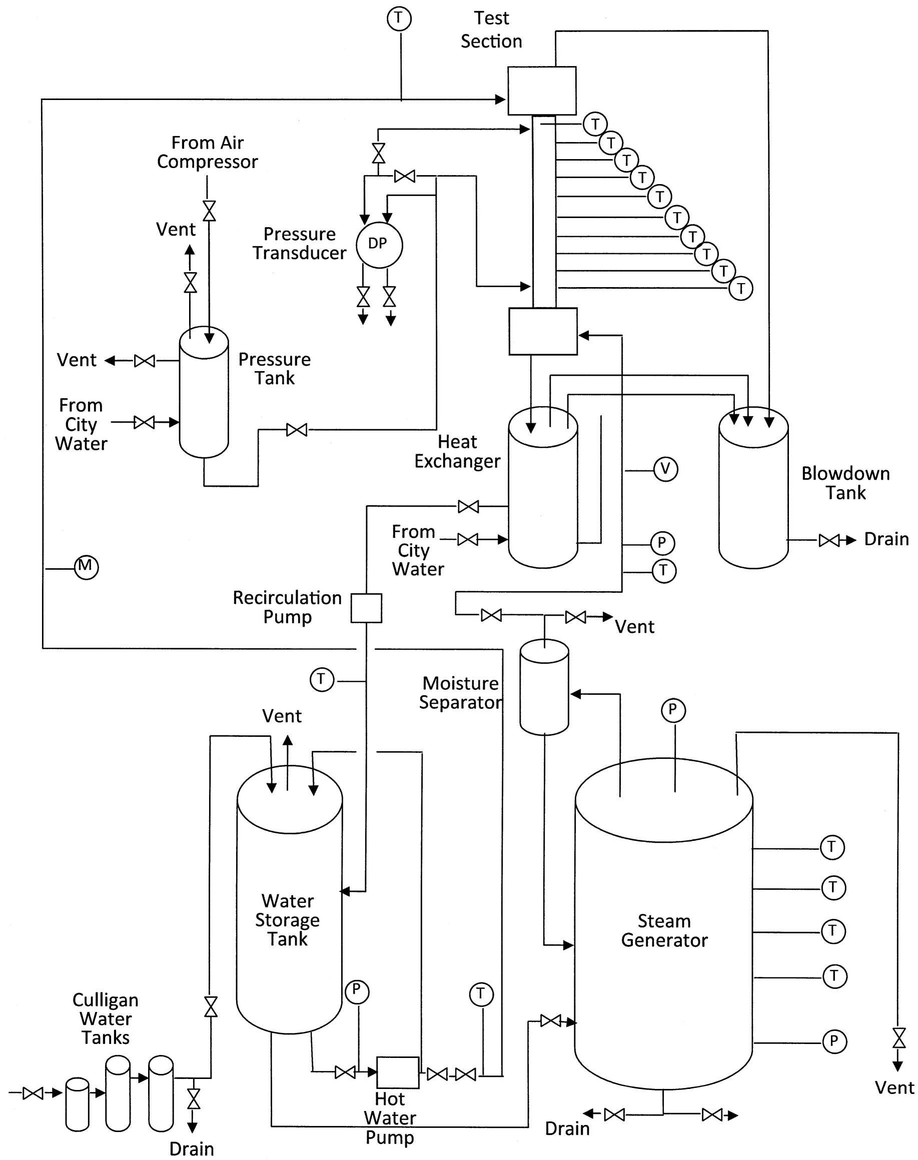

Fig. 3.6.: A diagram depicting the location of instrumentation throughout the facility.

temperature, and steam temperature. Finally, there are 4 probe type thermocouples inserted into 1/8-inch NPT instrument ports spaced axially along the steam generator. These thermocouples measure the temperature within the steam generator at different heights.

3.5.2 Flow Measurements

The water flow rate and steam flow rate are measured independently by separate instruments. The water flow rate is measured by a Yamatake Magnew 3000 plus magnetic flow meter (Model MGG14C). The flow meter uses Faraday's law to measure the velocity of the water. The meter consists of a ring which is installed around the outside of the pipe. The supplied DC voltage is used to generate a uniform magnetic field around the pipe. The water is a current carrying conductor which flows through the magnetic field inducing a voltage proportional to the velocity of the water. The velocity is converted to a volumetric flow rate by the meter circuitry and displayed locally in units of gallons per minute. The maximum working pressure of the meter is 2068 kPa and the maximum fluid temperature is 120°F.

The steam flow rate is measured by a Foxboro vortex flow meter (Model 83W-A). The steam is dry saturated steam; however, some condensate could be present in the system due to the throttling effects of the steam isolation valve. The meter uses a flow obstruction to create vortices which produce oscillations downstream in the flow path. These oscillations are sensed and converted to voltage proportional to steam velocity. The maximum working pressure of the vortex flow meter is 1500 psi with a maximum temperature of 400°F.

3.5.3 Pressure and Differential Pressure Measurements

Pressure measurements are taken in several different areas throughout the facility. All of the pressure indications are measured using Honeywell ST3000 absolute pressure transducers (Model STA-940). The pressure instruments measure level in the water storage tank, steam pressure and ambient pressure. The pressure transducer calibration does not drift with ambient temperature fluctuations between -40°C and 85°. Each individual pressure instrument is connected to the system through separate instrument ports and 1/4-inch stainless steel tubing which is ensured to be completely filled with water prior to testing.

A differential pressure measurement is taken across the test section during flooding tests. This is the most important identifying feature of the occurrence of flooding. The differential pressure instrument is a Honeywell ST3000 differential pressure transducer (Model STD-924). The transducer is connected to the test section via 2 instrument ports which are welded onto the test section and stainless steel tubing. The top port is 55.75 inches above the bottom port yielding a nominal differential pressure reading of 55.75 inches of water with no steam or water flowing through the test section.

An example of the differential pressure measurement throughout the duration of a flooding test is shown in Figure 3.7. Once water flow is initiated through the test section, the differential pressure increases slightly to approximately 56 inches of water. The exact value of the differential pressure varies with the water flow rate. As seen in Figure 3.7, as the steam flow rate is increased, the differential pressure also increases. The steam flow rate is incrementally increased until the flooding point which occurs at approximately 105 seconds in Figure 3.6. This marks to transition from counter-current flow to co-current flow. At the flooding point, the steam flow rate remains constant and disturbances in the water film from flow reversals cause the test section differential pressure to oscillate. After a period of time, the steam flow rate is reduced to zero and the flooding ceases as indicated at approximately

135 seconds in Figure 3.7. This transition is called deflooding and the differential pressure returns approximately to its original value before any steam flow through the test section. The flow regime returns to counter-current flow.

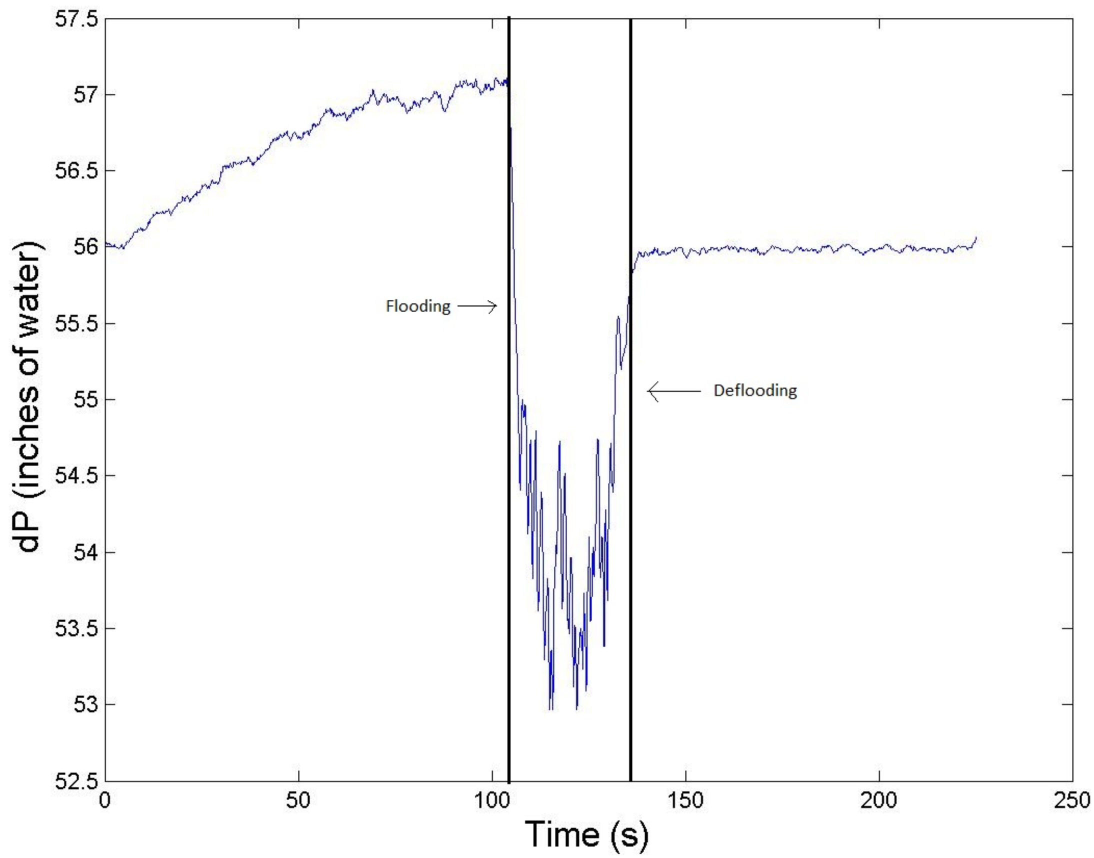

Fig. 3.7.: Differential pressure measurement for a flooding test conducted at 4.5 GPM.

Table 3.1: Instrumentation models and ranges.

Instrument	Manufacturer and Model	Quantity	Range
Differential Pressure Transducer	Honeywell STD-924	1	0 to 400 inches of water
Magnetic Flow Meter	Yamatake MagneW 3000 Plus 1/2-inch	1	0 to 28 GPM
Pressure Transducer (Atmospheric Pressure)	Honeywell STA-940	1	0 to 500 kPa
Pressure Transducer (Steam Pressure)	Honeywell STA-940	1	0 to 100 psig
Pressure Transducer (Water Tank Level)	Honeywell STA-940	1	0 to 100 psig
Thermocouple (Type T copper-constantan)	Omega	17	-250 to 350°C
Vortex Flow Meter	Foxboro 83W-A	1	0 to 30 g/s

3.5.4 Data Acquisition

The output of each instrument is wired into a National Instruments SCXI-1102b module which is connected to a SCXI-1000 chassis. This is the hardware which serves as the data acquisition system. The software component of the data acquisition system is a Labview virtual interface on a Dell Precision desktop computer. The Labview program senses all inputs on the National Instruments modules and samples the data at 200 Hz. The Labview program averages every 20 data points using a root mean square method and records this value for each input channel. The output of each channel is printed in a data file 10 times every second. The virtual interface, shown in Figure 3.8, allows the experimenter to see real-time data and adjust parameters accordingly for each test.

3.5.5 Calibrations

The calibration of every measuring instrument in the facility was checked with the exception of the temperature instruments. The thermocouples do have calibrations associated with them since their output correlates directly to a temperature value. The absolute pressure transducers and the differential pressure transducer were sent off to a facility to be calibrated since the proper calibration tools were not available in the lab. Upon re-installation in the system, the output was verified with a portable pressure tester and high accuracy pressure gage. Based on these results, a calibration curve was developed and incorporated into the Labview program.

The vortex flow meter, which measures steam flow in the system, was calibrated using an energy balance relationship. First, the system heat loss was determined. To perform this measurement, the steam generator was warmed up and pressurized to 50 psig. The steam generator was then maintained for two hours at this pressure to establish an equilibrium. Once the equilibrium was maintained, it was observed that leaving a 2 kW heater energized exactly maintained the pressure in the system. Therefore, the heat loss of the steam generator was assumed to be 2 kW. Next, the steam flow rate was adjusted to three different values corresponding to a low, medium and high steam flow rate. For each adjustment, the heaters were operated to maintain the steam generator at a constant pressure. The knowledge of the heater power for each steam flow rate allowed for the determination of the amount of steam production in the steam generator which was then used to calculate the steam flow rate. These different steam flow rates were plotted to obtain the calibration curve

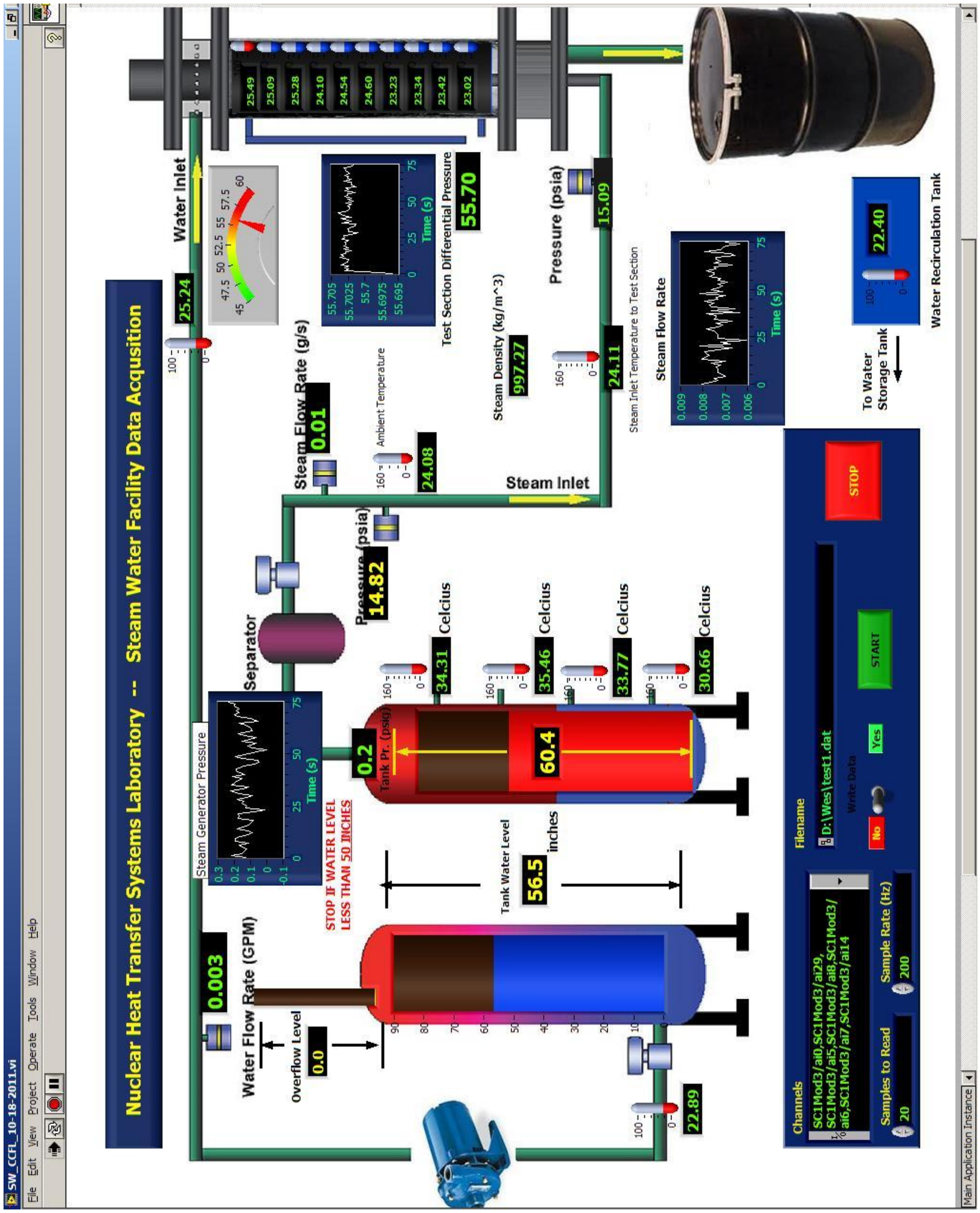

Fig. 3.8.: The Labview program front panel user interface.

for the steam flow detector. The data from these tests is shown in Appendix E Table E.1 and the calibration curve is shown in Figure E.1.

4. OPERATING PROCEDURES

The steam and water flooding facility at Texas A&M University contains several valves, pumps and instruments. To ensure consistency in operation and data collection, a series of procedures were developed. These procedures are also intended to ensure the safety of the lab equipment and personnel operating the facility. The procedures detailed in this section include operation of the steam generator, data acquisition system, recirculation system, cooling system and other important aspects of the experiment. All valve numbers referenced in these procedures correlate with those shown in Figure 3.1.

4.1 Data Acquisition System

The data aquisition system serves to collect all instrumentation data from the experiment and record these values into a text file at predetermined intervals. This procedure describes how to record data during a flooding test using the Labview front panel interface.

1. Open the Labview file titled “SWCCFL.vi” to display the facility front panel interface.

2. Turn on the 24 VDC power supply to the pressure transducers and flow detectors.

3. Turn on the National Instrument SCXI chassis to enable real time data capturing.

4. On the Labview front panel, click the “Run” button to start real time data display.

5. Ensure that all instruments are displaying expected values on the front panel.

6. On the Labview front panel, click the “Write Data” switch to yes.

7. Type the desired filename and path in the “Filename” box on the front panel.

8. Click the “Start” button on the front panel to begin recording data.

9. Click the “Stop” button on the front panel to end the data recording.

10. Repeat steps 7 through 9 for each subsequent test.

4.2 Filling the Water Storage Tank

After several tests have been performed, it may be necessary to refill the water storage tank or the steam generator. Since the steam generator is filled from the water storage tank, the operator must first fill the water storage tank in order to fill the steam generator. The water storage tank level should be maintained above 50 inches as indicated on the Labview front panel display to provide adequate net positive suction head for the hot water pump.

1. Ensure the Labview front panel is actively displaying data.

2. Open the valve V1.

3. Open the valve V3.

4. Check the indicating light on the Culligan tank. If the light is red, stop filling the water storage tank and coordinate with Culligan to change the DI tanks. If the light is green, continue filling the water storage tank until the water storage tank level on the front panel is approximately 70 inches.

5. Close the valve V3.

4.3 Filling the Steam Generator

Level in the steam generator should be maintained such that the magnetic float stays greater than 35 inches to ensure that all heaters in the steam generator remain covered with water. Since steam generator is filled from the water storage tank, follow the procedures detailed in Section 4.2 if necessary prior to filling the steam generator to ensure that there is adequate level in the water storage tank.

1. Ensure the Labview front panel is running and actively displaying data.
2. Ensure the steam generator is depressurized.
3. If the steam generator has been recently operated, ensure that the water temperature is below saturation.
4. Open valve V10.
5. Ensure that the level in the water storage tank is greater than the level in the steam generator. If water level in the steam generator is below the level in the water storage tank, fill the water storage tank.
6. Open valve V7.
7. Open valve V3 and fill the steam generator to approximately 60 inches.
8. Close valve V3.
9. Close valve V7.
10. Close valve V10.

4.4 Purging the Pressure Transducer Piping

From time to time, the piping to the pressure transducers must be flushed to ensure that the pipes are full of water. If they are not, it will cause erroneous readings during experimentation. Additionally, if testing is not performed frequently, the water in the detector piping can evaporate which will also produce undesirable readings. Therefore, the operator must ensure that the detector piping is properly filled.

4.4.1 Differential Pressure Transducer

The test section differential pressure transducer is prone to having the lines partially drained by evaporation after high temperature tests have been performed. Additionally, this detector is filled with unfiltered city water which increases the concern for dirt and debris to foul the piping. This procedure should be performed weekly or whenever the pressure transducer is reading greater than ±5% of 55.75 inches of water.

1. Turn on the air compressor to achieve a pressure of at least 30 psig.
2. Connect the air hose from the air compressor to the pressure tank.
3. Open valve V21.
4. Open valve V19 to fill the pressure tank with water.
5. When the pressure tank is full of water indicated by water coming out of the vent valve V21, close valve V19.
6. Close valve V21.
7. Open valves V22 and V29 to pressurize the pressure tank.
8. Open valves V25 and V26.
9. Open valve V18 to allow the water in the pressure tank to flow through the piping to the transducer.

10. Holding a bucket below valves V23 and V24, open valves V23 and V24 to purge the lines of air.

11. Close valves V23 and V24 when a continuous stream of water is observed to flow out of valves V23 and V24.

12. Close valve V18.

13. Close valve V25.

14. Close valves V22 and V29.

15. Slowly open valve V21 to vent the pressure tank.

16. Disconnect the air hose from the pressure tank.

4.4.2 Steam Pressure Transducer

The steam pressure transducer is filled with water collected from condensed steam as steam passing through the piping. Therefore, the water in this piping is pure and assumed to have minimal debris. This procedure to fill the detector piping should only be performed if the detector reads significantly different than expected or after the detector has been removed for maintenance and subsequently replaced.

1. Warm up and pressurize the steam generator to approximately 30 psig.

2. Start recirculation water flowing through the test section.

3. Open valve V28.

4. Ensure valve V27 is open.

5. Open V14 to initiate steam flow to the test section.

6. Allow steam to flow through the piping until water issues from valve V28.

7. Using a heat resistant glove, close valve V28.

8. Close valve V14 to secure steam flow.

9. If flooding tests will be conducted, leave the steam generator pressurized and recirculation flow enabled. If not, secure recirculation flow and vent the steam generator.

4.5 Water Recirculation

To initiate flooding tests, water circulation flow must be established and the flow rate must be adjusted to the desired level for testing. This procedure describes how to initiate water flow through the test section and adjust the flow rate of water traveling through the test section.

1. Ensure the water storage tank level is above 50 inches on the Labview front panel display.

2. Start the hot water pump.

3. Adjust the position of valves V5 and V6 to achieve the desired water flow rate. Valves V5 and V6 are both globe valves used to control the volumetric flow rate of water through the test section. One valve should remain fully open while the other should be used to adjust the system flow rate.

4. Start the recirculation pump.

5. Adjust valve V16 to maintain adequate water level in the heat exchanger and water storage tank.

4.6 Operating the Steam Generator

This procedure describes how to warm up the steam generator to produce steam for steam and water flooding tests. The water in the steam generator must be heated to the saturation temperature to induce boiling. Then, the steam generator must be purged of air to remove non-condensable gases from the system. The operating steam generator pressure may then be established.

1. Verify that valve V10 is open.

2. Turn the main breaker for the heater control panel on.

3. Turn the main switch on the heater control panel on.

4. Close valve V12.

5. Energize the appropriate number of heaters to heat the water in the steam generator. Avoid using the lowest 50kW heater as possible, although use of the lowest heater allows for better water mixing.

6. Allow the heaters to heat the water to the saturation temperature.

7. Continue to allow steam to generate and exit through valve V10 to purge the steam generator of air.

8. Close valve V10.

9. Ensure that the top thermocouple in the steam generator indicates approximately the same temperature as the bottom thermocouple. This verifies that the steam generator is adequately purged of air. If the thermocouple temperatures are not the same, open and close valve V10 to purge the air.

10. When the steam generator pressure reaches the desired value, turn off all heaters.

4.7 Cooling the Facility

After high temperature tests are conducted, the facility must be cooled to a safe temperature for safety concerns. This is accomplished by recirculating water though the heat exchanger with cooling water flowing through the copper coils to reduce the recirculation water temperature. This ensures that the tubing and connection joints are cooled to well below their design temperature limits to prevent failure from long term high temperature exposure.

1. Open valve V15 as needed to provide the appropriate amount of cooling flow.

2. Open valve V17 as needed to control the water level in the blowdown tank.

4.8 Performing a Flooding Test With Water Inlet Temperature < 80°C

To perform a flooding test, a series of steps must be performed to prepare the system and establish the proper initial conditions. This procedure describes the necessary steps to perform flooding tests at low water inlet temperatures.

1. Establish the proper water levels in the water storage tank and steam generator. Refer to sections 4.2 and 4.3.

2. Heat up the steam generator as detailed in section 4.6.

3. Establish water recirculation flow at the desired water flow rate for the flooding test as described in Section 4.5.

4. Initiate a moderate amount of steam flow to heat the water inlet temperature to the desired value for the flooding test.

5. Secure the steam flow to the test section once the desired temperature is achieved.

6. Record data for a period of approximately 10 seconds as a baseline to ensure that all instruments are functioning properly. Stop recording data after 10 seconds.

7. Begin recording data for the flooding test.

8. Establish cooling water flow to facilitate steam condensation in the blowdown tank.

9. Slowly open the steam flow valve, V14, in small increments until flooding is achieved. Flooding is marked by a sudden decrease in the test section differential pressure.

10. Allow flooding to continue for 10 to 20 seconds and then close V14.

11. Continue to record data until the test section temperatures stabilize.

12. Stop the data acquisition.

4.9 Performing a Flooding Test With Water Inlet Temperature > 80°C

High temperature tests are slightly different than low temperature tests. The procedural differences between the low temperature tests and high temperature tests are described in this section.

1. Follow the procedure of the low temperature testing in Section 4.8 with the modified steps below.

2. Establishing cooling water flow is optional and it depends on the test temperature. For tests close to the saturation temperature, cooling water flow should be off during the test.

3. Prior to commencing the test, turn on both heater tapes in the water piping from the water storage tank to the test section. This provides added heating

to ensure the testing temperature is reached. The heater tapes may or may not be necessary depending on the test temperature.

4.10 Facility Shutdown

When all testing has been completed for the day, the experimental facility must be shutdown properly. This includes turning off all pumps, heaters, and instrumentation along with ensuring that all valves are in their proper shutdown position. The steam generator is also allowed to vent and cool. The shutdown procedure ensures that the experiment is left in a safe condition prior to the experimenter leaving for the day.

1. Ensure all steam generator heaters are off.
2. Turn off the main switch on the heater panel.
3. Open the main breaker for the heater control panel.
4. Open valve V10 to vent the steam from the steam generator. Leave the steam generator vent valve open until the thermocouples in the steam generator are all below the saturation temperature.
5. Close valve V10
6. Leave the recirculation system running as necessary with cooling flow initiated until the test section water inlet temperature is less than 50°C.
7. When water temperature is below 50°C, turn off the recirculation pump.
8. Close valve V16.
9. Turn off the hot water pump.
10. Turn off the SCXI chassis and 24 VDC power supply.
11. Open valve V12.

12. Close valves V17 and V15 to secure cooling water flow.

5. RESULTS AND DISCUSSION

In this section, the collection of data is described along with the method to reduce the data from each test to a single point in order to analyze flooding trends on a large scale. The ranges for testing parameters and the program scripts used to reduce the data are explained in detail. Finally, the data results are presented with a discussion of the findings.

5.1 Test Ranges and Parameters

The important parameters for flooding experiments include the steam flow rate, water flow rate and density of the liquid and gas phases. The ranges of these parameters along with a few other parameters of interest are given for the full testing range in Table B.1.

For each test, the water flow rate was set to a predetermined value before the test was conducted. Then the steam flow rate was slowly and incrementally increased to the flooding point. Once flooding was achieved the steam flow rate remained constant for approximately 10 seconds and then the steam isolation valve was shut. As indicated in Table B.1, the water flow rate was varied between 3.5 and 12.0 GPM during the course of testing. Additionally, the water inlet temperature was varied in 5°C increments from 35°C to 90°C. Lastly, tests were also performed at numerous water flow rates at 97°C. A simplified test matrix of important parameters is shown in Table 5.1

5.2 Data Reduction

The data collected during each test was printed to a data file for storage. These data files were processed using two different MATLAB scripts. The MATLAB scripts used in each process are shown in Appendix A. The first MATLAB script determined

Table 5.1: Test matrix for the current research.

Parameter	Range
Volumetric Water Flow Rate	3.5 to 12.0 GPM
Water Inlet Temperature	35 to 97°C
Steam Mass Flow Rate	22 to 37 g/s
System Pressure	1 atm
Steam Generator Pressure	20 to 62 psig

the value of each measured parameter at the time of flooding. The script determined the time of flooding by a drop in the test section differential pressure.

These parameters were used to calculate the superficial velocities of the vapor and steam at the onset of flooding. Using the superficial velocities, each flooding test can be represented as a single data point at the time of flooding for the test conditions. This data provided the means for analysis to determine the effects of water inlet subcooling on flooding conditions. The reduced data is provided in Table B.1 located in Appendix B.

The second MATLAB script converted the tabular data into graphical data according to each test parameter as a function of time. The graphs for each test section temperature, steam flow rate, water flow rate and test section differential pressure are shown in Appendix D. The graphs for each test show the behavior of measured parameters as a function of time. The water flow rates remain fairly constant for the duration of each test since the desired water flow rate was achieved prior to the start of each test. The steam flow rate increases slowly over time until flooding is achieved. Flooding is indicated by a sharp decrease in the test section differential pressure followed by rapid fluctuations. After a brief period of time spent in the flooding condition, the steam flow rate is reduced to zero and the test section defloods. The deflooding is marked by the increase and subsequent steadiness of the test section differential pressure correlating to the decrease in steam flow rate. The data recording continued for a period of time after the steam flow rate was reduced to zero to allow the system to return to equilibrium. Figures 5.1 through 5.4 are example graphs of flooding tests conducted at a water flow rate of 4.5 GPM and water inlet temperature of 70°C.

The drop in the differential pressure can be seen in Figure 5.1 at approximately the 90 second mark. This indicates the flooding point. Flooding is followed by rapid fluctuations in the test section differential pressure. These fluctuations are due to the chaotic nature of flooding as waves form and travel upward along the water film. The test section temperatures shown in Figure 5.2 correlate with the differential pressure trends. The thermocouple reading inside the test section rises rapidly as the steam flow rate increases in the test section. A graph of the steam flow rate is shown in Figure 5.4. At approximately 40 seconds, the temperature inside the test section reaches saturation temperature. The surface thermocouple readings follow the inside temperature with some time delay due to the conduction through the wall of the test section. At the time of flooding, the inside thermocouple reading oscillates similar to the differential pressure oscillations.

The temperature oscillations of the thermocouple inside the test section are due to parts of the water film breaking off and becoming entrained in the steam. As the water impinges on the thermocouple, the temperature indication oscillates. Most of the surface thermocouple reading trends are close to each other with the exception of the top surface thermocouple. The top surface thermocouple tends to be lower than the other readings which could be due to the proximity of the thermocouple to the water inlet.

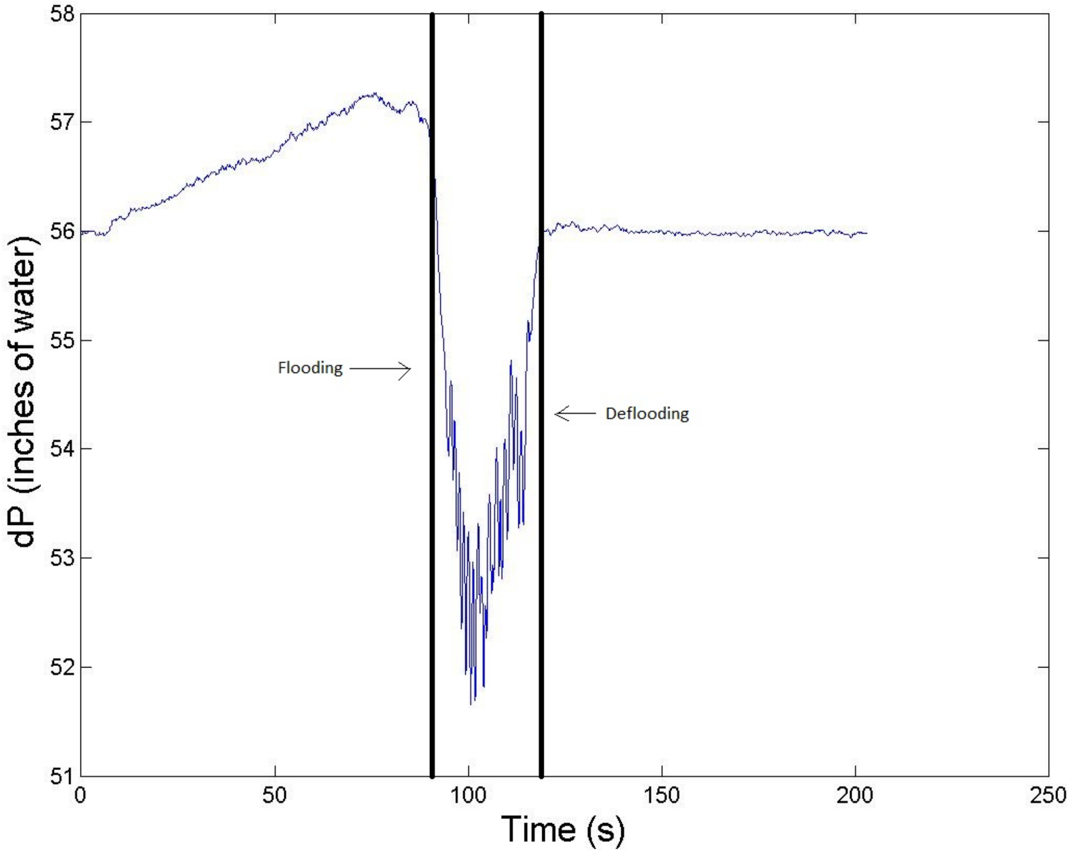

Fig. 5.1.: Differential pressure measurement for a flooding test conducted at 4.5 GPM.

The water flow rate is plotted on a narrow ordinate range in Figure 5.3. For all tests the water flow rate remains fairly constant throughout the duration of the test. This is because the water flow rate is adjusted to the desired value before the data recording is started. Minor fluctuations can be observed during flooding tests depending on the water flow rate and the extent of the fluctuations in the test section differential pressure.

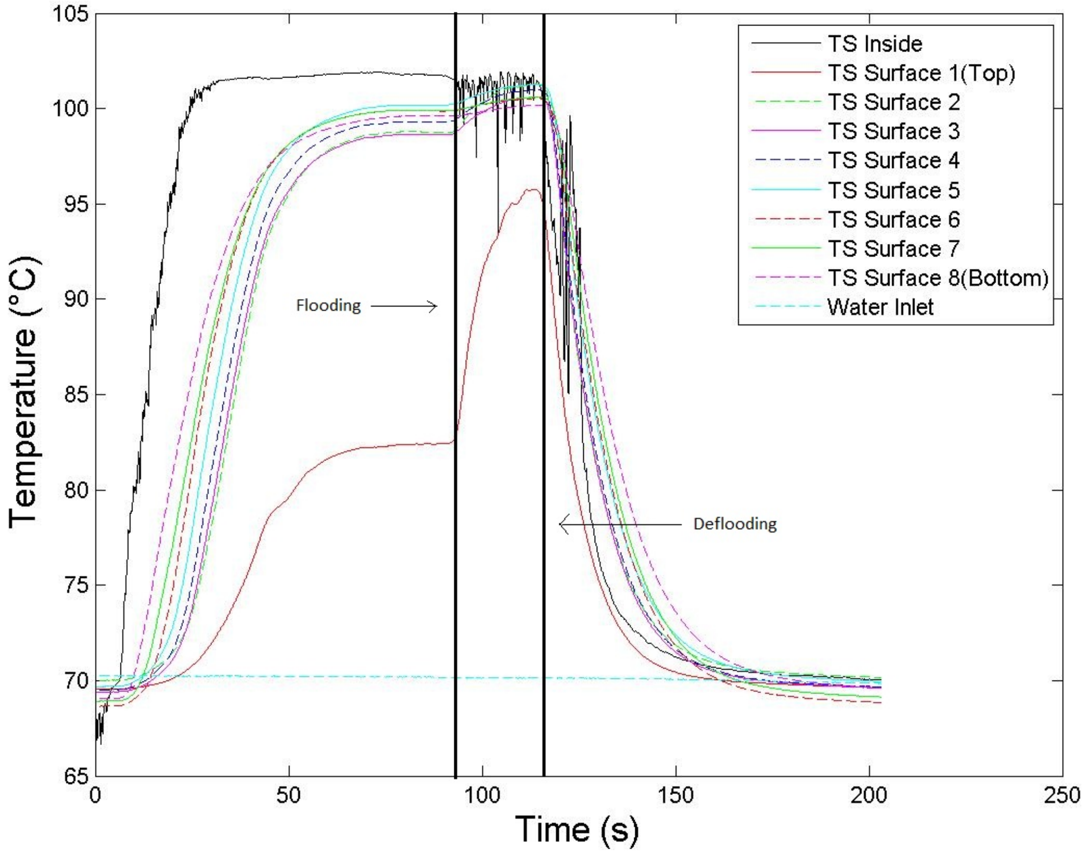

Fig. 5.2.: Test section temperatures for a flooding test conducted at 4.5 GPM.

5.3 Comparison of Low Subcooling Flooding Tests to Air-Water Flooding Data

The purpose of conducting flooding tests of varying water inlet temperature was to determine the effect of water subcooling on the flooding phenomenon. As described in Section 2, several researchers have performed steam-water flooding tests at a few different water temperatures. The most widely used method to account for the water subcooling has been the steam condensation correction proposed by Wallis using Equations 2.8 and the empirical correlation in Equation 2.9. Since this method did

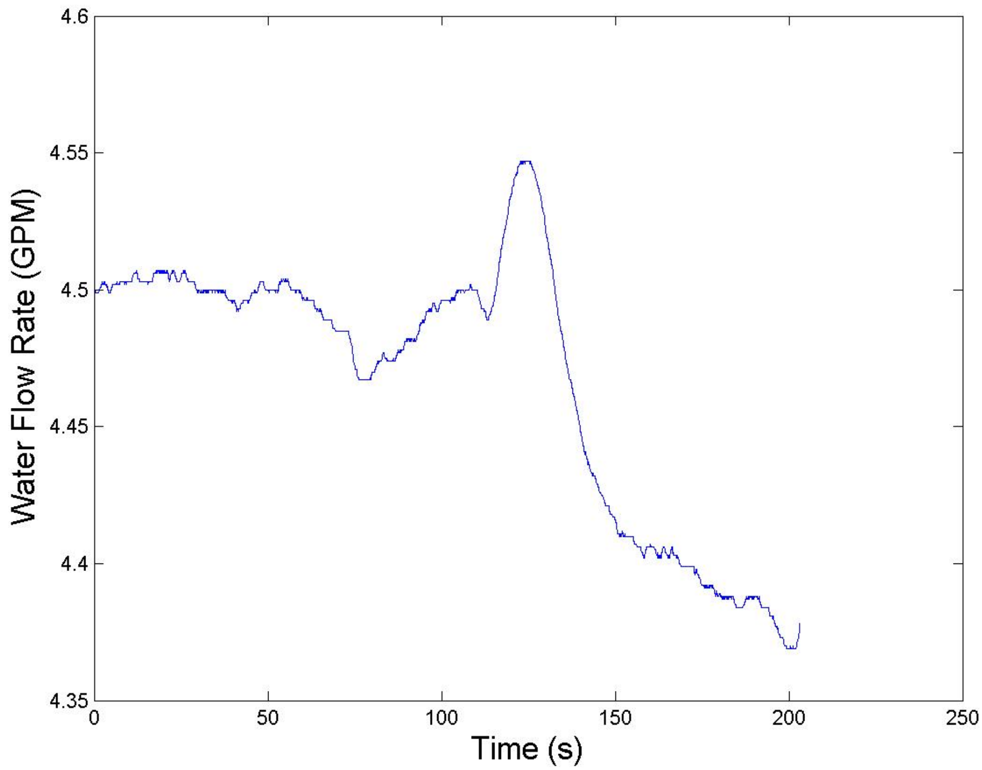

Fig. 5.3.: Water flow rate measurement for a flooding test conducted at 4.5 GPM.

not produced good results with the current facility as stated in Williams's thesis, Equations 2.11 and 2.12 are used to analyze the data. Even though the previous researchers have performed similar experiments, tests need to be conducted with the current geometry to analyze the behavior of flooding in the pressurizer surge line. Additionally, the results of the previous experiments have not been compared with air-water data. Comparing the steam-water data to air-water data provides an important benchmark; especially for steam-water experiments performed with water near saturation temperature. The correlations developed by Wallis and Williams both indicate that in the absence of steam condensation the data should follow the same trend as the Wallis air-water correlation shown in Figure 2.1. A comparison

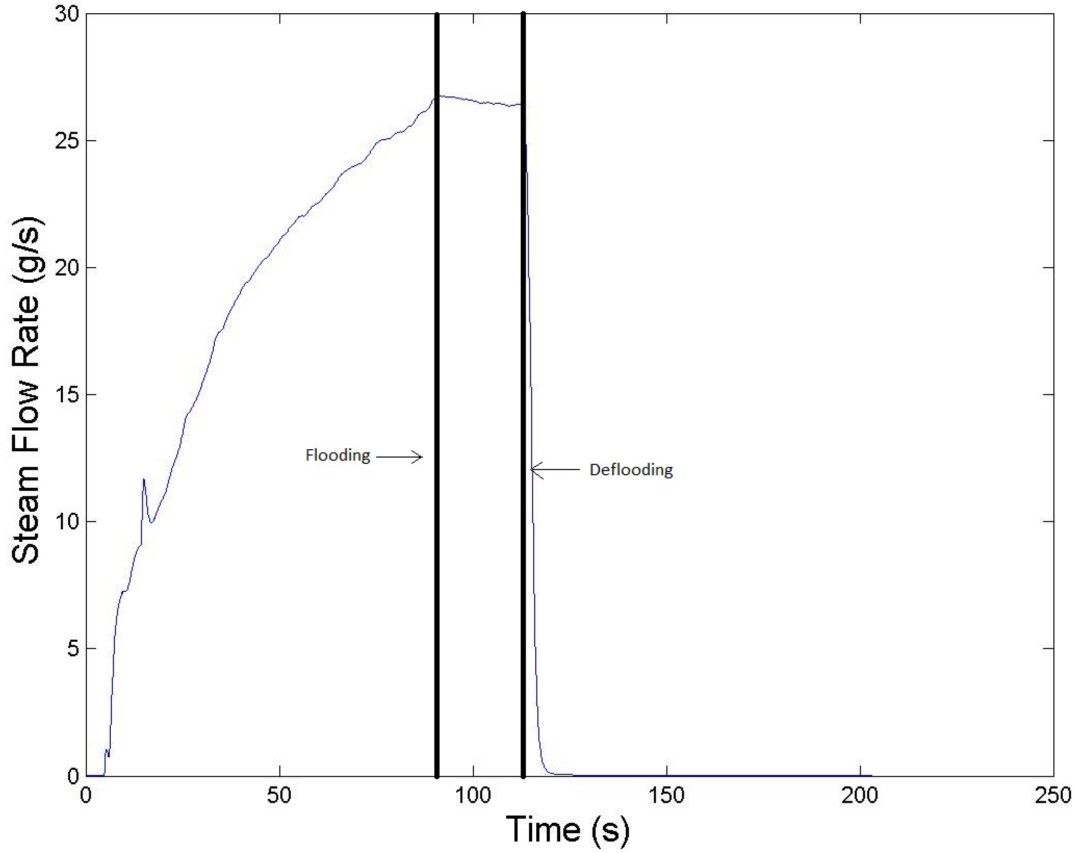

Fig. 5.4.: Steam flow measurement for a flooding test conducted at 4.5 GPM.

between the air-water data obtained by Williams and the current steam-water data at a water inlet temperature of approximately 97°C is shown in Figure 5.5.

The data from the 97°C tests has a similar linear trend and slope to that of the air-water data however it is shifted above the air-water data. The data is shifted upward because the water is still slightly subcooled which causes some steam condensation. Therefore, more steam flow is needed to initiate a flooding event. The method Williams developed was used to account for the steam condensation to obtain the effective Kutateladze number for the steam flow. The corrected data using

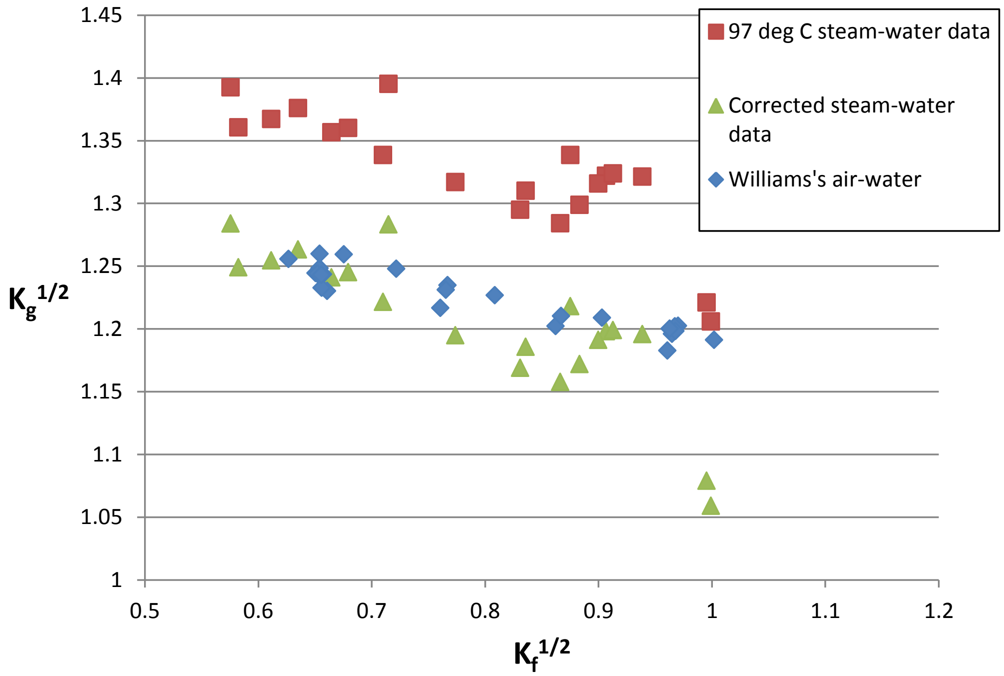

Fig. 5.5.: Comparison of current data with Williams air-water data.

the effective Kutateladze number for the vapor phase overlaps the air water data. This verifies that in the event of saturated water and steam flooding tests, the data matches with air and water flooding tests. This makes sense because there is no mass transfer in either situation so flooding should happen at the same flow rate for either scenario. The corrected data does seem to have a slightly different slope which can be attributed to the modifications made to the facility between the collection of the air-water and the current data. *This comparison validates the current data and serves as the basis of this research.*

5.4 Comparison of 70°C Data

Another important benchmark is achieved by comparing the current data for 70°C flooding tests to data obtained by Williams and Draznin at 70°C. The results of the comparison are shown in Figure 5.6. The current data obtained during the experiments shows a departure from the previous data, especially in the range of K_f between 0.7 and 0.9, while the data at low and high water flow rates match with that of Draznin and Williams. The maximum deviation between the current and previous data is approximately 10.5% which is less than the experimental error of 11% as quantified in Section 5.6. Therefore, the deviation is considered acceptable. The most likely cause for this departure in the data is because of the facility modification described in Section 3.4. This modification changed the geometry of the test section outlet which influences the constants, m and c, in the Wallis and Kutateladze correlations. A change in these constants changes the shape of the curve which is seen in Figure 5.6.

The approach to flooding can change the point at which flooding is achieved. This is shown in Figure 5.6 at the mark where K_f is equal to 0.8. There are three data points at slightly different K_g values. These indicated three different tests where the approach to flooding was varied. The point with the lowest K_g value was the fastest approach to flooding and the point with the highest K_g was the slowest approach to flooding. This indicates that there is a factor associated with the repeatability of each flooding test. Different approaches to flooding can affect the steam flow rate in which flooding is achieved.

Another comparison was made to the data obtained by Williams at a water temperature of 70°C after the data was corrected using the steam condensation factor. This data is shown in Figure 5.7 with linear trend lines for each data set.

The current data has a larger magnitude slope which, again, can be attributed to the facility alteration. The constants for a new correlation based on the facility

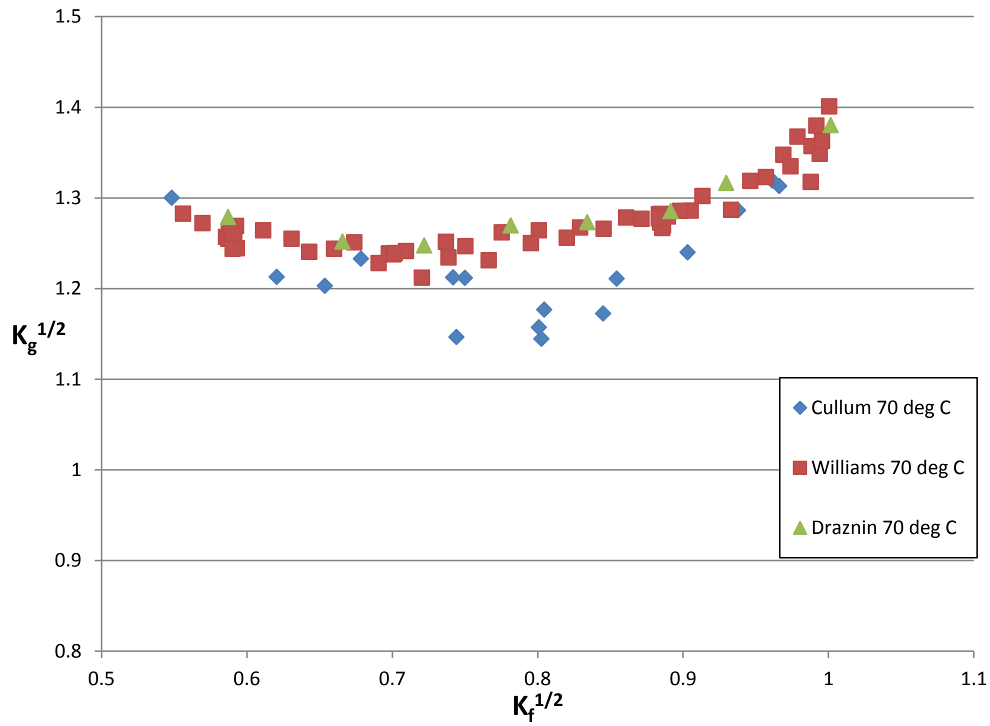

Fig. 5.6.: Comparison of current data with Williams and Draznin data for 70°C.

alteration can be determined directly from the linear trend line for the current data; however, analysis of the complete data set will show that this is not necessary.

5.5 Reduced Data Results

The steam flow rate and water flow rate raw data is plotted in Figure 5.8. The data is plotted separately for each water inlet temperature to show different trends as the water inlet temperature is varied.

The data at 35°C shows a fairly linearly increasing trend from low water flow rates to high water flow rates. As the water inlet temperature increases, the data shifts clockwise to a concave down trend between 85°C and 90°C. This data trend shows good agreement with the trends observed by Wallis in Figure 2.2. At the

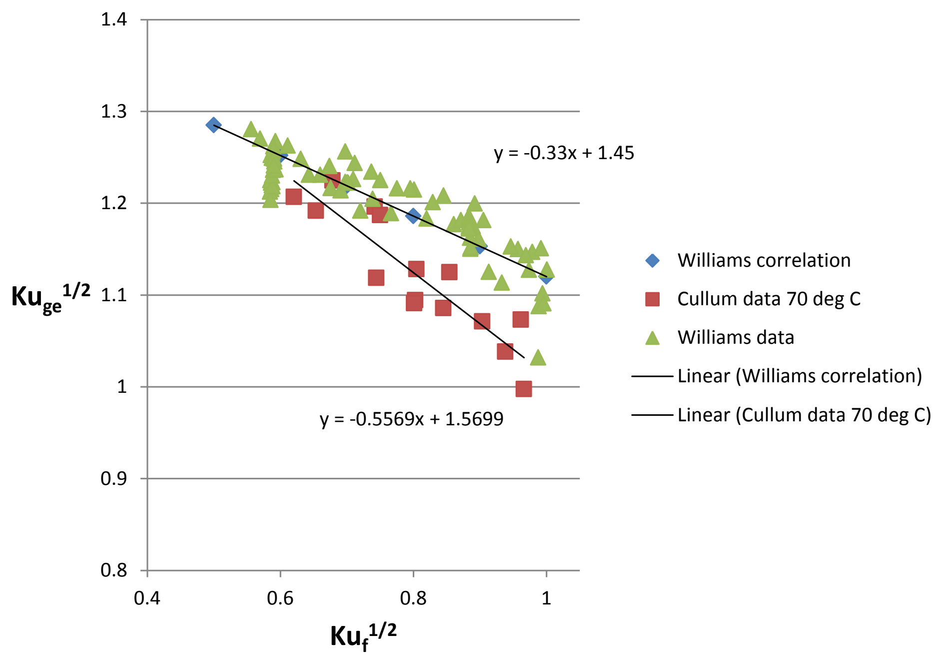

Fig. 5.7.: Comparison of 70°C data between current data and Williams when corrected for steam condensation.

lowest water inlet temperature of 35°C, the data is governed entirely by Boundary 2. This data follows closely with the line $R_T = 1$. This line represents the water flow rate required to condense all of the steam sent through the test section. Once the water inlet temperature reaches 55°C, the data represents the lines formed by Boundary 1 and Boundary 2. First, the steam flow rate decreases as the water flow rate increases. Then, the required steam flow rate needed to induce flooding increases as the water flow rate increases. As the water inlet temperature continues to increase, the turning point when the steam flow rate changes from a downward trend to an upward trend shifts to the right. The 97°C data represents the data closest to saturation conditions. The data was expected to be represented closely by

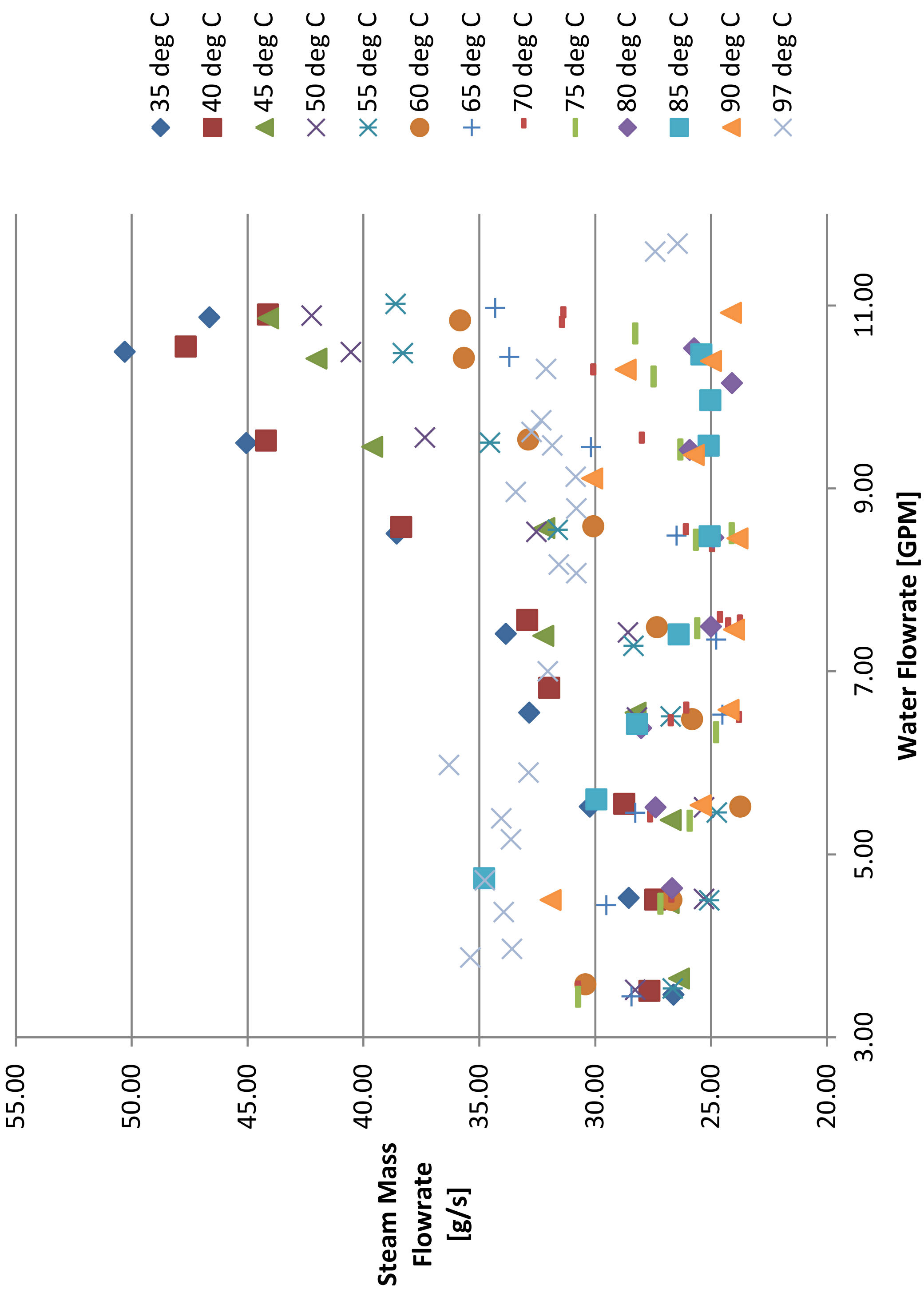

Fig. 5.8.: Raw experimental data at flooding conditions for each test.

the Wallis flooding line with a negative slope. This expectation is confirmed by the data in Figure 5.5.

At water temperatures close to saturation, a downward trend is observed. This indicates the the flooding phenomenon is governed by a purely hydrodynamic process. As the water temperature decreases, there becomes a transition point where the data trend changes from a downward direction to an upward direction. This indicates that thermal parameters influence the onset of flooding and it is not a solely hydrodynamic process. The thermal influence produces a marked shift in the data trend.

The reduced data was used to calculate the Kutateladze parameters, using Equations 2.4 and 2.5, at the time of flooding for each test. This data is shown in Figure 5.9. The same trends are observed in this data as were observed in Figure 5.8 since the water flow rate and steam flow rate are directly proportional to the Kutateladze parameters. The data was represented in terms of the Kutateladze parameters because the test section is classified as a large diameter tube.

Due to the large amount of data plotted in Figure 5.8 and 5.9, the data from each temperature is plotted individually in Appendix C. The figures in Appendix C provide better clarity of the trend shift from low temperatures to high temperatures.

5.6 Data Error Analysis

An analysis was conducted to determine the approximate amount of error in the current flooding data. In this analysis, several sources of error were considered. First, data was examined for several tests at the same water flow rate to test the repeatability and randomness associated with flooding tests. The tests were selected from the 70°C water inlet temperature since this was approximately the midpoint of the temperature range analyzed for this research. Three tests were analyzed at a water flow rate of 6.5 GPM and three other tests were analyzed at a flow rate of 10.5 GPM to determine the randomness. The tests conducted at 6.5 GPM had an error of 4.5 percent which was higher than the error for the 10.5 GPM tests.

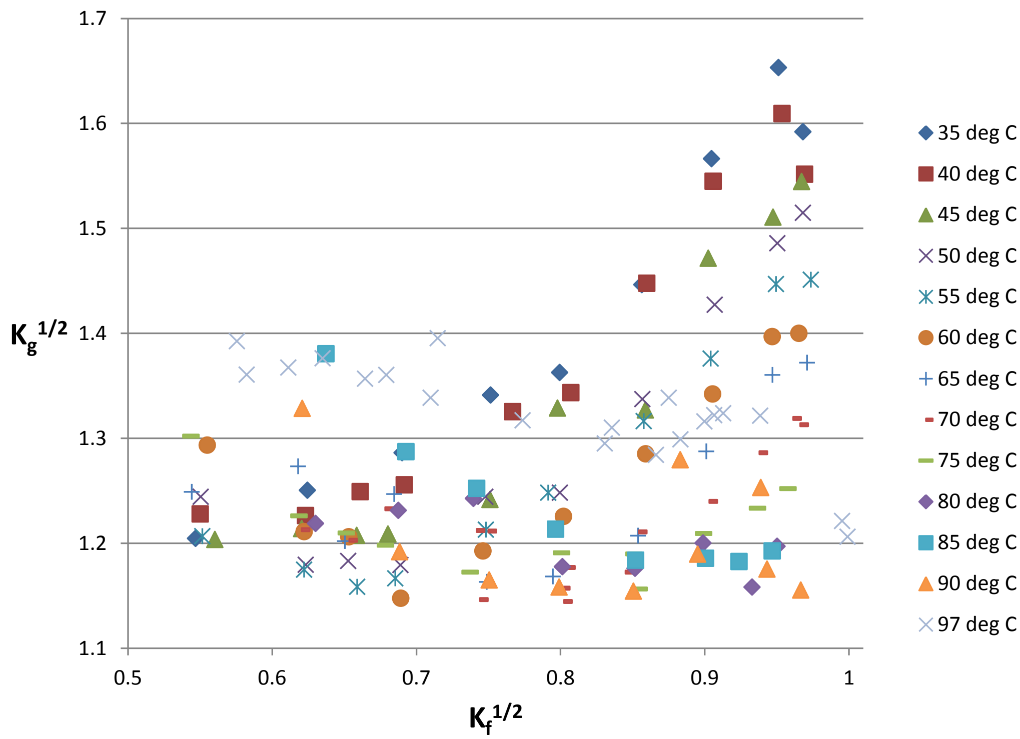

Fig. 5.9.: Raw data plotted in terms of the Kutateladze parameters.

As a conservative estimate, the higher error was used in the analysis for random fluctuations. A second source of error is due to the instrumentation used in the facility. While each instrument has its own associated error, the combined instrument error is approximately 1 percent using the values quoted by the manufactures of the instruments. Lastly, there is a small error associated with converting the data from analog values to digital values. This error was determined to be extremely small and was neglected for this analysis. The total error was calculated to be approximately 5.5 percent of the measured values. The raw data with error bars is shown in Figure 5.10.

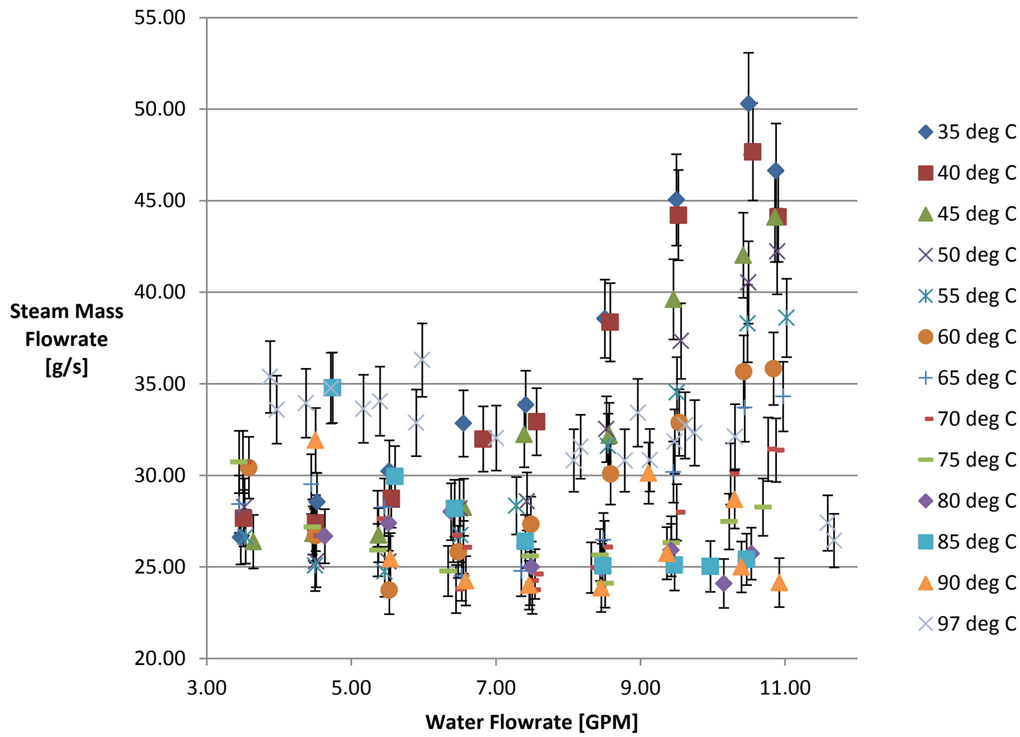

Fig. 5.10.: Raw data plotted with error bars.

5.7 Steam Condensation Correction

Finally, the data was analyzed using the method developed by Williams to account for the fraction of steam which condenses on the water film during a flooding test. This fraction is calculated using Equation 2.11 and implemented in K_ge, the effective Kutateladze number for the vapor.

The net result of using this fraction yields the modified Wallis correlation using the fraction of condensed steam and Kutateladze parameters as shown in Equation 2.12. This methodology was applied to the current data to obtain Figure 5.11. The data in Figure 5.11 is plotted in separate series for each water inlet temperature. The trend for each water inlet temperature is a line with a negative slope which ultimately resembles the correlation obtained by Williams. Even though each water

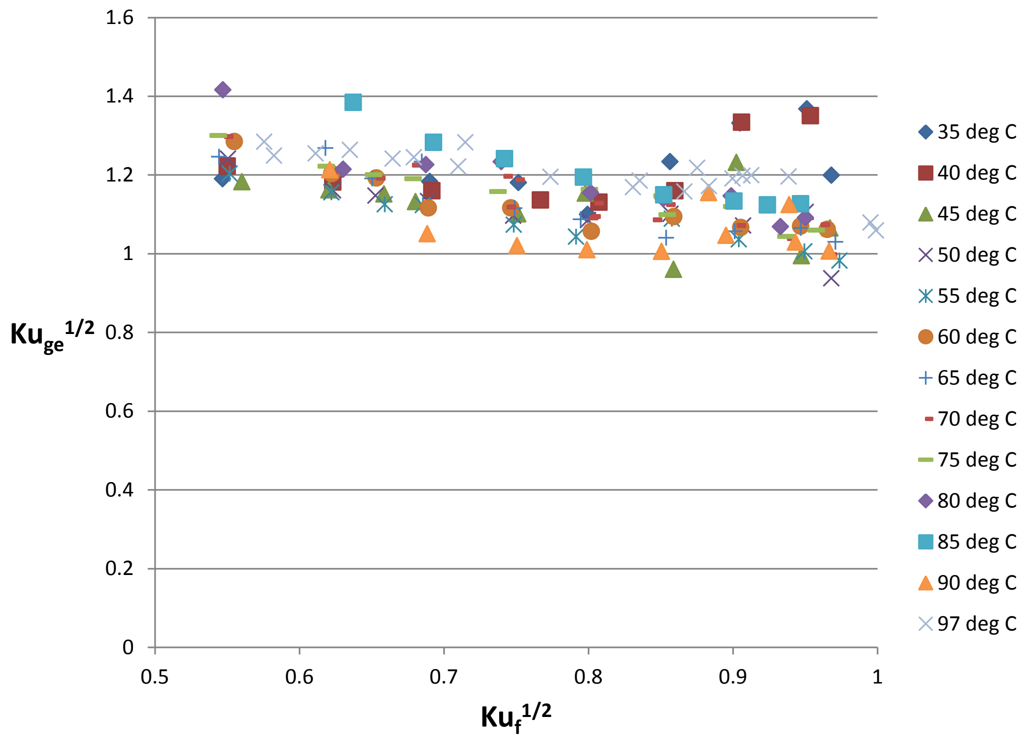

Fig. 5.11.: Final data with steam condensation correction plotted for each water inlet temperature.

inlet temperature produced a different trend when plotted with the standard Kutateladze parameters as shown in Appendix C, the final data shown in Figure 5.11 all shows approximately the same relationship. The data is all plotted in the same series in Figure 5.12 to facilitate the use of a trend line.

The trend line indicates an extremely close relationship with the correlation developed by Williams for the 70°C data. The correlation developed by Williams is shown in Figure 5.7. Due to the close relationship between Williams correlation and the data obtained from the subcooled experiments, it is concluded that the steam condensation fraction provides a good prediction of flooding over a range of subcooled water temperatures. A new correlation is not necessary even with the facility

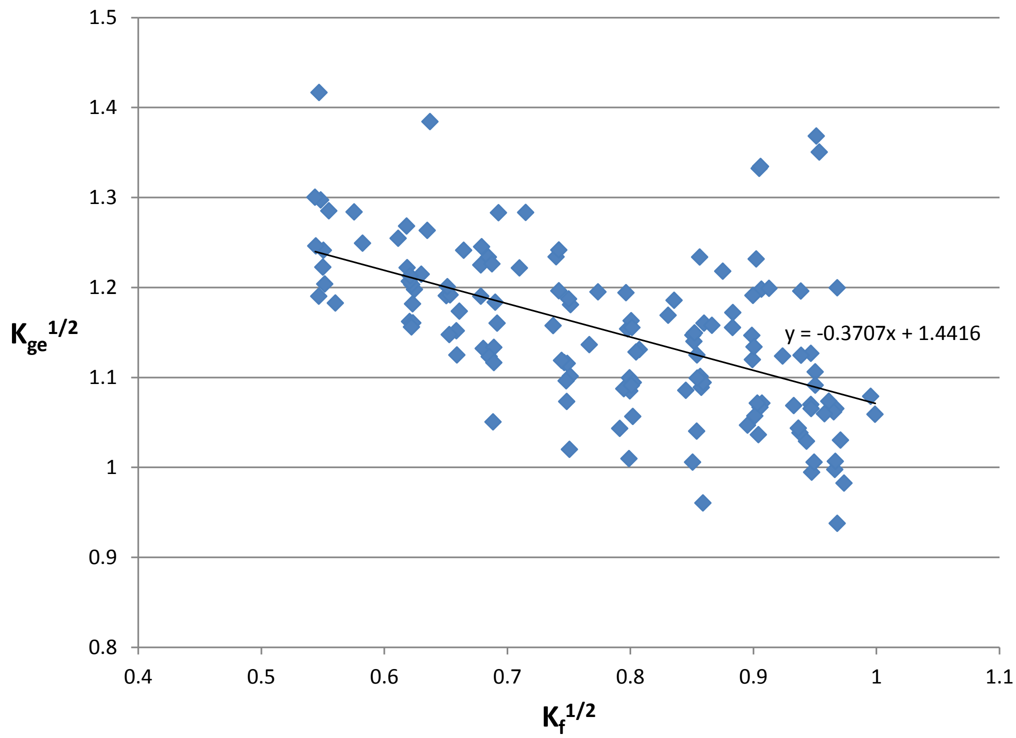

Fig. 5.12.: Final data with steam condensation correction and linear trend line.

modification based on this data. Williams correlation accurately accounts for varying degrees of subcooling by correcting the vapor Kutateladze parameter for the faction of steam which condenses on the water film.

6. CONCLUSIONS AND FUTURE WORK

6.1 Conclusions

Flooding experiments were performed to analyze the effect of subcooled water on the phenomenon in the pressurizer surge line of a PWR. The motivation for this research was to provide a flooding correlation which accounts for varying degrees of subcooling. In a PWR, reactor accidents could produce a wide range of water inlet temperatures in the pressurizer surge line yielding the need for an analytic means to determine the behavior of flooding under these conditions. A flooding correlation accounting for the subcooling effects of the inlet water can be used in reactor analysis computer codes to provide better predictions of flooding in the pressurizer surge line. Furthermore, a more accurate prediction of a pressurizer surge line rupture due to high temperature creep can be assessed.

In this research, flooding tests using steam and water were conducted at varying degrees of water subcooling. The lowest subcooling tests were performed at 97°C and compared to air-water data obtained using the same facility. The steam water data agreed with the air-water data which provided an important benchmark. From high subcooling to low subcooling tests, the same patterns were observed as Wallis noted in Figure 2.2. At low water temperatures, a significant amount of steam condensed on the water film while at high water temperatures, a minimal amount of steam condenses in the test section. To account for the steam condensation caused by water subcooling, the correlation developed by Williams was used to analyze the data. This method collapsed all of the tests conducted at various water temperatures into a trend which corresponds to the air-water data. Therefore, the work performed during this research was benchmarked by air-water data and proved that the correlation developed by Williams accounts for varying degrees of water subcooling. The flooding correlation developed by Williams can be appropriately used for water subcooling values between 0 and 65°C in large diameter tubes using steam and water.

6.2 Future Work

Although extensive research has been performed in the area of flooding in a vertical tube, there is still more work which can be done to improve flooding models in the future. The main aspect of flooding which has not been addressed in this research is the significance of varying pressure on the phenomenon. All tests conducted during this research were performed at atmospheric pressure. In order to provide a correlation which can truly predict flooding conditions in a PWR pressurizer surge line, a pressure scaling analysis must be performed.

Another aspect of flooding which needs to be addressed is the location of the origin of flooding events. This could provide better data in terms of heat transfer during the flooding event and insight to the propagation of the event. Determining the exact location of the onset of the flow reversal could lead to better knowledge of the time required for other parts of the film to reverse direction. The velocity and direction of the water film directly affects the heat transfer from the steam to the liquid film.

Lastly, the mechanism of flooding must be determined. While there are several theories about what causes flooding, no one theory has been proven. The determination of the cause of flooding would be a tremendous asset to this research and could be used to develop a better prediction of flooding in all applications.

REFERENCES

[1] T. K. Sherwood, G. H. Shipley, and F. A. L. Holloway. Flooding velocities in packed columns. Industrial and Engineering Chemistry, 30(7):765–769, 1938.

[2] W. E. Lobo, L. Friend, F. Hashmall, and F. Zenz. Limiting capacity of dumped tower packings. American Institute of Chemical Engineers, 42(3):693–710, 1946.

[3] G. B. Wallis, D. C. deSieyes, R. J. Rosselli, and J. Lacombe. Countercurrent annular flow regimes for steam and subcooled water in a vertical tube. Technical report, Electric Power Research Institute, 1980.

[4] G. B. Wallis. One-dimensional Two-phase Flow. McGraw-Hill, Inc., New York, 1969.

[5] G. B. Wallis. Flooding velocities for air and water in vertical tubes. Technical report, Reactor Developement Division, Atomic Energy Establishment, 1961.

[6] O. L. Pushinka and YU. L. Sorokin. Breakdown of liquid film motion in vertical tubes. In Heat Transfer - Soviet Research, volume 1. 1969.

[7] S. S. Kutateladze and I. G. Malenkov. Experimental investigation of the analogy between the process of boiling and bubbling. Journal of Applied Mechanics and Technical Physics, 1966.

[8] S. S. Kutateladze. Boiling heat transfer. In Proceedings of Heat Transfer Conference Number SC-957, Minsk, USSR, 1961.

[9] S. S. Kutateladze. Elements of the hydrodynamics of gas-liquid systems. In Fluid Mechanics - Soviet Research, volume 1, pages 29–50. 1972.

[10] G. B. Wallis and S. Makkenchery. The hanging film phenomenon in vertical annular two-phase flow. Journal of Fluids Engineering (1974) 297–298, .

[11] M. Vijayan, S. Jayanti, and A. R. Balakrishnan. Effect of tube diameter on flooding. International Journal of Multiphase Flow 27 (2001) 797–816.

[12] C. L. Tien. A Simple Analytical Model for Counter-current Flow Limiting Phenomena with Vapor Condensation, volume 4, pages 231–238. Pergamon Press, Great Britain, 1977.

[13] P. Rothe and C. Crowley. Scaling of pressure and subcooling for countercurrent flow. NUREG CR-0464, Nuclear Regulatory Commission, 1978.

[14] G. B. Wallis, C. J. Crowley, and J. A.Block. ECC bypass studies. In Proceedings of American Institue of Chemical Engineers 80th National Meeting, Boston, MA, 1975.

[15] J. A. Block and G. B. Wallis. Heat transfer and fluid flows limited by flooding. The American Institute of Chemical Engineers, pages 73–82, 1978.

[16] S. N. Williams. Flooding experiments with steam and water in a large diameter vertical tube. Master's thesis, Texas A&M University, 2009.

[17] O. Draznin, S. N. Ritchey, and K. Vierow. Experimental study of water subcooling effect on steam-water flooding in a large diameter vertical tube. In Proceedings of ICAPP 2010, San Diego, CA, 2010.

[18] K. W. McQuillan and P. B. Whalley. A comparison between flooding correlations and experimental flooding data for gas-liquid flow in vertical circular tubes. Chemical Engineering Science, 1985.

[19] D. Bharathan and G. B. Wallis. Air-water countercurrent annular flow. International Journal of Multiphase Flow 9 (4) (1983) 349–366.

[20] K. W. McQuillan, P. B. Whalley, and G. F. Hewitt. Flooding in vertical two-phase flow. International Journal of Multiphase Flow 11 (6) (1985) 741–760.

[21] Y. Cheng, C. Shih, J. Wang, and H. Lin. An investigation of steam-water countercurrent flow model in trace. Annal of Nuclear Energy, (37):1378–1383, 2010.

APPENDIX A
MATLAB SCRIPTS

The MATLAB script used to reduce the data from a flooding test to a single data point is given below.

```
clear all


datafile='test1f.dat';
rootname='C:\Users\wcullum\Documents\Raw data\thesis tests\';


for i = 1:1
    filename=[rootname datafile];
    M = load(filename);
    dp = M(:,6);
    % mass_flow = data(:,2);
    len = length(dp);
    dx = 1.0;
    vel_cmpr = dp(1);
    for j = 1:len-1
       if (((dp(j+1)-vel_cmpr))>2*dx)
            vel_cmpr = dp(j+1);
       end
       if (dp(j+1)<(vel_cmpr - 1*dx))
           (j-1)/10                  % time at onset of flooding
           M(j-1,:)             % parameters at flooding
           min(M(j-1:j+200,6))  % min dp
           mean(M(j-1:j+200,6)) % mean dp
           % flooding_velocity = dp(j-1)
```

```
            % flooding_massFlow = mass_flow(j-1)
            % waterExitPr = mean(data(1:j-1,8))
            break
        end
    end
end
```

The MATLAB script used to generate all of the graphical data in APPENDIX C is given below.

```
clear;
clc;

listoffiles=dir('*.dat');
[numoffiles one]=size(listoffiles);

for i=1:numoffiles

    cvin = load(listoffiles(i).name);
    namewithoutdatisone=regexp(listoffiles(i).name, 'test\w*','match');
    %break
    fileidentifier=namewithoutdatisone(1);
    steamflow=cvin(:,1);
    ambp=cvin(:,2);
    ambt=cvin(:,3);
    steamp=cvin(:,4);
    steamt=cvin(:,5);
    dp=cvin(:,6);
    wstouttemp=cvin(:,7);
    wstlevel=cvin(:,8);
    waterf=cvin(:,9);
    sgp=cvin(:,10);
    sgt4=cvin(:,11);
    sgt3=cvin(:,12);
    sgt2=cvin(:,13);
    sgt1=cvin(:,14);
```

```
    tsinside=cvin(:,15);
    ts1=cvin(:,16);
    ts3=cvin(:,17);
    ts8=cvin(:,18);
    tswaterin=cvin(:,19);
    ts2=cvin(:,21);
    ts4=cvin(:,22);
    ts5=cvin(:,23);
    ts6=cvin(:,24);
    ts7=cvin(:,25);
    hxout=cvin(:,26);

    namesteamflow=char(strcat(fileidentifier,'_steamflow.jpg'));
    nameambp=char(strcat(fileidentifier,'_ambp.jpg'));
    nameambt=char(strcat(fileidentifier,'_ambt.jpg'));
    namesteamp=char(strcat(fileidentifier,'_steamp.jpg'));
    namesteamt=char(strcat(fileidentifier,'_steamt.jpg'));
    namedp=char(strcat(fileidentifier,'_dp.jpg'));
    namewaterf=char(strcat(fileidentifier,'_waterf.jpg'));
    namesgp=char(strcat(fileidentifier,'_sgp.jpg'));
    namesgt4=char(strcat(fileidentifier,'_sgt4.jpg'));
    namesgt3=char(strcat(fileidentifier,'_sgt3.jpg'));
    namesgt2=char(strcat(fileidentifier,'_sgt2.jpg'));
    namesgt1=char(strcat(fileidentifier,'_sgt1.jpg'));
    namealltemps=char(strcat(fileidentifier,'_alltemps.jpg'));


time=0:0.1:(.1*(size(steamflow)-1));
```

```
time=time';
plot(time,steamflow);
xlabel('Time (s)','fontsize',16);
ylabel('Steam Flow Rate (g/s)','fontsize',16);
print('-djpeg',namesteamflow);

aaaambp=plot(time,ambp);
xlabel('Time (s)','fontsize',16);
ylabel('Ambient Pressure (psia)','fontsize',16);
print('-djpeg', nameambp);
aaaambt=plot(time,ambt);
xlabel('Time (s)','fontsize',16);
ylabel('Ambient Temperature (C)','fontsize',16);
print('-djpeg', nameambt);
aaasteamp=plot(time,steamp);
xlabel('Time (s)','fontsize',16);
ylabel('Steam Pressure (psia)','fontsize',16);
print('-djpeg', namesteamp);
aaasteamt=plot(time,steamt);
xlabel('Time (s)','fontsize',16);
ylabel('Steam Temperature (C)','fontsize',16);
print('-djpeg', namesteamt);
aaadp=plot(time,dp);
xlabel('Time (s)','fontsize',16);
ylabel('dP (inches of water)','fontsize',16);
print('-djpeg', namedp);
aaawaterf=plot(time,waterf);
xlabel('Time (s)','fontsize',16);
```

```
ylabel('Water Flow Rate (GPM)','fontsize',16);
print('-djpeg', namewaterf);
aaasgp=plot(time,sgp);
xlabel('Time (s)','fontsize',16);
ylabel('Steam Generator Pressure (psig)','fontsize',16);
print('-djpeg', namesgp);
aaasgt1=plot(time,sgt1);
xlabel('Time (s)','fontsize',16);
ylabel('Steam Generator Temperature (C)','fontsize',16);
print('-djpeg', namesgt1);
aaasgt2=plot(time,sgt2);
xlabel('Time (s)','fontsize',16);
ylabel('Steam Generator Temperature 2 (C)','fontsize',16);
print('-djpeg', namesgt2);
aaasgt3=plot(time,sgt3);
xlabel('Time (s)','fontsize',16);
ylabel('Steam Generator Temperature 3 (C)','fontsize',16);
print('-djpeg', namesgt3);
aaasgt4=plot(time,sgt4);
xlabel('Time (s)','fontsize',16);
ylabel('Steam Generator Temperature 4 (C)','fontsize',16);
print('-djpeg', namesgt4);

aaatsinside=plot(time,tsinside,'k');
xlabel('Time (s)','fontsize',16);
ylabel('Temperature (C)','fontsize',16);
hold on;
aaats1=plot(time,ts1,'r');
```

```
aaats2=plot(time,ts2,'--g');
    aaats3=plot(time,ts3,'m');
aaats4=plot(time,ts4,'--b');
    aaats5=plot(time,ts5,'c');
    aaats6=plot(time,ts6,'--r');
    aaats7=plot(time,ts7,'g');
    aaats8=plot(time,ts8,'--m');
    aaatswaterin=plot(time,tswaterin,'--c');
hold off;
legend('TS Inside', 'TS Surface 1(Top)', 'TS Surface 2',

 'TS Surface 3', 'TS Surface 4', 'TS Surface 5',

'TS Surface 6', 'TS Surface 7', 'TS Surface 8(Bottom)',

 'Water Inlet',1);
%legend('Location',1);
    print('-djpeg', namealltemps);
end
```

APPENDIX B
REDUCED DATA

This appendix contains the tabular results of every flooding test conducted during this research. The test matrix contains flooding test performed at varying water inlet temperatures and water flow rates. This table contains the data used to analyze the effects of water subcooling on flooding.

Table B.1: Reduced data from all steam and water flooding tests.

Test Number	Water Inlet Temp [°C]	Steam Flow Rate [g/s]	Water Flow Rate [g/s]	TC Inside [°C]	TC 1 [°C]	TC 2 [°C]	TC 3 [°C]	TC 4 [°C]	TC 5 [°C]	TC 6 [°C]	TC 7 [°C]	TC 8 [°C]	DP [Inches of Water]
1	35.13	35.13	3.47	101.16	90.68	92.06	93.93	96.63	98.08	97.57	97.52	98.60	55.28
2	35.03	35.03	4.53	98.03	64.58	69.18	74.36	82.21	89.78	90.53	92.85	94.52	55.27
3	35.14	35.14	5.53	94.16	50.48	53.97	59.12	67.85	78.53	82.22	87.80	90.81	55.39
4	35.31	35.31	6.55	57.50	42.79	44.80	48.51	56.65	68.66	75.44	83.14	87.55	55.51
5	35.15	35.15	7.41	92.45	38.86	39.73	42.09	47.58	56.28	64.59	75.62	82.21	57.35
6	35.05	35.05	8.51	35.72	36.09	35.49	36.11	37.04	41.24	59.75	80.50	86.60	57.43
7	35.14	35.14	9.50	50.55	35.87	35.46	35.98	37.07	43.12	60.92	81.94	85.83	57.96
8	35.23	35.23	10.50	58.55	35.74	35.43	35.86	38.16	46.18	62.11	82.26	83.70	58.09
9	35.62	35.62	10.88	58.28	35.95	35.65	35.81	36.47	38.44	52.65	73.70	79.82	59.73
10	40.38	40.38	3.51	101.51	97.49	97.61	98.48	99.71	99.80	99.62	99.21	100.07	55.13
11	40.21	40.21	4.51	98.78	70.09	74.27	78.72	85.59	91.44	91.92	93.88	95.54	55.17
12	40.19	40.19	5.55	98.42	56.28	59.58	64.03	71.87	81.04	84.10	89.04	91.71	55.53

Test Number	Water Inlet Temp [°C]	Steam Flow Rate [g/s]	Water Flow Rate [g/s]	TC Inside [°C]	TC 1 [°C]	TC 2 [°C]	TC 3 [°C]	TC 4 [°C]	TC 5 [°C]	TC 6 [°C]	TC 7 [°C]	TC 8 [°C]	DP [Inches of Water]
13	40.07	40.07	6.82	52.23	45.43	46.55	49.99	56.77	66.59	73.17	81.33	86.09	55.41
14	40.24	40.24	7.56	87.67	42.86	42.84	44.78	49.76	58.63	68.98	80.39	85.89	57.53
15	40.02	40.02	8.58	47.99	41.41	41.33	41.83	44.04	50.20	60.16	74.35	82.20	57.74
16	39.83	39.83	9.53	44.41	40.60	40.08	40.87	43.27	53.94	69.20	84.18	87.25	57.43
17	40.05	40.05	10.55	63.86	40.63	40.28	40.57	42.11	50.15	64.01	82.15	85.54	57.95
18	39.97	39.97	10.91	57.29	40.74	39.88	40.39	40.76	40.29	43.69	54.50	70.30	59.61
19	40.01	40.01	5.07	97.51	61.56	65.37	69.82	77.55	85.69	87.26	90.72	92.88	55.34
20	45.45	45.45	3.65	99.85	86.43	88.49	91.08	94.21	96.36	96.21	96.21	97.72	55.38
21	45.01	45.01	4.47	99.18	70.91	74.33	78.39	84.48	90.03	91.04	92.95	94.61	55.17
22	45.02	45.02	5.38	99.07	62.65	66.08	70.85	77.90	85.11	87.44	91.14	93.39	55.38
23	45.10	45.10	6.55	71.80	52.98	55.17	58.95	65.92	74.94	80.01	86.45	89.77	55.54
24	44.98	44.98	7.39	90.40	47.74	48.33	50.59	56.27	65.40	74.26	83.21	88.09	57.33
25	44.82	44.82	8.57	73.74	46.57	46.19	47.11	50.08	55.92	62.17	72.16	79.78	57.37

Test Number	Water Inlet Temp [°C]	Steam Flow Rate [g/s]	Water Flow Rate [g/s]	TC Inside [°C]	TC 1 [°C]	TC 2 [°C]	TC 3 [°C]	TC 4 [°C]	TC 5 [°C]	TC 6 [°C]	TC 7 [°C]	TC 8 [°C]	DP [Inches of Water]
26	45.04	45.04	9.46	68.96	45.75	45.60	45.74	46.74	50.53	62.88	78.74	86.22	57.71
27	44.96	44.96	10.42	78.71	45.72	45.27	45.51	45.97	46.36	51.00	61.43	74.36	59.66
28	44.61	44.61	10.86	71.11	45.32	44.90	45.10	45.52	45.72	50.44	62.96	76.27	59.65
29	45.27	45.27	5.04	98.91	69.13	73.03	77.38	84.08	90.10	81.29	93.27	95.04	55.33
30	50.26	50.26	3.52	101.80	99.12	99.15	99.67	100.54	100.20	100.18	99.88	100.39	55.17
31	50.03	50.03	4.51	99.95	89.92	91.50	93.38	95.97	97.45	97.39	97.70	98.66	55.26
32	49.78	49.78	5.52	98.24	92.18	93.84	96.27	96.76	95.28	97.38	95.48	96.58	55.46
33	49.65	49.65	6.50	67.37	56.58	58.77	62.52	68.67	76.02	80.05	85.41	89.05	55.44
34	50.04	50.04	7.43	64.74	53.83	54.86	57.34	63.34	73.06	79.49	85.86	89.56	55.25
35	49.89	49.89	8.53	58.98	53.28	54.52	56.76	61.65	69.16	74.54	81.90	86.26	55.82
36	49.71	49.71	9.56	64.46	51.19	51.04	51.84	54.53	59.46	64.68	73.53	80.79	57.83
37	50.02	50.02	10.49	53.63	51.33	50.87	51.43	53.16	57.28	63.12	72.60	80.73	58.09

Test Number	Water Inlet Temp [°C]	Steam Flow Rate [g/s]	Water Flow Rate [g/s]	TC Inside [°C]	TC 1 [°C]	TC 2 [°C]	TC 3 [°C]	TC 4 [°C]	TC 5 [°C]	TC 6 [°C]	TC 7 [°C]	TC 8 [°C]	DP [Inches of Water]
38	49.99	49.99	10.89	66.62	50.57	50.12	50.29	50.67	50.39	53.27	60.67	72.96	59.91
39	50.18	50.18	4.95	100.36	81.34	84.22	87.33	91.65	94.73	95.10	85.90	97.14	55.21
40	55.01	55.01	3.54	101.63	99.33	99.16	99.70	100.54	100.26	100.20	99.77	100.45	55.09
41	55.24	55.24	4.50	101.29	90.65	91.98	93.89	96.31	97.53	97.50	97.60	98.64	55.14
42	54.60	54.60	5.46	100.92	79.33	82.08	85.36	89.82	93.39	94.05	95.45	96.76	55.48
43	54.88	54.88	6.51	71.95	63.31	65.58	69.08	74.56	80.64	82.71	86.85	89.90	55.06
44	55.17	55.17	7.28	71.39	59.63	60.97	63.79	68.63	74.35	77.56	82.70	86.58	55.45
45	54.80	54.80	8.55	72.43	58.96	60.23	63.08	67.93	74.02	77.22	82.73	86.87	55.49
46	54.65	54.65	9.50	71.16	56.59	56.67	58.34	61.73	66.52	70.17	76.48	82.16	57.58
47	54.84	54.84	10.48	67.83	55.85	55.51	56.14	58.11	61.51	65.34	71.79	78.58	57.79
48	54.82	54.82	11.02	54.85	55.82	55.42	55.82	57.19	59.94	64.11	70.89	78.58	58.02
49	55.02	55.02	5.05	100.76	84.62	86.81	89.33	92.88	95.35	95.57	96.22	97.45	55.47
50	60.47	60.47	3.58	100.91	98.18	97.89	98.59	99.24	99.03	99.00	98.34	99.45	54.99

Test Number	Water Inlet Temp [°C]	Steam Flow Rate [g/s]	Water Flow Rate [g/s]	TC Inside [°C]	TC 1 [°C]	TC 2 [°C]	TC 3 [°C]	TC 4 [°C]	TC 5 [°C]	TC 6 [°C]	TC 7 [°C]	TC 8 [°C]	DP [Inches of Water]
51	60.14	60.14	4.51	101.59	97.20	97.37	98.27	99.51	99.53	99.54	99.28	99.94	55.24
52	59.96	59.96	5.53	101.36	87.40	89.11	91.20	94.24	96.20	96.30	96.96	98.02	55.23
53	59.70	59.70	6.48	98.15	77.33	79.52	82.24	86.45	90.30	90.88	92.78	94.75	55.33
54	60.09	60.09	7.48	76.18	68.84	70.58	73.11	77.20	81.69	82.96	86.17	89.37	55.49
55	59.72	59.72	8.59	66.13	64.77	66.67	69.69	74.39	79.62	81.78	86.03	89.22	55.47
56	60.01	60.01	9.54	74.02	62.42	63.22	65.44	69.24	73.84	76.43	81.35	85.62	57.70
57	59.86	59.86	10.43	64.74	61.65	61.72	63.18	66.35	70.39	73.64	79.00	84.03	58.43
58	60.18	60.18	10.84	59.92	61.94	61.89	63.34	66.47	70.38	73.93	79.17	84.18	58.41
59	59.86	59.86	4.96	100.73	95.48	95.98	97.02	98.49	98.75	98.83	98.74	99.37	55.32
60	64.98	64.98	3.45	100.24	100.49	100.04	100.46	101.00	100.37	100.40	100.02	100.44	55.07
61	65.20	65.20	4.45	100.70	98.35	98.38	99.13	100.09	99.92	99.92	99.58	100.26	55.43
62	64.80	64.80	5.46	100.47	95.32	95.76	96.91	98.39	98.75	98.80	98.67	99.54	55.22

Test Number	Water Inlet Temp [°C]	Steam Flow Rate [g/s]	Water Flow Rate [g/s]	TC Inside [°C]	TC 1 [°C]	TC 2 [°C]	TC 3 [°C]	TC 4 [°C]	TC 5 [°C]	TC 6 [°C]	TC 7 [°C]	TC 8 [°C]	DP [Inches of Water]
63	64.81	64.81	6.53	101.18	86.91	88.24	90.10	92.90	94.87	94.94	95.81	97.14	55.47
64	64.89	64.89	7.35	96.53	80.52	82.42	84.78	88.29	91.34	92.09	93.83	95.32	55.32
65	64.65	64.65	8.49	74.63	71.09	73.17	75.79	79.78	83.83	85.36	88.60	91.06	55.34
66	65.29	65.29	9.46	97.68	69.25	70.44	72.60	76.07	79.83	81.38	85.01	88.28	55.57
67	64.67	64.67	10.44	74.65	67.17	67.63	69.40	72.37	75.79	78.02	82.00	85.89	57.97
68	64.76	64.76	10.98	74.27	66.66	66.80	68.26	70.81	73.61	76.06	80.09	84.56	58.00
69	64.75	64.75	4.93	100.83	96.66	96.97	97.87	99.10	99.11	99.18	99.06	99.62	55.17
70	69.64	69.64	3.50	101.36	100.63	100.06	100.50	100.92	100.30	100.38	99.79	100.40	55.01
71	70.16	70.16	4.49	100.93	98.96	98.81	99.47	100.29	99.91	99.94	99.64	100.15	55.05
72	70.56	70.56	5.36	101.54	97.38	97.53	98.40	99.56	99.54	99.57	99.43	100.06	55.17
73	70.01	70.01	6.41	101.37	94.77	95.35	96.30	98.03	98.51	98.65	98.95	99.54	55.47
74	69.96	69.96	6.45	101.51	93.14	93.75	94.96	96.81	97.60	97.64	97.90	98.69	55.59

Test Number	Water Inlet Temp [°C]	Steam Flow Rate [g/s]	Water Flow Rate [g/s]	TC Inside [°C]	TC 1 [°C]	TC 2 [°C]	TC 3 [°C]	TC 4 [°C]	TC 5 [°C]	TC 6 [°C]	TC 7 [°C]	TC 8 [°C]	DP [Inches of Water]
75	69.94	69.94	6.55	100.83	94.16	94.66	95.66	97.39	97.91	98.01	98.34	98.90	55.67
76	70.43	70.43	7.50	101.45	89.62	90.57	91.93	94.20	95.54	95.78	96.66	97.52	55.41
77	70.11	70.11	7.47	101.23	87.20	88.23	89.77	92.25	94.04	94.11	95.09	96.40	55.55
78	69.55	69.55	7.54	100.79	91.09	91.75	92.92	95.04	96.12	96.23	96.87	97.62	55.47
79	69.91	69.91	8.32	94.43	85.14	86.32	87.99	90.56	92.55	92.87	94.17	95.61	55.37
80	69.98	69.98	8.50	97.09	86.30	87.24	88.73	91.20	93.00	93.24	94.41	95.72	55.28
81	69.57	69.57	9.50	79.08	77.00	78.30	80.31	83.29	86.09	87.02	89.46	91.77	55.82
82	69.68	69.68	10.25	93.11	73.29	74.10	75.69	78.43	81.24	82.56	85.51	88.48	57.78
83	69.45	69.45	10.88	80.48	71.48	71.73	73.07	75.44	77.82	79.70	82.82	86.16	58.12
84	70.44	70.44	10.77	92.39	74.69	75.25	77.10	79.74	82.25	83.47	86.09	88.96	57.76
85	70.03	70.03	4.98	101.30	97.41	97.56	98.24	99.36	99.22	99.32	99.30	99.69	55.17
86	74.94	74.94	3.45	101.69	101.23	100.53	100.96	101.42	100.64	100.65	100.28	100.56	54.94

Test Number	Water Inlet Temp [°C]	Steam Flow Rate [g/s]	Water Flow Rate [g/s]	TC Inside [°C]	TC 1 [°C]	TC 2 [°C]	TC 3 [°C]	TC 4 [°C]	TC 5 [°C]	TC 6 [°C]	TC 7 [°C]	TC 8 [°C]	DP [Inches of Water]
87	74.85	74.85	4.46	101.65	99.67	99.36	99.94	100.72	100.21	100.24	100.01	100.37	55.19
88	75.59	75.59	5.37	101.08	98.36	98.24	98.98	100.03	99.75	99.80	99.70	100.08	55.24
89	74.75	74.75	6.34	101.61	96.51	96.64	97.47	98.89	98.99	99.02	99.15	99.65	55.23
90	74.75	74.75	7.47	101.54	94.23	94.49	95.49	97.25	97.98	97.82	98.30	98.92	55.37
91	74.48	74.48	8.51	101.42	91.31	91.70	92.80	94.77	95.78	95.86	96.63	97.49	55.50
92	74.92	74.92	8.44	101.23	92.34	92.77	93.80	95.71	96.57	96.83	97.59	98.24	55.34
93	74.56	74.56	9.43	101.35	88.40	88.93	90.25	92.24	93.51	93.83	94.81	96.00	55.91
94	74.98	74.98	10.70	99.51	82.35	82.82	84.19	86.14	87.72	88.22	89.76	91.74	56.00
95	74.39	74.39	10.23	98.91	81.41	81.90	83.33	85.51	87.36	87.83	89.56	91.55	57.23
96	75.41	75.41	4.95	101.25	98.33	98.32	98.89	99.84	99.50	99.58	99.57	99.87	55.10
97	80.77	80.77	3.49	102.20	101.85	101.01	101.49	102.00	101.23	101.21	100.89	101.19	57.16
98	79.39	79.39	4.63	101.45	100.13	99.67	100.21	100.92	100.30	100.32	100.14	100.41	55.06

Test Number	Water Inlet Temp [°C]	Steam Flow Rate [g/s]	Water Flow Rate [g/s]	TC Inside [°C]	TC 1 [°C]	TC 2 [°C]	TC 3 [°C]	TC 4 [°C]	TC 5 [°C]	TC 6 [°C]	TC 7 [°C]	TC 8 [°C]	DP [Inches of Water]
99	80.03	80.03	5.52	101.56	99.02	98.74	99.41	100.37	100.02	100.04	99.96	100.37	55.21
100	79.80	79.80	6.38	101.48	97.74	97.64	98.39	99.59	99.54	99.58	99.63	100.11	55.21
101	79.75	79.75	7.49	101.67	95.75	95.87	96.66	98.08	98.36	98.46	98.81	99.32	55.50
102	79.75	79.75	8.46	101.57	94.36	94.48	95.36	96.94	97.39	97.54	98.08	98.69	55.53
103	79.51	79.51	9.43	101.53	92.75	92.97	93.91	95.56	96.18	96.48	97.28	97.93	55.63
104	79.66	79.66	10.53	101.68	91.46	90.43	91.26	92.95	93.65	94.03	94.75	95.82	56.96
105	79.78	79.78	10.15	101.47	91.27	91.42	92.44	93.98	94.65	94.96	95.62	96.55	55.37
106	85.25	85.25	4.74	102.70	101.25	100.82	101.18	101.88	101.31	101.38	101.33	101.50	57.03
107	84.86	84.86	5.60	101.50	100.04	99.71	100.11	100.76	100.20	100.28	100.22	100.46	54.94
108	85.04	85.04	6.43	101.43	98.44	98.28	98.78	99.78	99.49	99.58	99.72	99.95	55.22
109	84.73	84.73	7.41	101.08	97.11	97.05	97.64	98.83	98.74	98.86	99.22	99.49	55.23
110	84.40	84.40	8.48	101.29	95.69	95.69	96.38	97.66	97.76	97.99	98.42	98.78	55.47

Test Number	Water Inlet Temp [°C]	Steam Flow Rate [g/s]	Water Flow Rate [g/s]	TC Inside [°C]	TC 1 [°C]	TC 2 [°C]	TC 3 [°C]	TC 4 [°C]	TC 5 [°C]	TC 6 [°C]	TC 7 [°C]	TC 8 [°C]	DP [Inches of Water]
111	84.93	84.93	9.47	101.29	94.76	94.74	95.44	96.71	96.88	97.11	97.63	98.07	55.46
112	84.83	84.83	10.47	101.16	93.81	93.82	94.57	95.86	96.08	96.49	97.13	97.66	55.14
113	84.68	84.68	9.97	101.16	94.18	94.20	94.94	96.23	96.47	96.78	97.37	97.87	55.50
114	89.67	89.67	4.51	101.84	101.28	100.68	101.01	101.52	100.73	100.77	100.59	100.77	57.10
115	90.28	90.28	5.54	101.51	100.68	100.09	100.43	100.96	100.18	100.24	100.10	100.21	54.97
116	89.67	89.67	6.58	101.37	99.42	99.04	99.44	100.24	99.69	99.79	99.81	99.97	55.41
117	89.88	89.88	7.46	101.31	98.83	98.51	98.94	99.83	99.42	99.52	99.65	99.79	54.96
118	90.28	90.28	8.46	101.32	98.08	97.77	98.27	99.20	98.90	99.04	99.24	99.49	55.29
119	89.41	89.41	9.11	102.54	98.14	97.94	98.52	99.60	99.47	99.60	99.99	100.38	57.07
120	90.08	90.08	9.37	101.45	97.67	97.28	97.92	98.95	98.76	98.87	99.14	99.53	55.08
121	90.61	90.61	10.30	102.21	97.35	97.10	97.69	98.65	98.48	98.73	99.00	99.46	57.10
122	90.18	90.18	10.40	101.40	96.93	96.57	97.25	98.25	98.09	98.31	98.63	99.03	54.97

Test Number	Water Inlet Temp [°C]	Steam Flow Rate [g/s]	Water Flow Rate [g/s]	TC Inside [°C]	TC 1 [°C]	TC 2 [°C]	TC 3 [°C]	TC 4 [°C]	TC 5 [°C]	TC 6 [°C]	TC 7 [°C]	TC 8 [°C]	DP [Inches of Water]
123	90.23	90.23	10.92	101.43	96.60	96.24	96.92	97.89	97.67	97.96	98.25	98.69	55.17
124	97.12	97.12	5.17	102.97	102.71	101.98	102.24	102.75	101.97	101.99	101.84	101.98	57.09
125	96.48	96.48	5.98	103.94	103.15	102.44	102.70	103.34	102.76	102.74	102.69	102.87	57.07
126	96.71	96.71	7.01	103.80	102.66	101.96	102.18	102.87	102.45	102.44	102.48	102.68	57.10
127	97.33	97.33	8.08	103.04	101.78	101.20	101.55	102.25	101.68	101.72	101.76	102.00	57.11
128	97.19	97.19	8.78	103.87	102.12	101.51	101.82	102.61	102.22	102.28	102.42	102.73	57.10
129	97.36	97.36	9.62	104.05	101.99	101.37	101.63	102.42	102.20	102.22	102.37	102.64	56.82
130	96.70	96.70	11.59	101.91	99.60	99.07	99.42	100.06	99.20	99.31	98.92	99.71	55.37
131	96.87	96.87	11.68	101.63	99.46	98.91	99.25	99.86	98.96	98.88	98.65	99.31	54.99
132	97.51	97.51	8.96	104.06	101.92	101.44	101.64	102.53	101.17	101.17	100.83	101.76	57.23
133	97.18	97.18	8.17	102.65	101.23	100.70	100.98	101.65	100.87	100.68	100.70	100.92	56.83
134	96.94	96.94	9.13	102.51	100.68	100.16	100.48	101.16	100.40	100.40	100.08	100.79	56.92

Test Number	Water Inlet Temp [°C]	Steam Flow Rate [g/s]	Water Flow Rate [g/s]	TC Inside [°C]	TC 1 [°C]	TC 2 [°C]	TC 3 [°C]	TC 4 [°C]	TC 5 [°C]	TC 6 [°C]	TC 7 [°C]	TC 8 [°C]	DP [Inches of Water]
135	96.75	96.75	9.47	103.01	100.91	100.41	100.75	101.49	100.68	100.57	100.24	101.07	57.02
136	96.76	96.76	9.75	103.12	101.04	100.55	100.87	101.69	100.88	100.89	100.61	101.69	56.79
137	96.80	96.80	10.31	103.06	100.80	100.29	100.64	101.42	100.63	100.63	100.28	101.11	56.87
138	97.53	97.53	3.97	102.11	102.26	101.43	101.64	102.06	100.97	100.69	100.11	100.73	57.17
139	97.36	97.36	3.88	102.38	102.42	101.64	101.84	102.26	101.16	100.92	100.26	100.81	57.01
140	97.61	97.61	4.37	102.24	102.37	101.54	101.72	102.07	100.73	100.66	100.07	100.64	57.06
141	96.83	96.83	5.90	103.07	102.40	101.73	101.95	102.57	101.35	101.22	100.72	101.63	57.51
142	96.87	96.87	5.40	103.41	102.74	102.09	102.29	102.91	101.69	101.41	100.82	101.56	57.03
143	97.16	97.16	4.72	103.38	102.90	102.22	102.39	102.97	101.67	101.52	100.97	101.53	56.89

APPENDIX C

GRAPHS ACCORDING TO TEMPERATURE

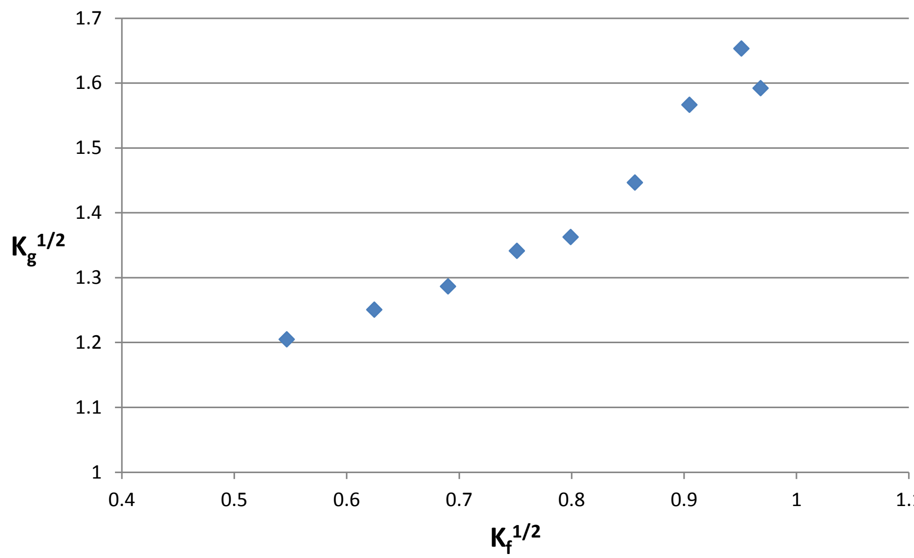

Fig. C.1.: Raw data plotted in terms of the Kutateladze parameters for 35°C tests.

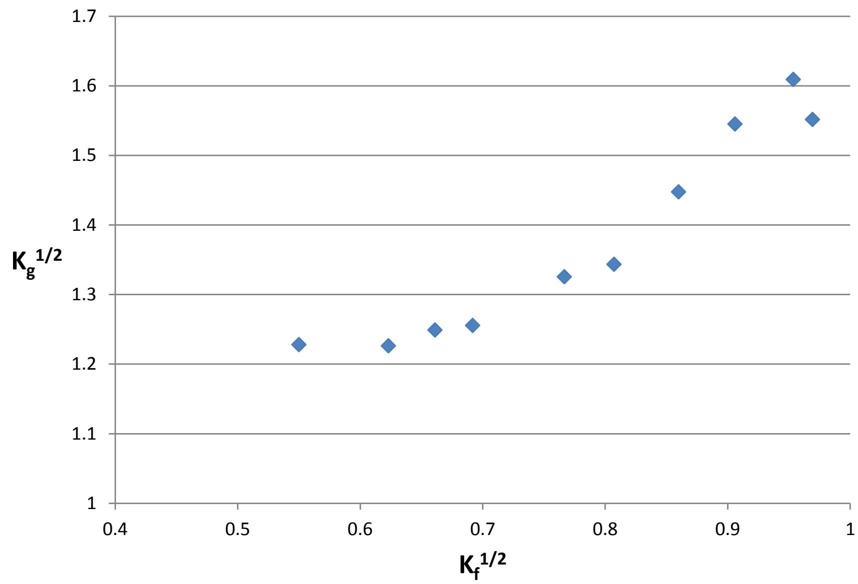

Fig. C.2.: Raw data plotted in terms of the Kutateladze parameters for 40°C tests.

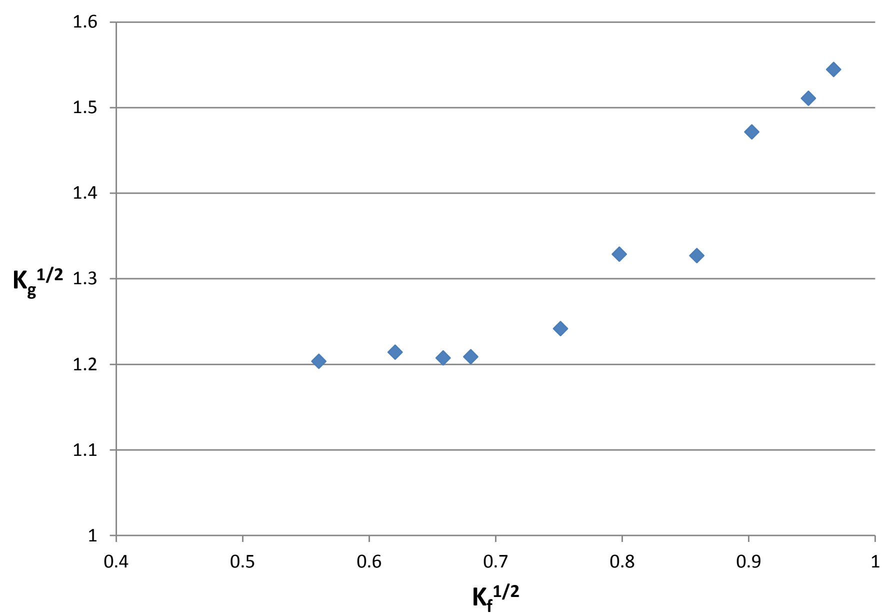

Fig. C.3.: Raw data plotted in terms of the Kutateladze parameters for 45°C tests.

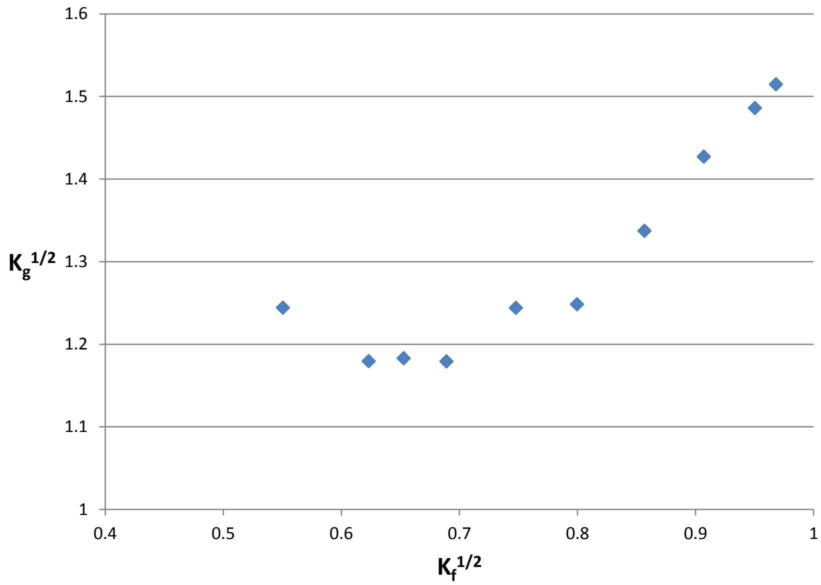

Fig. C.4.: Raw data plotted in terms of the Kutateladze parameters for 50°C tests.

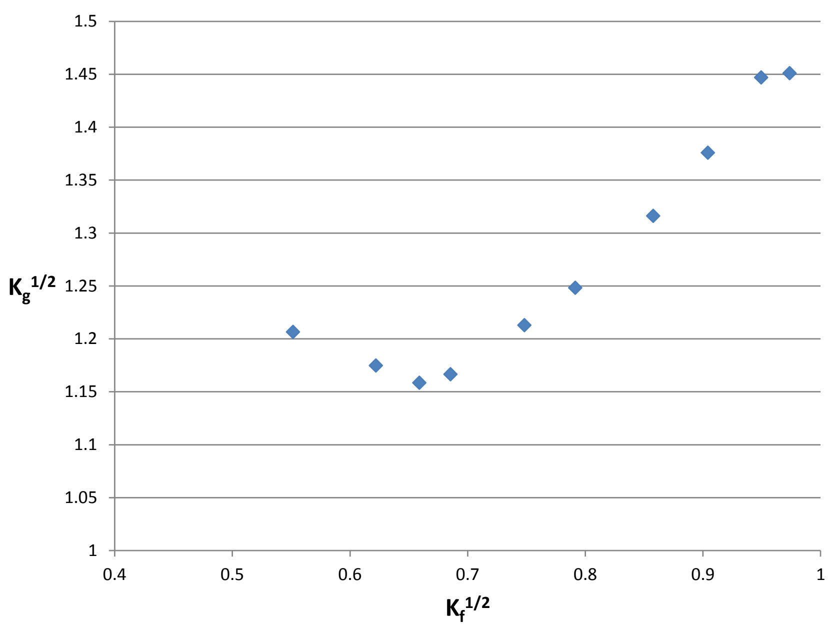

Fig. C.5.: Raw data plotted in terms of the Kutateladze parameters for 55°C tests.

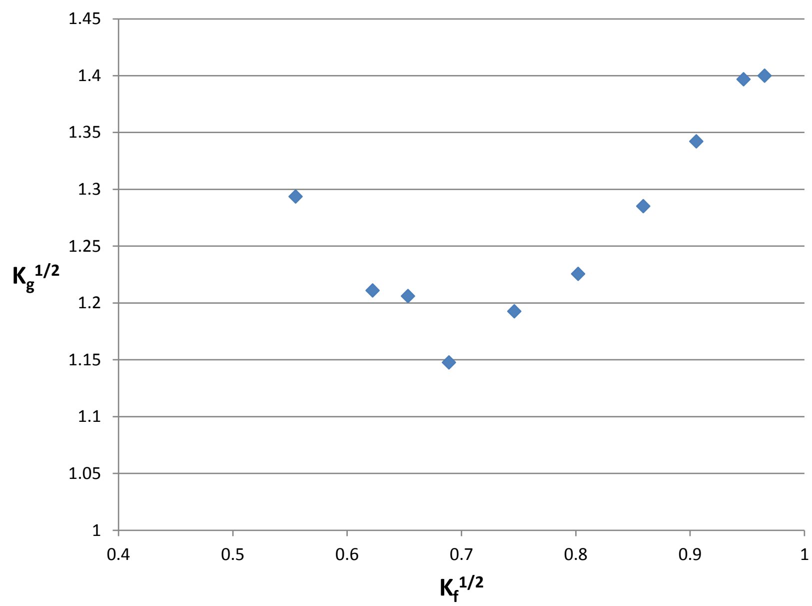

Fig. C.6.: Raw data plotted in terms of the Kutateladze parameters for 60°C tests.

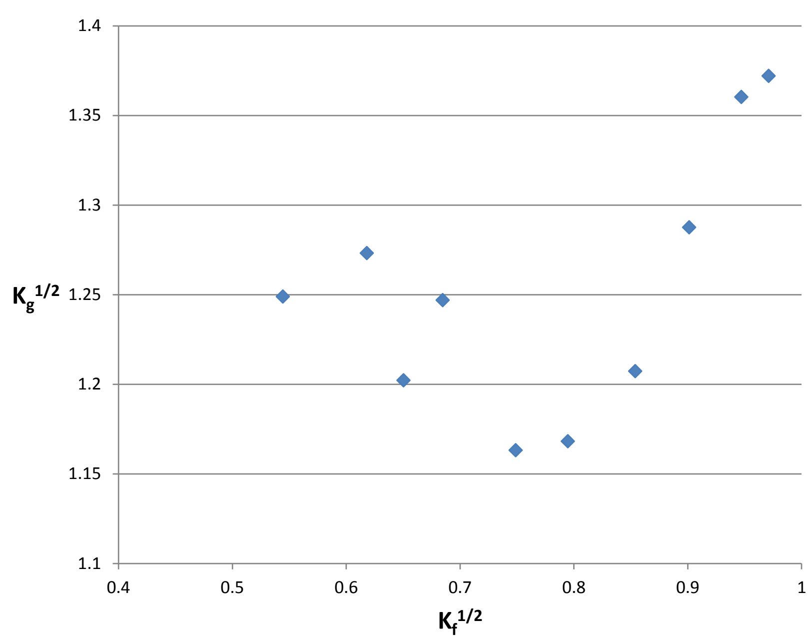

Fig. C.7.: Raw data plotted in terms of the Kutateladze parameters for 65°C tests.

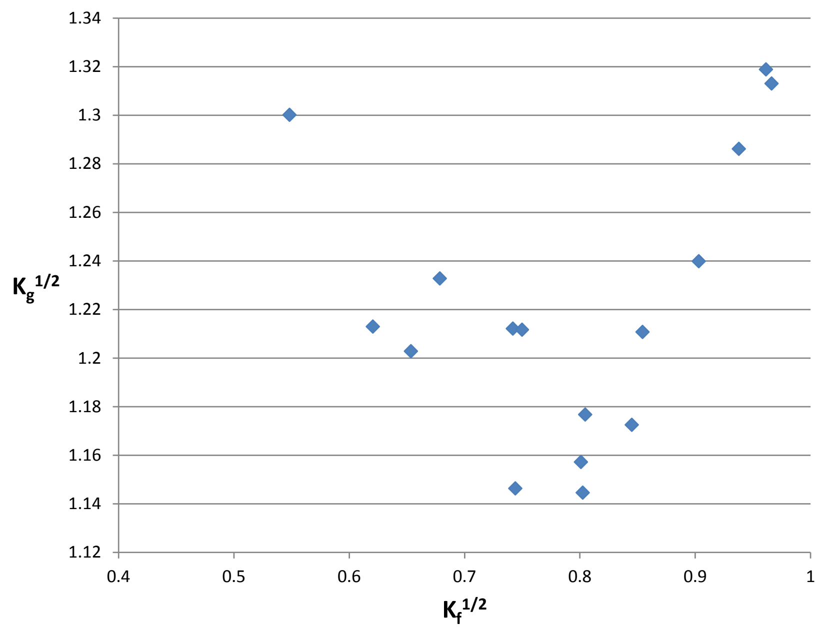

Fig. C.8.: Raw data plotted in terms of the Kutateladze parameters for 70°C tests.

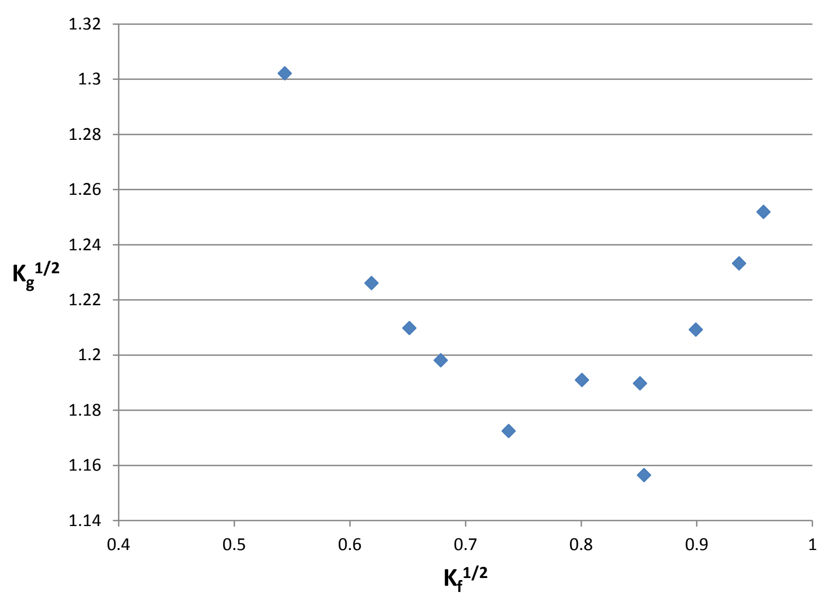

Fig. C.9.: Raw data plotted in terms of the Kutateladze parameters for 75°C tests.

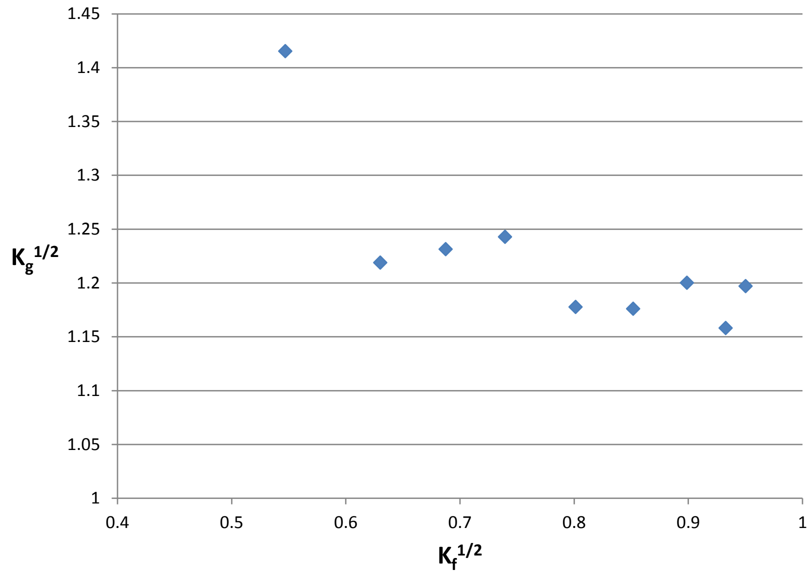

Fig. C.10.: Raw data plotted in terms of the Kutateladze parameters for 80°C tests.

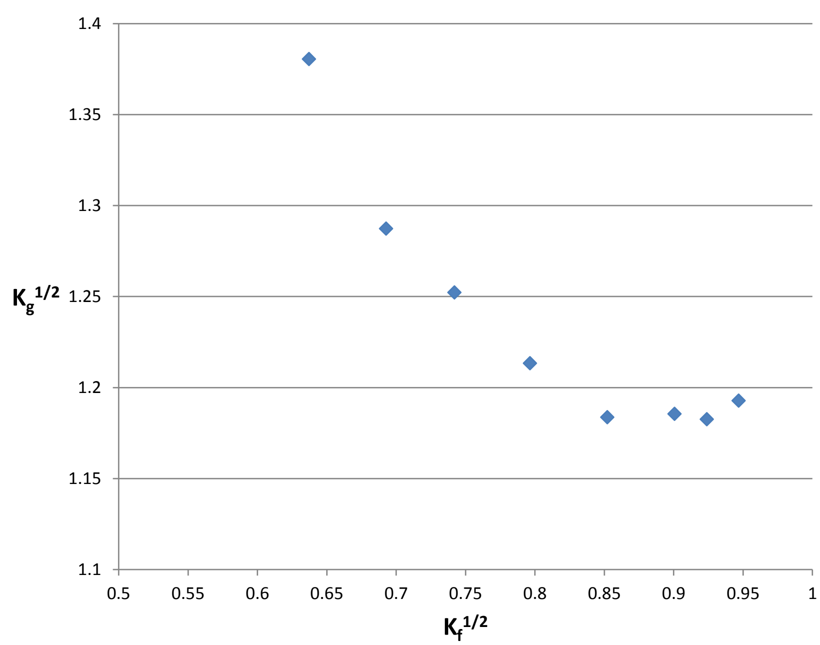

Fig. C.11.: Raw data plotted in terms of the Kutateladze parameters for 85°C tests.

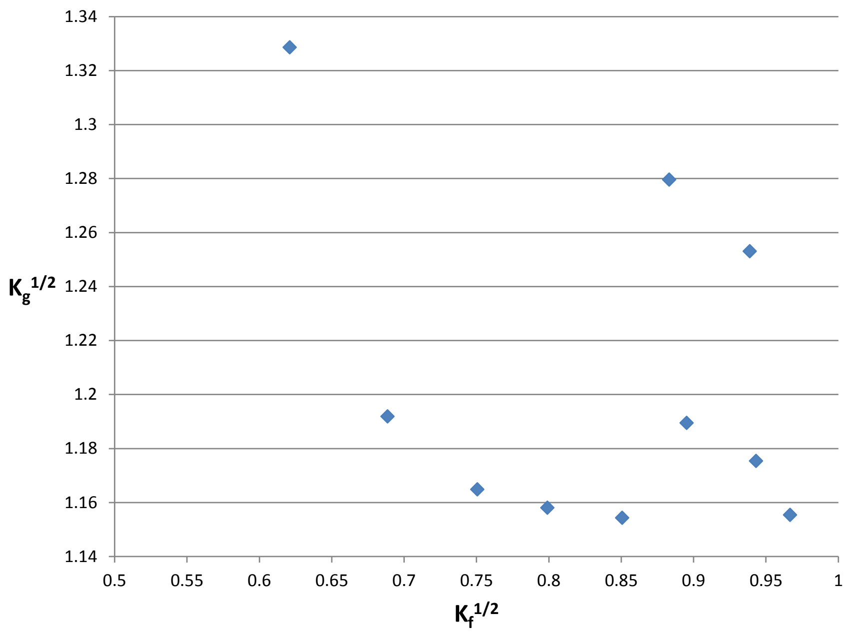

Fig. C.12.: Raw data plotted in terms of the Kutateladze parameters for 90°C tests.

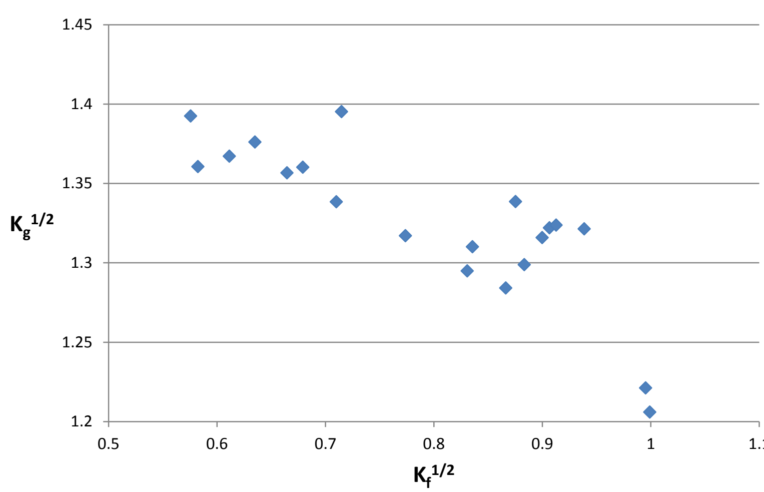

Fig. C.13.: Raw data plotted in terms of the Kutateladze parameters for 97°C tests.

APPENDIX D
FLOODING TEST GRAPHS

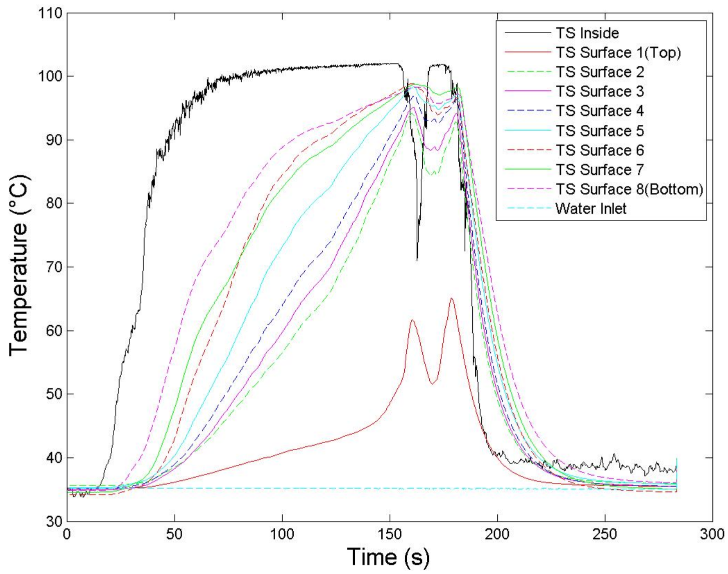

Fig. D.1.: Test section temperatures for test 1.

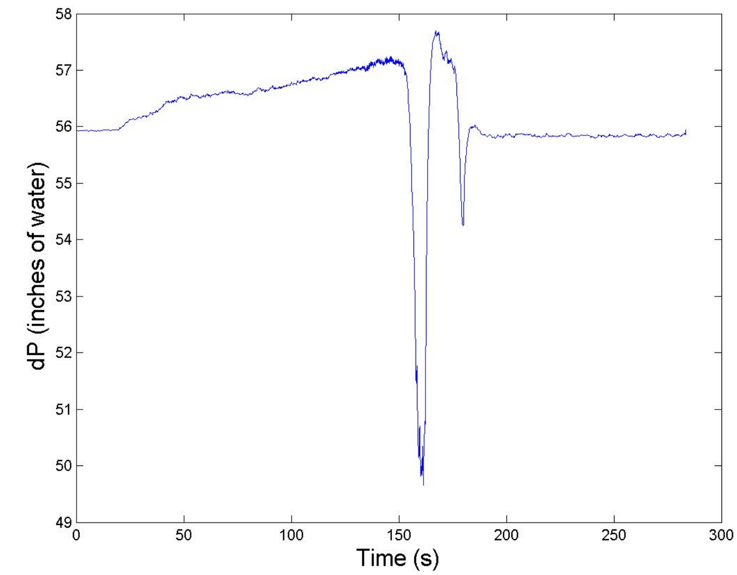

Fig. D.2.: Test section differential pressure for test 1.

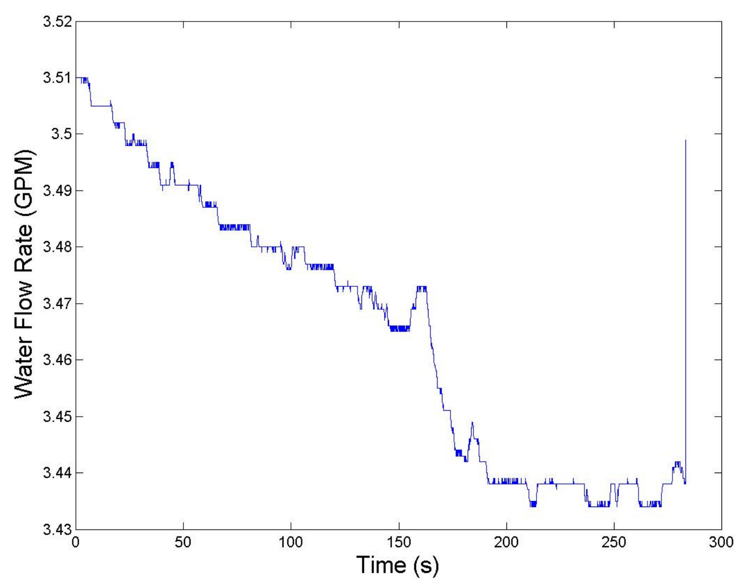

Fig. D.3.: Water flow rate for test 1.

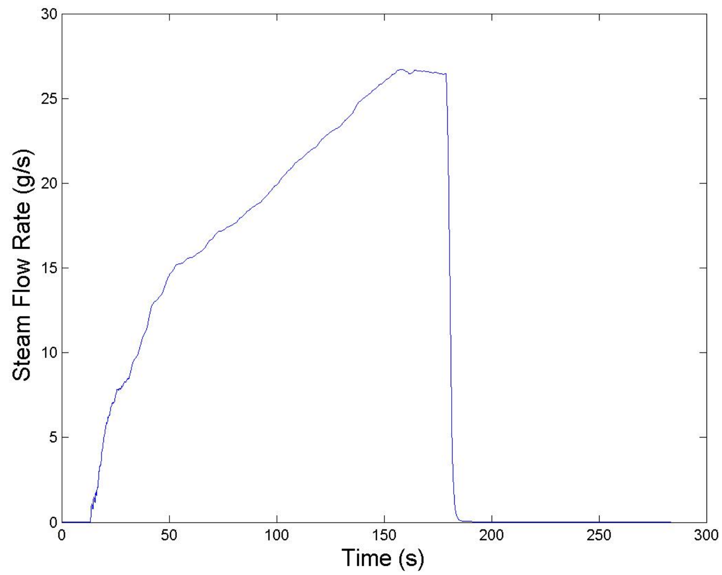

Fig. D.4.: Steam flow rate for test 1.

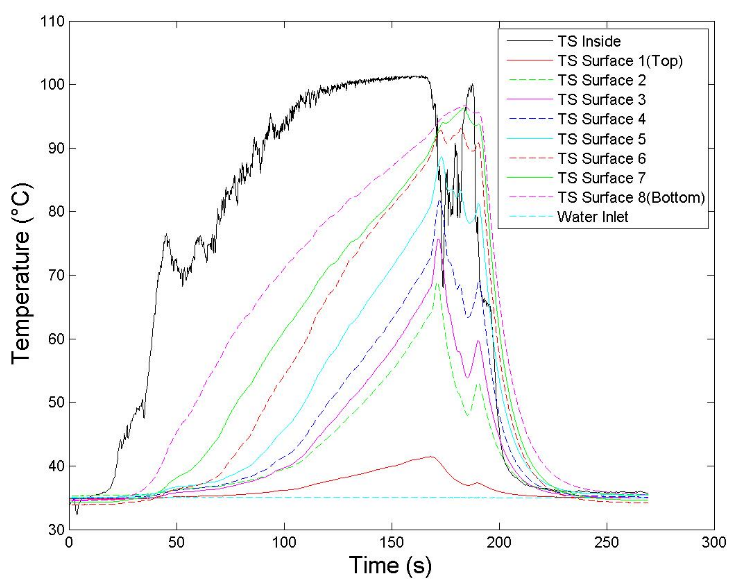

Fig. D.5.: Test section temperatures for test 2.

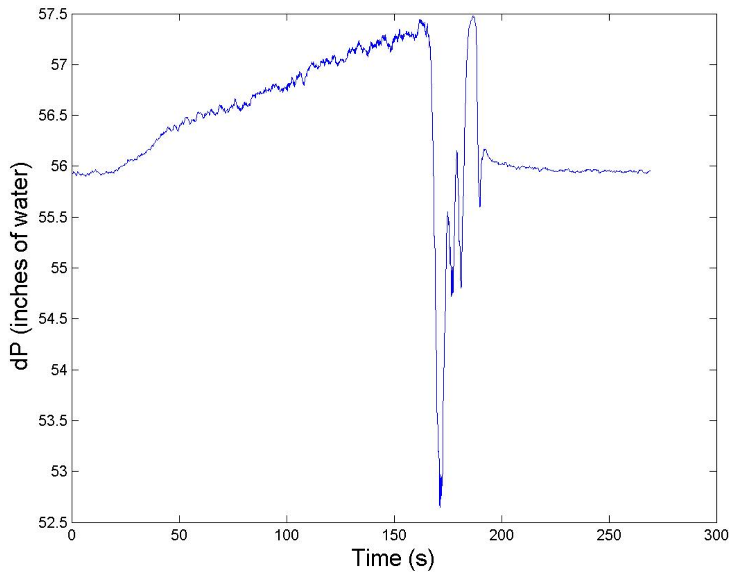

Fig. D.6.: Test section differential pressure for test 2.

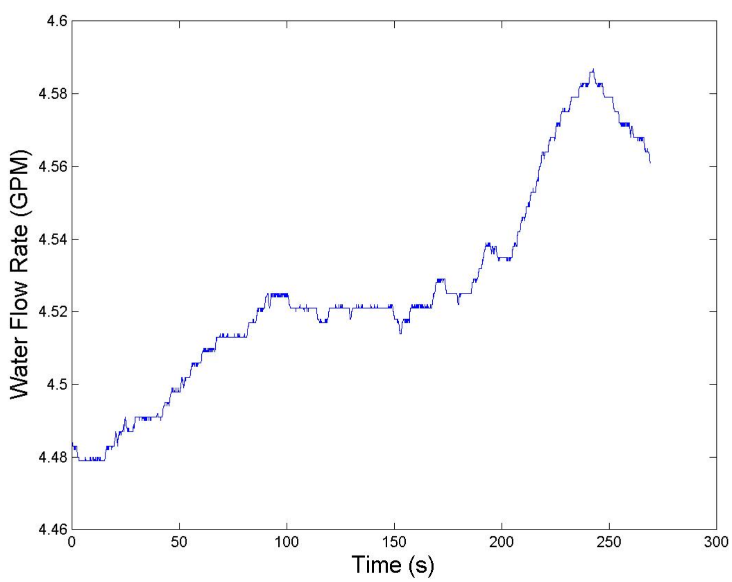

Fig. D.7.: Water flow rate for test 2.

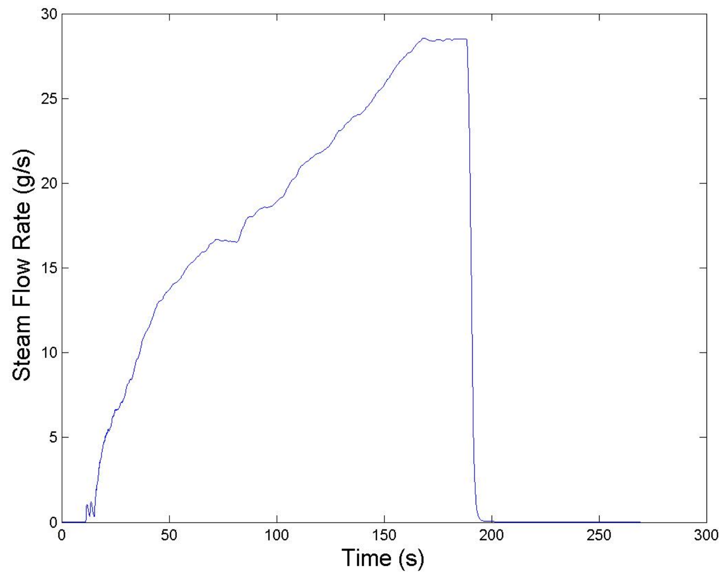

Fig. D.8.: Steam flow rate for test 2.

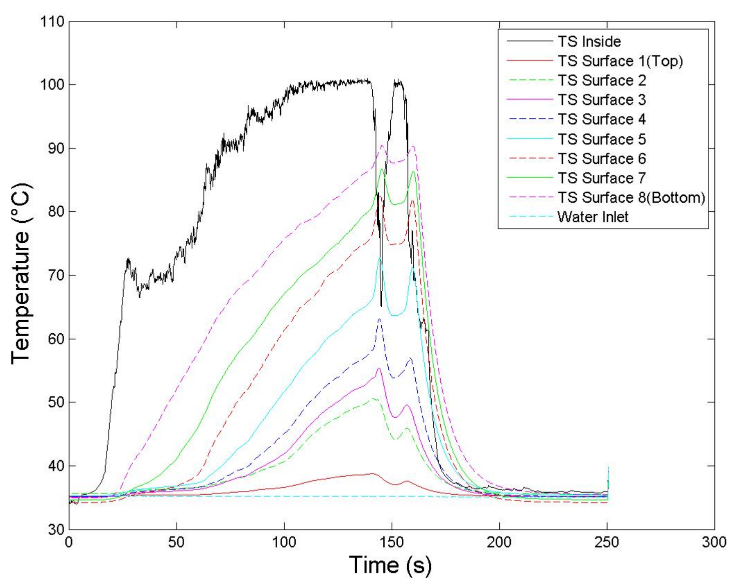

Fig. D.9.: Test section temperatures for test 3.

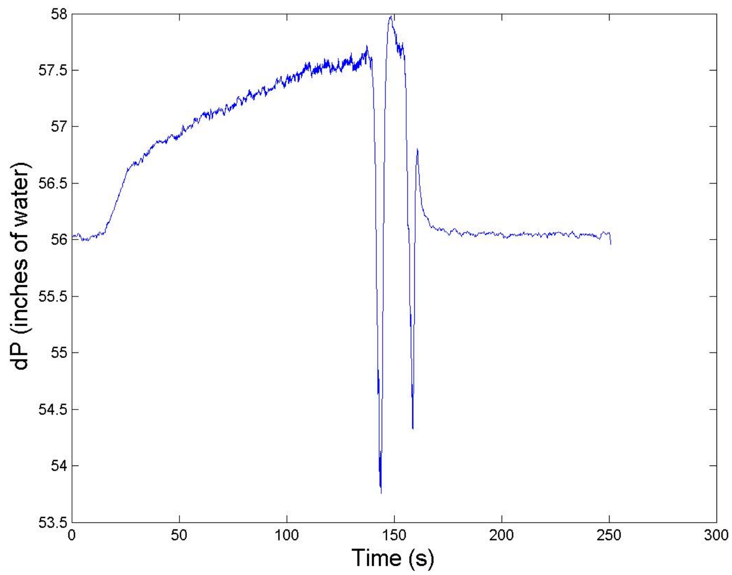

Fig. D.10.: Test section differential pressure for test 3.

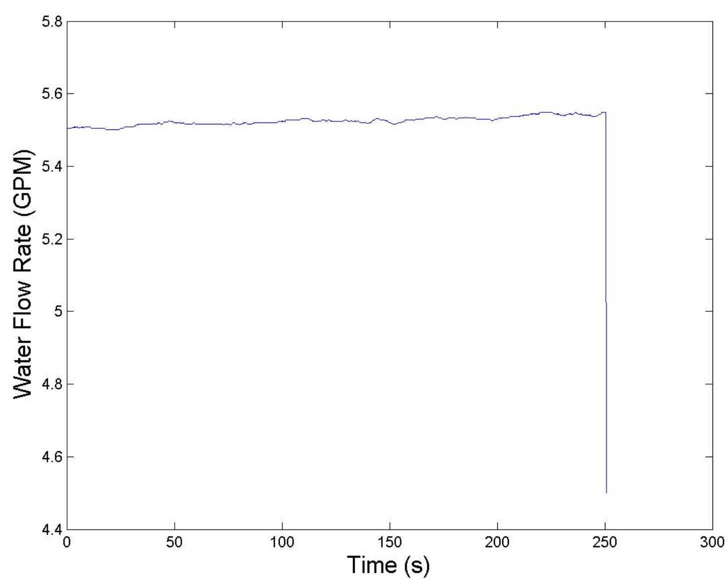

Fig. D.11.: Water flow rate for test 3.

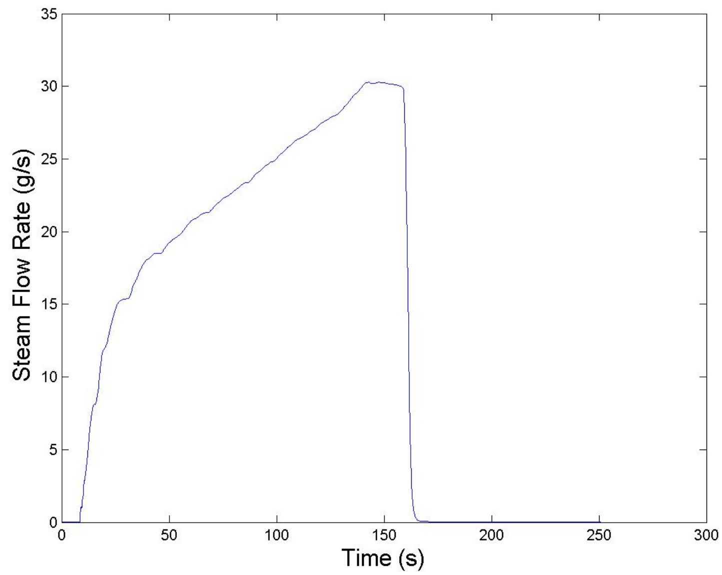

Fig. D.12.: Steam flow rate for test 3.

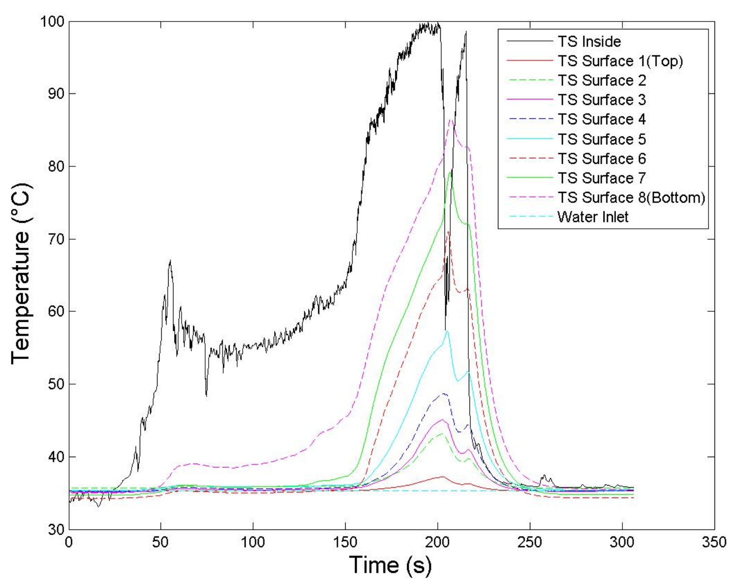

Fig. D.13.: Test section temperatures for test 4.

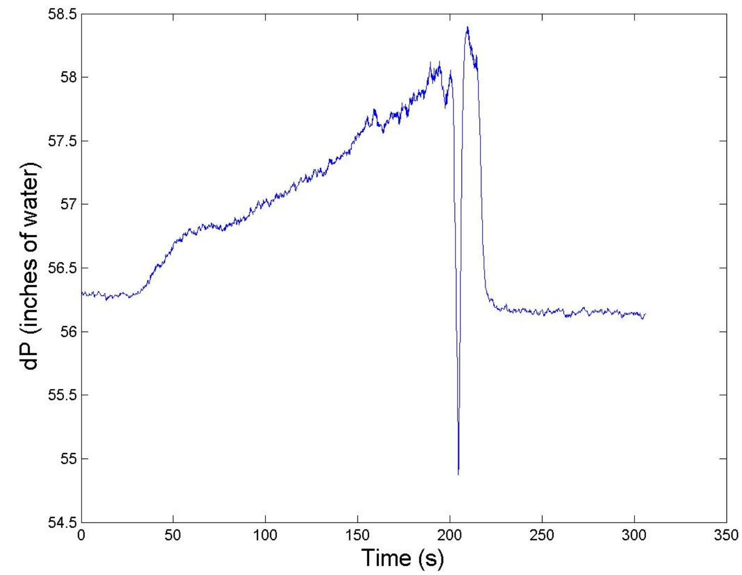

Fig. D.14.: Test section differential pressure for test 4.

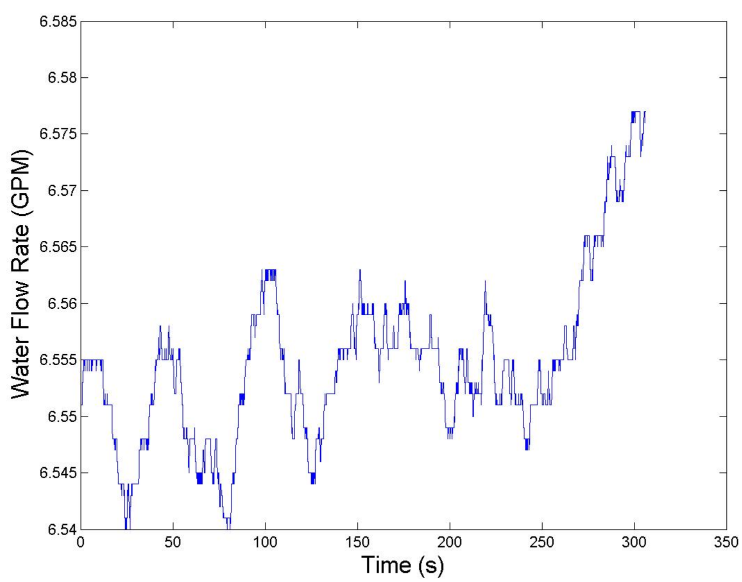

Fig. D.15.: Water flow rate for test 4.

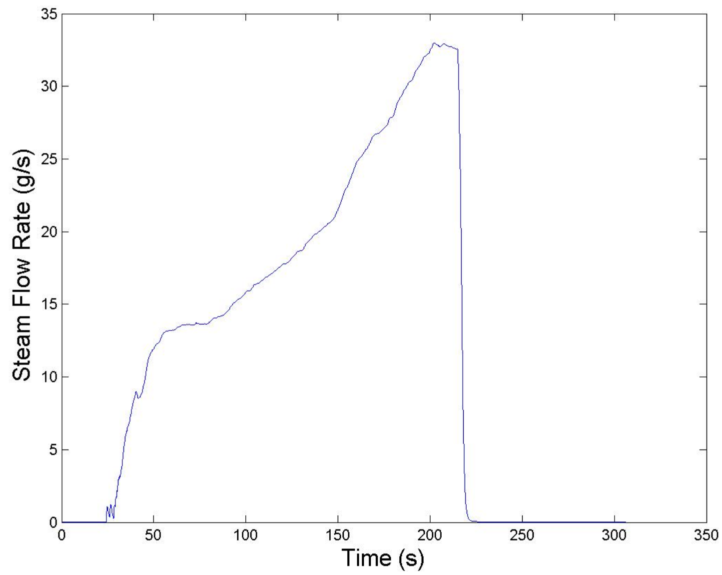

Fig. D.16.: Steam flow rate for test 4.

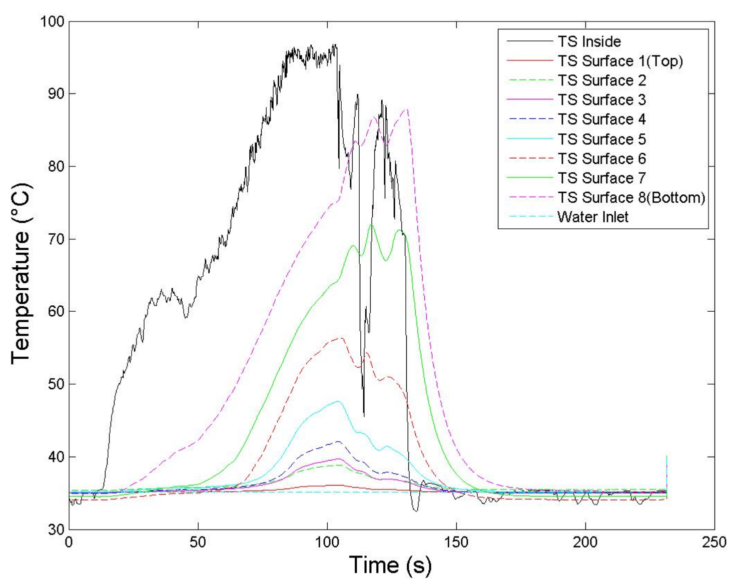

Fig. D.17.: Test section temperatures for test 5.

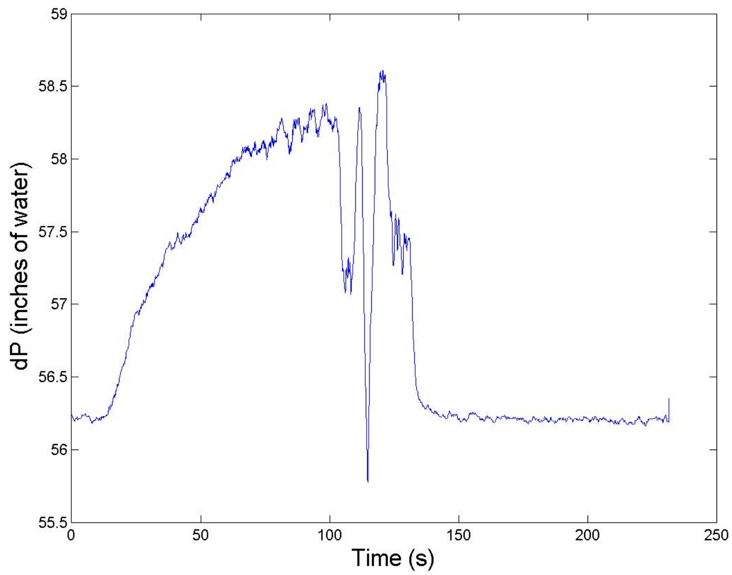

Fig. D.18.: Test section differential pressure for test 5.

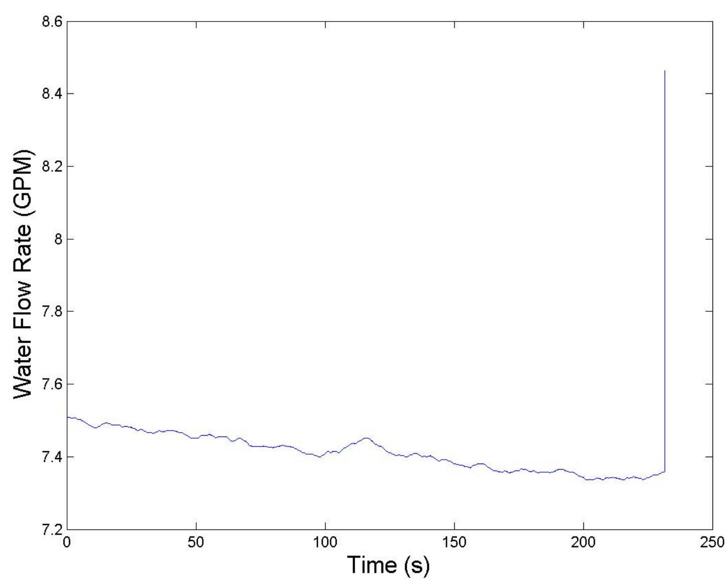

Fig. D.19.: Water flow rate for test 5.

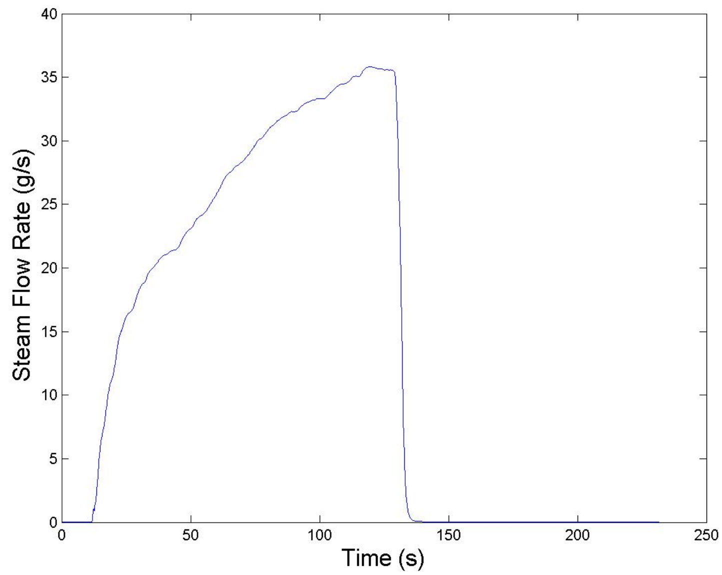

Fig. D.20.: Steam flow rate for test 5.

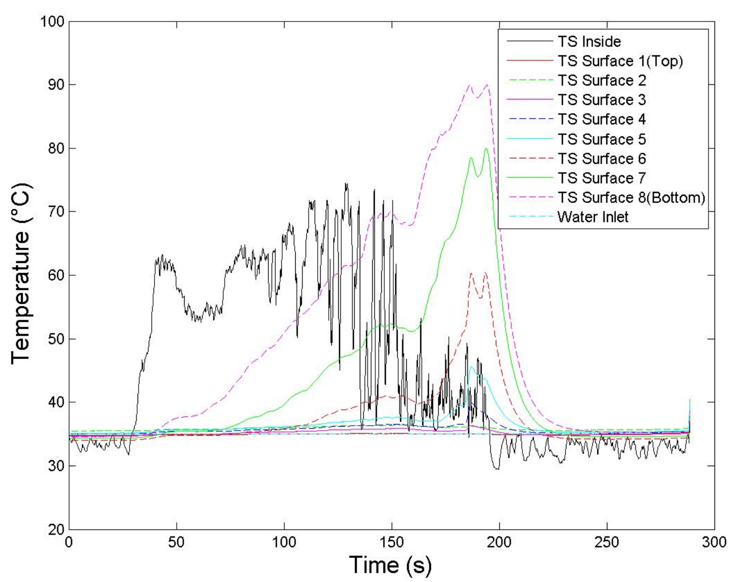

Fig. D.21.: Test section temperatures for test 6.

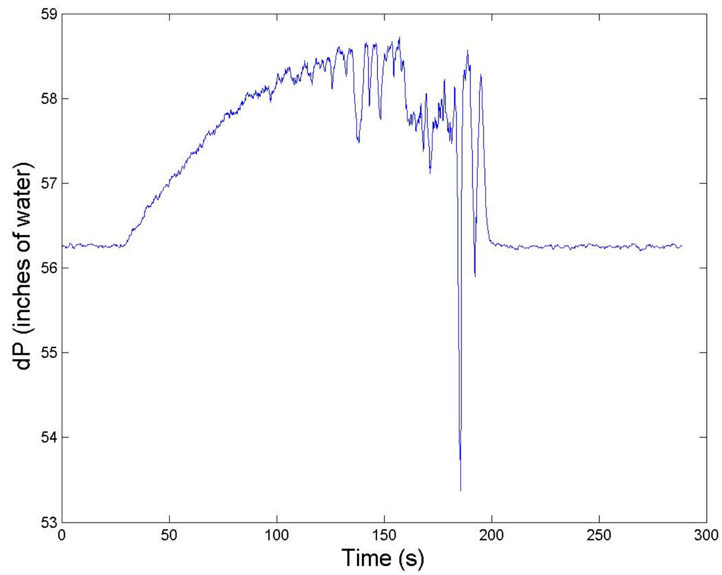

Fig. D.22.: Test section differential pressure for test 6.

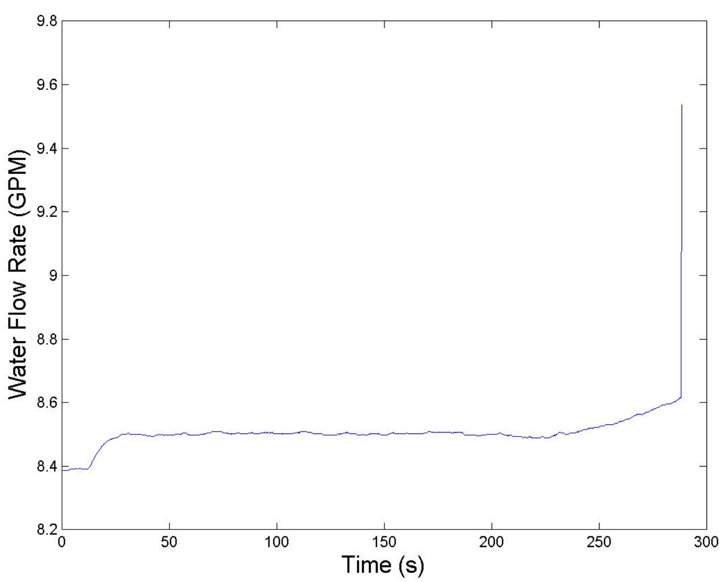

Fig. D.23.: Water flow rate for test 6.

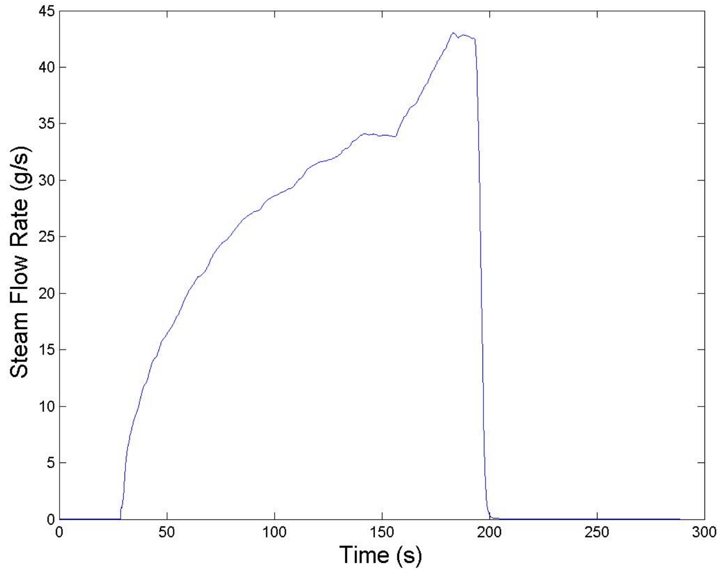

Fig. D.24.: Steam flow rate for test 6.

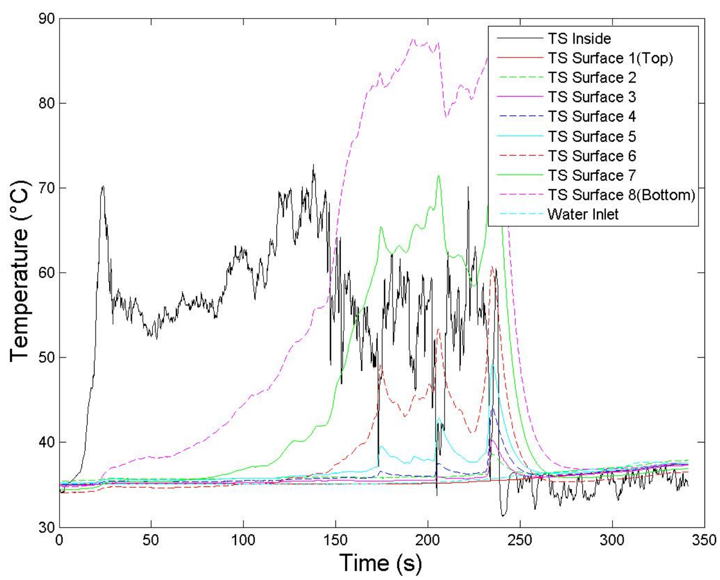

Fig. D.25.: Test section temperatures for test 7.

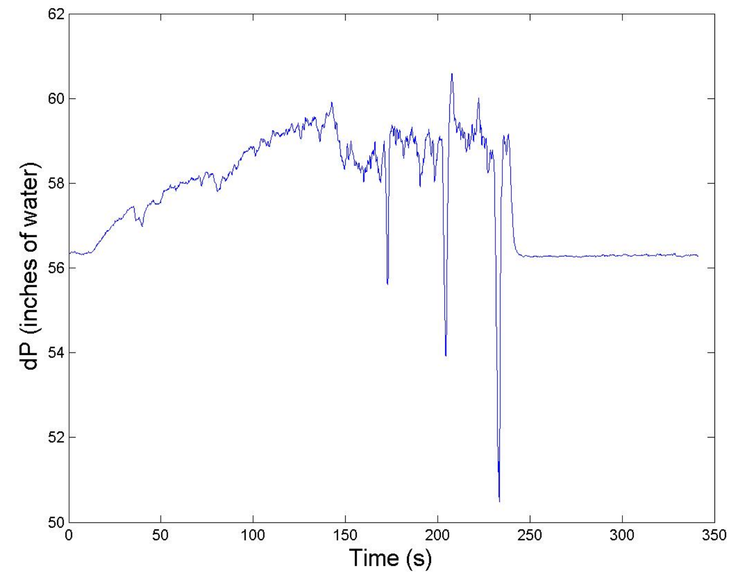

Fig. D.26.: Test section differential pressure for test 7.

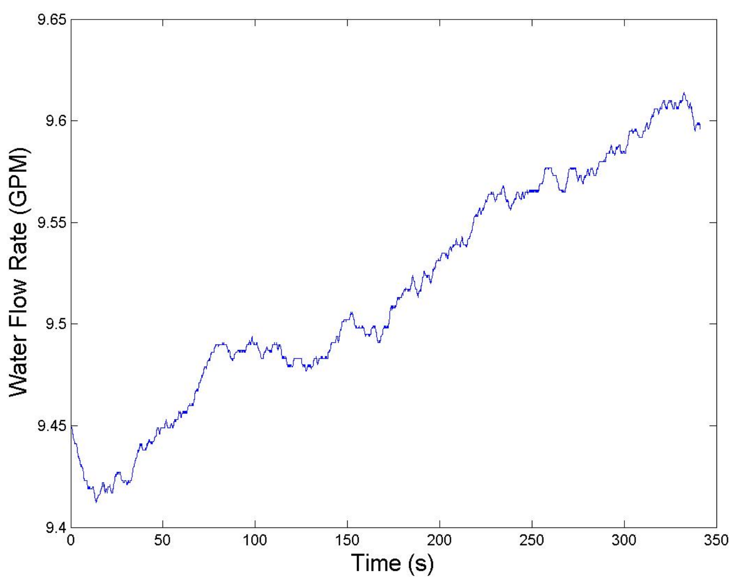

Fig. D.27.: Water flow rate for test 7.

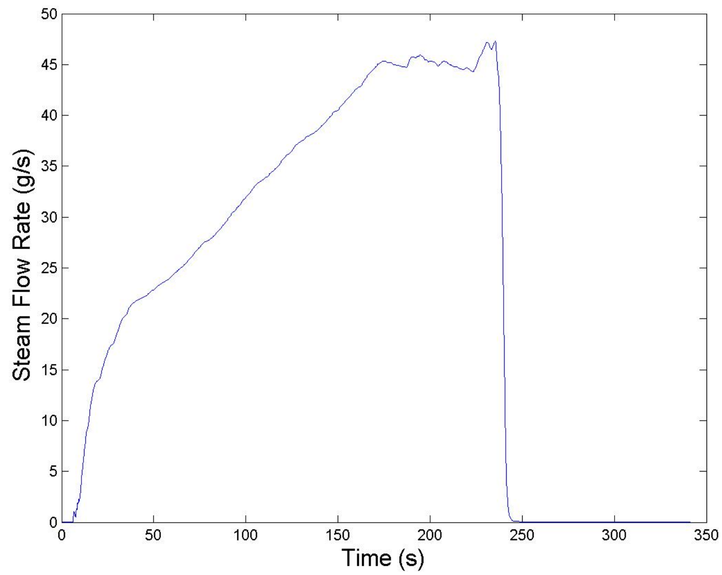

Fig. D.28.: Steam flow rate for test 7.

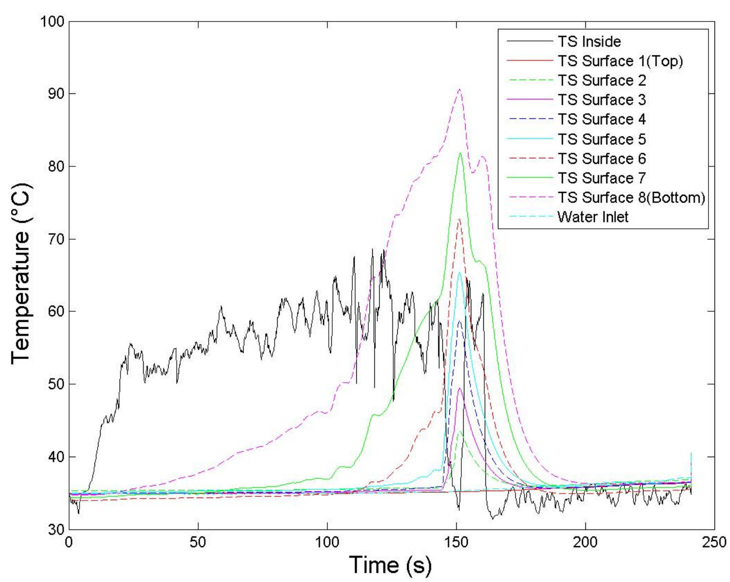

Fig. D.29.: Test section temperatures for test 8.

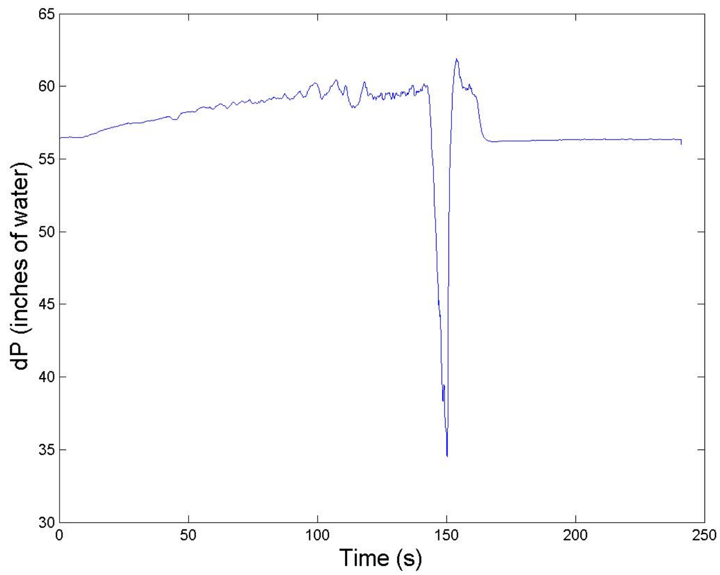

Fig. D.30.: Test section differential pressure for test 8.

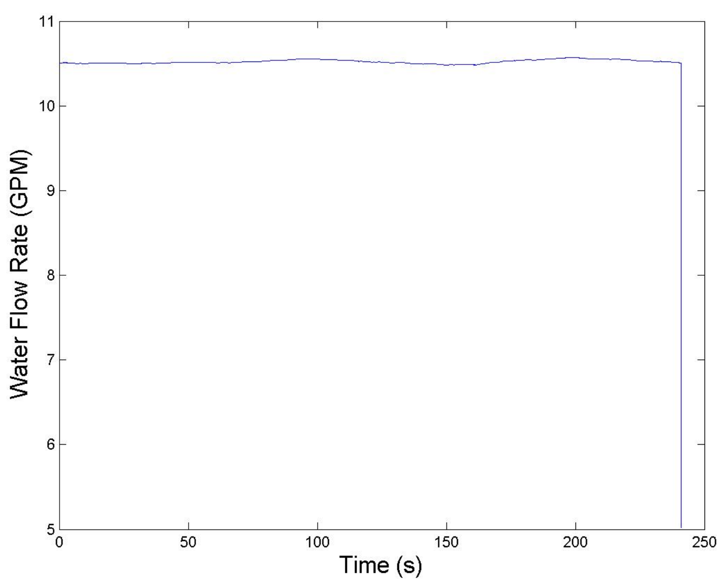

Fig. D.31.: Water flow rate for test 8.

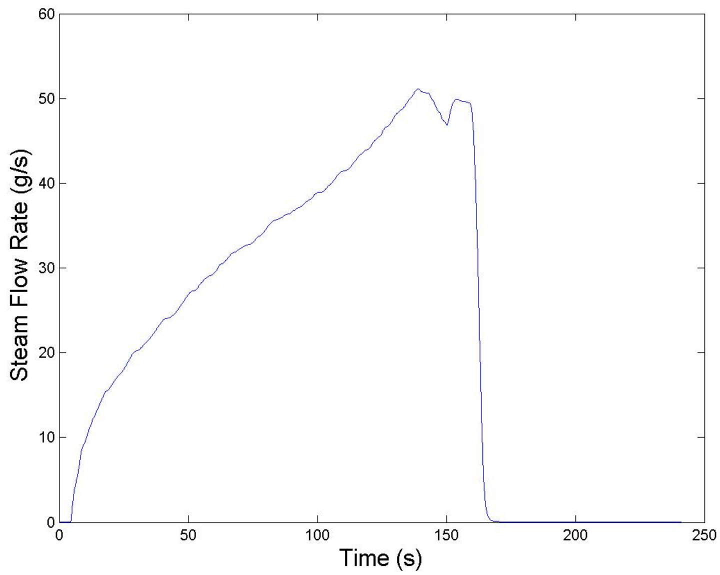

Fig. D.32.: Steam flow rate for test 8.

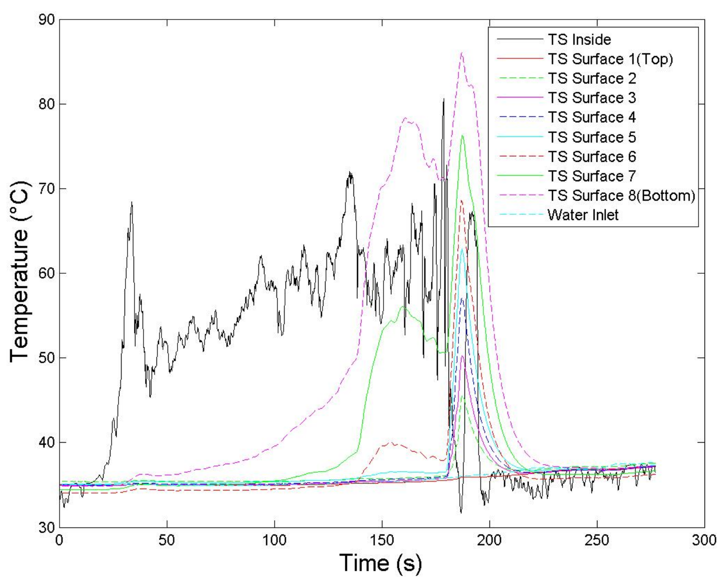

Fig. D.33.: Test section temperatures for test 9.

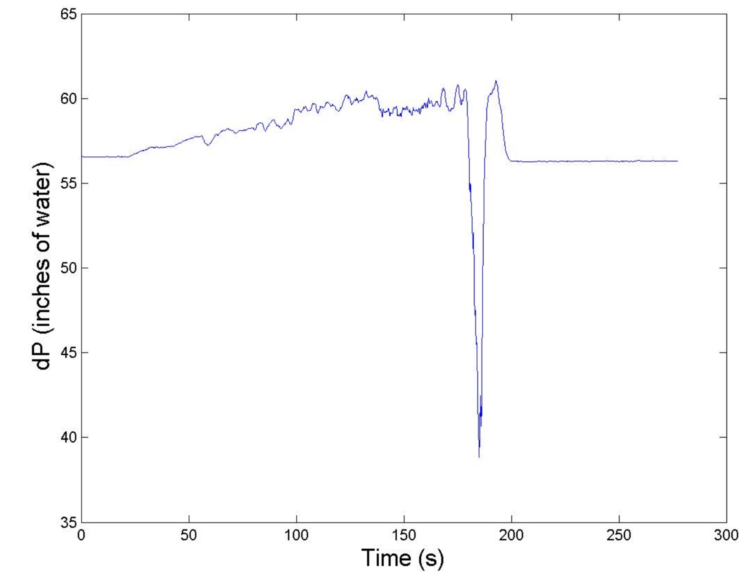

Fig. D.34.: Test section differential pressure for test 9.

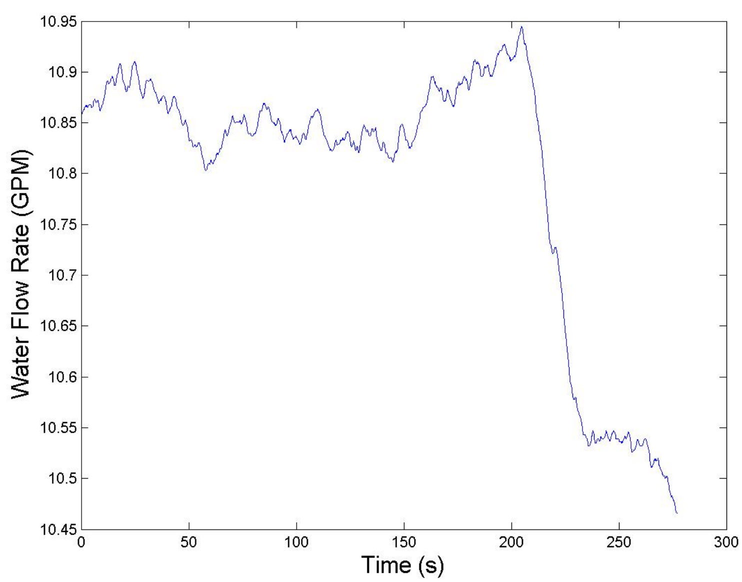

Fig. D.35.: Water flow rate for test 9.

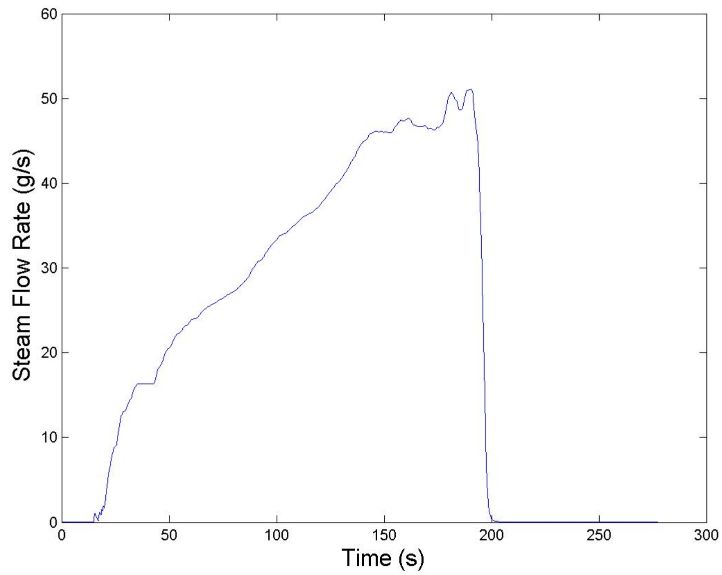

Fig. D.36.: Steam flow rate for test 9.

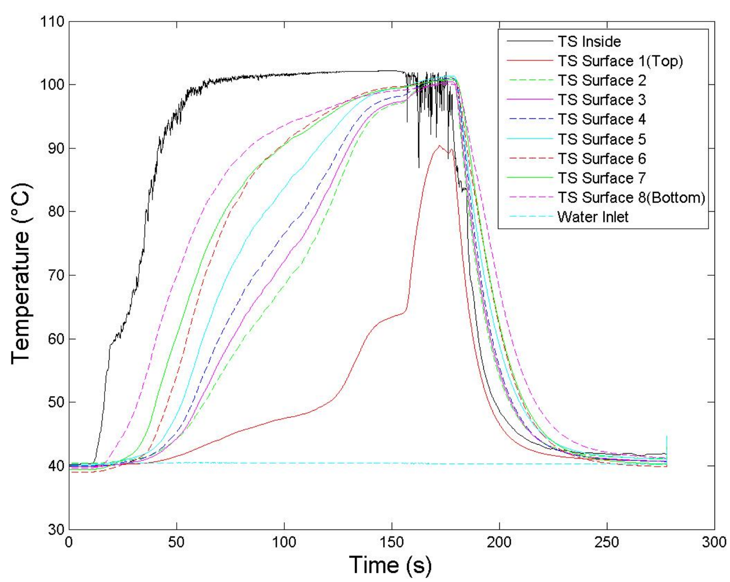

Fig. D.37.: Test section temperatures for test 10.

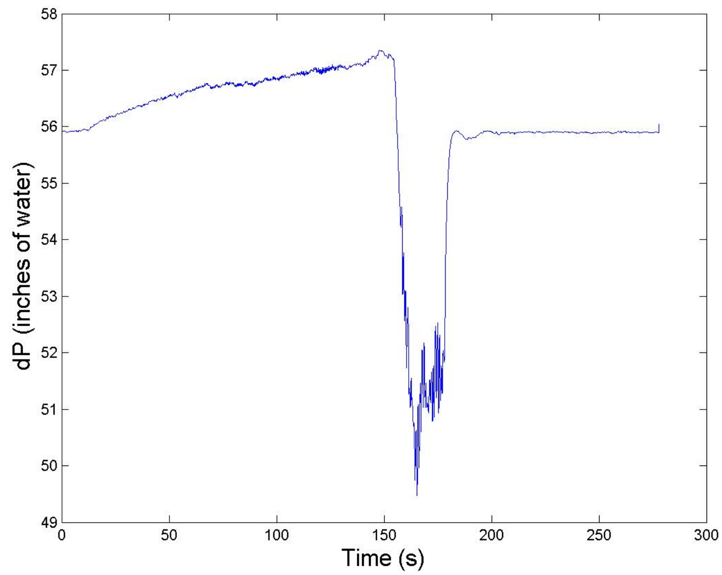

Fig. D.38.: Test section differential pressure for test 10.

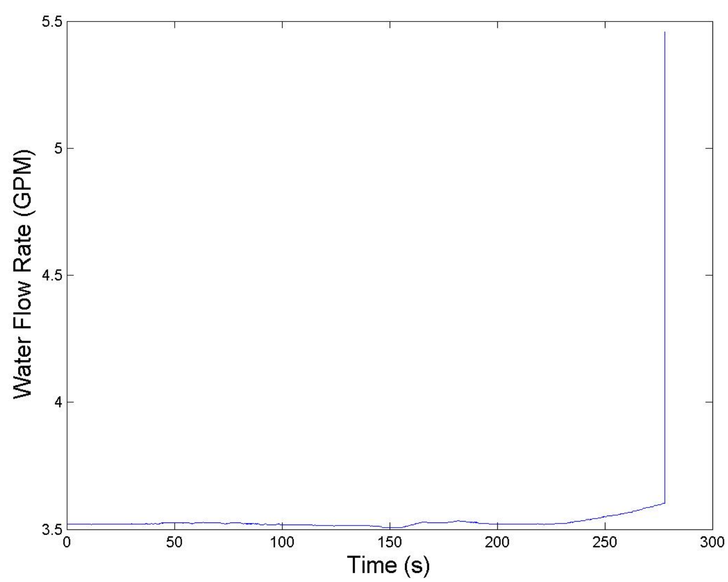

Fig. D.39.: Water flow rate for test 10.

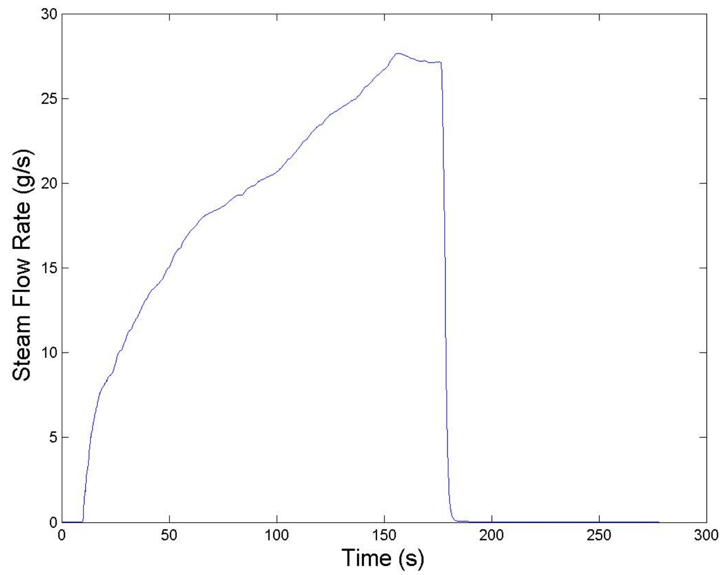

Fig. D.40.: Steam flow rate for test 10.

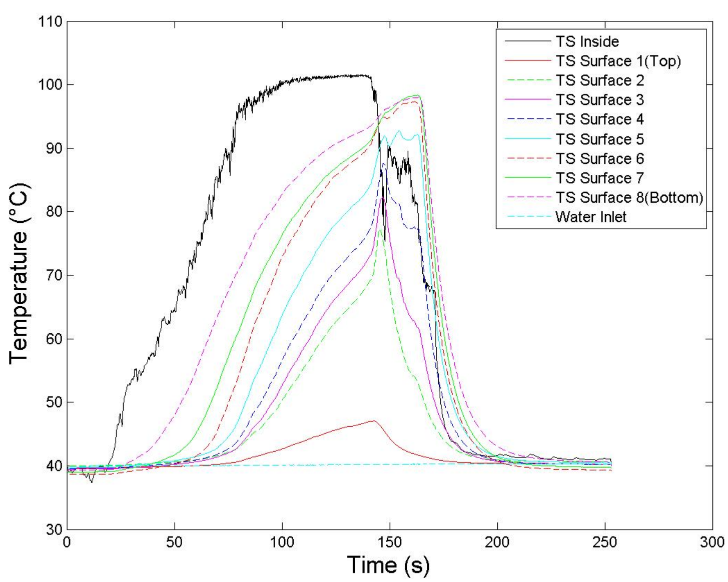

Fig. D.41.: Test section temperatures for test 11.

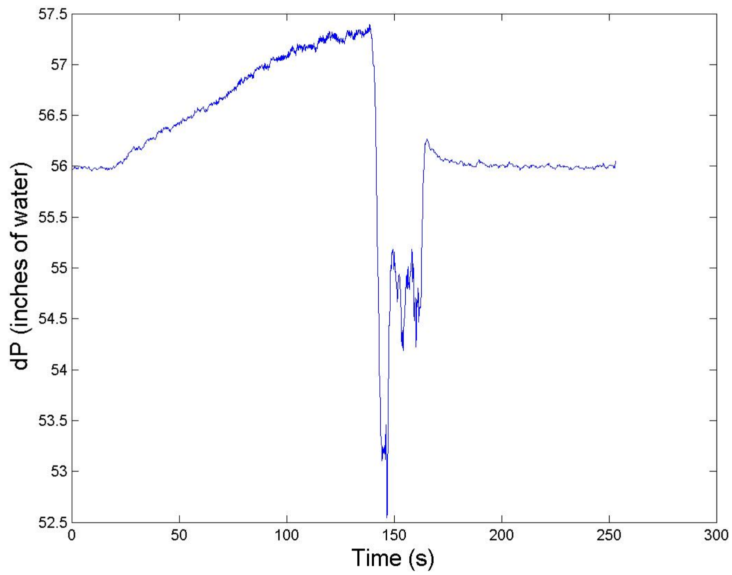

Fig. D.42.: Test section differential pressure for test 11.

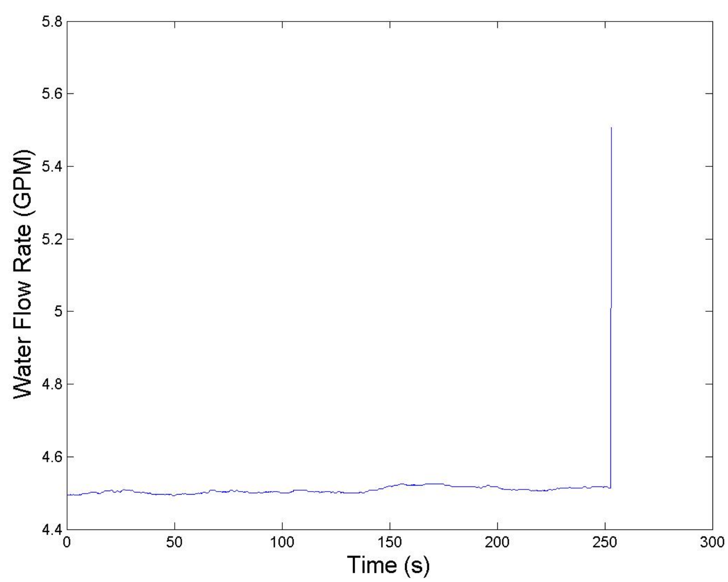

Fig. D.43.: Water flow rate for test 11.

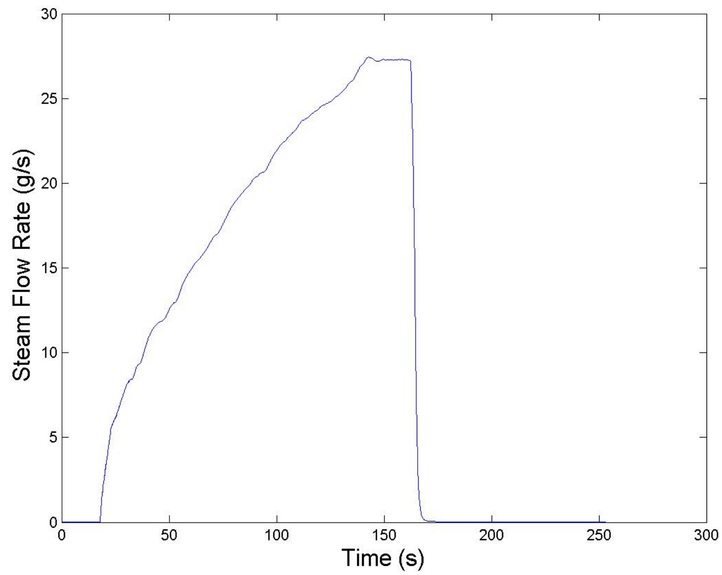

Fig. D.44.: Steam flow rate for test 11.

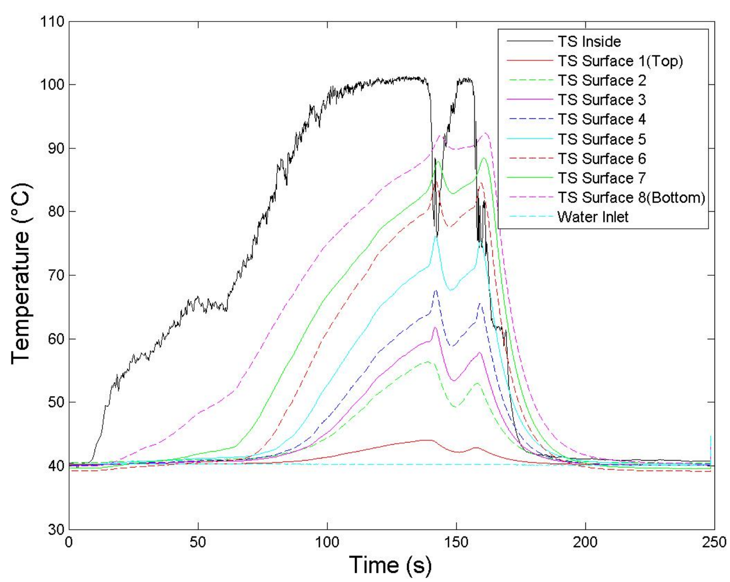

Fig. D.45.: Test section temperatures for test 12.

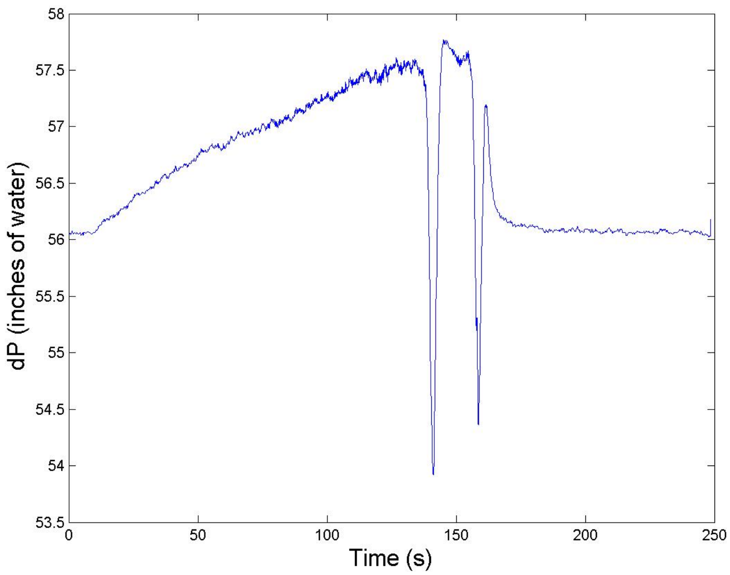

Fig. D.46.: Test section differential pressure for test 12.

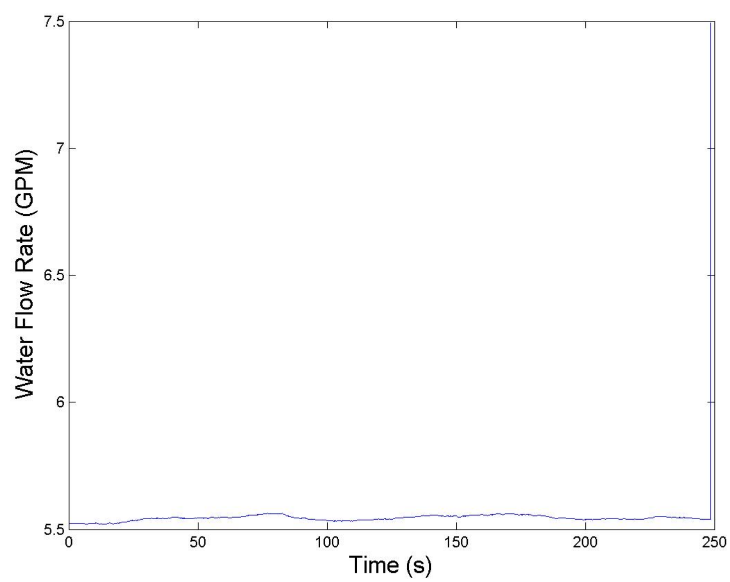

Fig. D.47.: Water flow rate for test 12.

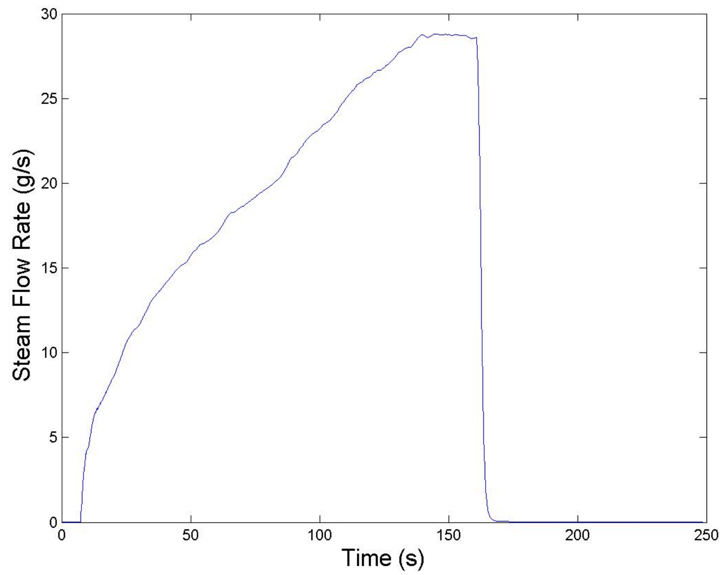

Fig. D.48.: Steam flow rate for test 12.

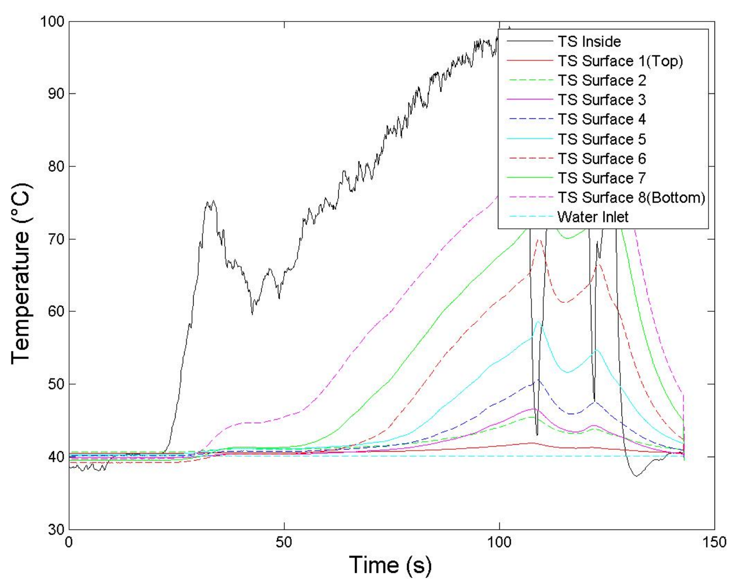

Fig. D.49.: Test section temperatures for test 13.

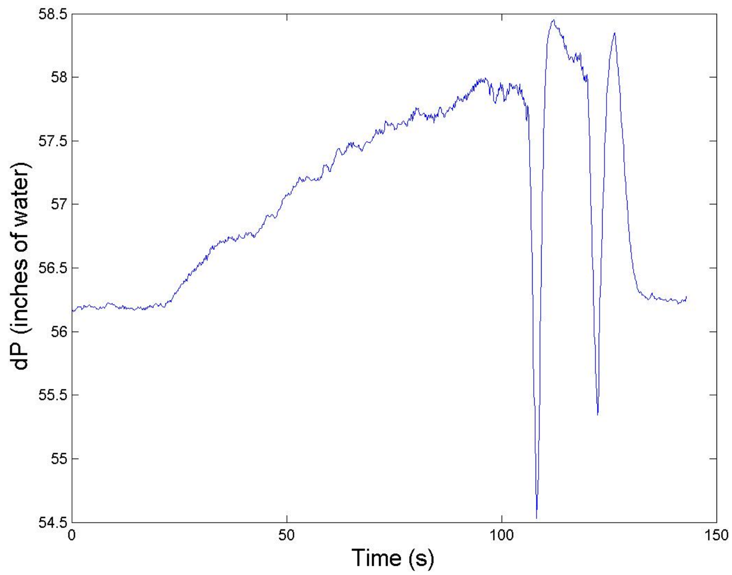

Fig. D.50.: Test section differential pressure for test 13.

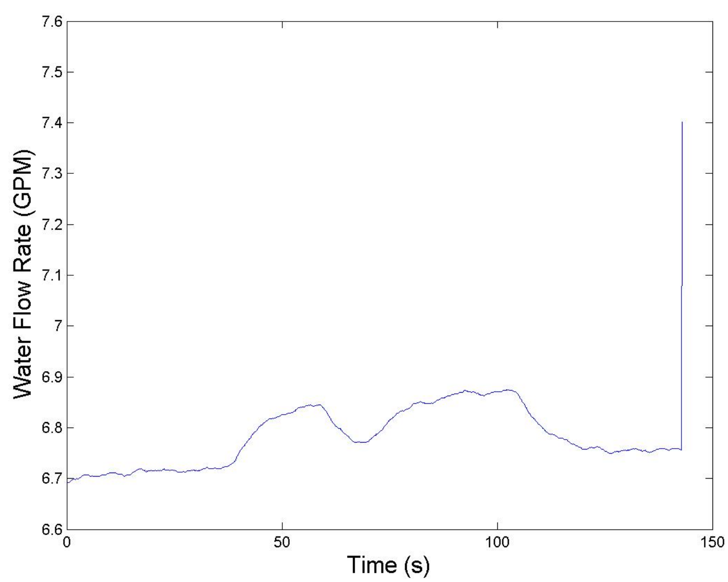

Fig. D.51.: Water flow rate for test 13.

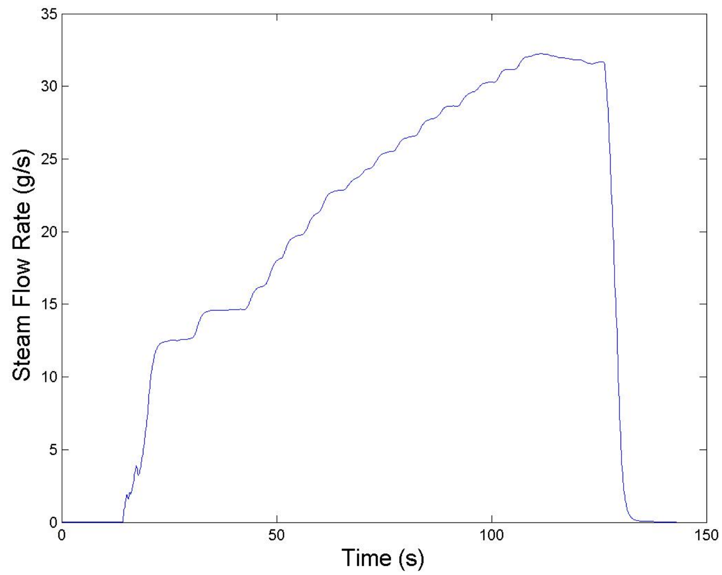

Fig. D.52.: Steam flow rate for test 13.

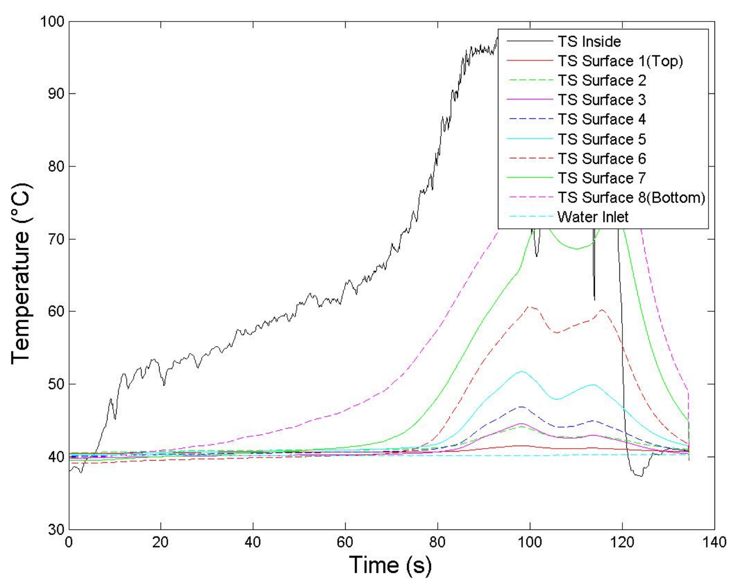

Fig. D.53.: Test section temperatures for test 14.

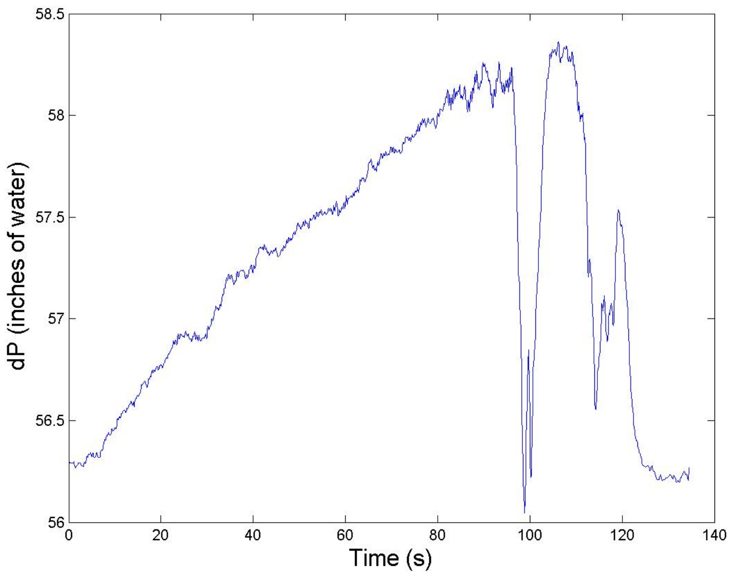

Fig. D.54.: Test section differential pressure for test 14.

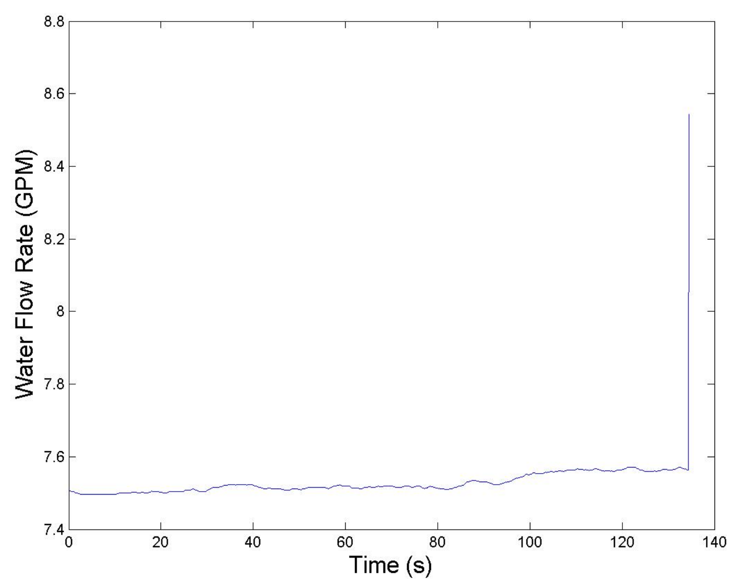

Fig. D.55.: Water flow rate for test 14.

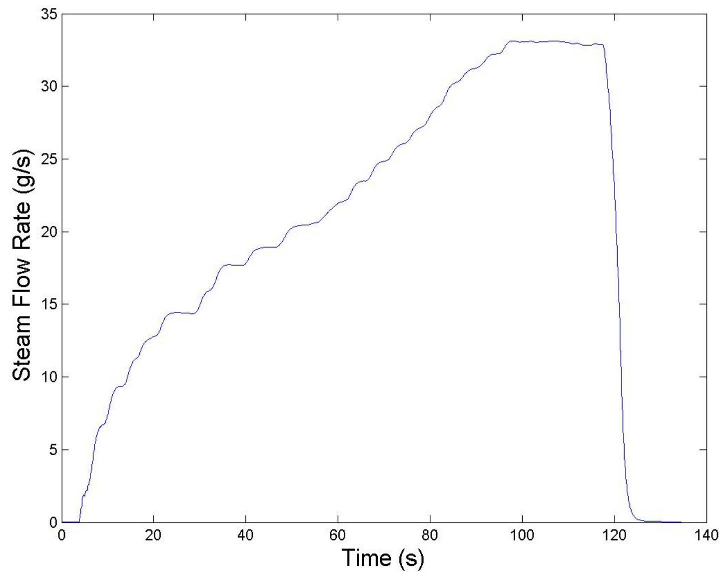

Fig. D.56.: Steam flow rate for test 14.

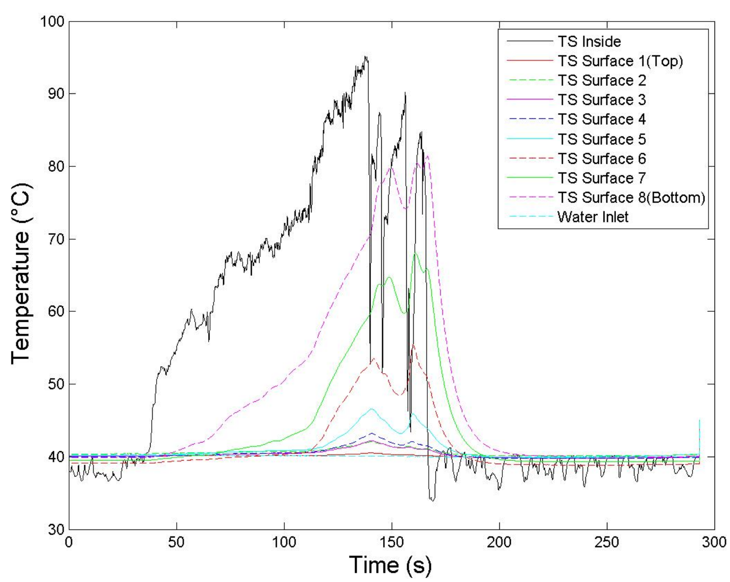

Fig. D.57.: Test section temperatures for test 15.

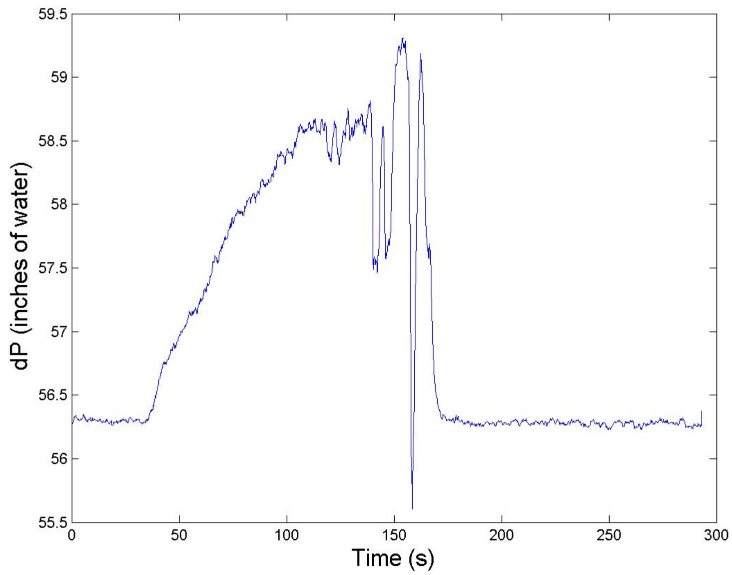

Fig. D.58.: Test section differential pressure for test 15.

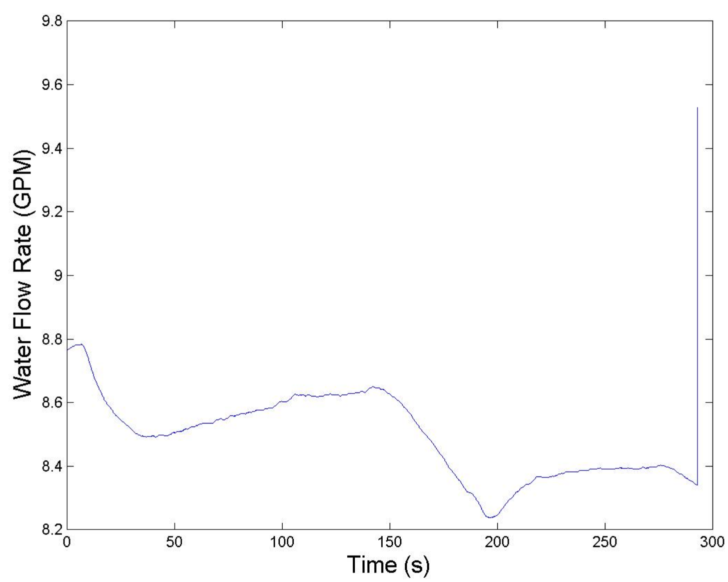

Fig. D.59.: Water flow rate for test 15.

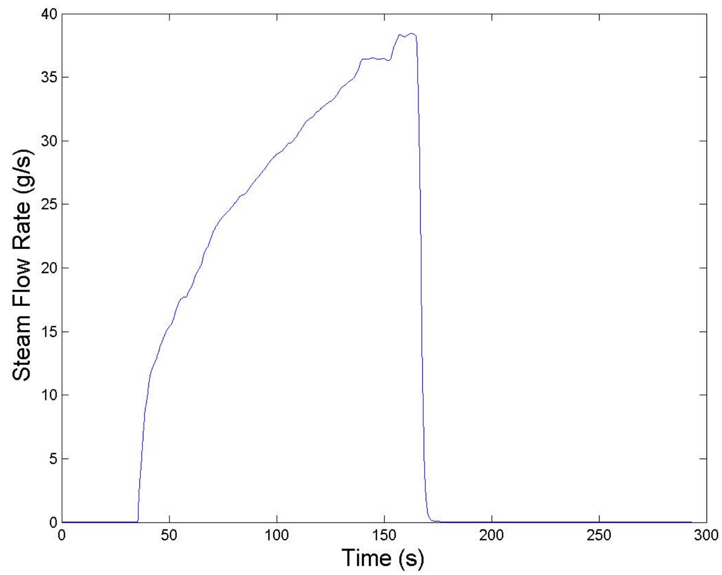

Fig. D.60.: Steam flow rate for test 15.

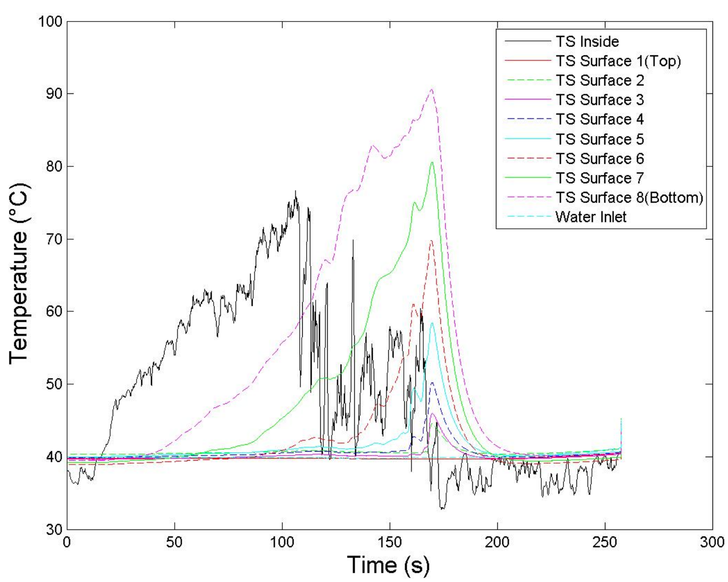

Fig. D.61.: Test section temperatures for test 16.

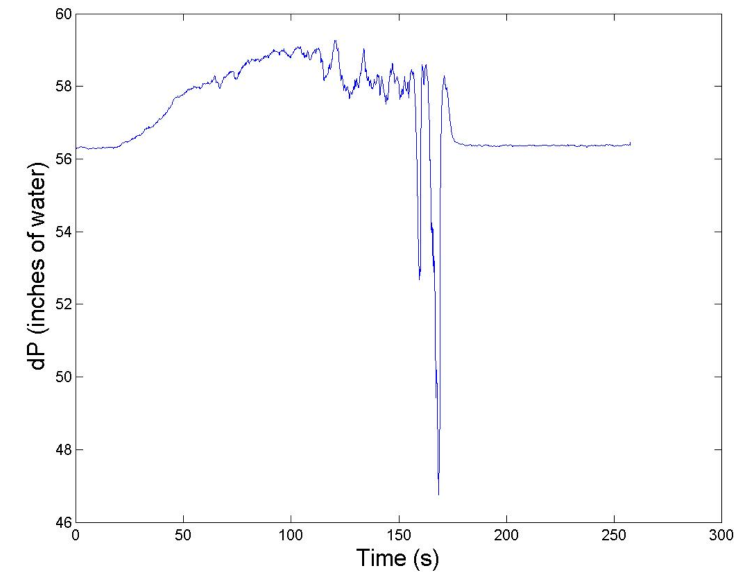

Fig. D.62.: Test section differential pressure for test 16.

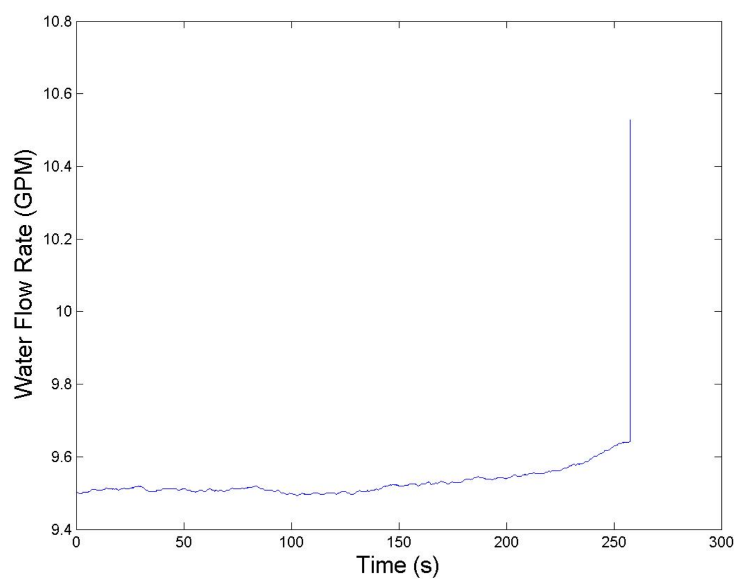

Fig. D.63.: Water flow rate for test 16.

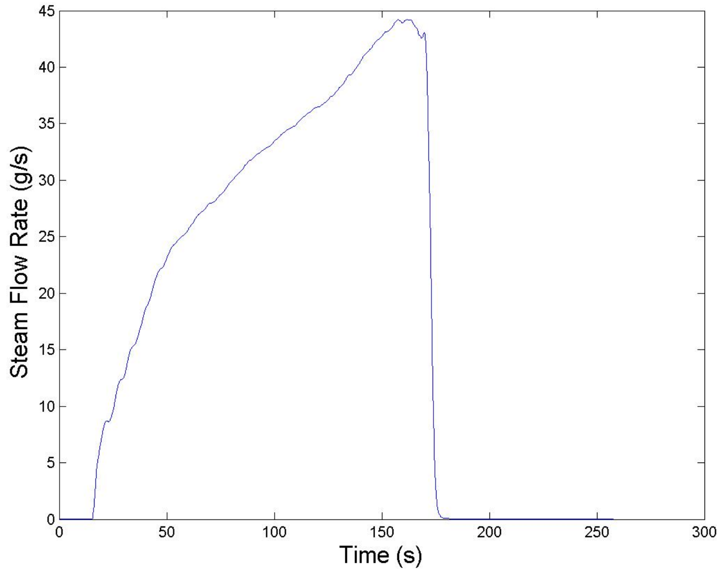

Fig. D.64.: Steam flow rate for test 16.

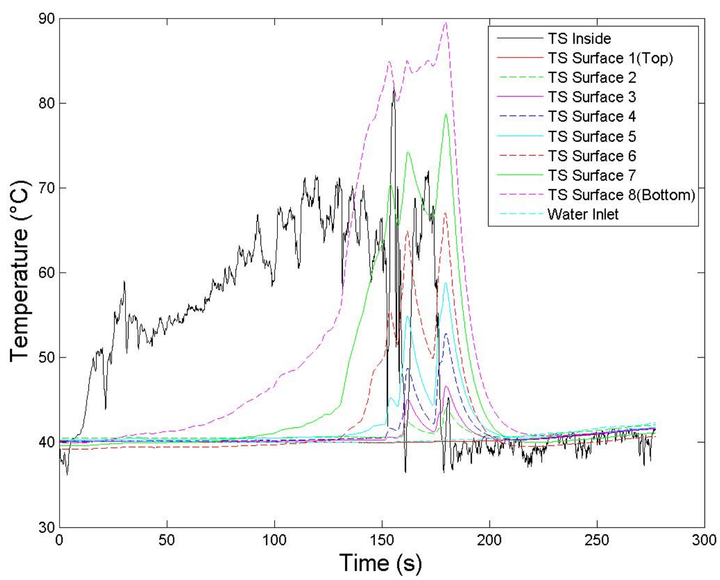

Fig. D.65.: Test section temperatures for test 17.

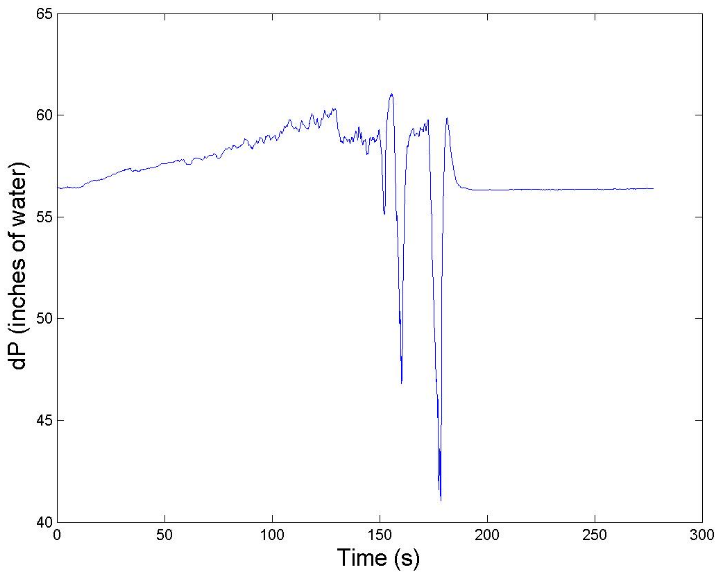

Fig. D.66.: Test section differential pressure for test 17.

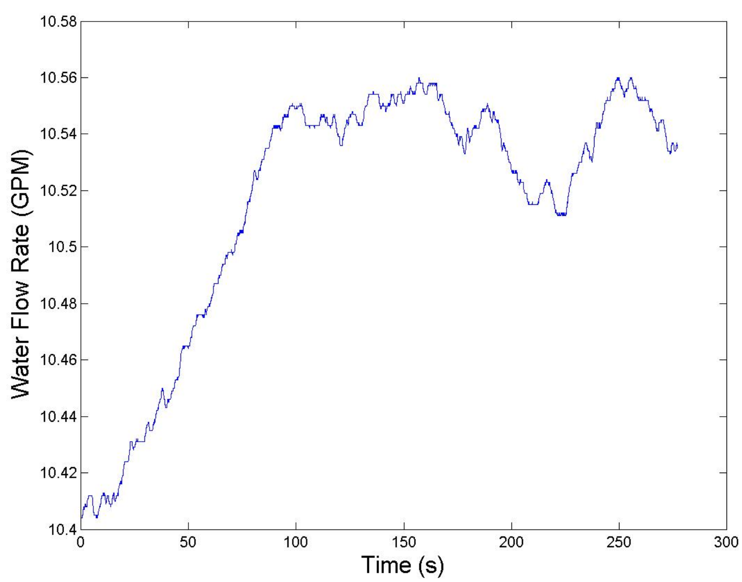

Fig. D.67.: Water flow rate for test 17.

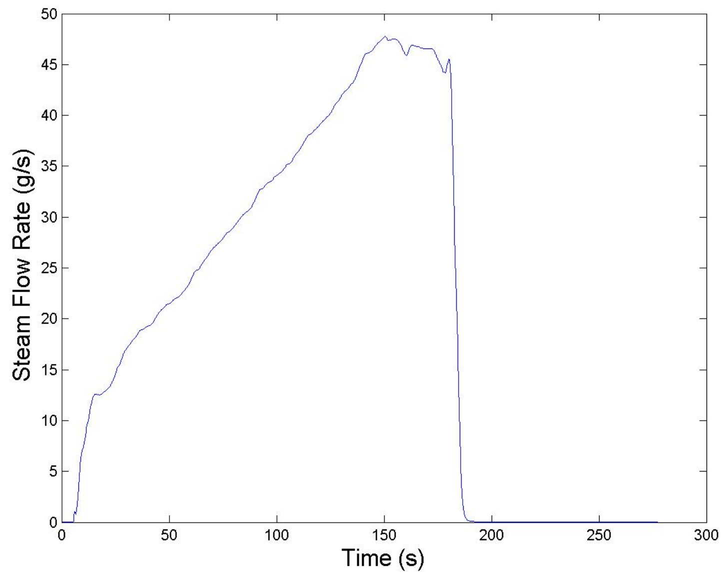

Fig. D.68.: Steam flow rate for test 17.

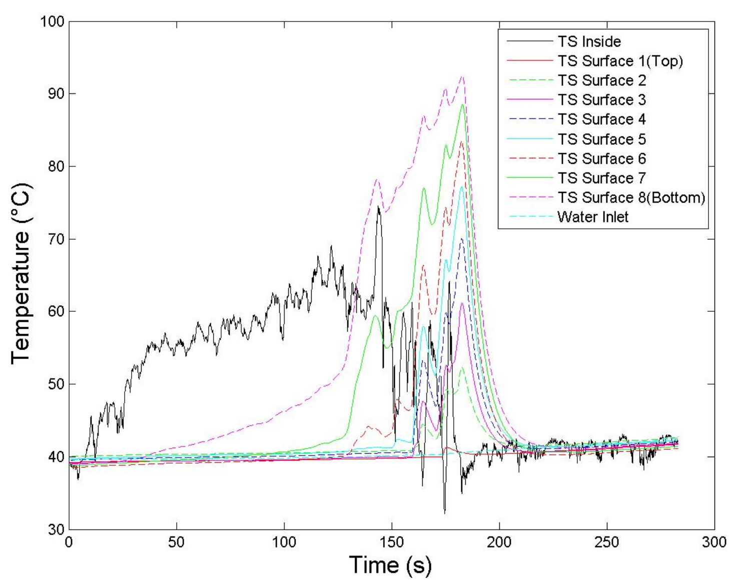

Fig. D.69.: Test section temperatures for test 18.

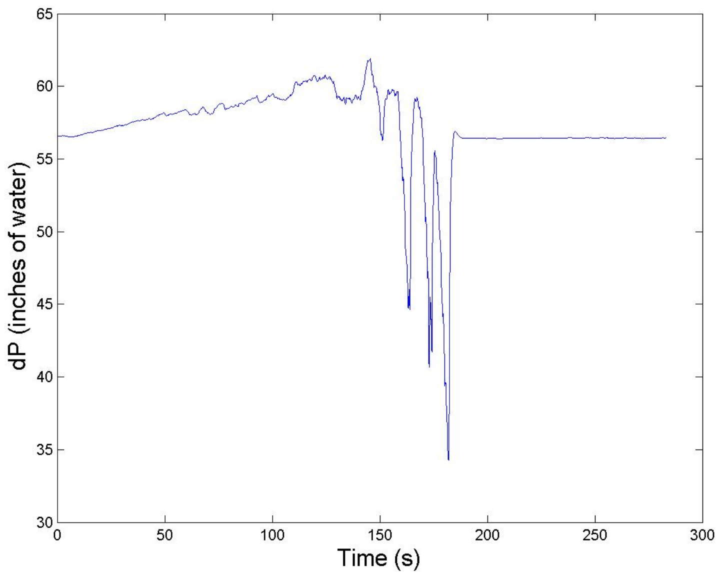

Fig. D.70.: Test section differential pressure for test 18.

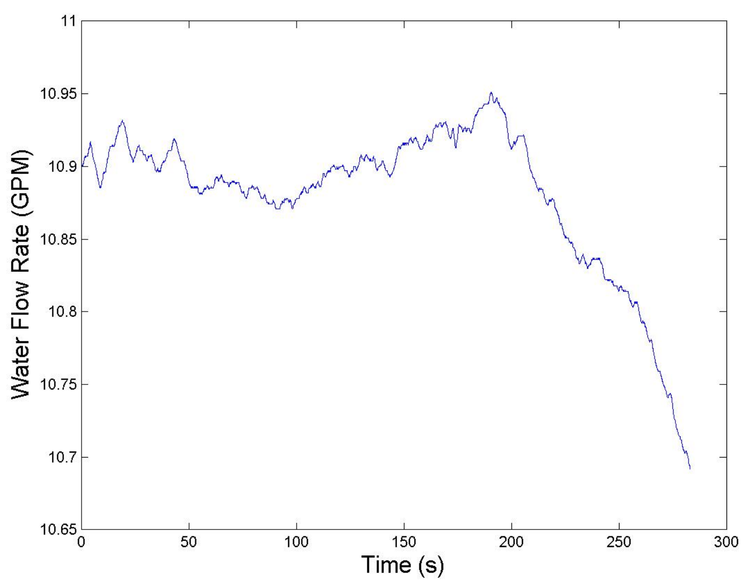

Fig. D.71.: Water flow rate for test 18.

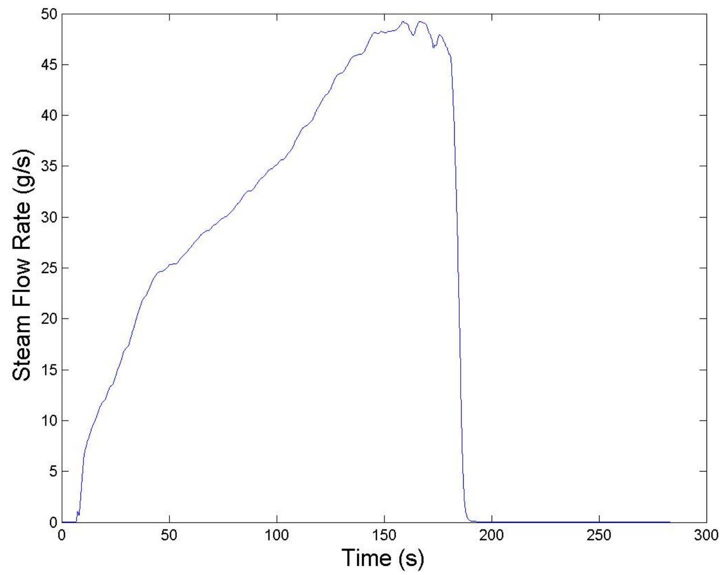

Fig. D.72.: Steam flow rate for test 18.

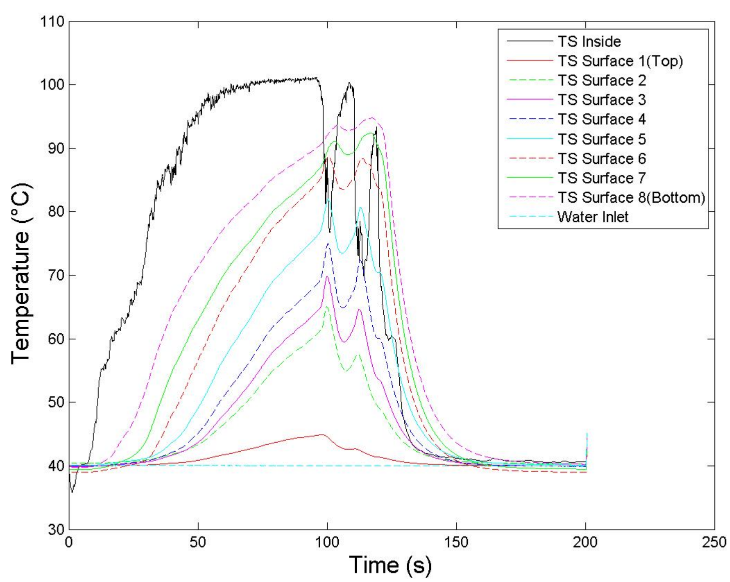

Fig. D.73.: Test section temperatures for test 19.

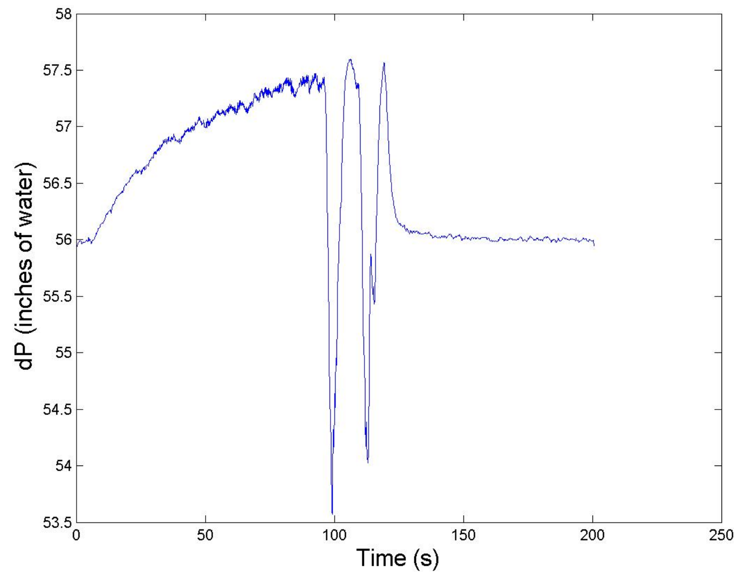

Fig. D.74.: Test section differential pressure for test 19.

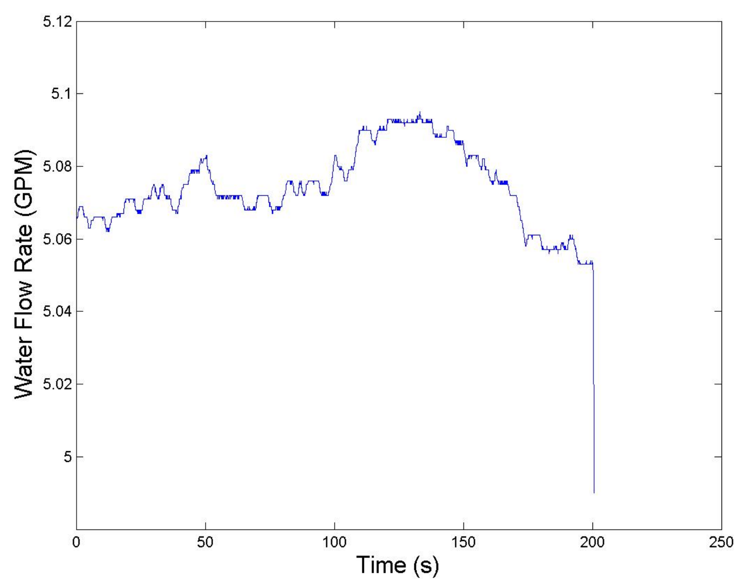

Fig. D.75.: Water flow rate for test 19.

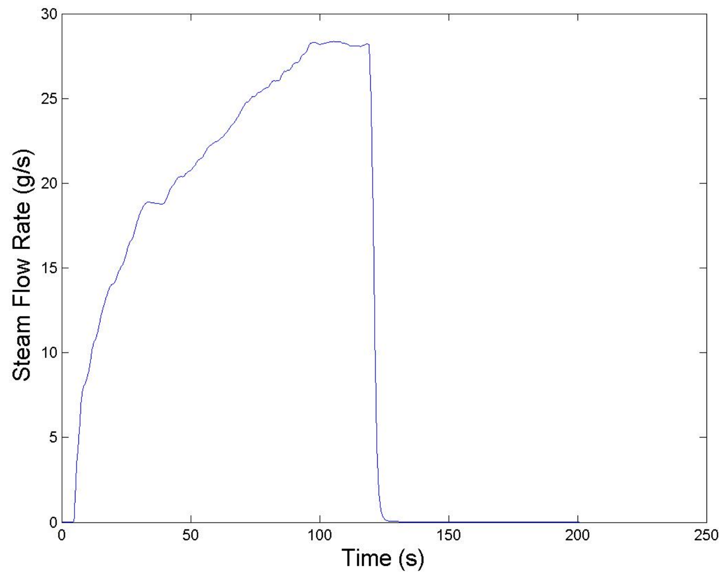

Fig. D.76.: Steam flow rate for test 19.

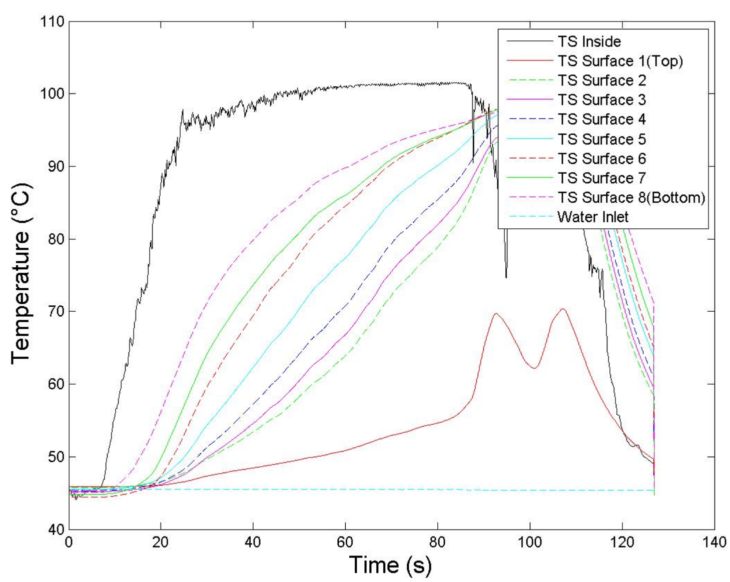

Fig. D.77.: Test section temperatures for test 20.

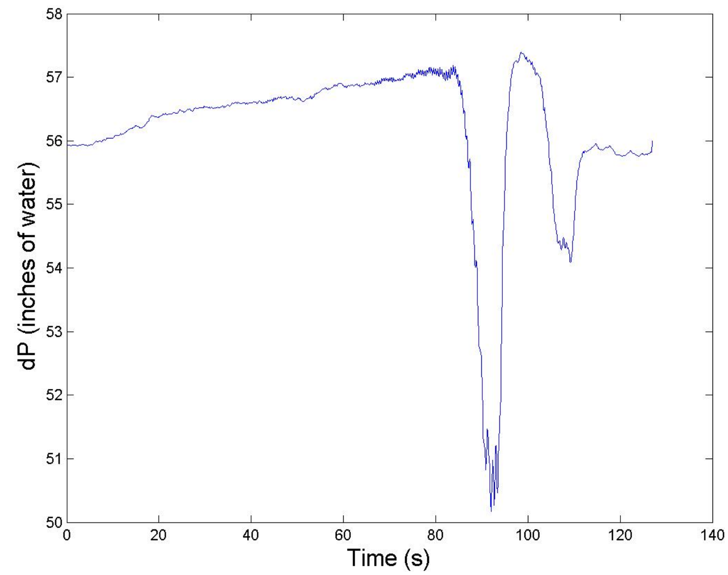

Fig. D.78.: Test section differential pressure for test 20.

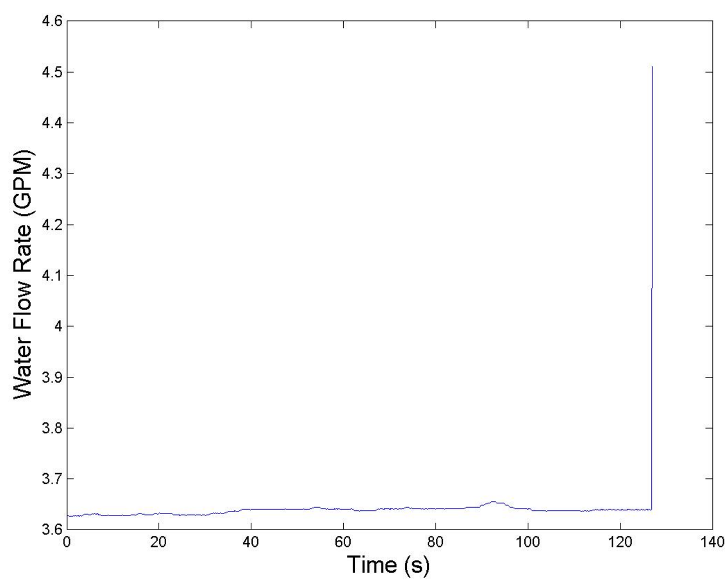

Fig. D.79.: Water flow rate for test 20.

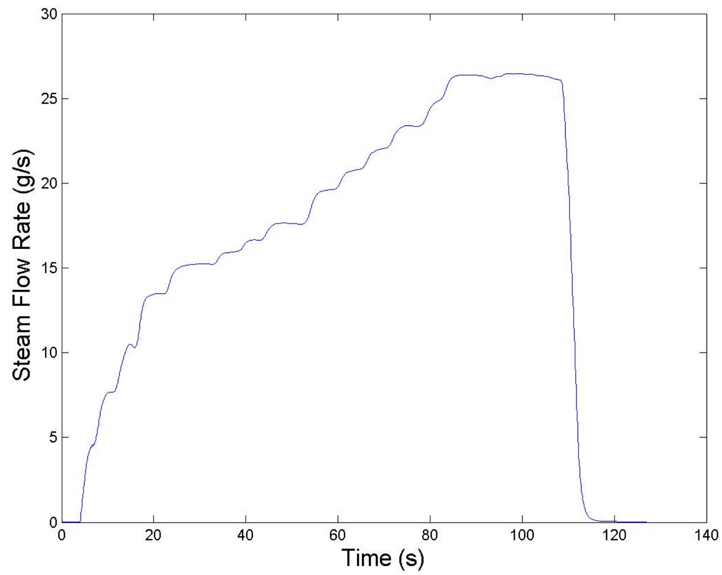

Fig. D.80.: Steam flow rate for test 20.

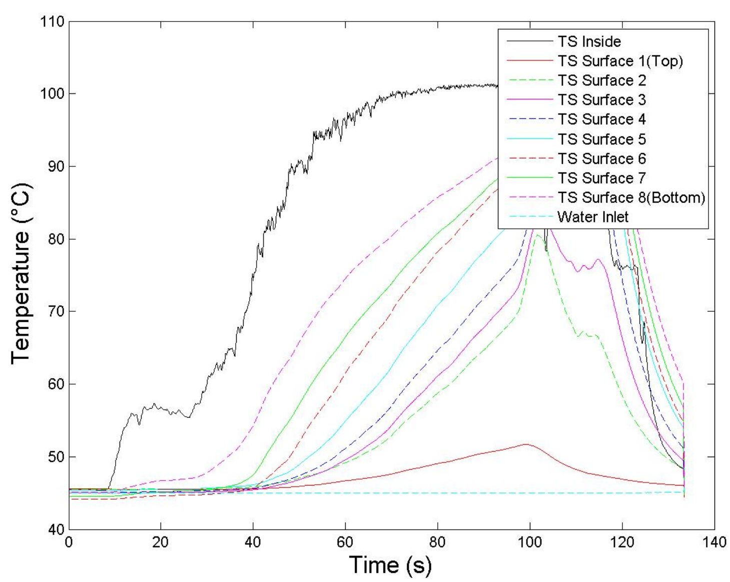

Fig. D.81.: Test section temperatures for test 21.

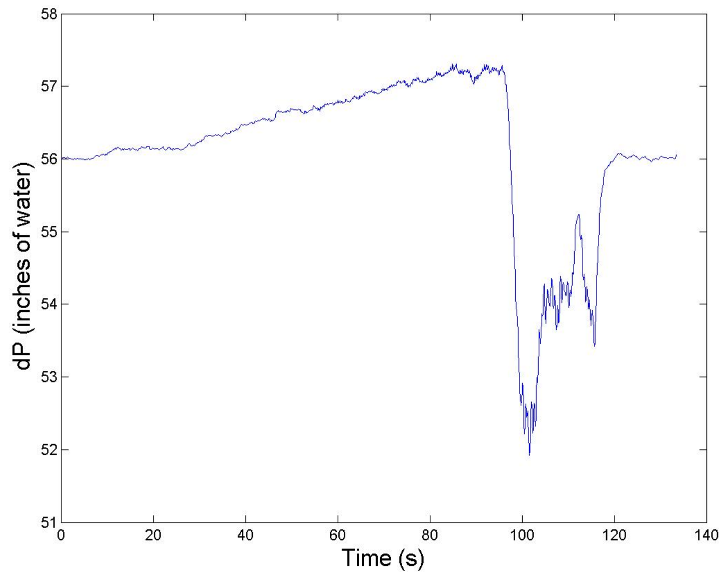

Fig. D.82.: Test section differential pressure for test 21.

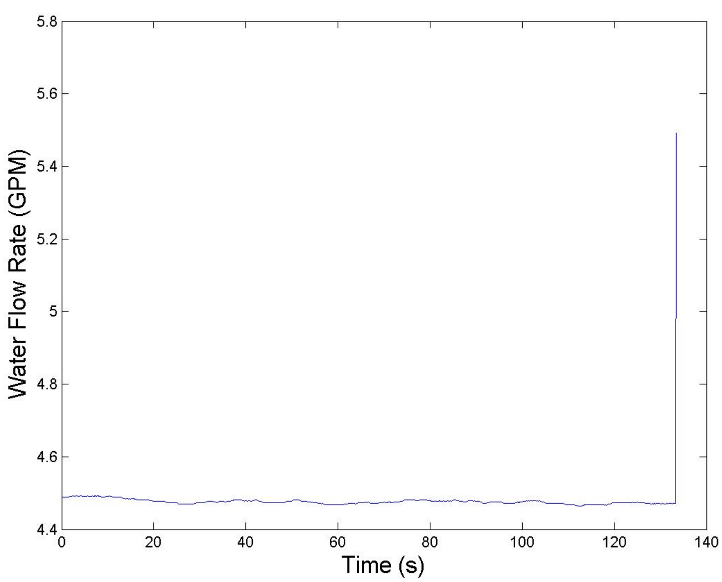

Fig. D.83.: Water flow rate for test 21.

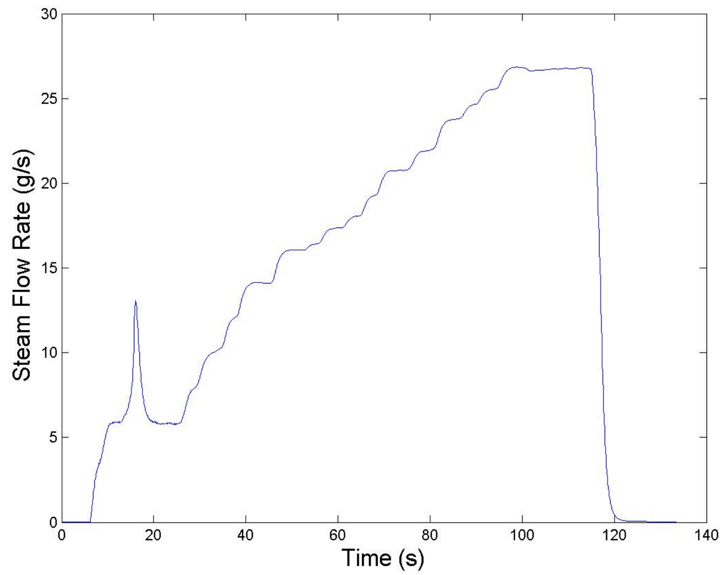

Fig. D.84.: Steam flow rate for test 21.

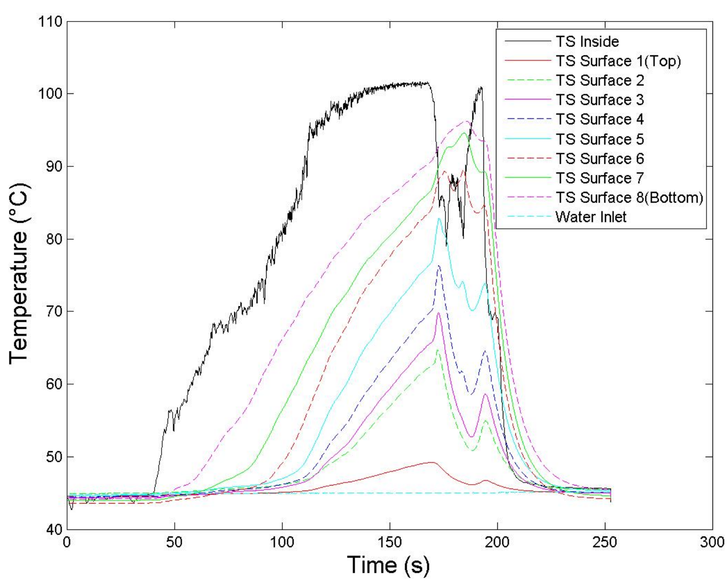

Fig. D.85.: Test section temperatures for test 22.

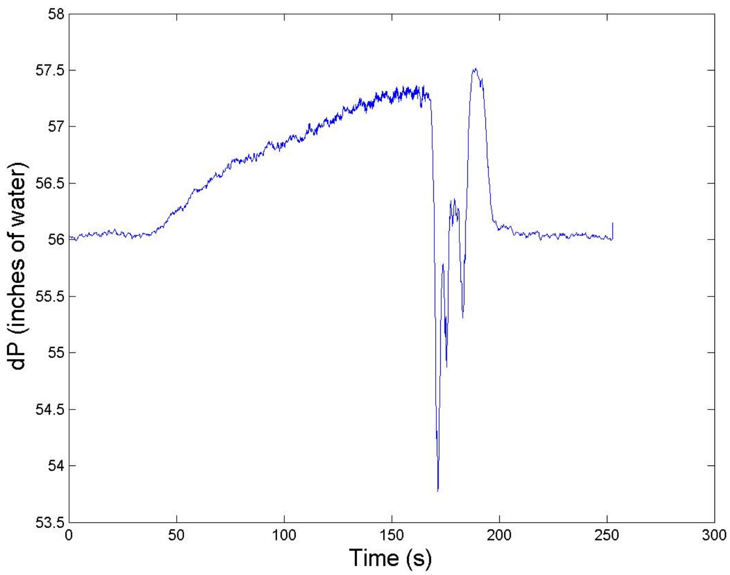

Fig. D.86.: Test section differential pressure for test 22.

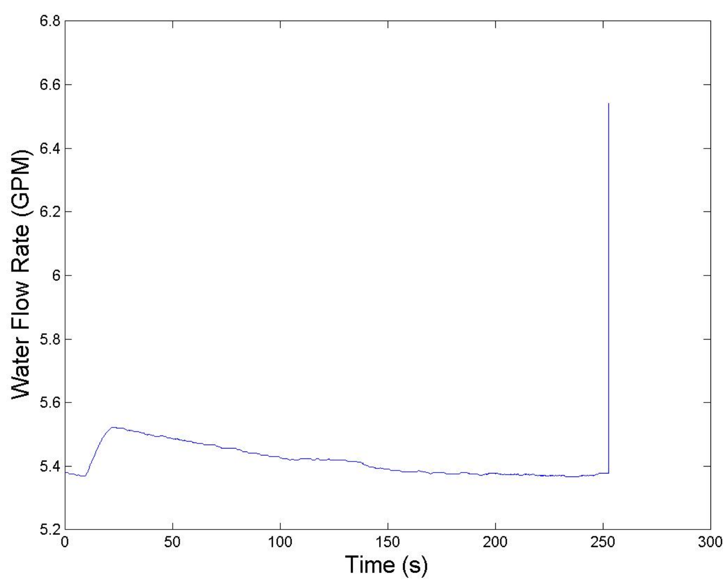

Fig. D.87.: Water flow rate for test 22.

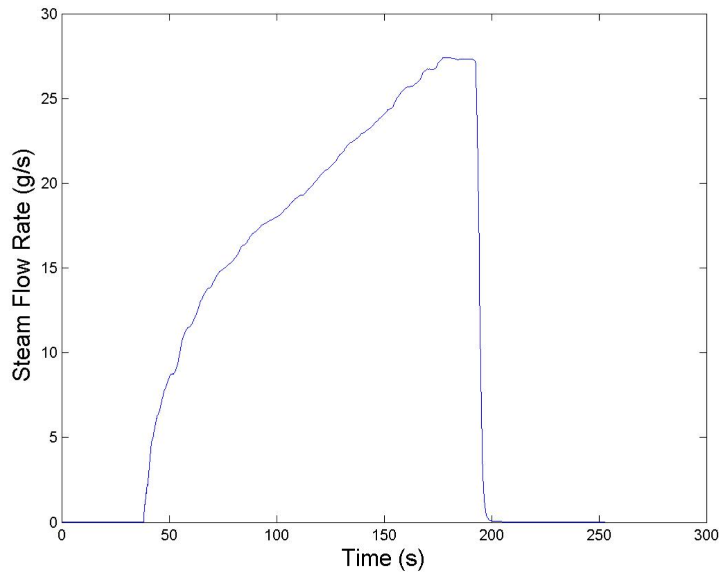

Fig. D.88.: Steam flow rate for test 22.

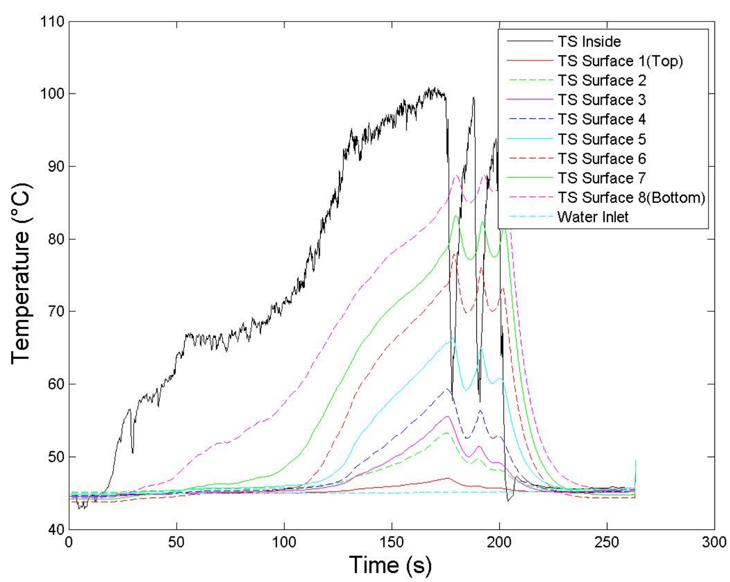

Fig. D.89.: Test section temperatures for test 23.

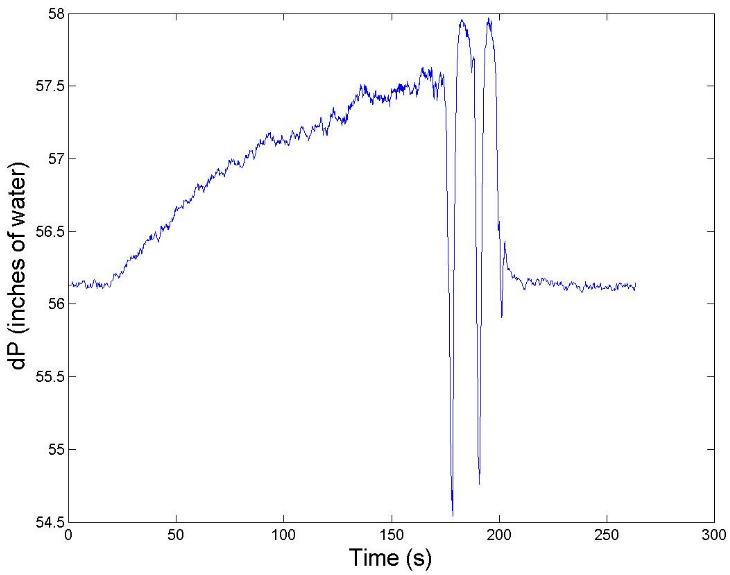

Fig. D.90.: Test section differential pressure for test 23.

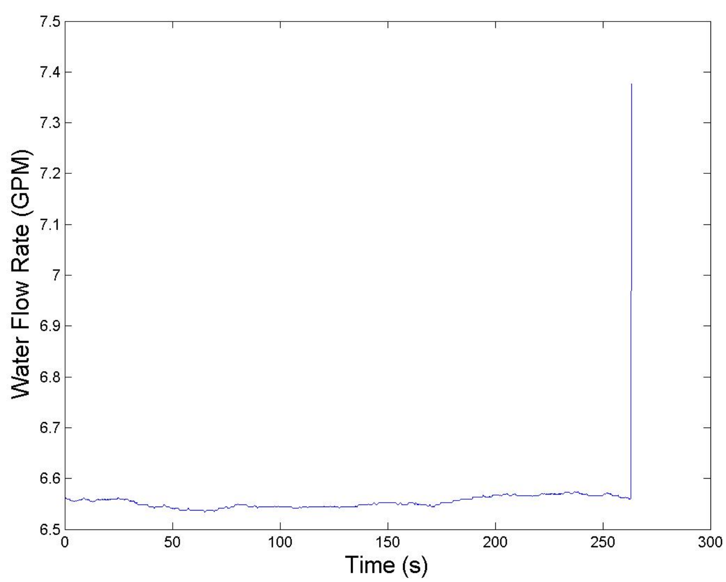

Fig. D.91.: Water flow rate for test 23.

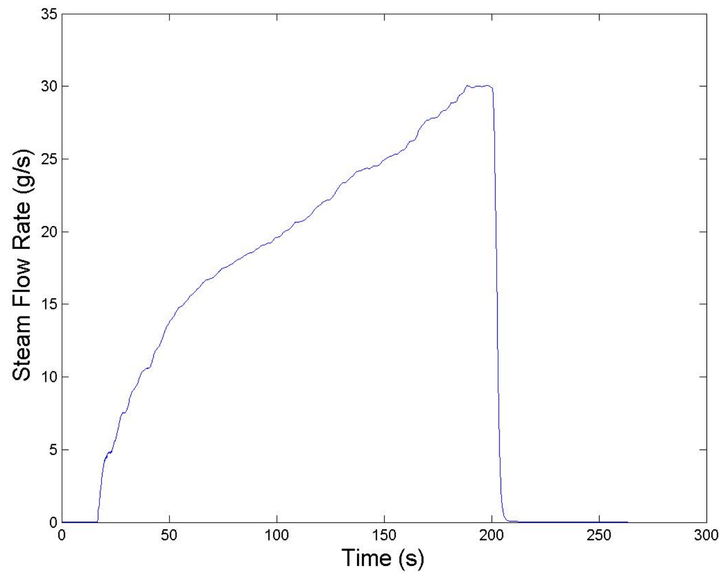

Fig. D.92.: Steam flow rate for test 23.

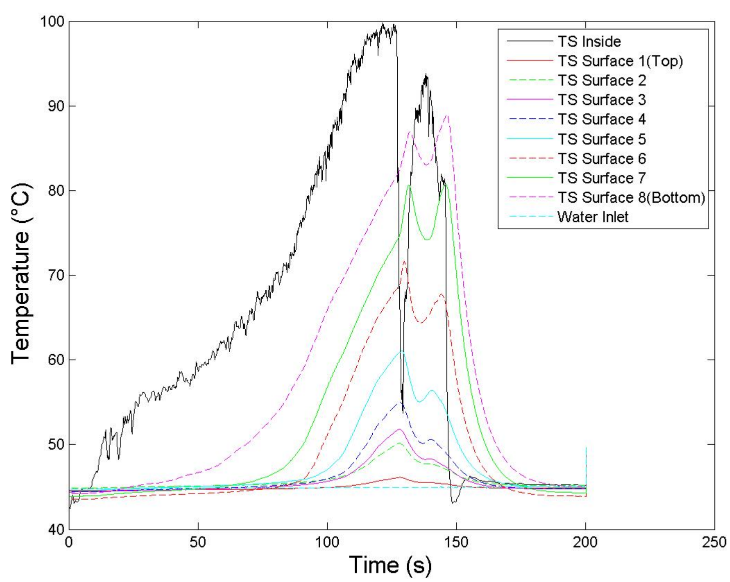

Fig. D.93.: Test section temperatures for test 24.

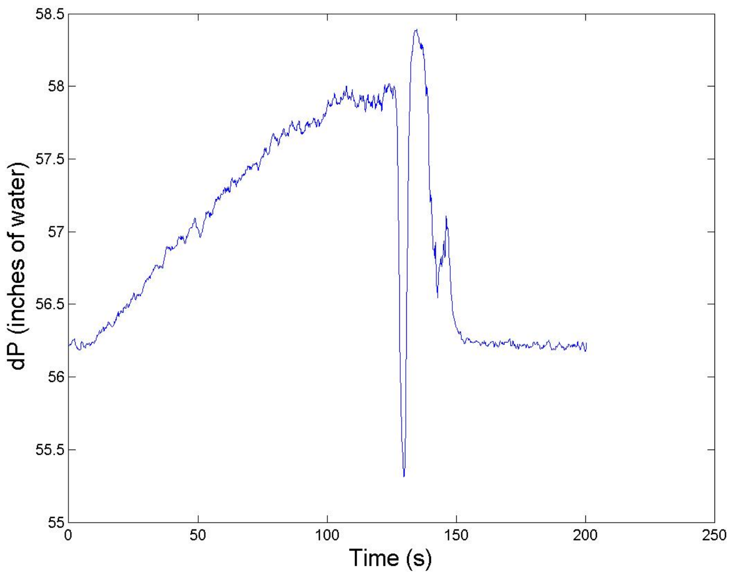

Fig. D.94.: Test section differential pressure for test 24.

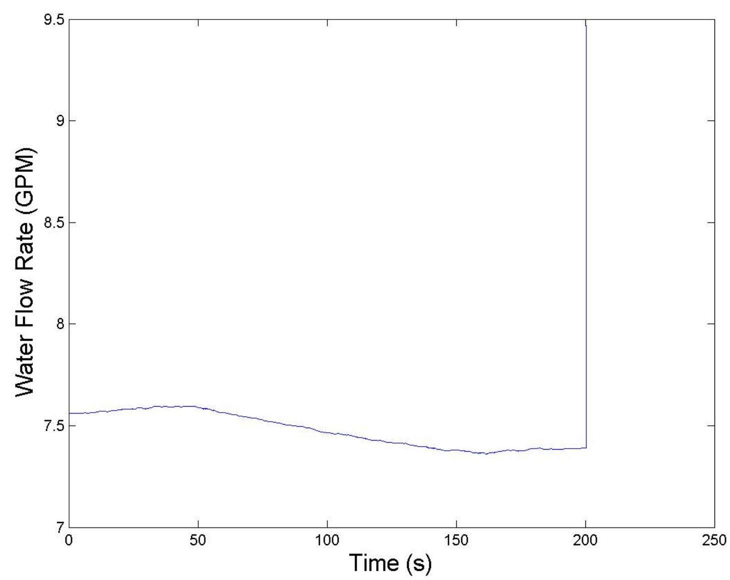

Fig. D.95.: Water flow rate for test 24.

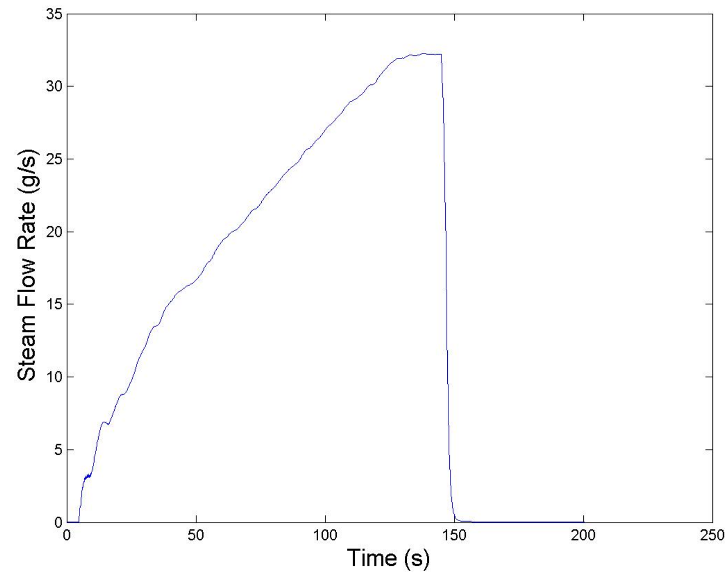

Fig. D.96.: Steam flow rate for test 24.

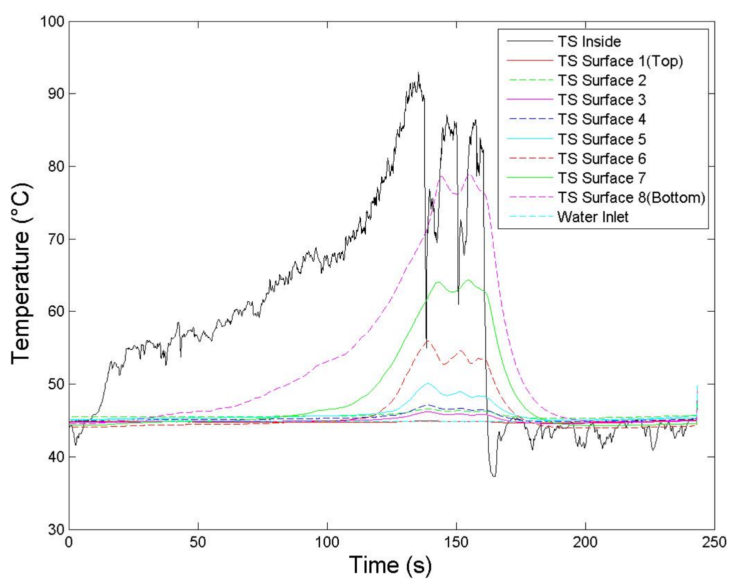

Fig. D.97.: Test section temperatures for test 25.

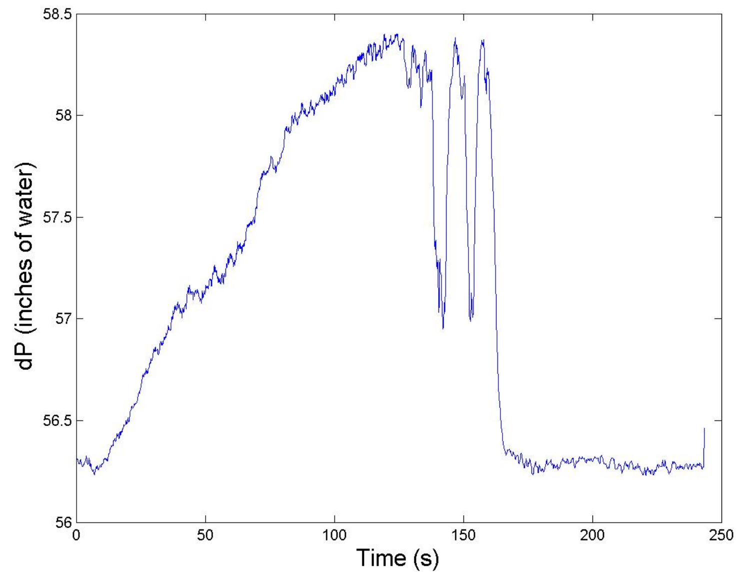

Fig. D.98.: Test section differential pressure for test 25.

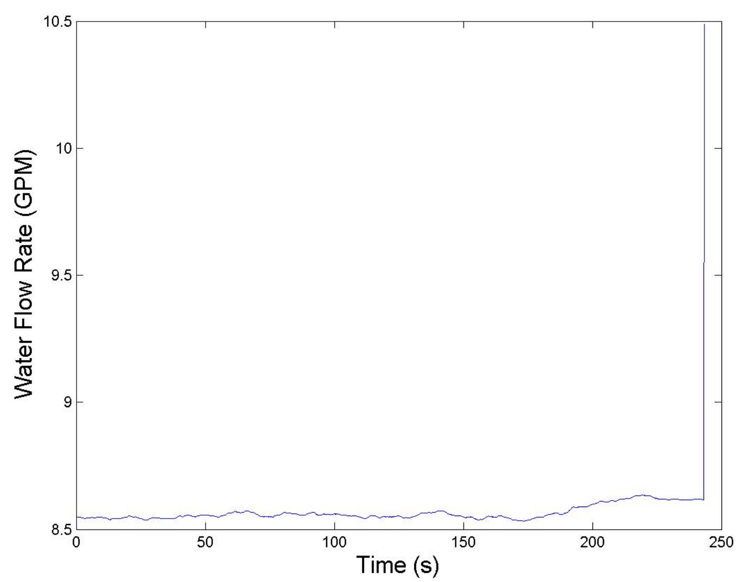

Fig. D.99.: Water flow rate for test 25.

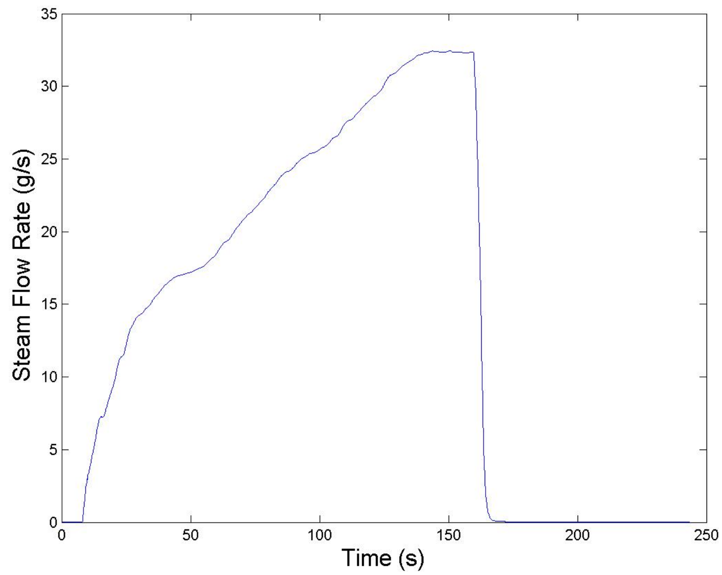

Fig. D.100.: Steam flow rate for test 25.

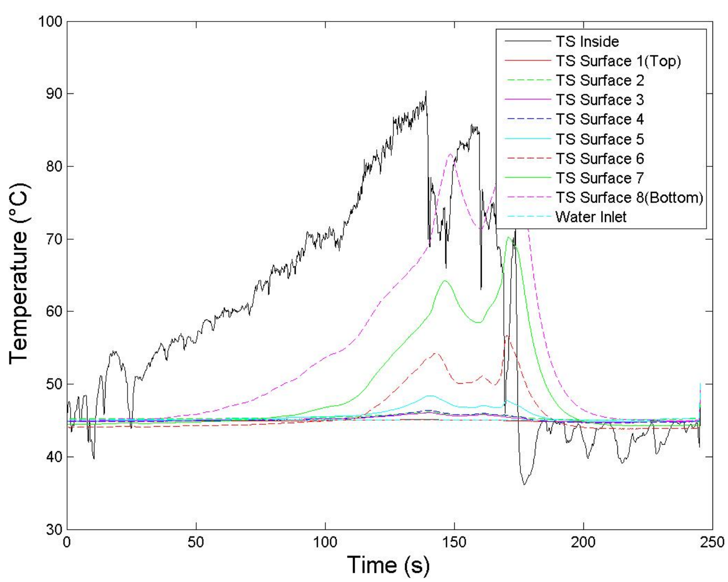

Fig. D.101.: Test section temperatures for test 26.

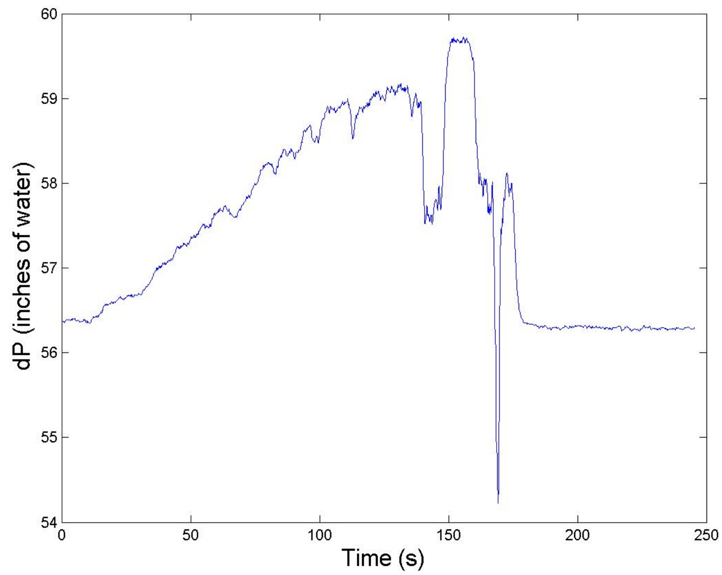

Fig. D.102.: Test section differential pressure for test 26.

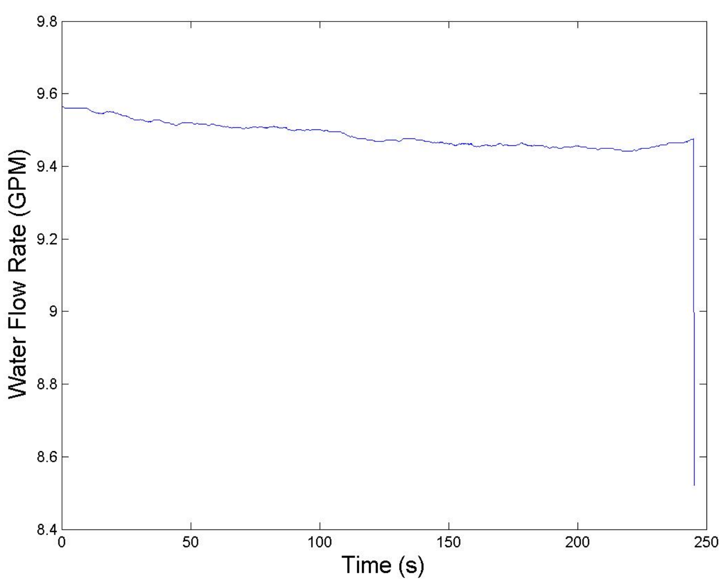

Fig. D.103.: Water flow rate for test 26.

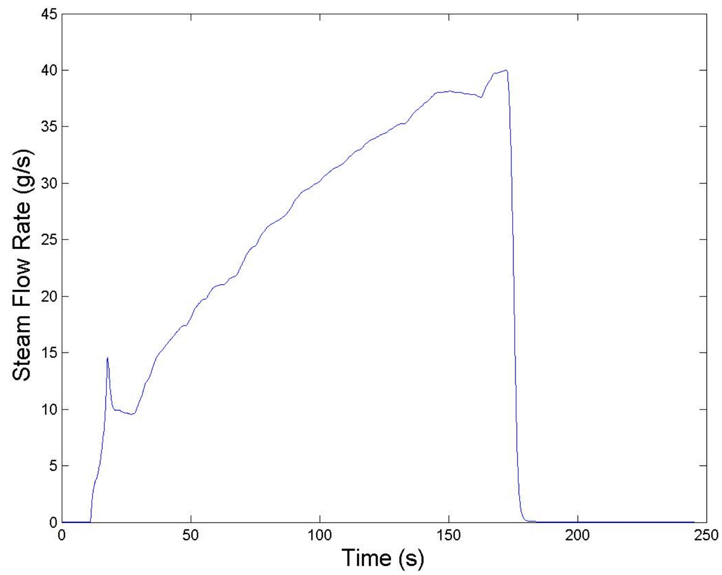

Fig. D.104.: Steam flow rate for test 26.

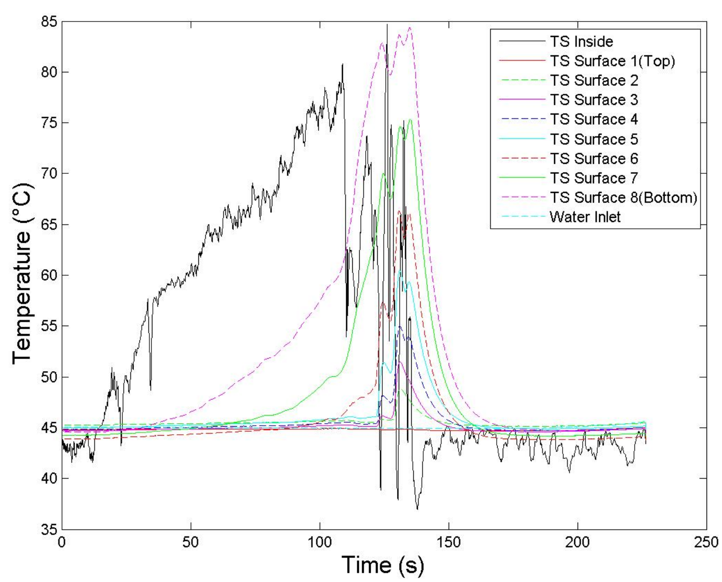

Fig. D.105.: Test section temperatures for test 27.

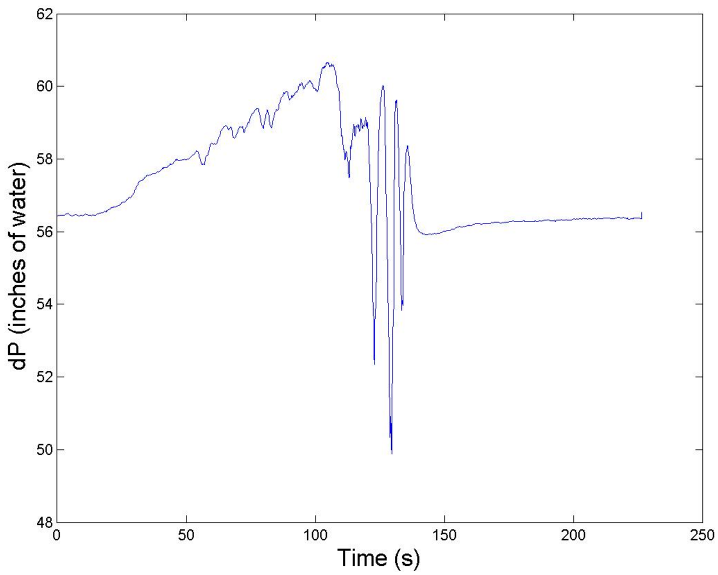

Fig. D.106.: Test section differential pressure for test 27.

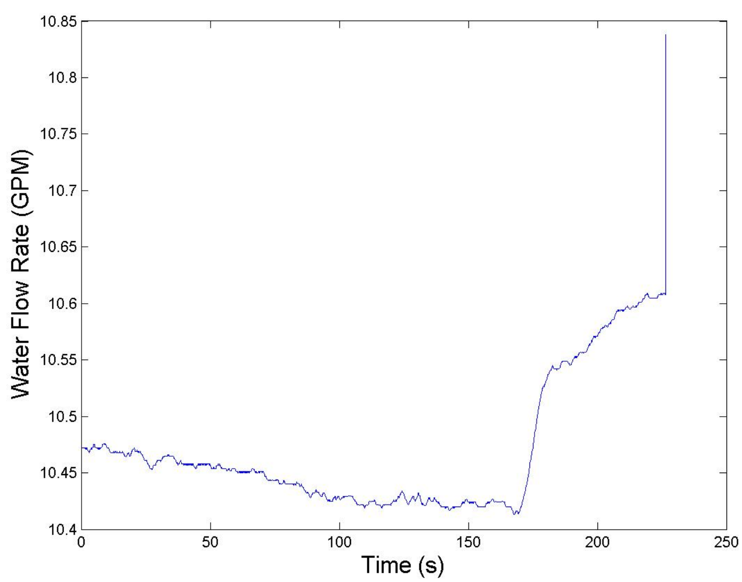

Fig. D.107.: Water flow rate for test 27.

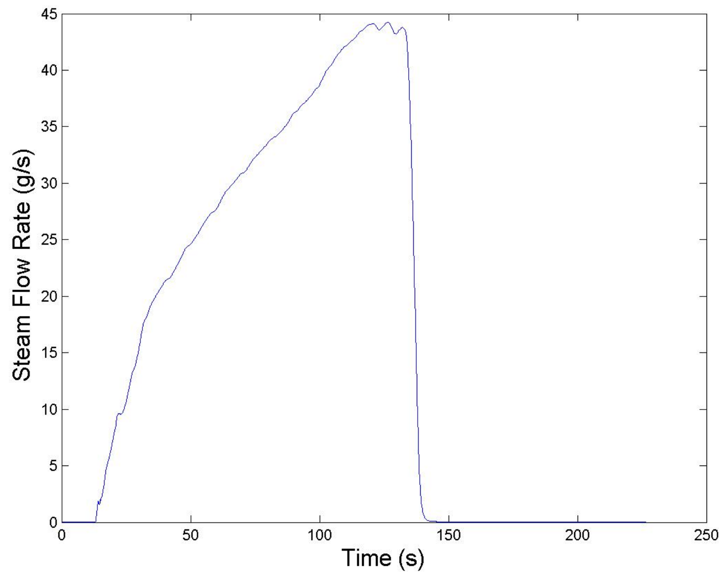

Fig. D.108.: Steam flow rate for test 27.

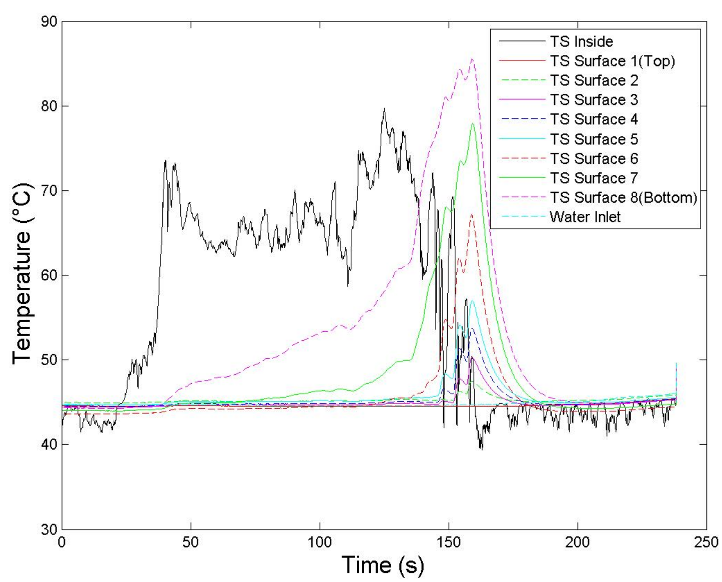

Fig. D.109.: Test section temperatures for test 28.

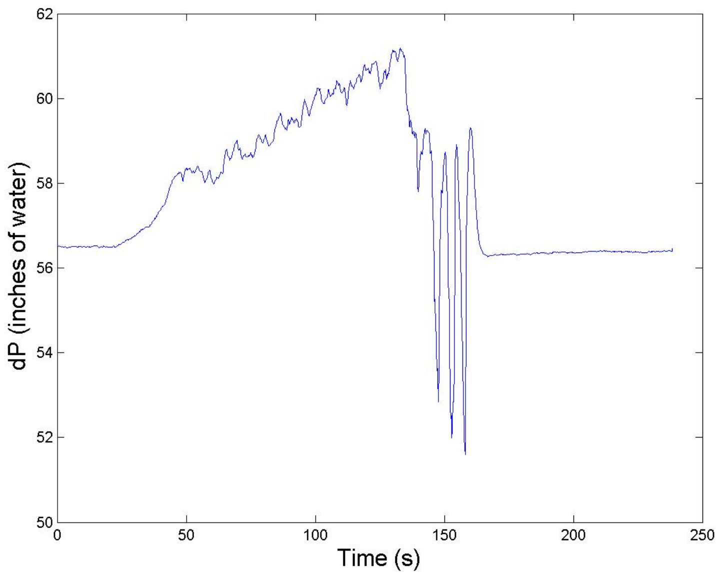

Fig. D.110.: Test section differential pressure for test 28.

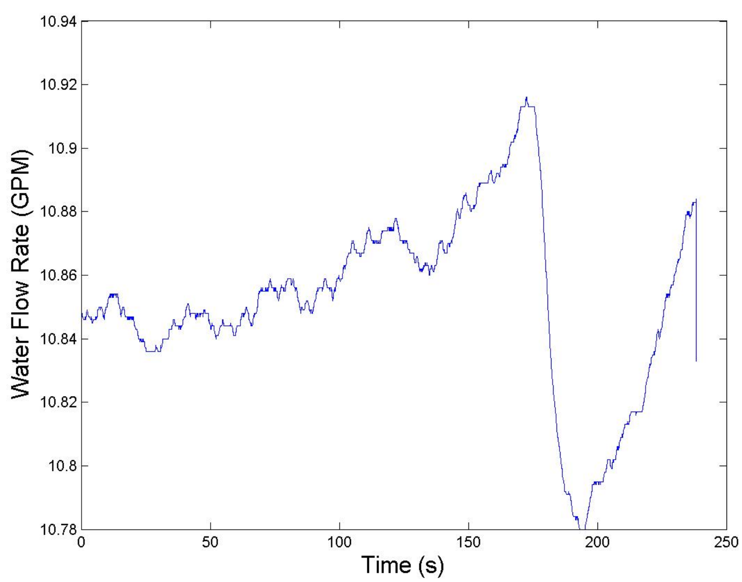

Fig. D.111.: Water flow rate for test 28.

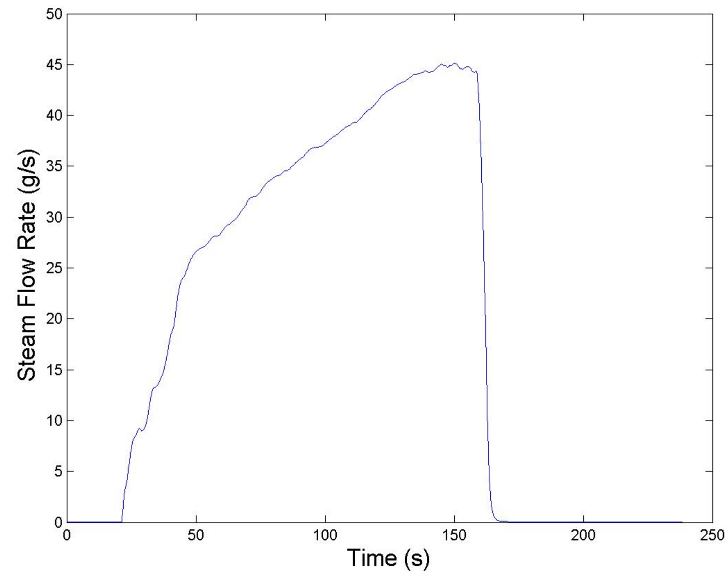

Fig. D.112.: Steam flow rate for test 28.

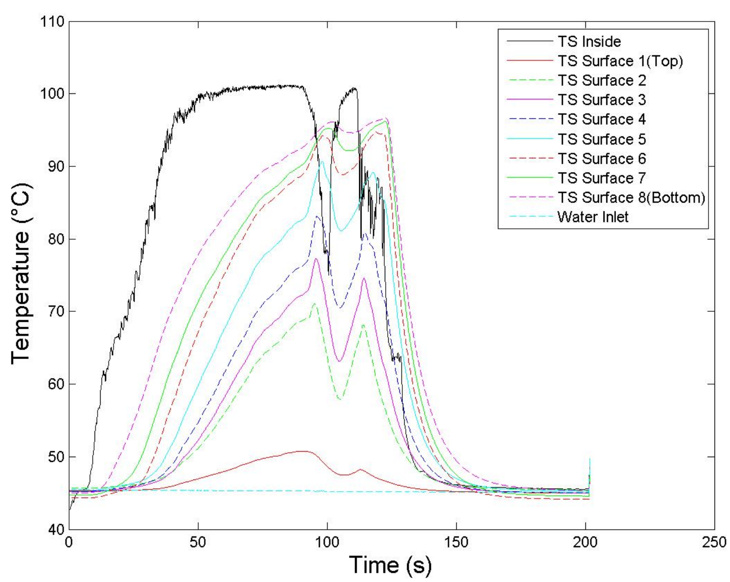

Fig. D.113.: Test section temperatures for test 29.

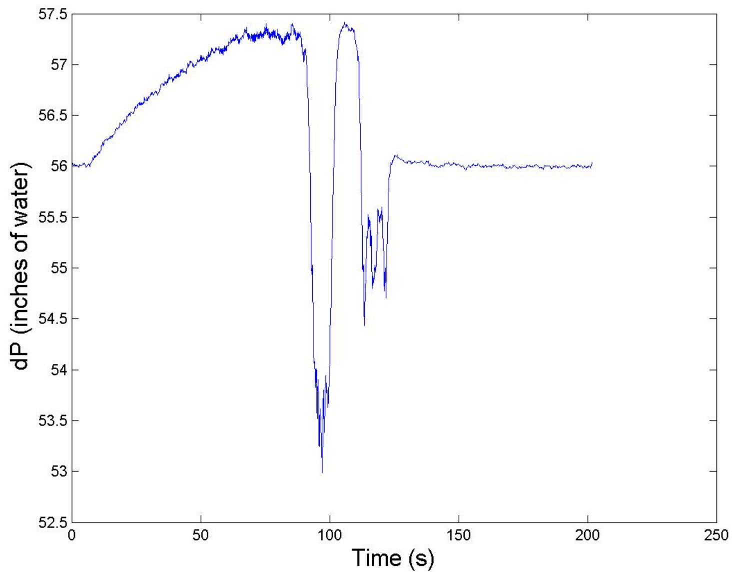

Fig. D.114.: Test section differential pressure for test 29.

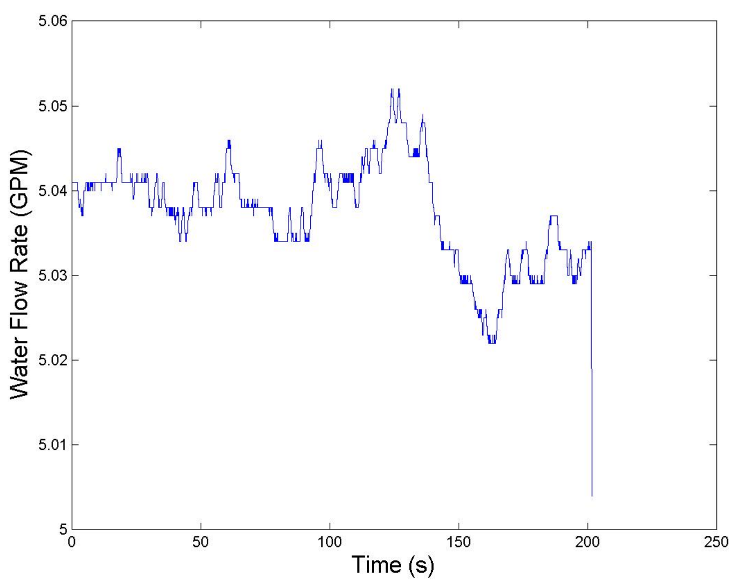

Fig. D.115.: Water flow rate for test 29.

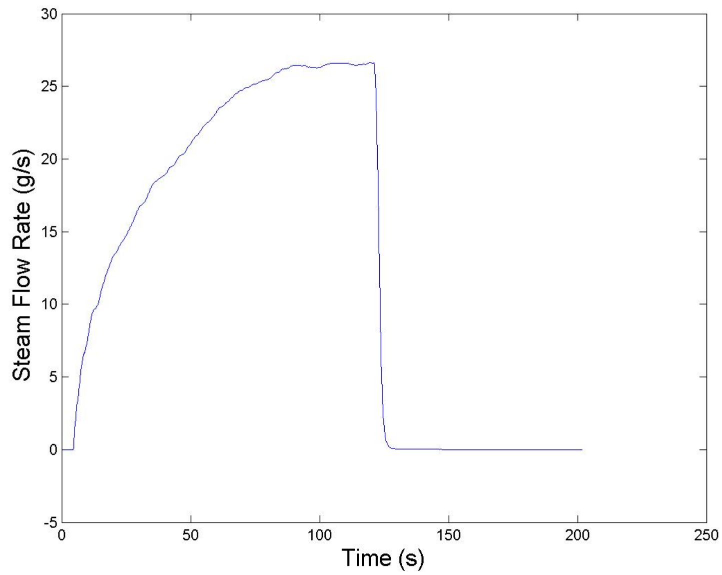

Fig. D.116.: Steam flow rate for test 29.

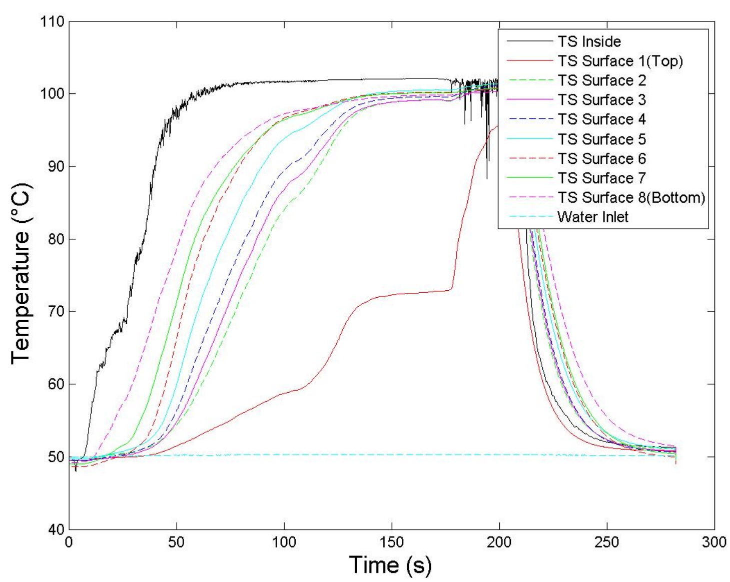

Fig. D.117.: Test section temperatures for test 30.

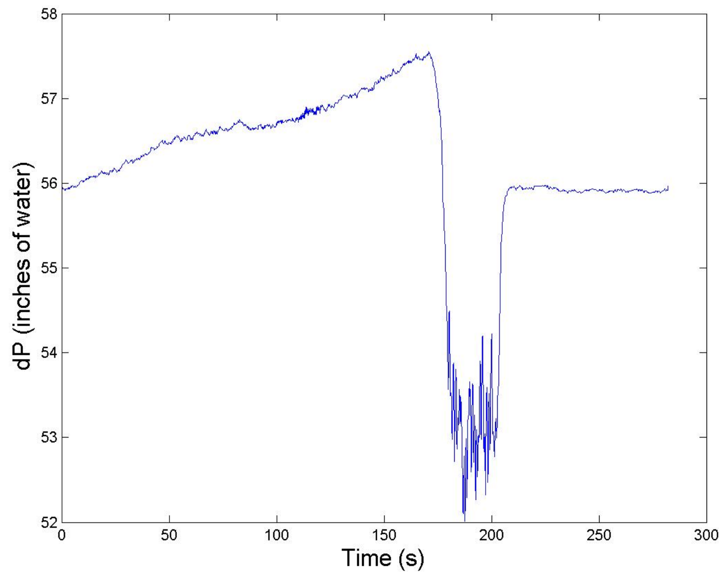

Fig. D.118.: Test section differential pressure for test 30.

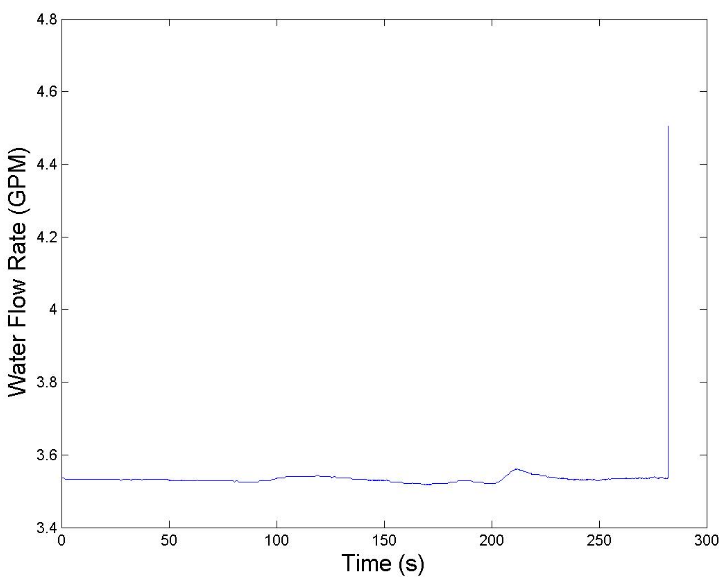

Fig. D.119.: Water flow rate for test 30.

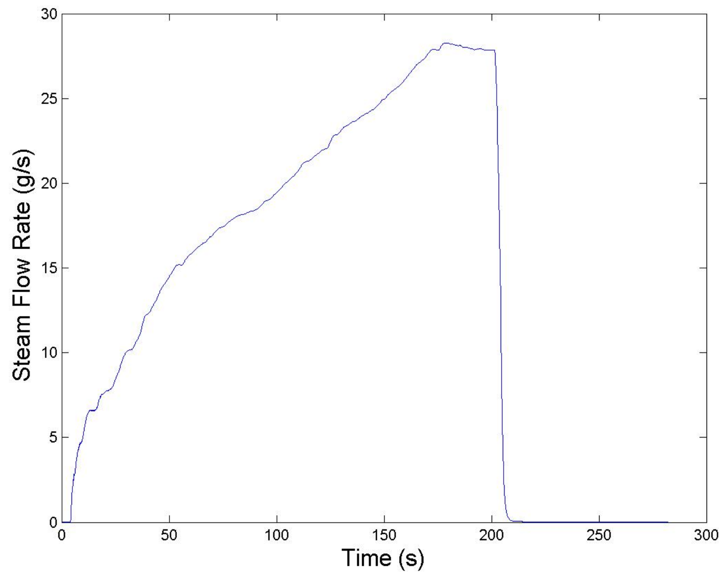

Fig. D.120.: Steam flow rate for test 30.

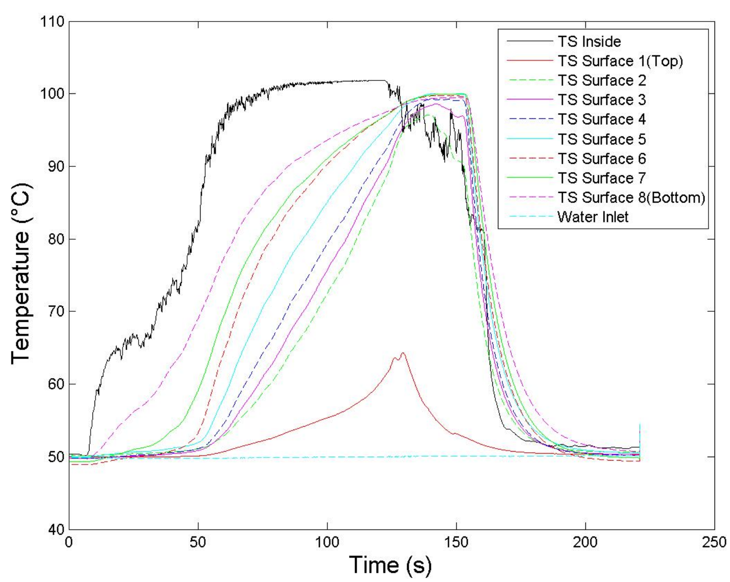

Fig. D.121.: Test section temperatures for test 31.

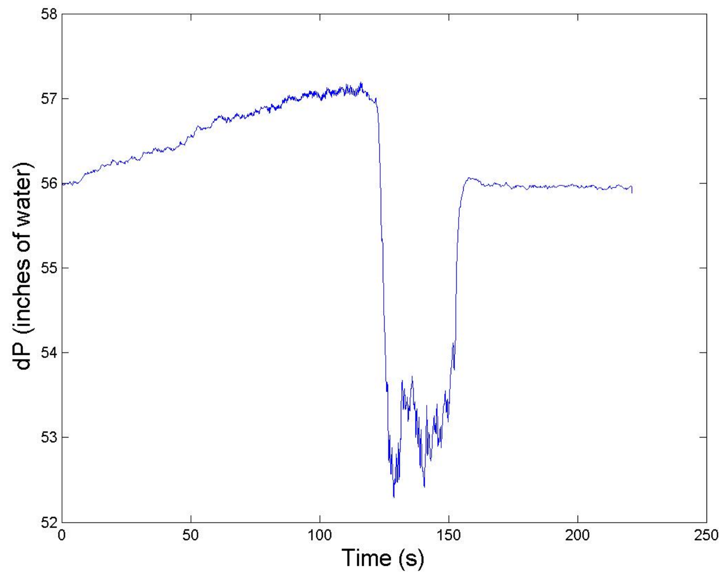

Fig. D.122.: Test section differential pressure for test 31.

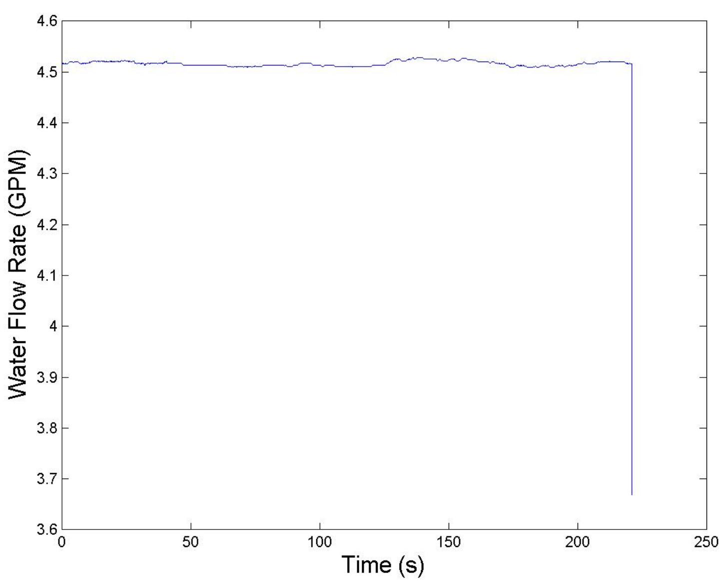

Fig. D.123.: Water flow rate for test 31.

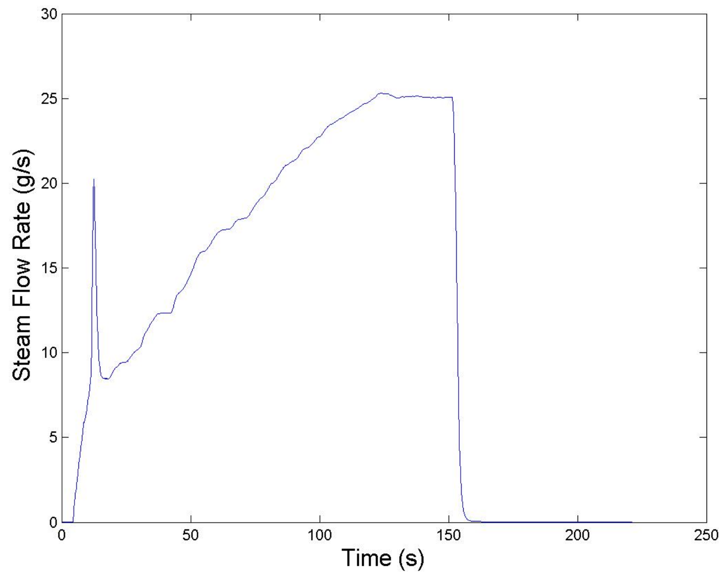

Fig. D.124.: Steam flow rate for test 31.

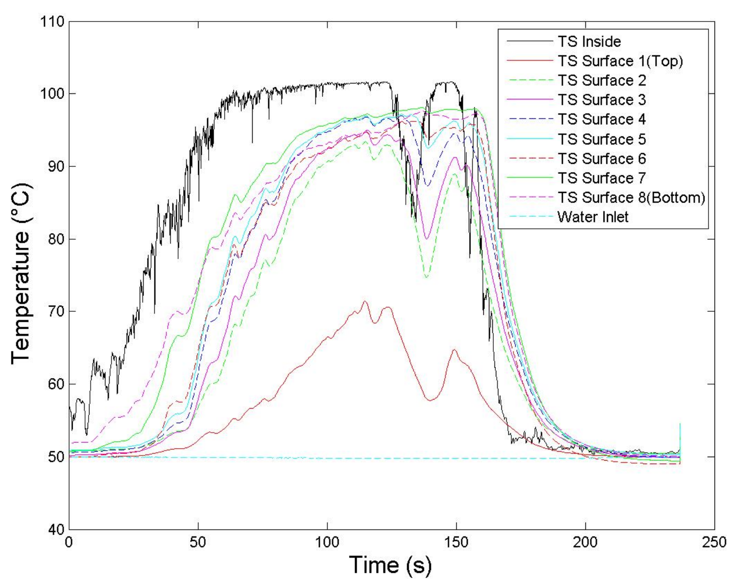

Fig. D.125.: Test section temperatures for test 32.

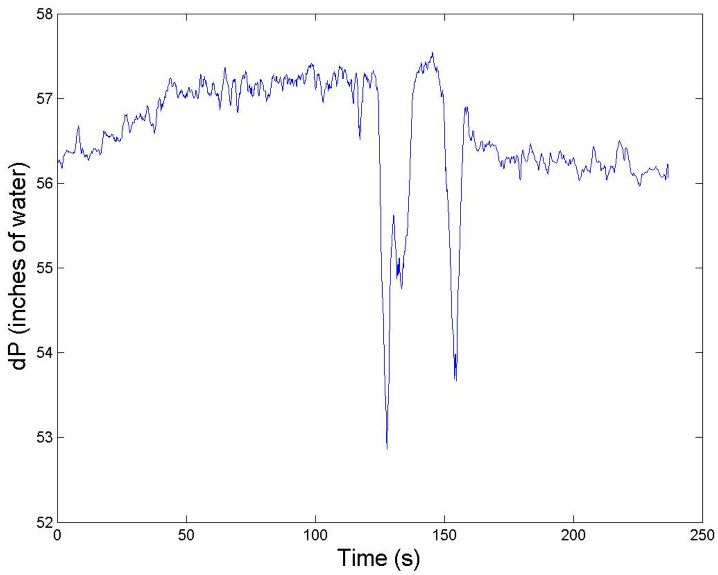

Fig. D.126.: Test section differential pressure for test 32.

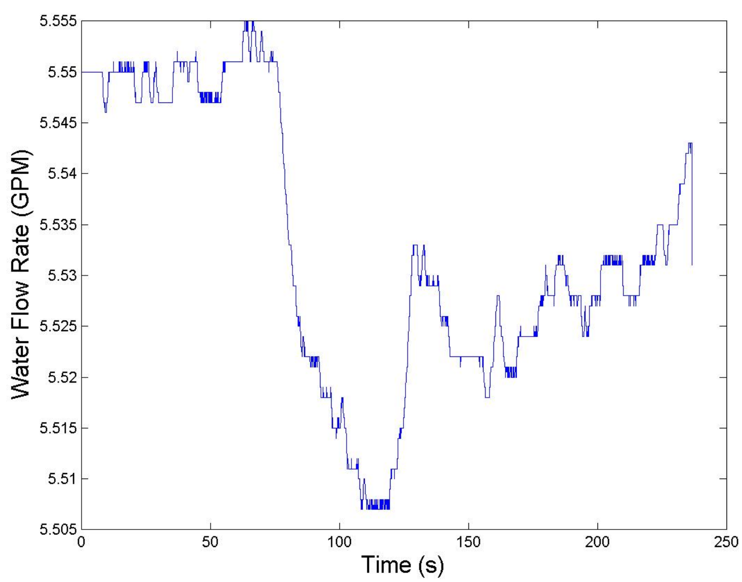

Fig. D.127.: Water flow rate for test 32.

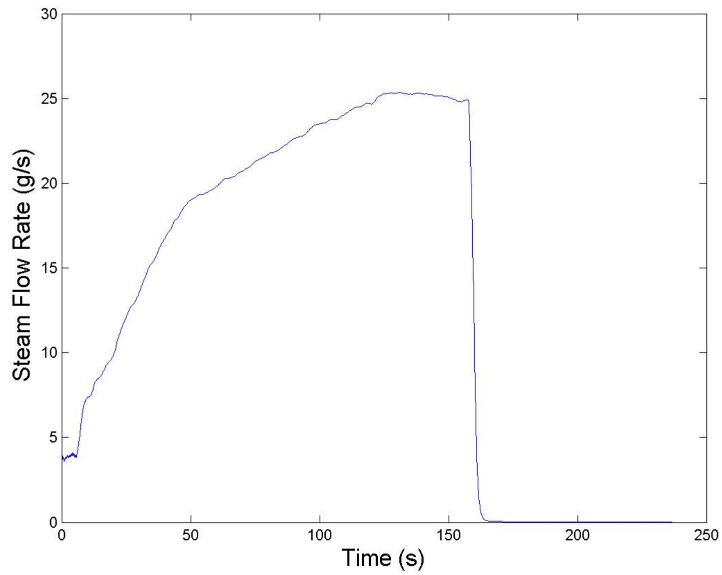

Fig. D.128.: Steam flow rate for test 32.

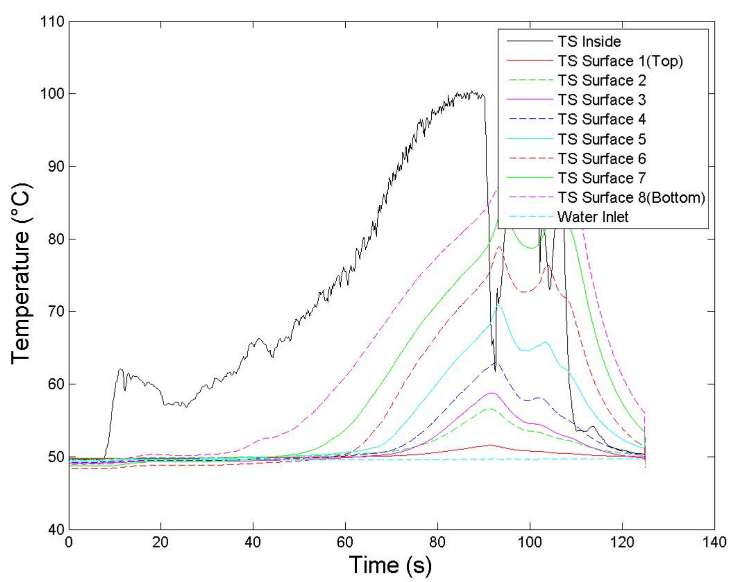

Fig. D.129.: Test section temperatures for test 33.

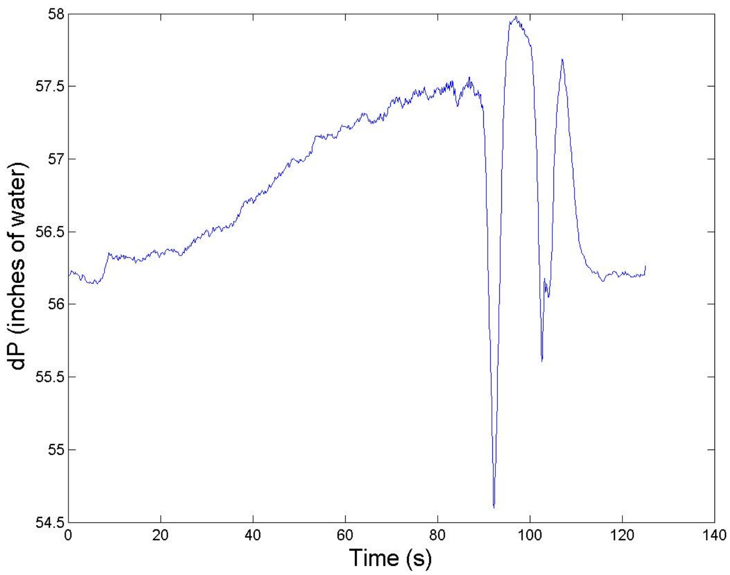

Fig. D.130.: Test section differential pressure for test 33.

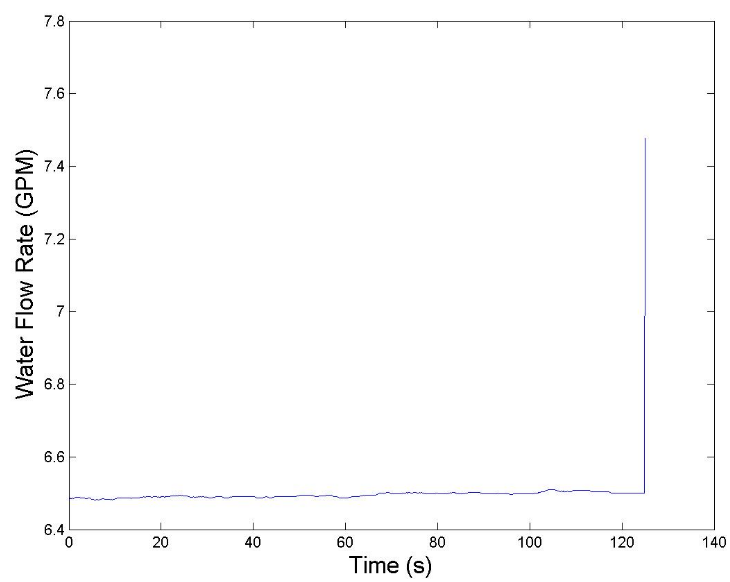

Fig. D.131.: Water flow rate for test 33.

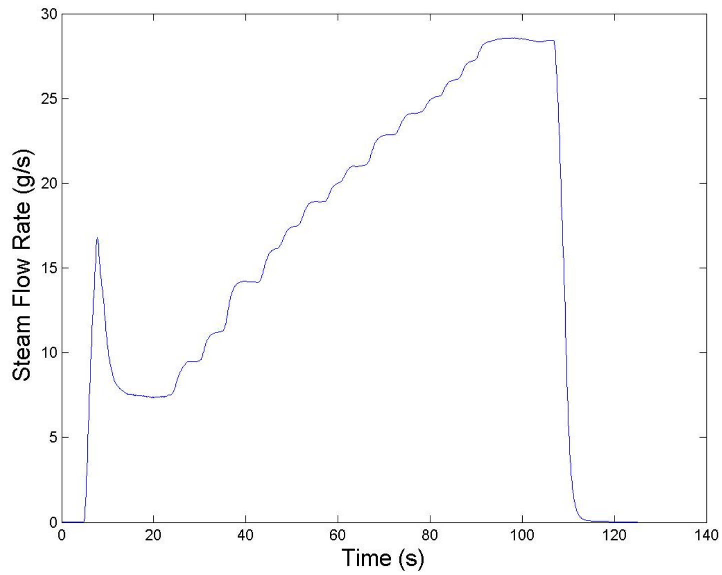

Fig. D.132.: Steam flow rate for test 33.

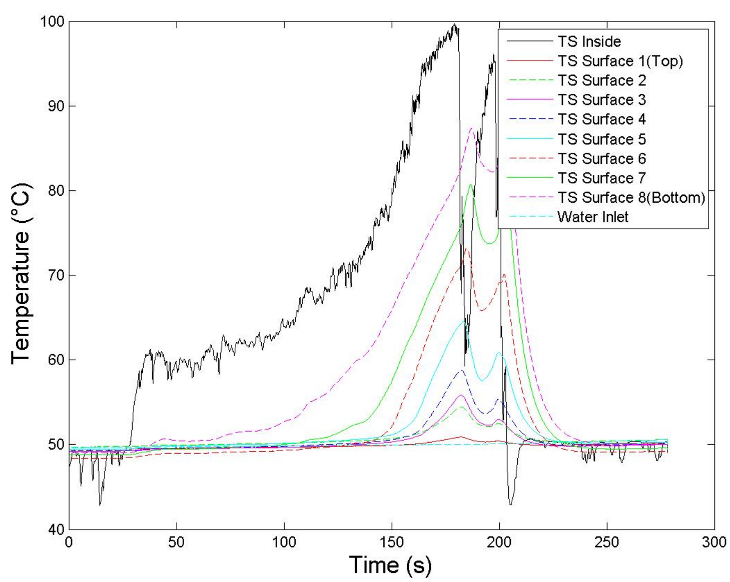

Fig. D.133.: Test section temperatures for test 34.

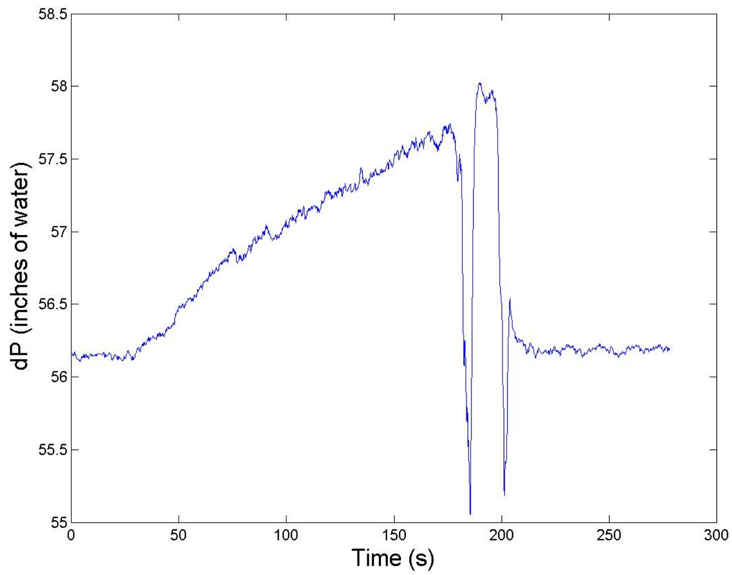

Fig. D.134.: Test section differential pressure for test 34.

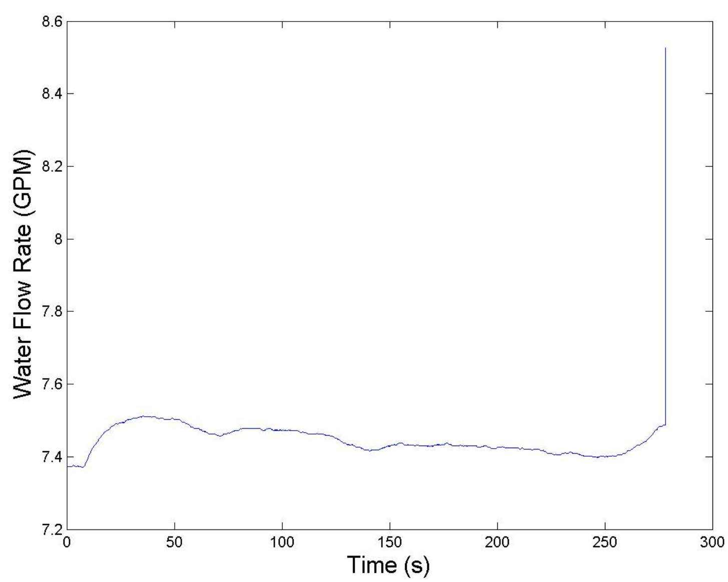

Fig. D.135.: Water flow rate for test 34.

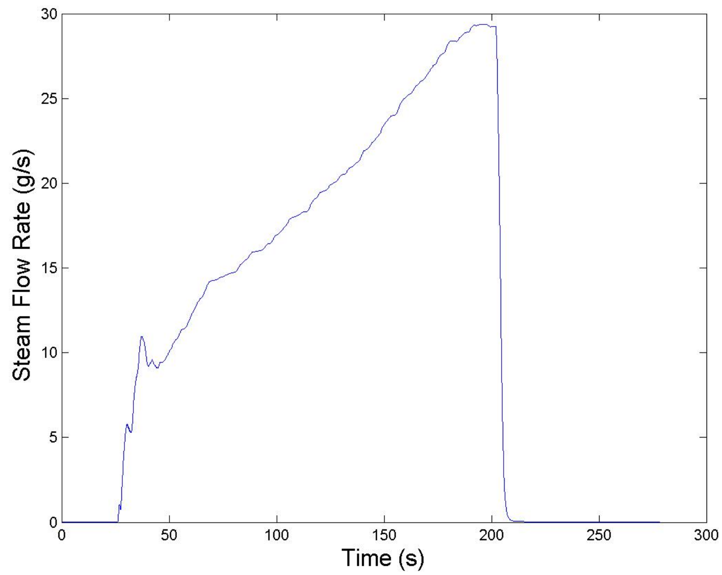

Fig. D.136.: Steam flow rate for test 34.

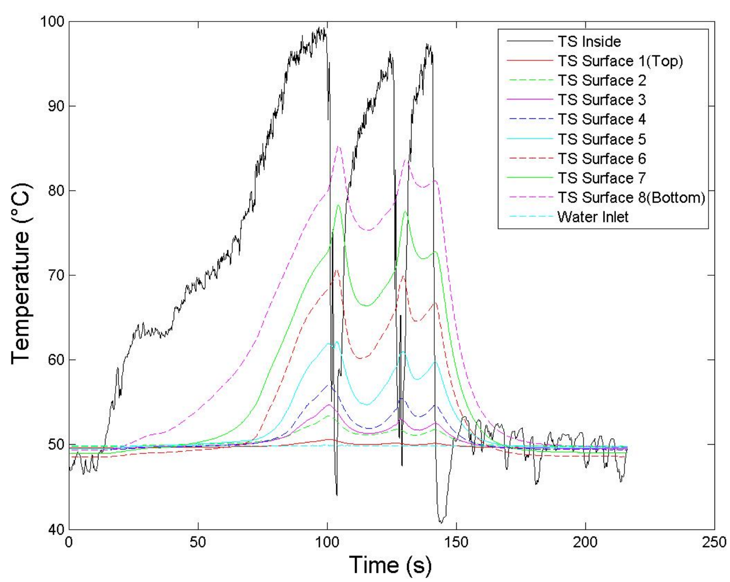

Fig. D.137.: Test section temperatures for test 35.

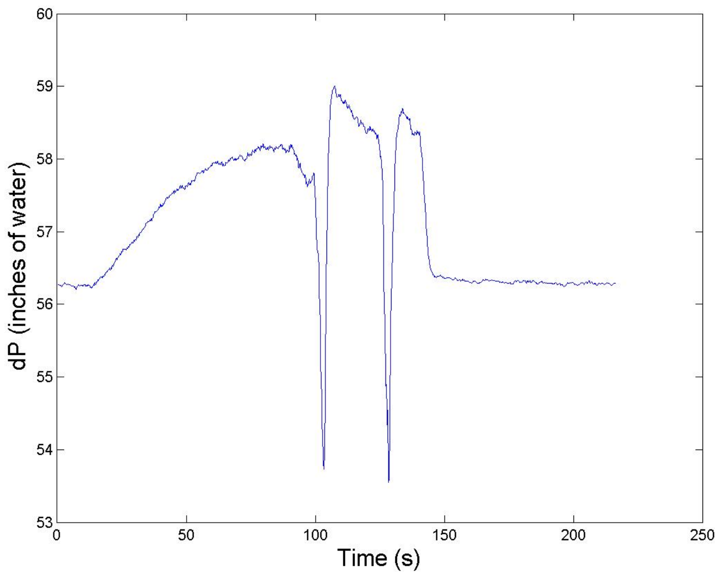

Fig. D.138.: Test section differential pressure for test 35.

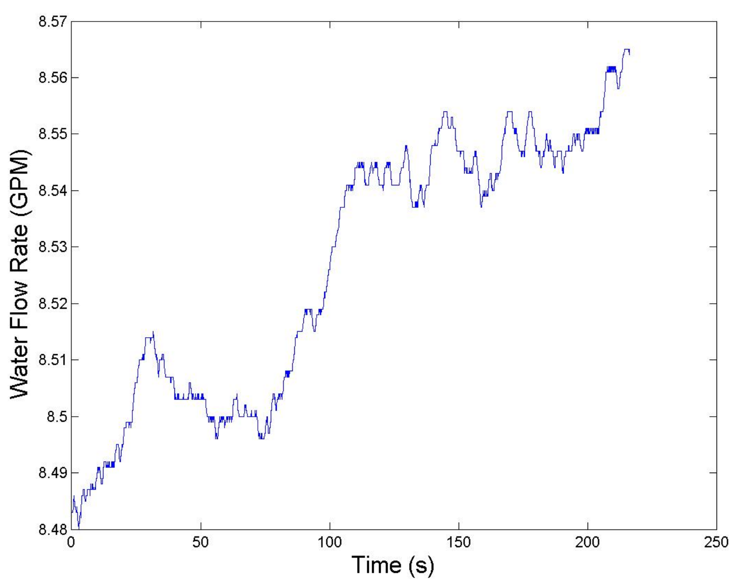

Fig. D.139.: Water flow rate for test 35.

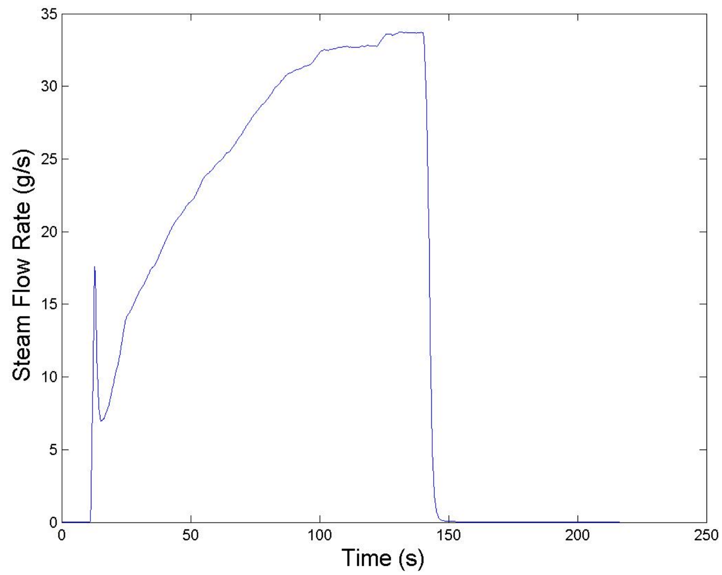

Fig. D.140.: Steam flow rate for test 35.

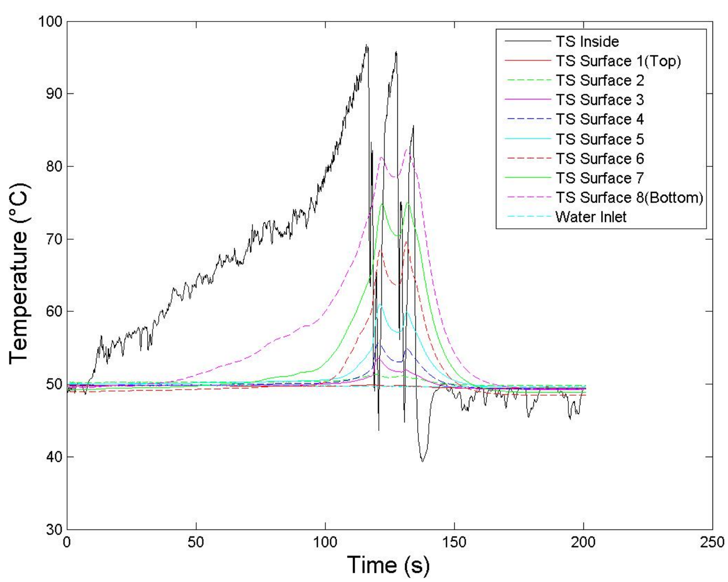

Fig. D.141.: Test section temperatures for test 36.

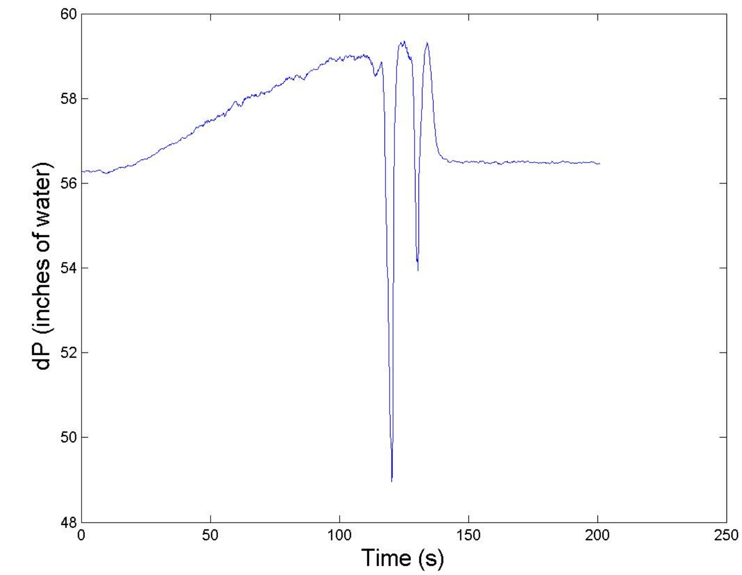

Fig. D.142.: Test section differential pressure for test 36.

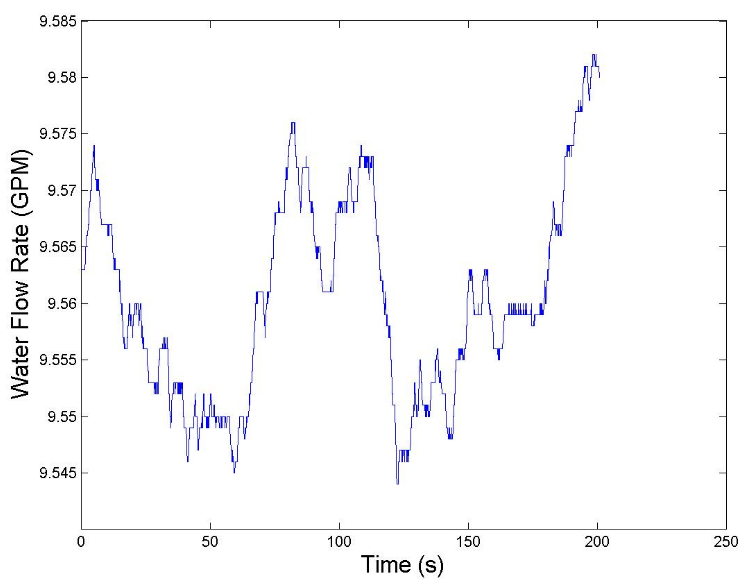

Fig. D.143.: Water flow rate for test 36.

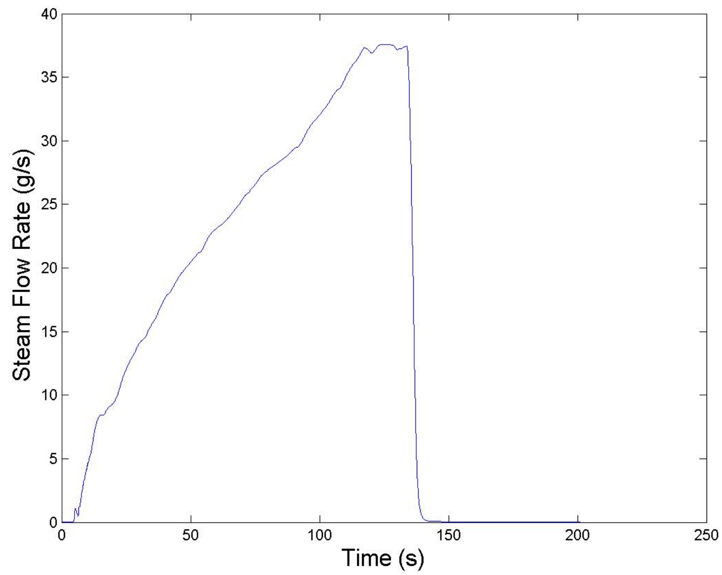

Fig. D.144.: Steam flow rate for test 36.

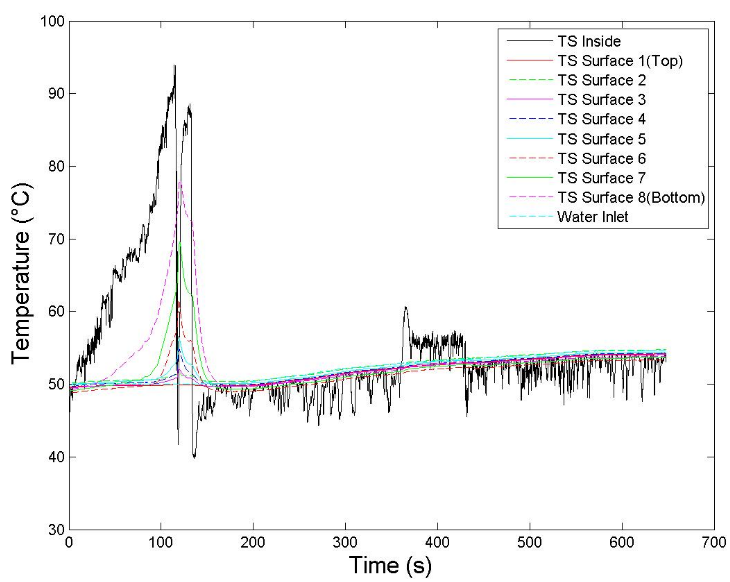

Fig. D.145.: Test section temperatures for test 37.

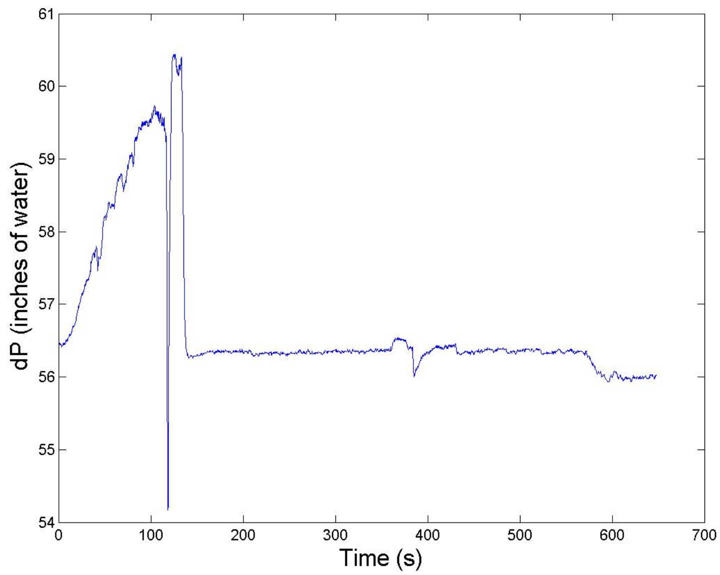

Fig. D.146.: Test section differential pressure for test 37.

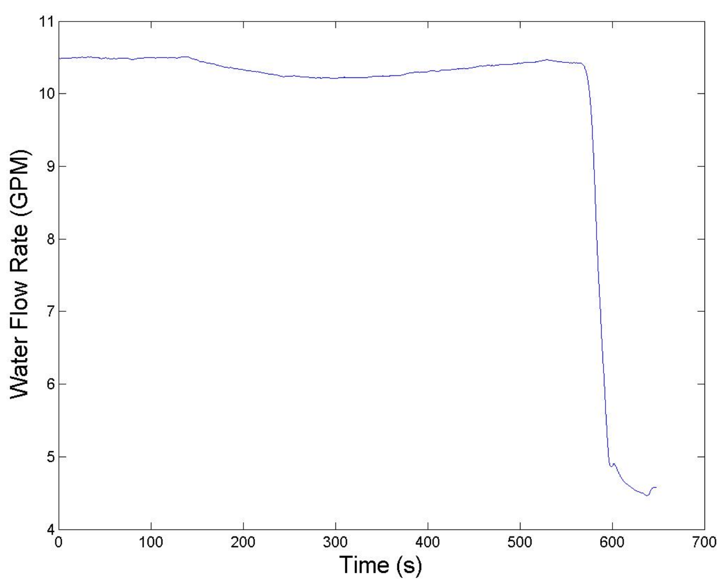

Fig. D.147.: Water flow rate for test 37.

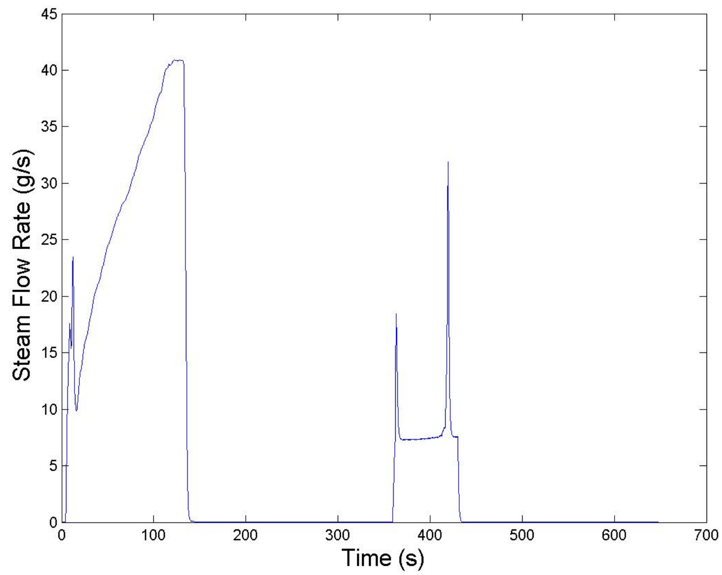

Fig. D.148.: Steam flow rate for test 37.

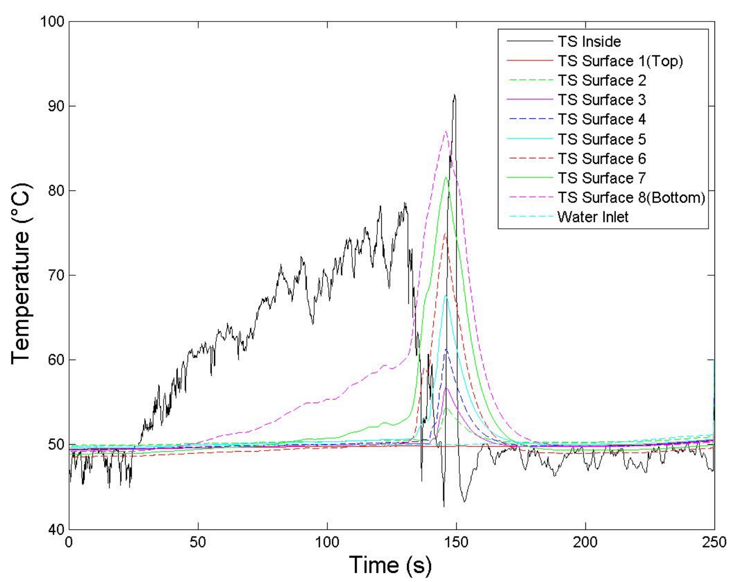

Fig. D.149.: Test section temperatures for test 38.

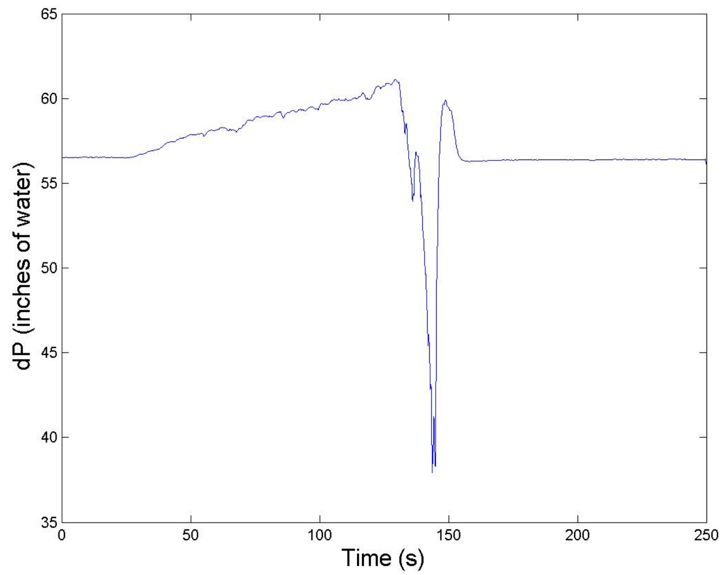

Fig. D.150.: Test section differential pressure for test 38.

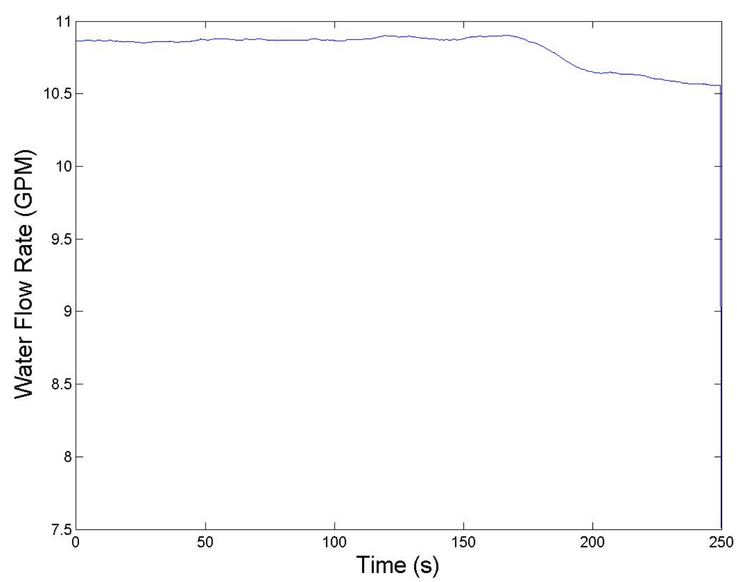

Fig. D.151.: Water flow rate for test 38.

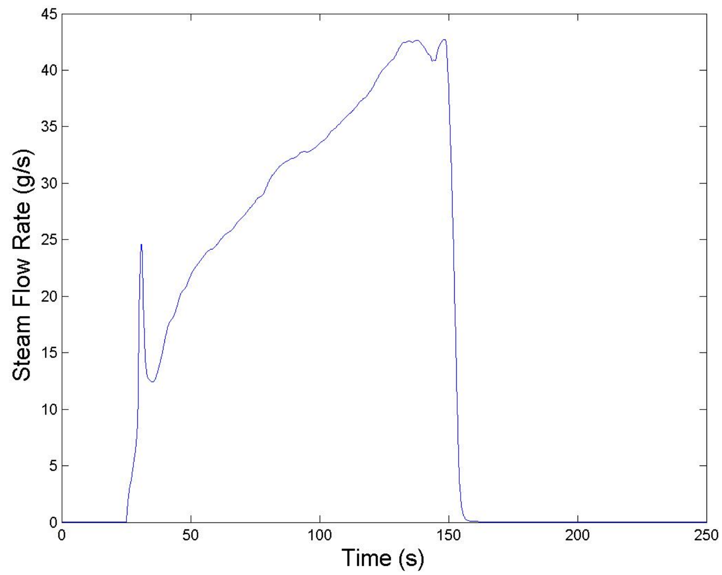

Fig. D.152.: Steam flow rate for test 38.

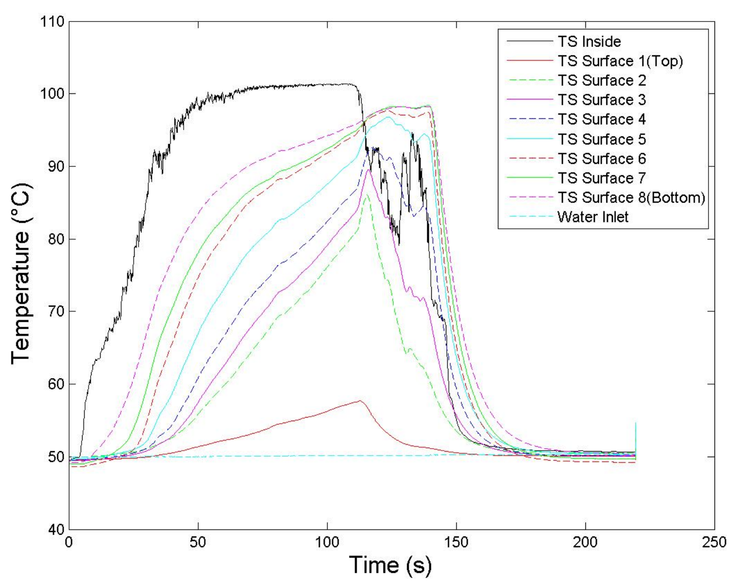

Fig. D.153.: Test section temperatures for test 39.

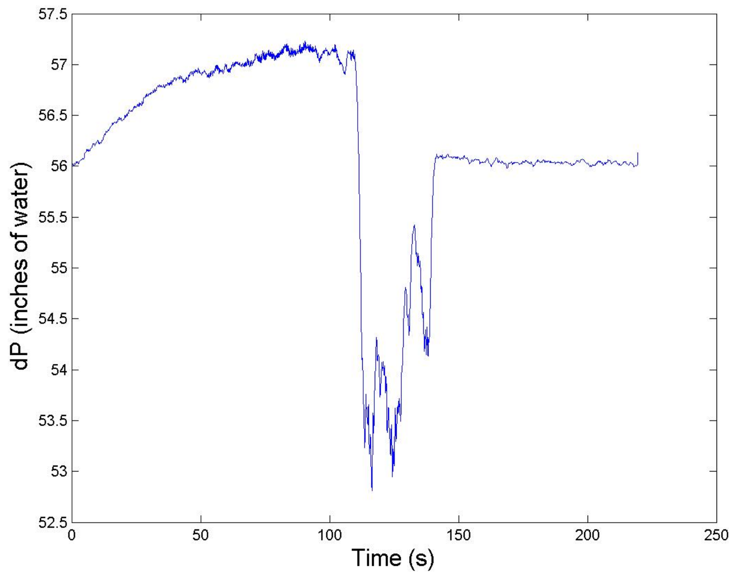

Fig. D.154.: Test section differential pressure for test 39.

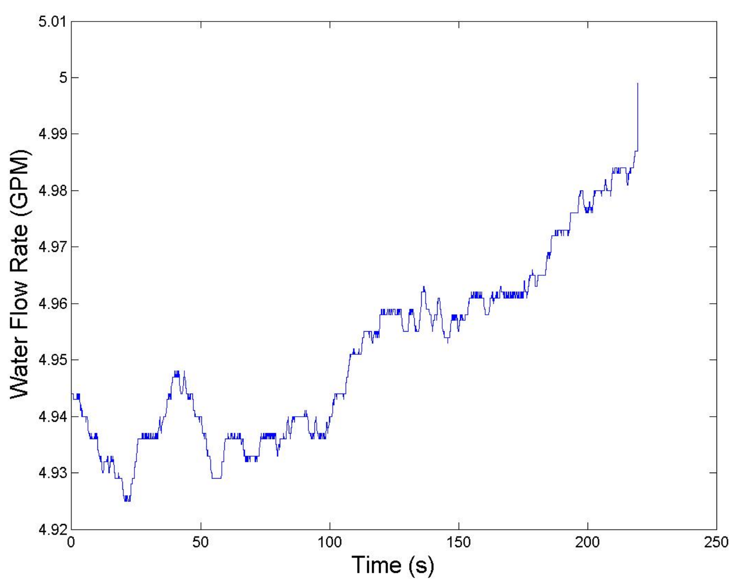

Fig. D.155.: Water flow rate for test 39.

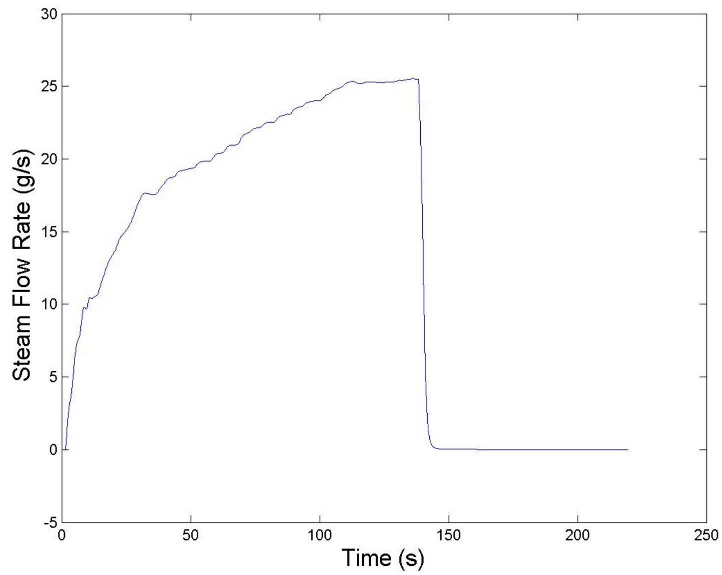

Fig. D.156.: Steam flow rate for test 39.

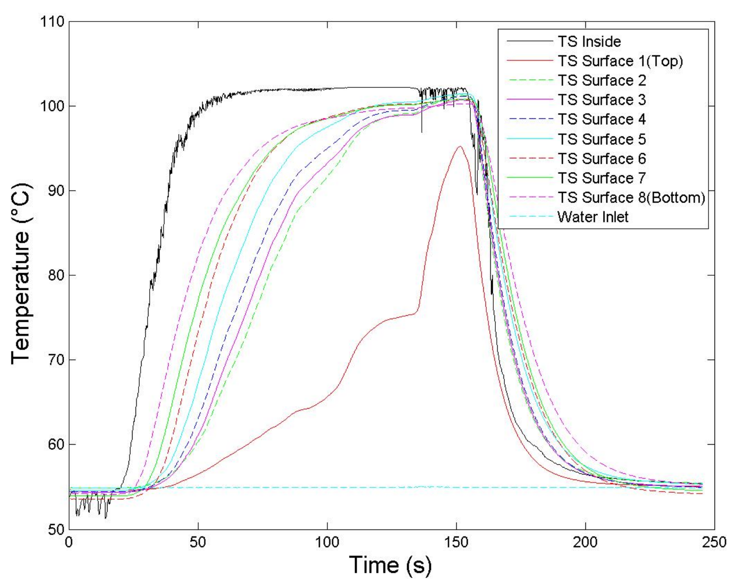

Fig. D.157.: Test section temperatures for test 40.

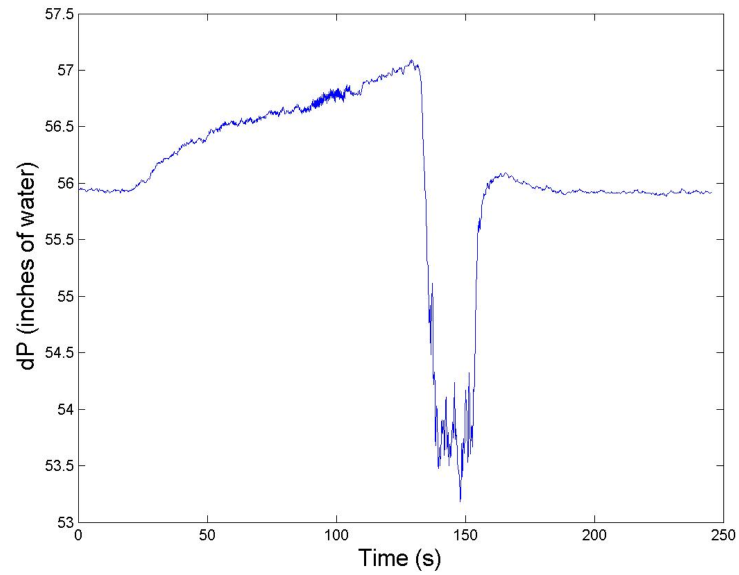

Fig. D.158.: Test section differential pressure for test 40.

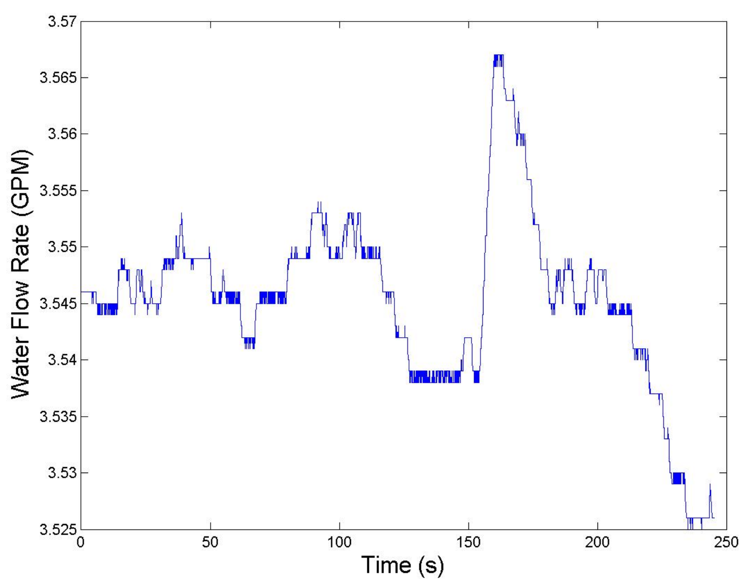

Fig. D.159.: Water flow rate for test 40.

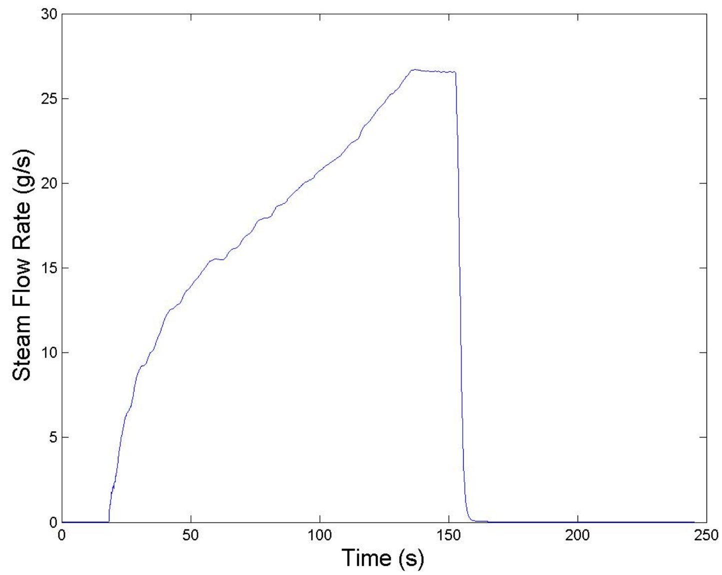

Fig. D.160.: Steam flow rate for test 40.

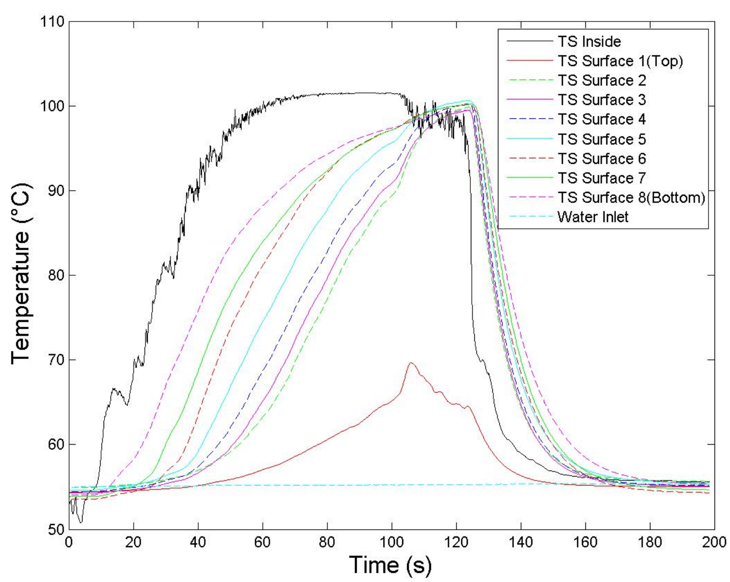

Fig. D.161.: Test section temperatures for test 41.

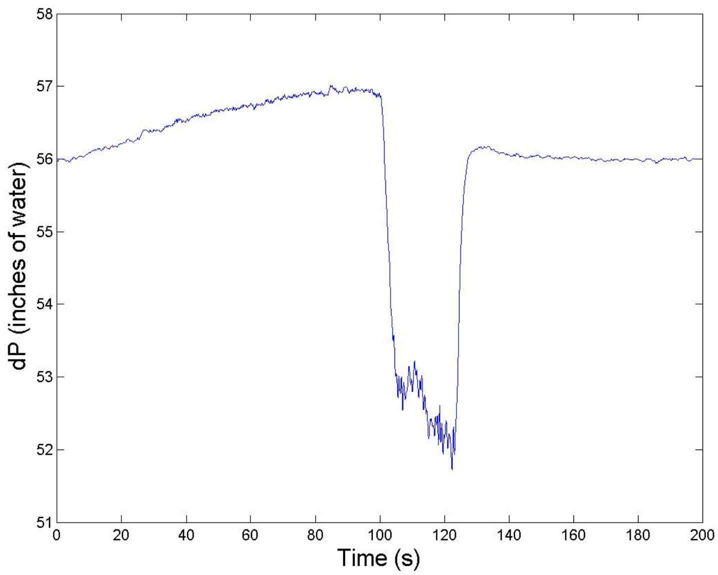

Fig. D.162.: Test section differential pressure for test 41.

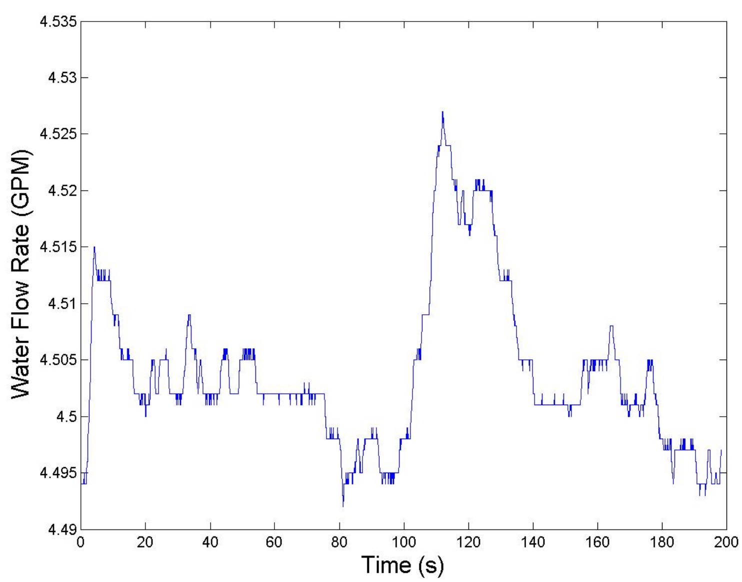

Fig. D.163.: Water flow rate for test 41.

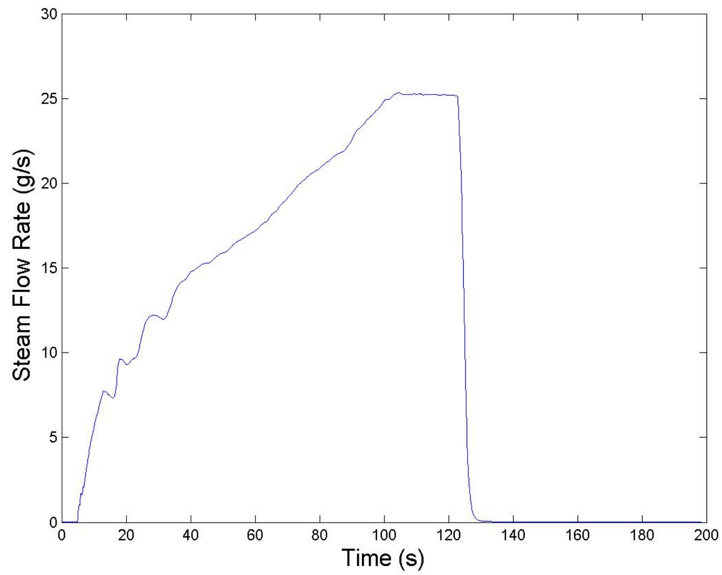

Fig. D.164.: Steam flow rate for test 41.

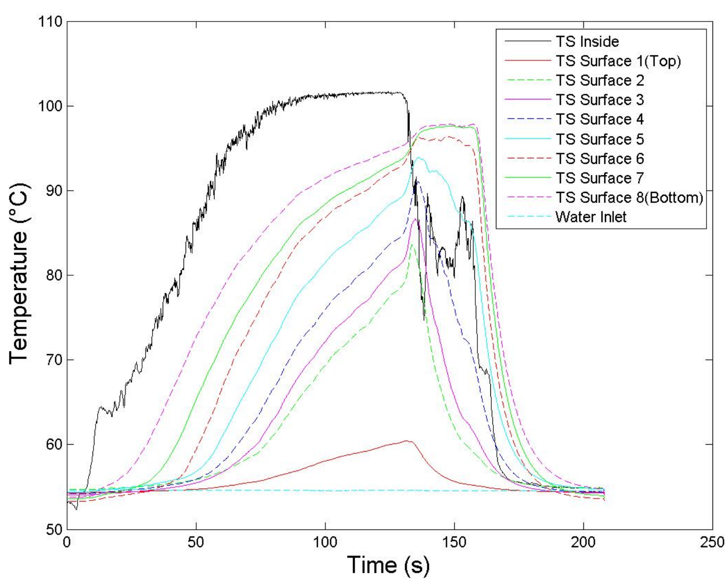

Fig. D.165.: Test section temperatures for test 42.

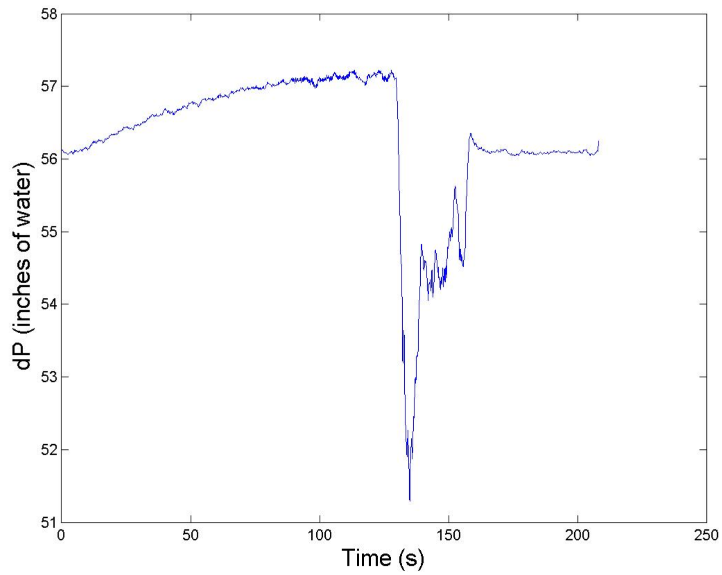

Fig. D.166.: Test section differential pressure for test 42.

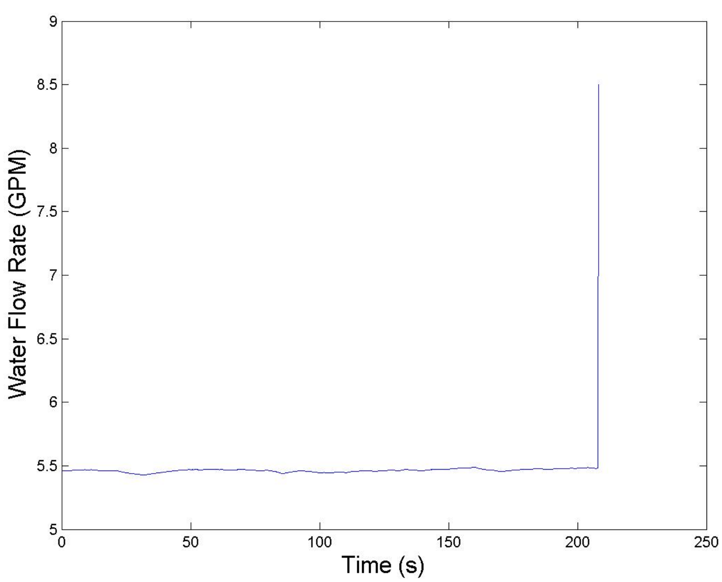

Fig. D.167.: Water flow rate for test 42.

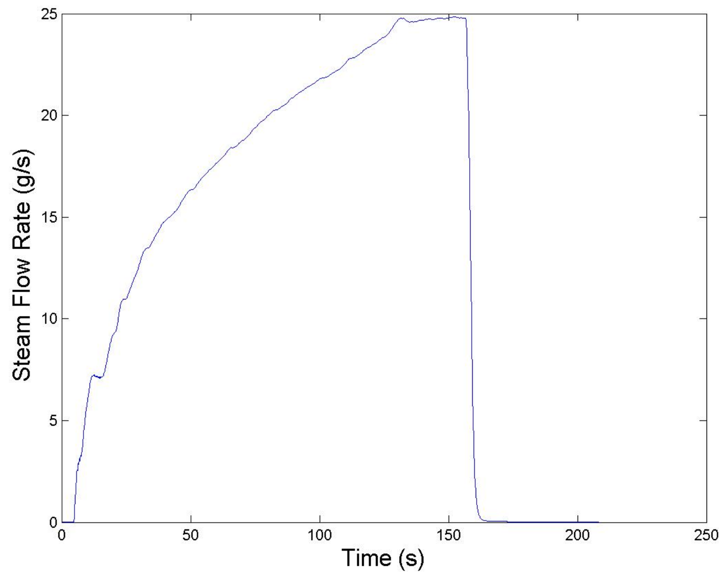

Fig. D.168.: Steam flow rate for test 42.

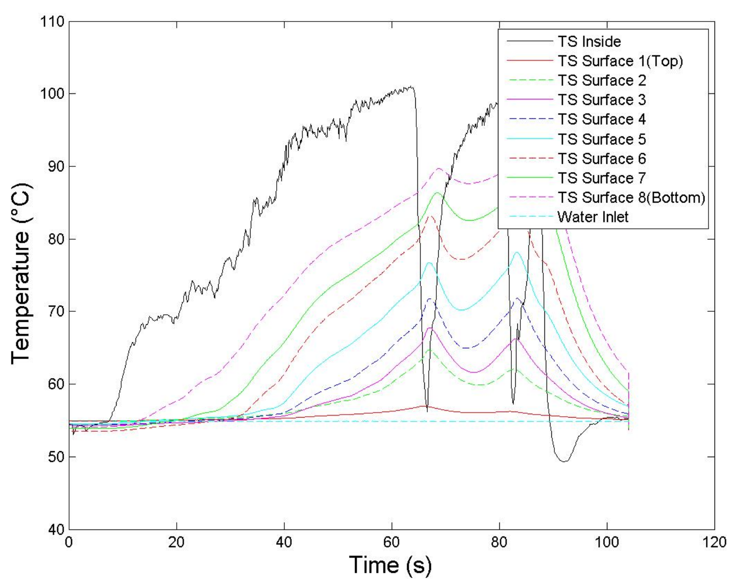

Fig. D.169.: Test section temperatures for test 43.

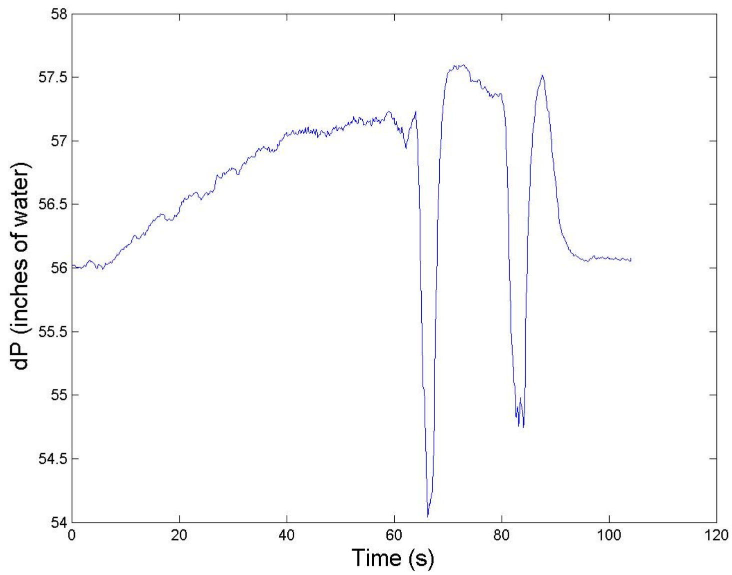

Fig. D.170.: Test section differential pressure for test 43.

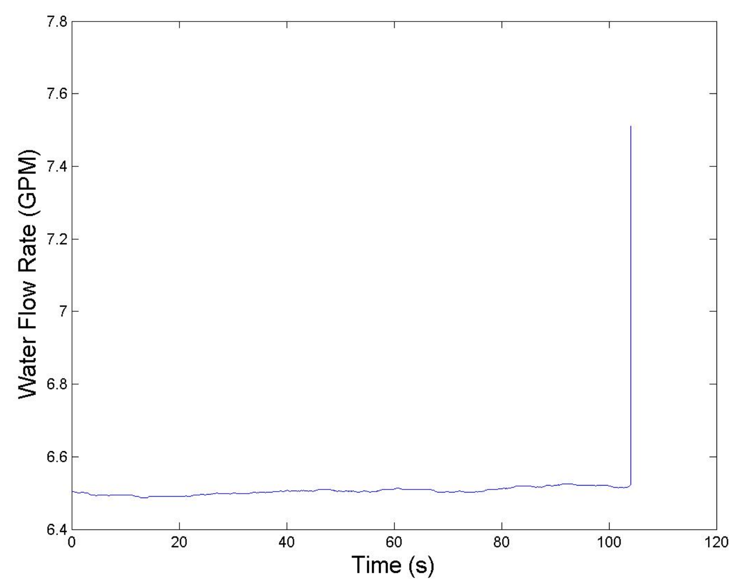

Fig. D.171.: Water flow rate for test 43.

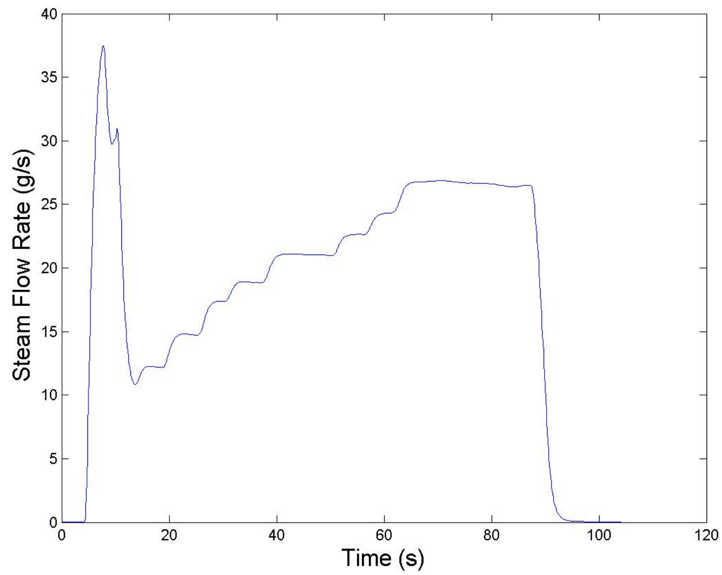

Fig. D.172.: Steam flow rate for test 43.

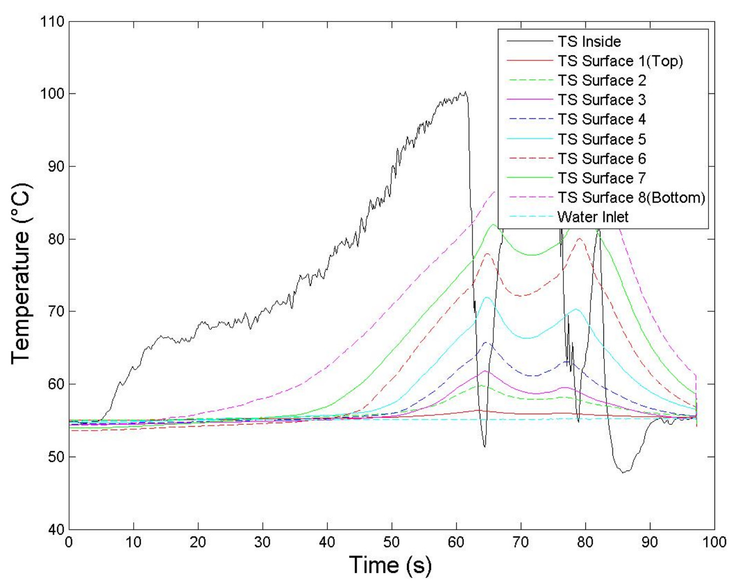

Fig. D.173.: Test section temperatures for test 44.

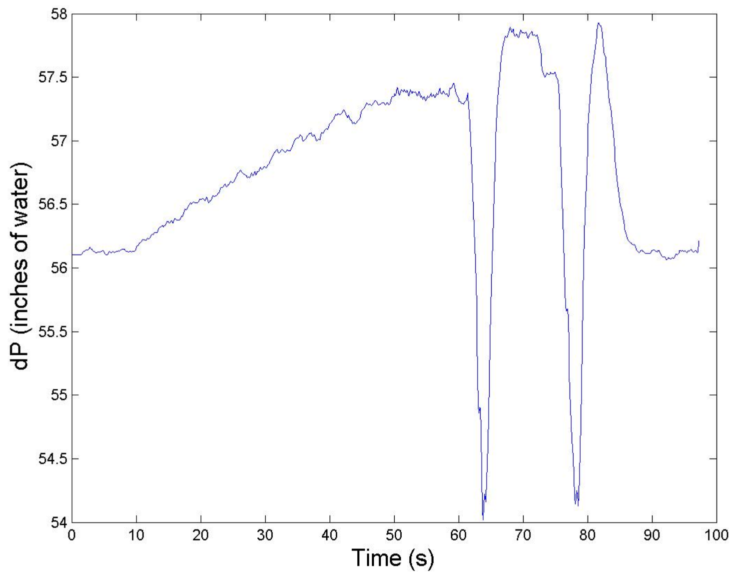

Fig. D.174.: Test section differential pressure for test 44.

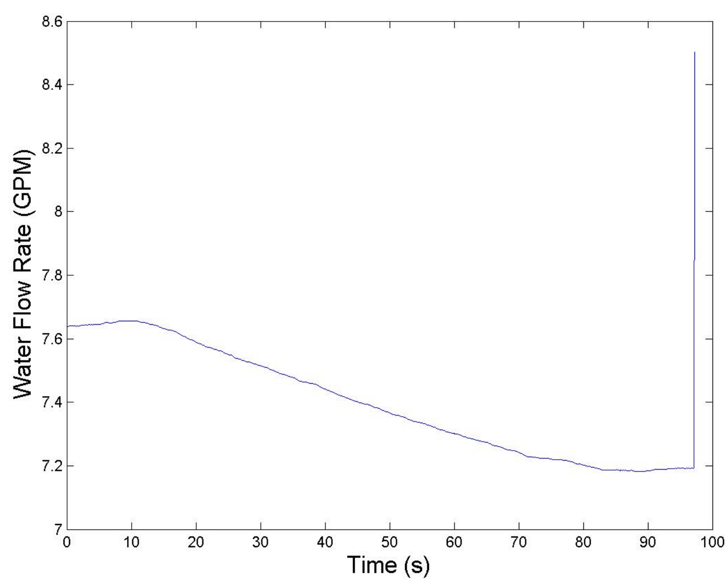

Fig. D.175.: Water flow rate for test 44.

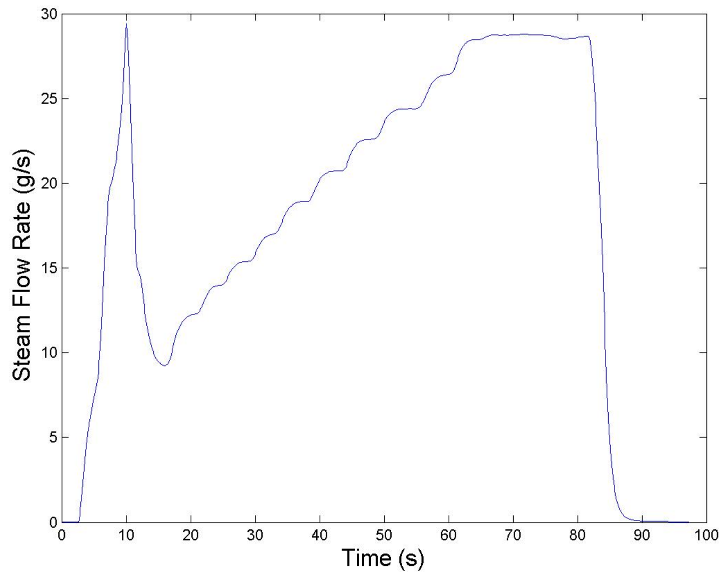

Fig. D.176.: Steam flow rate for test 44.

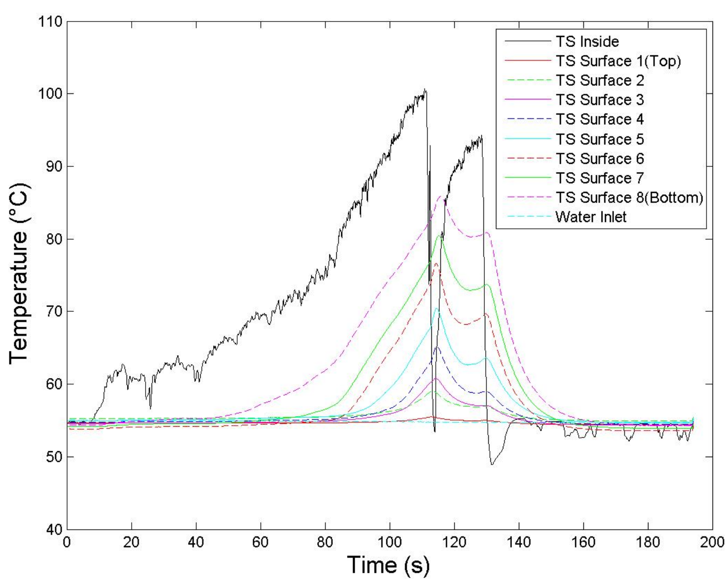

Fig. D.177.: Test section temperatures for test 45.

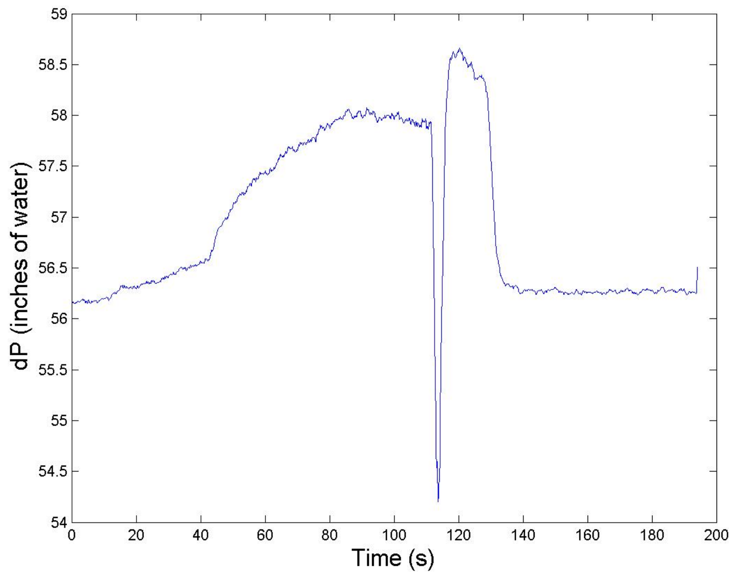

Fig. D.178.: Test section differential pressure for test 45.

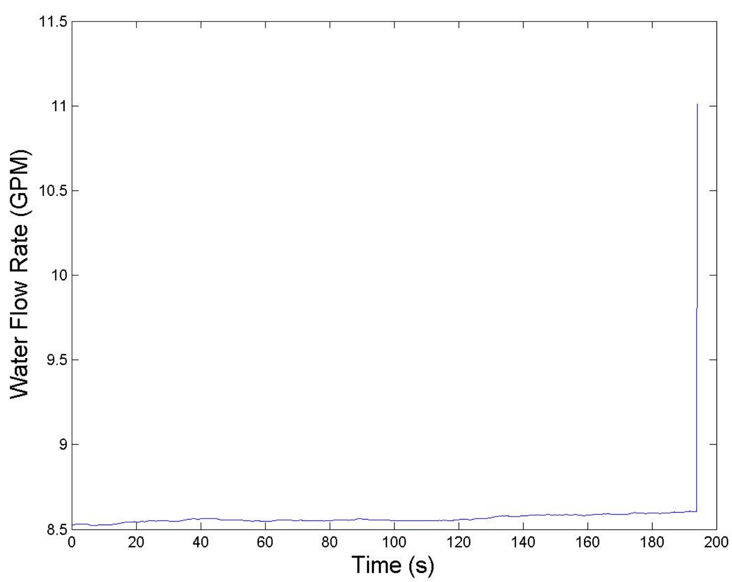

Fig. D.179.: Water flow rate for test 45.

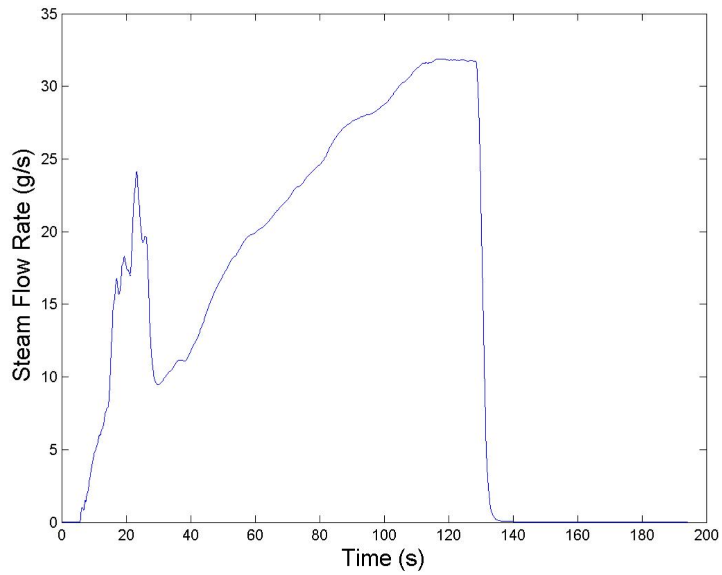

Fig. D.180.: Steam flow rate for test 45.

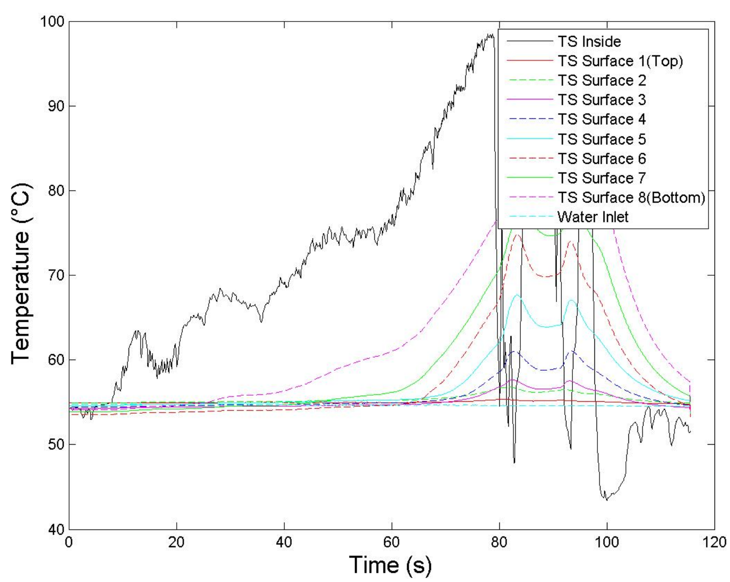

Fig. D.181.: Test section temperatures for test 46.

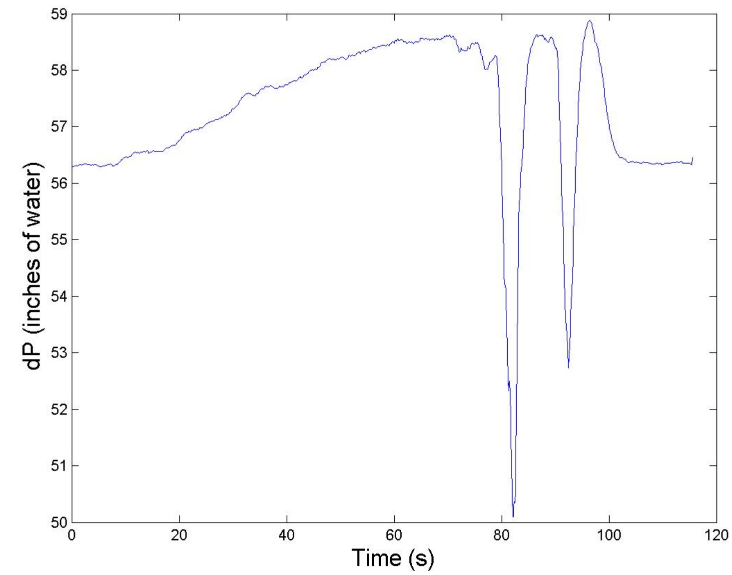

Fig. D.182.: Test section differential pressure for test 46.

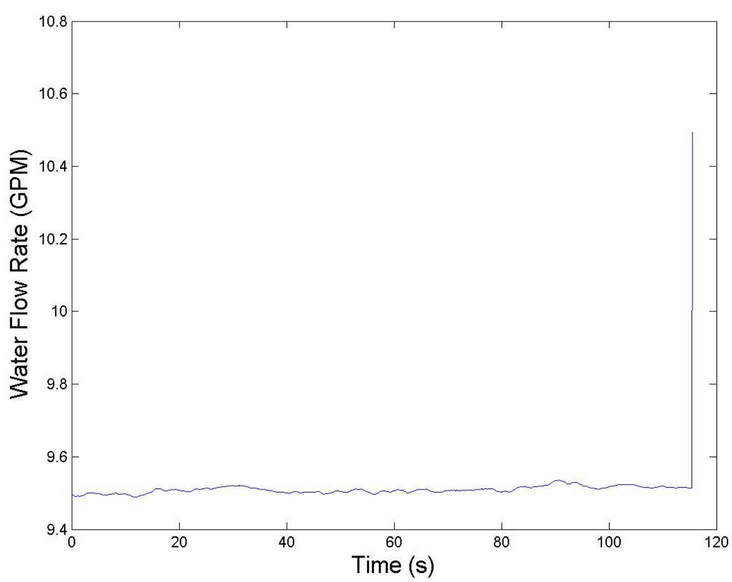

Fig. D.183.: Water flow rate for test 46.

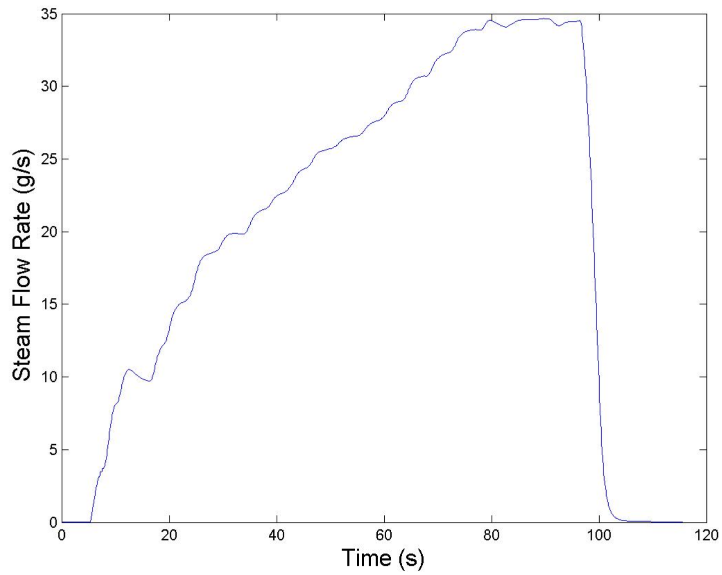

Fig. D.184.: Steam flow rate for test 46.

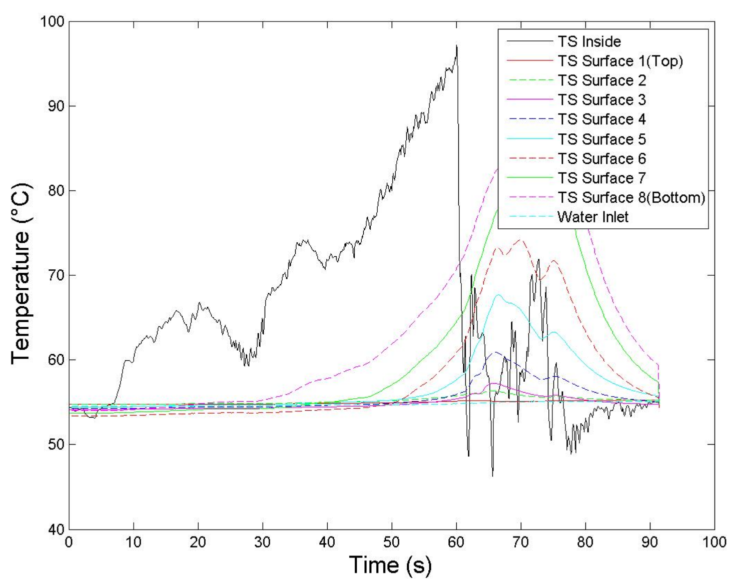

Fig. D.185.: Test section temperatures for test 47.

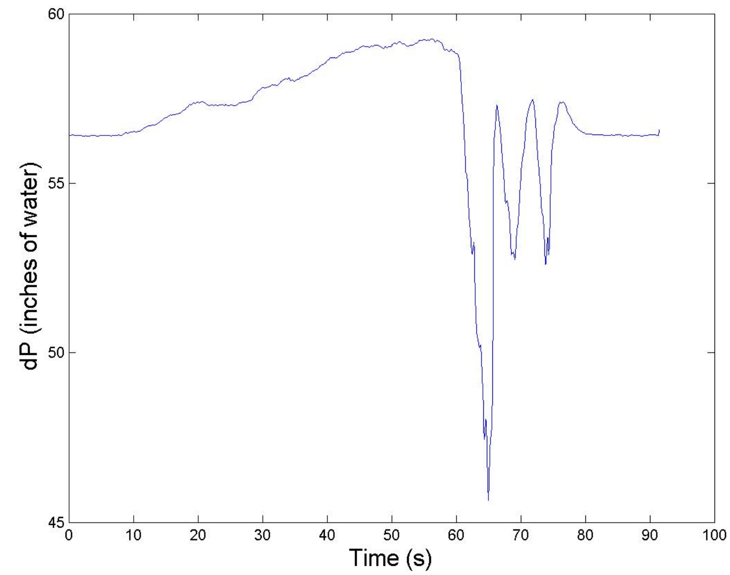

Fig. D.186.: Test section differential pressure for test 47.

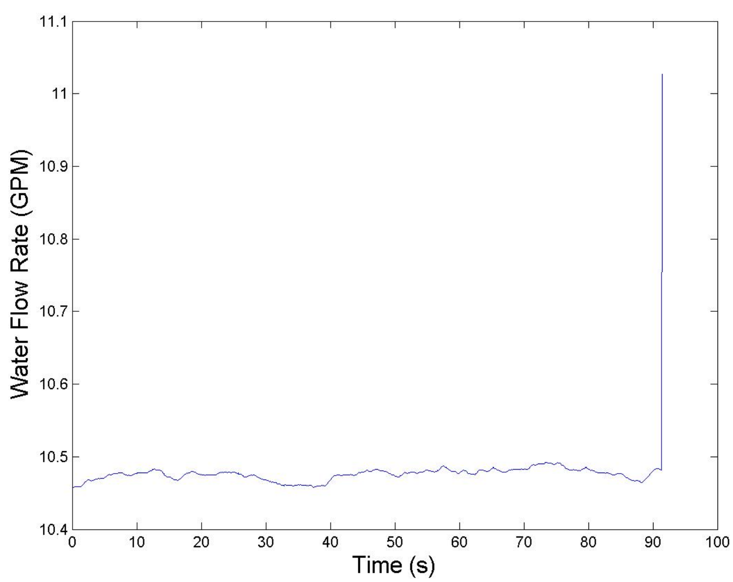

Fig. D.187.: Water flow rate for test 47.

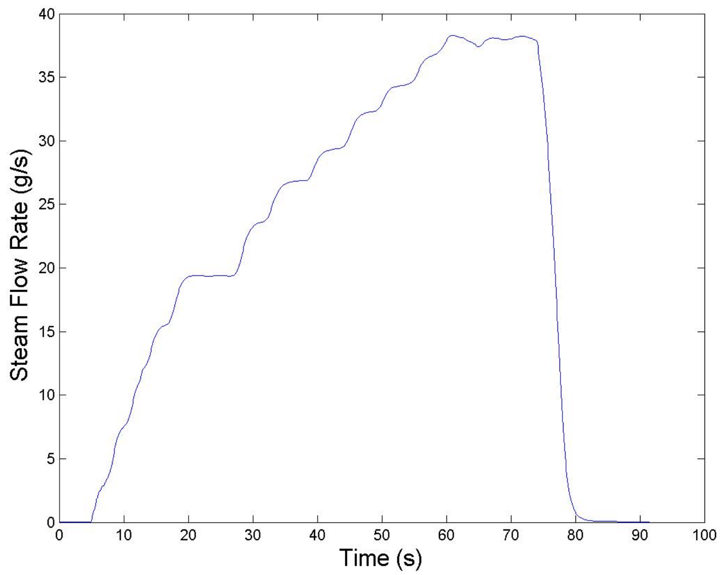

Fig. D.188.: Steam flow rate for test 47.

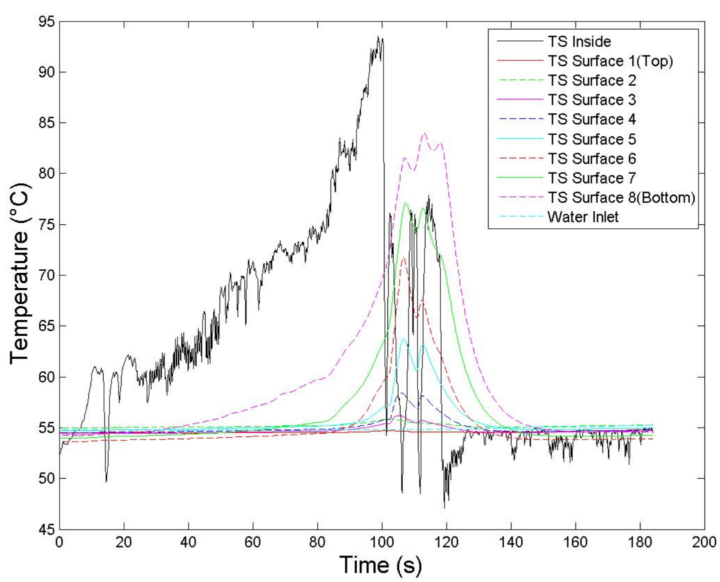

Fig. D.189.: Test section temperatures for test 48.

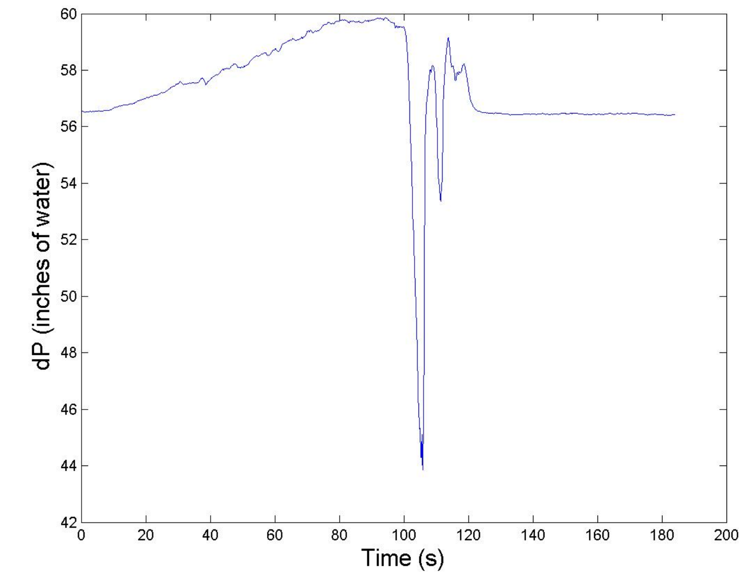

Fig. D.190.: Test section differential pressure for test 48.

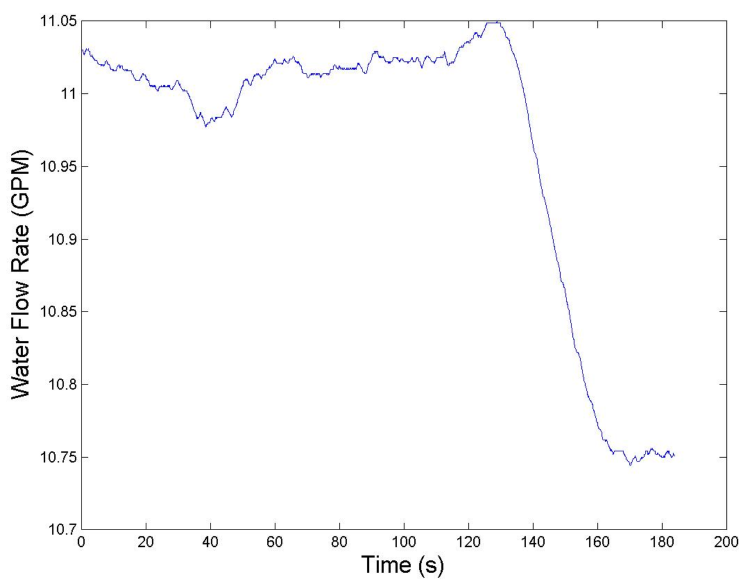

Fig. D.191.: Water flow rate for test 48.

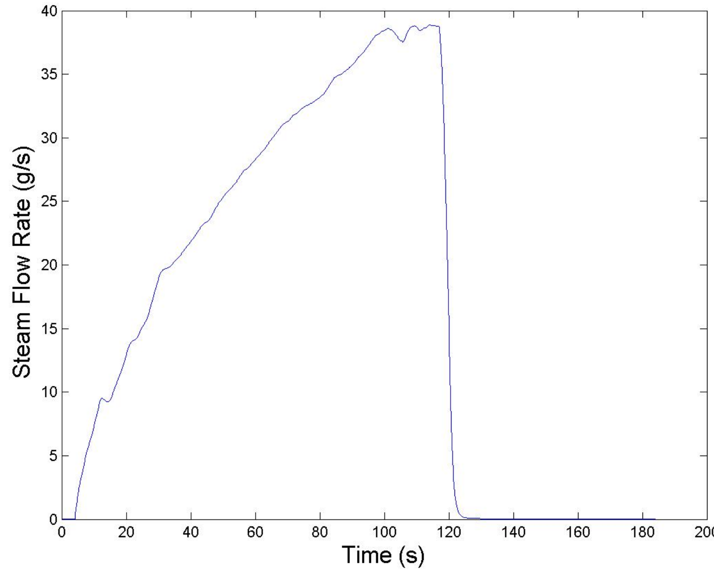

Fig. D.192.: Steam flow rate for test 48.

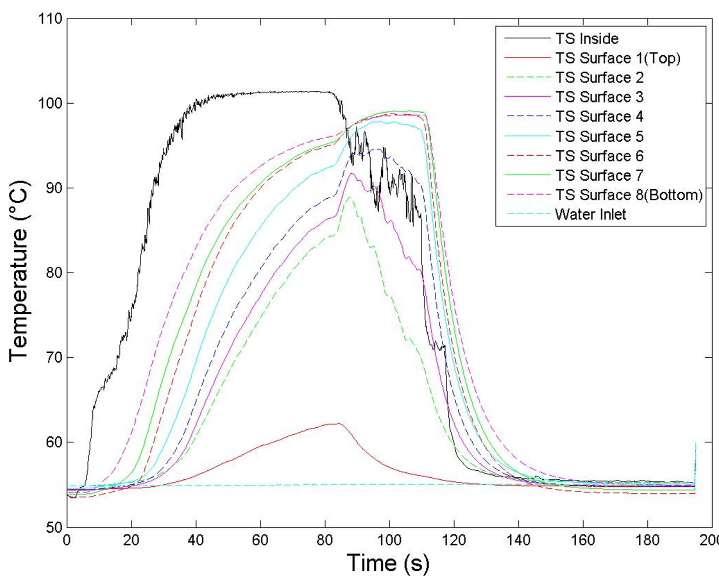

Fig. D.193.: Test section temperatures for test 49.

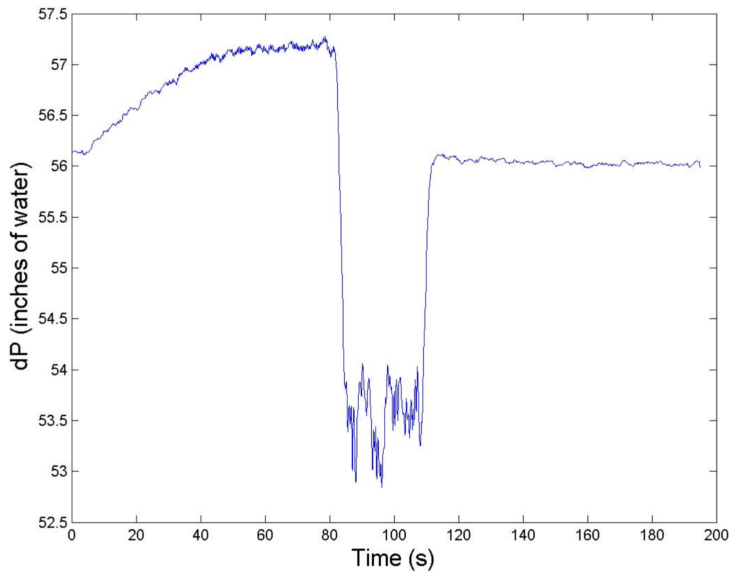

Fig. D.194.: Test section differential pressure for test 49.

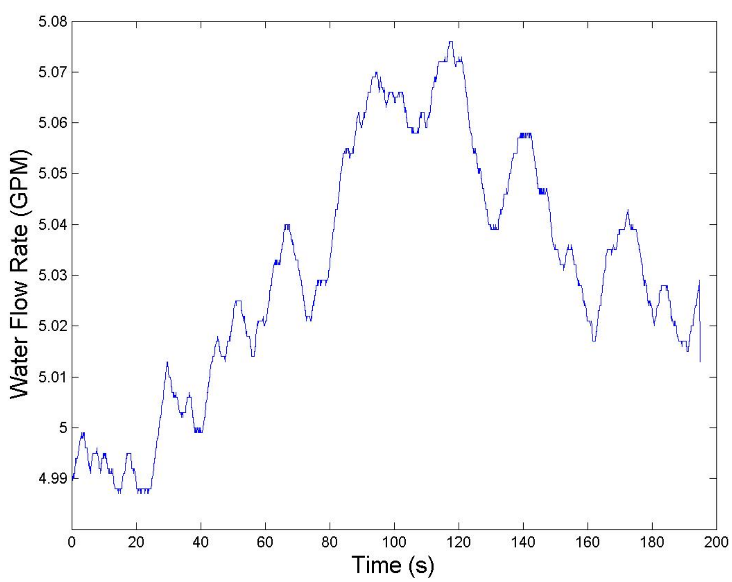

Fig. D.195.: Water flow rate for test 49.

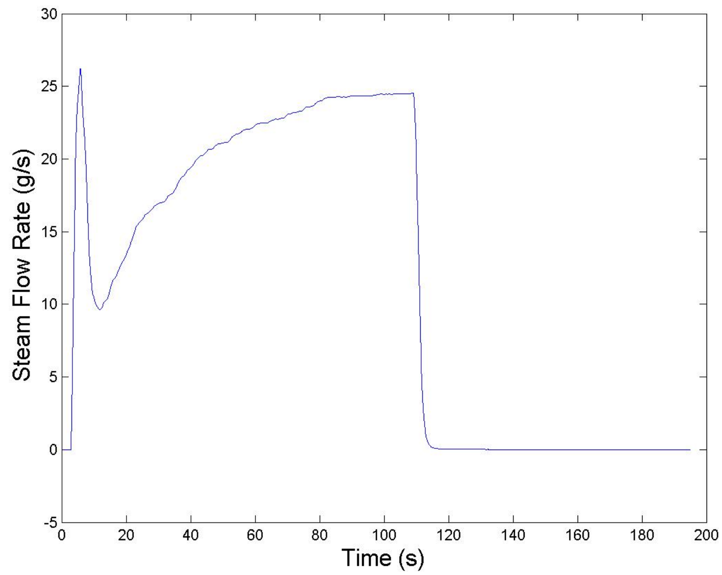

Fig. D.196.: Steam flow rate for test 49.

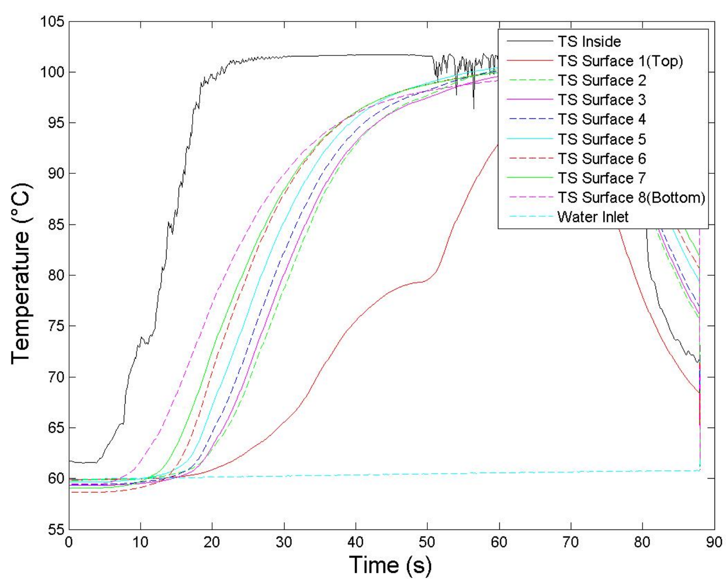

Fig. D.197.: Test section temperatures for test 50.

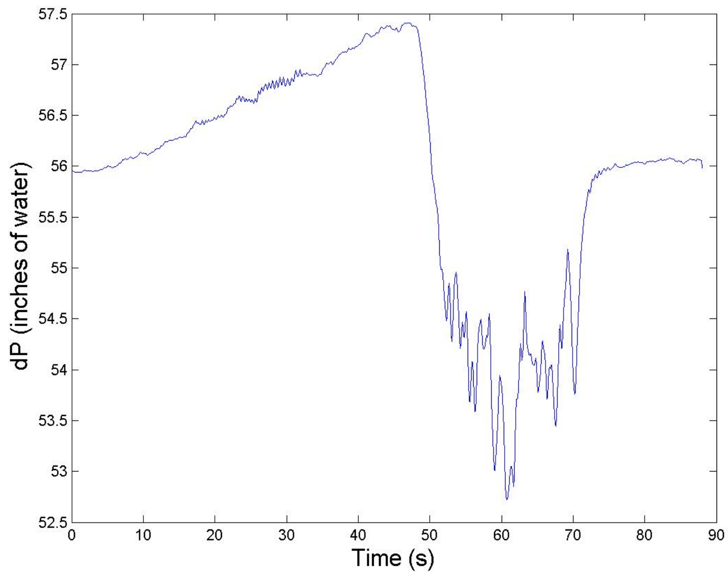

Fig. D.198.: Test section differential pressure for test 50.

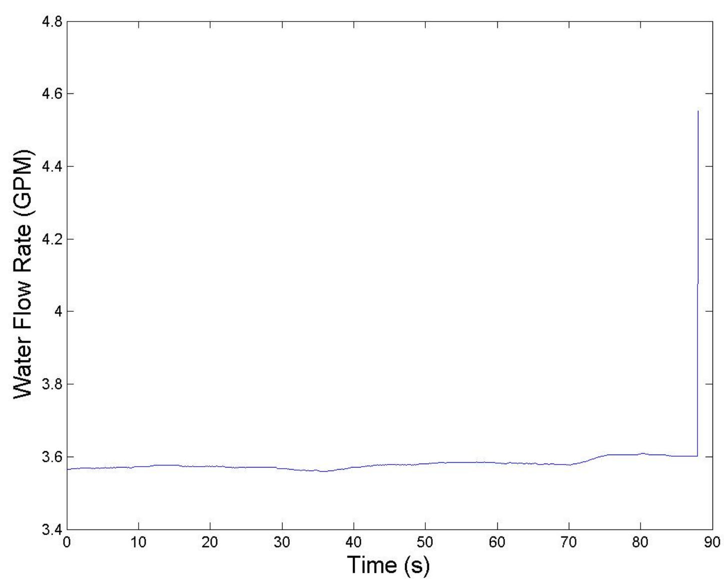

Fig. D.199.: Water flow rate for test 50.

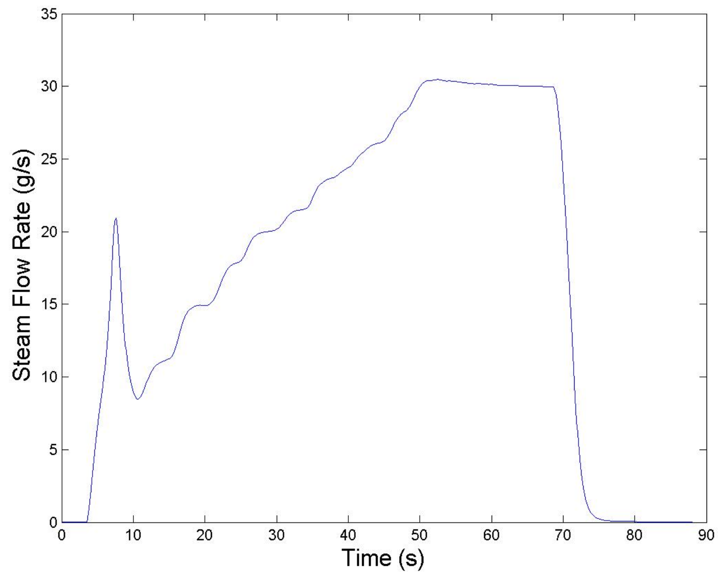

Fig. D.200.: Steam flow rate for test 50.

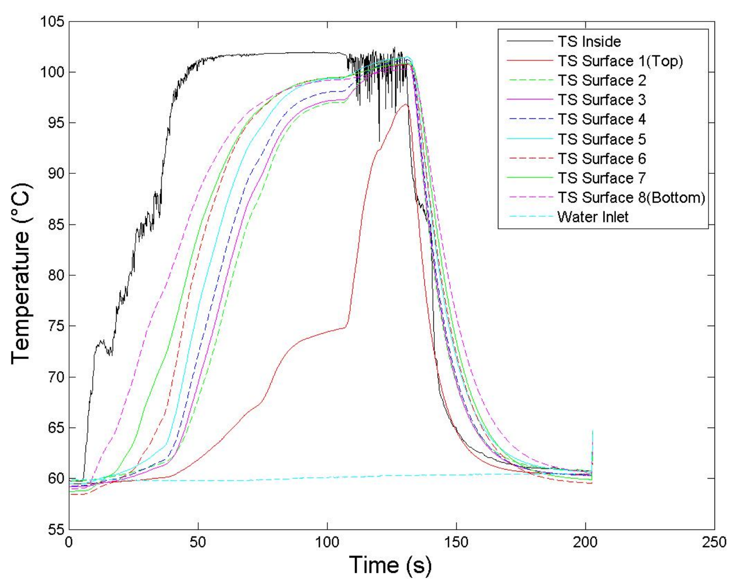

Fig. D.201.: Test section temperatures for test 51.

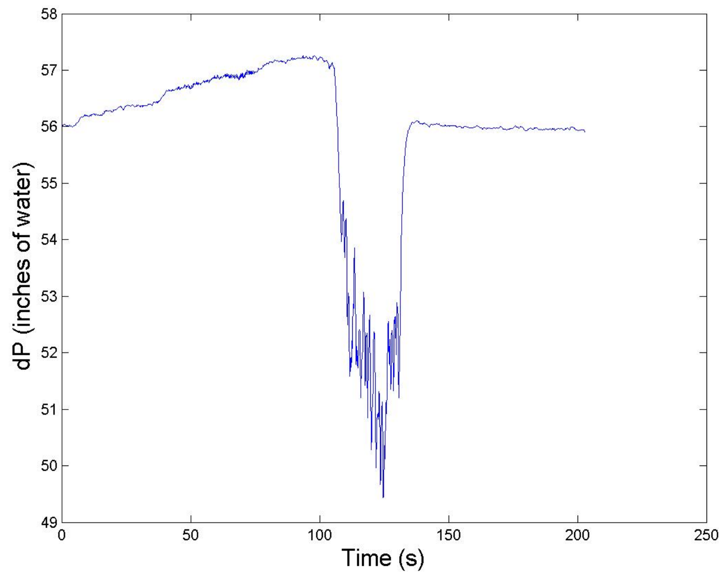

Fig. D.202.: Test section differential pressure for test 51.

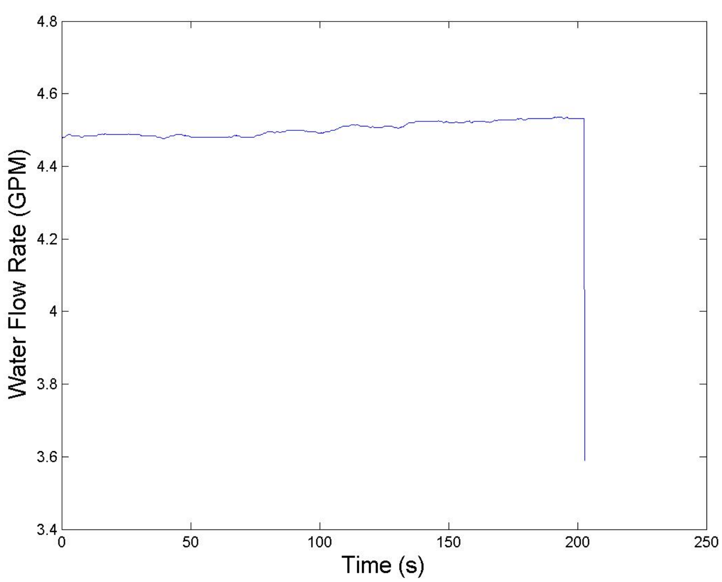

Fig. D.203.: Water flow rate for test 51.

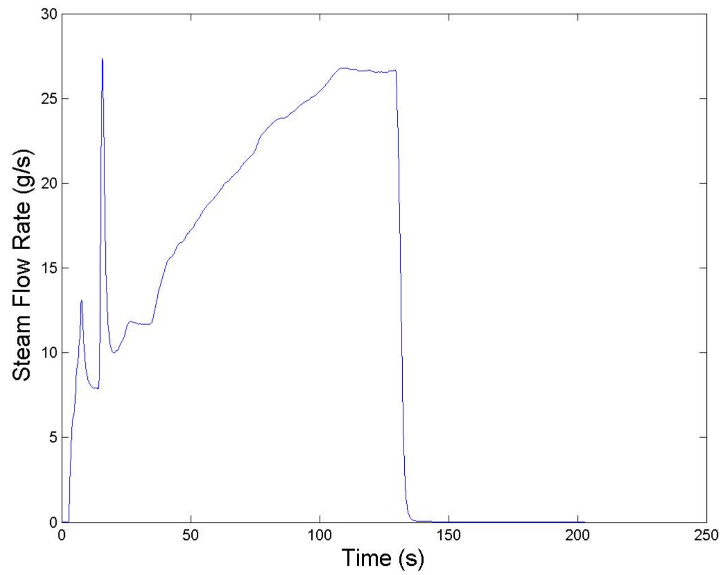

Fig. D.204.: Steam flow rate for test 51.

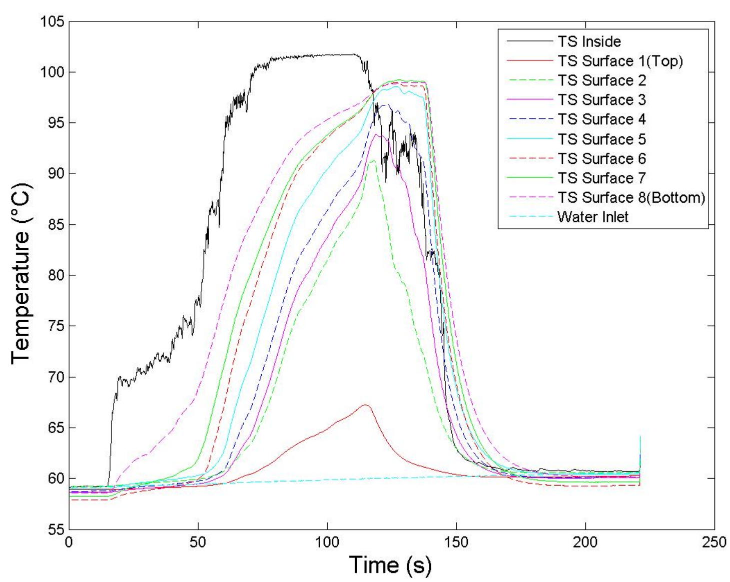

Fig. D.205.: Test section temperatures for test 52.

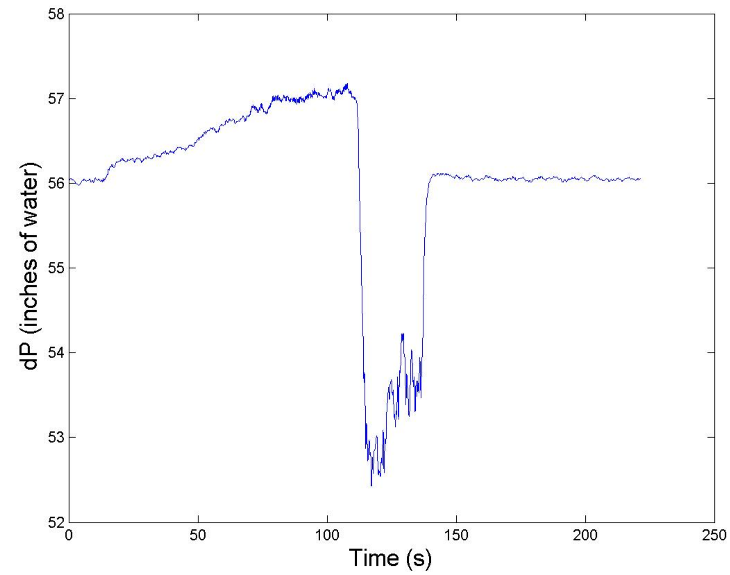

Fig. D.206.: Test section differential pressure for test 52.

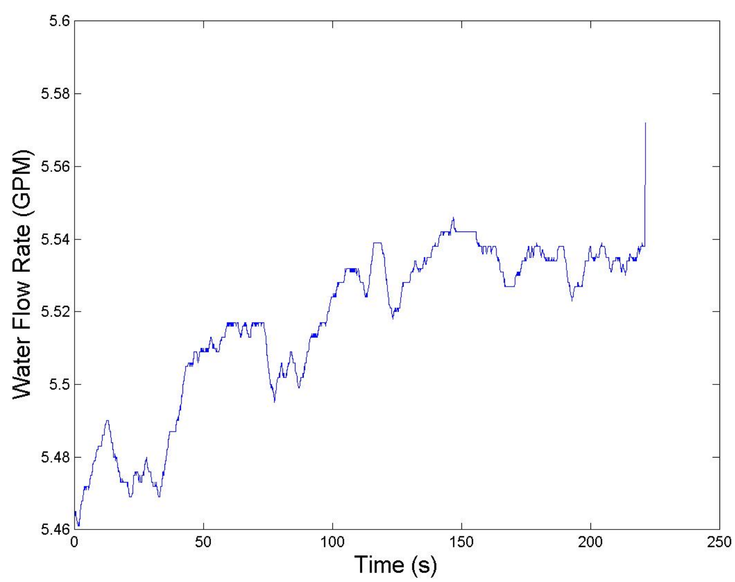

Fig. D.207.: Water flow rate for test 52.

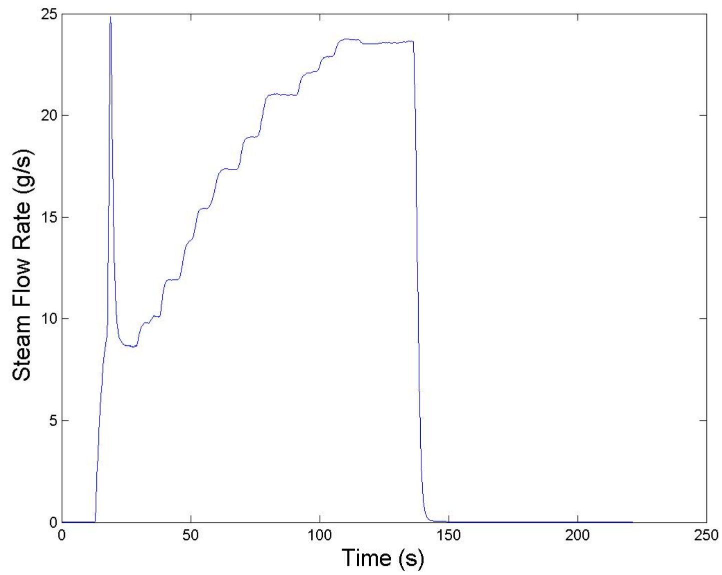

Fig. D.208.: Steam flow rate for test 52.

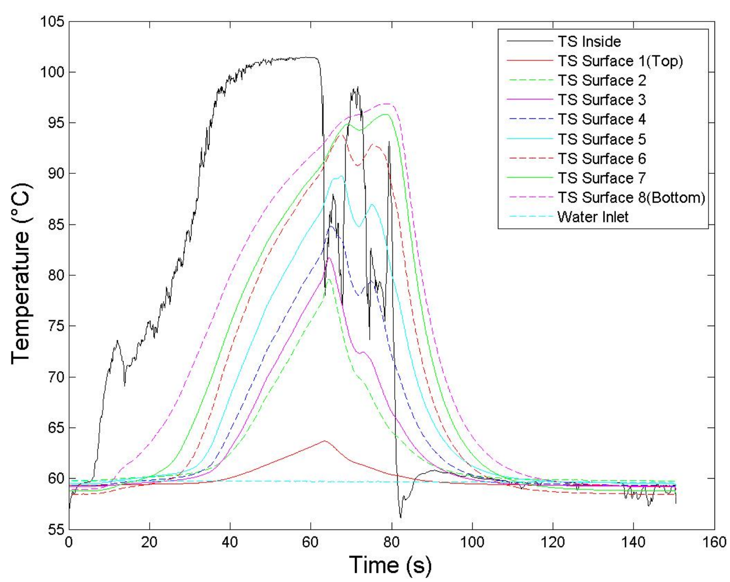

Fig. D.209.: Test section temperatures for test 53.

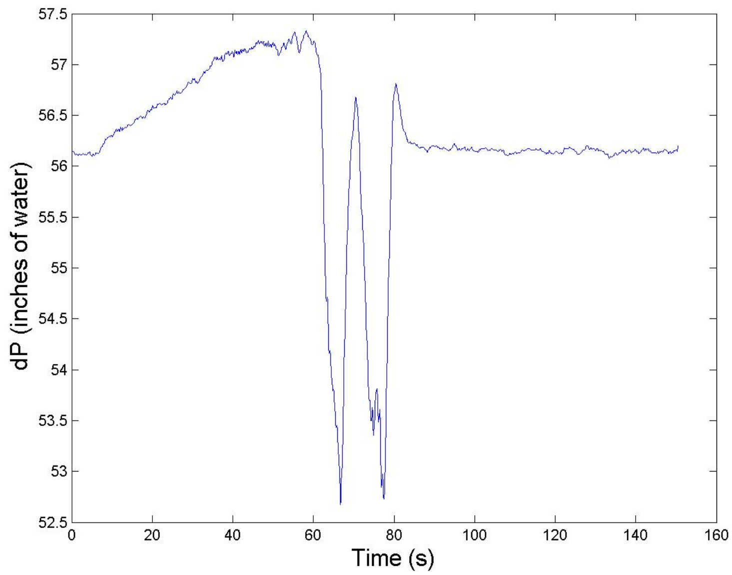

Fig. D.210.: Test section differential pressure for test 53.

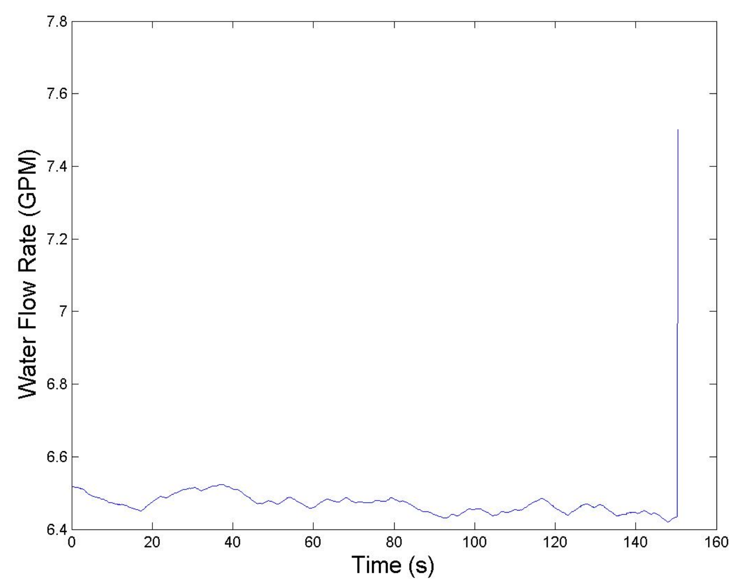

Fig. D.211.: Water flow rate for test 53.

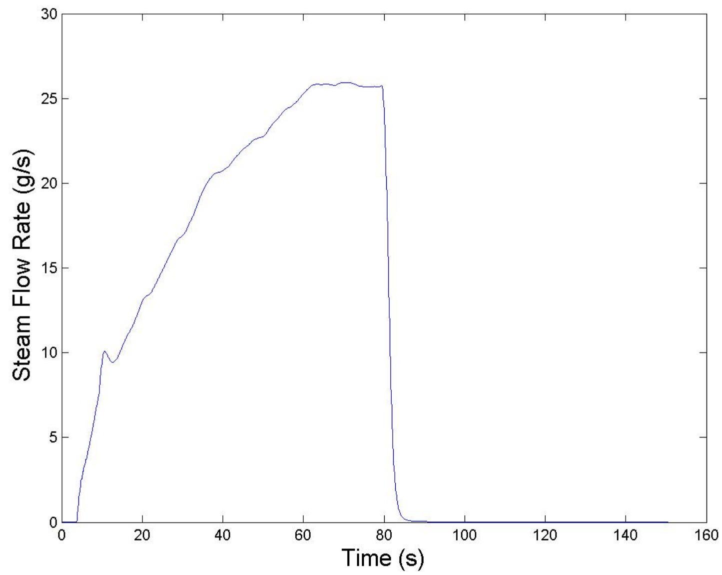

Fig. D.212.: Steam flow rate for test 53.

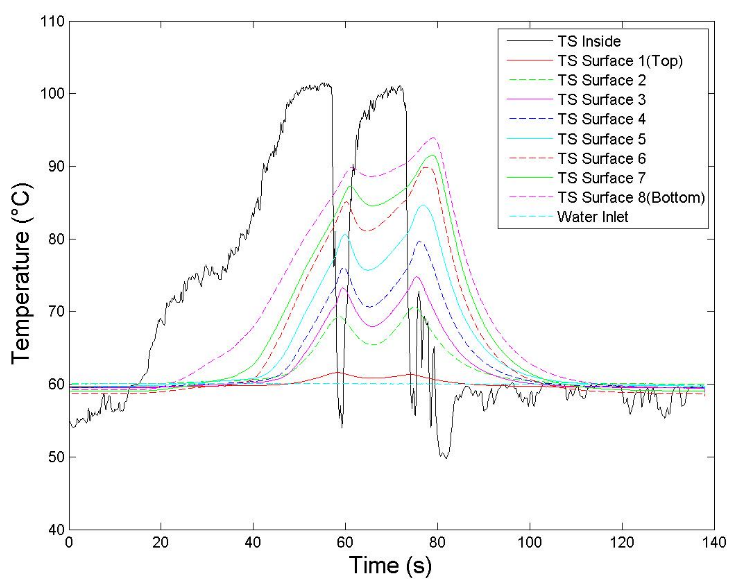

Fig. D.213.: Test section temperatures for test 54.

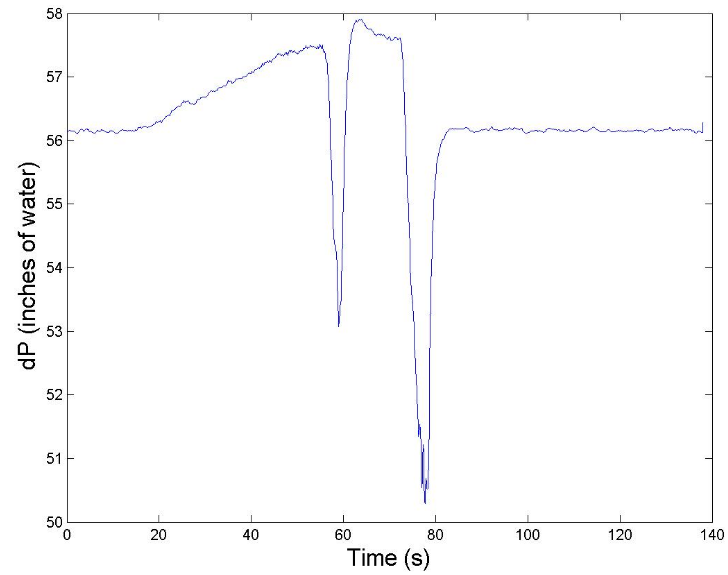

Fig. D.214.: Test section differential pressure for test 54.

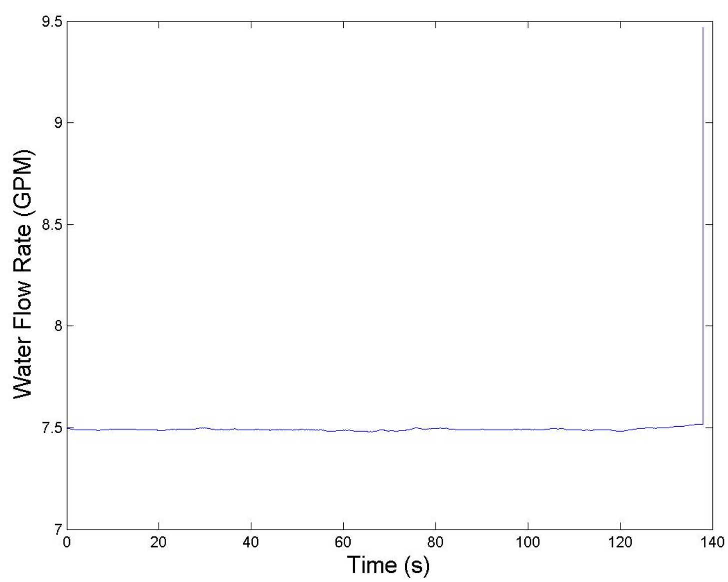

Fig. D.215.: Water flow rate for test 54.

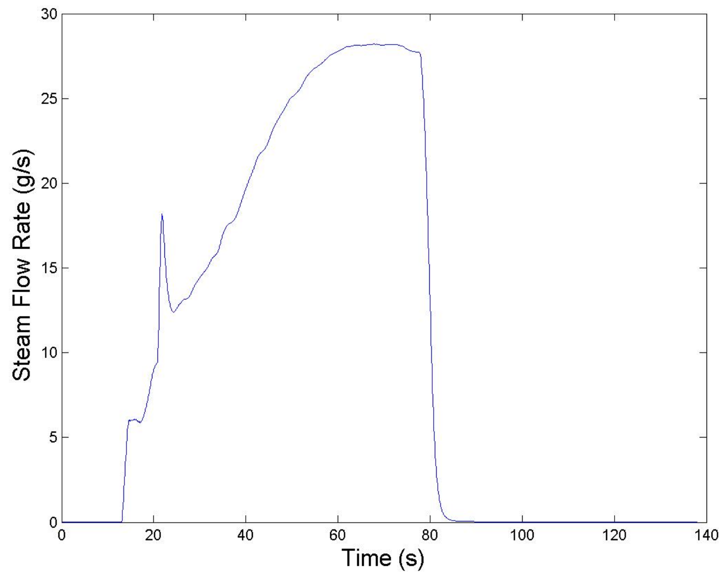

Fig. D.216.: Steam flow rate for test 54.

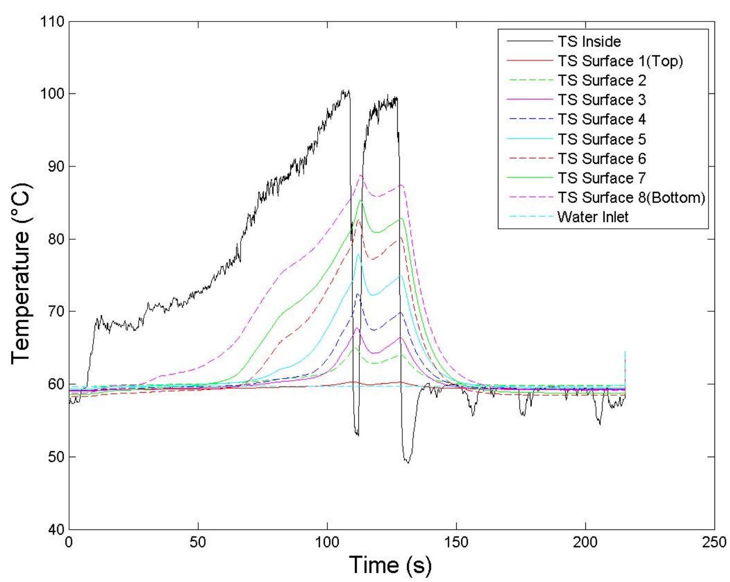

Fig. D.217.: Test section temperatures for test 55.

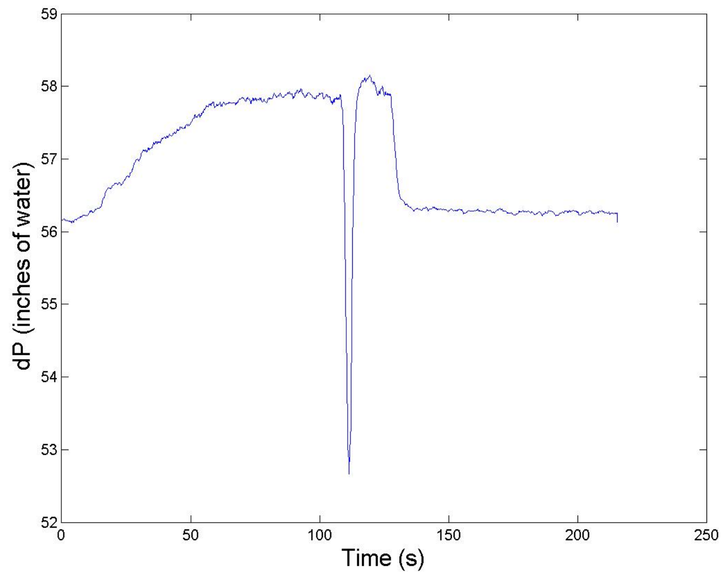

Fig. D.218.: Test section differential pressure for test 55.

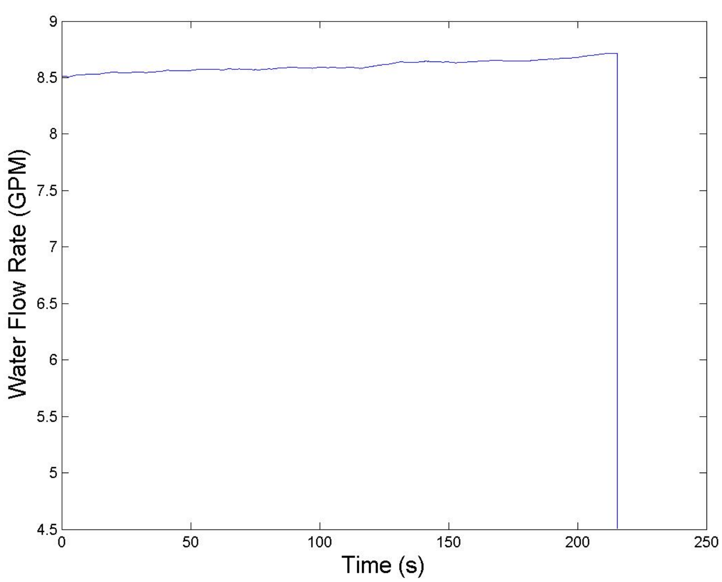

Fig. D.219.: Water flow rate for test 55.

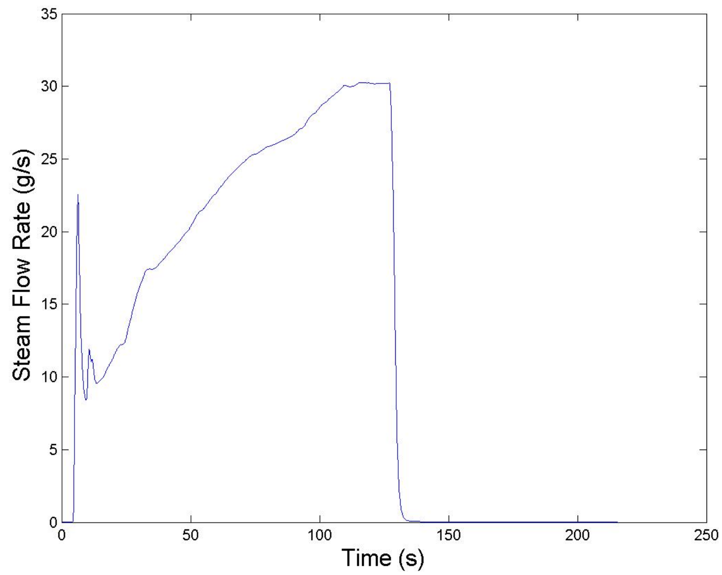

Fig. D.220.: Steam flow rate for test 55.

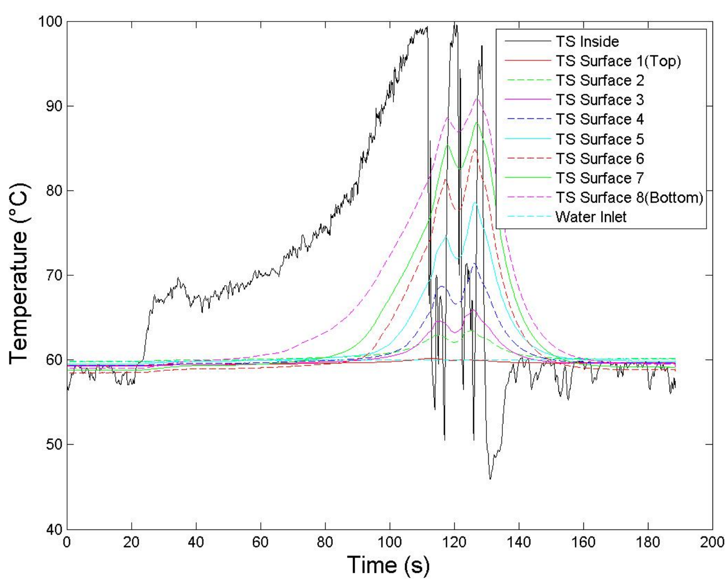

Fig. D.221.: Test section temperatures for test 56.

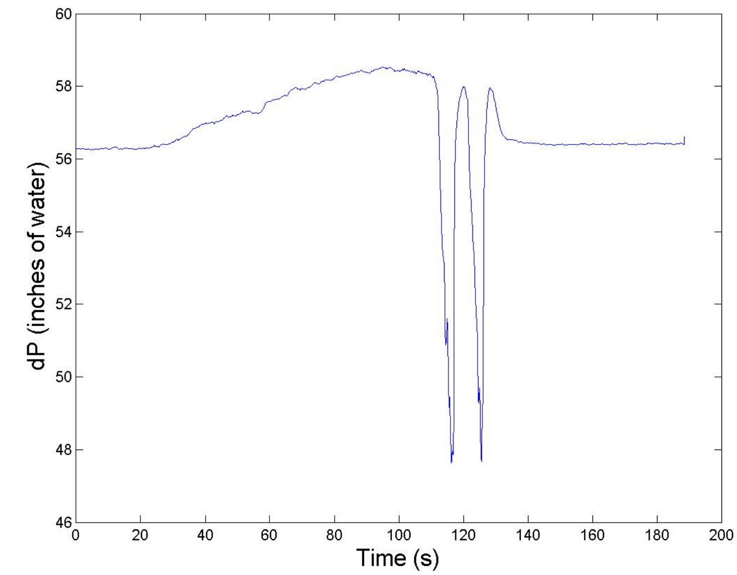

Fig. D.222.: Test section differential pressure for test 56.

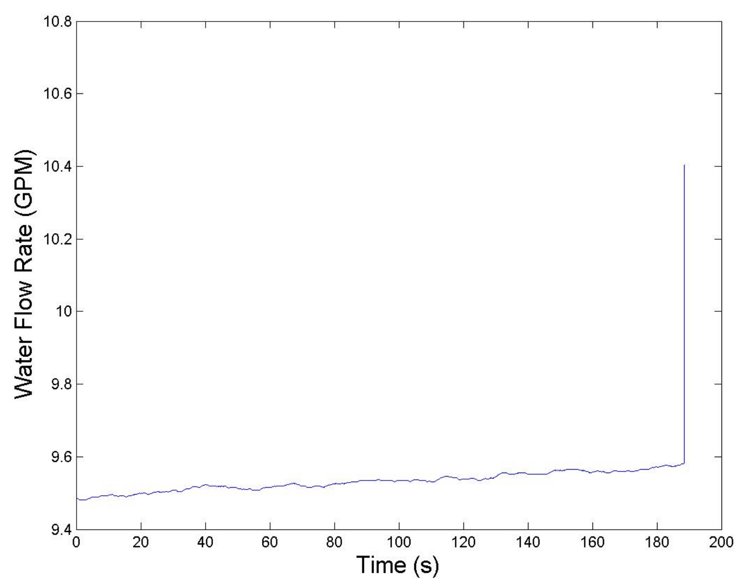

Fig. D.223.: Water flow rate for test 56.

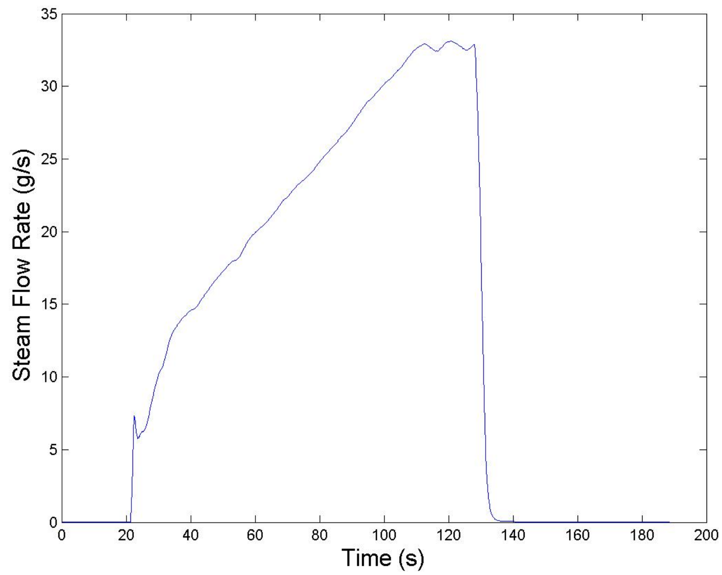

Fig. D.224.: Steam flow rate for test 56.

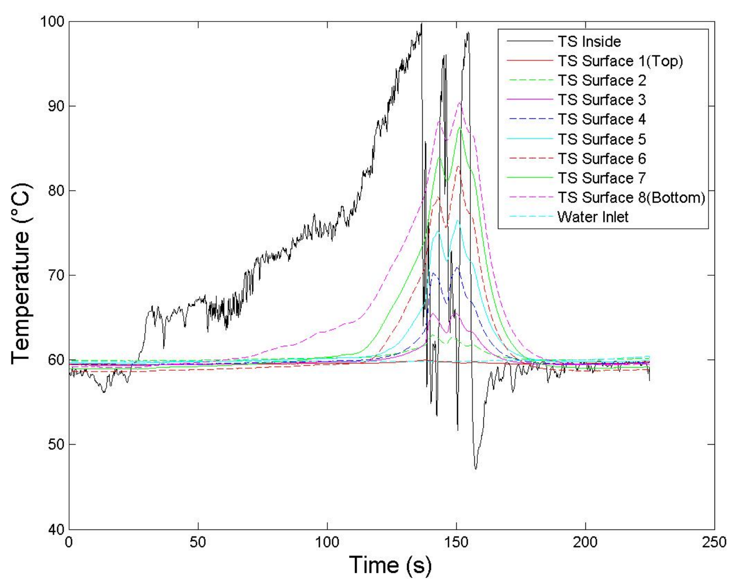

Fig. D.225.: Test section temperatures for test 57.

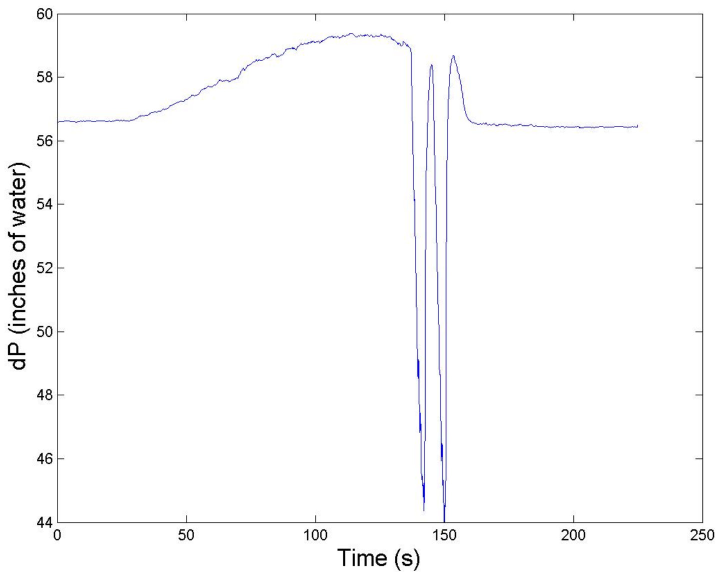

Fig. D.226.: Test section differential pressure for test 57.

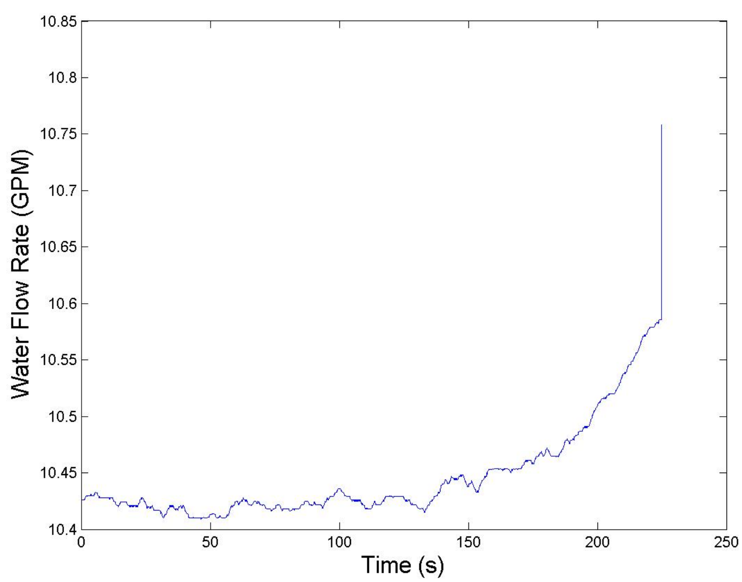

Fig. D.227.: Water flow rate for test 57.

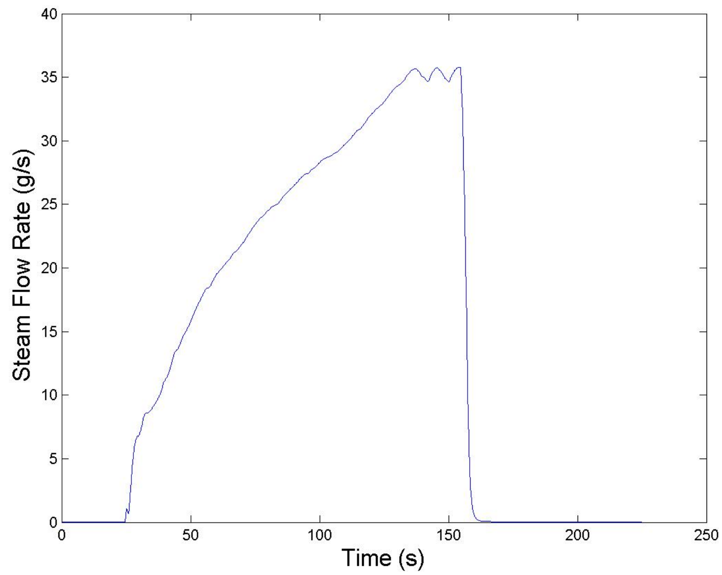

Fig. D.228.: Steam flow rate for test 57.

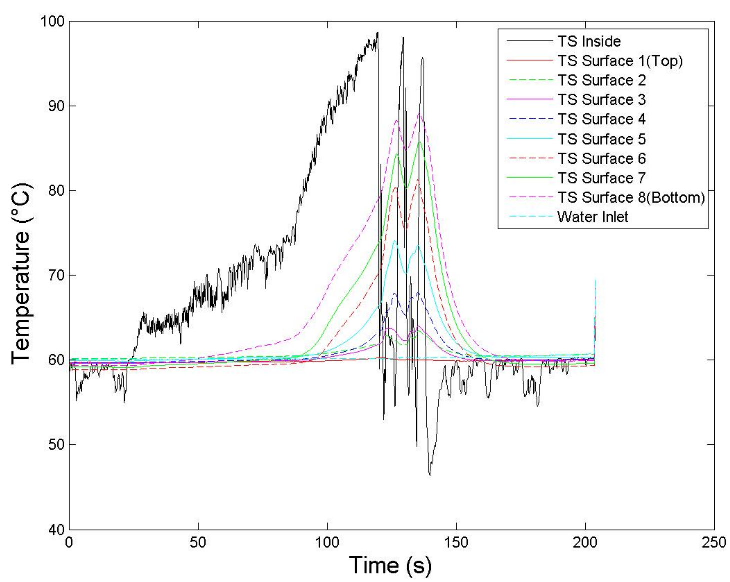

Fig. D.229.: Test section temperatures for test 58.

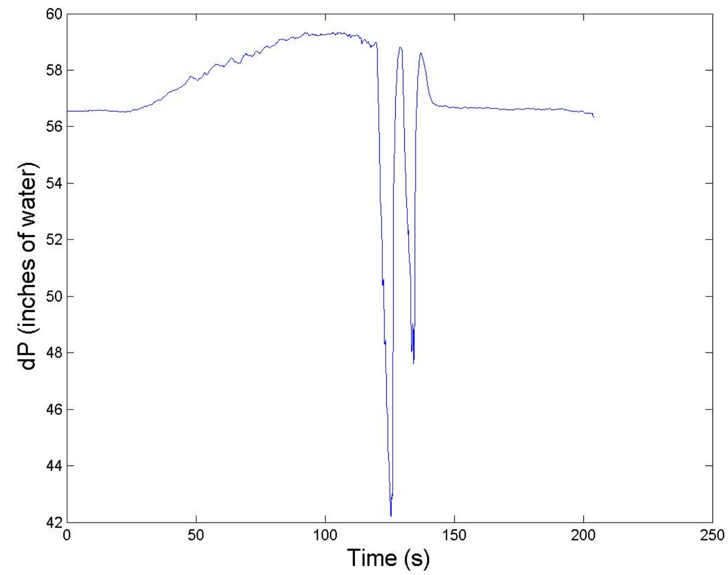

Fig. D.230.: Test section differential pressure for test 58.

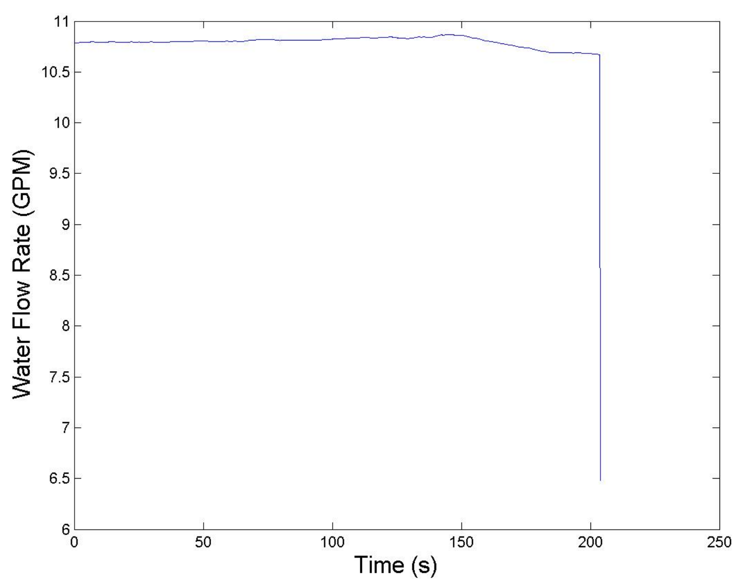

Fig. D.231.: Water flow rate for test 58.

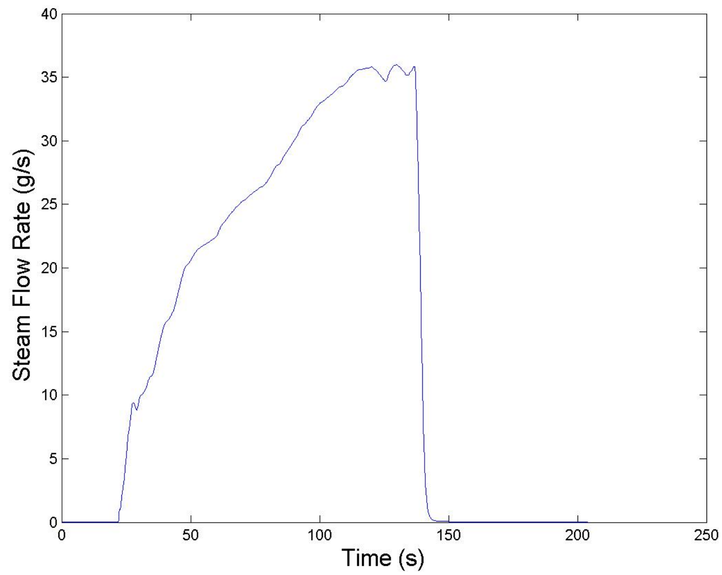

Fig. D.232.: Steam flow rate for test 58.

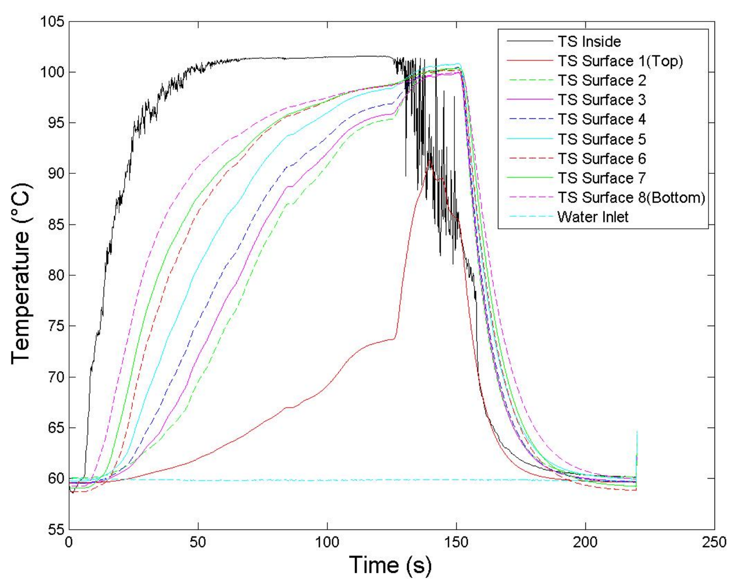

Fig. D.233.: Test section temperatures for test 59.

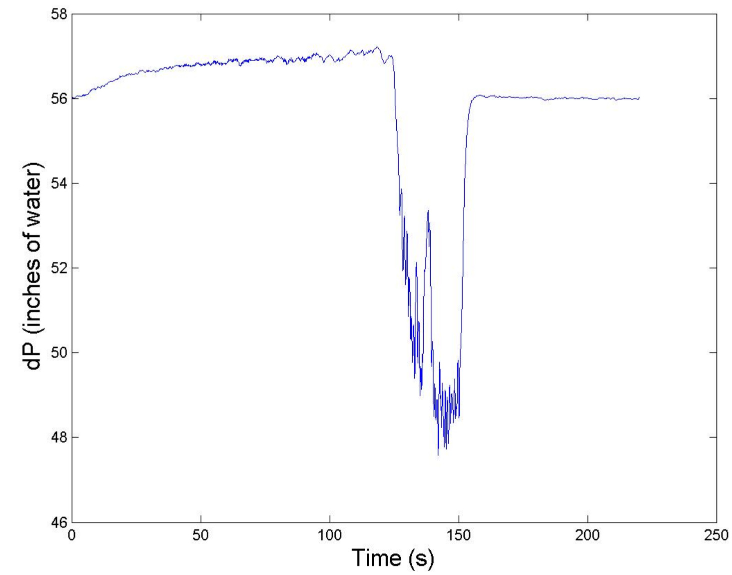

Fig. D.234.: Test section differential pressure for test 59.

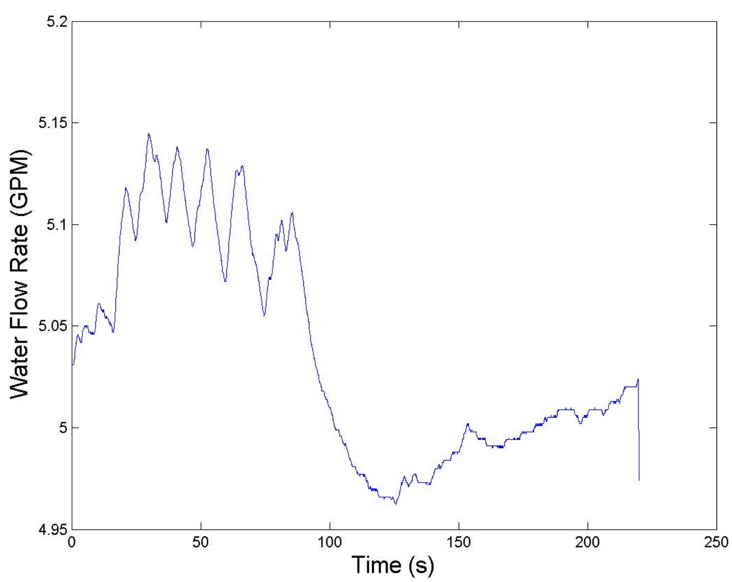

Fig. D.235.: Water flow rate for test 59.

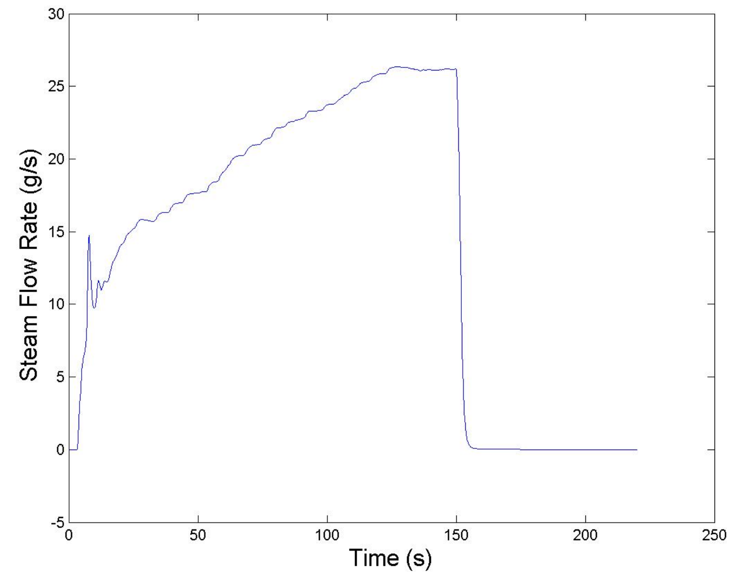

Fig. D.236.: Steam flow rate for test 59.

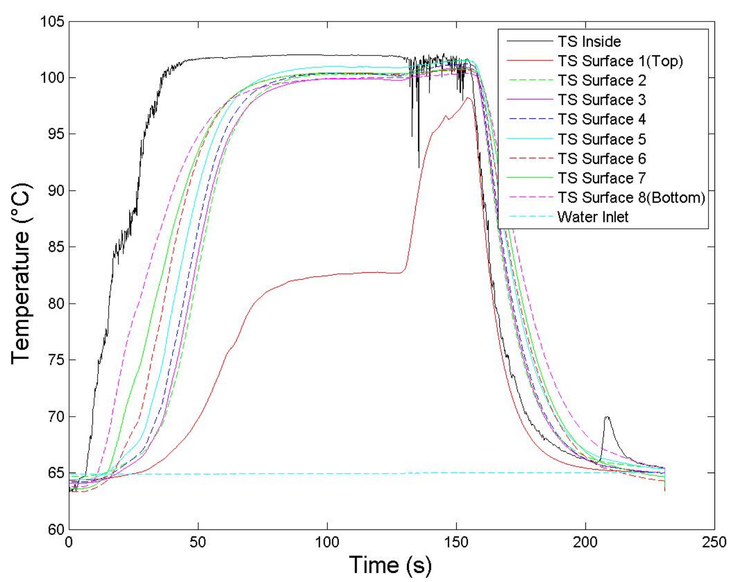

Fig. D.237.: Test section temperatures for test 60.

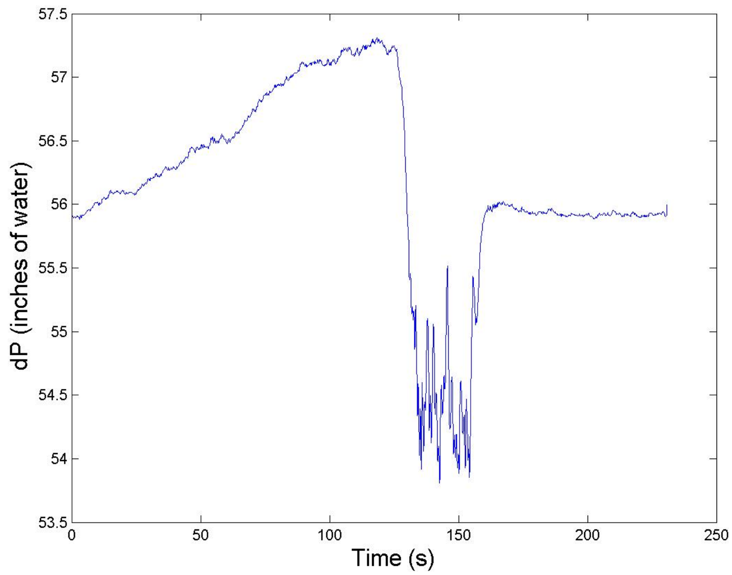

Fig. D.238.: Test section differential pressure for test 60.

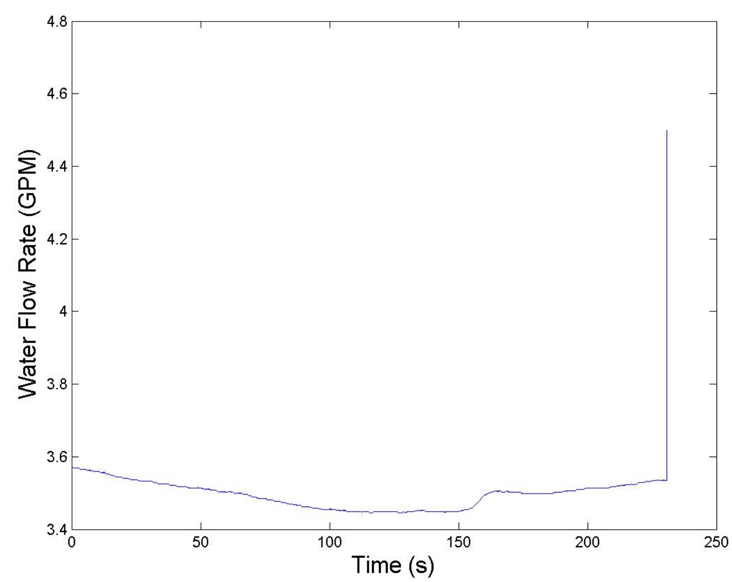

Fig. D.239.: Water flow rate for test 60.

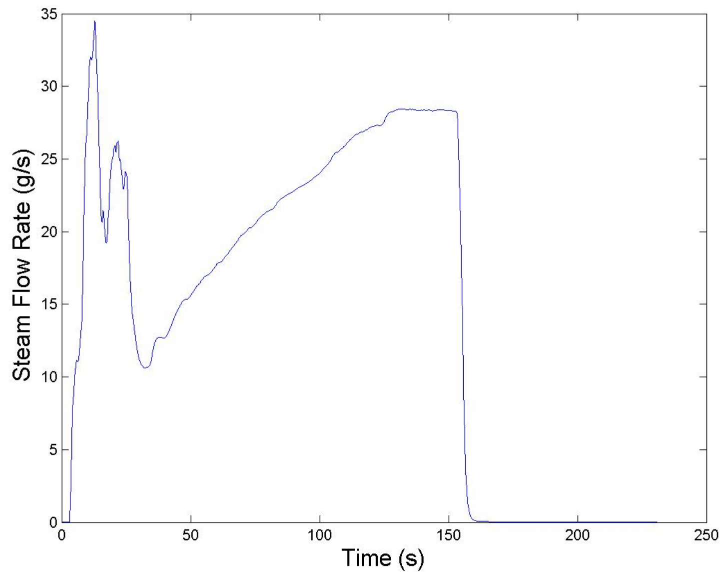

Fig. D.240.: Steam flow rate for test 60.

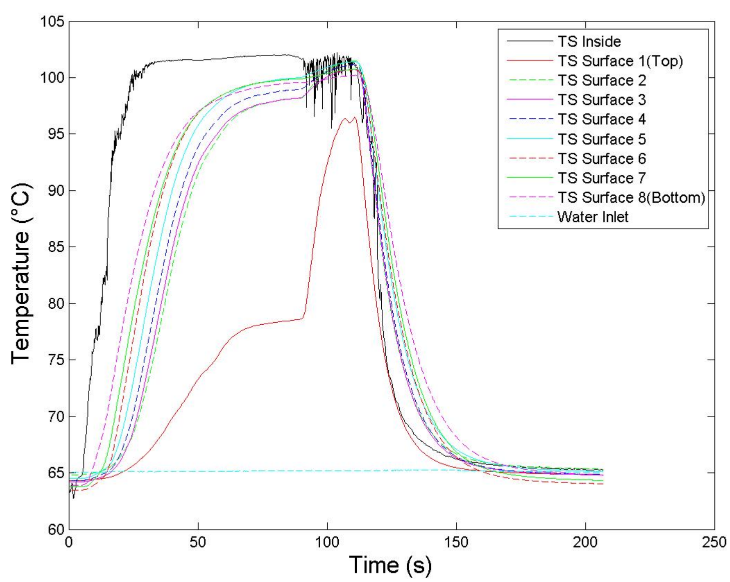

Fig. D.241.: Test section temperatures for test 61.

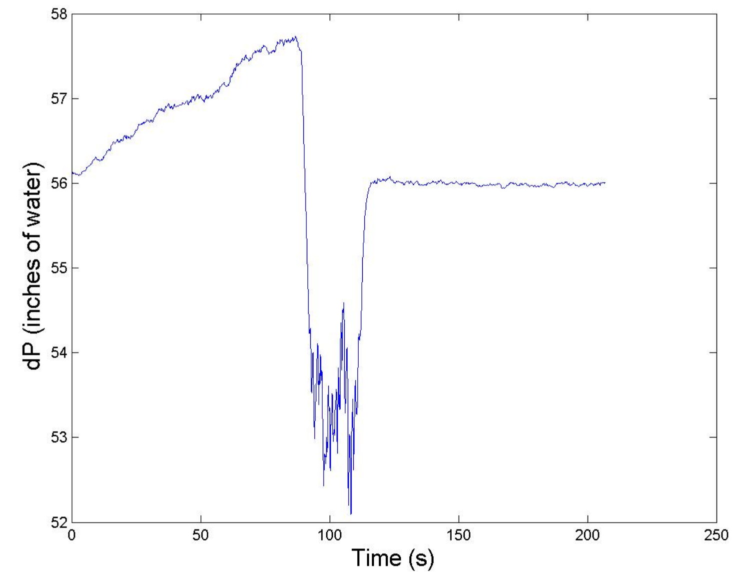

Fig. D.242.: Test section differential pressure for test 61.

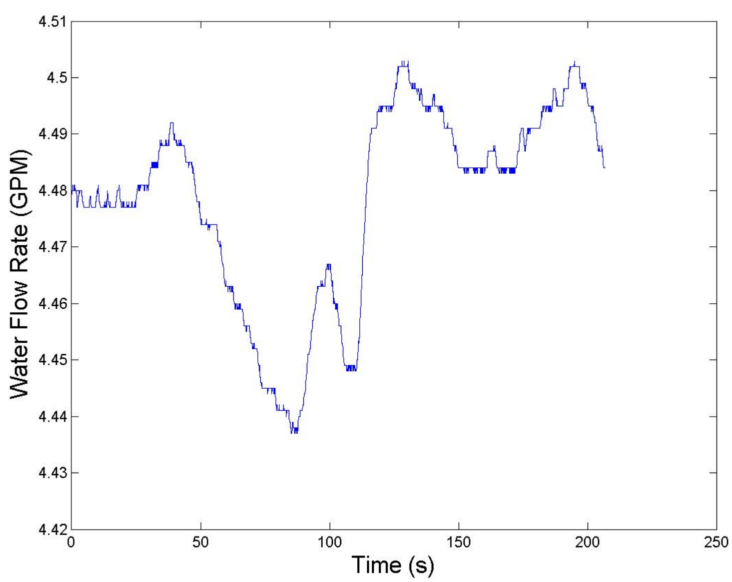

Fig. D.243.: Water flow rate for test 61.

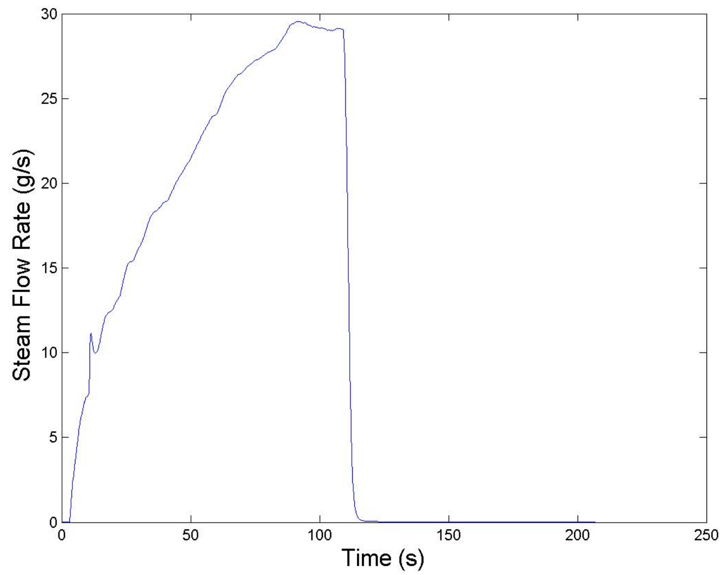

Fig. D.244.: Steam flow rate for test 61.

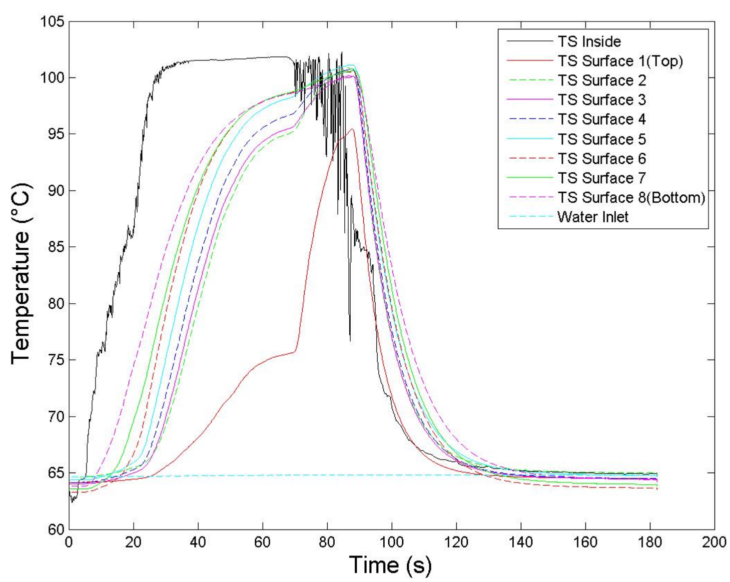

Fig. D.245.: Test section temperatures for test 62.

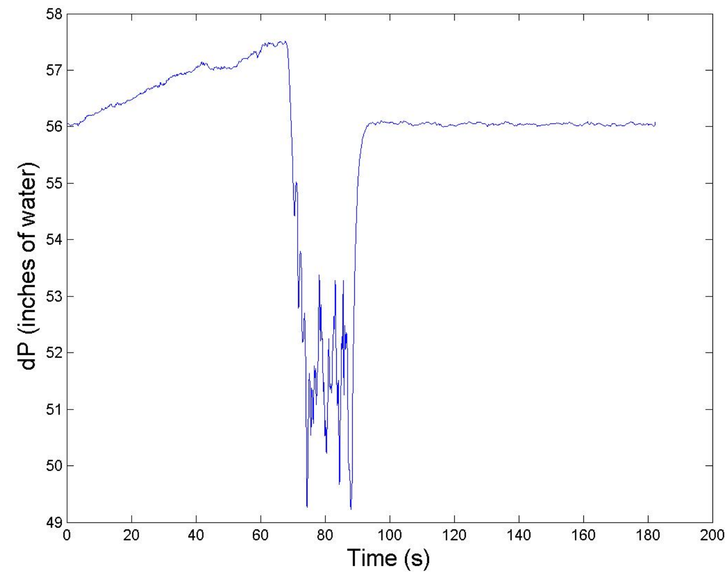

Fig. D.246.: Test section differential pressure for test 62.

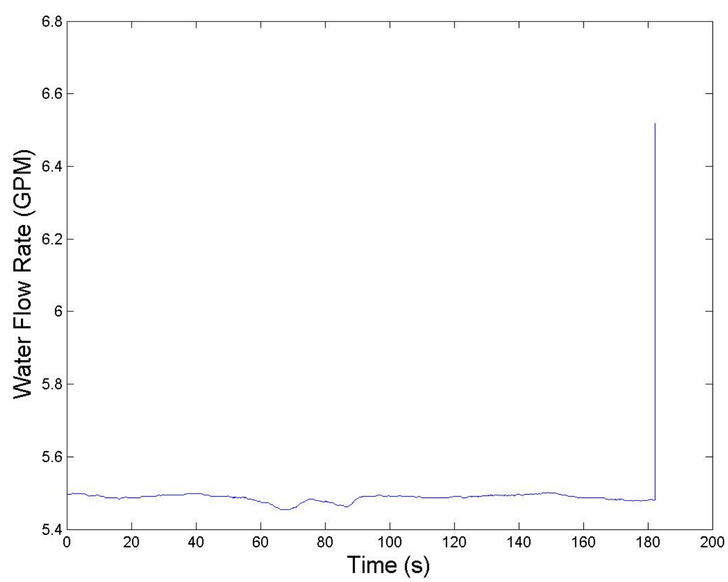

Fig. D.247.: Water flow rate for test 62.

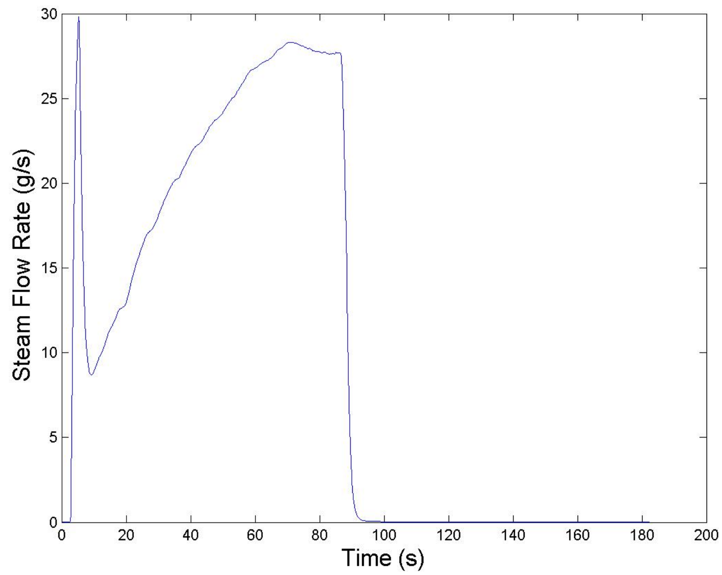

Fig. D.248.: Steam flow rate for test 62.

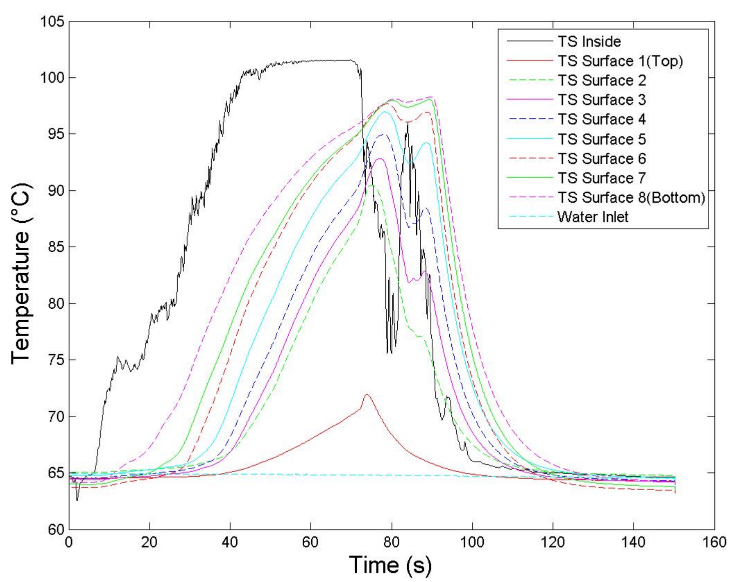

Fig. D.249.: Test section temperatures for test 63.

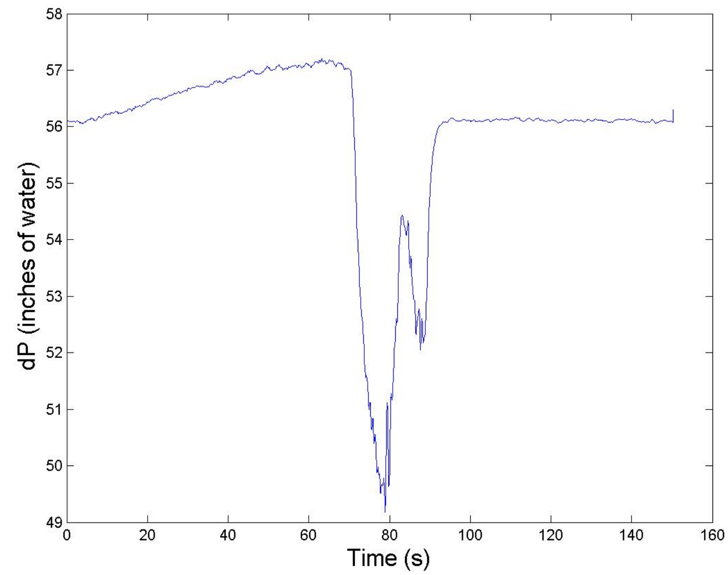

Fig. D.250.: Test section differential pressure for test 63.

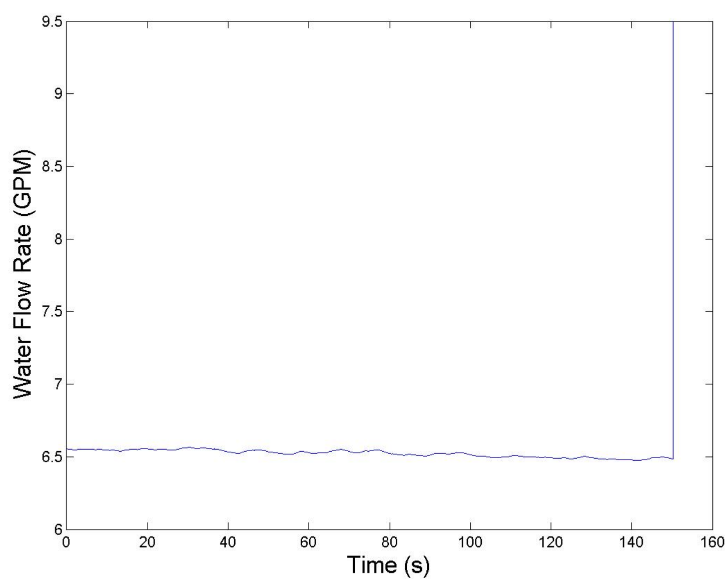

Fig. D.251.: Water flow rate for test 63.

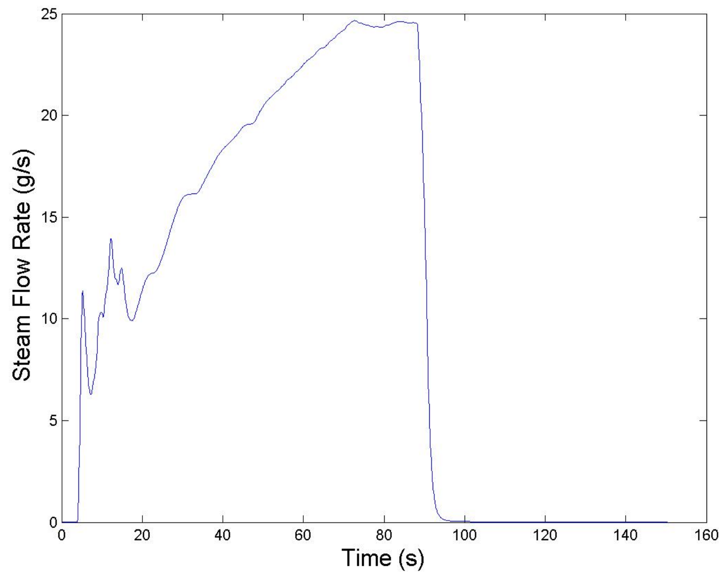

Fig. D.252.: Steam flow rate for test 63.

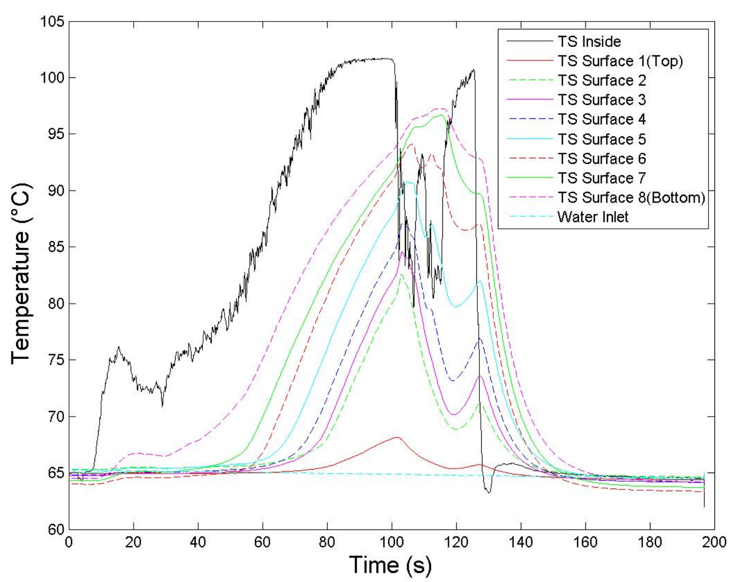

Fig. D.253.: Test section temperatures for test 64.

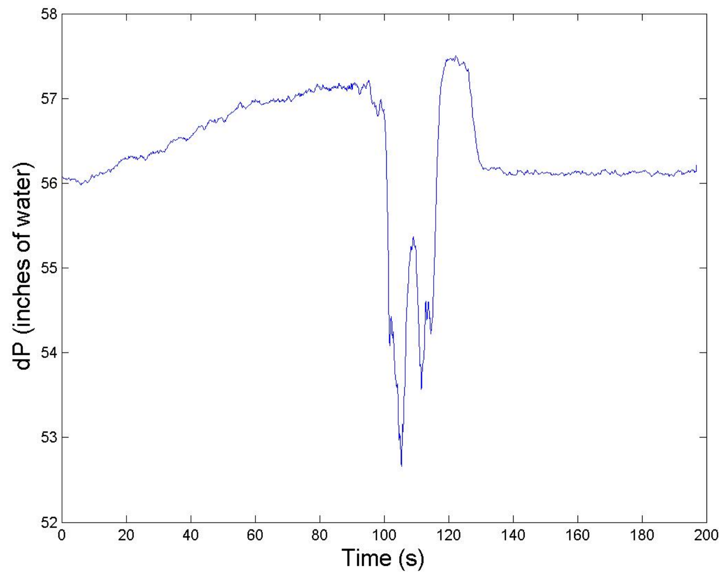

Fig. D.254.: Test section differential pressure for test 64.

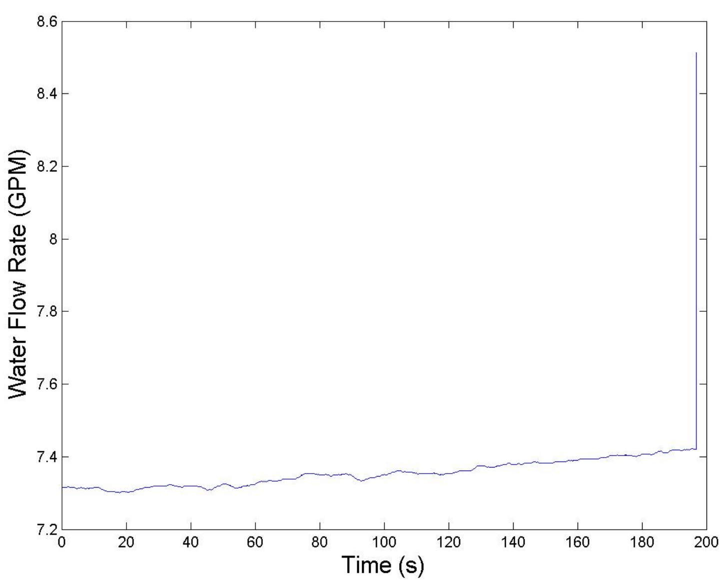

Fig. D.255.: Water flow rate for test 64.

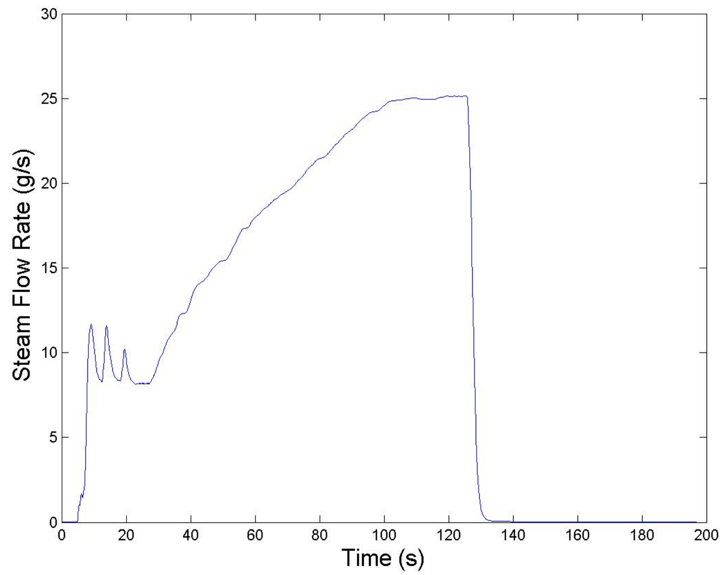

Fig. D.256.: Steam flow rate for test 64.

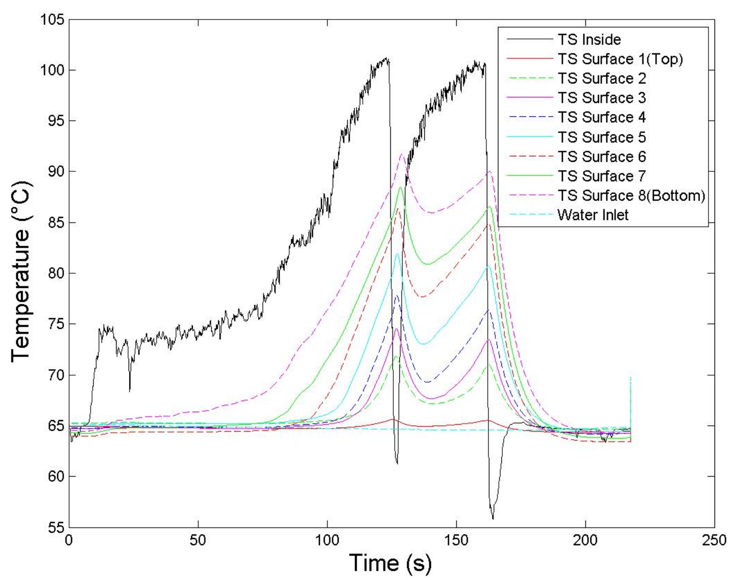

Fig. D.257.: Test section temperatures for test 65.

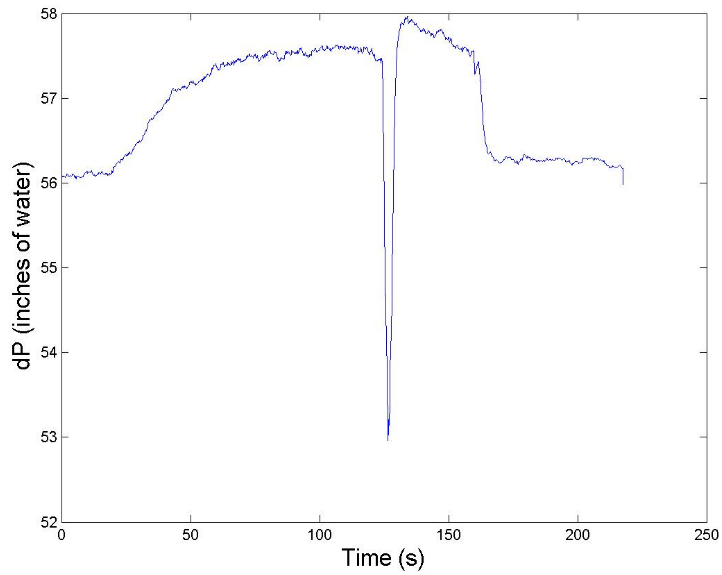

Fig. D.258.: Test section differential pressure for test 65.

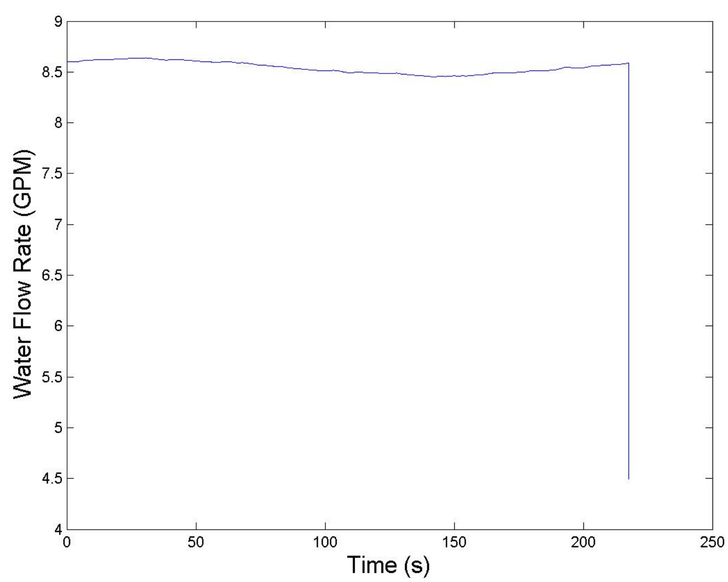

Fig. D.259.: Water flow rate for test 65.

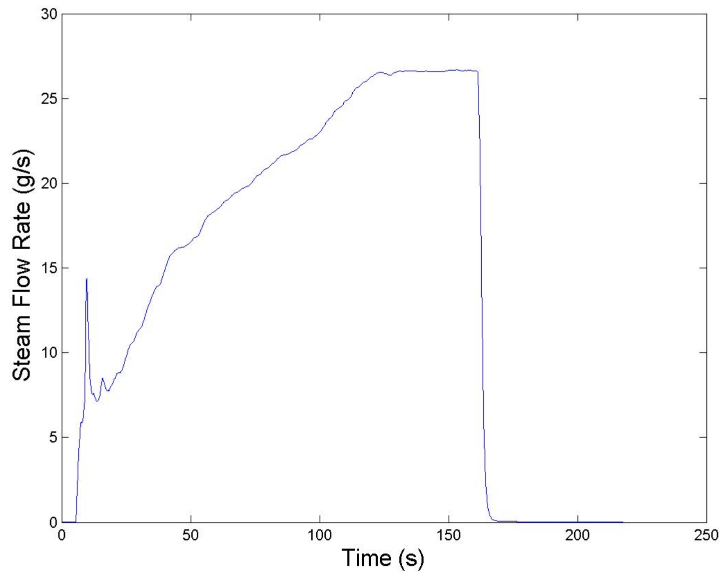

Fig. D.260.: Steam flow rate for test 65.

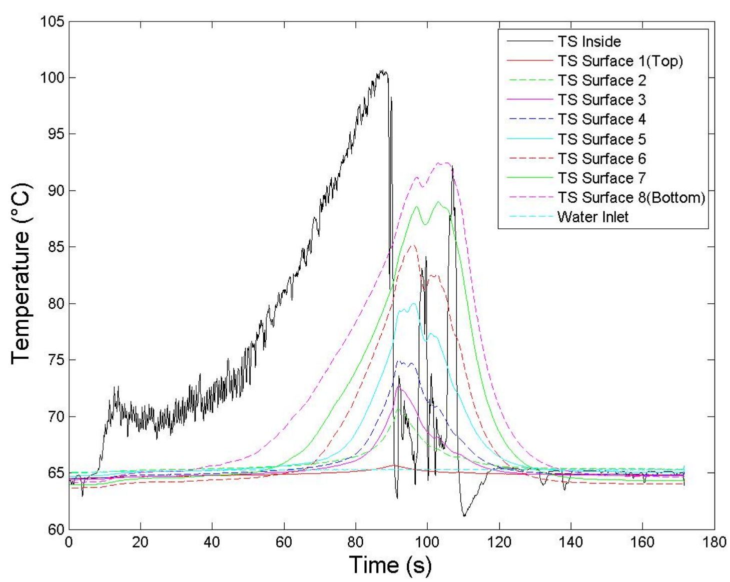

Fig. D.261.: Test section temperatures for test 66.

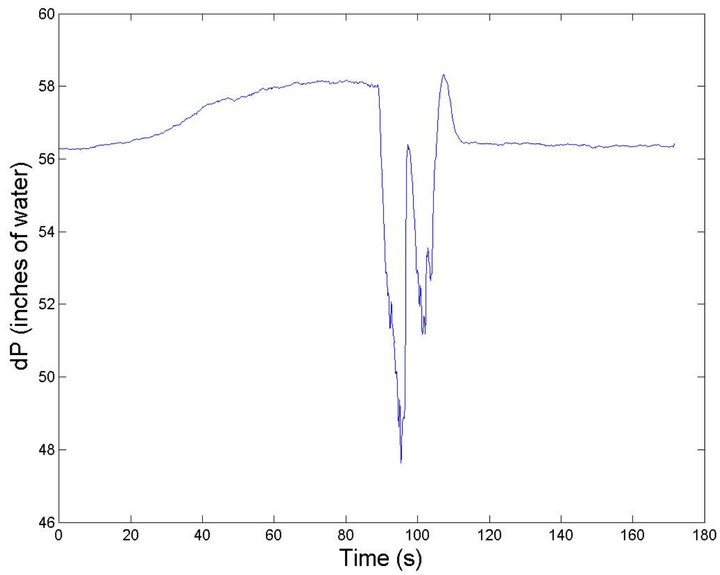

Fig. D.262.: Test section differential pressure for test 66.

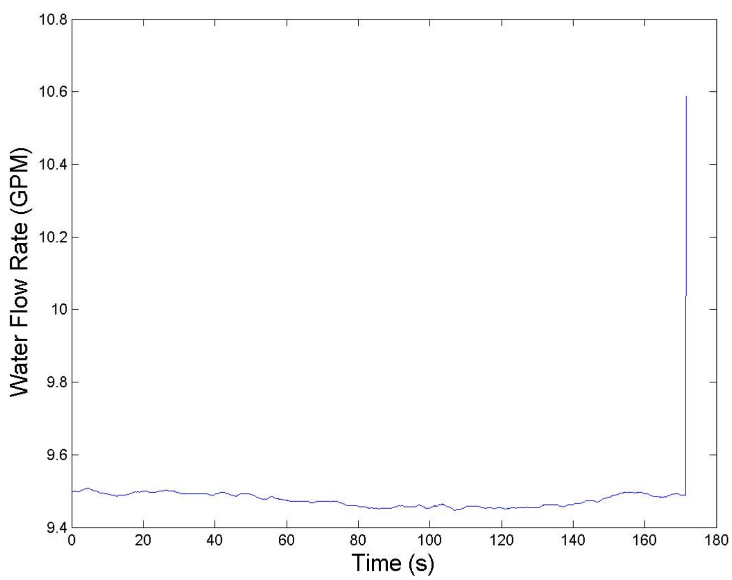

Fig. D.263.: Water flow rate for test 66.

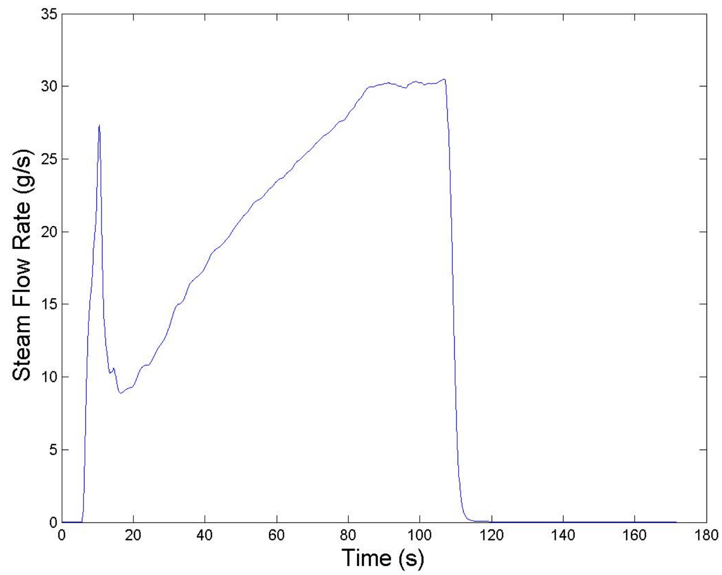

Fig. D.264.: Steam flow rate for test 66.

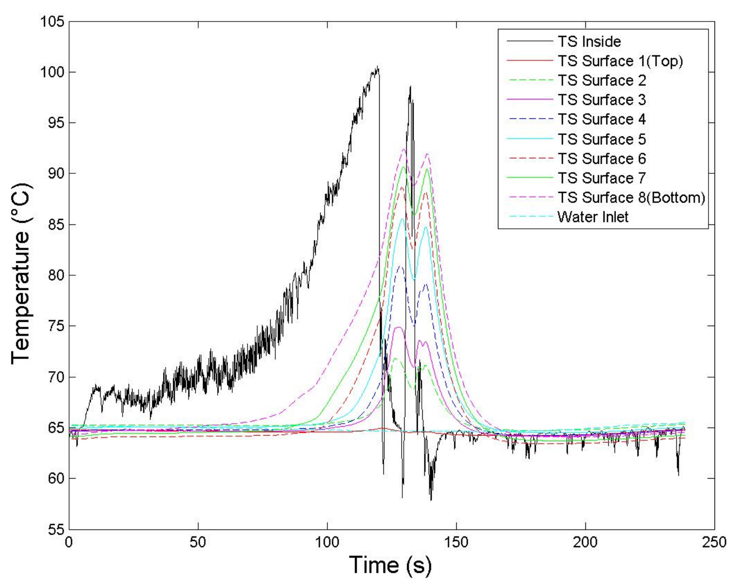

Fig. D.265.: Test section temperatures for test 67.

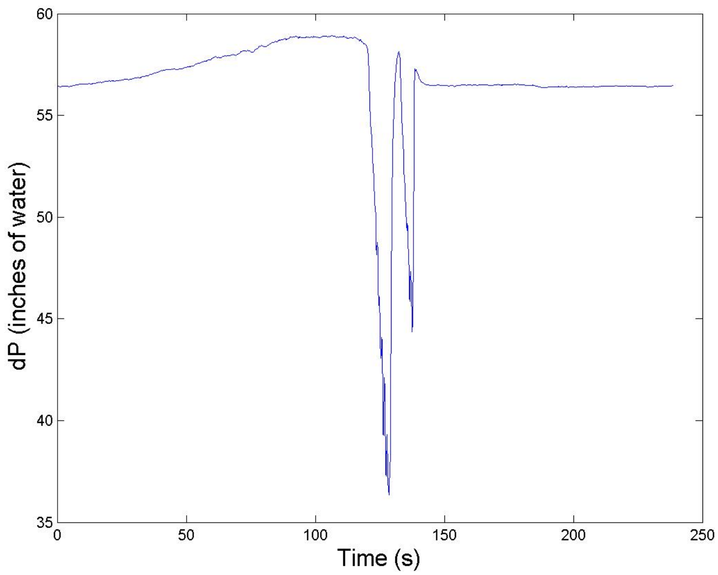

Fig. D.266.: Test section differential pressure for test 67.

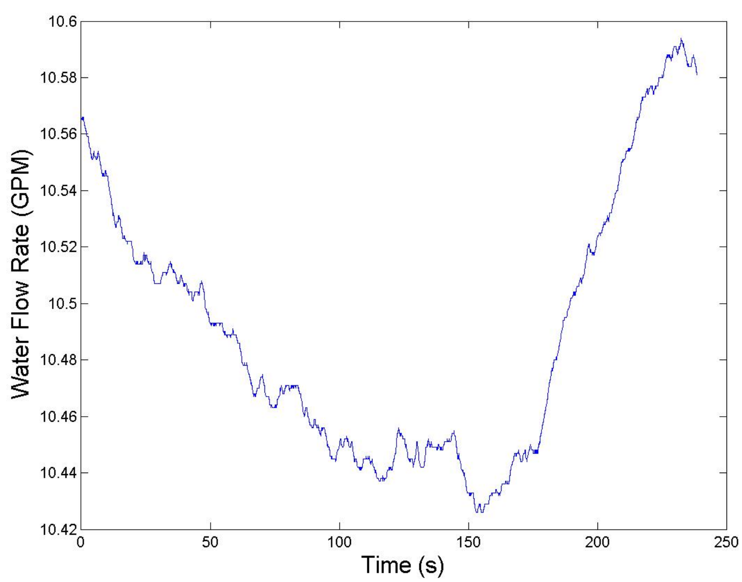

Fig. D.267.: Water flow rate for test 67.

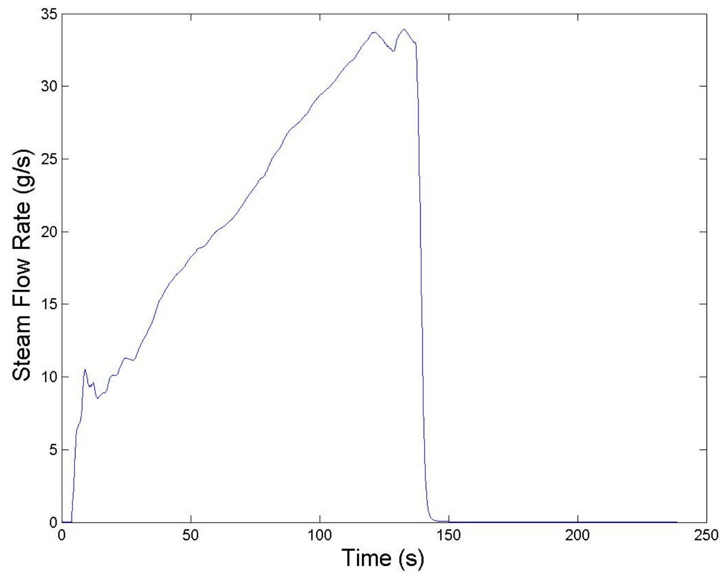

Fig. D.268.: Steam flow rate for test 67.

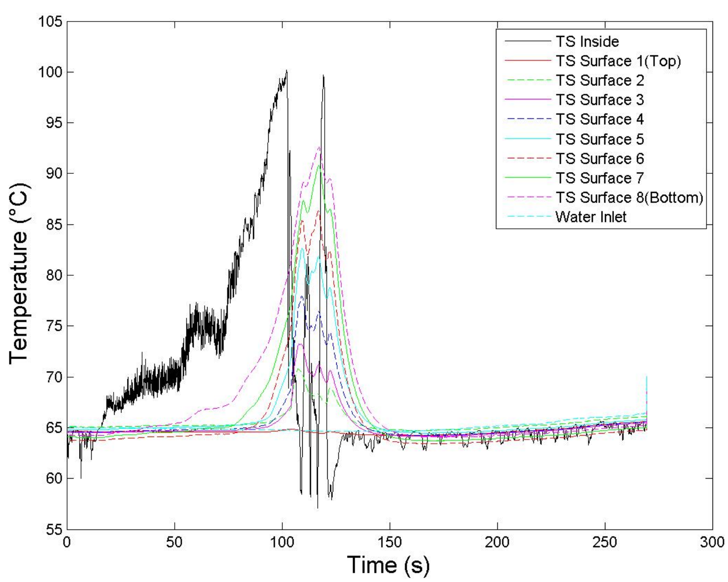

Fig. D.269.: Test section temperatures for test 68.

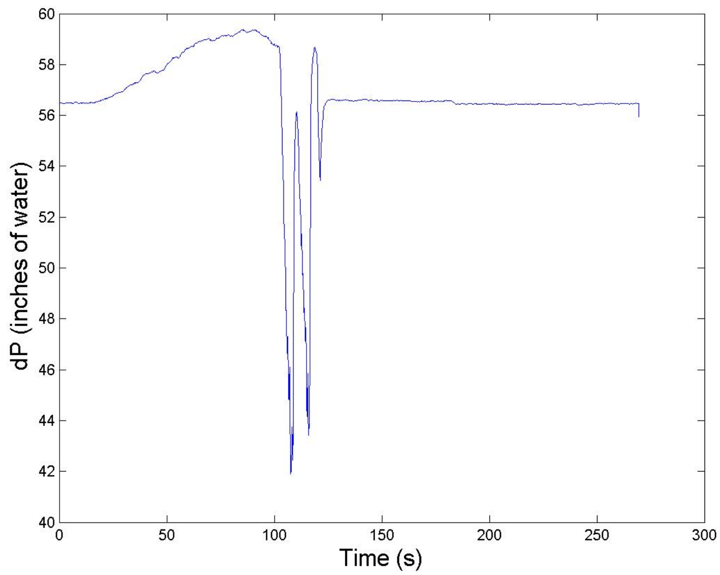

Fig. D.270.: Test section differential pressure for test 68.

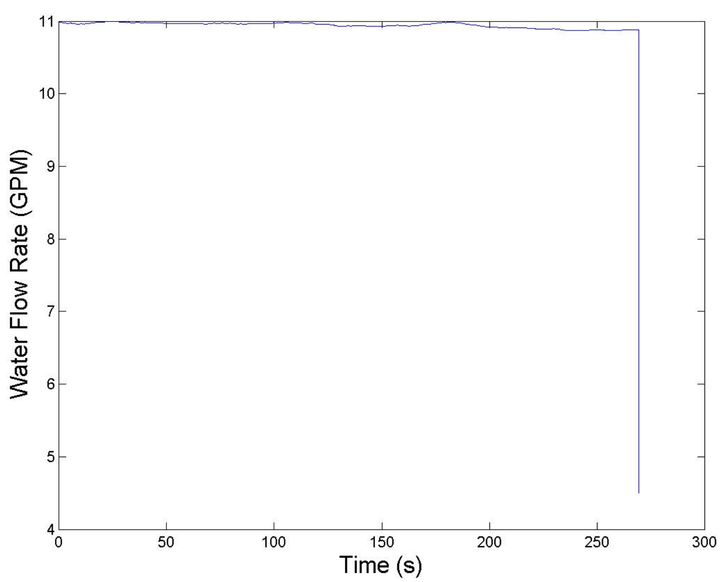

Fig. D.271.: Water flow rate for test 68.

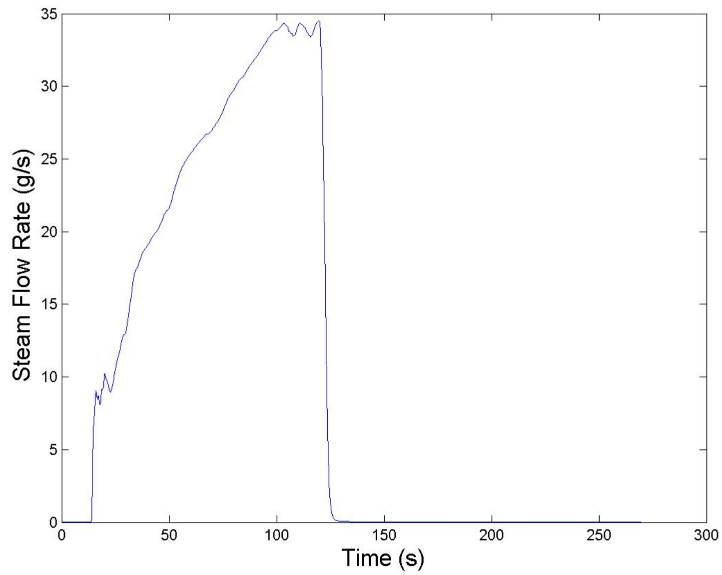

Fig. D.272.: Steam flow rate for test 68.

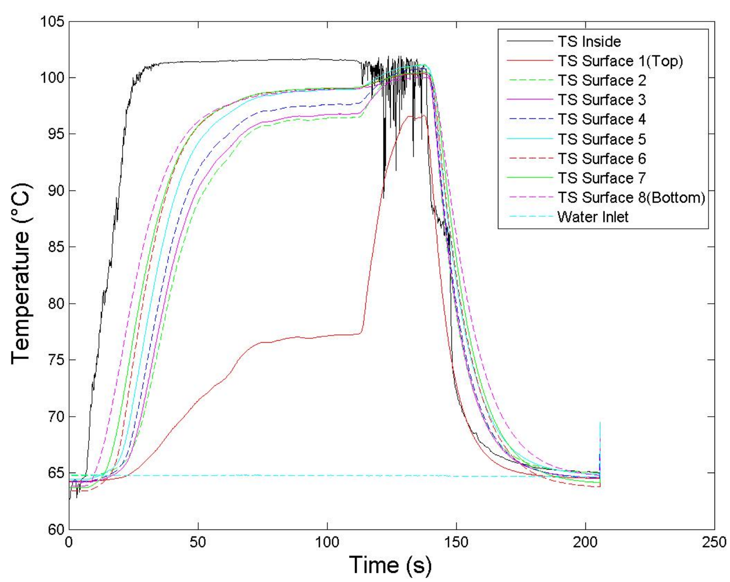

Fig. D.273.: Test section temperatures for test 69.

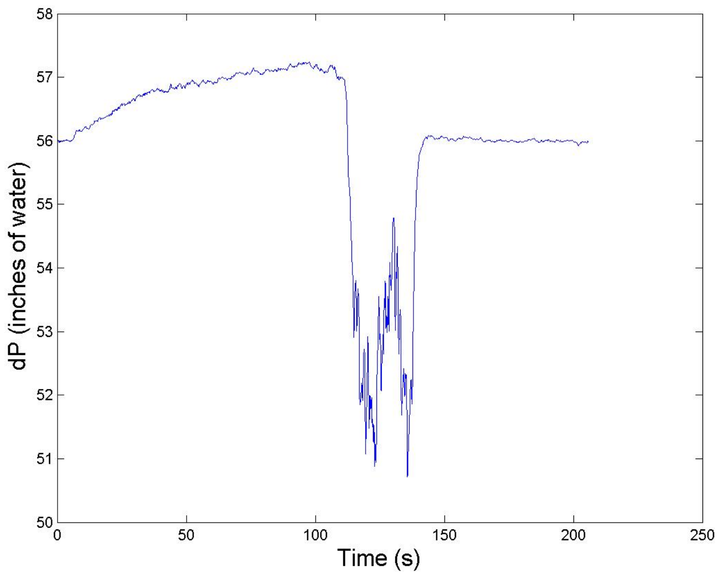

Fig. D.274.: Test section differential pressure for test 69.

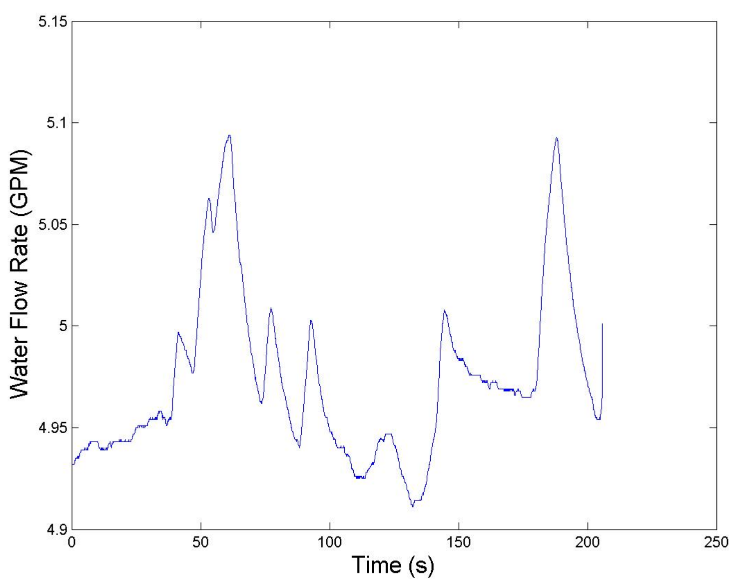

Fig. D.275.: Water flow rate for test 69.

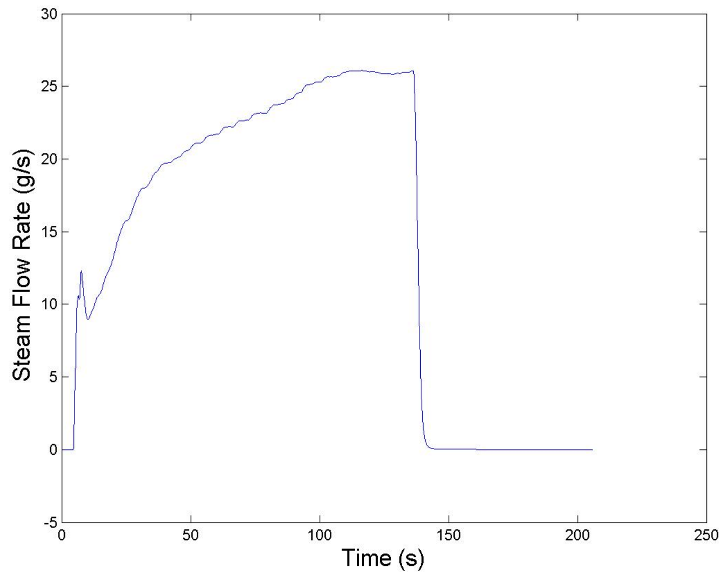

Fig. D.276.: Steam flow rate for test 69.

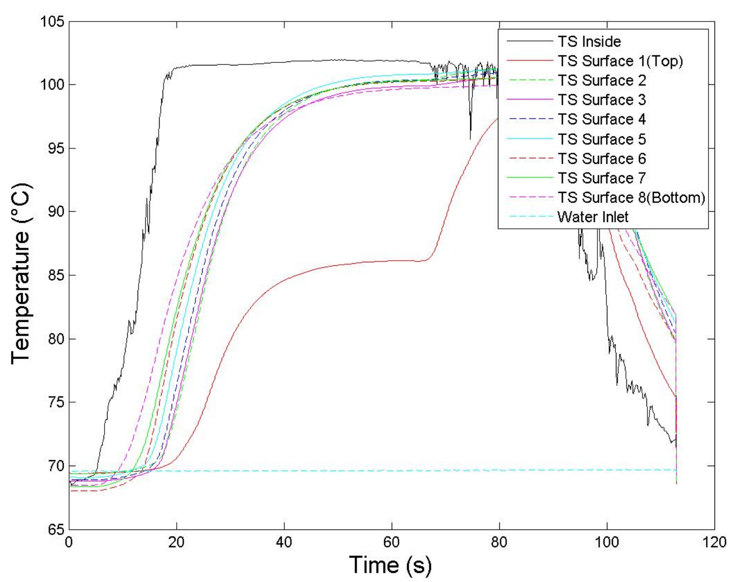

Fig. D.277.: Test section temperatures for test 70.

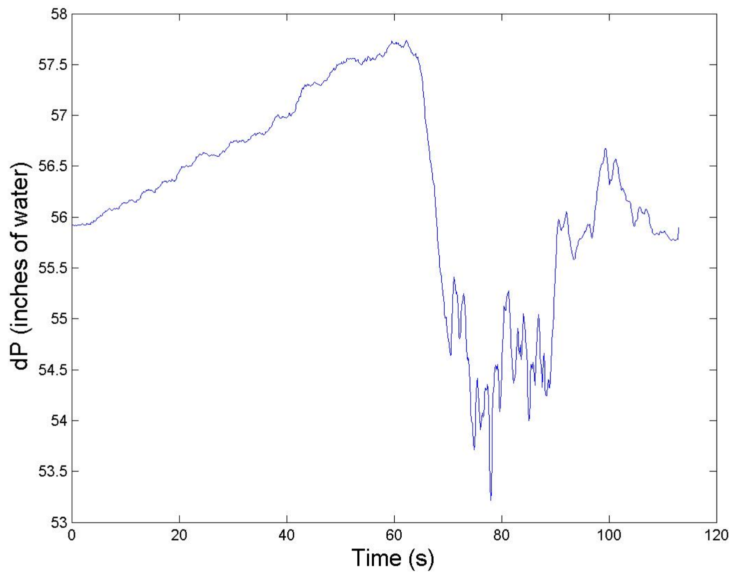

Fig. D.278.: Test section differential pressure for test 70.

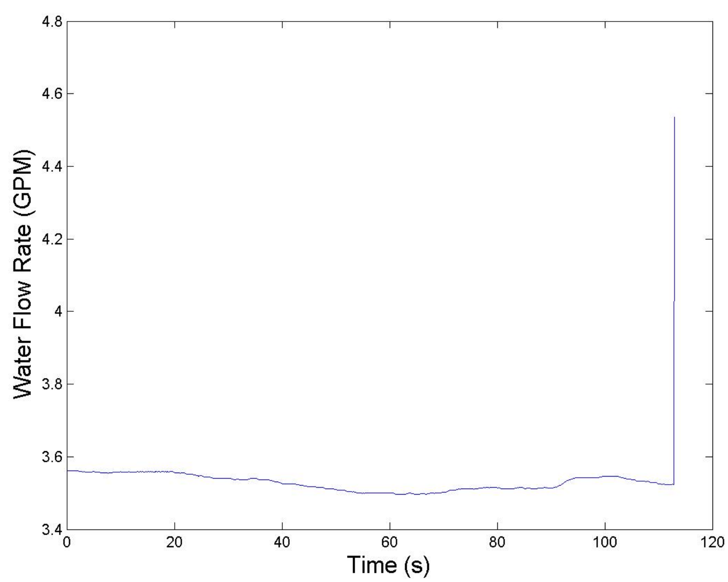

Fig. D.279.: Water flow rate for test 70.

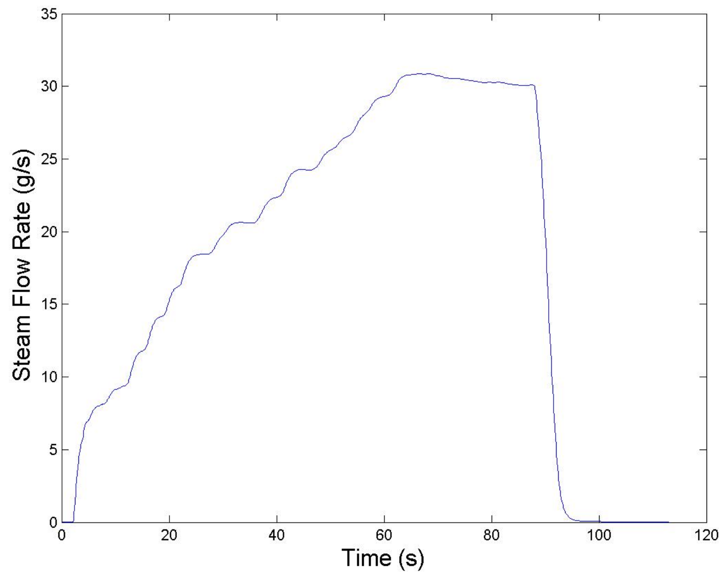

Fig. D.280.: Steam flow rate for test 70.

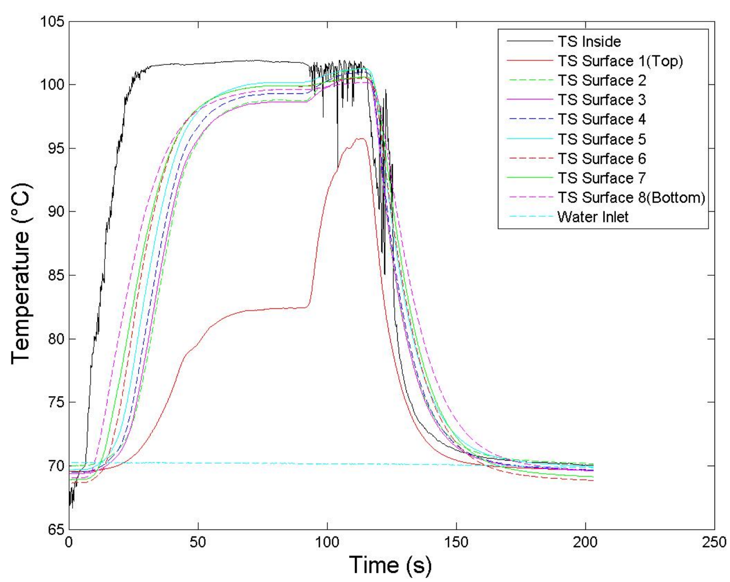

Fig. D.281.: Test section temperatures for test 71.

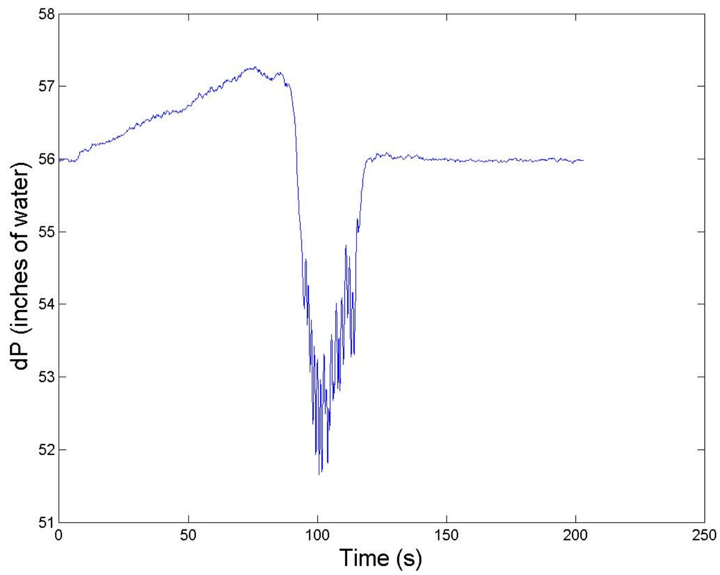

Fig. D.282.: Test section differential pressure for test 71.

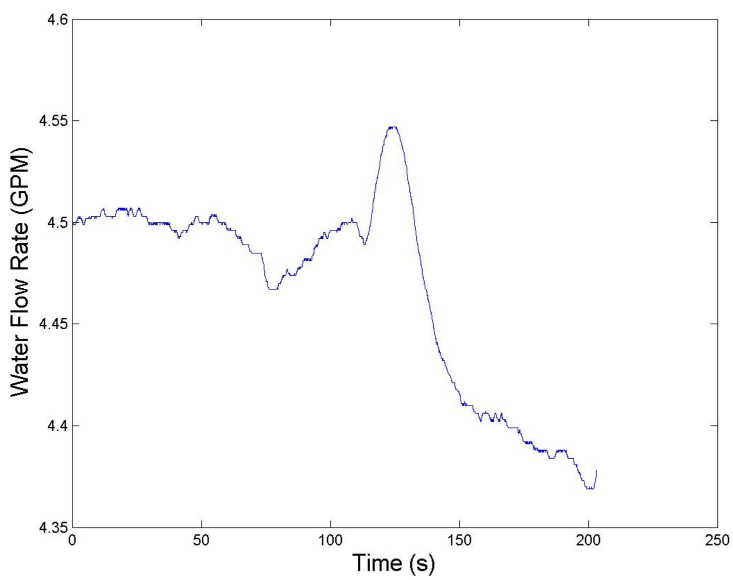

Fig. D.283.: Water flow rate for test 71.

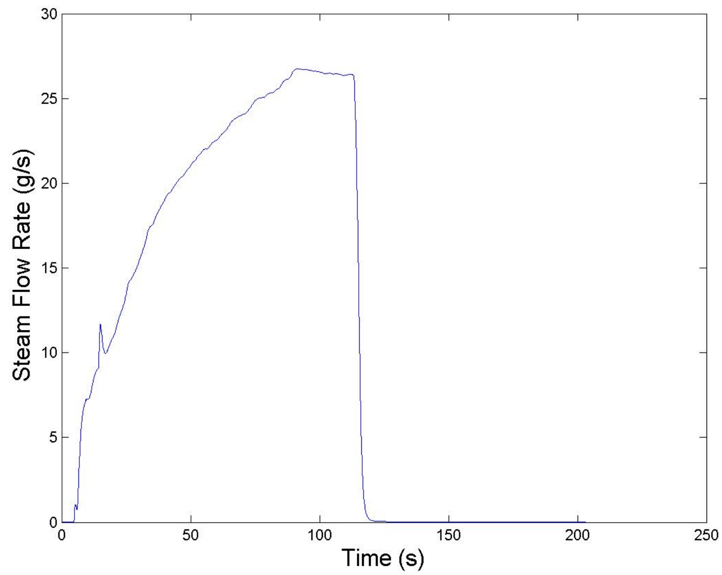

Fig. D.284.: Steam flow rate for test 71.

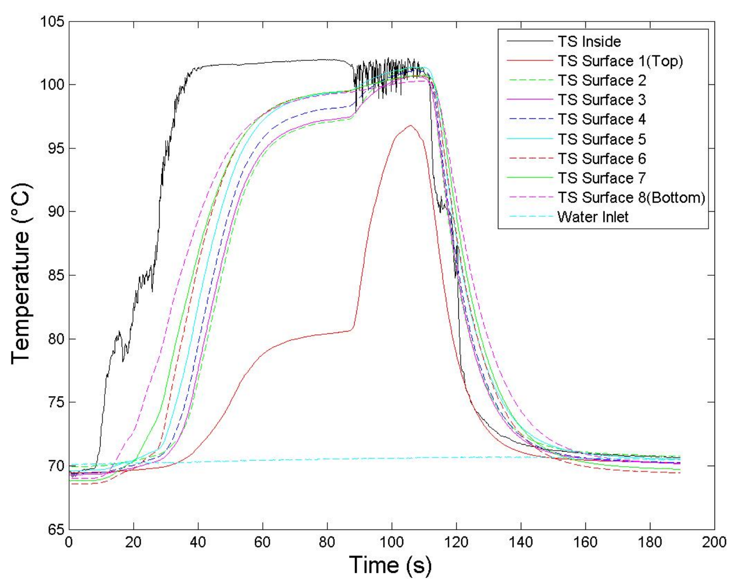

Fig. D.285.: Test section temperatures for test 72.

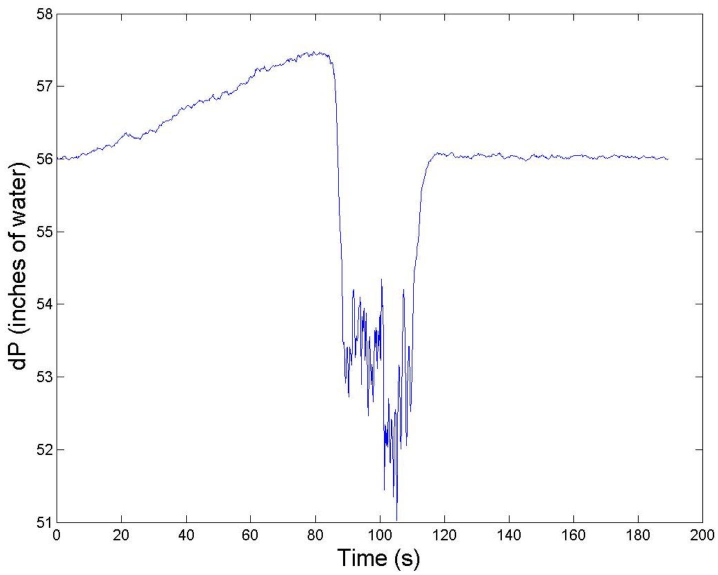

Fig. D.286.: Test section differential pressure for test 72.

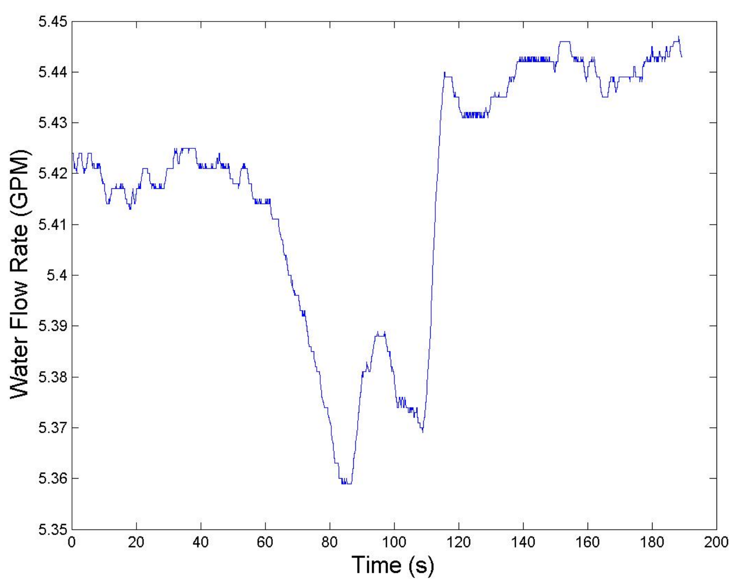

Fig. D.287.: Water flow rate for test 72.

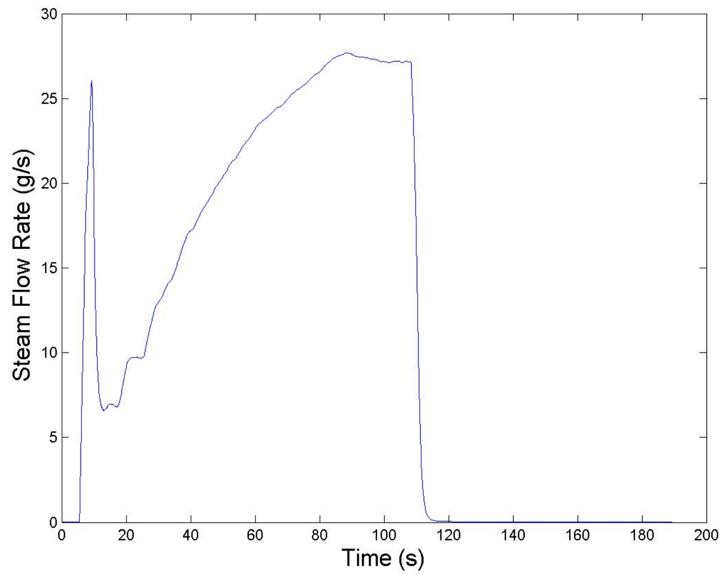

Fig. D.288.: Steam flow rate for test 72.

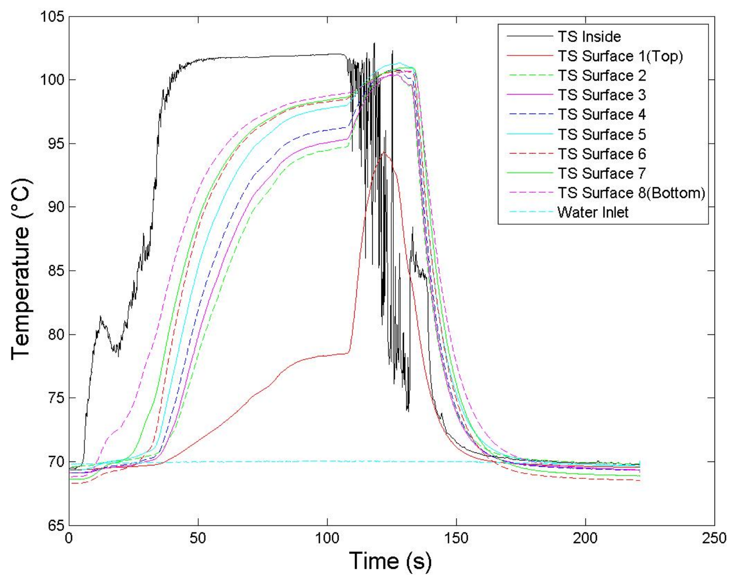

Fig. D.289.: Test section temperatures for test 73.

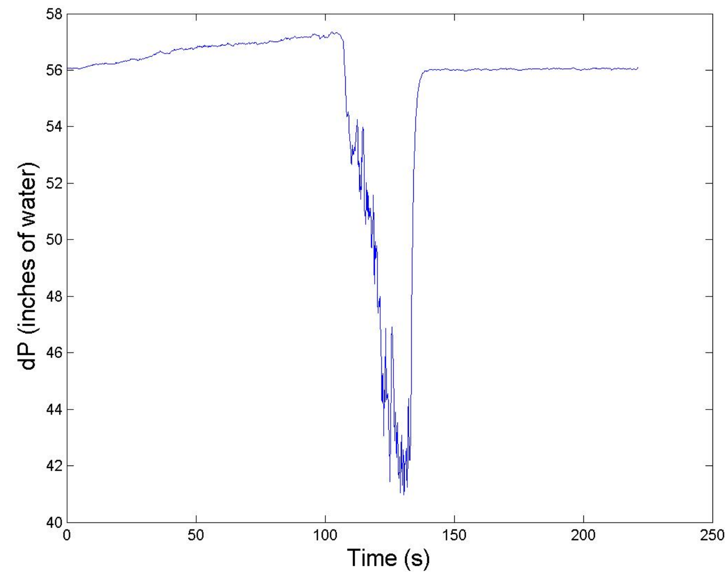

Fig. D.290.: Test section differential pressure for test 73.

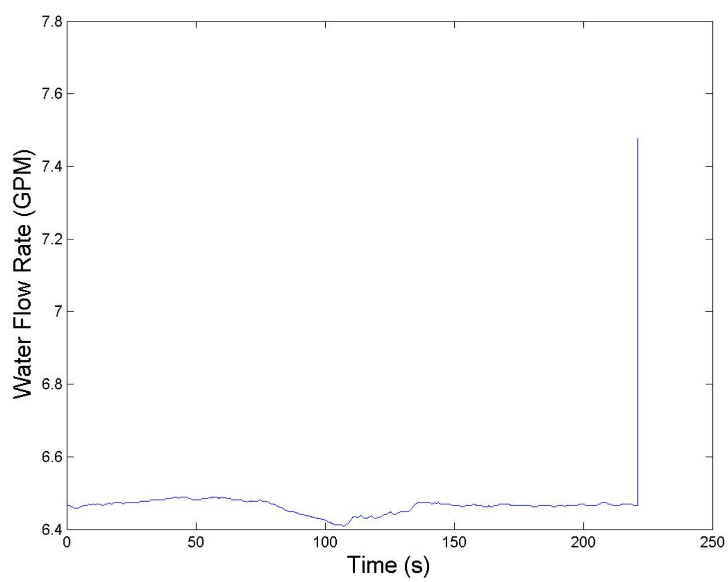

Fig. D.291.: Water flow rate for test 73.

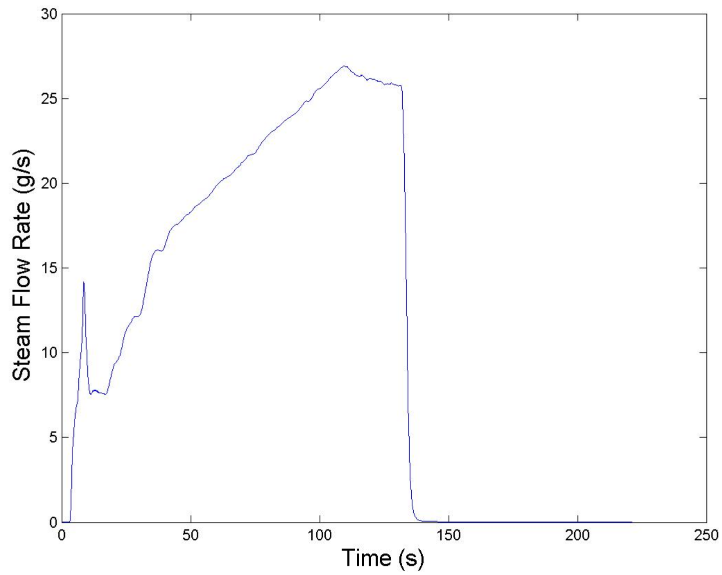

Fig. D.292.: Steam flow rate for test 73.

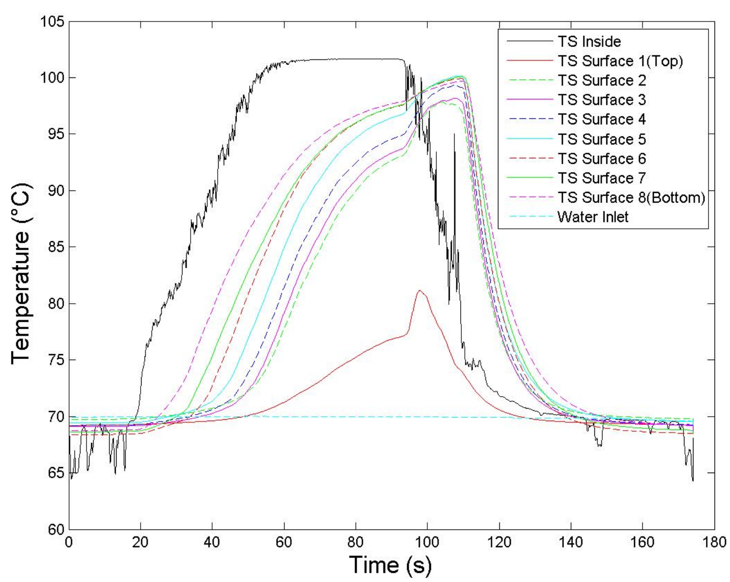

Fig. D.293.: Test section temperatures for test 74.

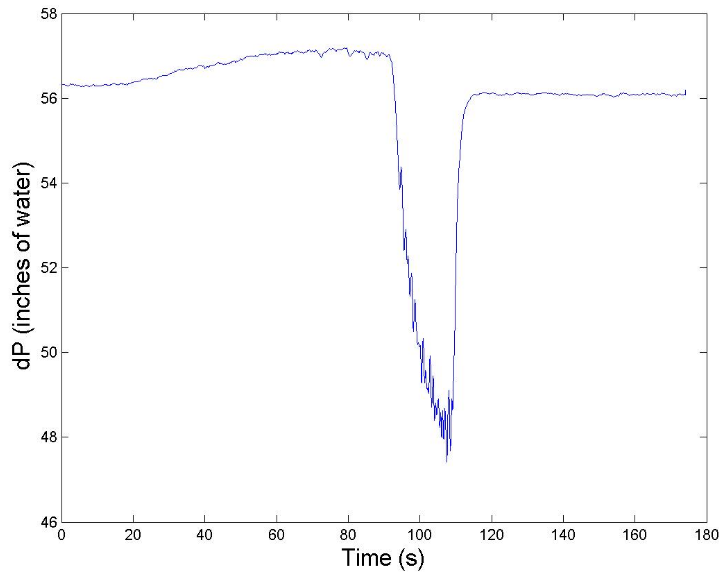

Fig. D.294.: Test section differential pressure for test 74.

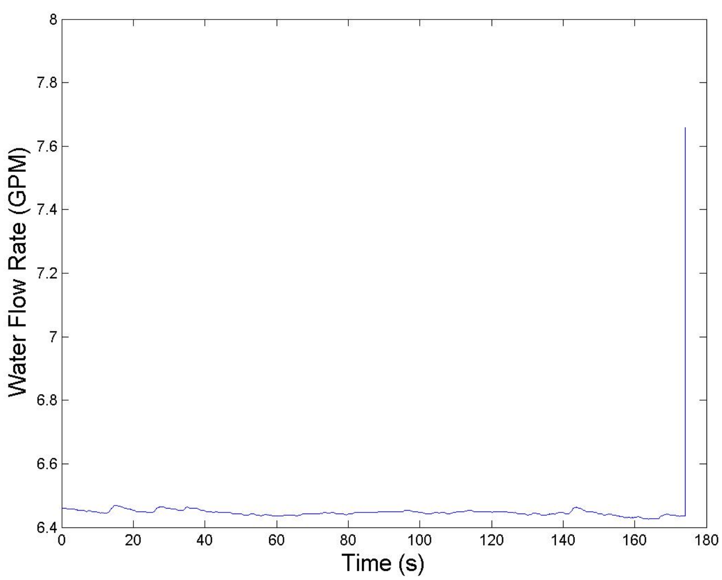

Fig. D.295.: Water flow rate for test 74.

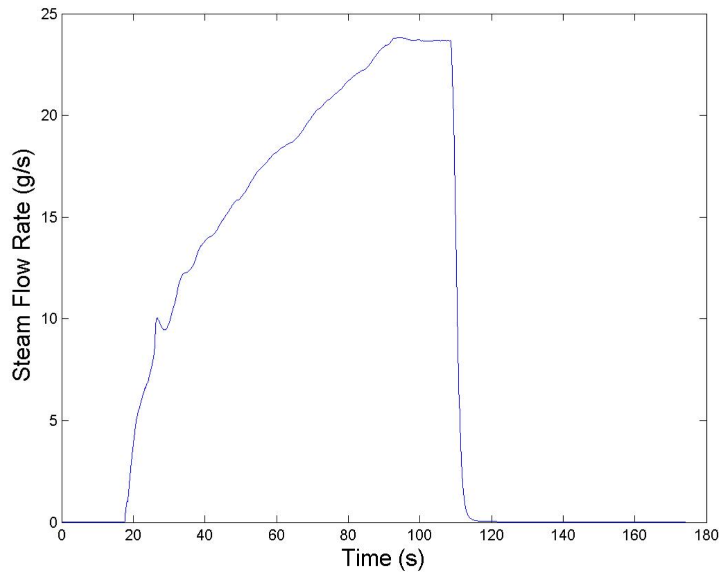

Fig. D.296.: Steam flow rate for test 74.

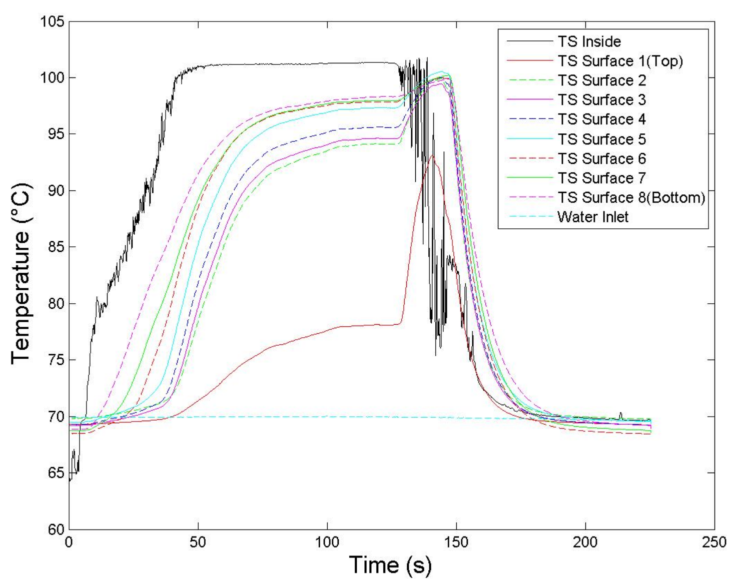

Fig. D.297.: Test section temperatures for test 75.

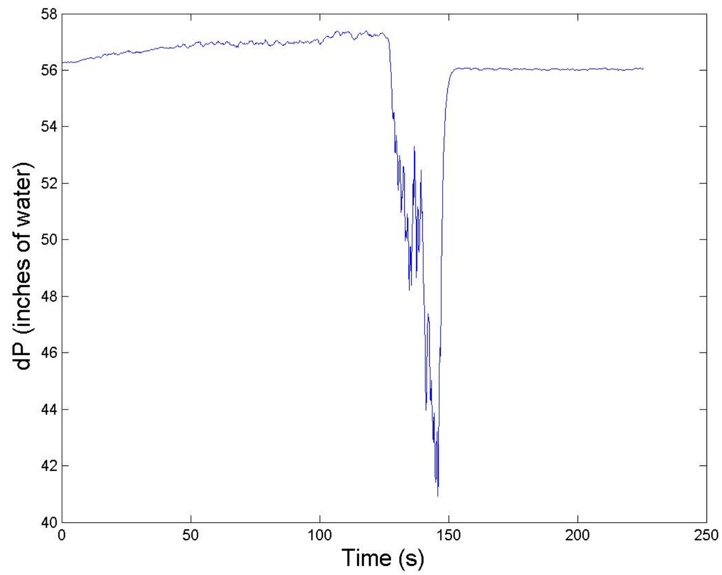

Fig. D.298.: Test section differential pressure for test 75.

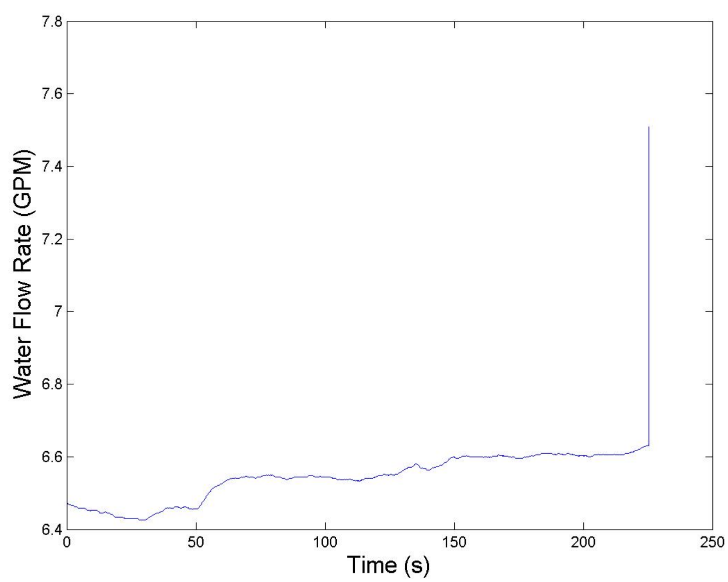

Fig. D.299.: Water flow rate for test 75.

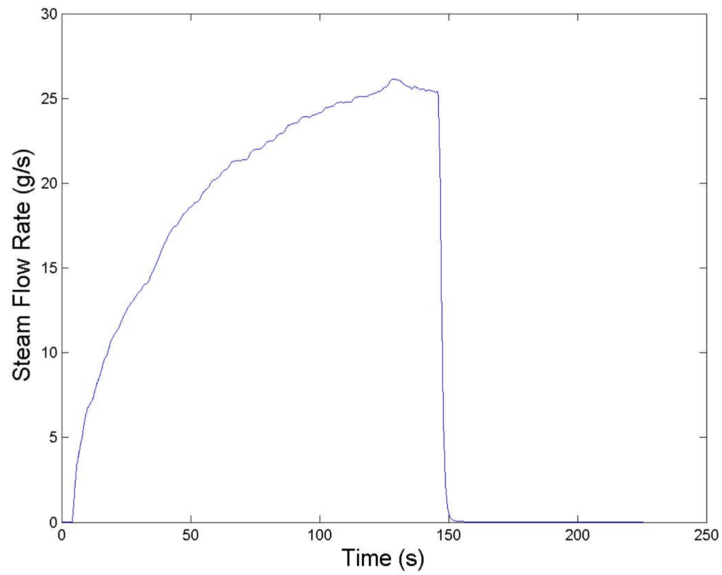

Fig. D.300.: Steam flow rate for test 75.

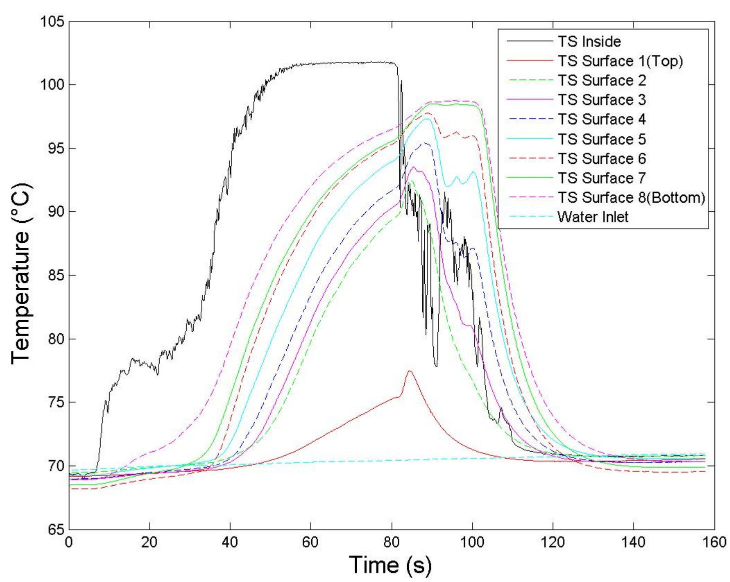

Fig. D.301.: Test section temperatures for test 76.

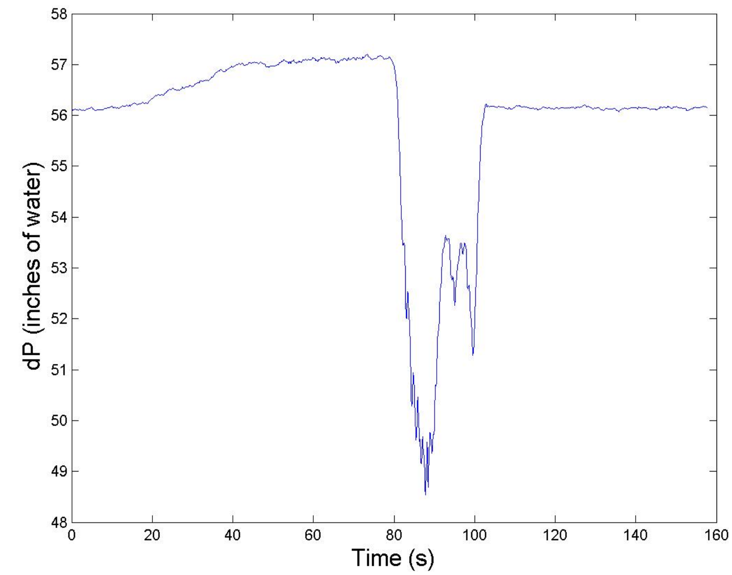

Fig. D.302.: Test section differential pressure for test 76.

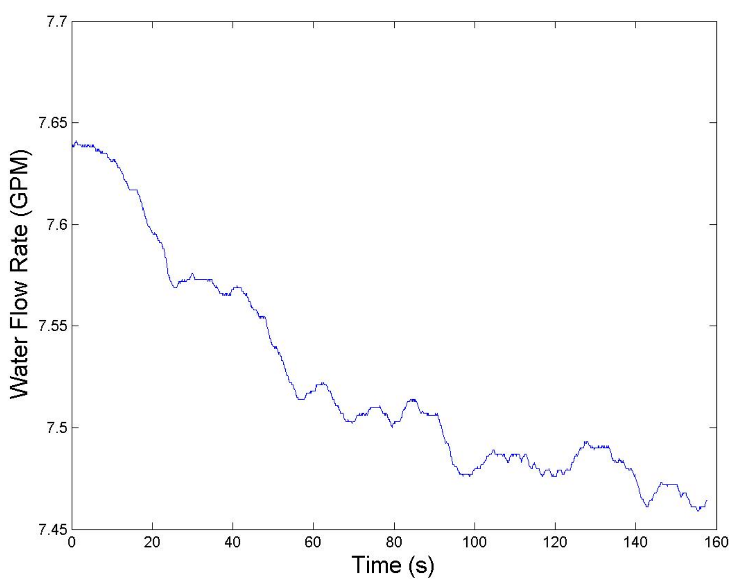

Fig. D.303.: Water flow rate for test 76.

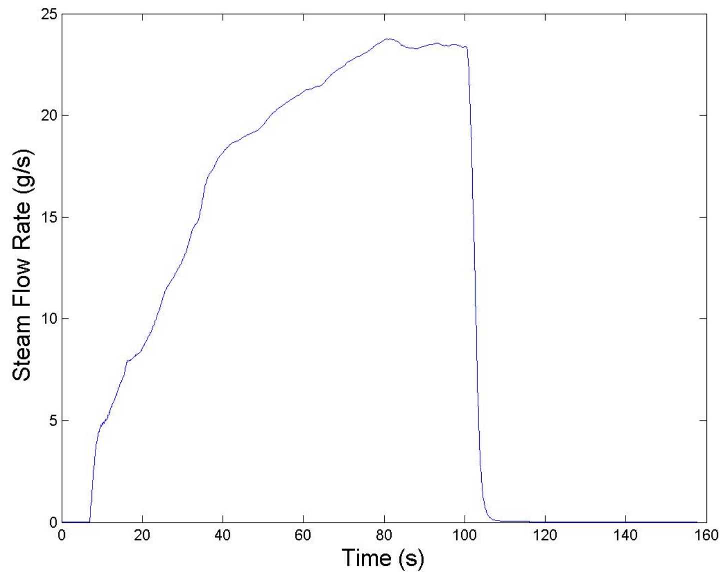

Fig. D.304.: Steam flow rate for test 76.

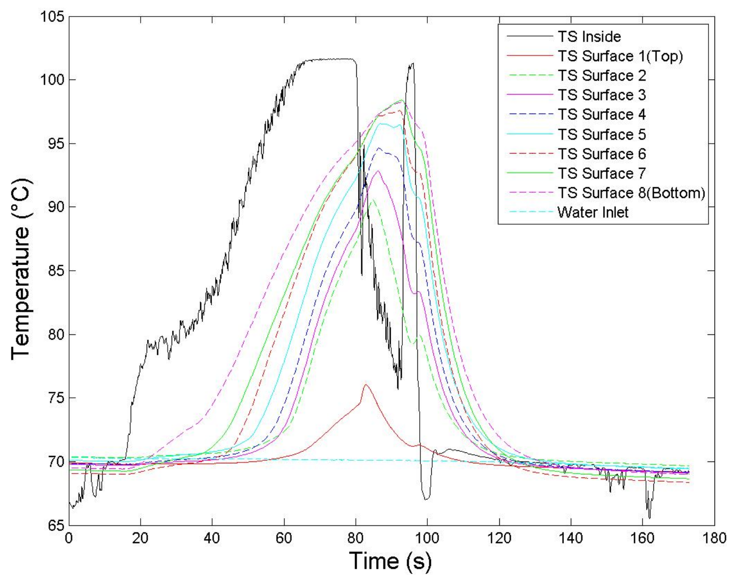

Fig. D.305.: Test section temperatures for test 77.

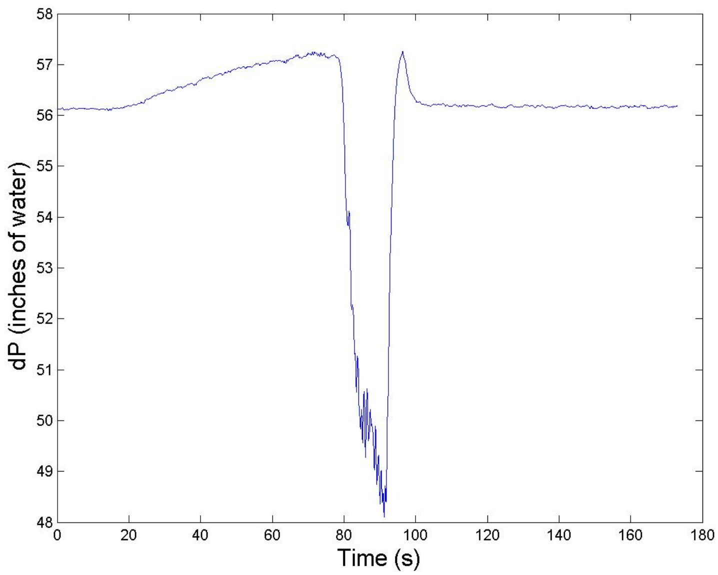

Fig. D.306.: Test section differential pressure for test 77.

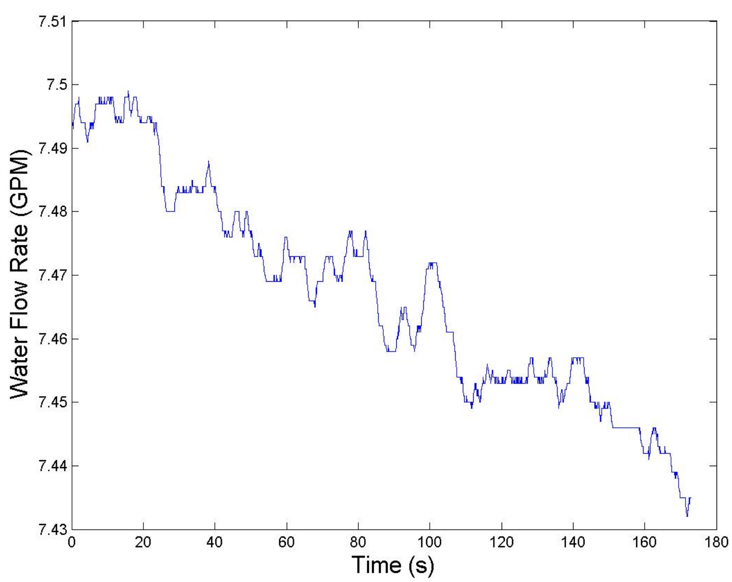

Fig. D.307.: Water flow rate for test 77.

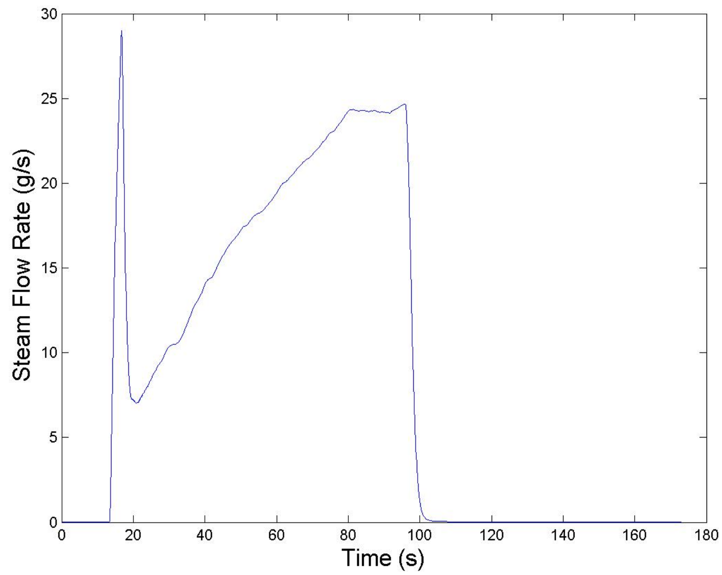

Fig. D.308.: Steam flow rate for test 77.

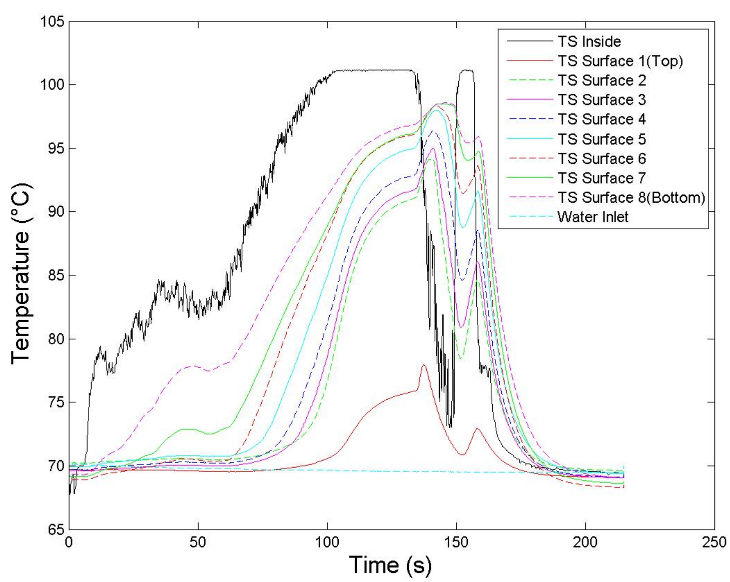

Fig. D.309.: Test section temperatures for test 78.

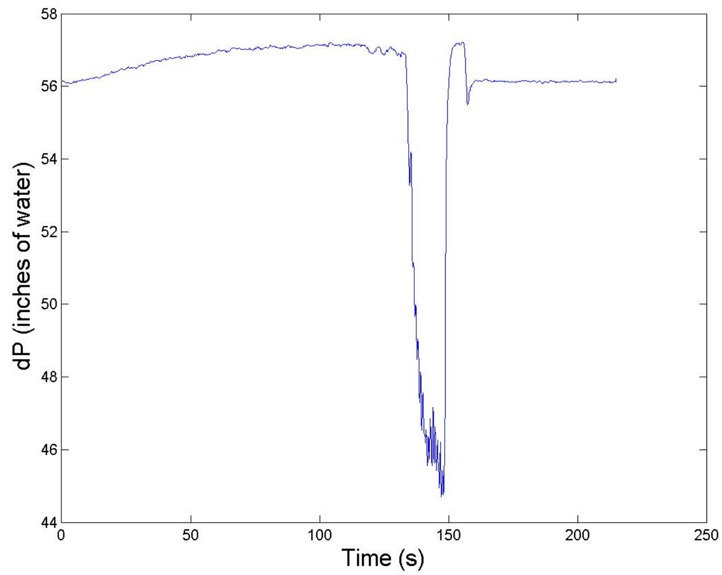

Fig. D.310.: Test section differential pressure for test 78.

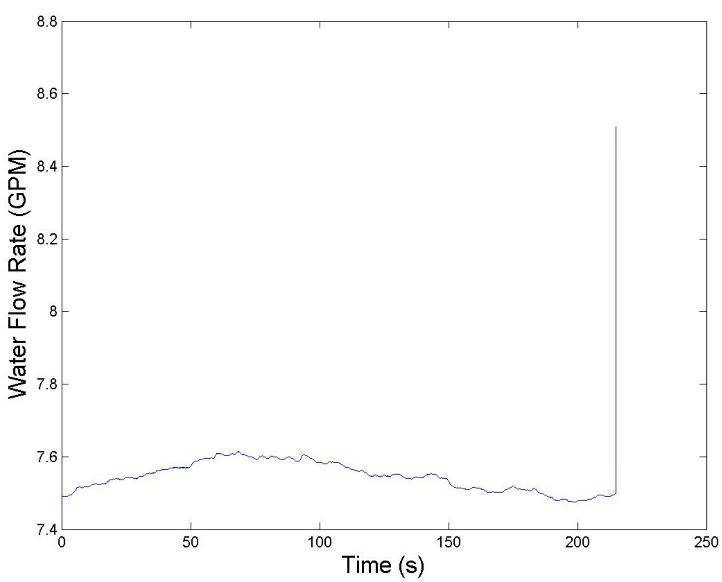

Fig. D.311.: Water flow rate for test 78.

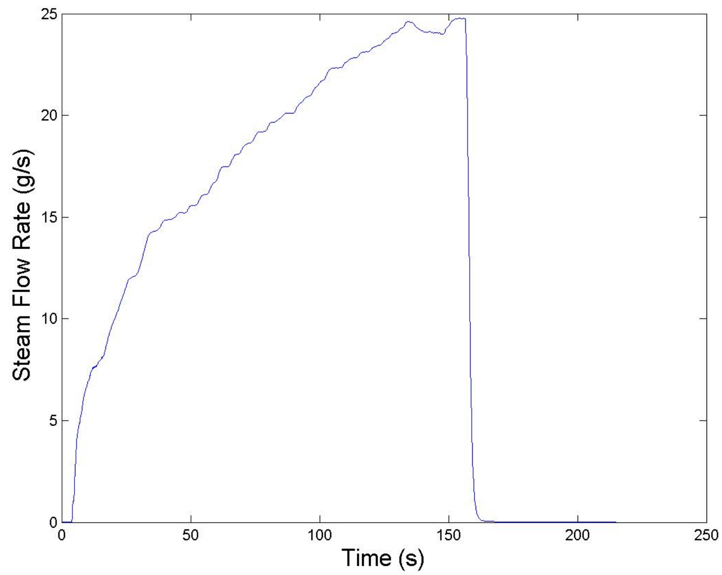

Fig. D.312.: Steam flow rate for test 78.

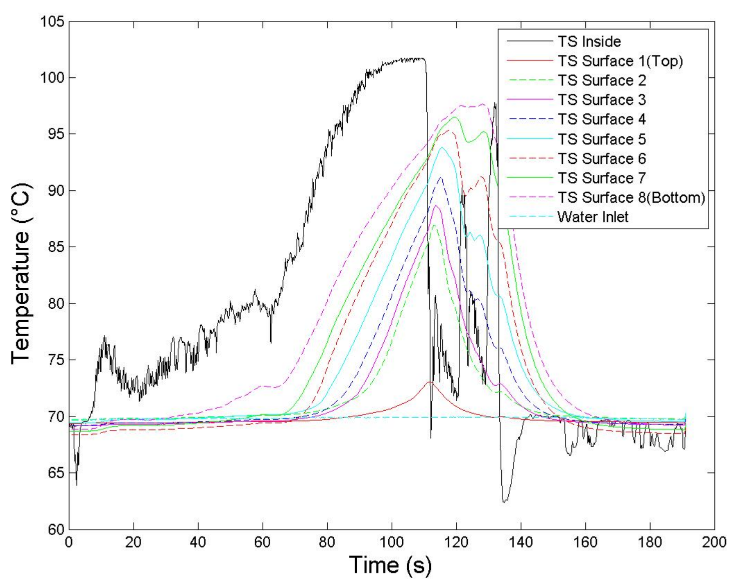

Fig. D.313.: Test section temperatures for test 79.

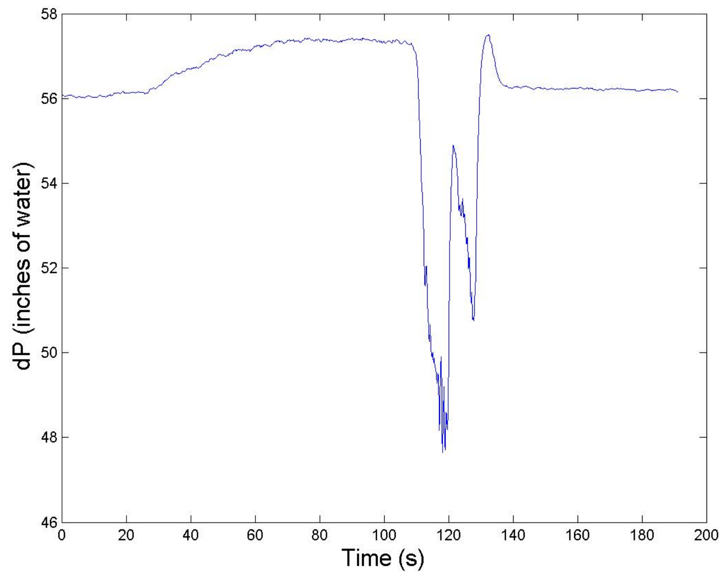

Fig. D.314.: Test section differential pressure for test 79.

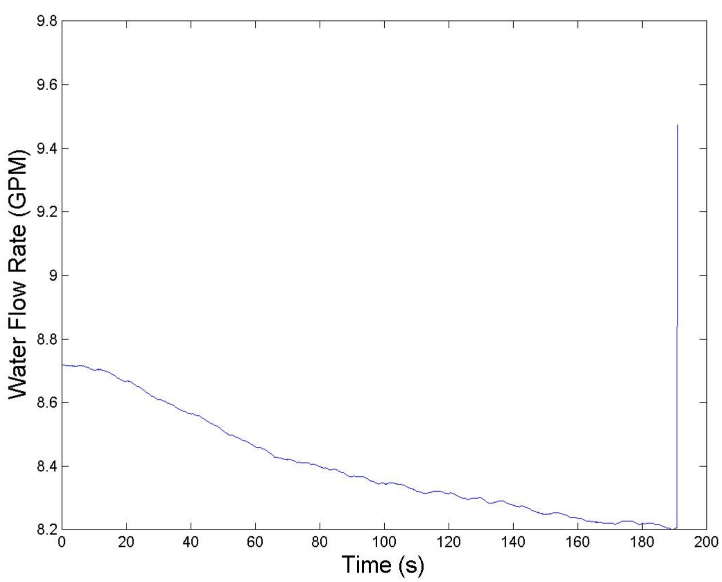

Fig. D.315.: Water flow rate for test 79.

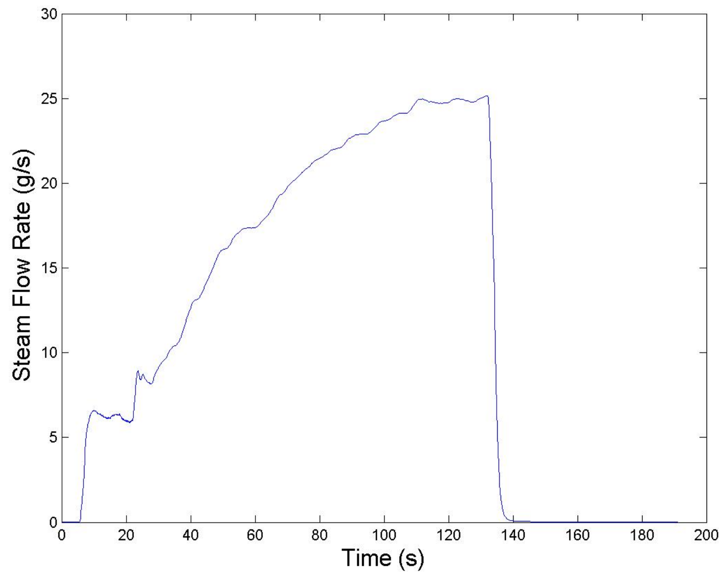

Fig. D.316.: Steam flow rate for test 79.

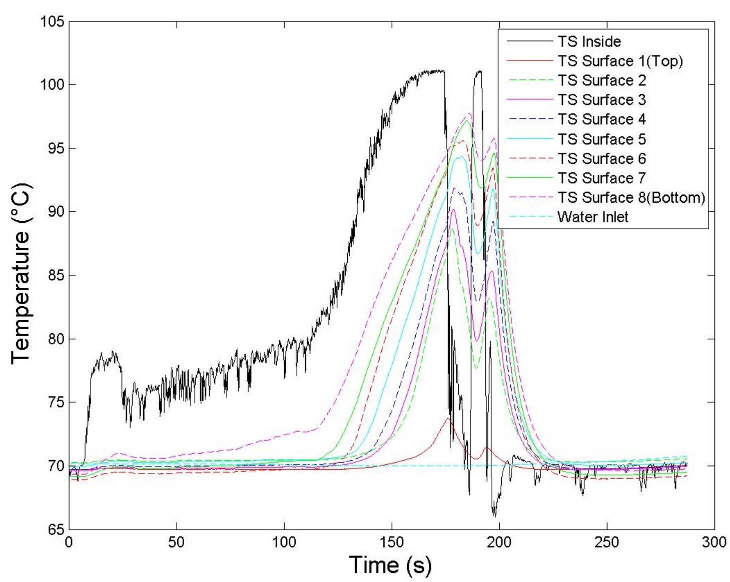

Fig. D.317.: Test section temperatures for test 80.

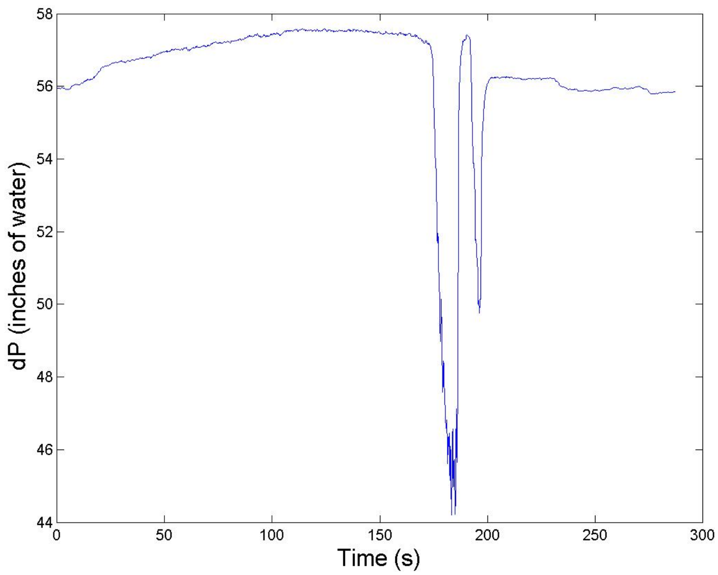

Fig. D.318.: Test section differential pressure for test 80.

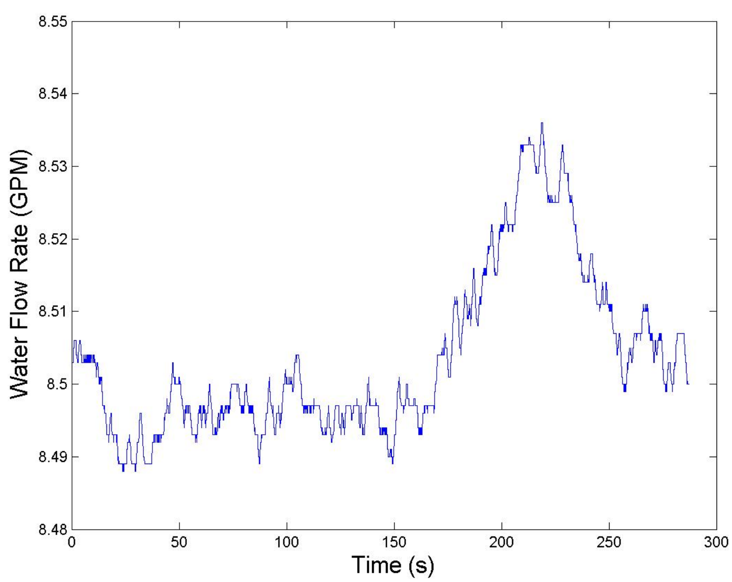

Fig. D.319.: Water flow rate for test 80.

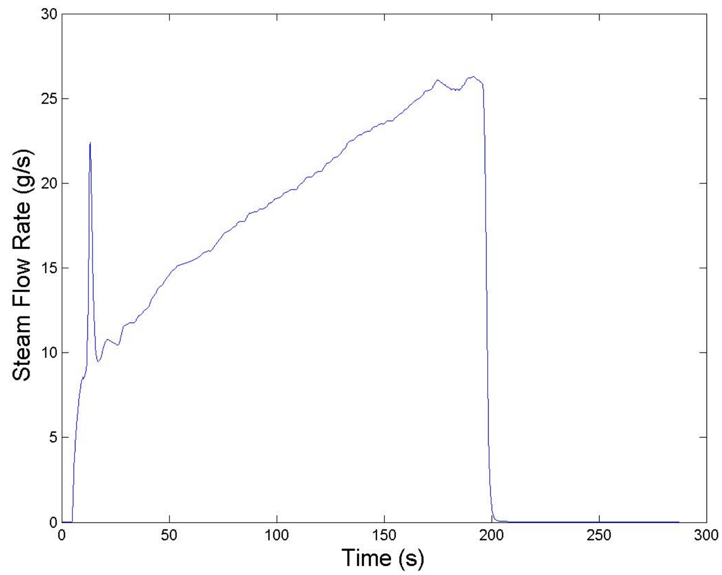

Fig. D.320.: Steam flow rate for test 80.

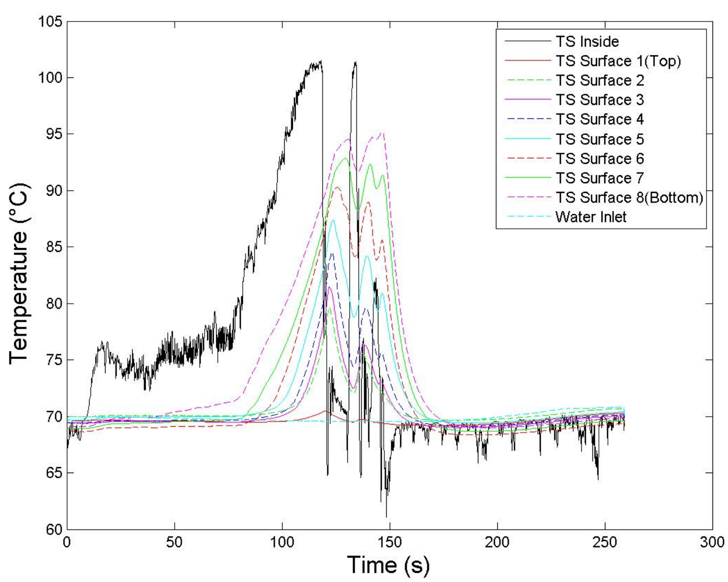

Fig. D.321.: Test section temperatures for test 81.

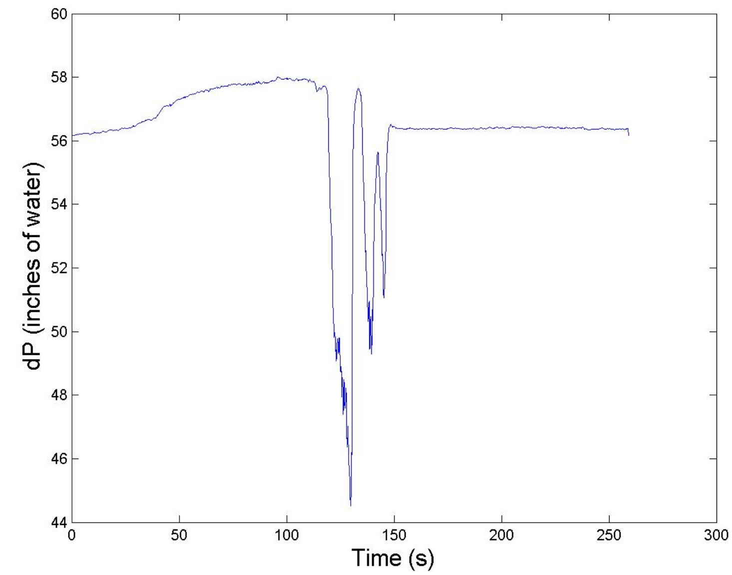

Fig. D.322.: Test section differential pressure for test 81.

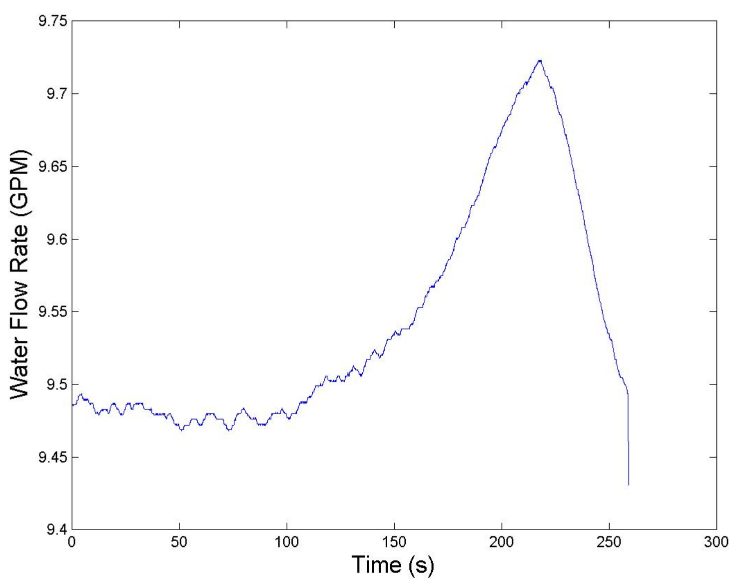

Fig. D.323.: Water flow rate for test 81.

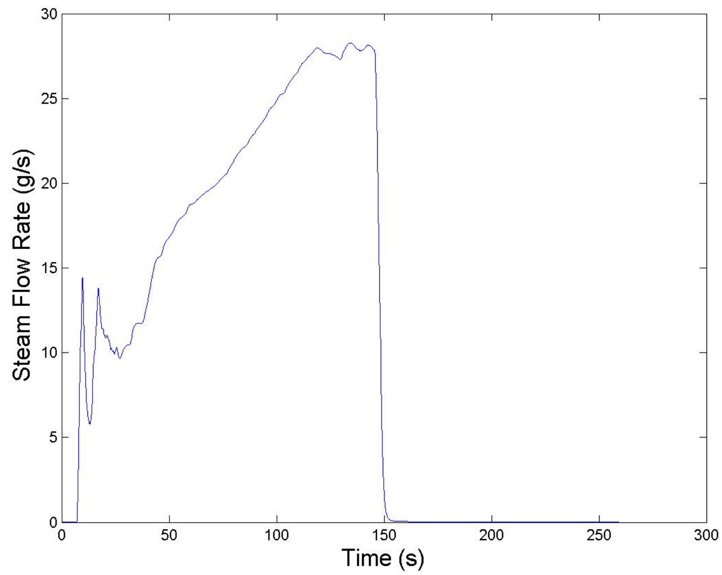

Fig. D.324.: Steam flow rate for test 81.

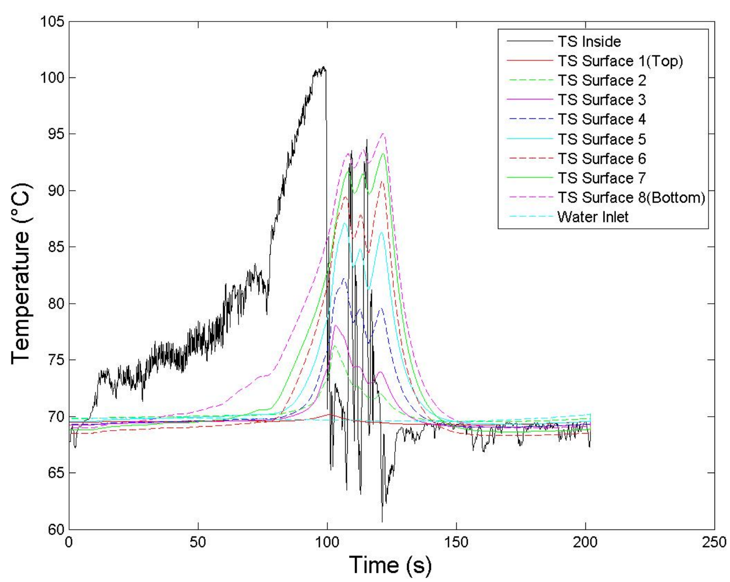

Fig. D.325.: Test section temperatures for test 82.

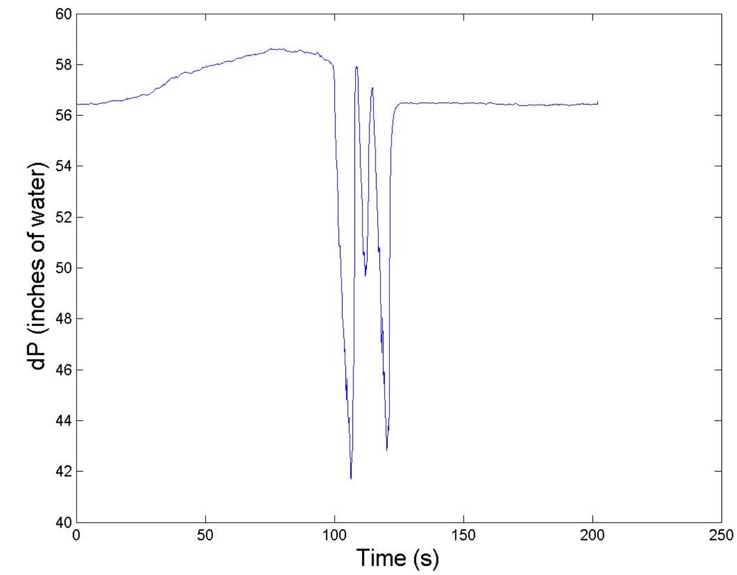

Fig. D.326.: Test section differential pressure for test 82.

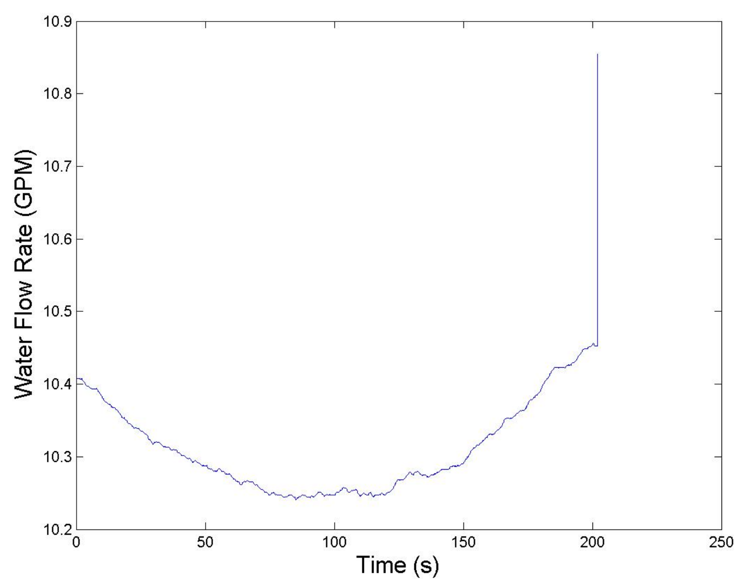

Fig. D.327.: Water flow rate for test 82.

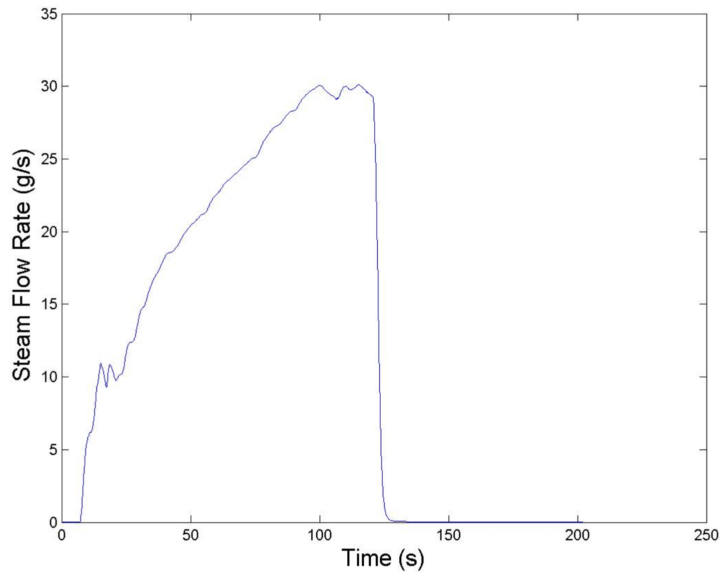

Fig. D.328.: Steam flow rate for test 82.

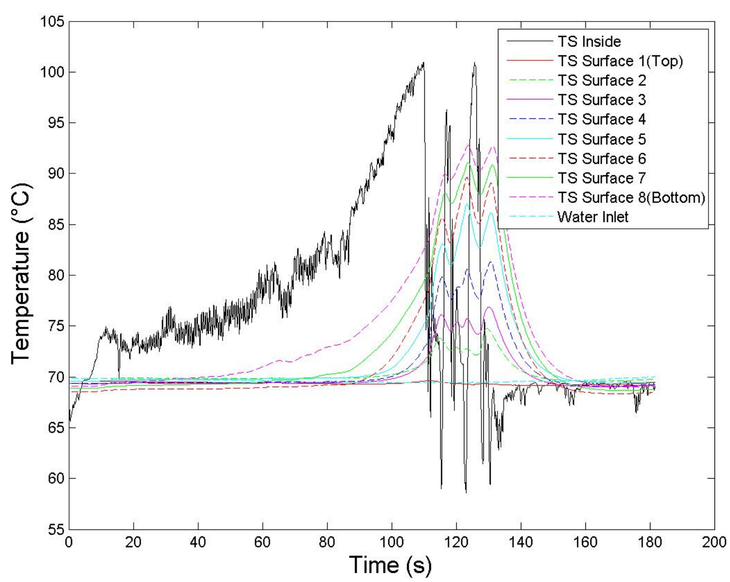

Fig. D.329.: Test section temperatures for test 83.

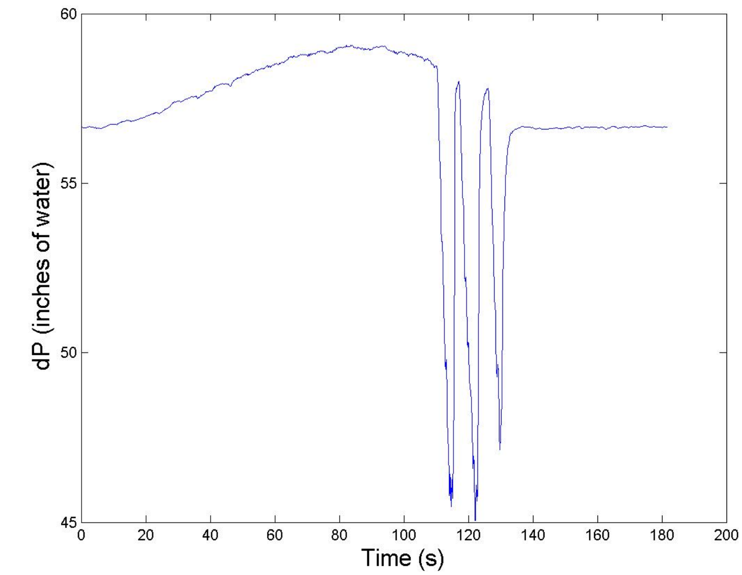

Fig. D.330.: Test section differential pressure for test 83.

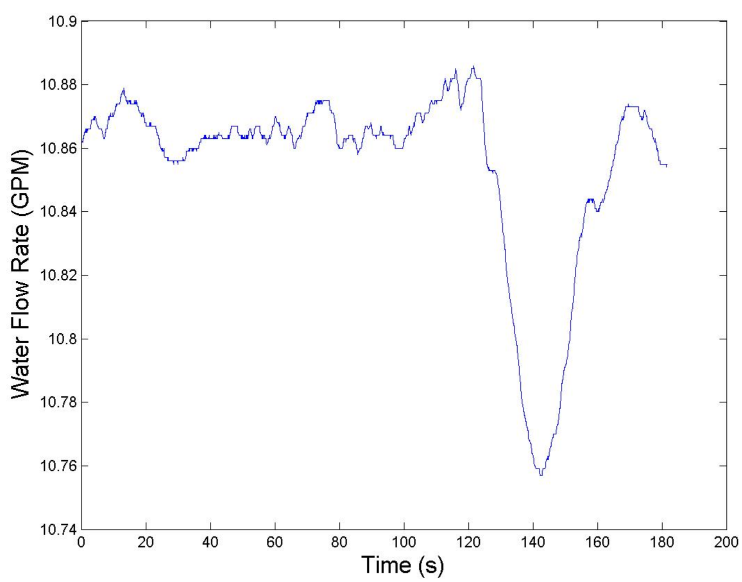

Fig. D.331.: Water flow rate for test 83.

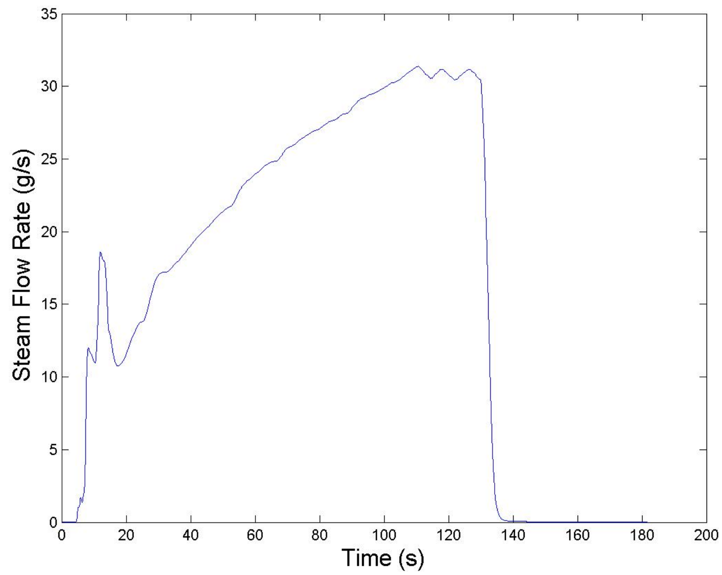

Fig. D.332.: Steam flow rate for test 83.

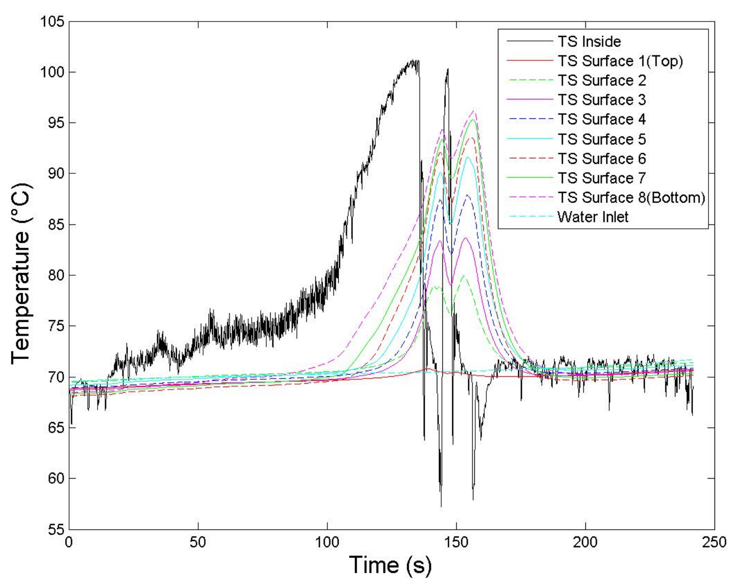

Fig. D.333.: Test section temperatures for test 84.

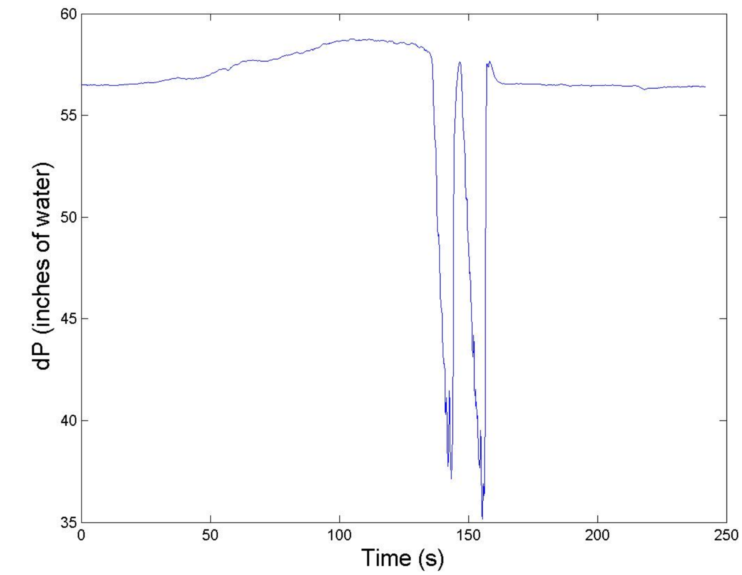

Fig. D.334.: Test section differential pressure for test 84.

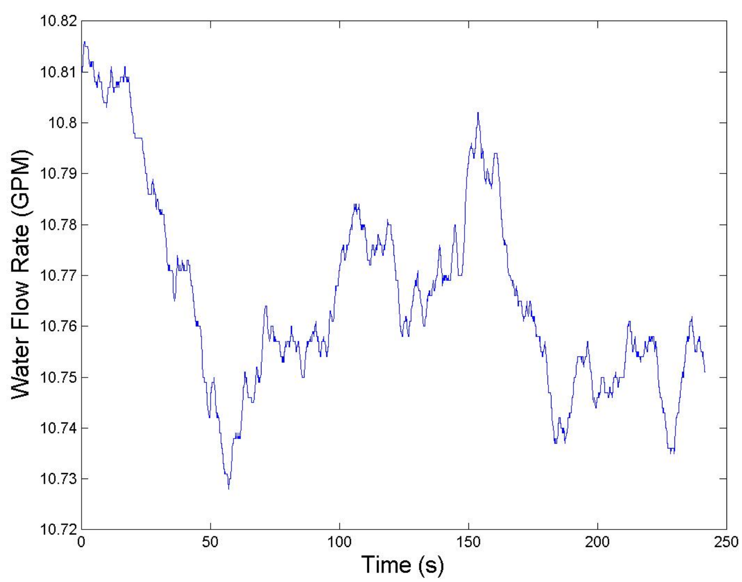

Fig. D.335.: Water flow rate for test 84.

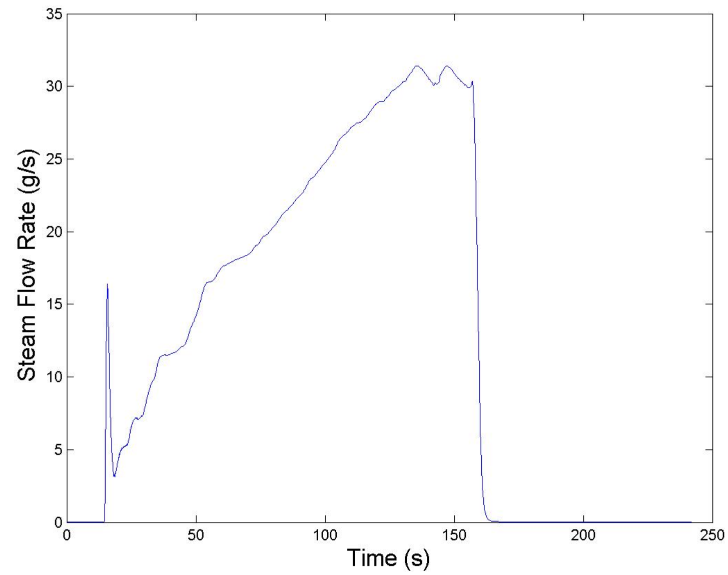

Fig. D.336.: Steam flow rate for test 84.

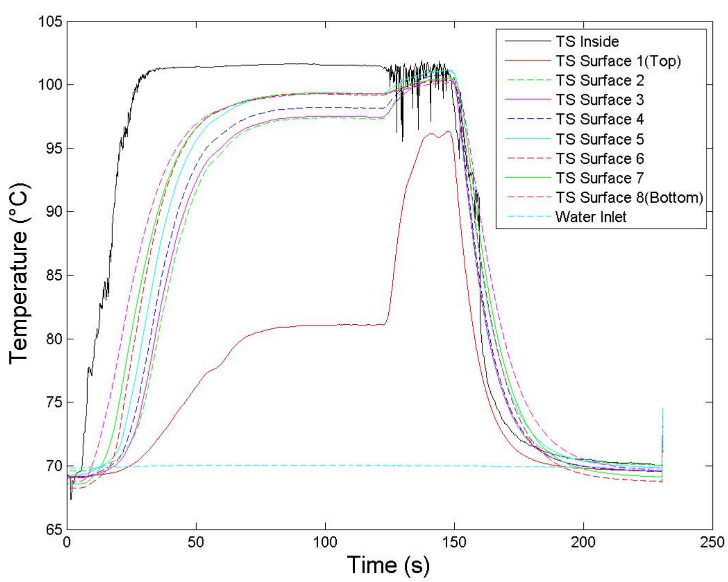

Fig. D.337.: Test section temperatures for test 85.

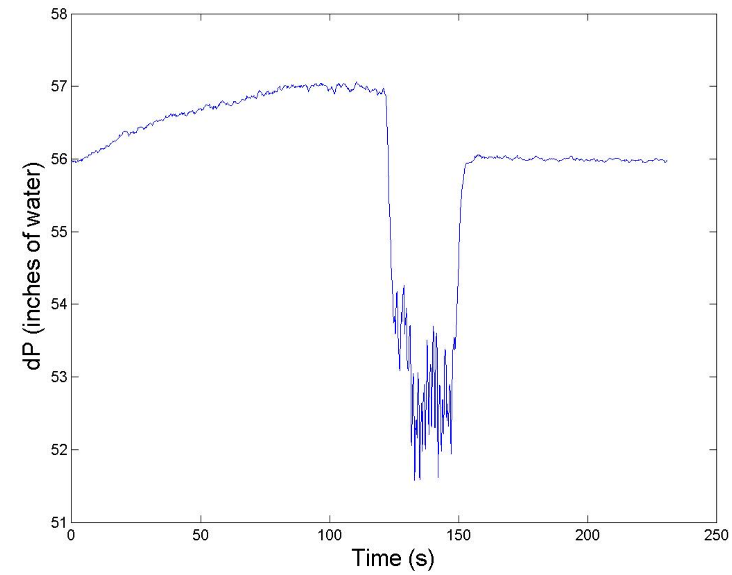

Fig. D.338.: Test section differential pressure for test 85.

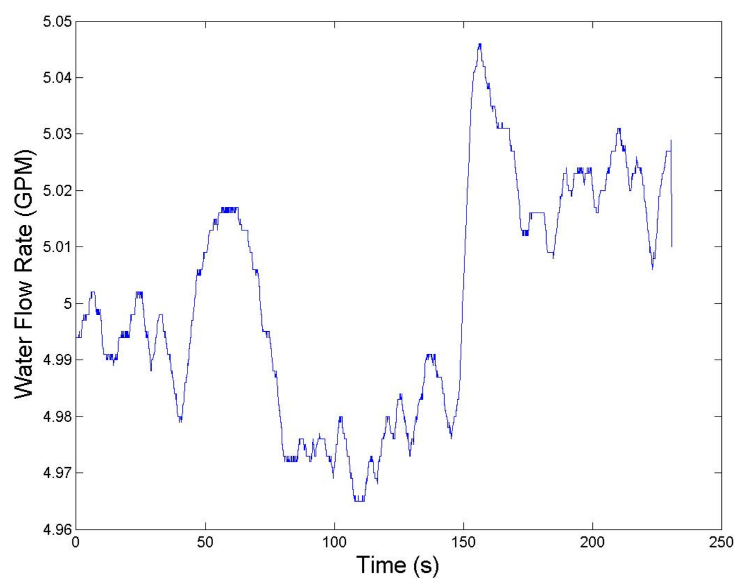

Fig. D.339.: Water flow rate for test 85.

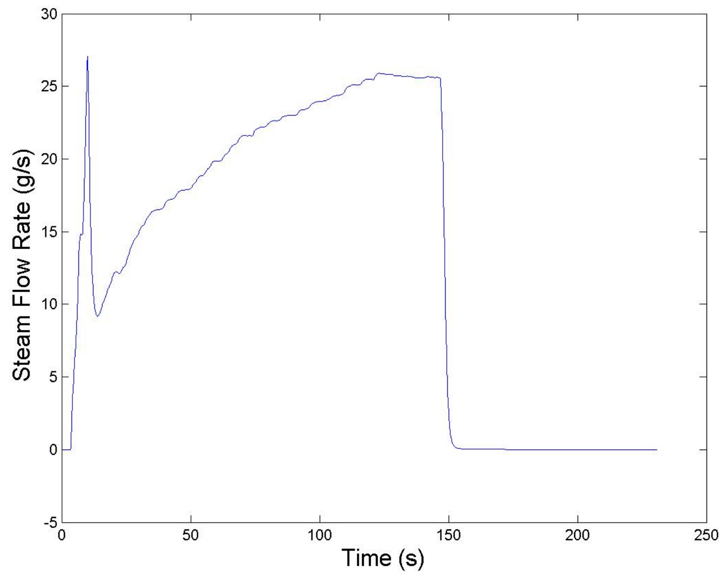

Fig. D.340.: Steam flow rate for test 85.

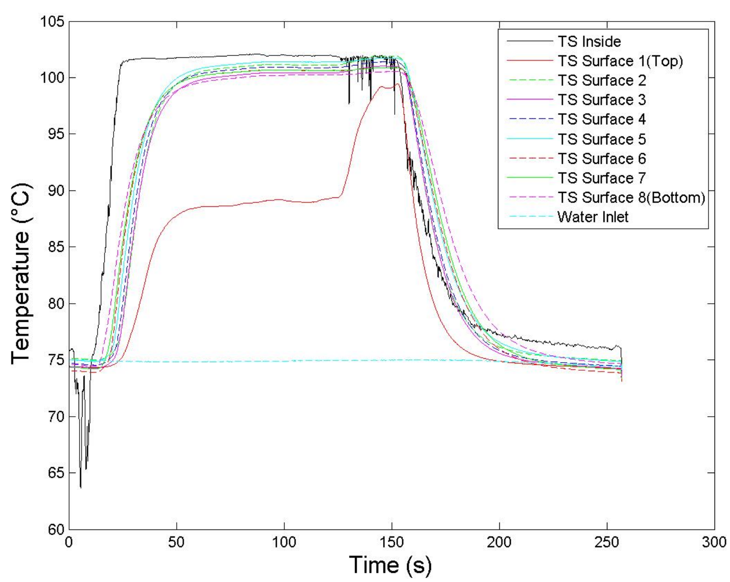

Fig. D.341.: Test section temperatures for test 86.

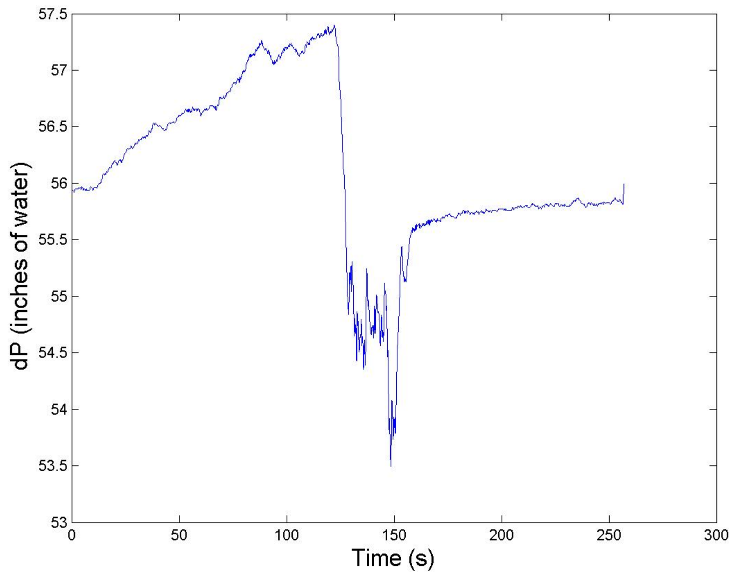

Fig. D.342.: Test section differential pressure for test 86.

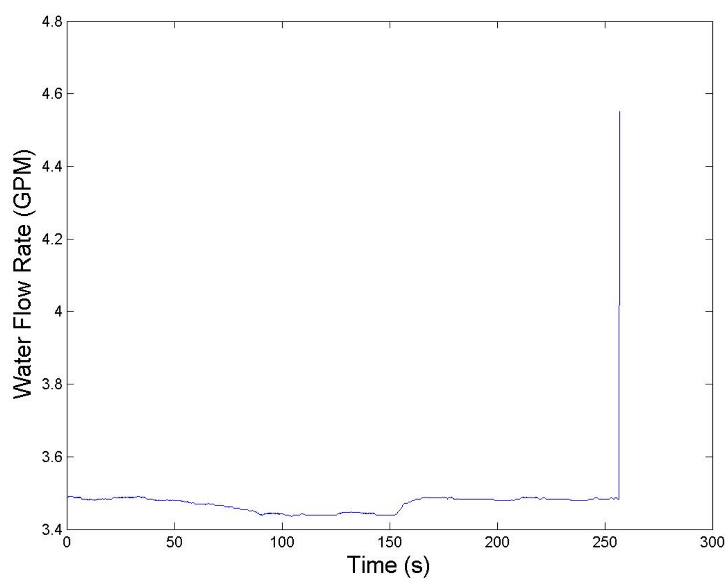

Fig. D.343.: Water flow rate for test 86.

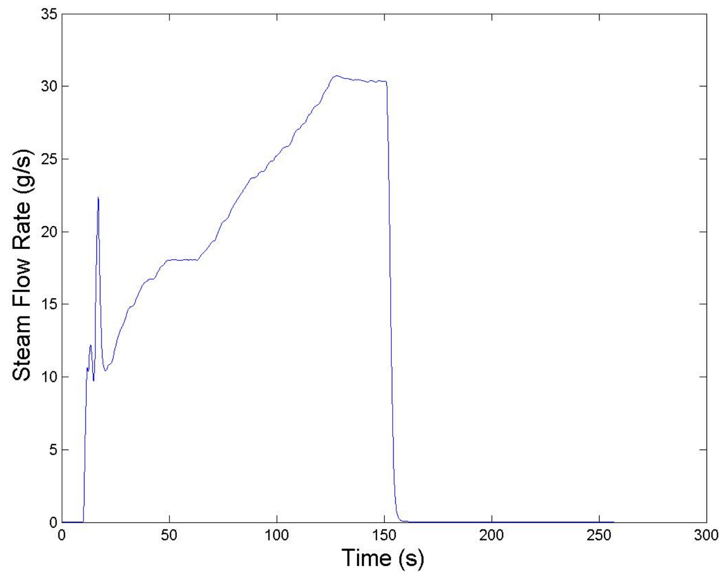

Fig. D.344.: Steam flow rate for test 86.

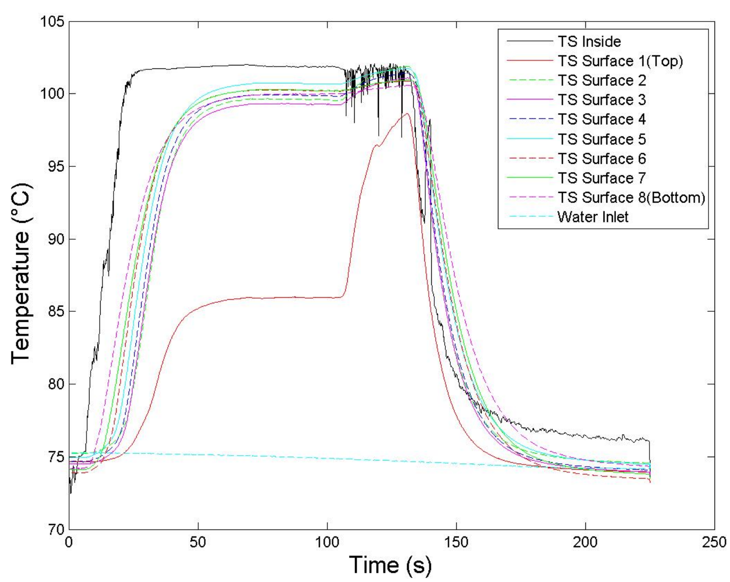

Fig. D.345.: Test section temperatures for test 87.

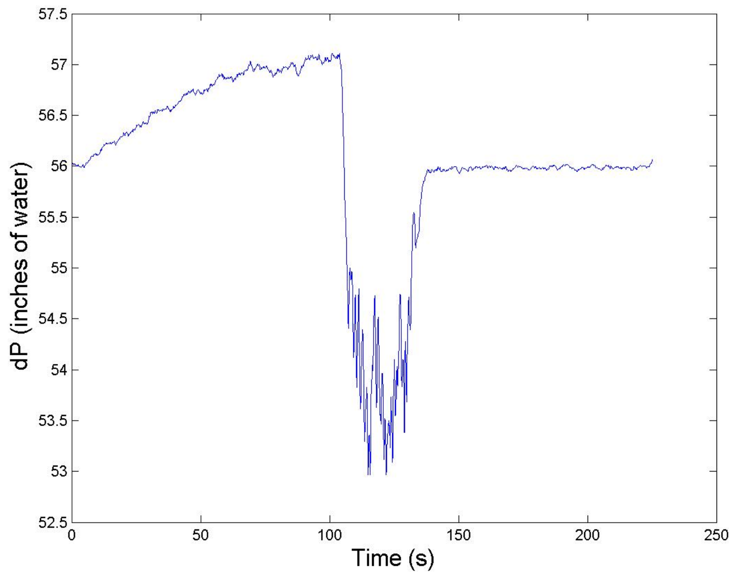

Fig. D.346.: Test section differential pressure for test 87.

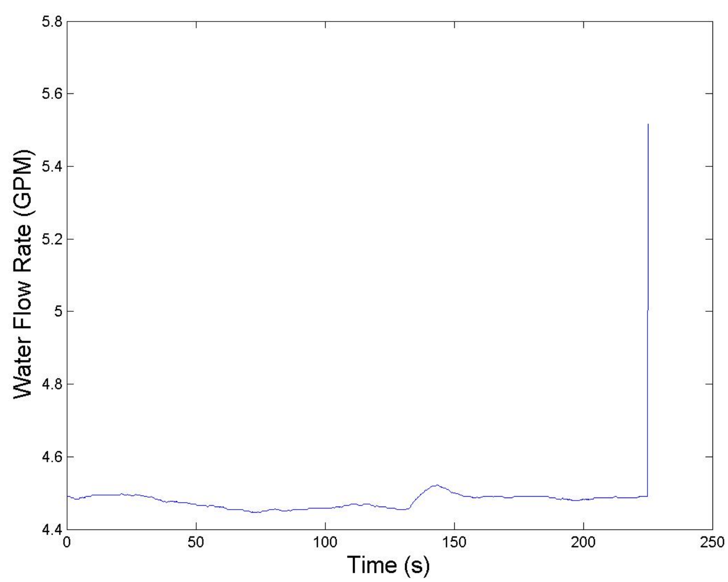

Fig. D.347.: Water flow rate for test 87.

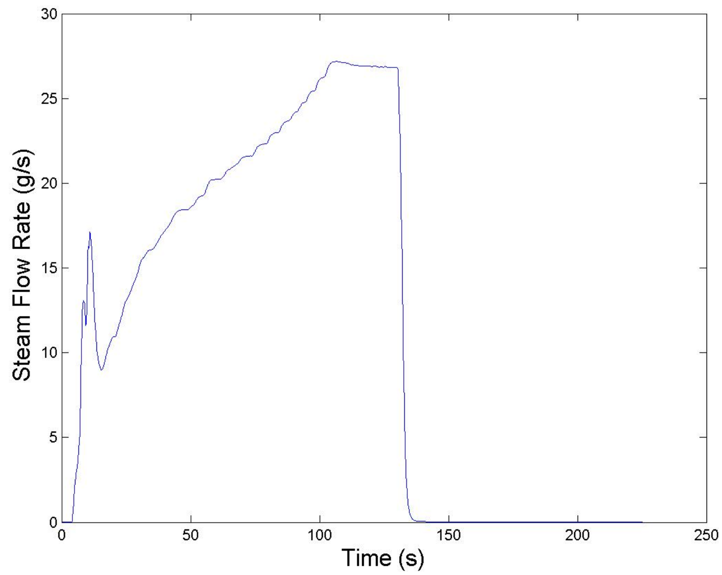

Fig. D.348.: Steam flow rate for test 87.

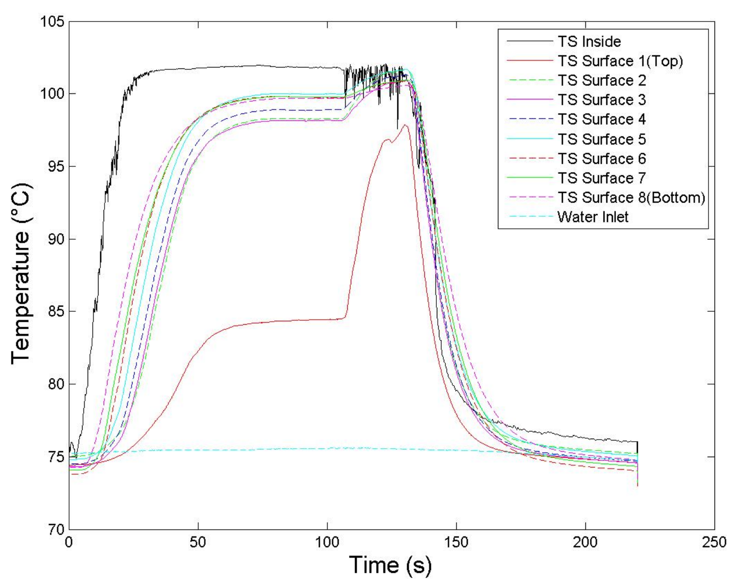

Fig. D.349.: Test section temperatures for test 88.

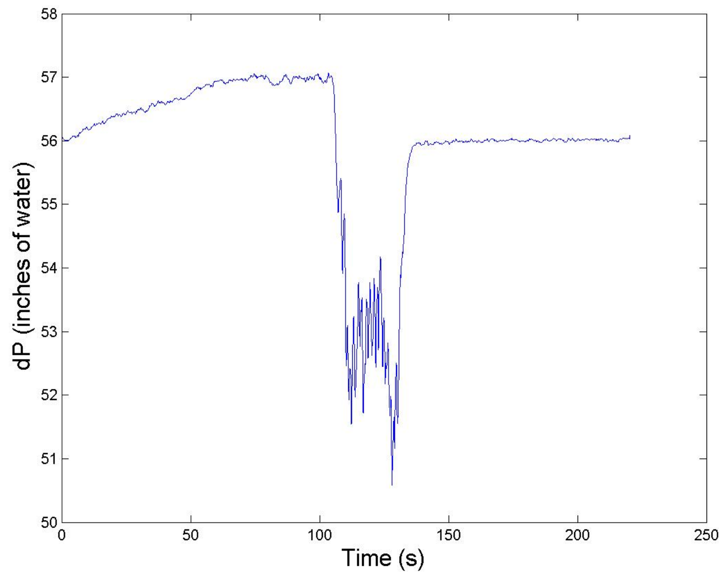

Fig. D.350.: Test section differential pressure for test 88.

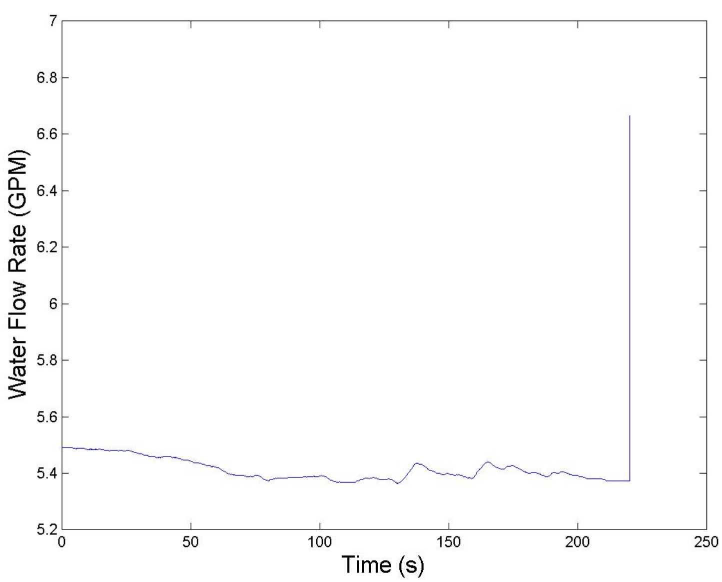

Fig. D.351.: Water flow rate for test 88.

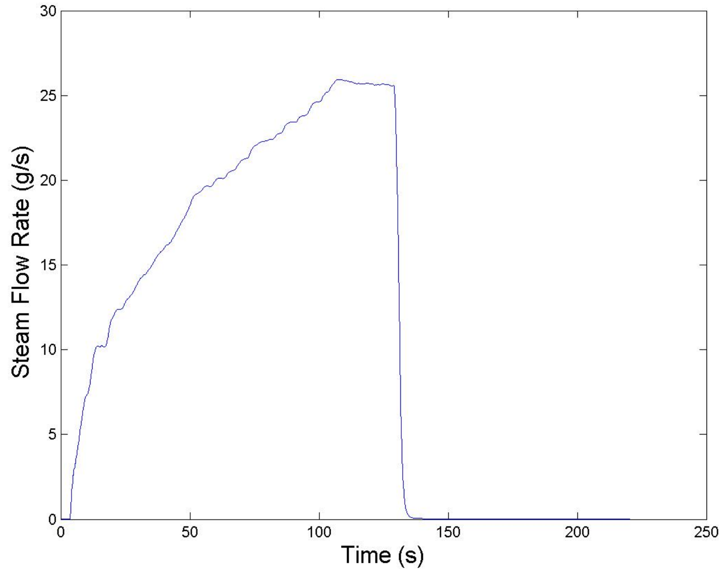

Fig. D.352.: Steam flow rate for test 88.

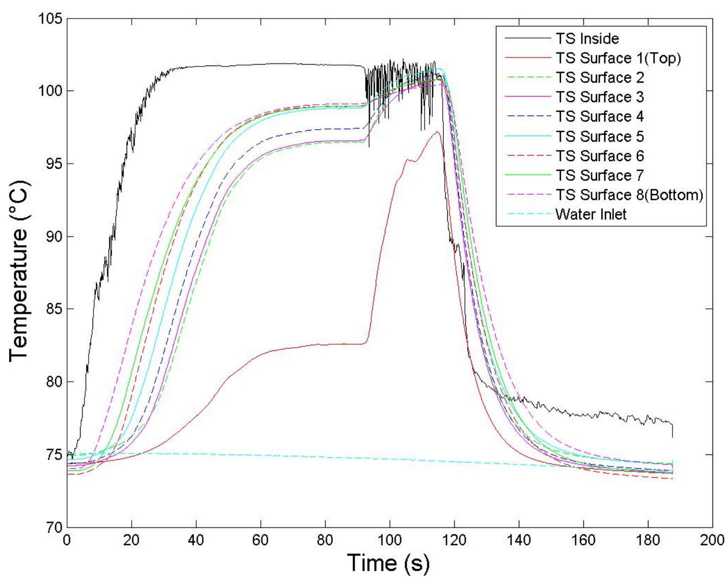

Fig. D.353.: Test section temperatures for test 89.

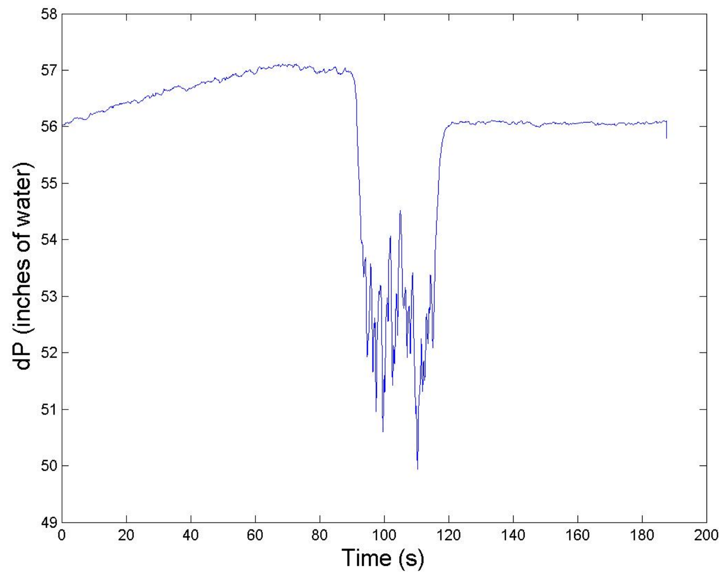

Fig. D.354.: Test section differential pressure for test 89.

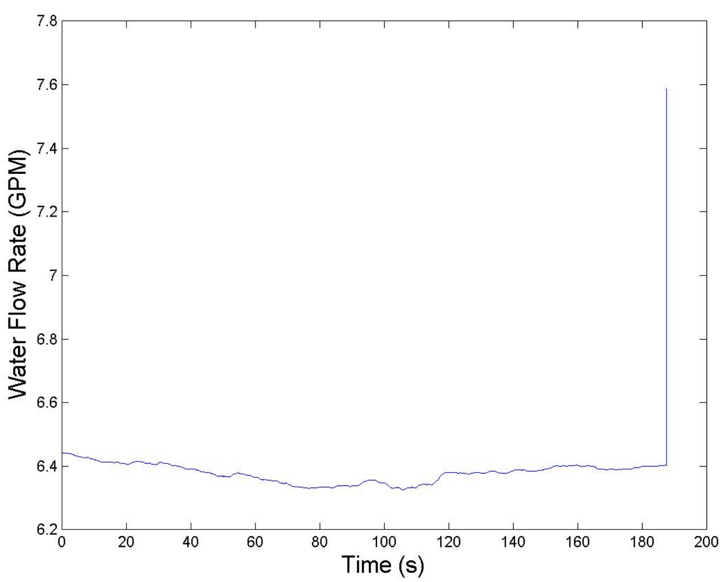

Fig. D.355.: Water flow rate for test 89.

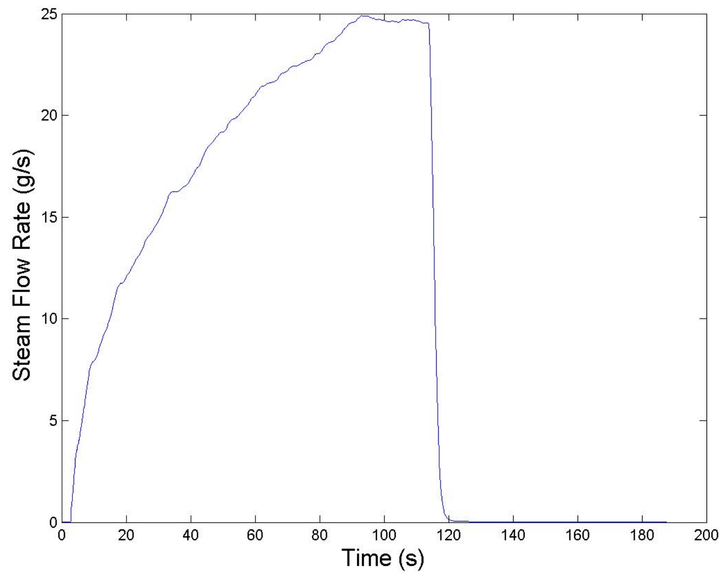

Fig. D.356.: Steam flow rate for test 89.

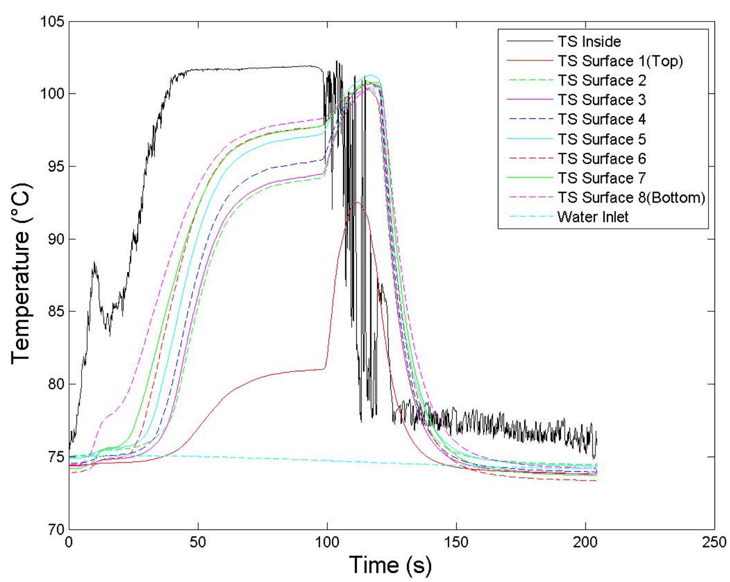

Fig. D.357.: Test section temperatures for test 90.

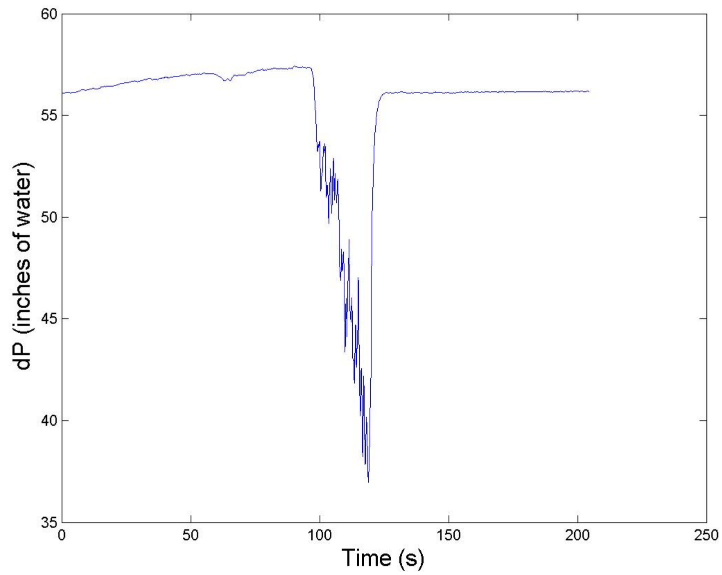

Fig. D.358.: Test section differential pressure for test 90.

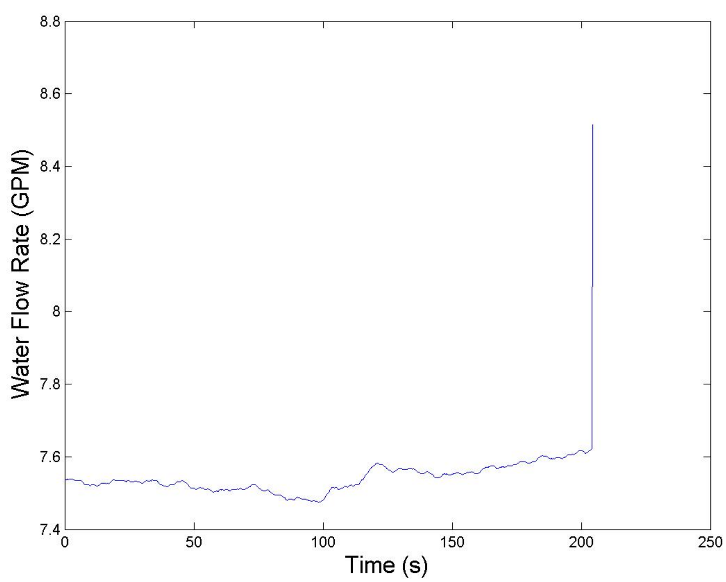

Fig. D.359.: Water flow rate for test 90.

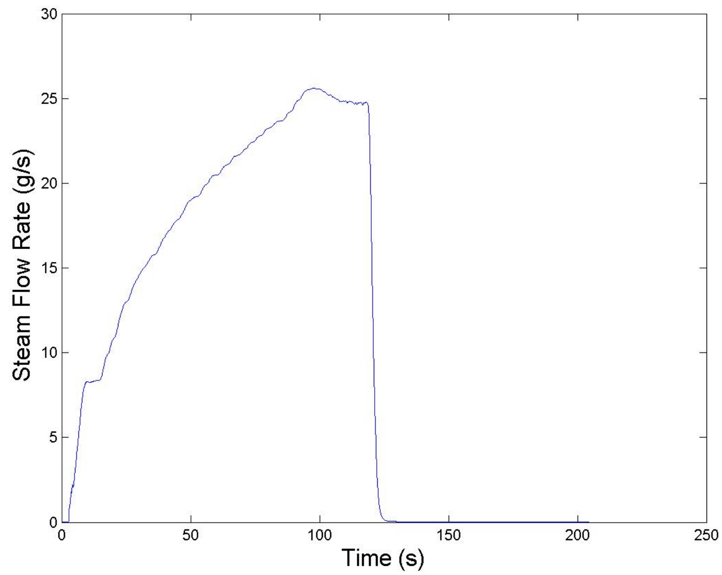

Fig. D.360.: Steam flow rate for test 90.

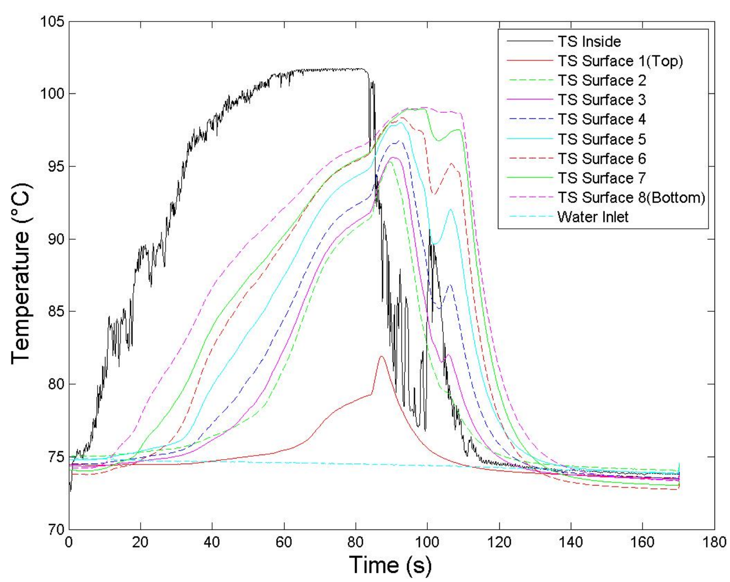

Fig. D.361.: Test section temperatures for test 91.

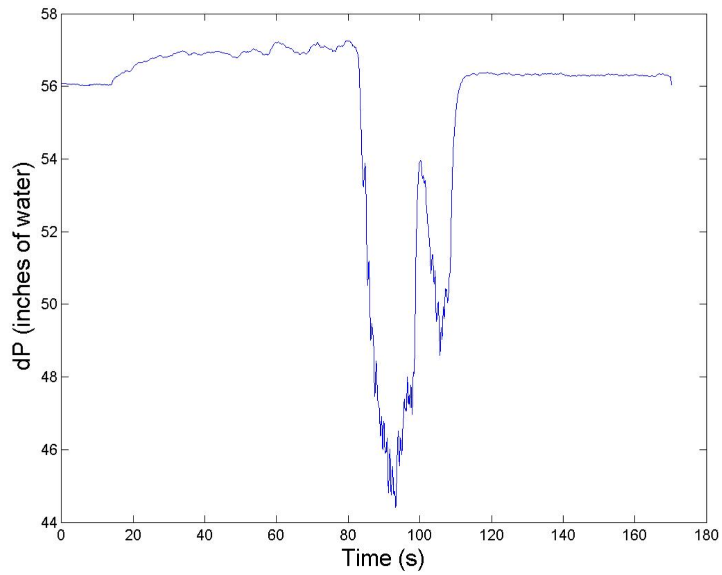

Fig. D.362.: Test section differential pressure for test 91.

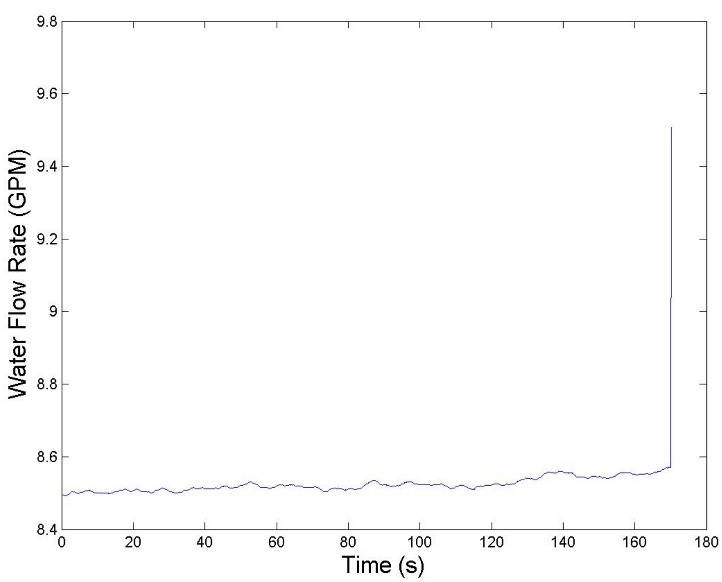

Fig. D.363.: Water flow rate for test 91.

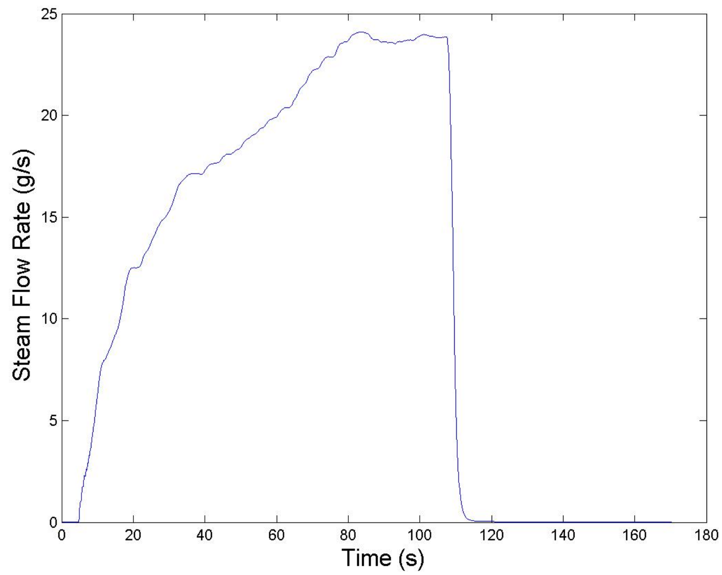

Fig. D.364.: Steam flow rate for test 91.

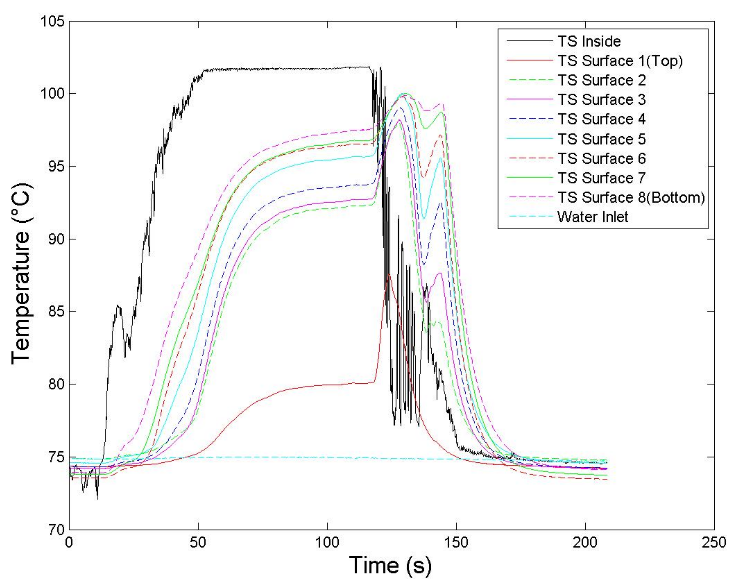

Fig. D.365.: Test section temperatures for test 92.

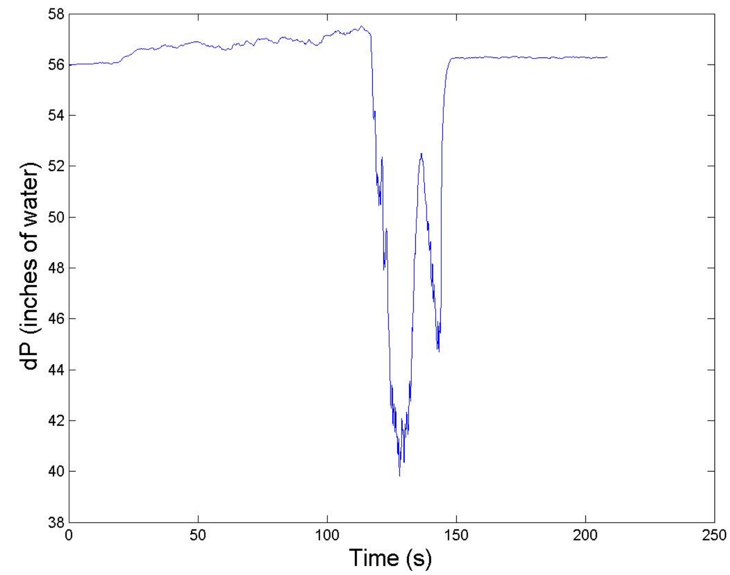

Fig. D.366.: Test section differential pressure for test 92.

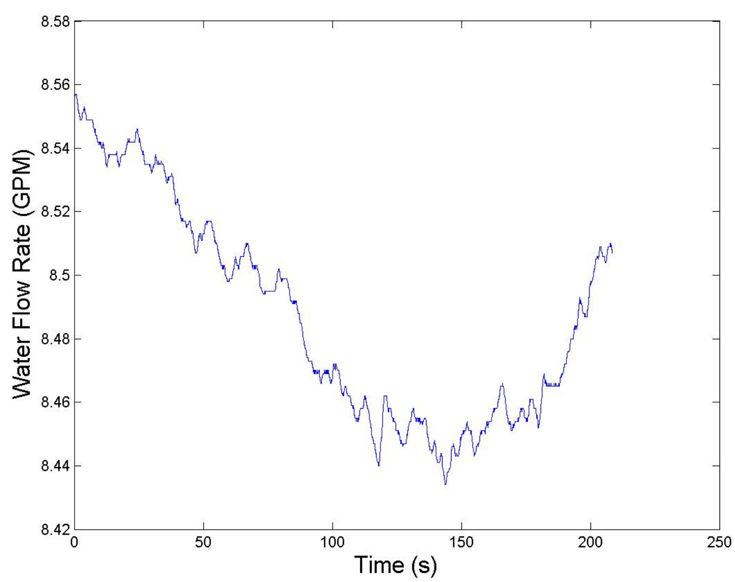

Fig. D.367.: Water flow rate for test 92.

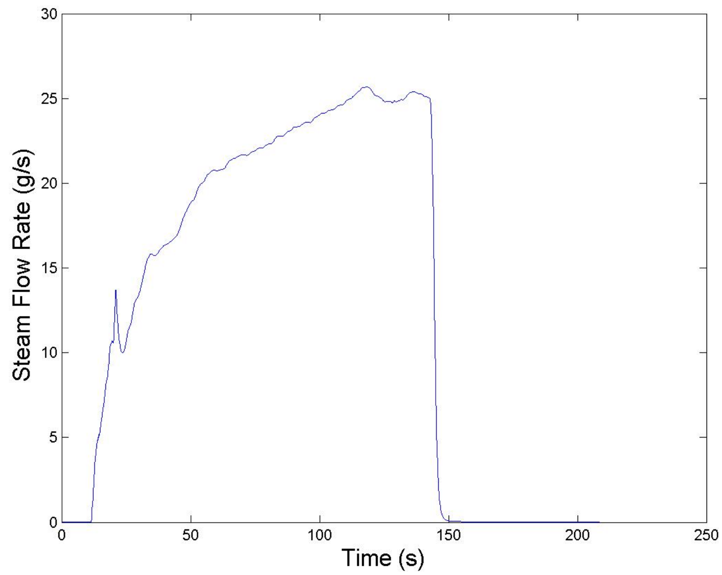

Fig. D.368.: Steam flow rate for test 92.

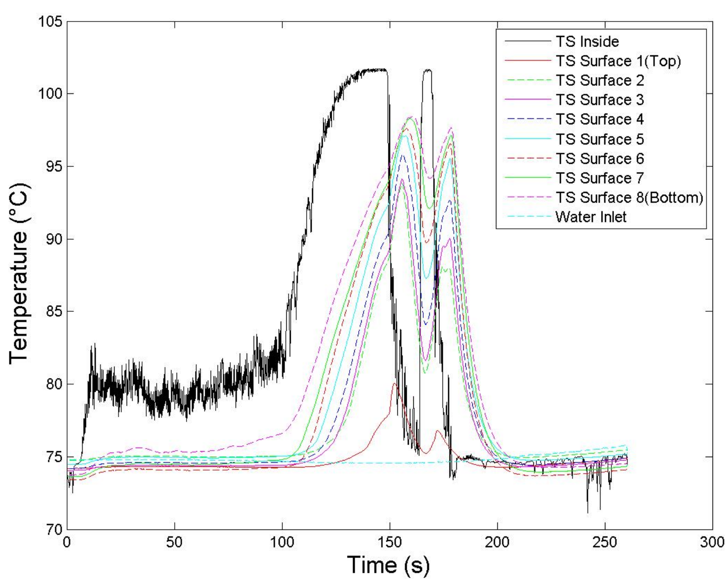

Fig. D.369.: Test section temperatures for test 93.

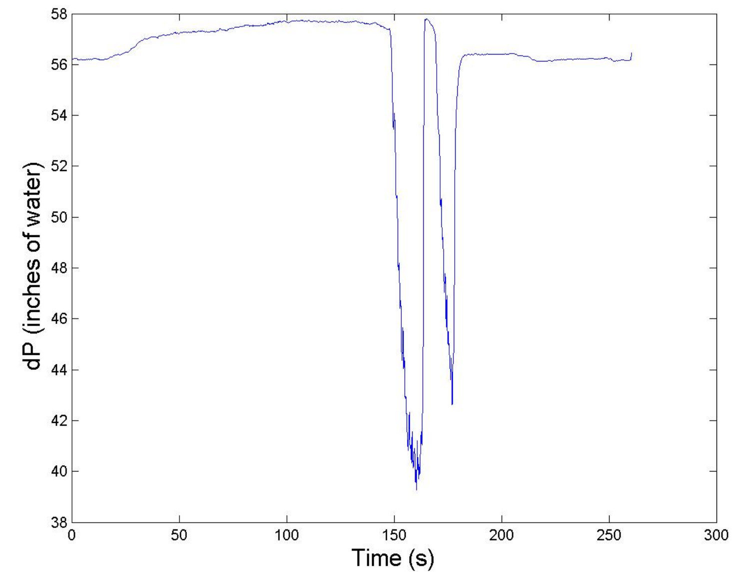

Fig. D.370.: Test section differential pressure for test 93.

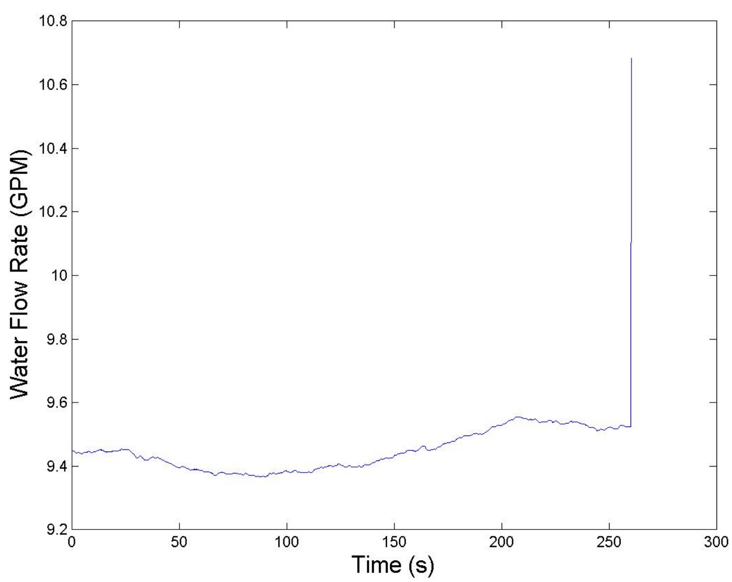

Fig. D.371.: Water flow rate for test 93.

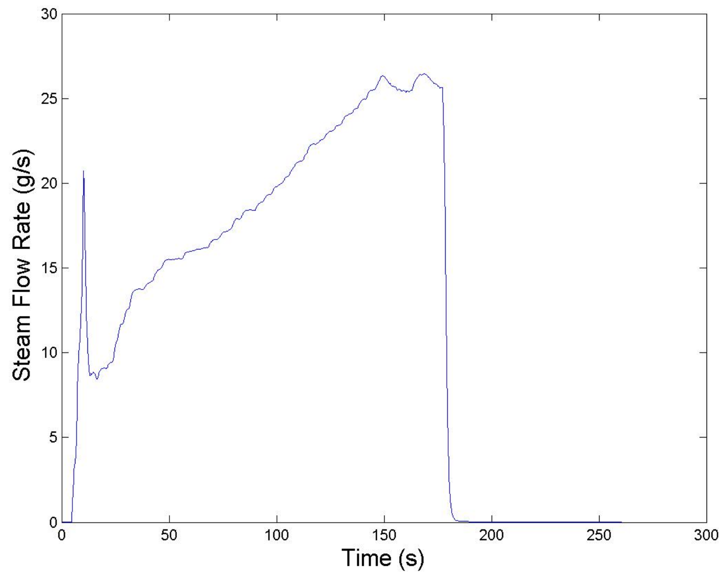

Fig. D.372.: Steam flow rate for test 93.

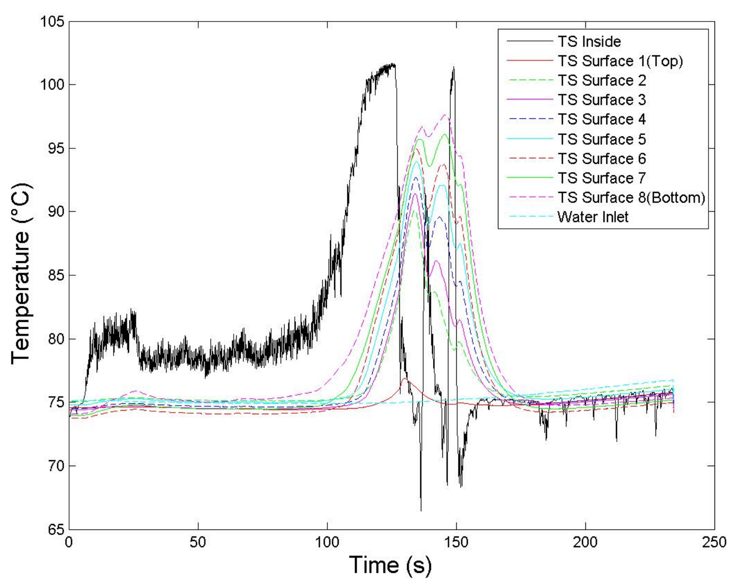

Fig. D.373.: Test section temperatures for test 94.

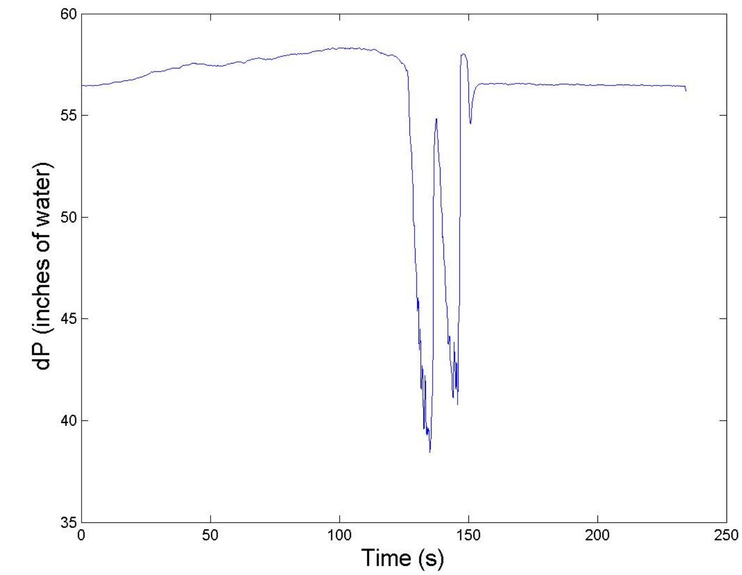

Fig. D.374.: Test section differential pressure for test 94.

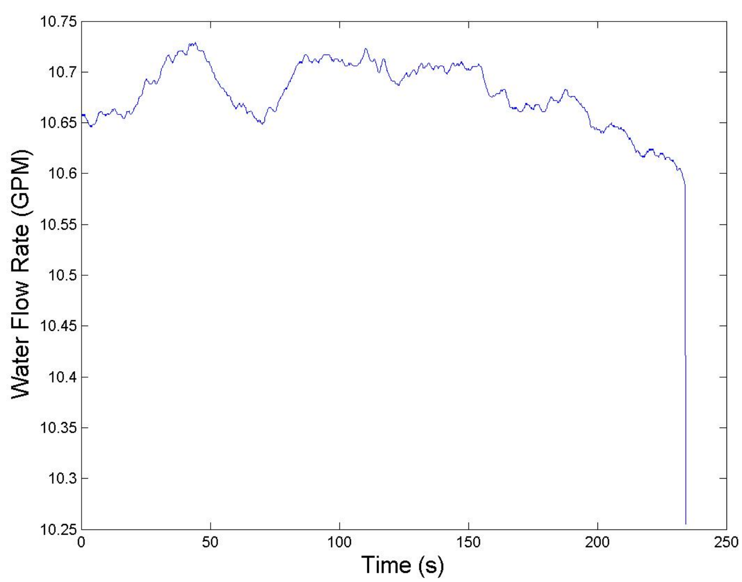

Fig. D.375.: Water flow rate for test 94.

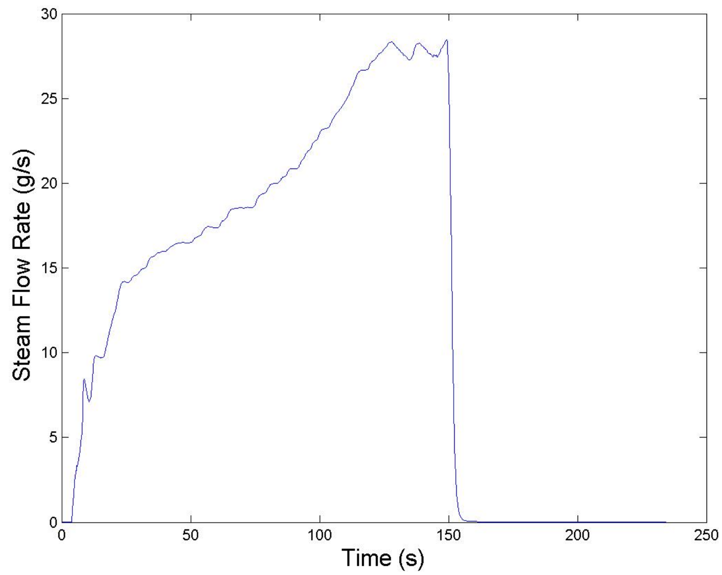

Fig. D.376.: Steam flow rate for test 94.

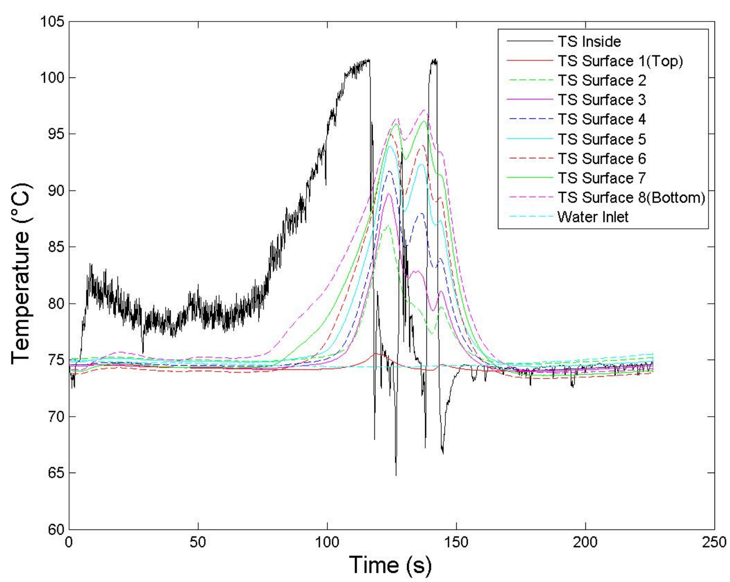

Fig. D.377.: Test section temperatures for test 95.

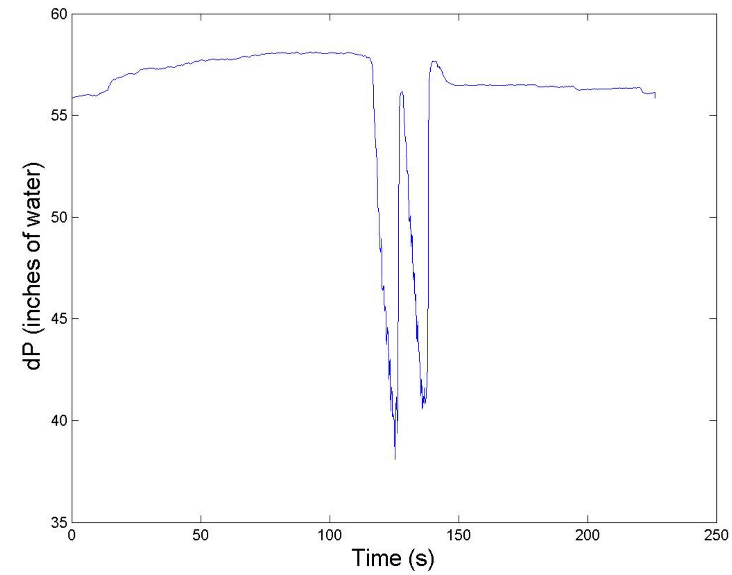

Fig. D.378.: Test section differential pressure for test 95.

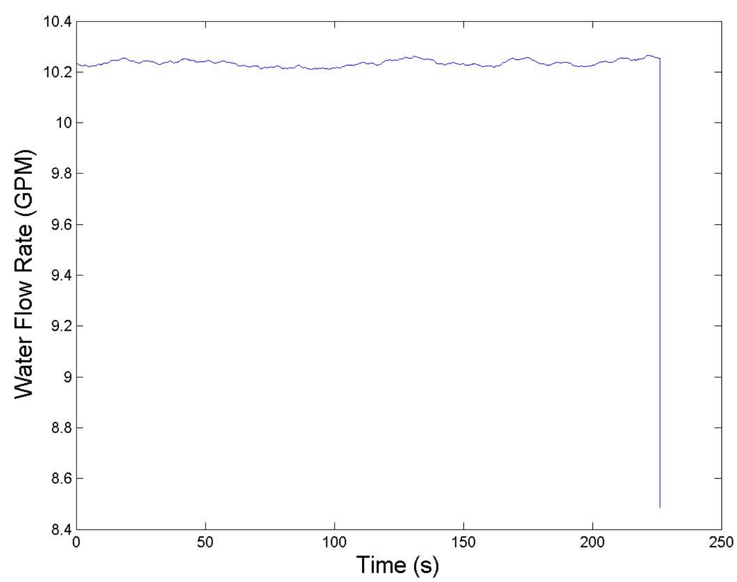

Fig. D.379.: Water flow rate for test 95.

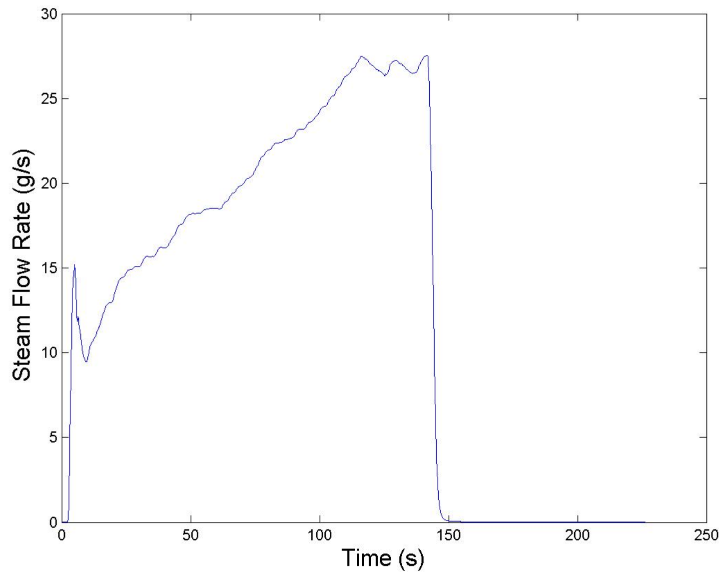

Fig. D.380.: Steam flow rate for test 95.

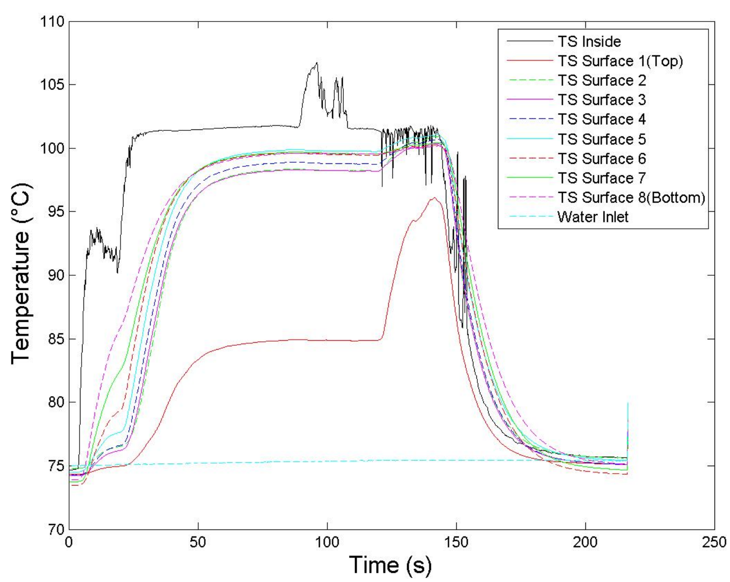

Fig. D.381.: Test section temperatures for test 96.

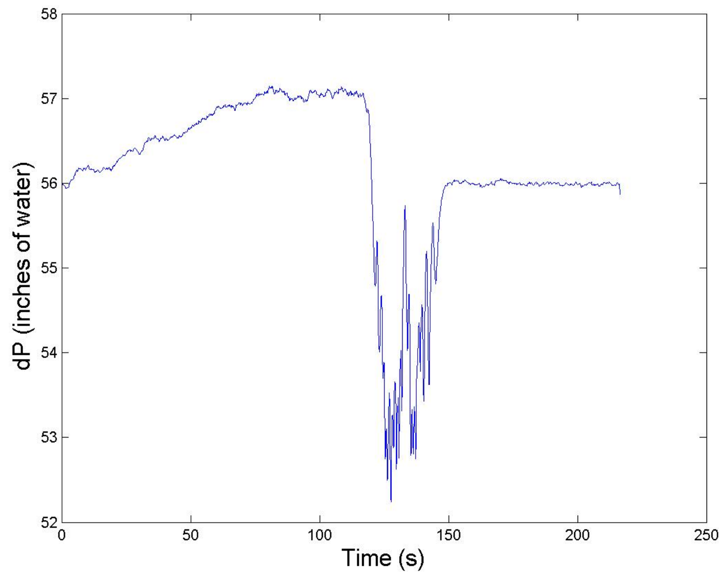

Fig. D.382.: Test section differential pressure for test 96.

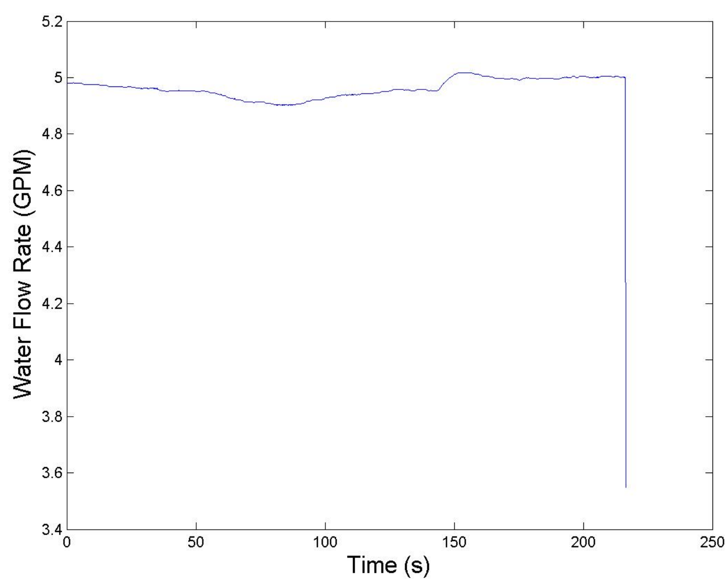

Fig. D.383.: Water flow rate for test 96.

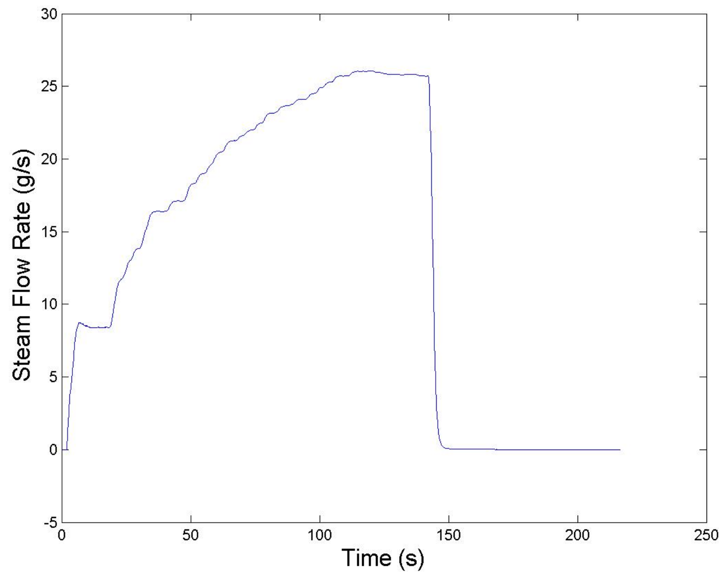

Fig. D.384.: Steam flow rate for test 96.

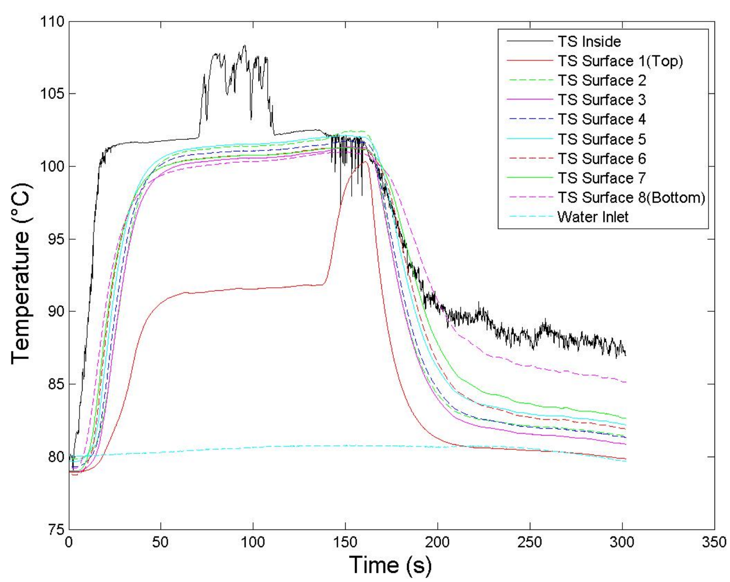

Fig. D.385.: Test section temperatures for test 97.

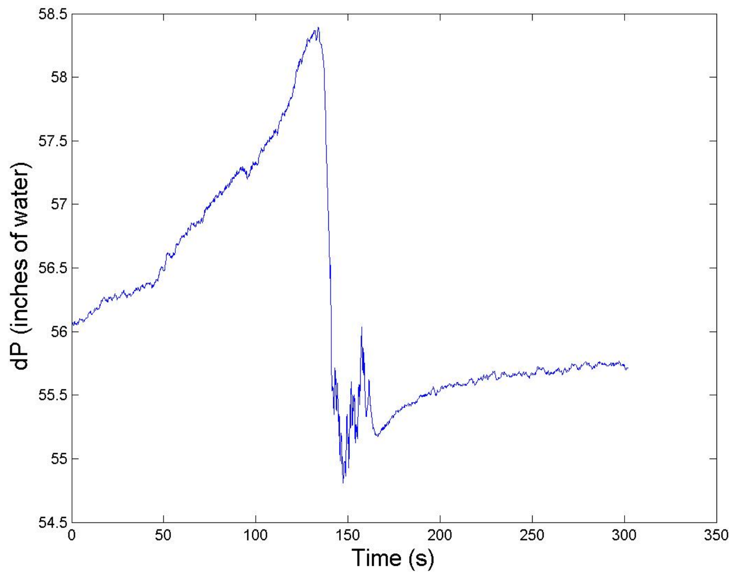

Fig. D.386.: Test section differential pressure for test 97.

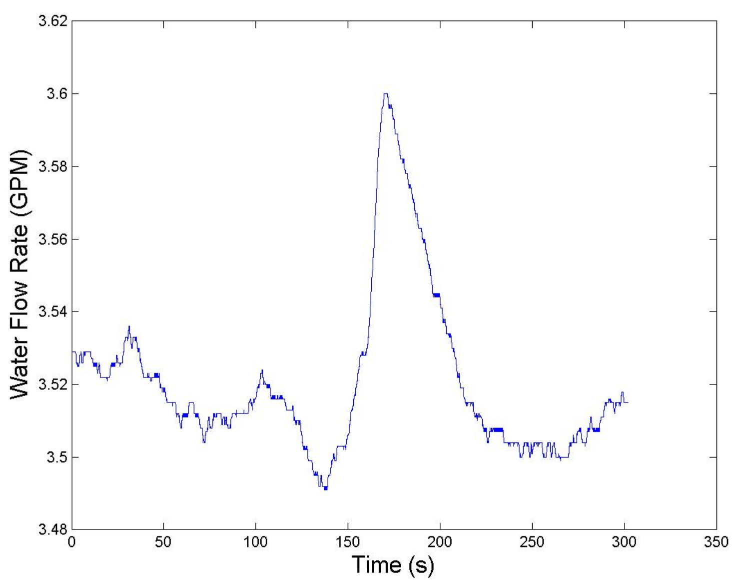

Fig. D.387.: Water flow rate for test 97.

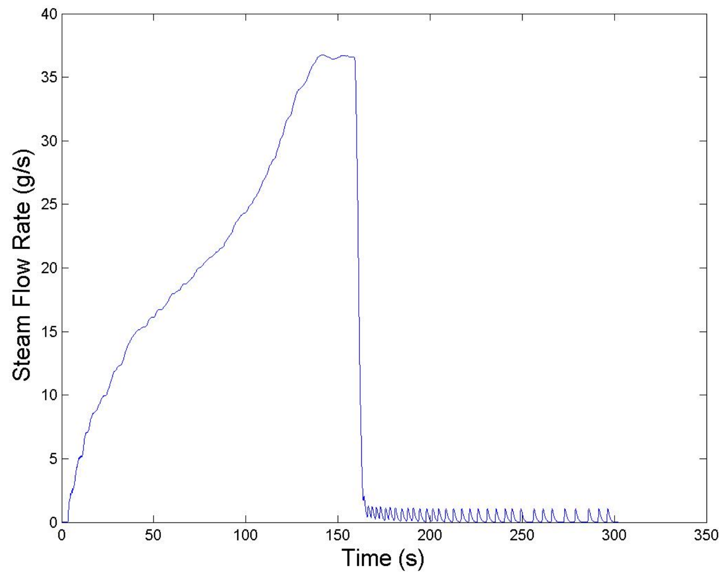

Fig. D.388.: Steam flow rate for test 97.

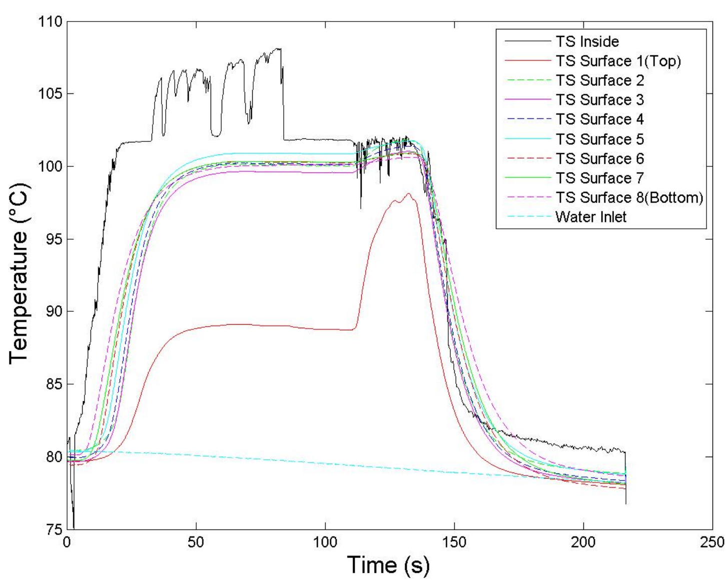

Fig. D.389.: Test section temperatures for test 98.

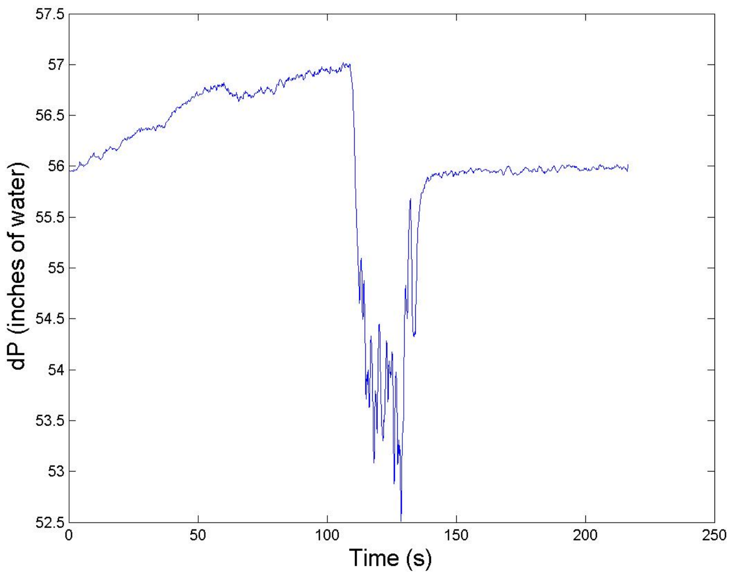

Fig. D.390.: Test section differential pressure for test 98.

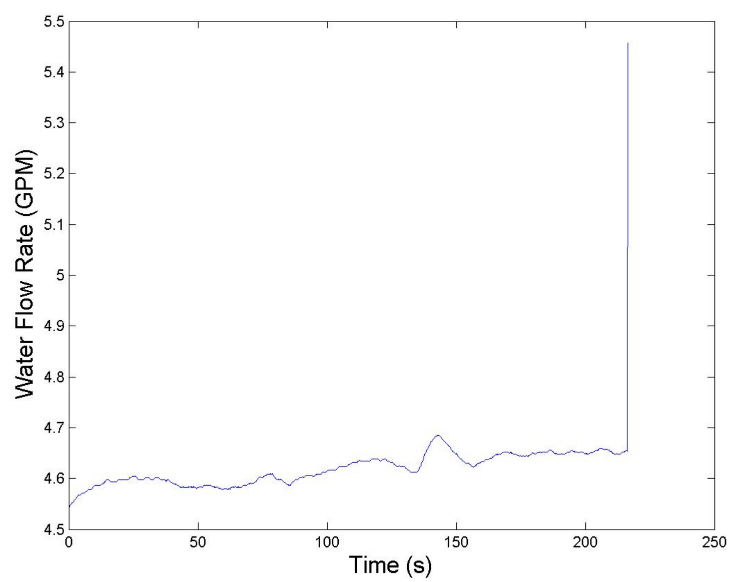

Fig. D.391.: Water flow rate for test 98.

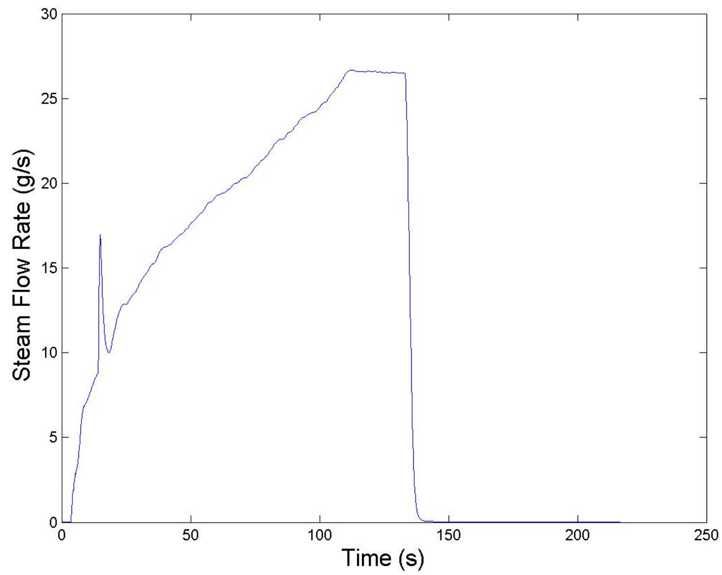

Fig. D.392.: Steam flow rate for test 98.

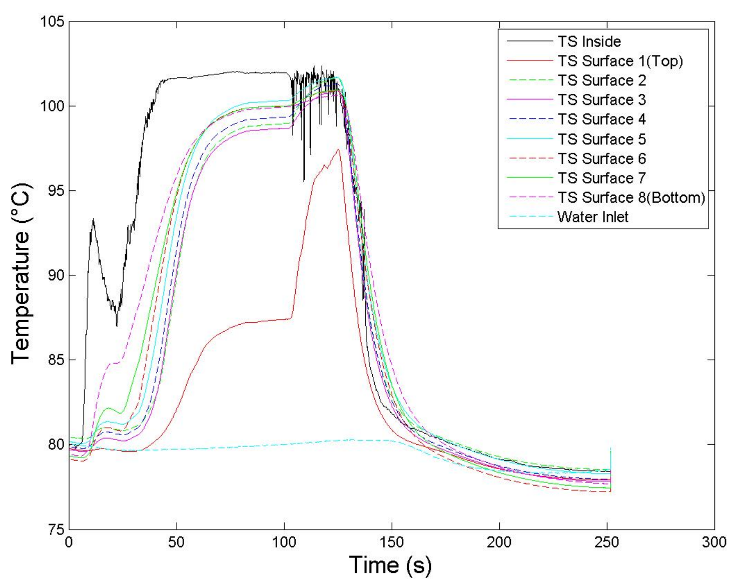

Fig. D.393.: Test section temperatures for test 99.

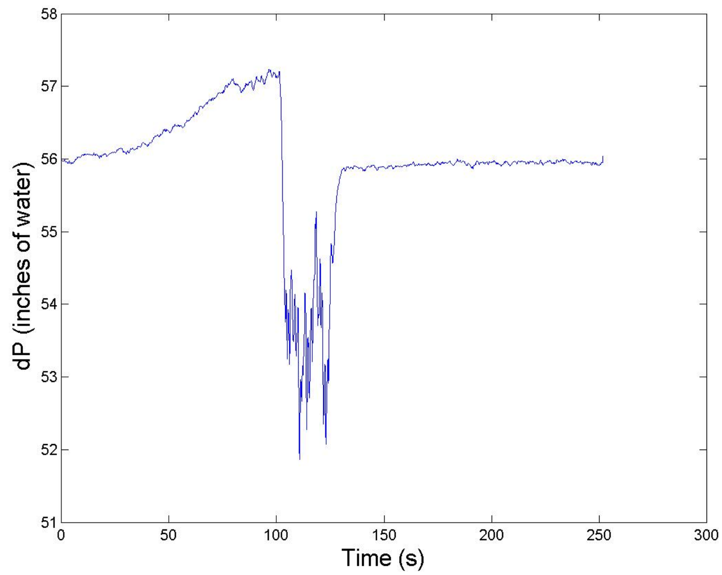

Fig. D.394.: Test section differential pressure for test 99.

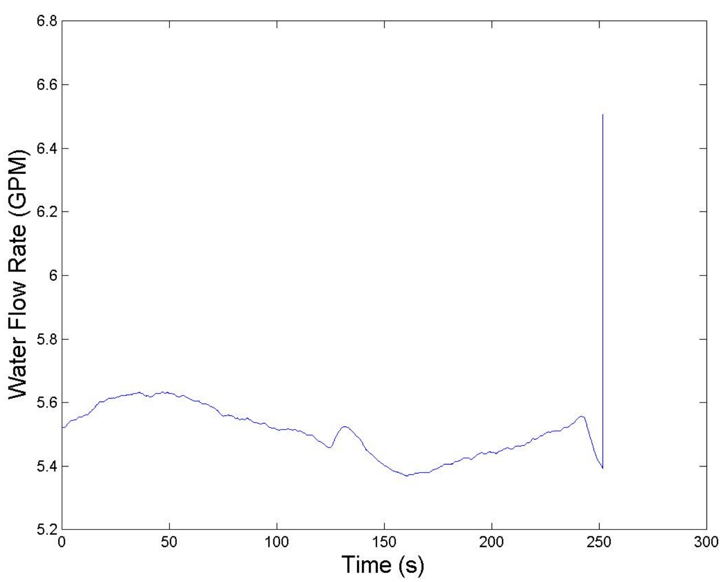

Fig. D.395.: Water flow rate for test 99.

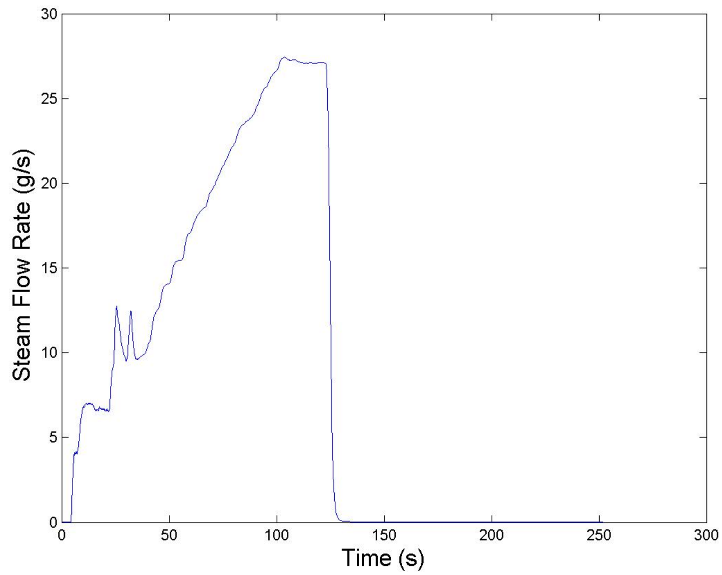

Fig. D.396.: Steam flow rate for test 99.

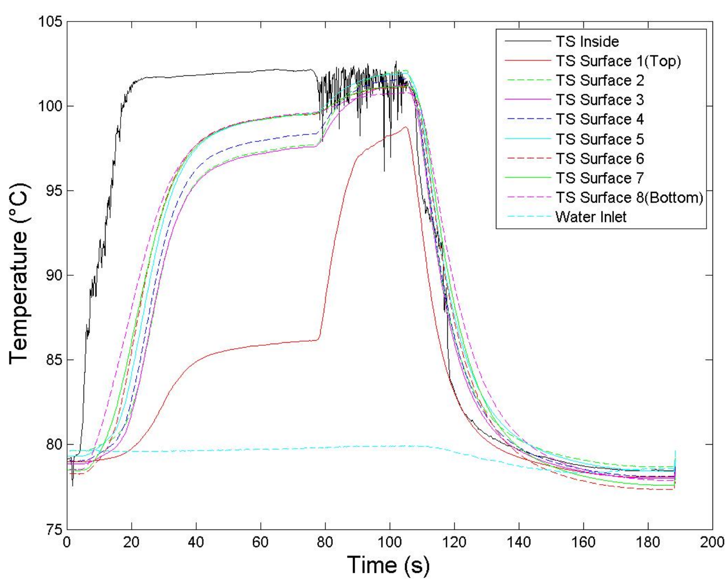

Fig. D.397.: Test section temperatures for test 100.

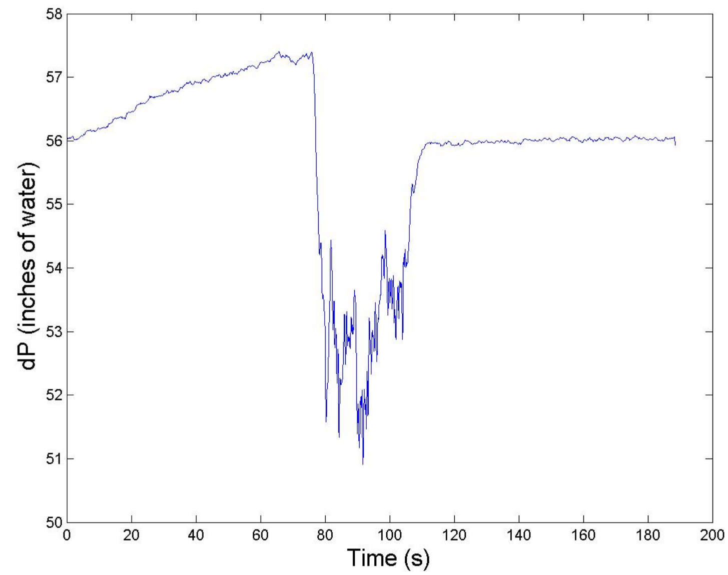

Fig. D.398.: Test section differential pressure for test 100.

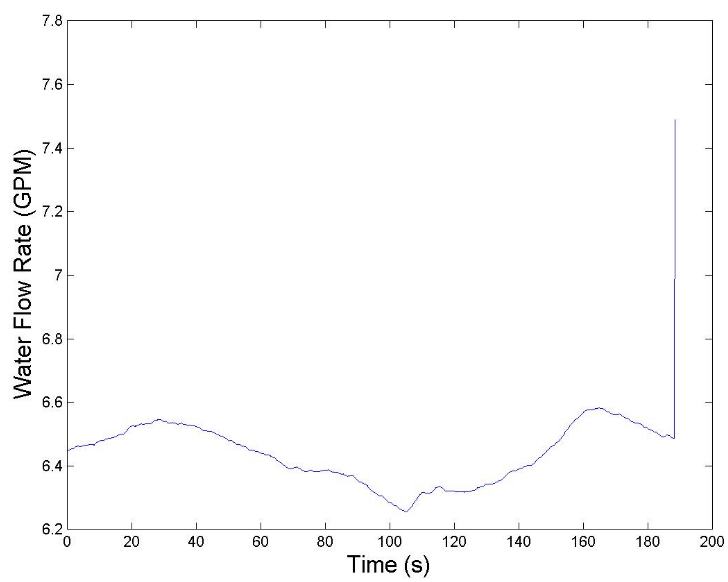

Fig. D.399.: Water flow rate for test 100.

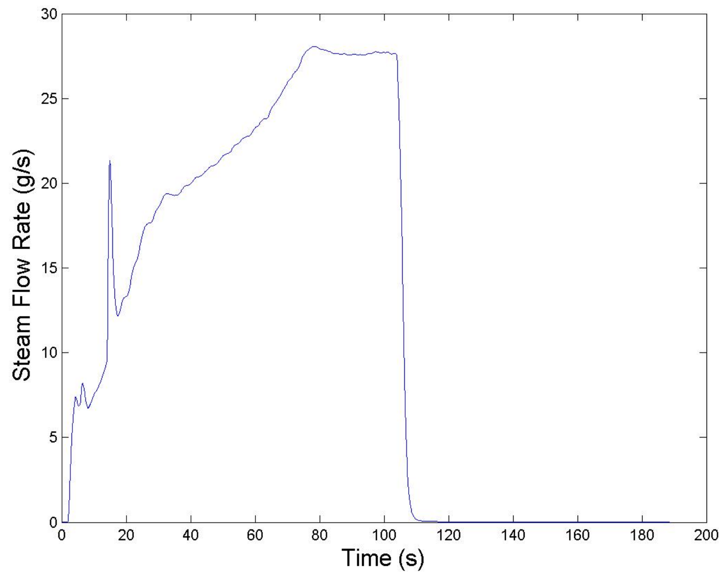

Fig. D.400.: Steam flow rate for test 100.

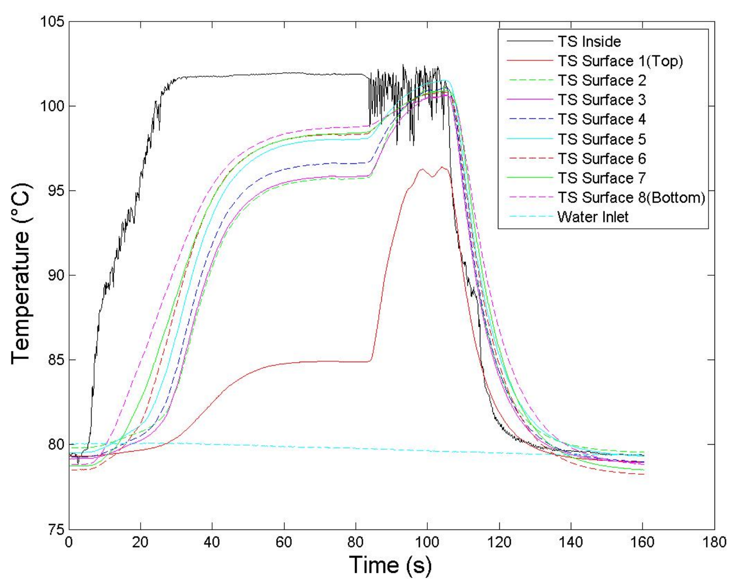

Fig. D.401.: Test section temperatures for test 101.

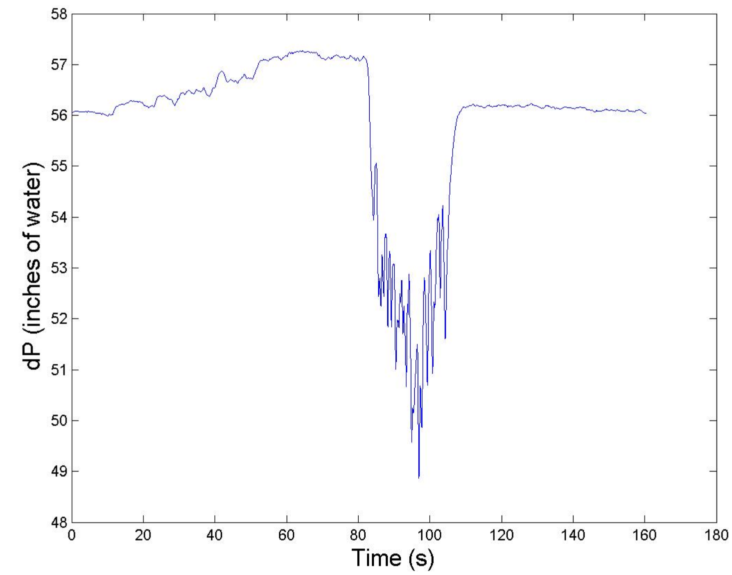

Fig. D.402.: Test section differential pressure for test 101.

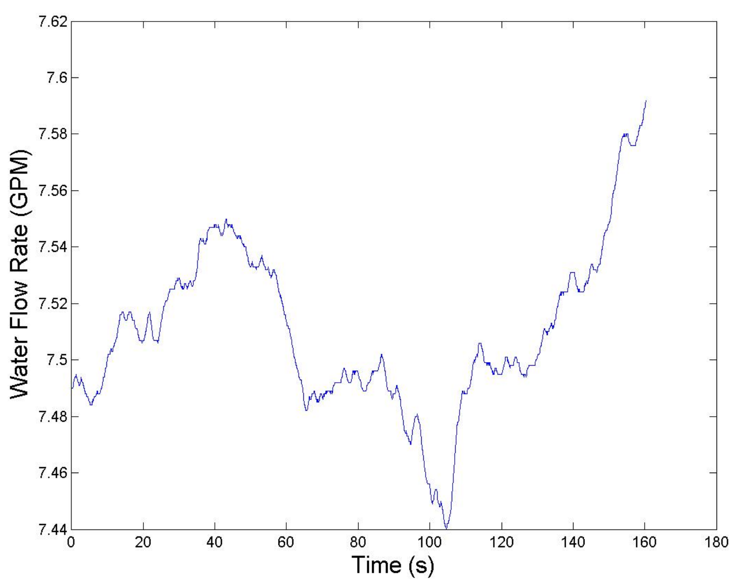

Fig. D.403.: Water flow rate for test 101.

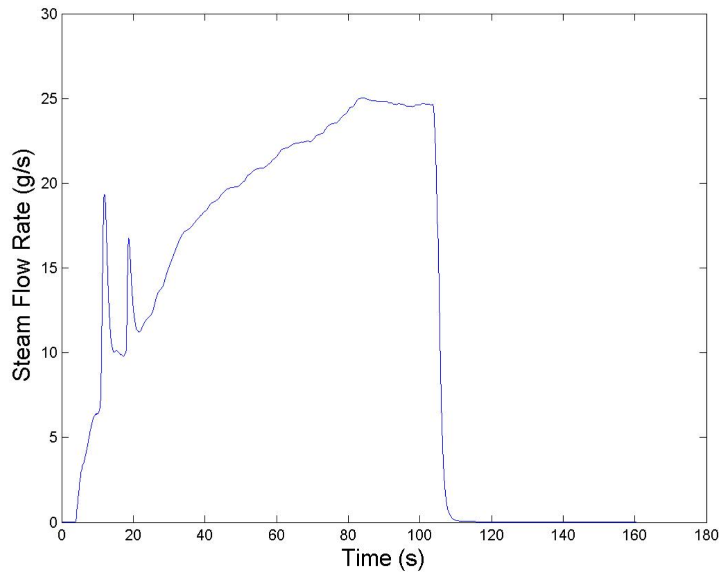

Fig. D.404.: Steam flow rate for test 101.

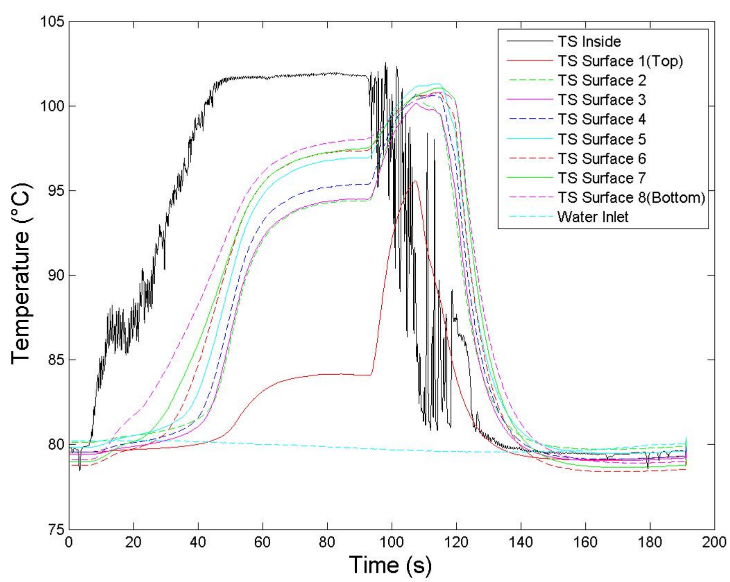

Fig. D.405.: Test section temperatures for test 102.

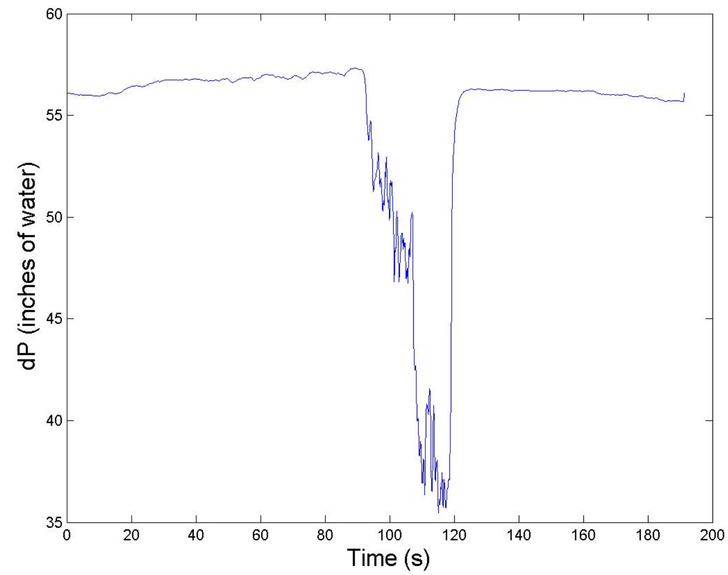

Fig. D.406.: Test section differential pressure for test 102.

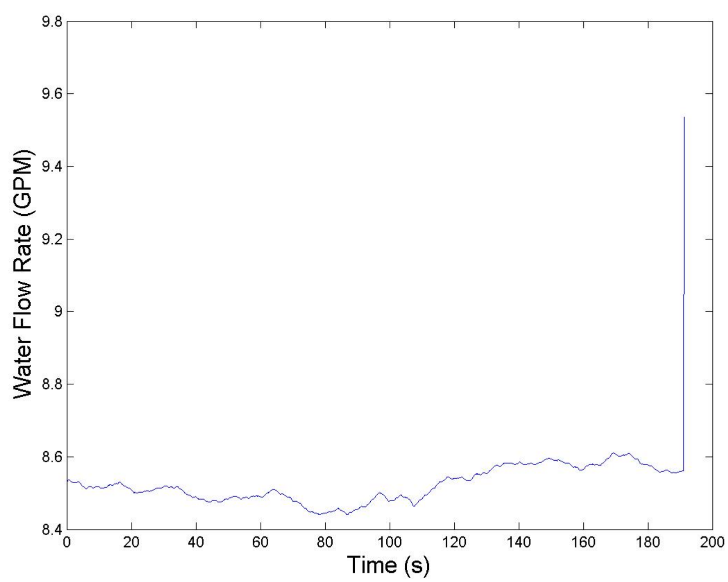

Fig. D.407.: Water flow rate for test 102.

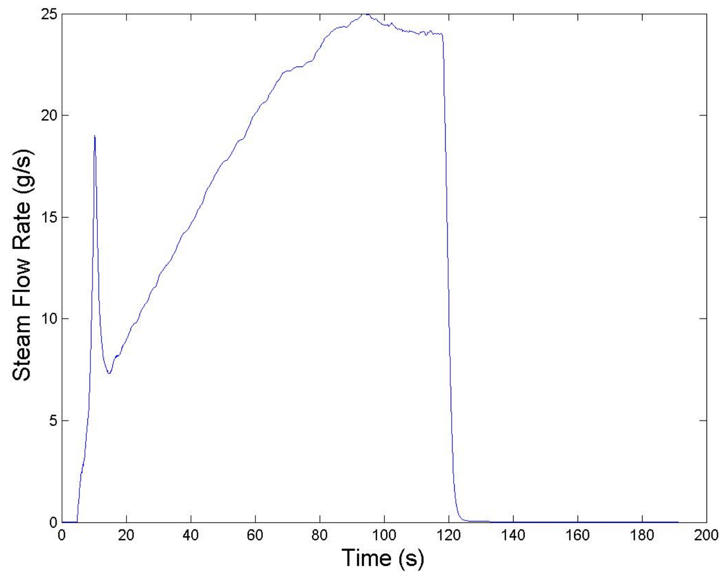

Fig. D.408.: Steam flow rate for test 102.

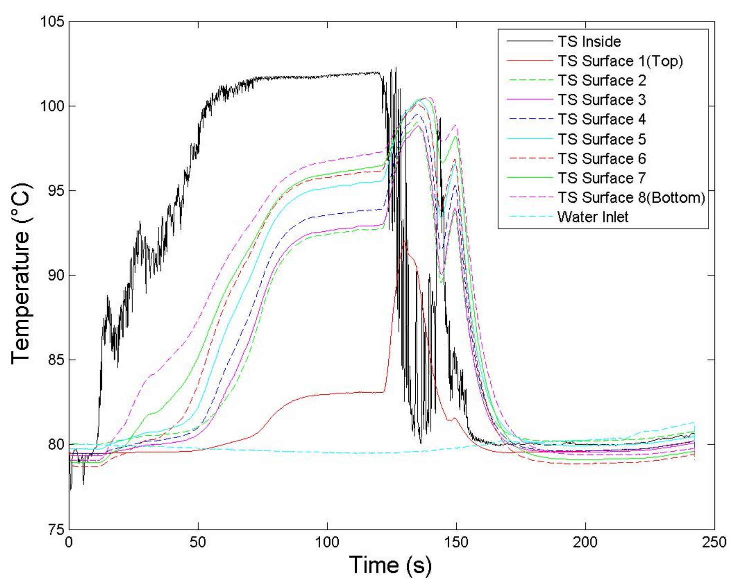

Fig. D.409.: Test section temperatures for test 103.

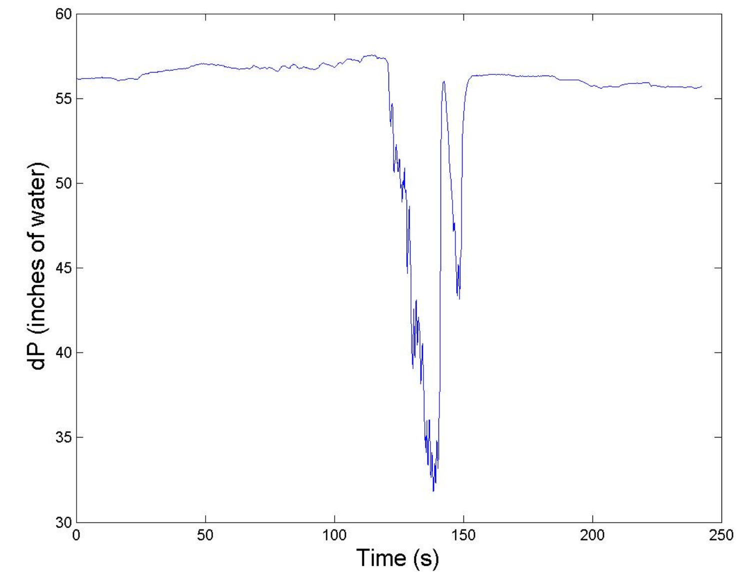

Fig. D.410.: Test section differential pressure for test 103.

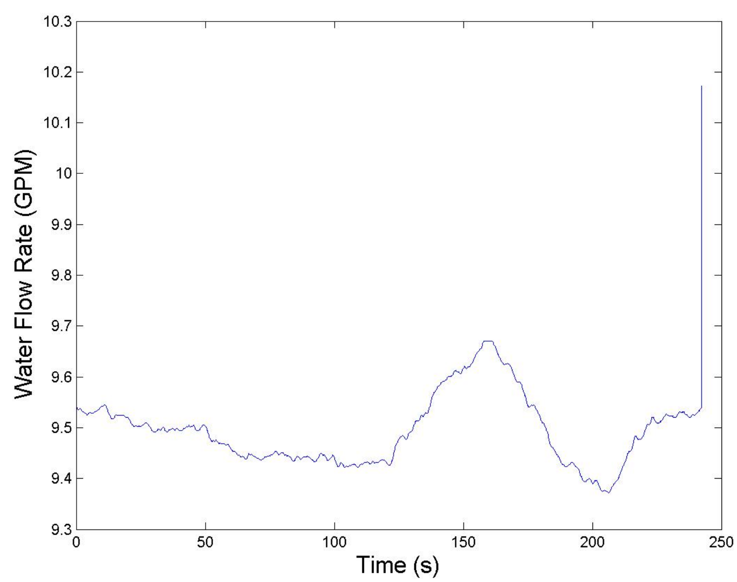

Fig. D.411.: Water flow rate for test 103.

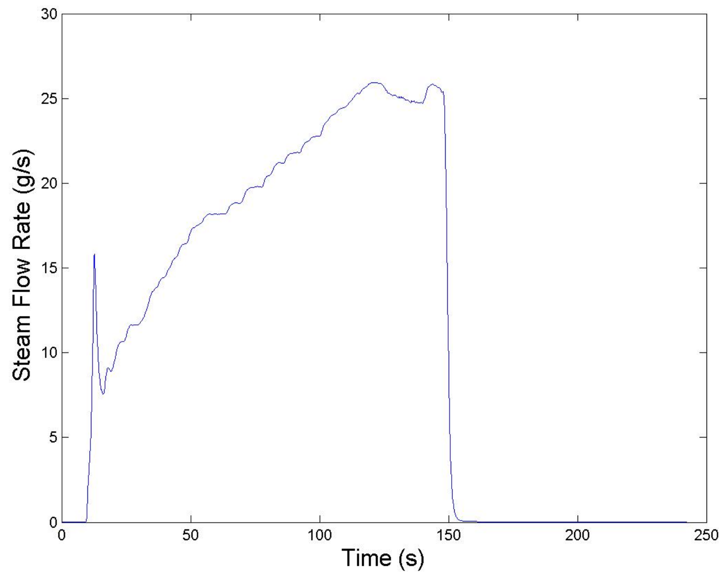

Fig. D.412.: Steam flow rate for test 103.

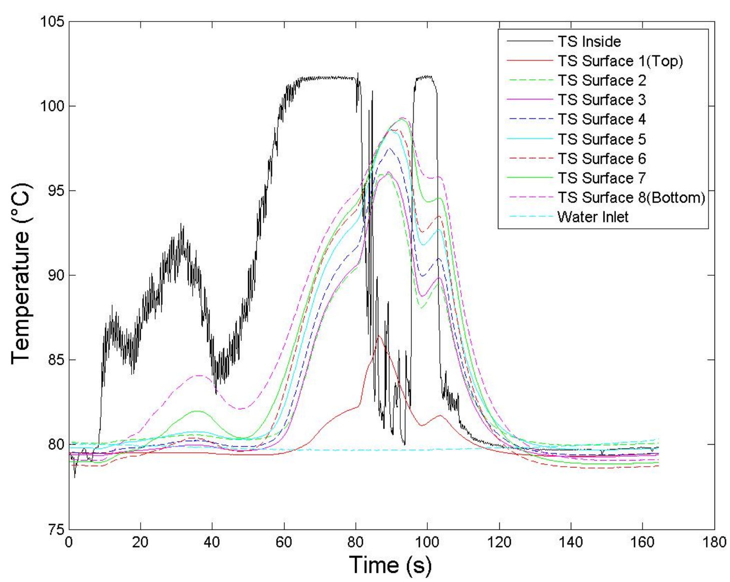

Fig. D.413.: Test section temperatures for test 104.

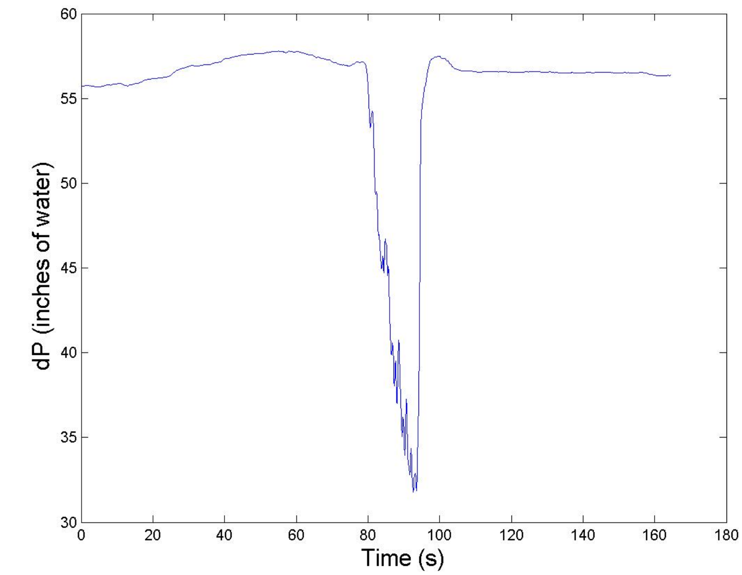

Fig. D.414.: Test section differential pressure for test 104.

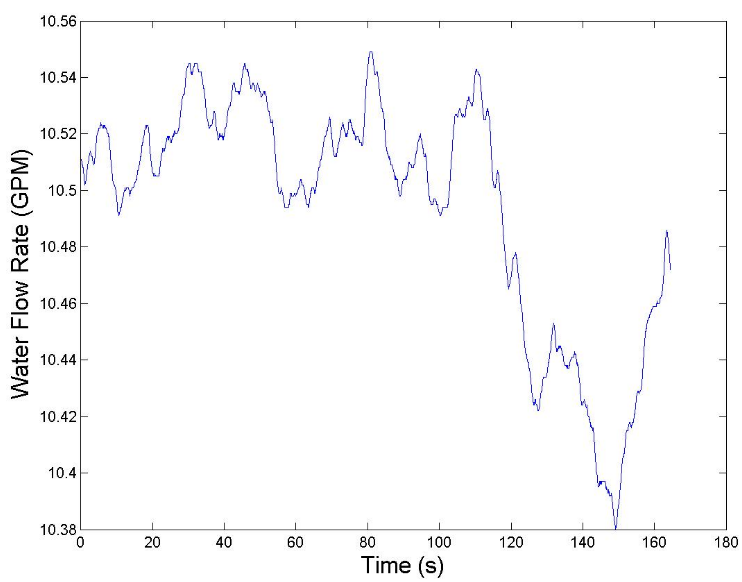

Fig. D.415.: Water flow rate for test 104.

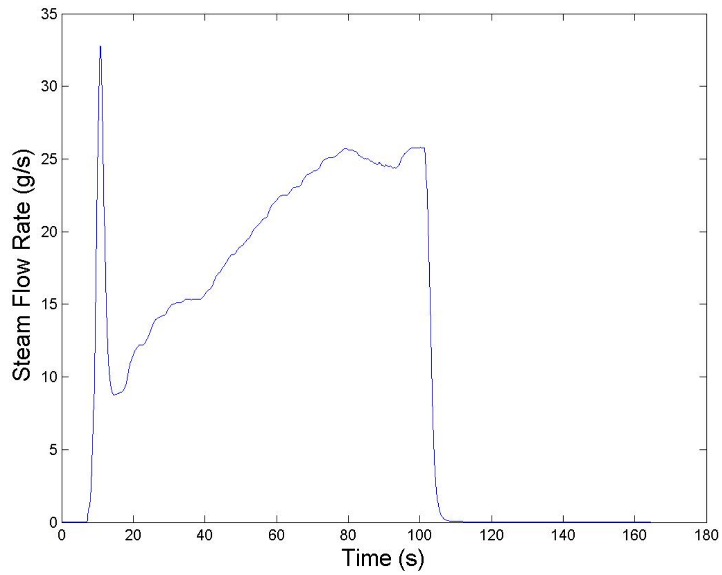

Fig. D.416.: Steam flow rate for test 104.

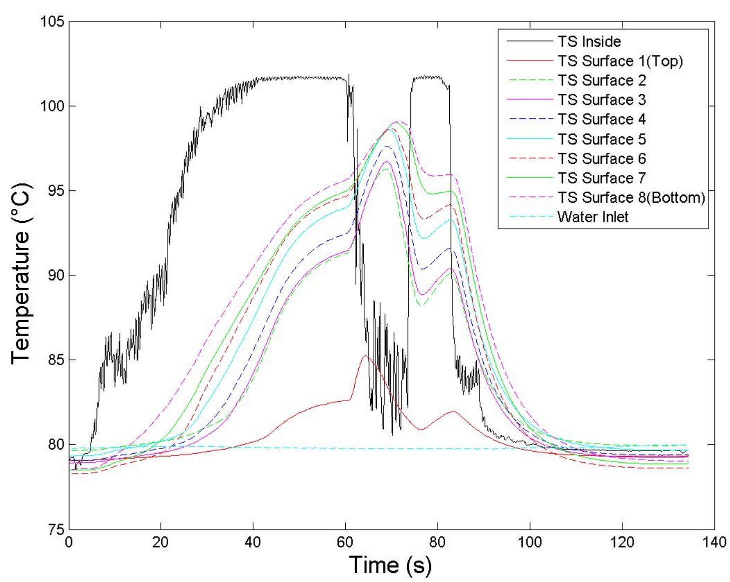

Fig. D.417.: Test section temperatures for test 105.

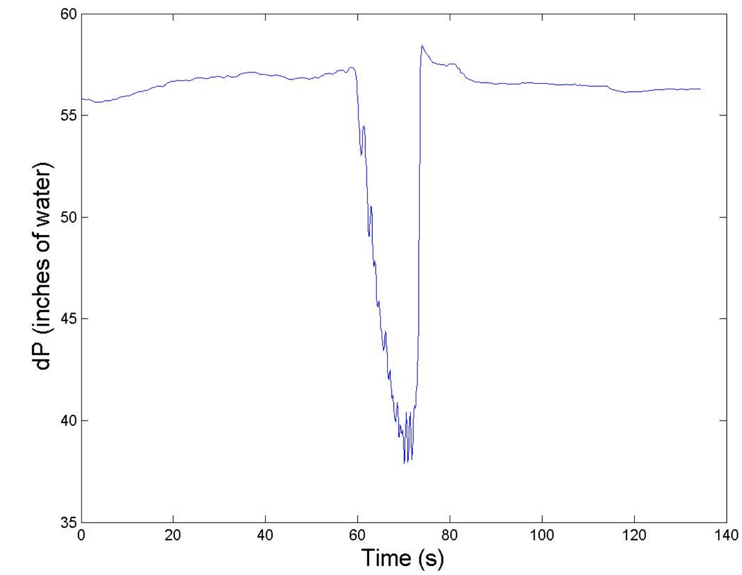

Fig. D.418.: Test section differential pressure for test 105.

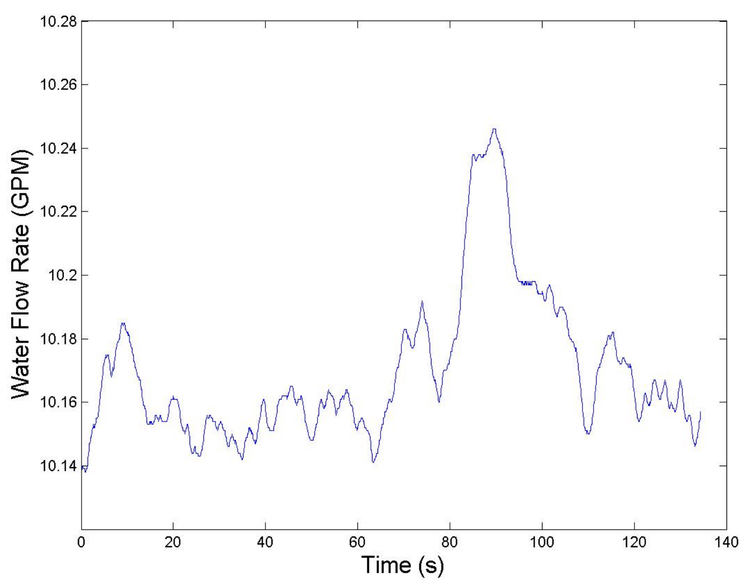

Fig. D.419.: Water flow rate for test 105.

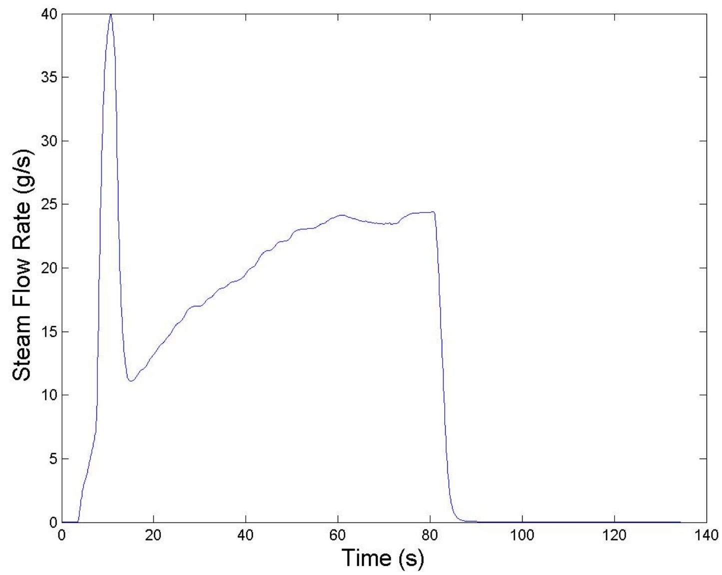

Fig. D.420.: Steam flow rate for test 105.

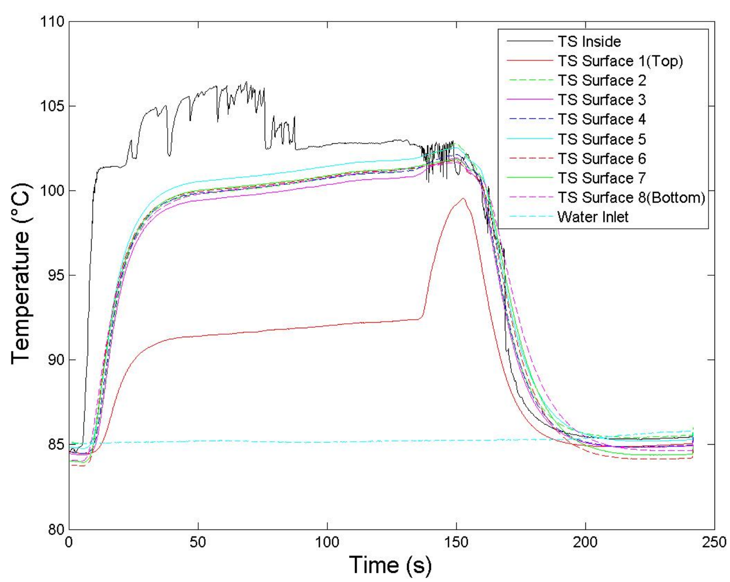

Fig. D.421.: Test section temperatures for test 106.

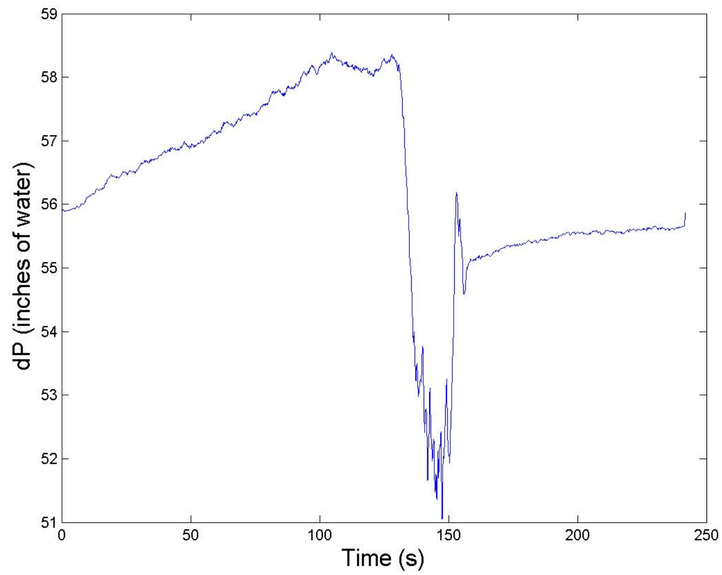

Fig. D.422.: Test section differential pressure for test 106.

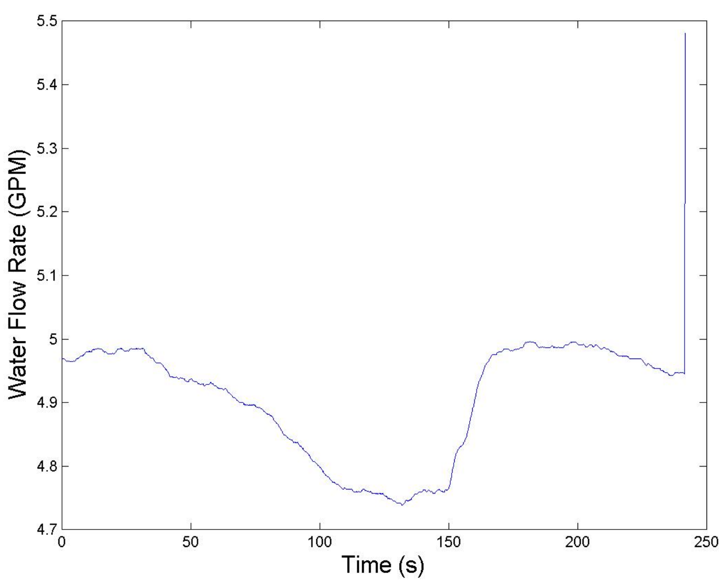

Fig. D.423.: Water flow rate for test 106.

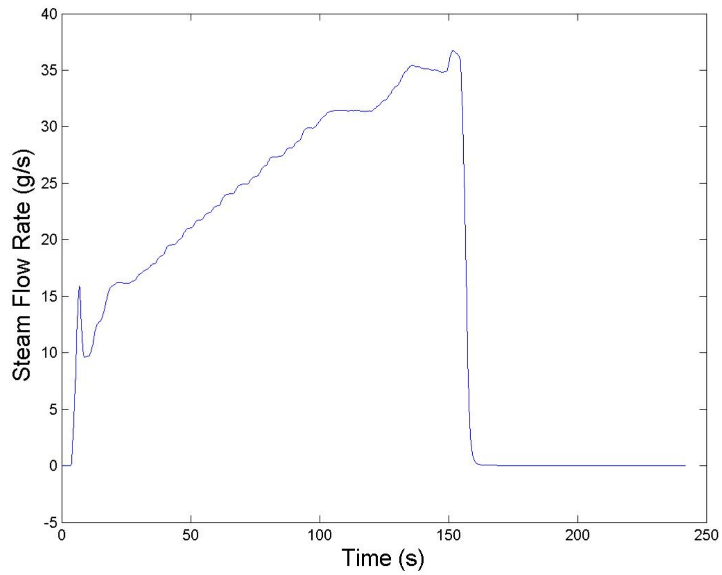

Fig. D.424.: Steam flow rate for test 106.

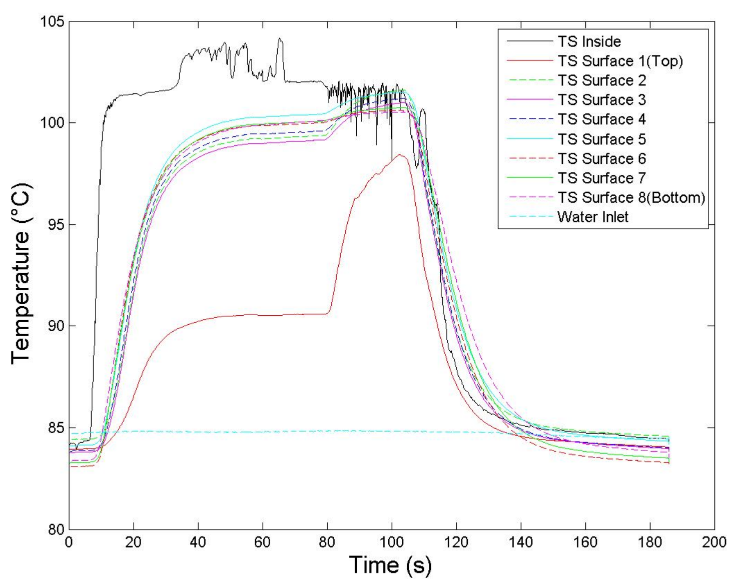

Fig. D.425.: Test section temperatures for test 107.

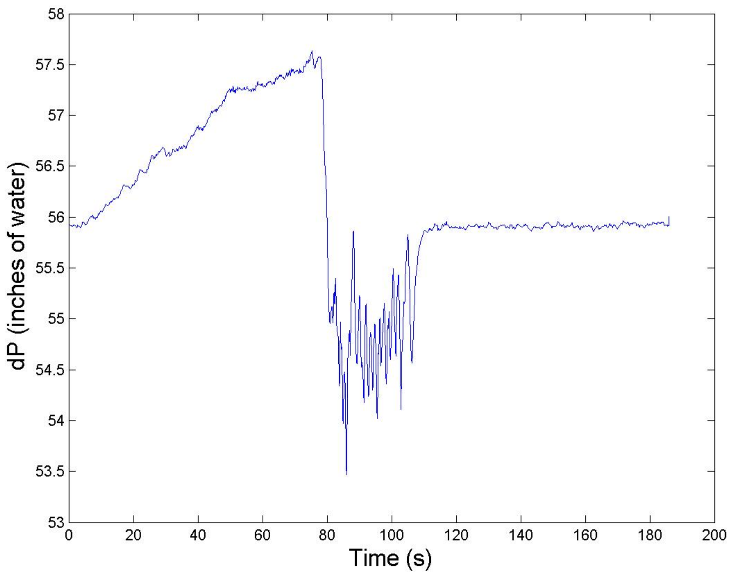

Fig. D.426.: Test section differential pressure for test 107.

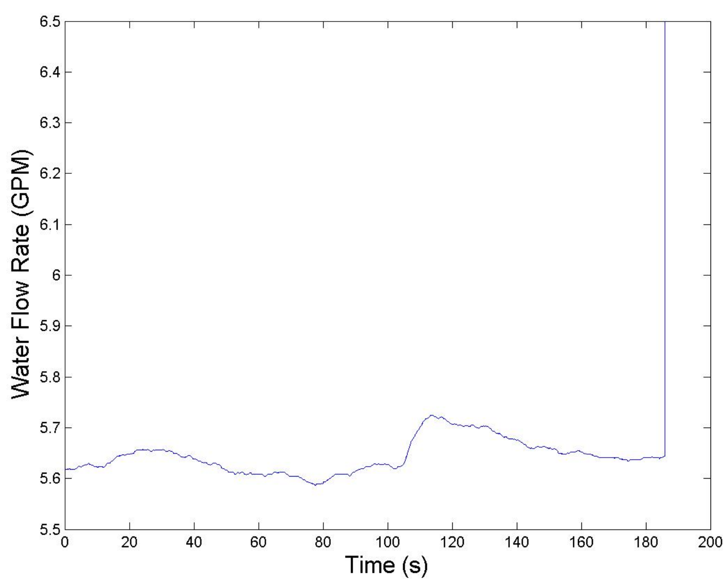

Fig. D.427.: Water flow rate for test 107.

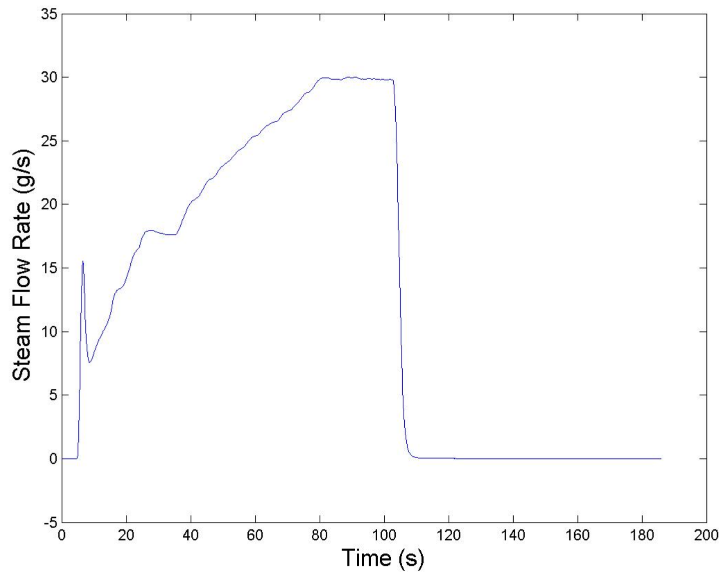

Fig. D.428.: Steam flow rate for test 107.

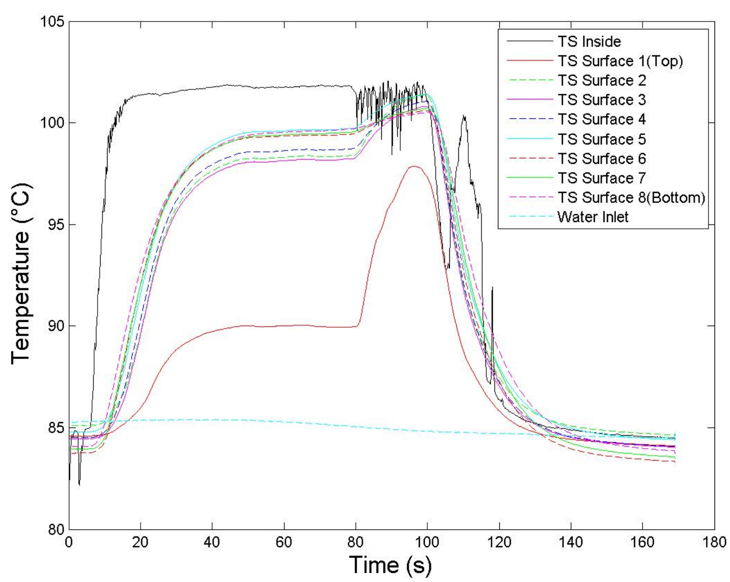

Fig. D.429.: Test section temperatures for test 108.

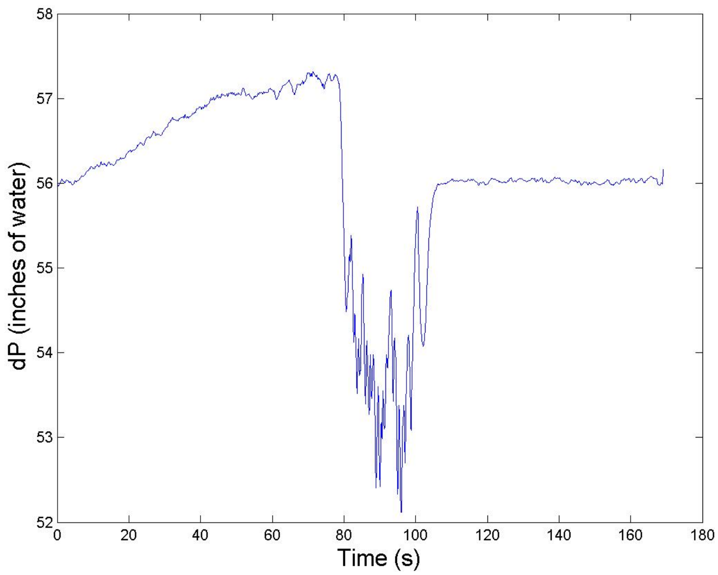

Fig. D.430.: Test section differential pressure for test 108.

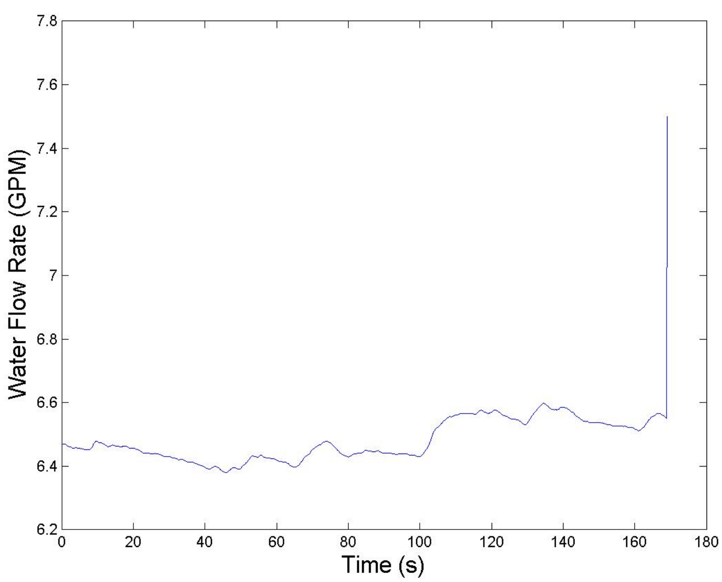

Fig. D.431.: Water flow rate for test 108.

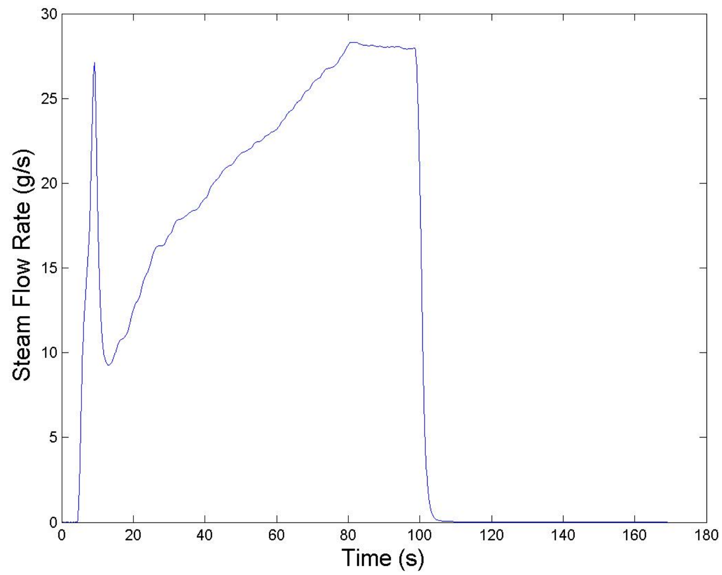

Fig. D.432.: Steam flow rate for test 108.

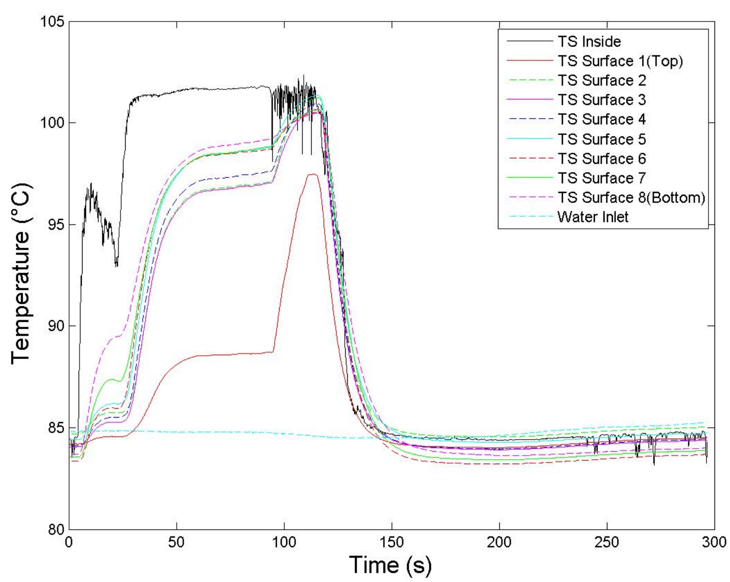

Fig. D.433.: Test section temperatures for test 109.

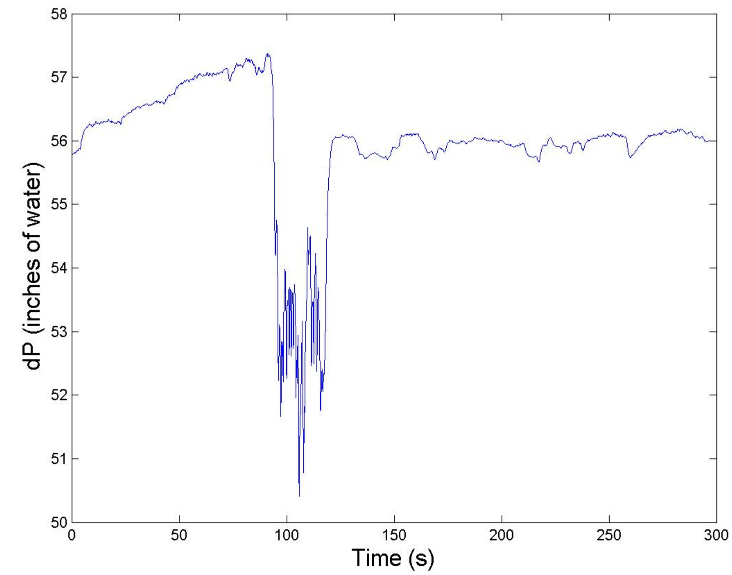

Fig. D.434.: Test section differential pressure for test 109.

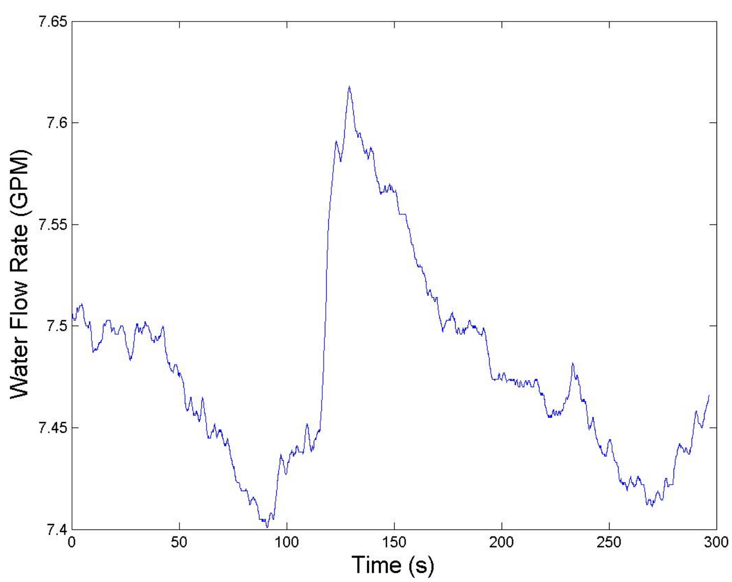

Fig. D.435.: Water flow rate for test 109.

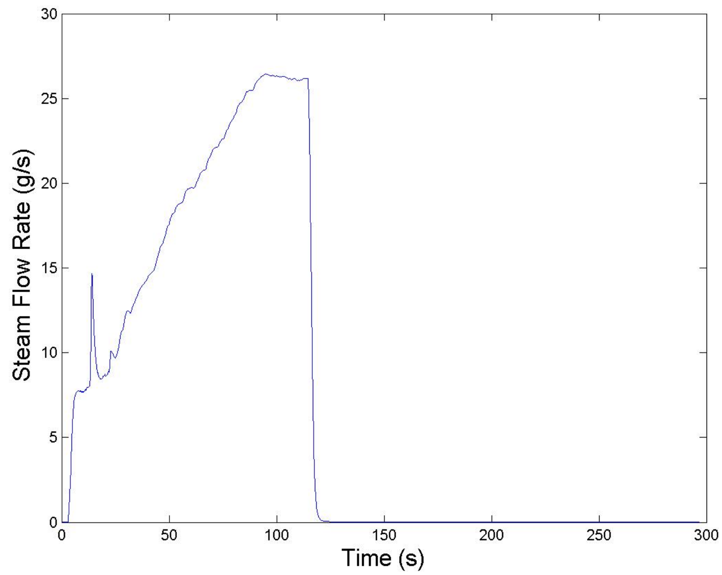

Fig. D.436.: Steam flow rate for test 109.

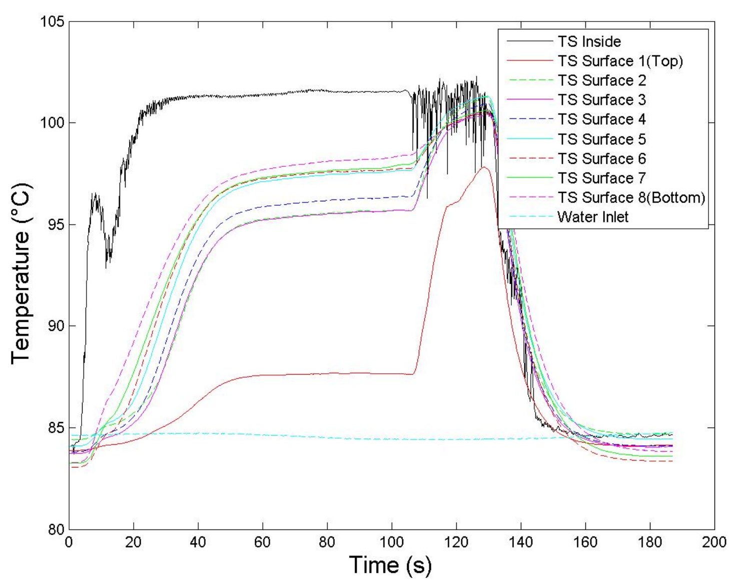

Fig. D.437.: Test section temperatures for test 110.

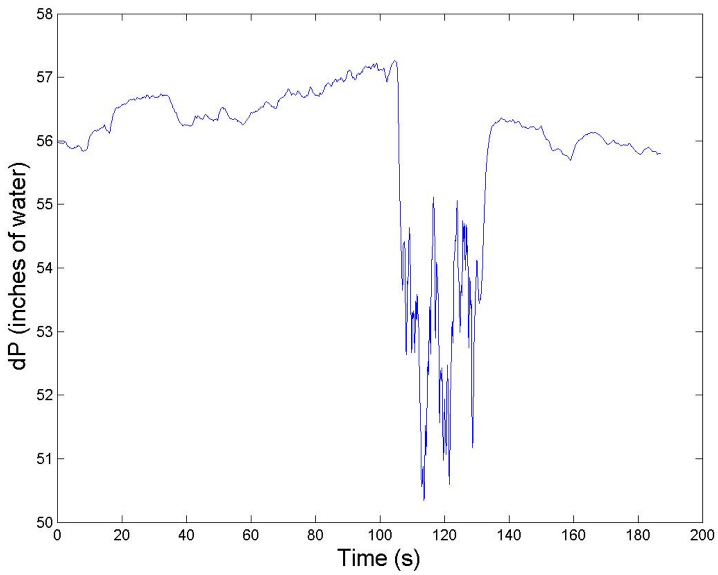

Fig. D.438.: Test section differential pressure for test 110.

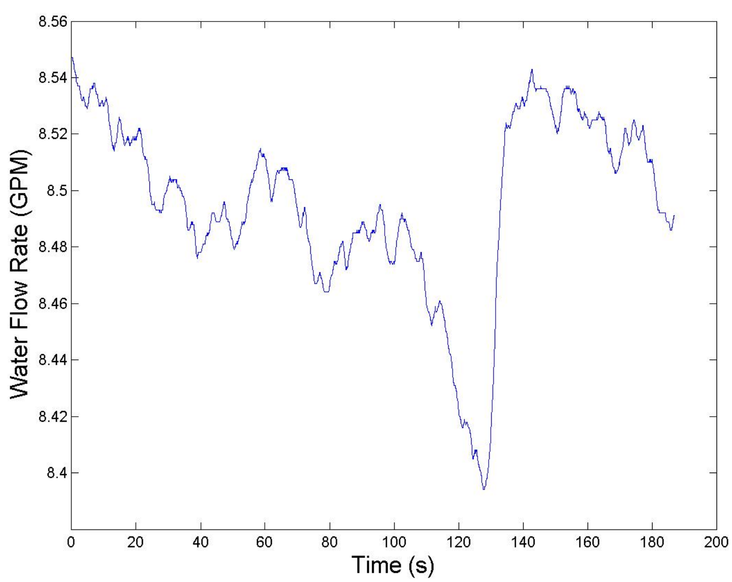

Fig. D.439.: Water flow rate for test 110.

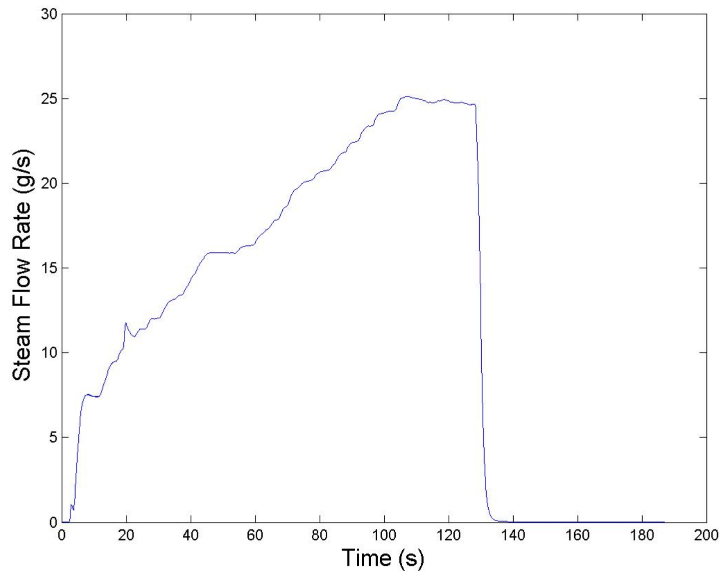

Fig. D.440.: Steam flow rate for test 110.

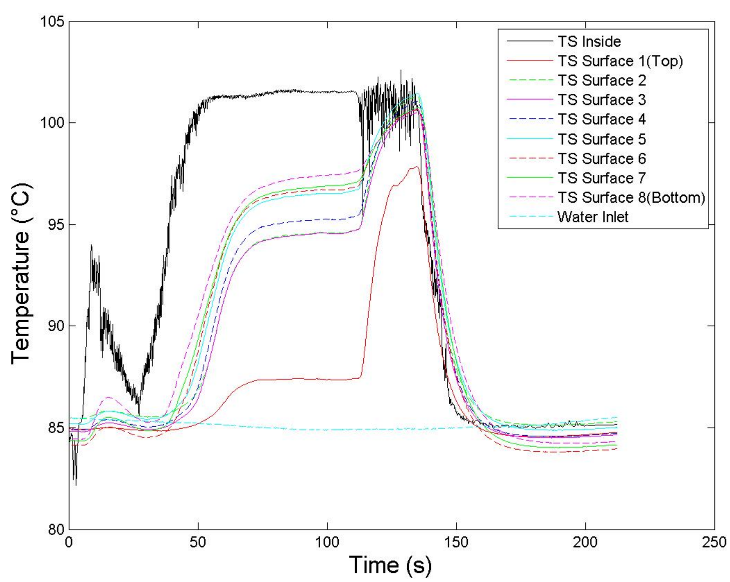

Fig. D.441.: Test section temperatures for test 111.

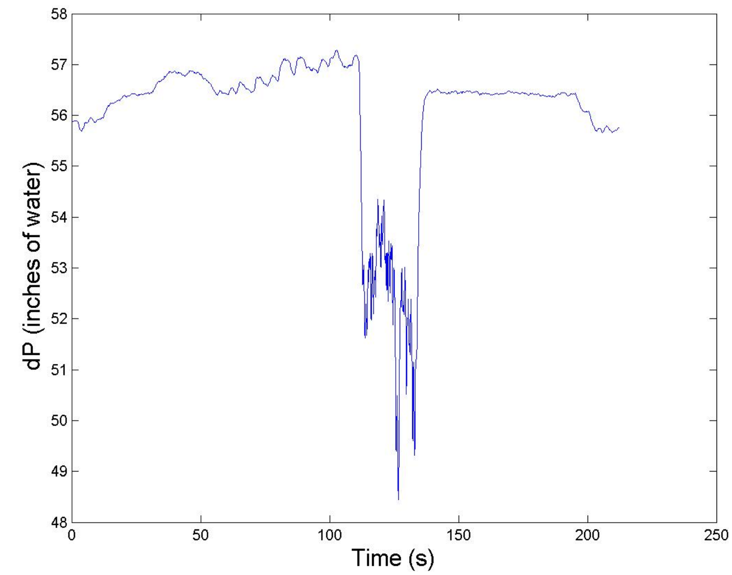

Fig. D.442.: Test section differential pressure for test 111.

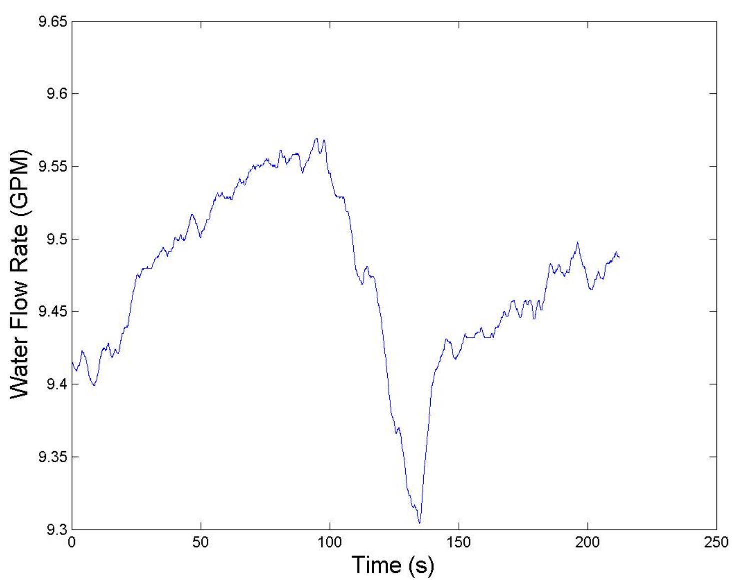

Fig. D.443.: Water flow rate for test 111.

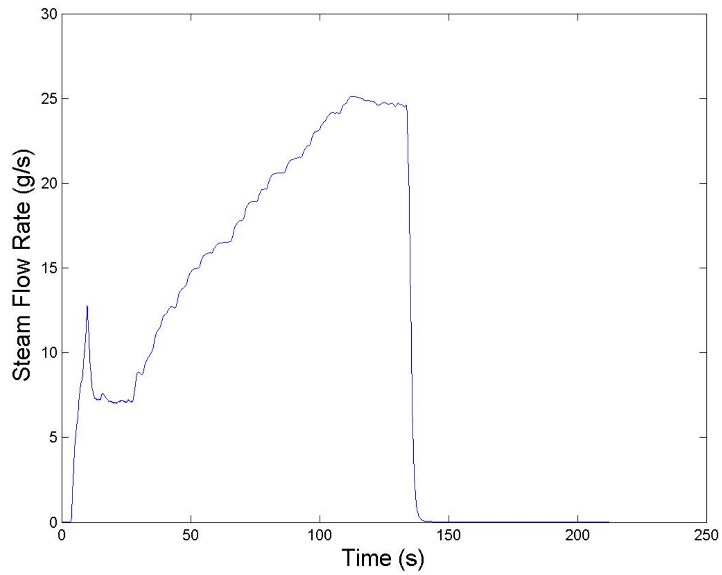

Fig. D.444.: Steam flow rate for test 111.

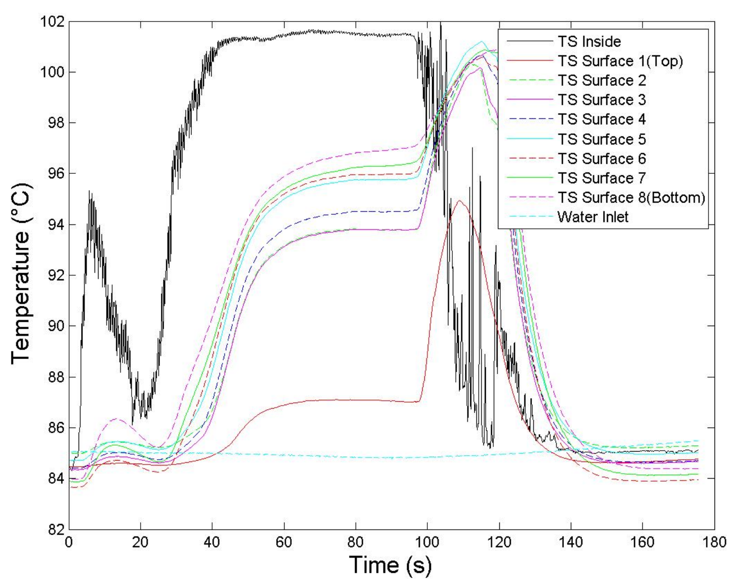

Fig. D.445.: Test section temperatures for test 112.

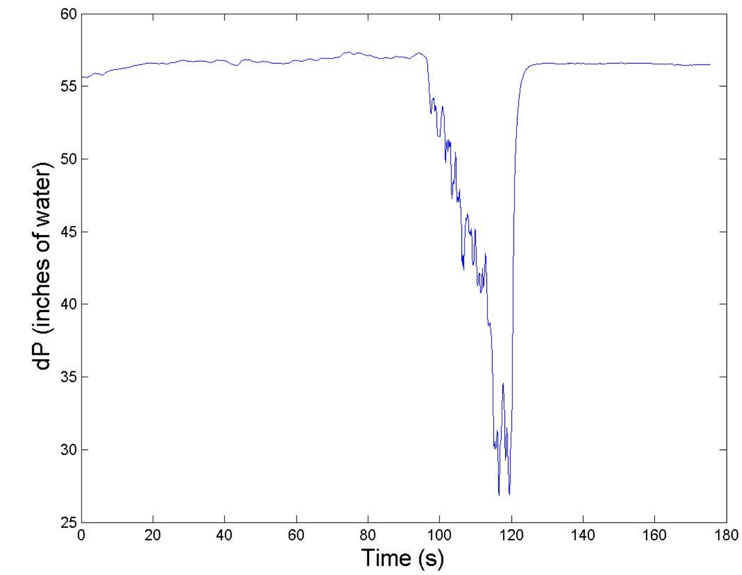

Fig. D.446.: Test section differential pressure for test 112.

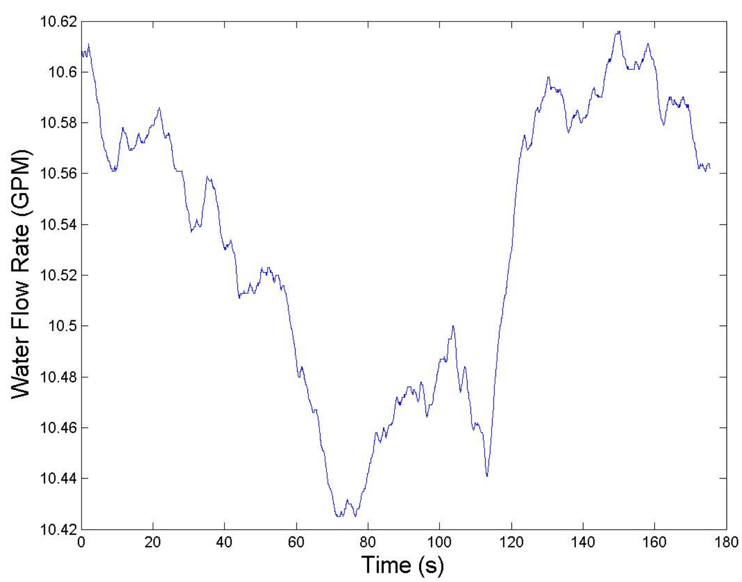

Fig. D.447.: Water flow rate for test 112.

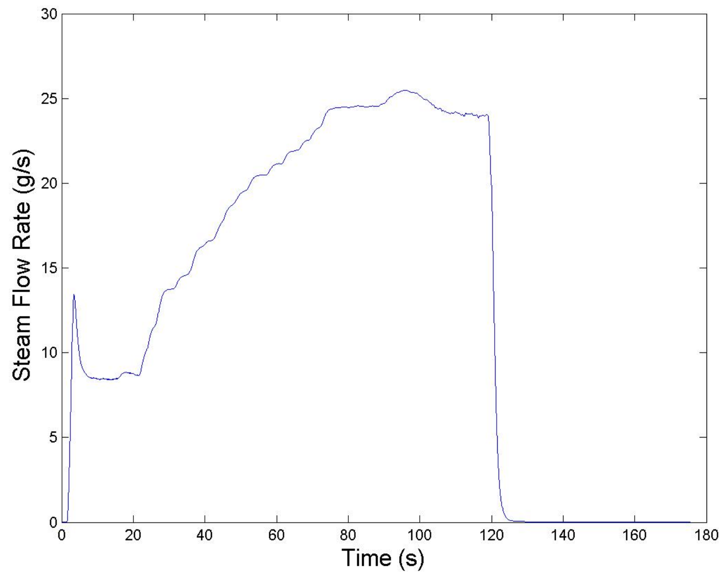

Fig. D.448.: Steam flow rate for test 112.

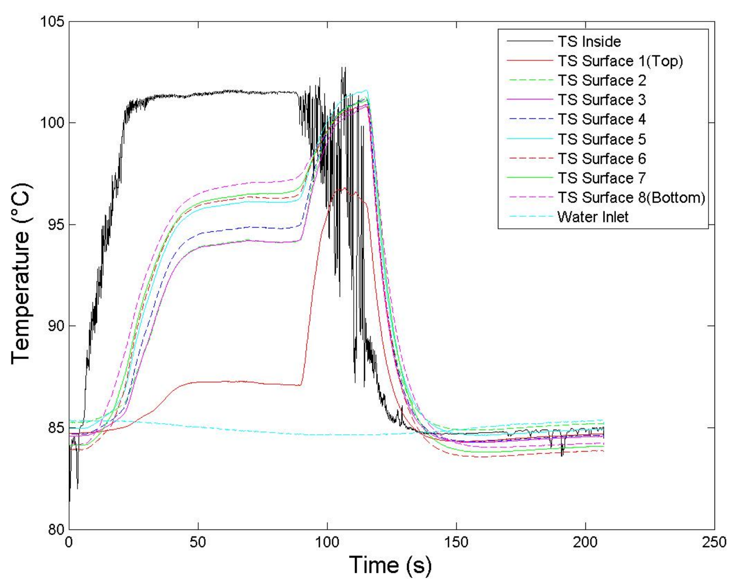

Fig. D.449.: Test section temperatures for test 113.

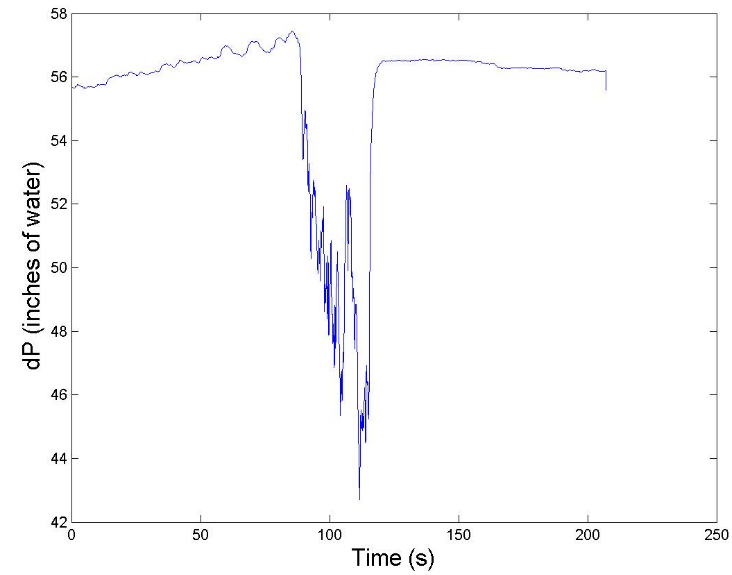

Fig. D.450.: Test section differential pressure for test 113.

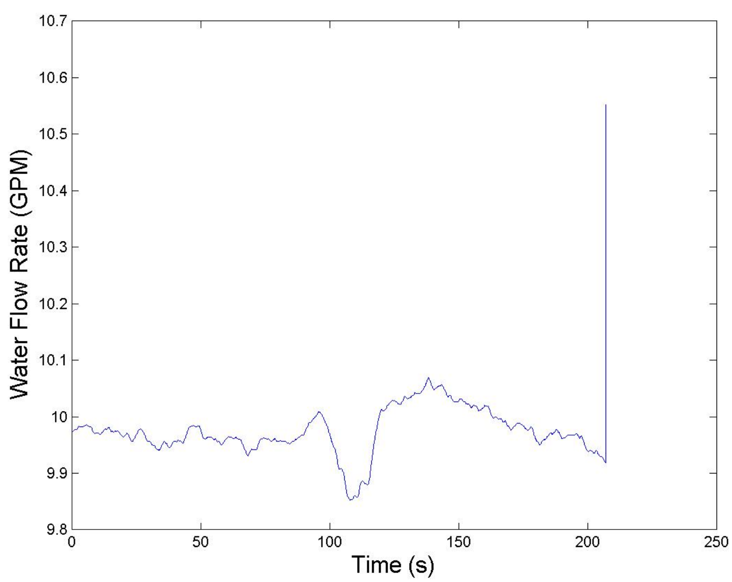

Fig. D.451.: Water flow rate for test 113.

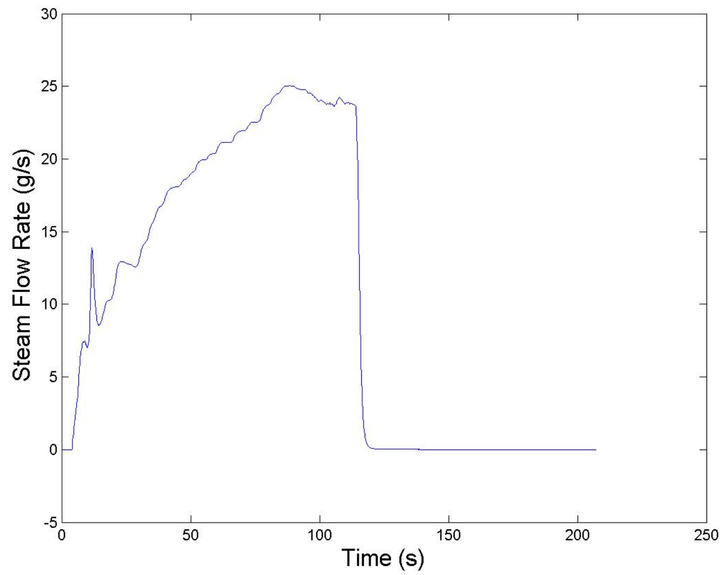

Fig. D.452.: Steam flow rate for test 113.

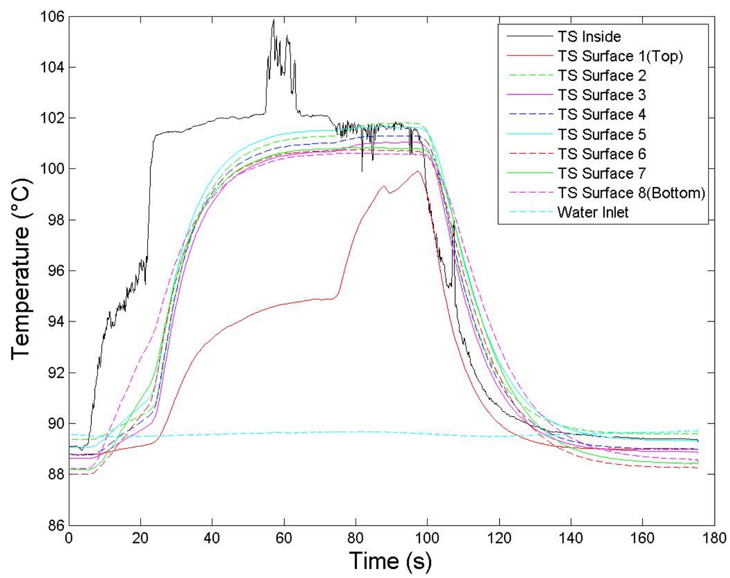

Fig. D.453.: Test section temperatures for test 114.

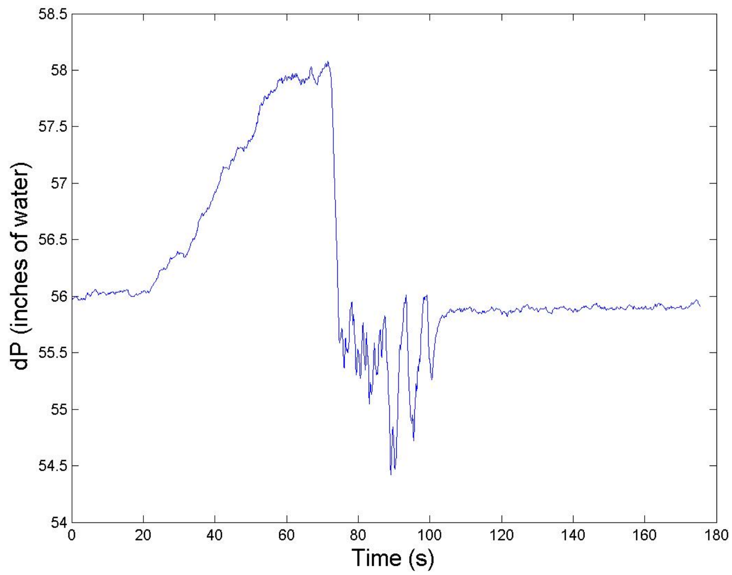

Fig. D.454.: Test section differential pressure for test 114.

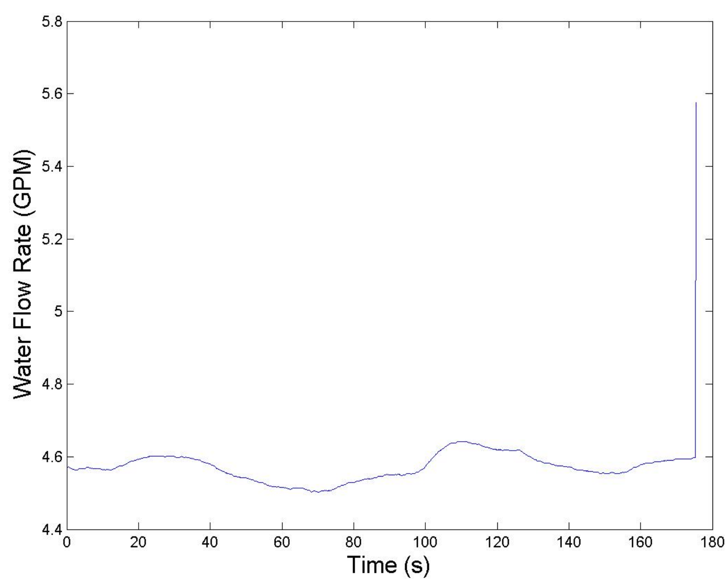

Fig. D.455.: Water flow rate for test 114.

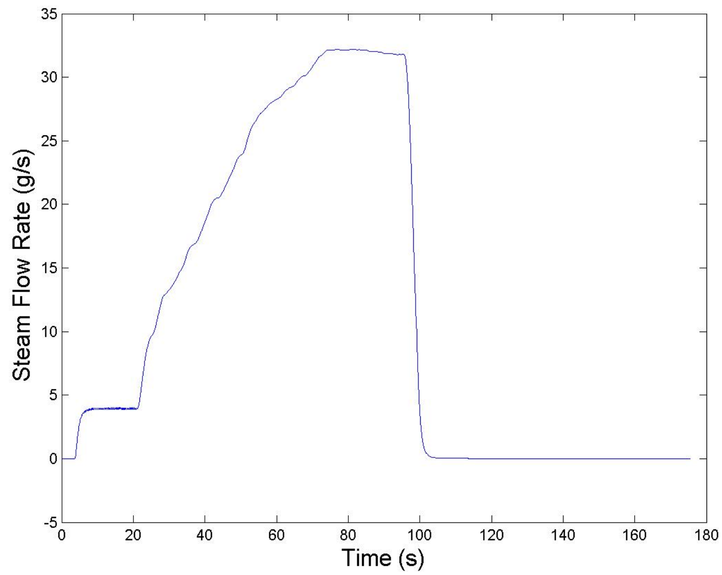

Fig. D.456.: Steam flow rate for test 114.

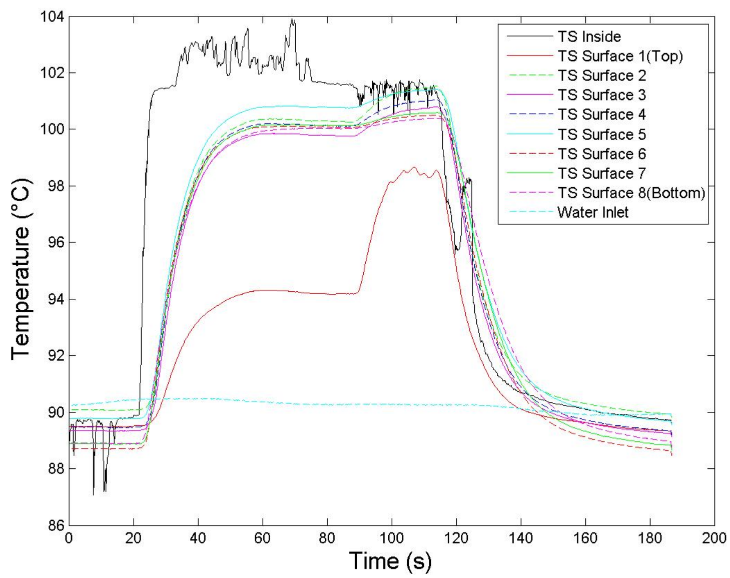

Fig. D.457.: Test section temperatures for test 115.

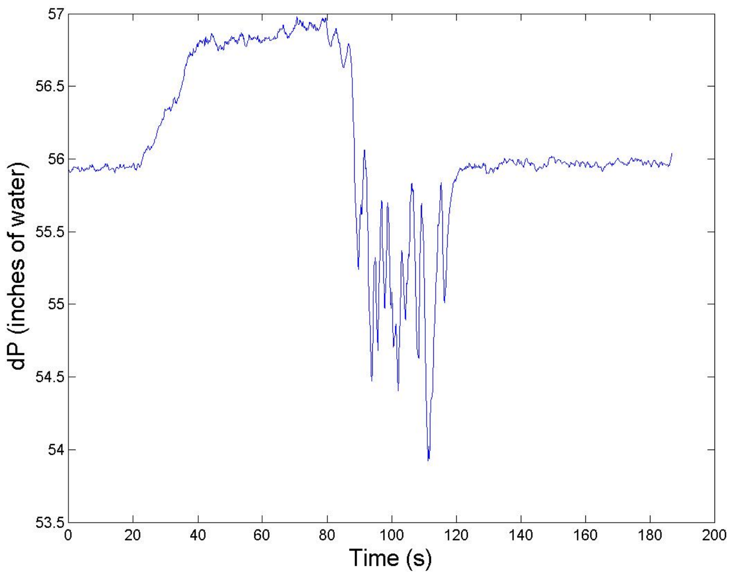

Fig. D.458.: Test section differential pressure for test 115.

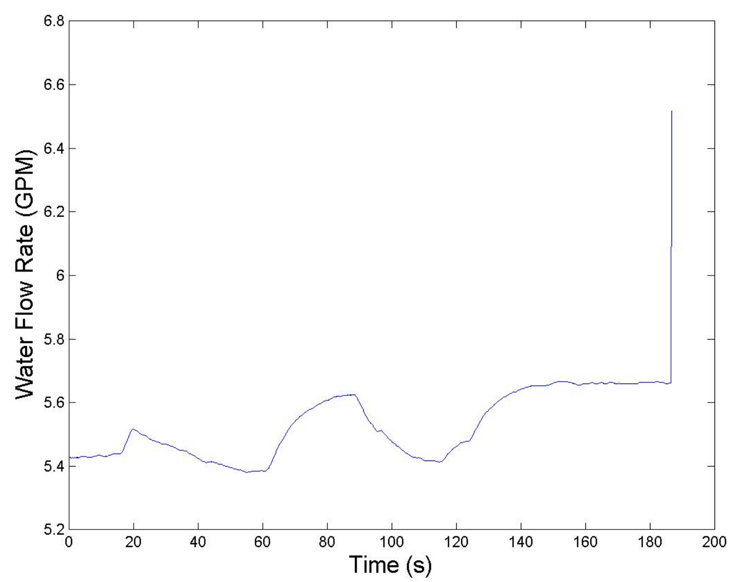

Fig. D.459.: Water flow rate for test 115.

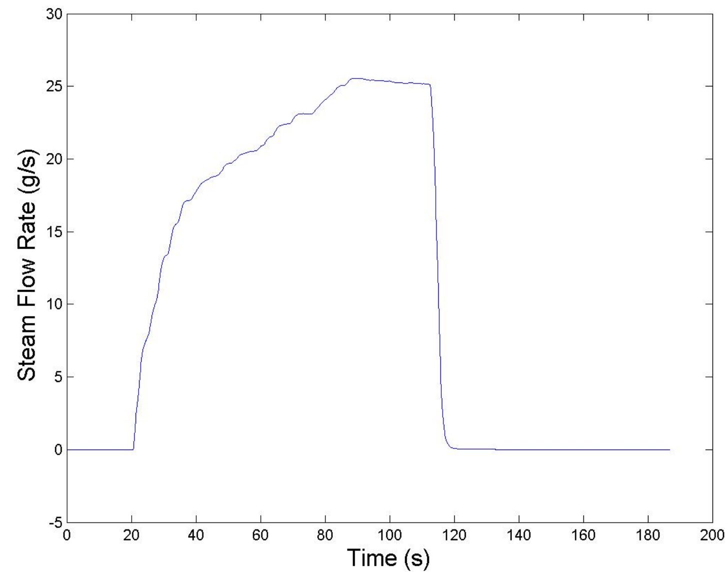

Fig. D.460.: Steam flow rate for test 115.

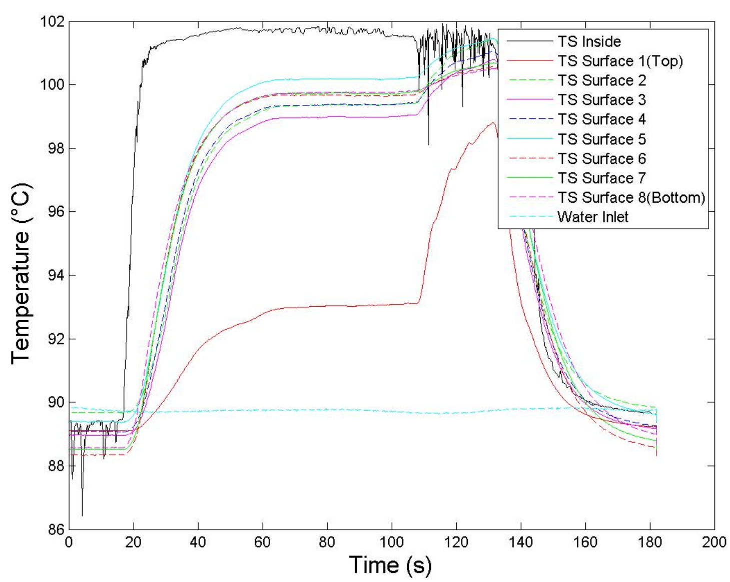

Fig. D.461.: Test section temperatures for test 116.

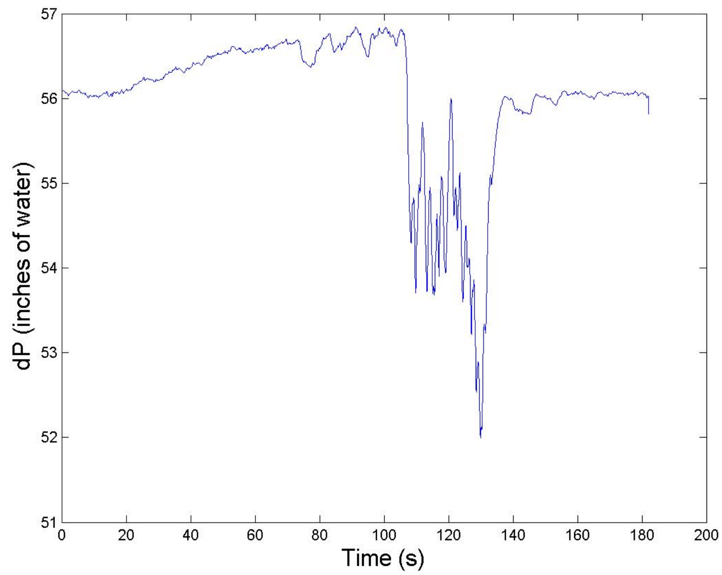

Fig. D.462.: Test section differential pressure for test 116.

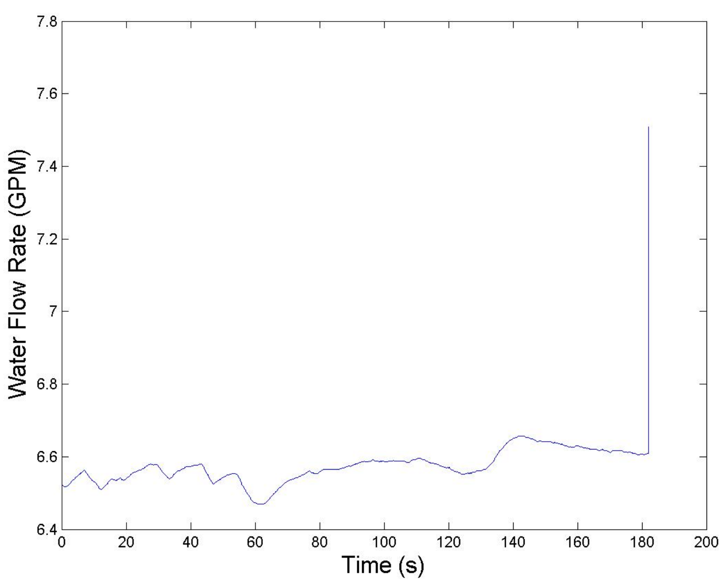

Fig. D.463.: Water flow rate for test 116.

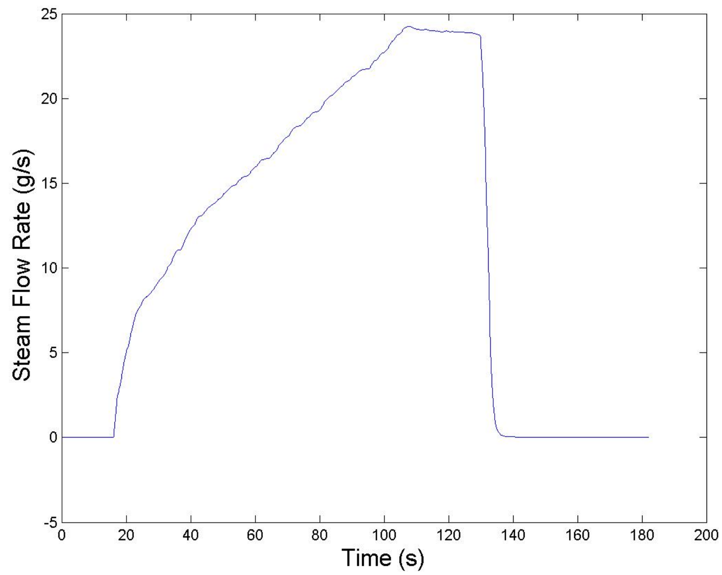

Fig. D.464.: Steam flow rate for test 116.

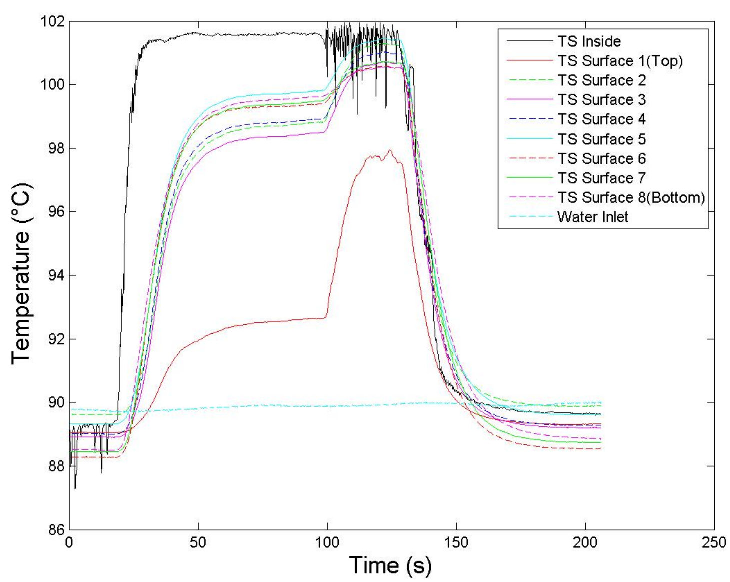

Fig. D.465.: Test section temperatures for test 117.

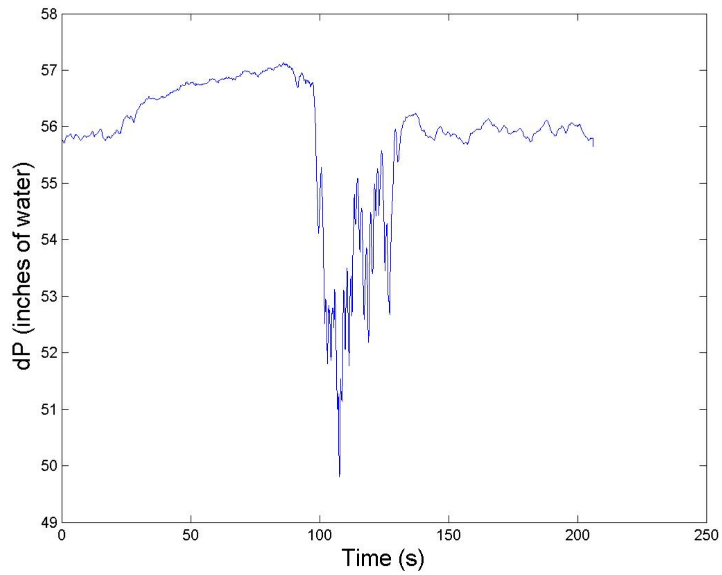

Fig. D.466.: Test section differential pressure for test 117.

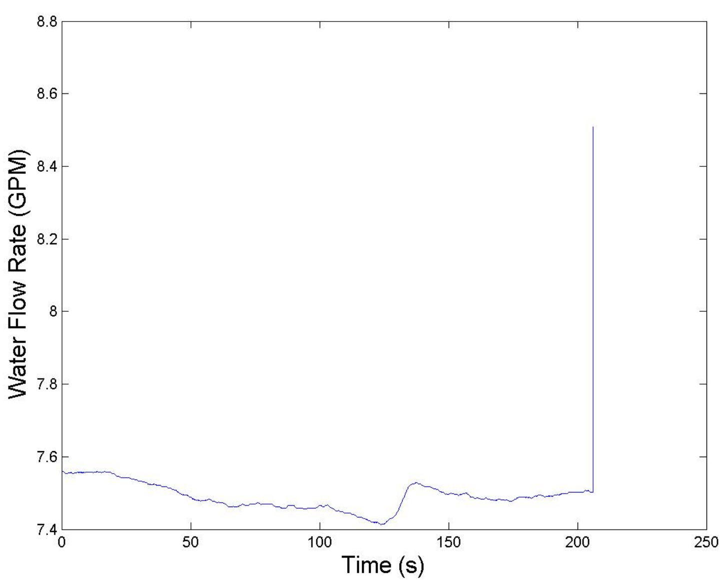

Fig. D.467.: Water flow rate for test 117.

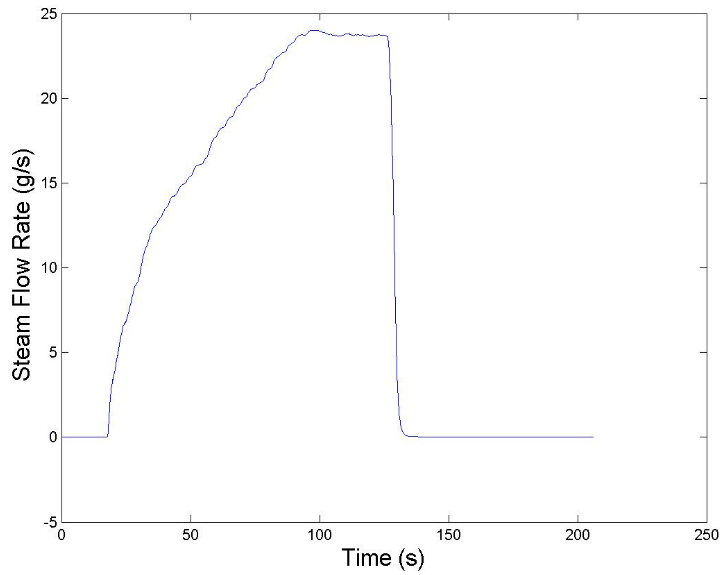

Fig. D.468.: Steam flow rate for test 117.

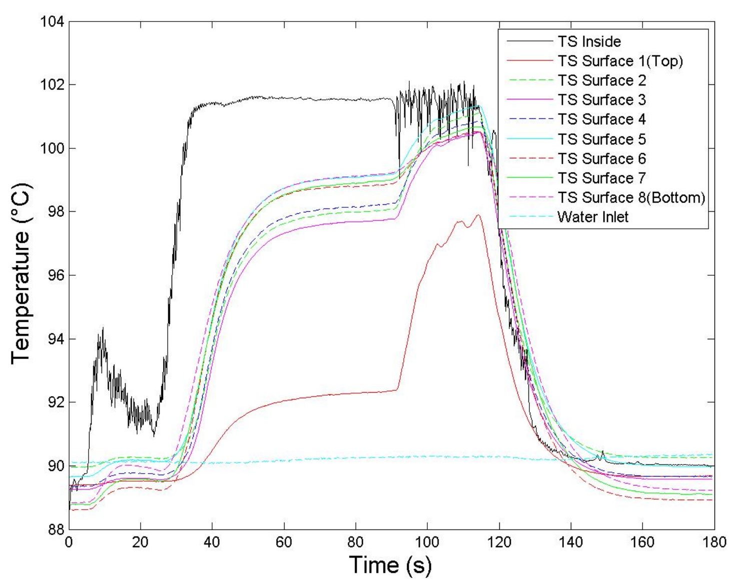

Fig. D.469.: Test section temperatures for test 118.

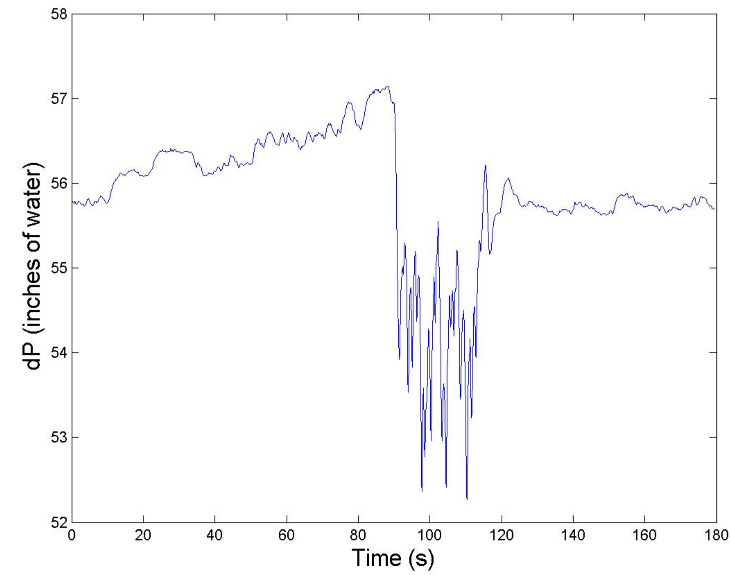

Fig. D.470.: Test section differential pressure for test 118.

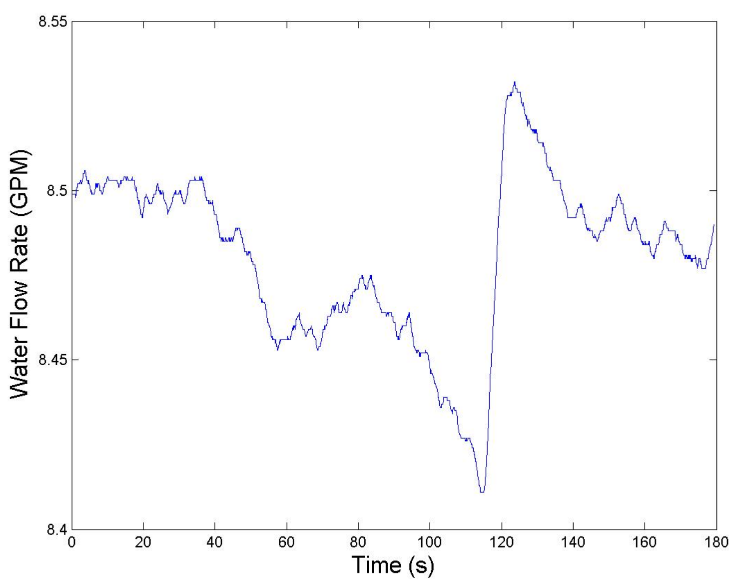

Fig. D.471.: Water flow rate for test 118.

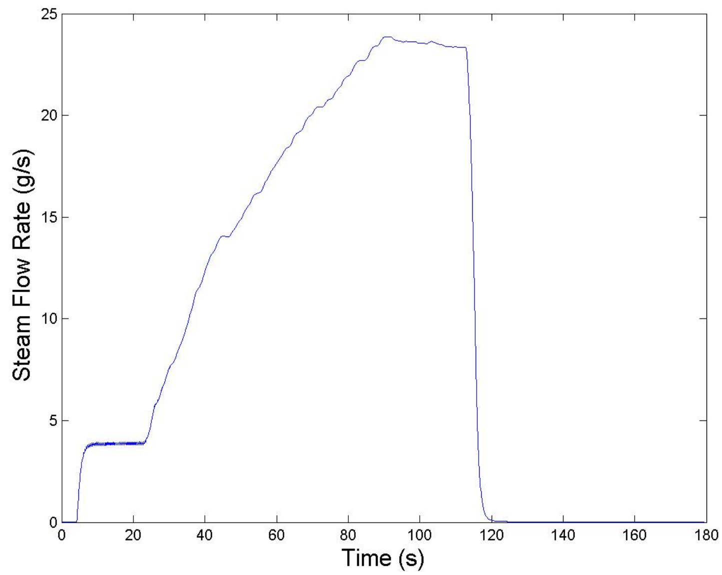

Fig. D.472.: Steam flow rate for test 118.

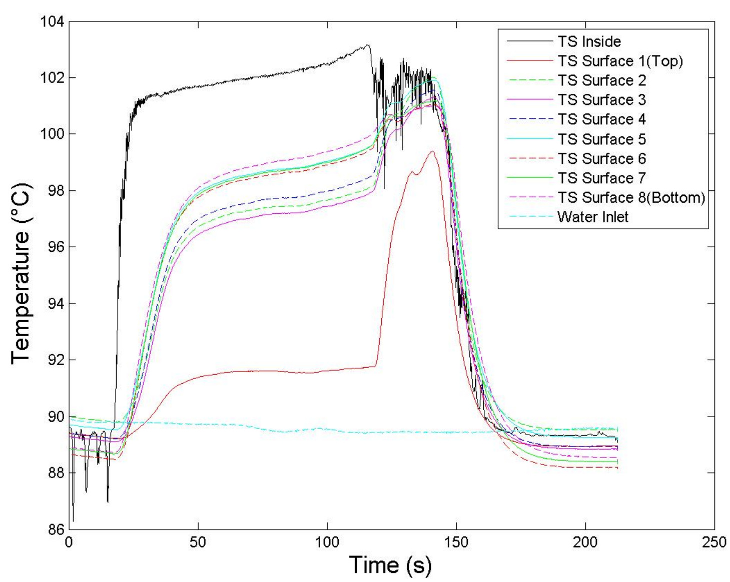

Fig. D.473.: Test section temperatures for test 119.

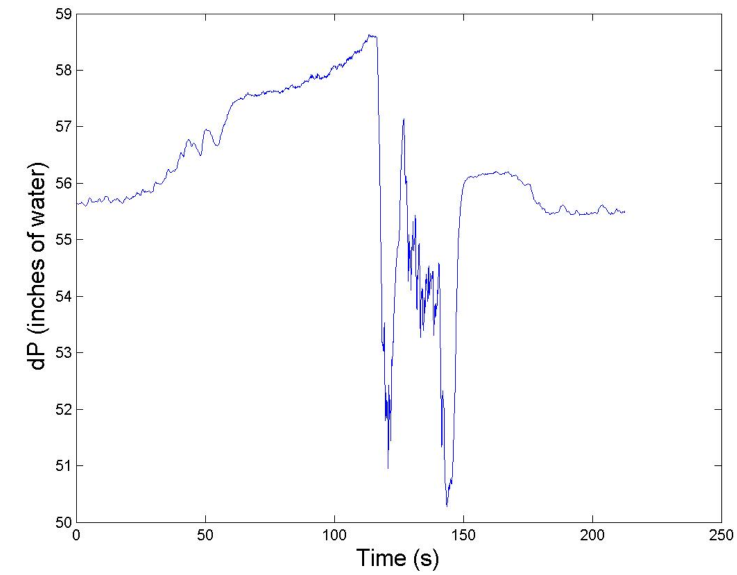

Fig. D.474.: Test section differential pressure for test 119.

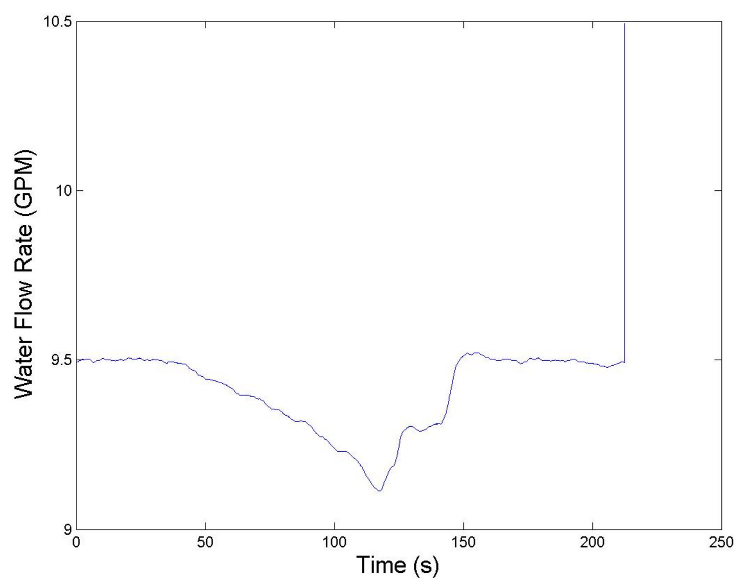

Fig. D.475.: Water flow rate for test 119.

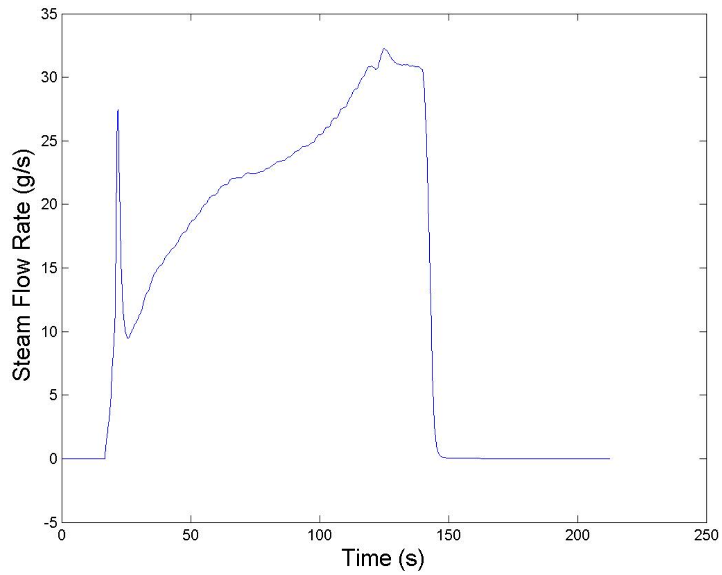

Fig. D.476.: Steam flow rate for test 119.

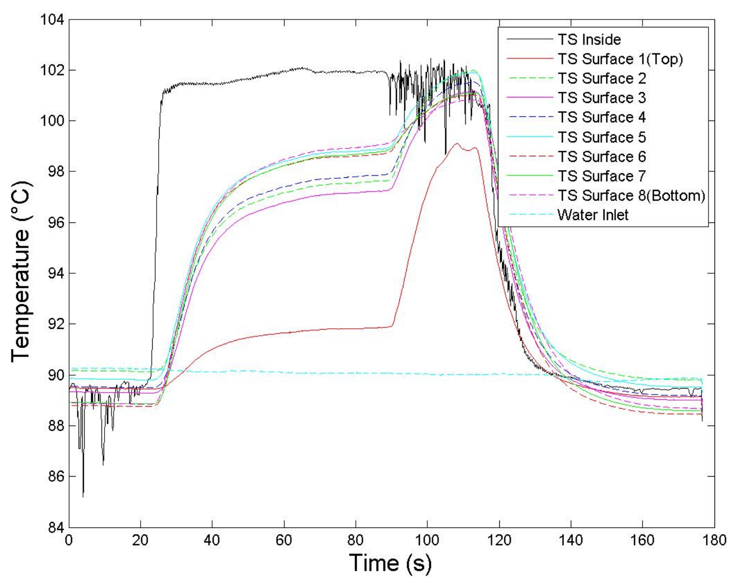

Fig. D.477.: Test section temperatures for test 120.

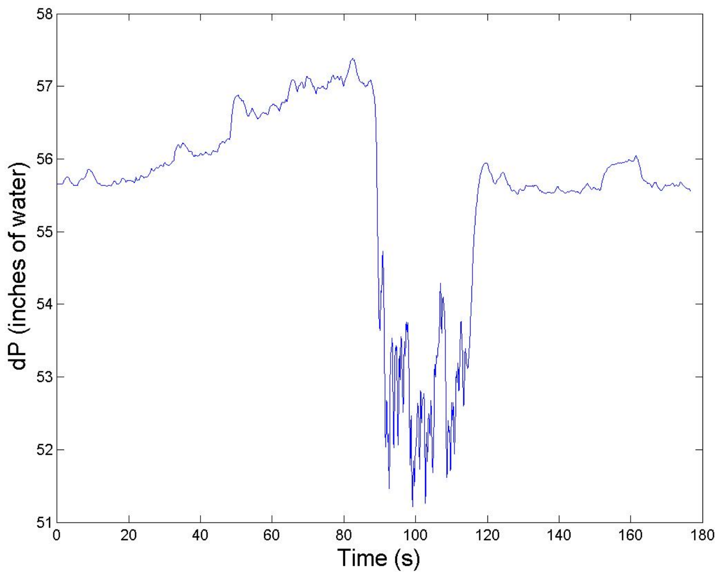

Fig. D.478.: Test section differential pressure for test 120.

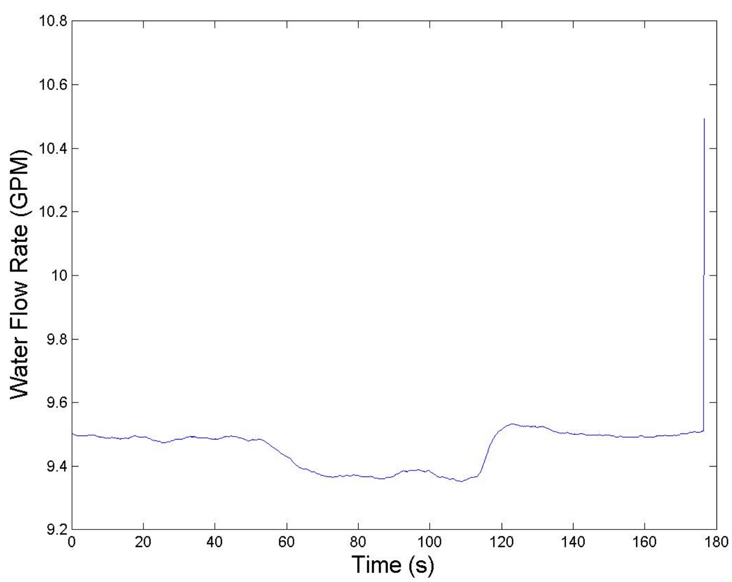

Fig. D.479.: Water flow rate for test 120.

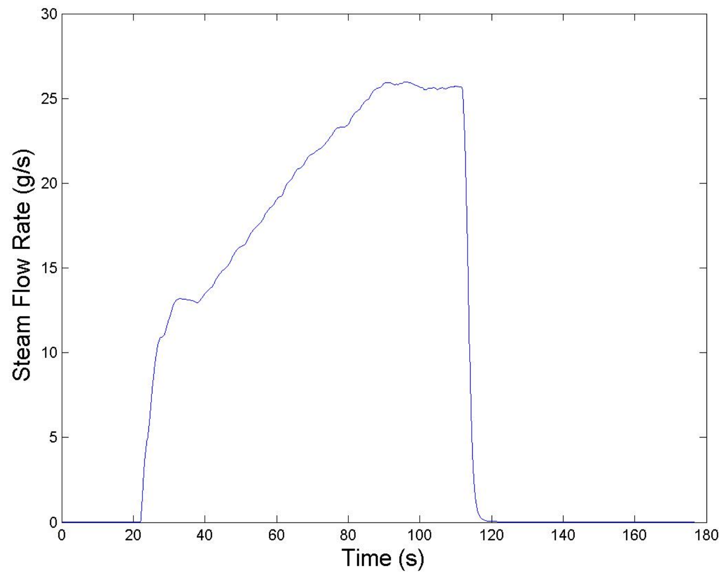

Fig. D.480.: Steam flow rate for test 120.

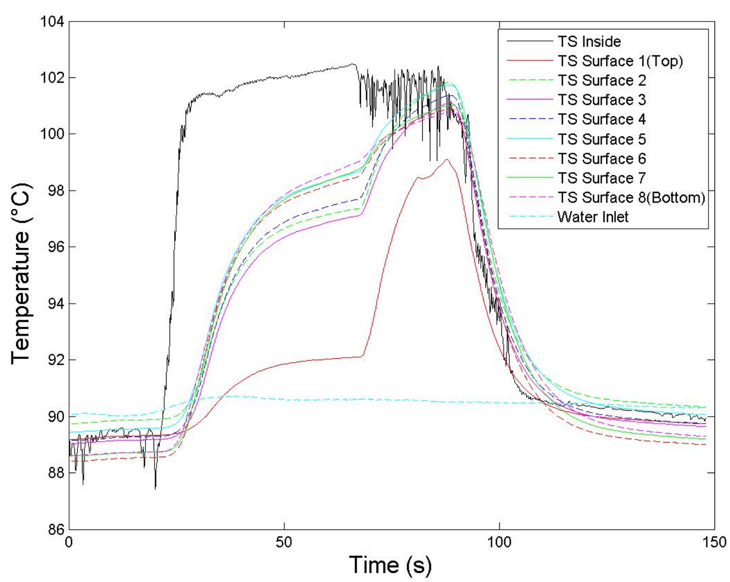

Fig. D.481.: Test section temperatures for test 121.

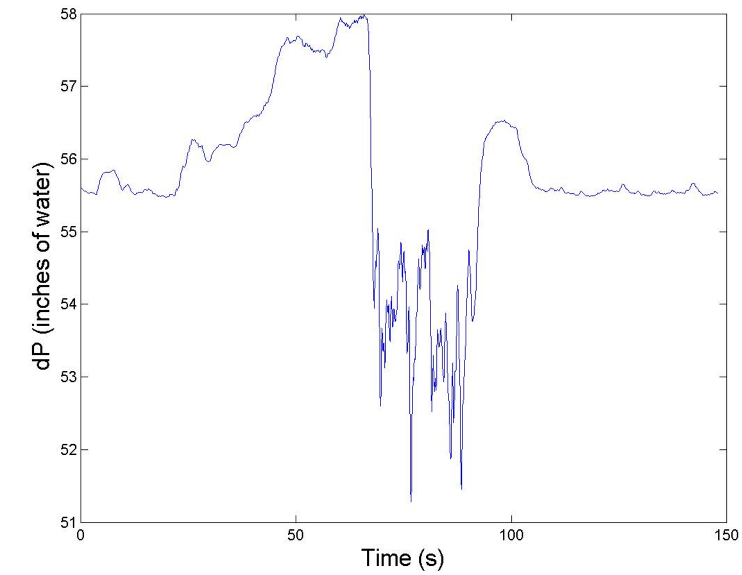

Fig. D.482.: Test section differential pressure for test 121.

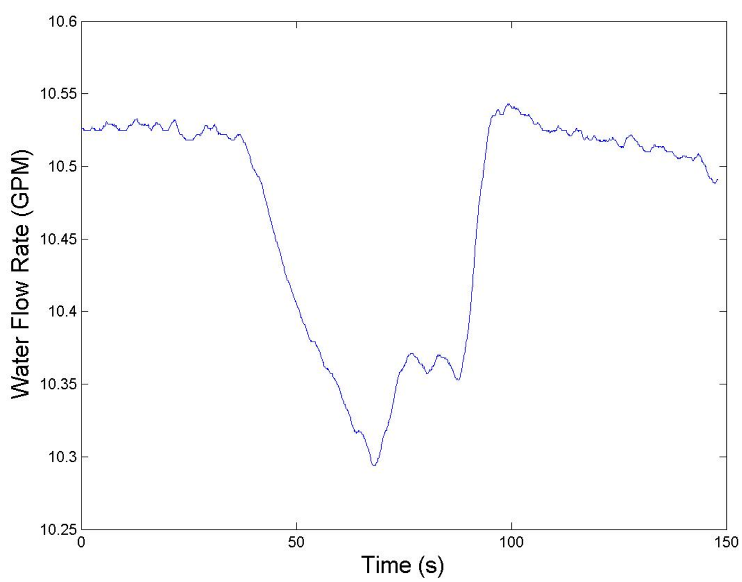

Fig. D.483.: Water flow rate for test 121.

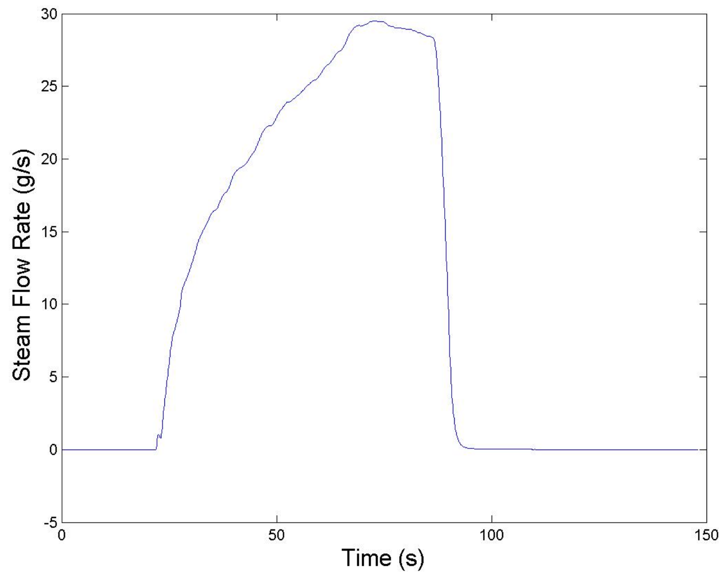

Fig. D.484.: Steam flow rate for test 121.

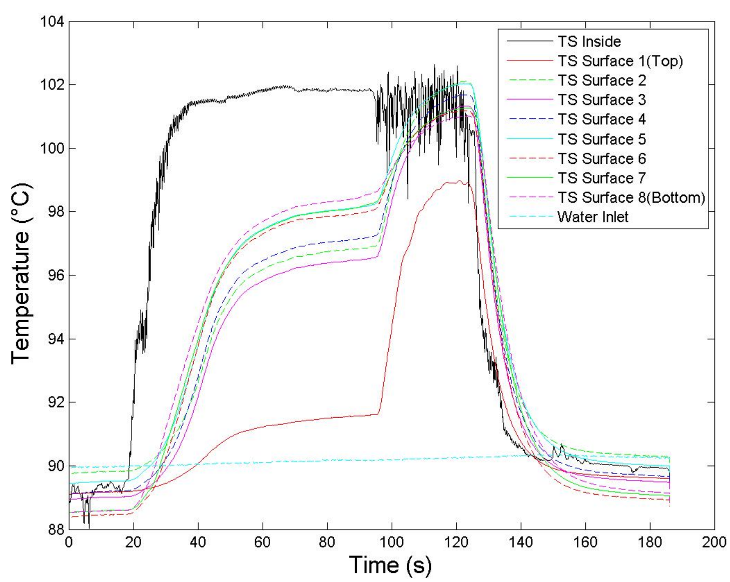

Fig. D.485.: Test section temperatures for test 122.

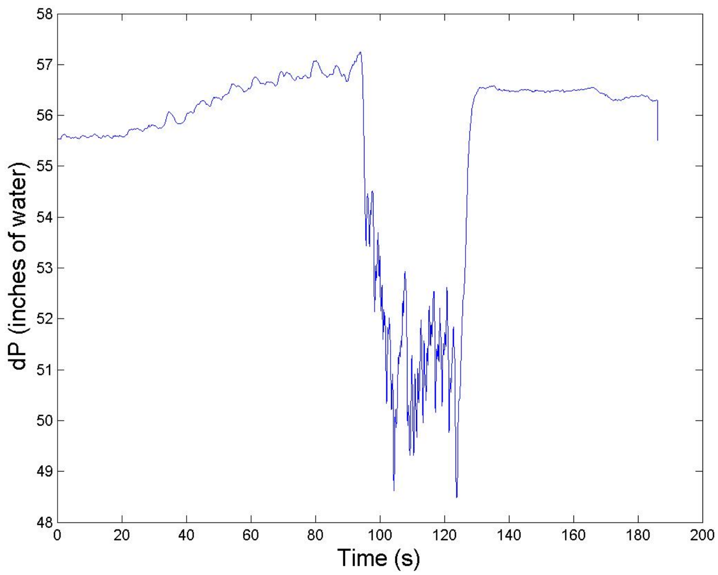

Fig. D.486.: Test section differential pressure for test 122.

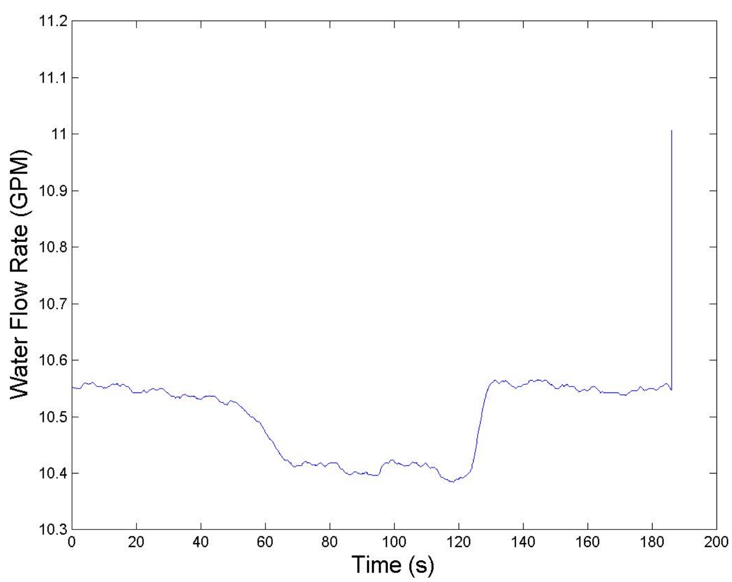

Fig. D.487.: Water flow rate for test 122.

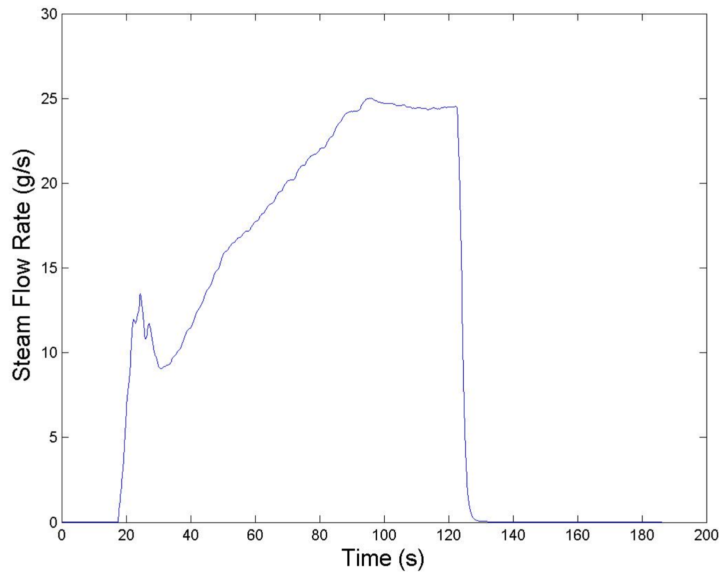

Fig. D.488.: Steam flow rate for test 122.

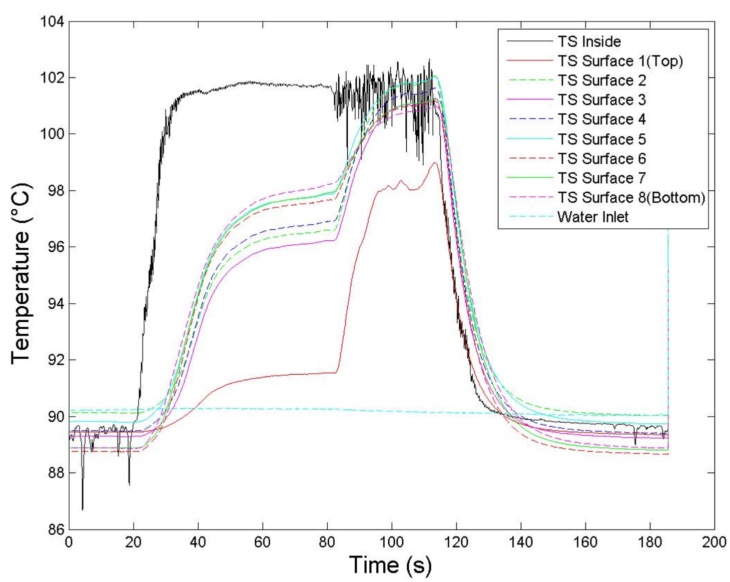

Fig. D.489.: Test section temperatures for test 123.

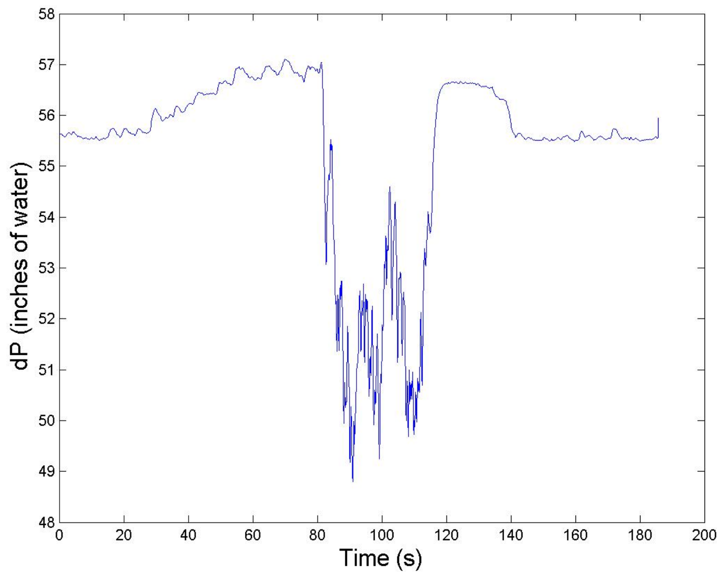

Fig. D.490.: Test section differential pressure for test 123.

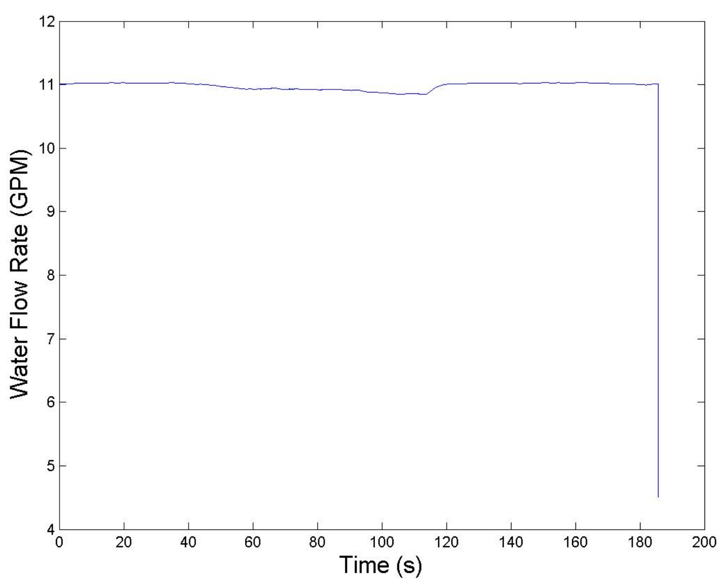

Fig. D.491.: Water flow rate for test 123.

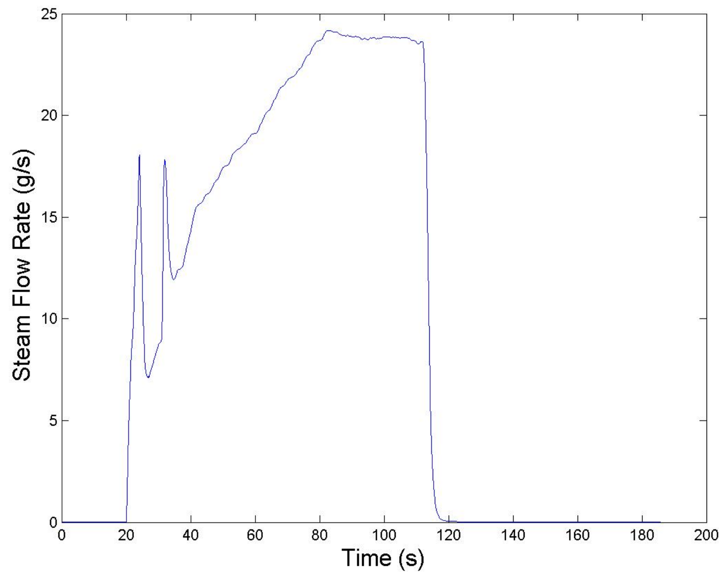

Fig. D.492.: Steam flow rate for test 123.

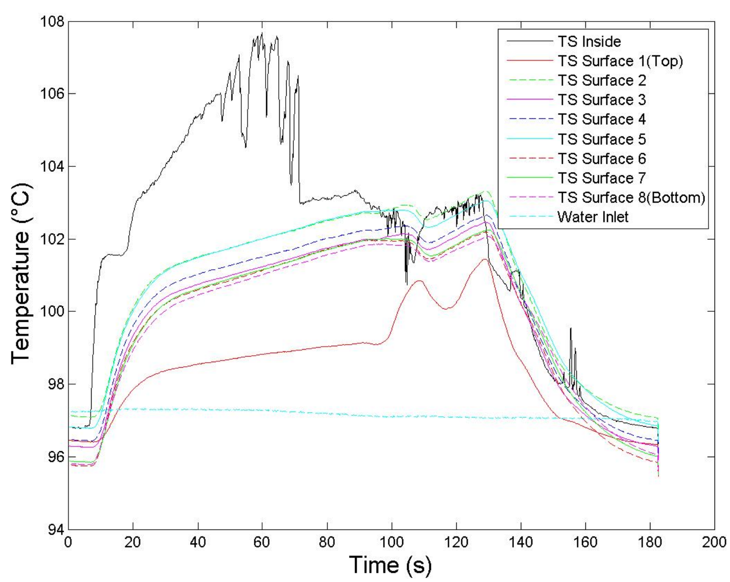

Fig. D.493.: Test section temperatures for test 124.

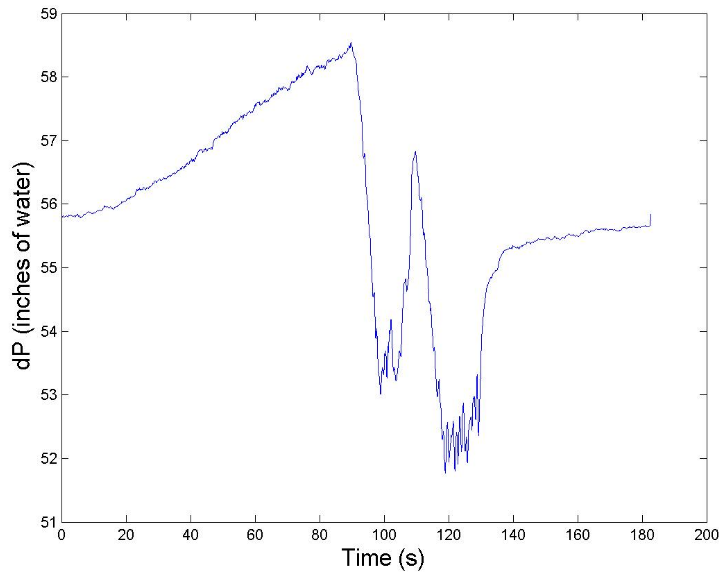

Fig. D.494.: Test section differential pressure for test 124.

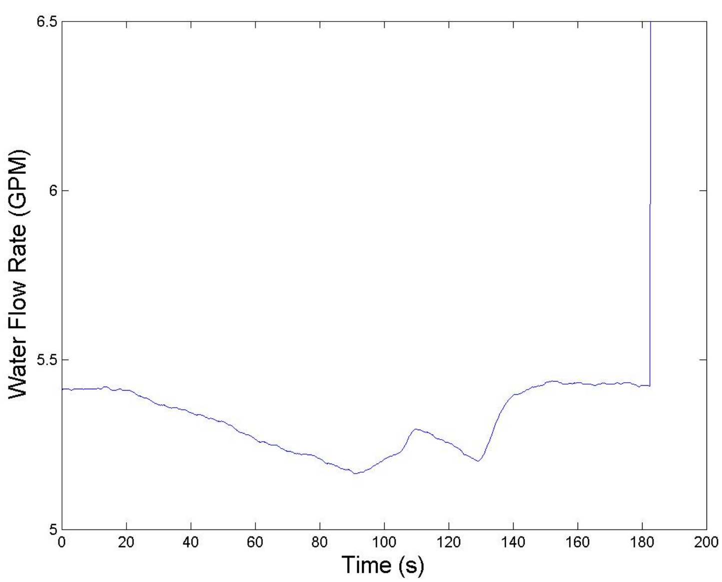

Fig. D.495.: Water flow rate for test 124.

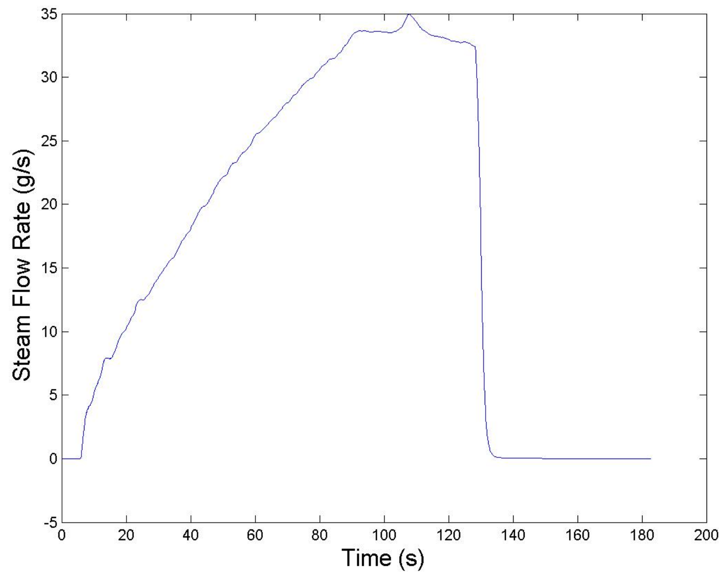

Fig. D.496.: Steam flow rate for test 124.

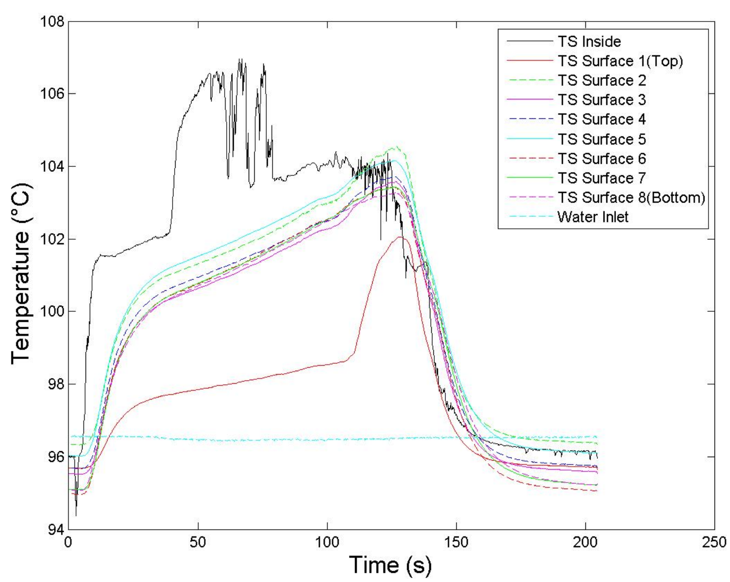

Fig. D.497.: Test section temperatures for test 125.

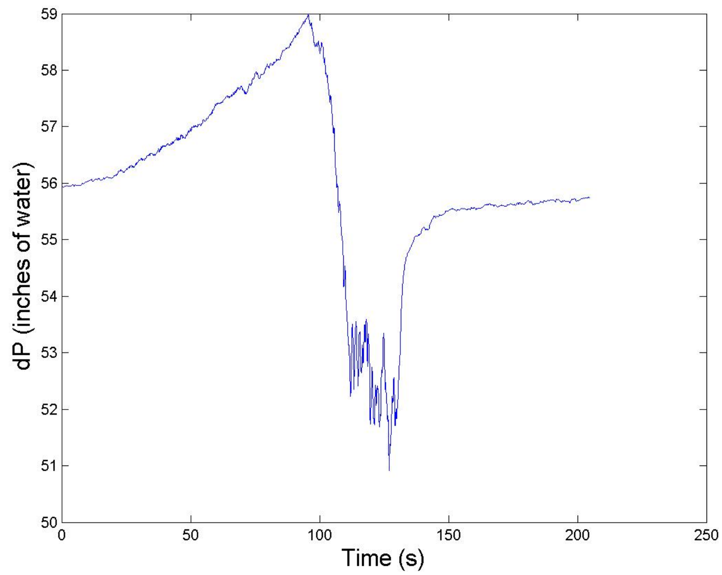

Fig. D.498.: Test section differential pressure for test 125.

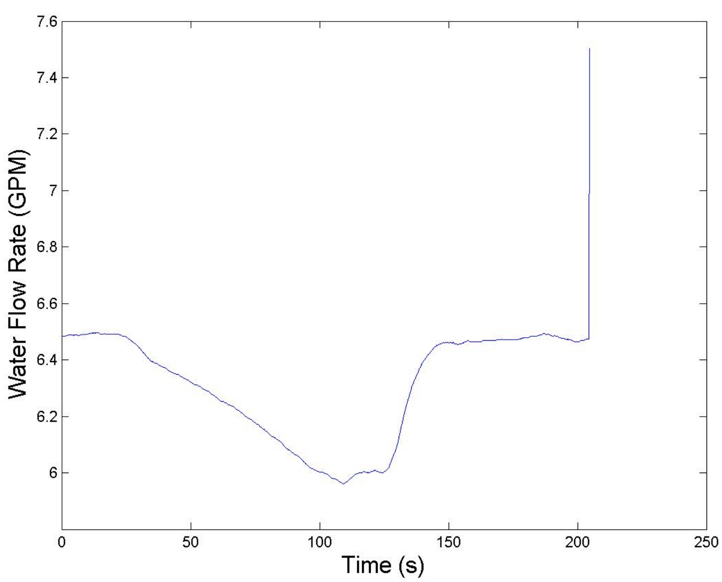

Fig. D.499.: Water flow rate for test 125.

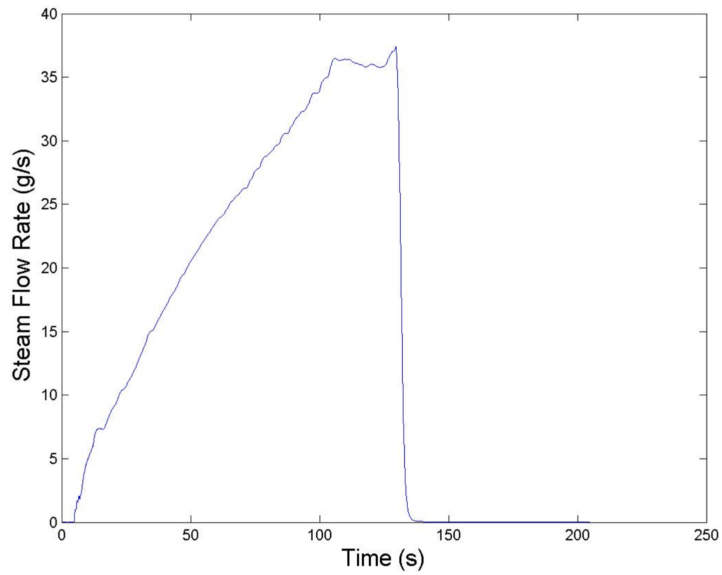

Fig. D.500.: Steam flow rate for test 125.

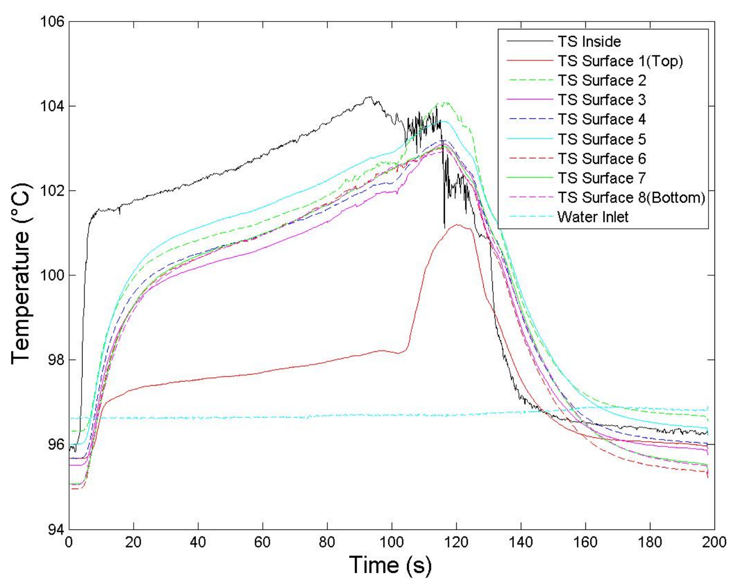

Fig. D.501.: Test section temperatures for test 126.

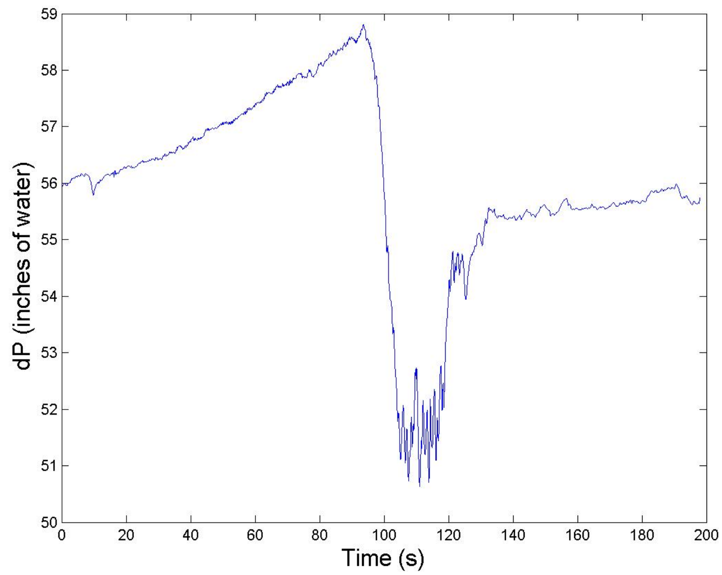

Fig. D.502.: Test section differential pressure for test 126.

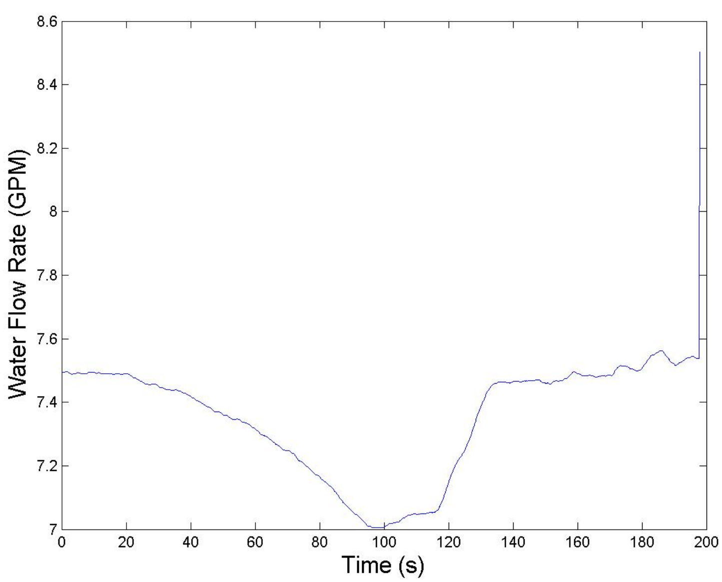

Fig. D.503.: Water flow rate for test 126.

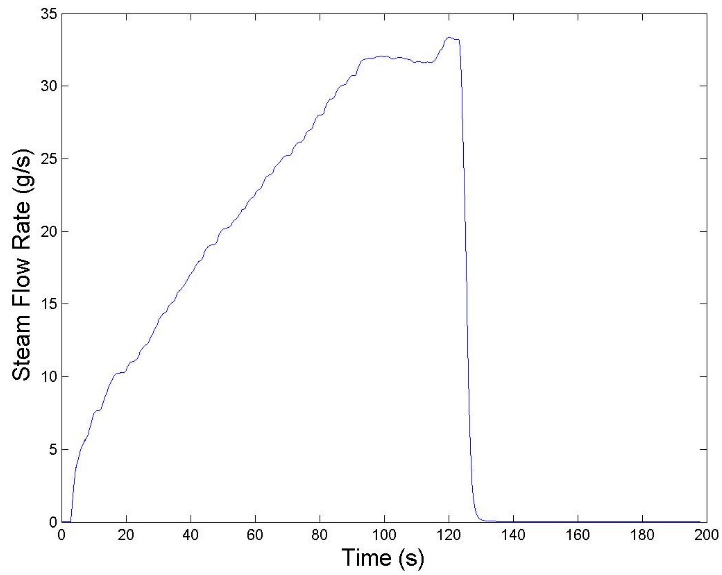

Fig. D.504.: Steam flow rate for test 126.

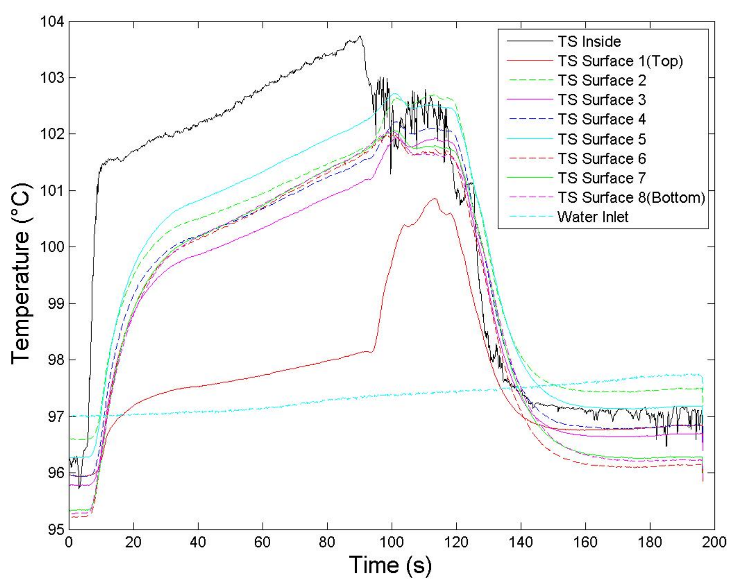

Fig. D.505.: Test section temperatures for test 127.

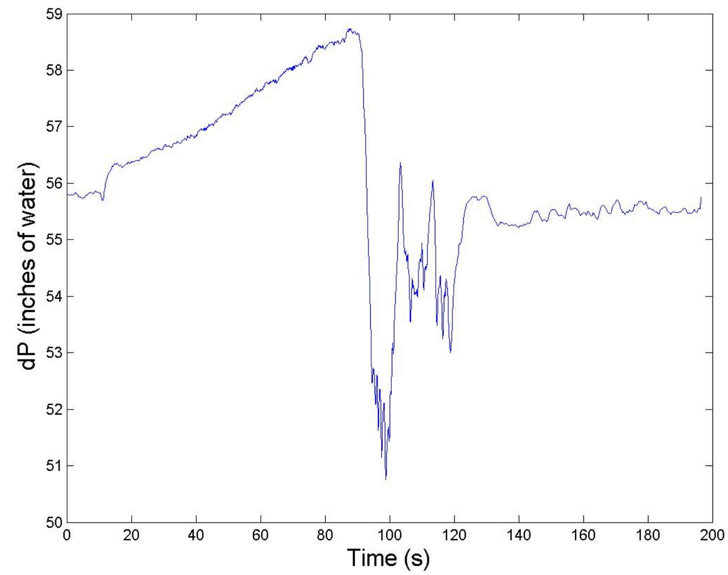

Fig. D.506.: Test section differential pressure for test 127.

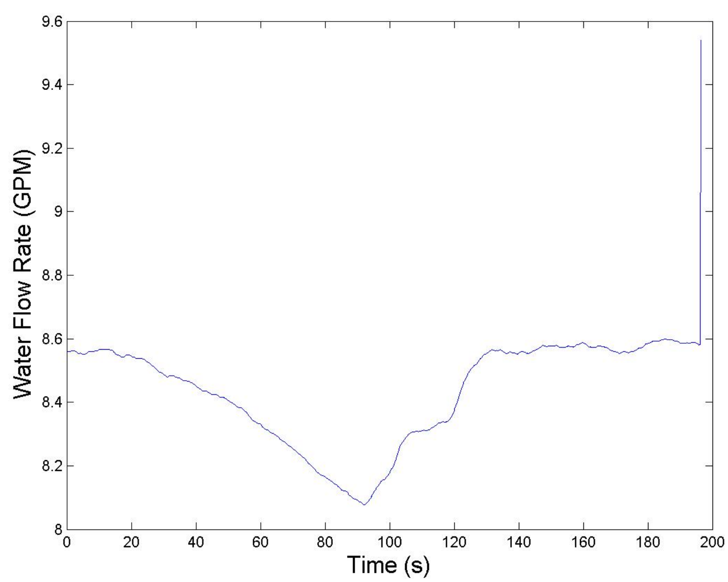

Fig. D.507.: Water flow rate for test 127.

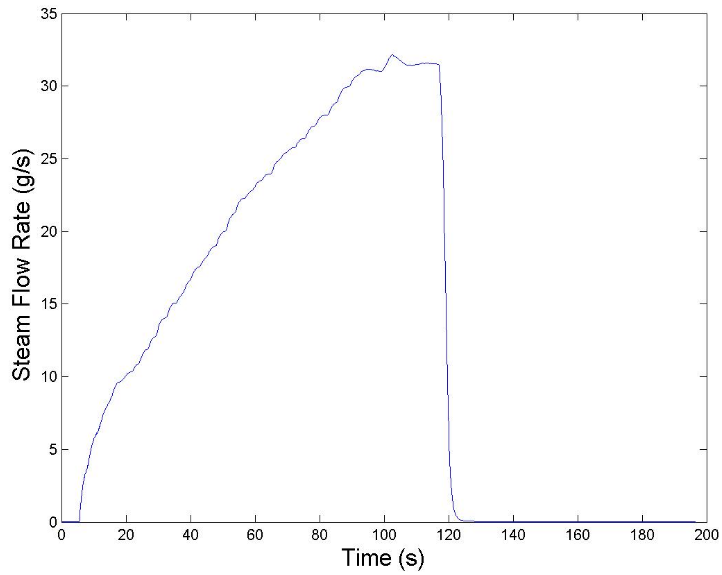

Fig. D.508.: Steam flow rate for test 127.

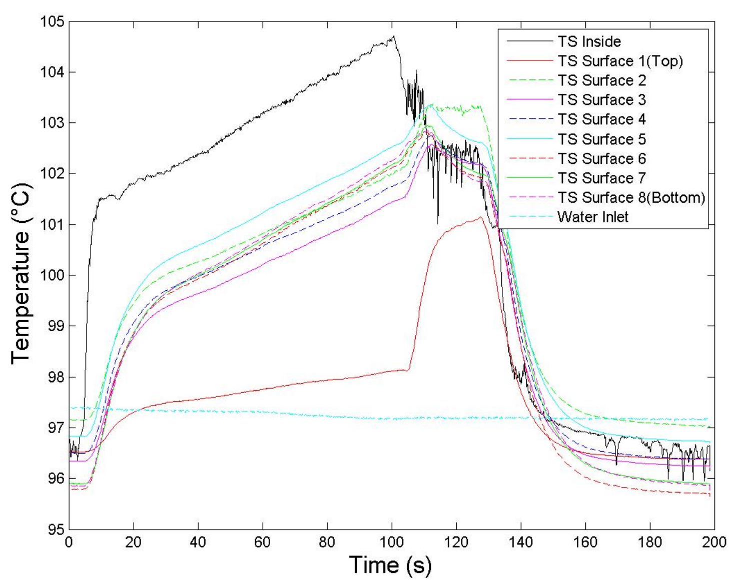

Fig. D.509.: Test section temperatures for test 128.

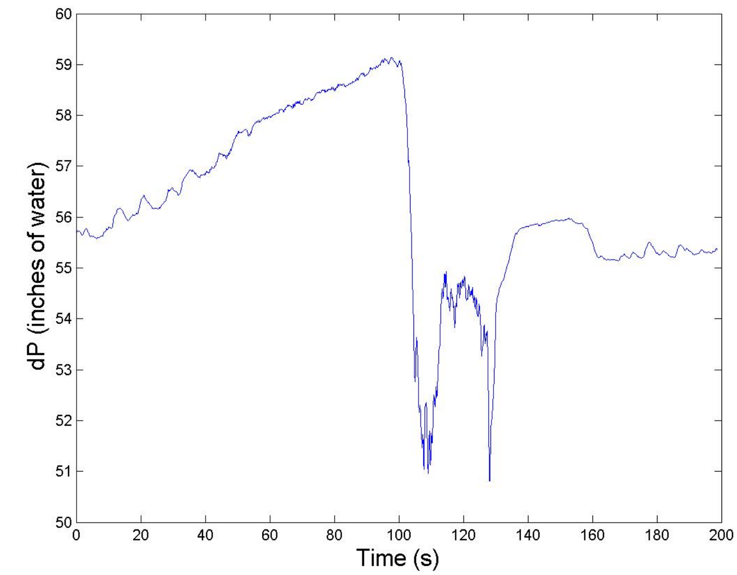

Fig. D.510.: Test section differential pressure for test 128.

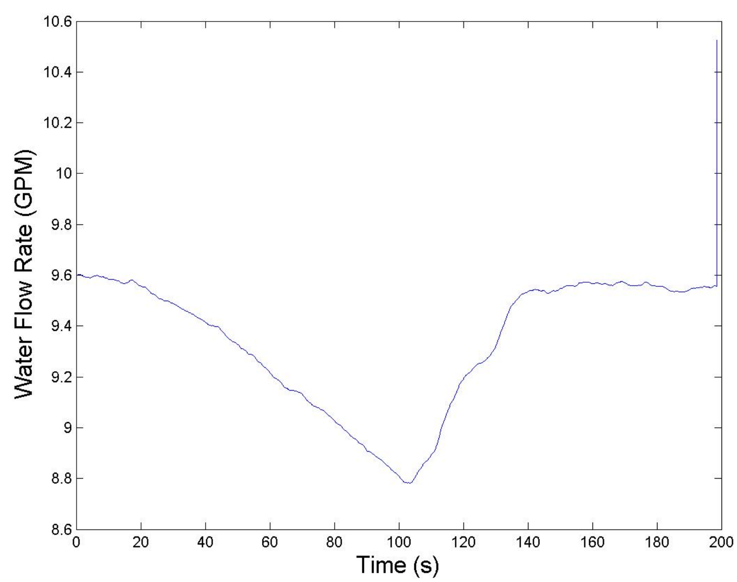

Fig. D.511.: Water flow rate for test 128.

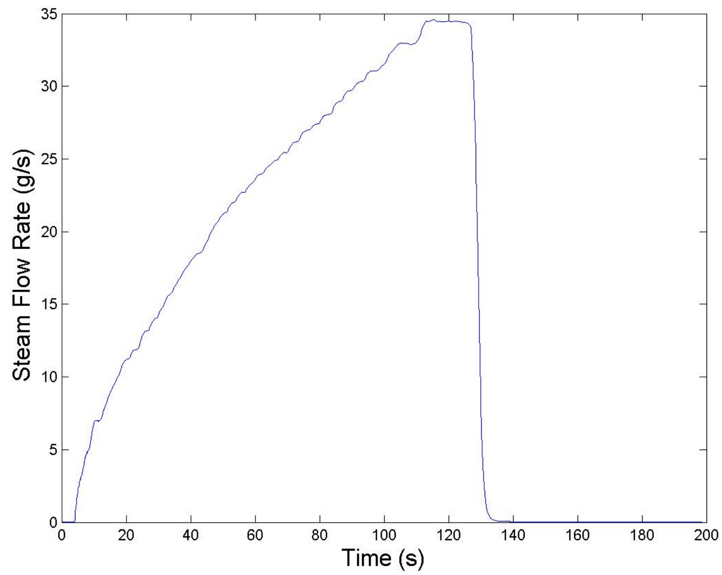

Fig. D.512.: Steam flow rate for test 128.

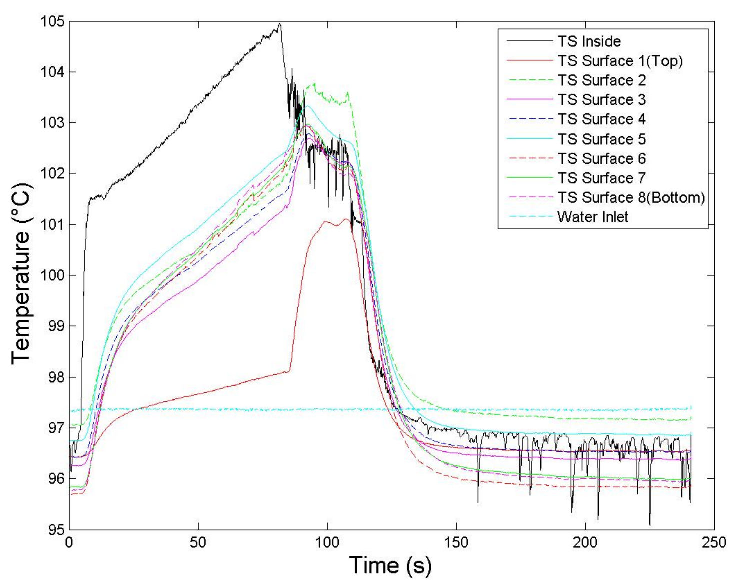

Fig. D.513.: Test section temperatures for test 129.

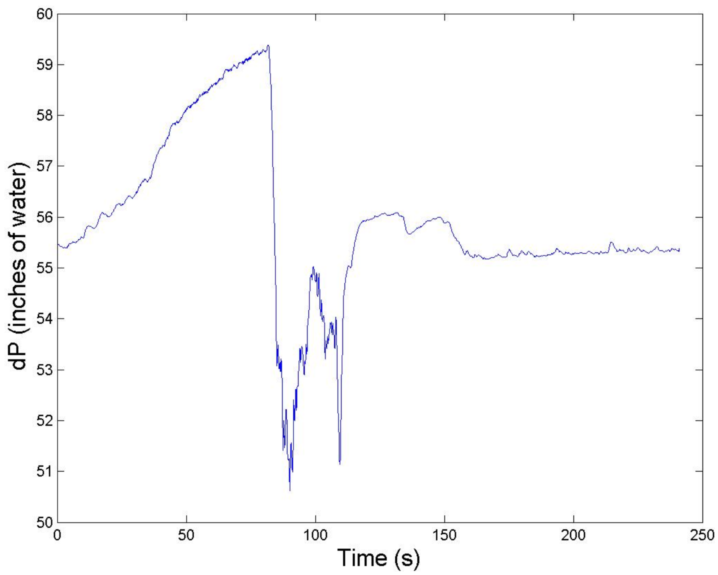

Fig. D.514.: Test section differential pressure for test 129.

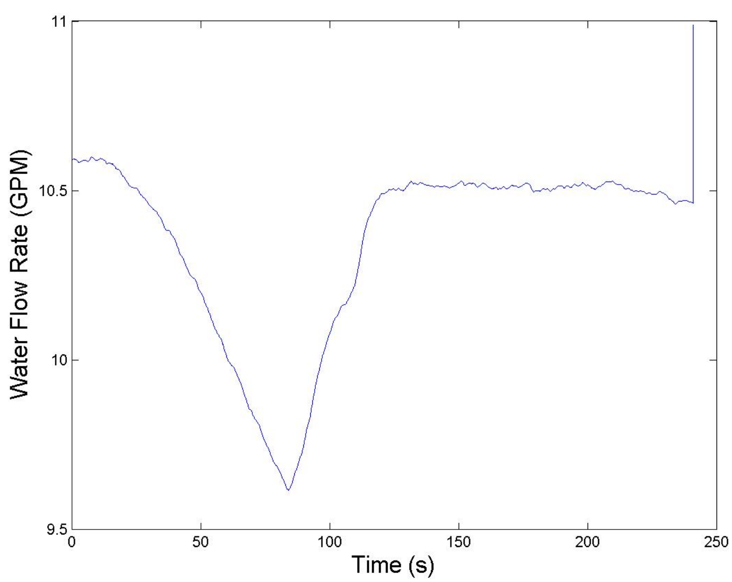

Fig. D.515.: Water flow rate for test 129.

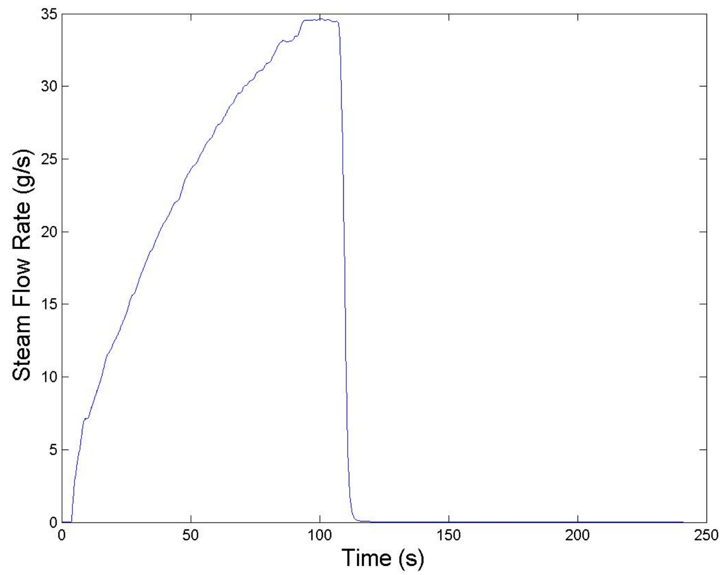

Fig. D.516.: Steam flow rate for test 129.

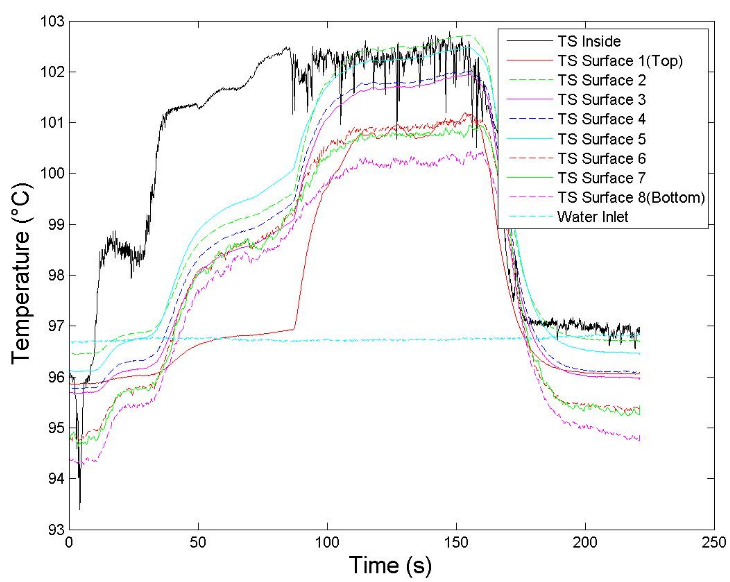

Fig. D.517.: Test section temperatures for test 130.

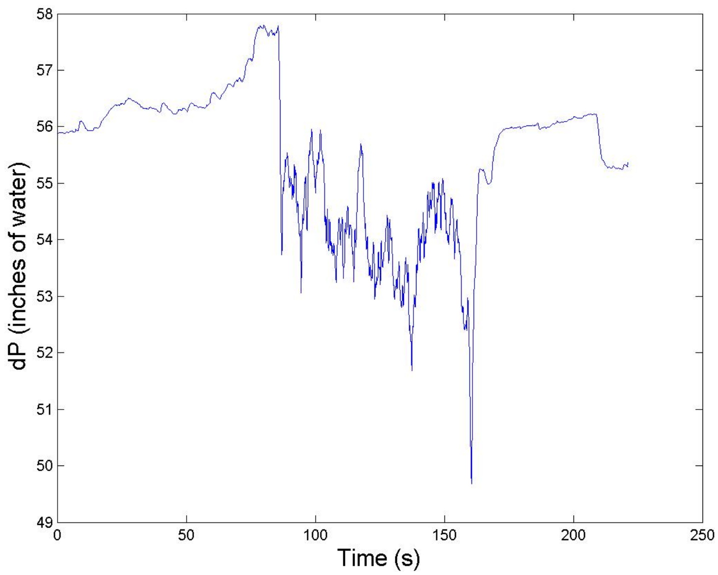

Fig. D.518.: Test section differential pressure for test 130.

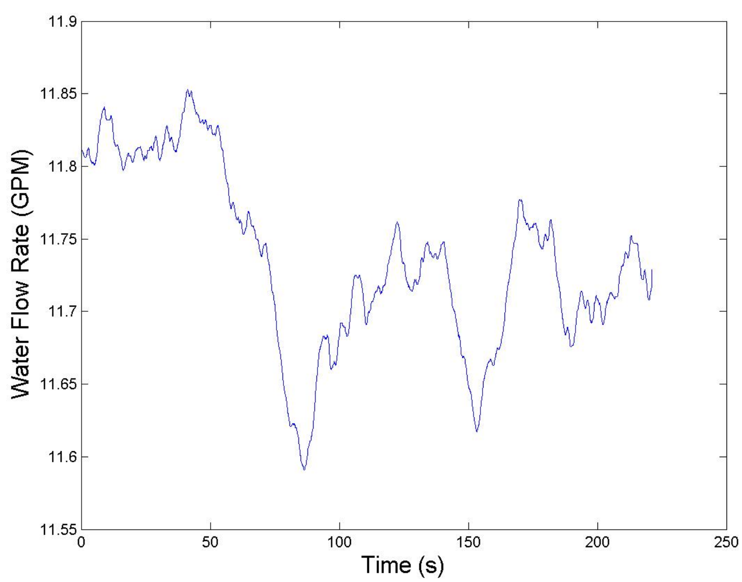

Fig. D.519.: Water flow rate for test 130.

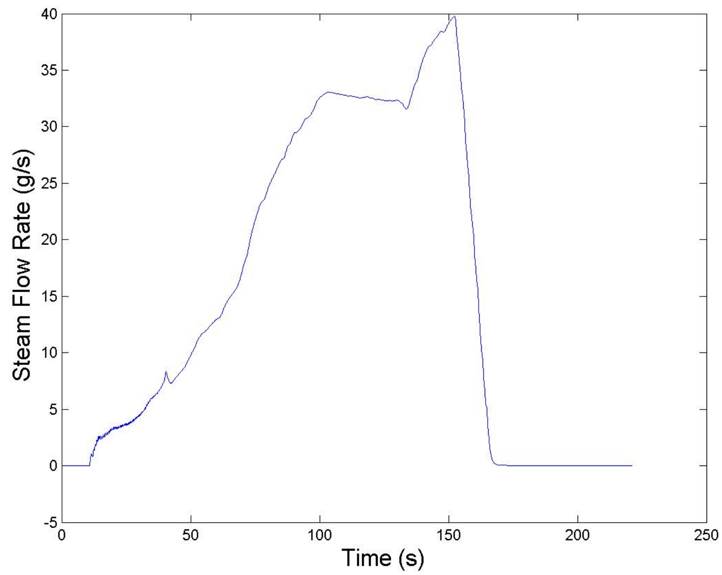

Fig. D.520.: Steam flow rate for test 130.

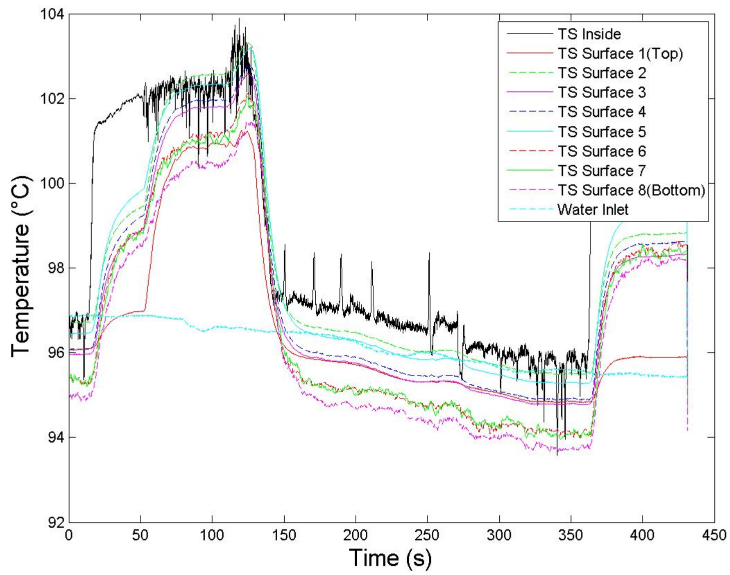

Fig. D.521.: Test section temperatures for test 131.

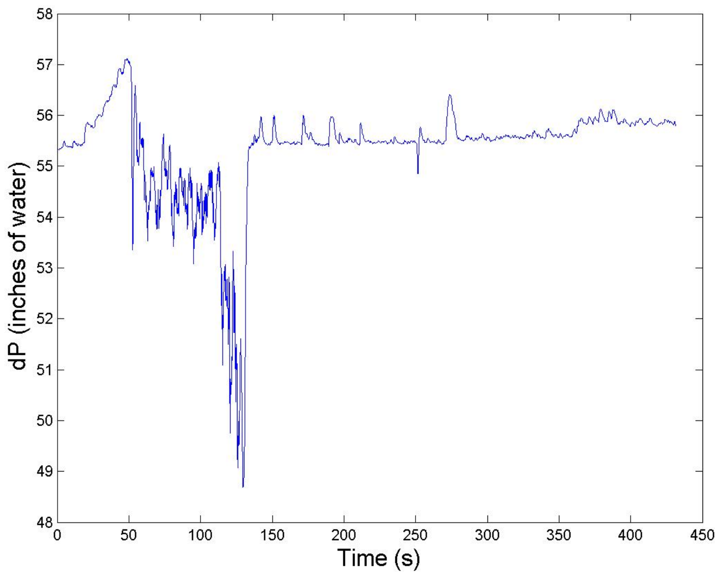

Fig. D.522.: Test section differential pressure for test 131.

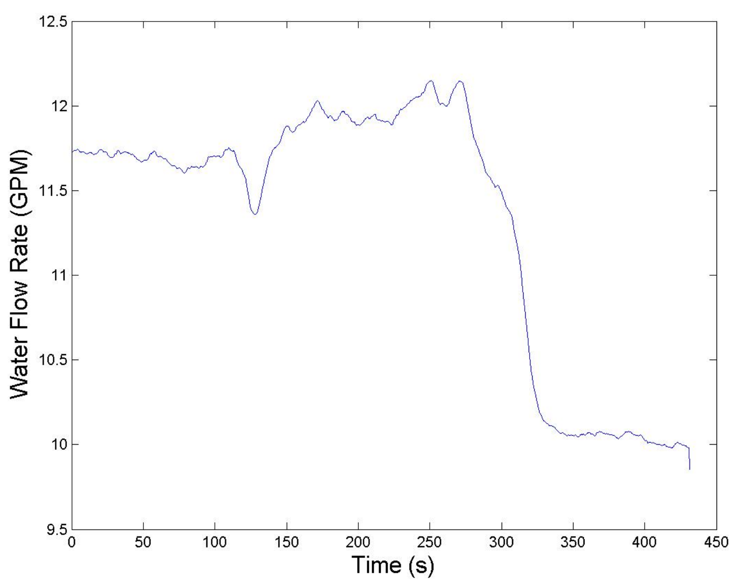

Fig. D.523.: Water flow rate for test 131.

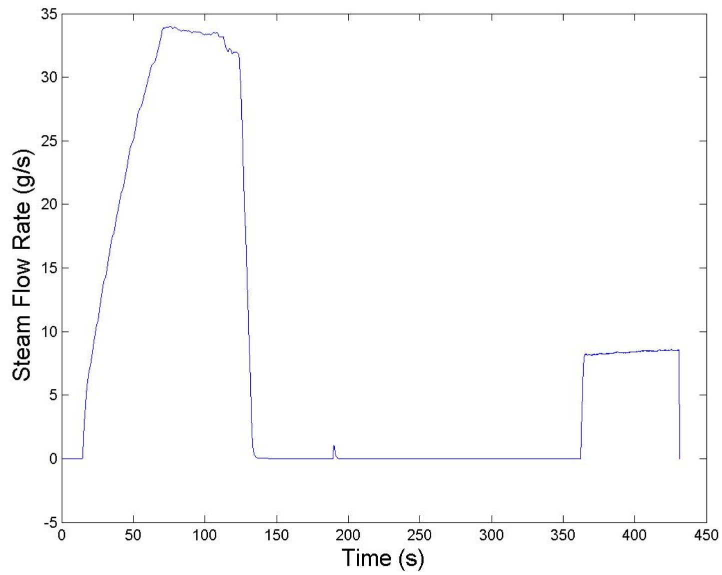

Fig. D.524.: Steam flow rate for test 131.

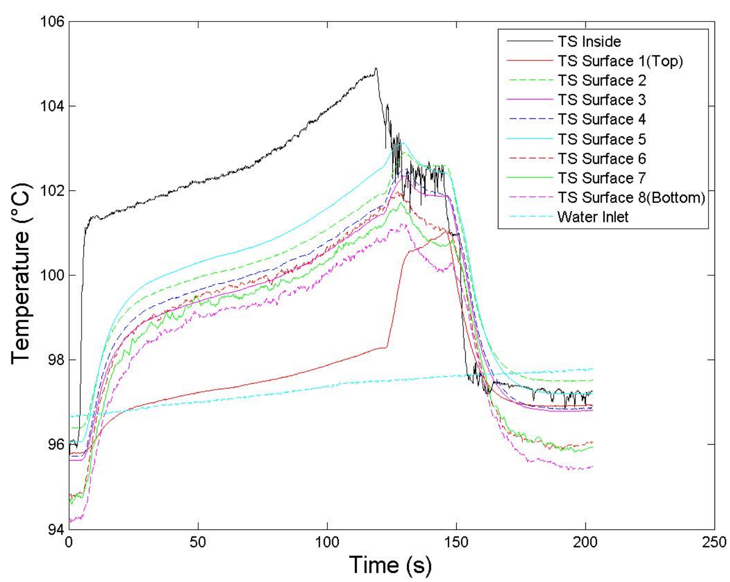

Fig. D.525.: Test section temperatures for test 132.

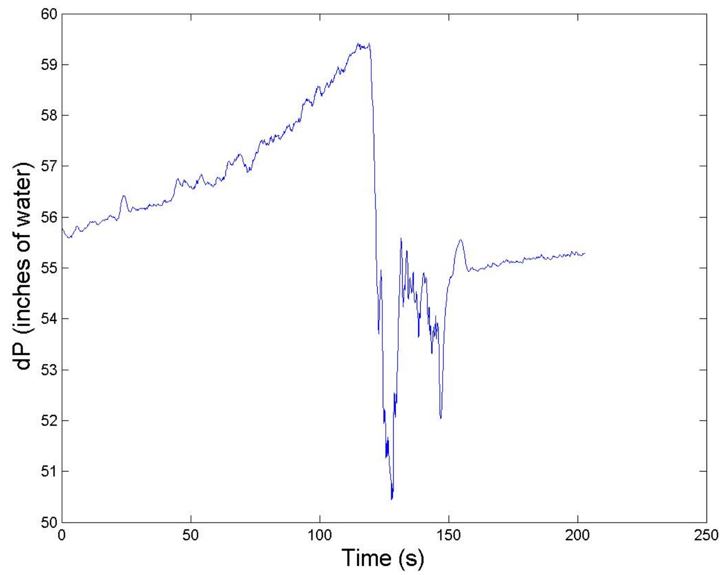

Fig. D.526.: Test section differential pressure for test 132.

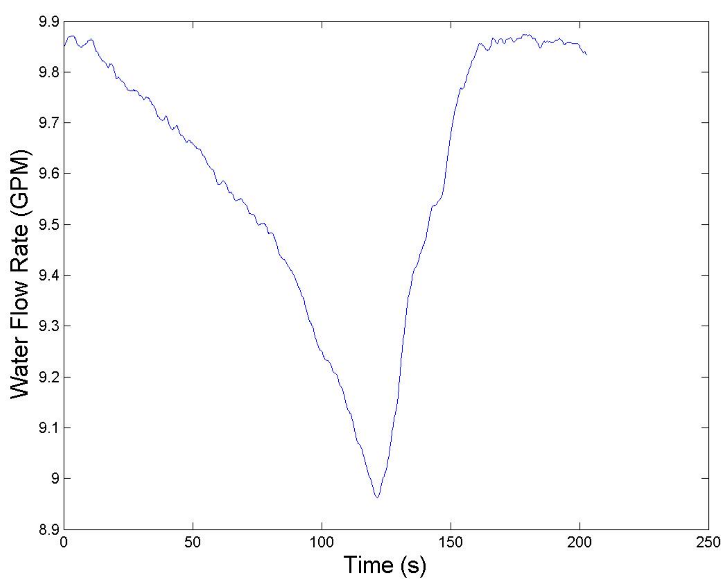

Fig. D.527.: Water flow rate for test 132.

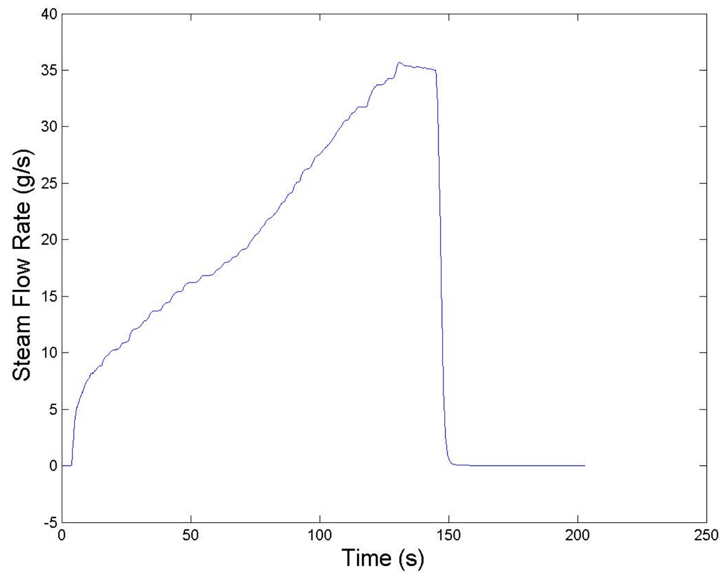

Fig. D.528.: Steam flow rate for test 132.

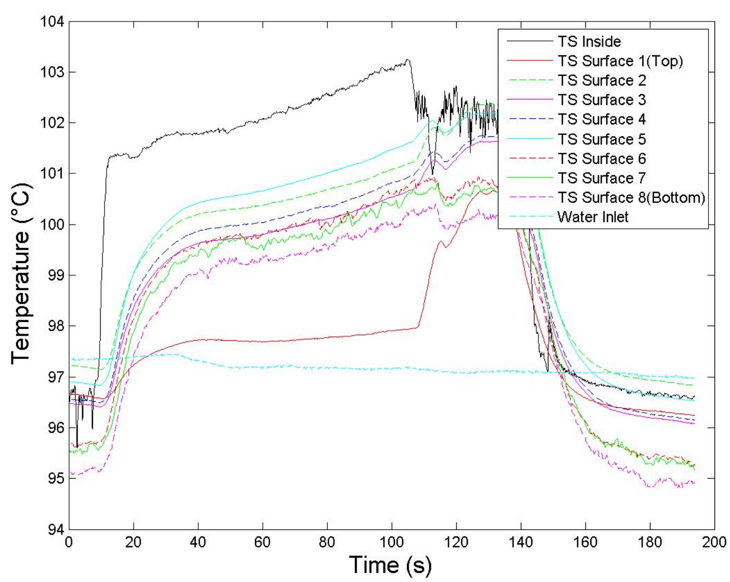

Fig. D.529.: Test section temperatures for test 133.

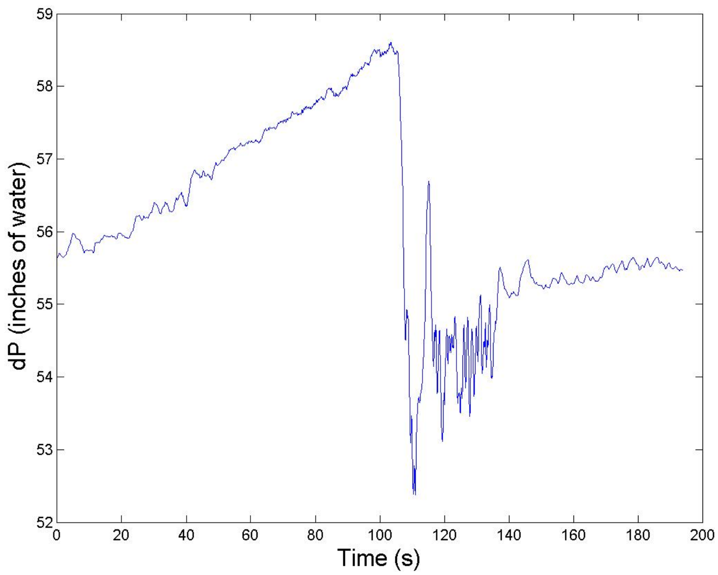

Fig. D.530.: Test section differential pressure for test 133.

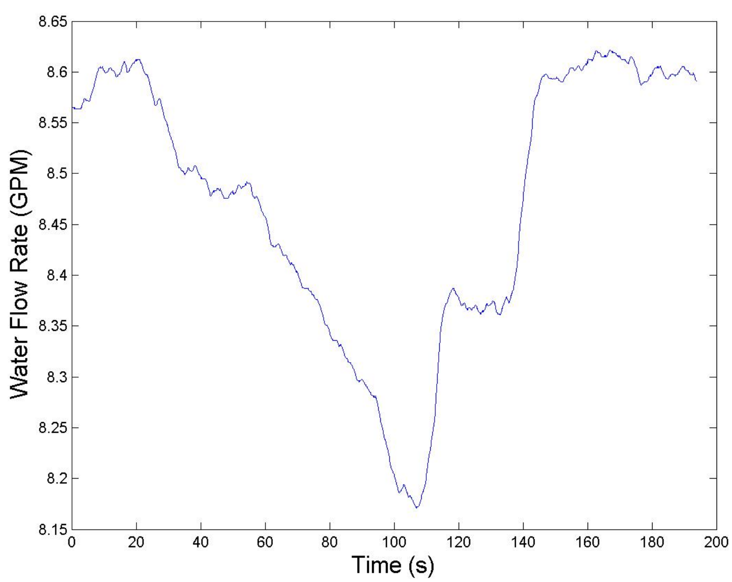

Fig. D.531.: Water flow rate for test 133.

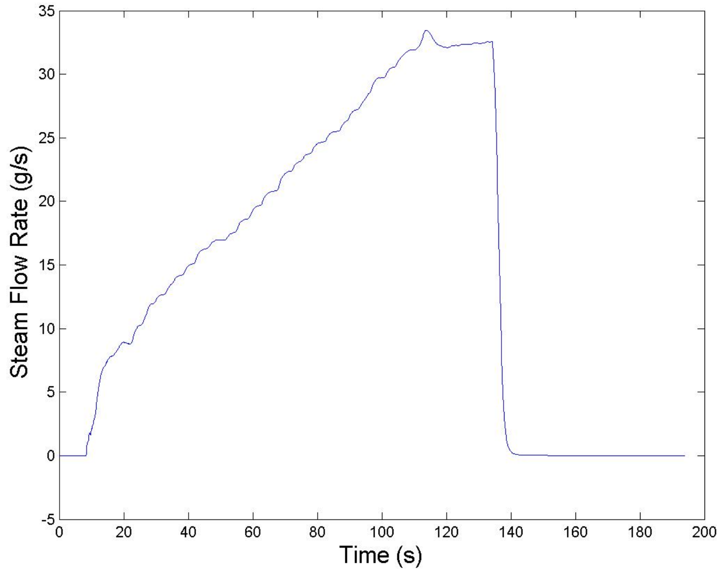

Fig. D.532.: Steam flow rate for test 133.

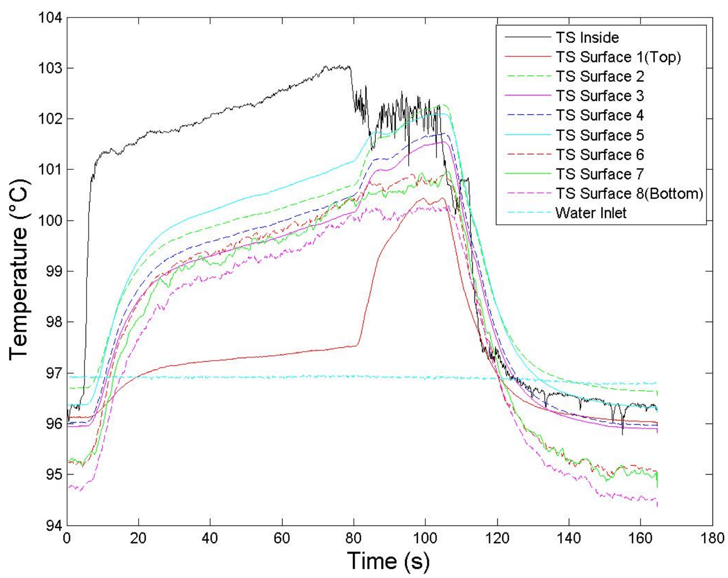

Fig. D.533.: Test section temperatures for test 134.

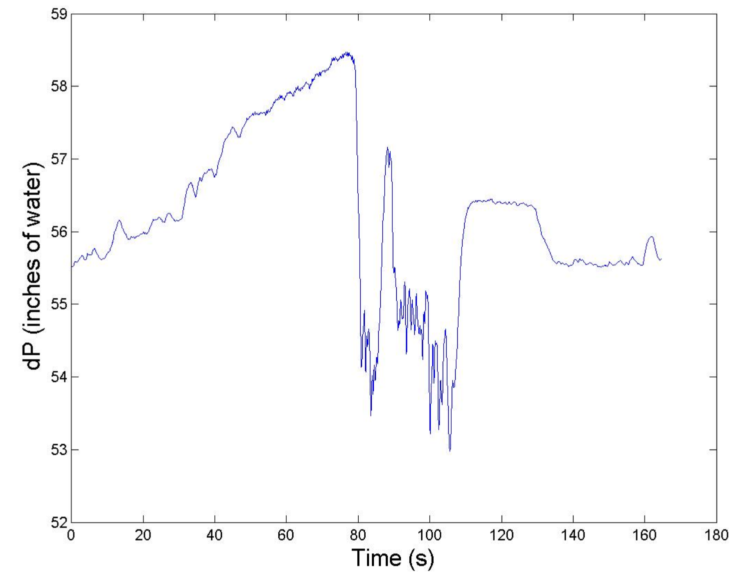

Fig. D.534.: Test section differential pressure for test 134.

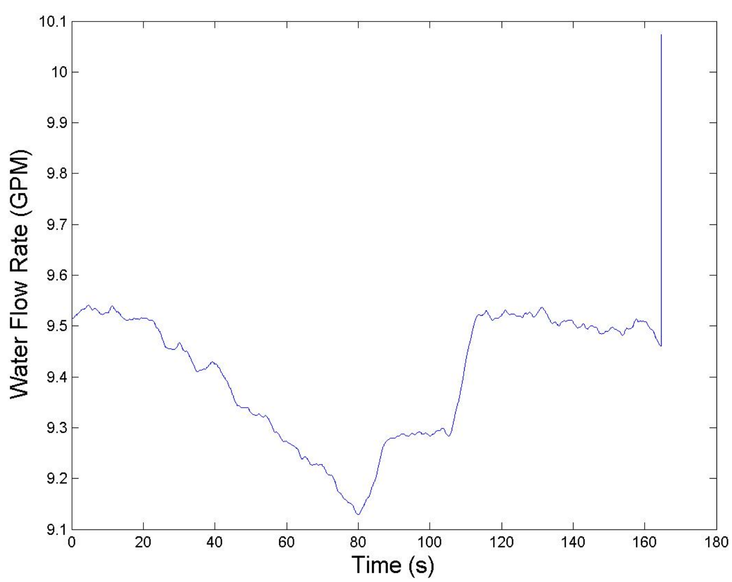

Fig. D.535.: Water flow rate for test 134.

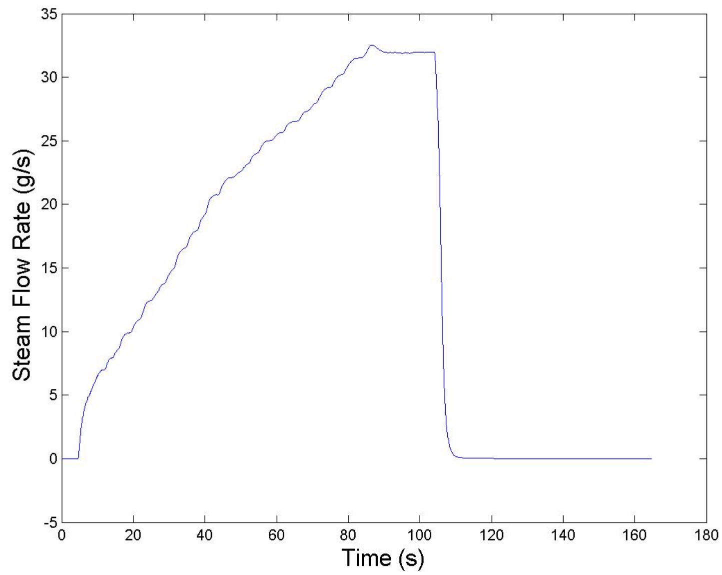

Fig. D.536.: Steam flow rate for test 134.

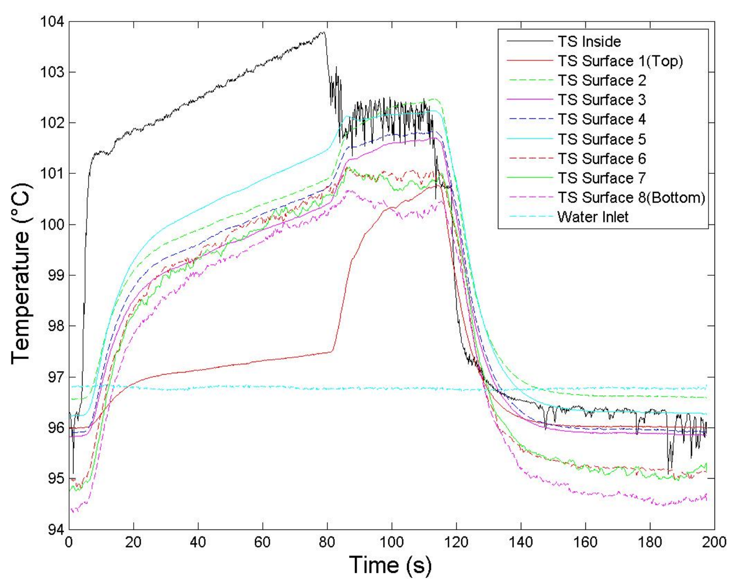

Fig. D.537.: Test section temperatures for test 135.

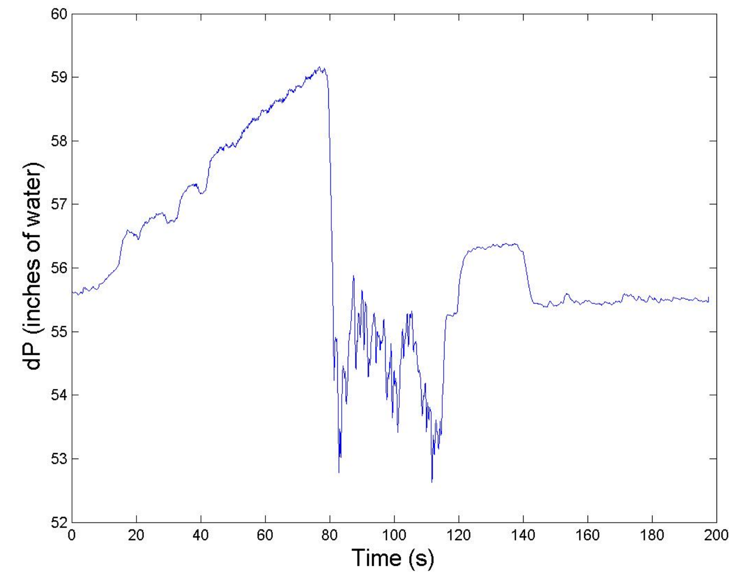

Fig. D.538.: Test section differential pressure for test 135.

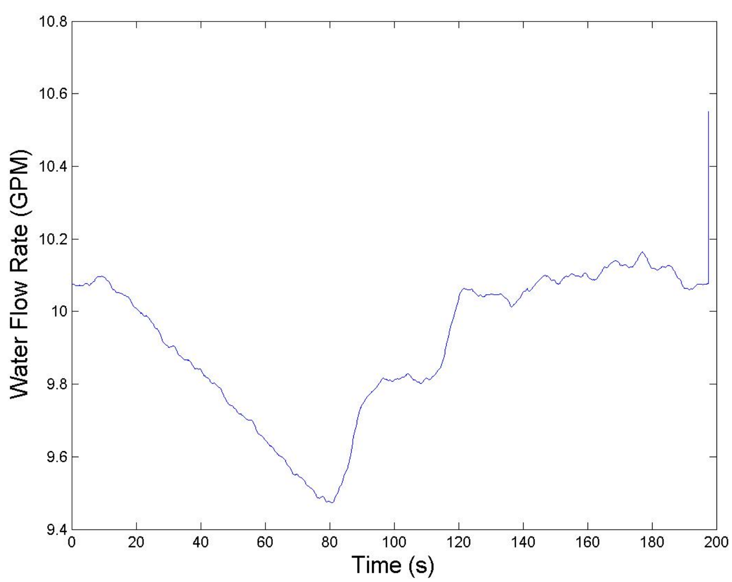

Fig. D.539.: Water flow rate for test 135.

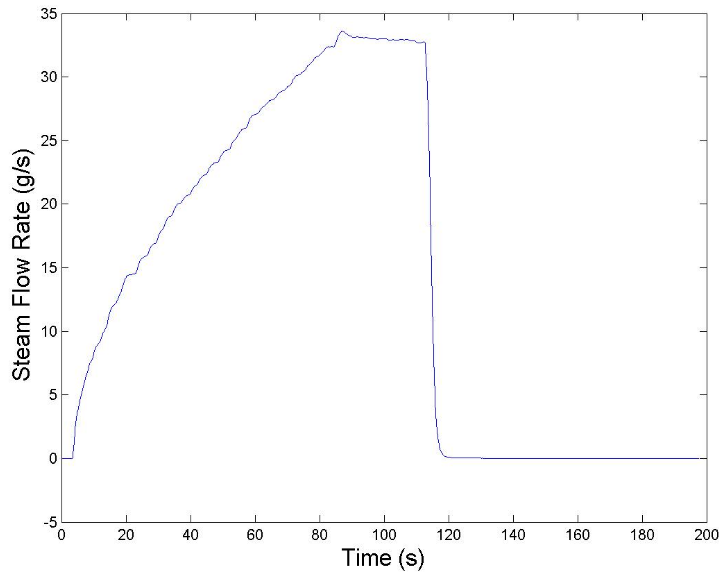

Fig. D.540.: Steam flow rate for test 135.

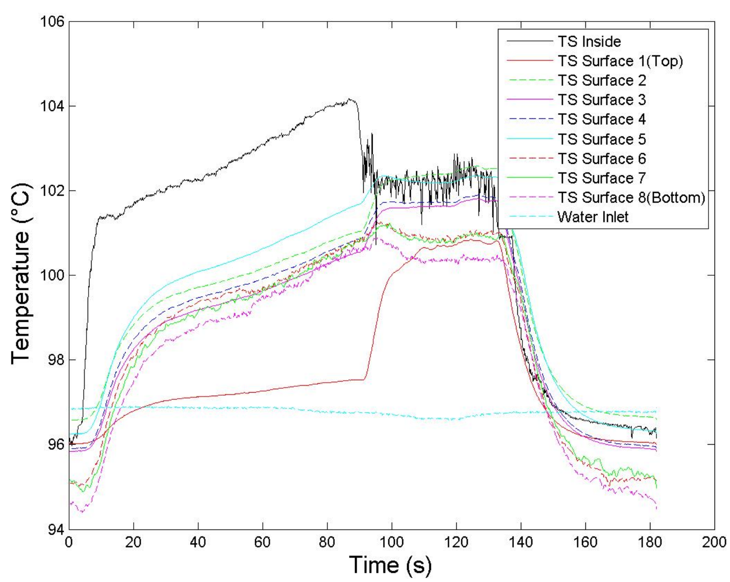

Fig. D.541.: Test section temperatures for test 136.

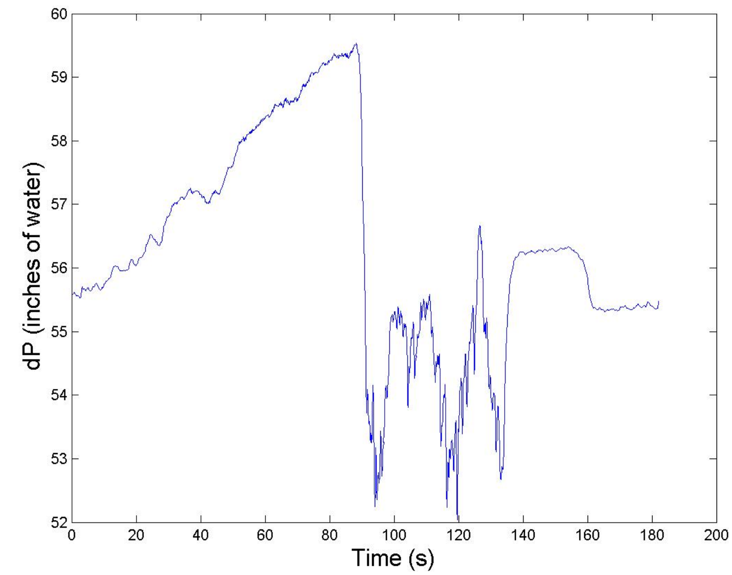

Fig. D.542.: Test section differential pressure for test 136.

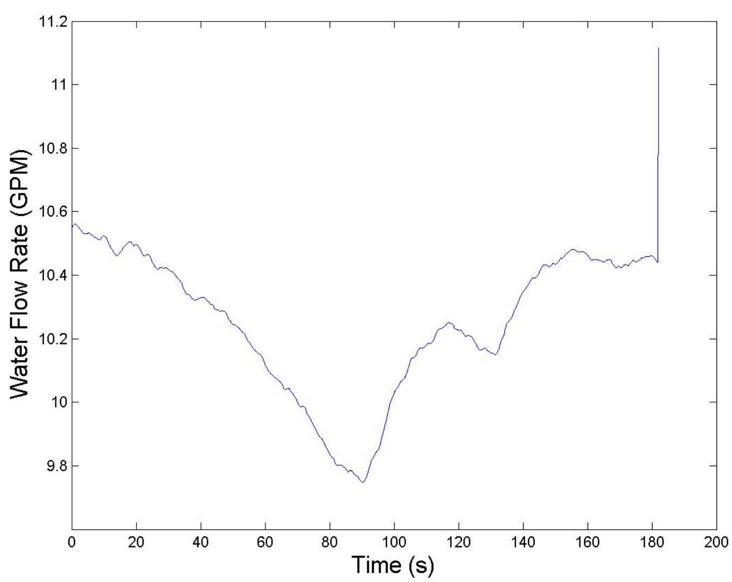

Fig. D.543.: Water flow rate for test 136.

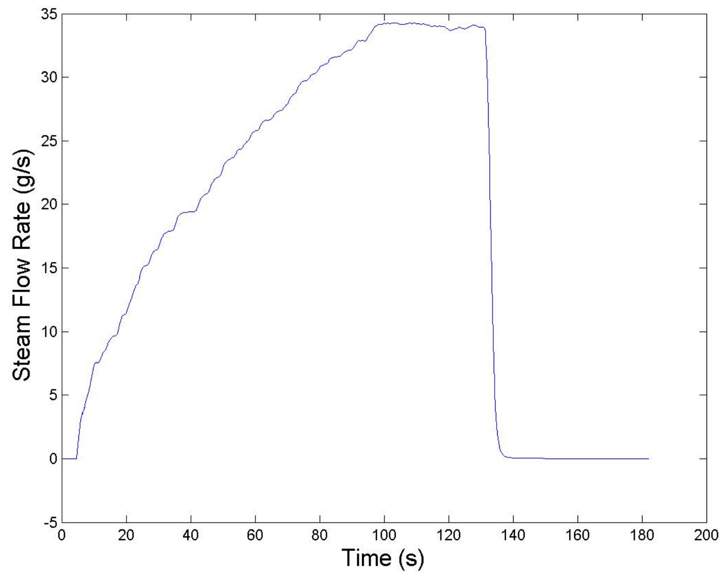

Fig. D.544.: Steam flow rate for test 136.

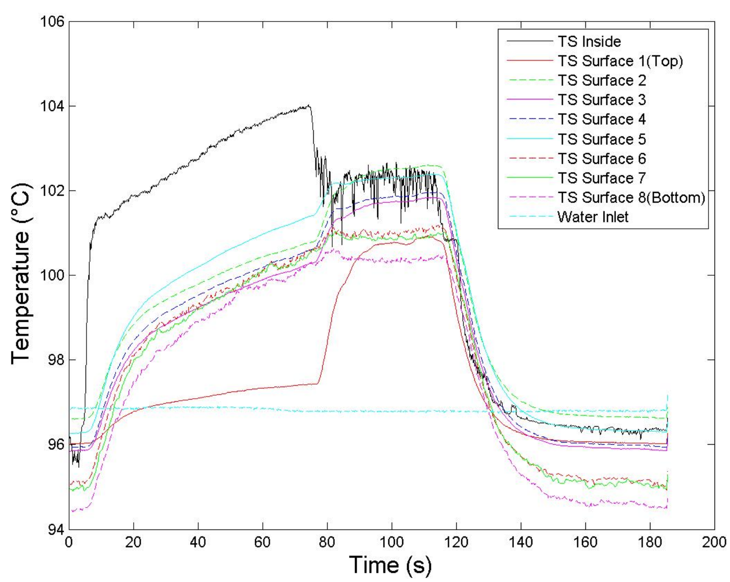

Fig. D.545.: Test section temperatures for test 137.

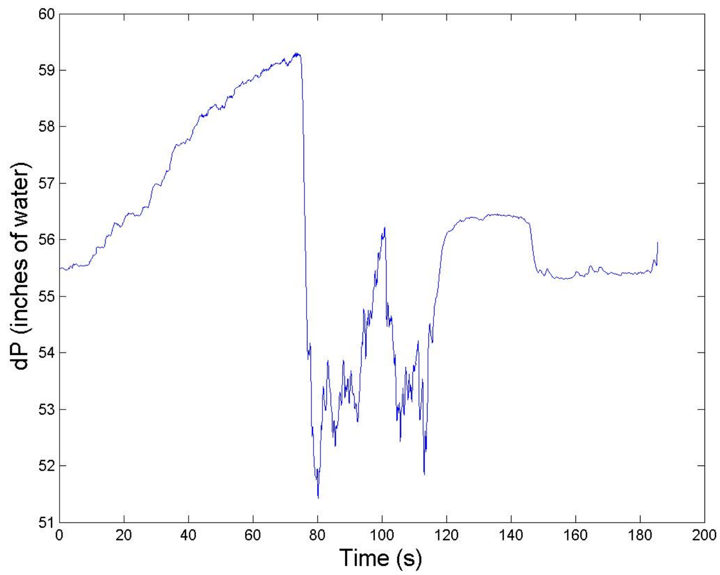

Fig. D.546.: Test section differential pressure for test 137.

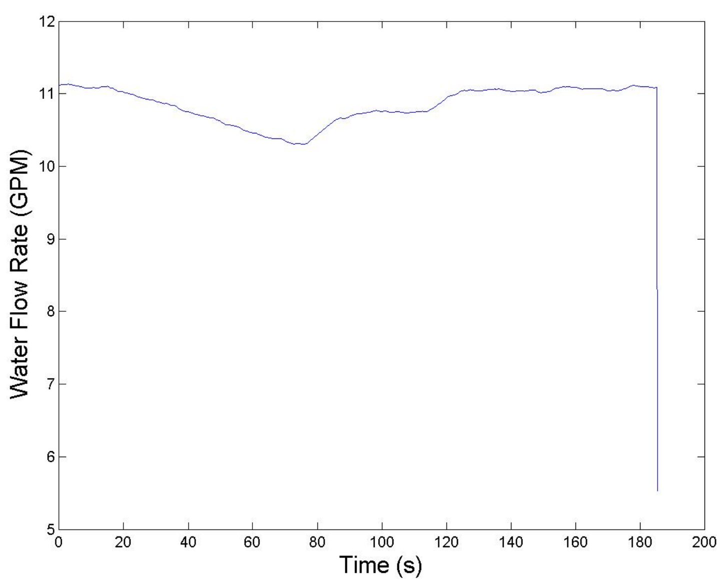

Fig. D.547.: Water flow rate for test 137.

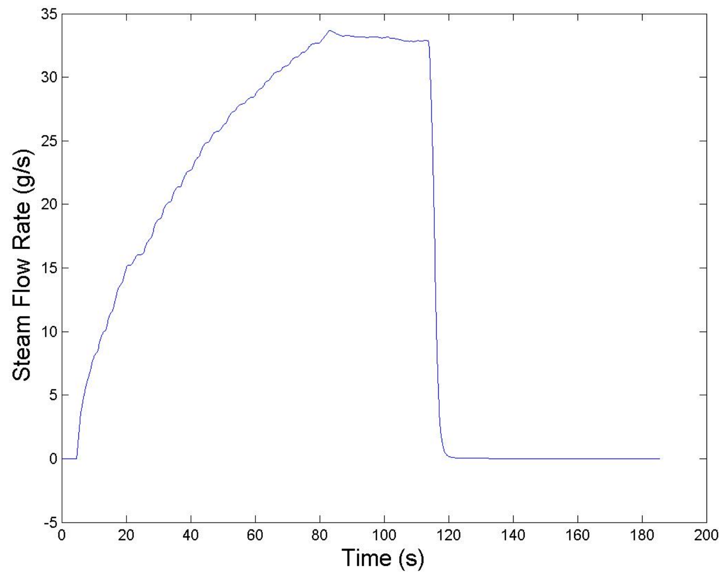

Fig. D.548.: Steam flow rate for test 137.

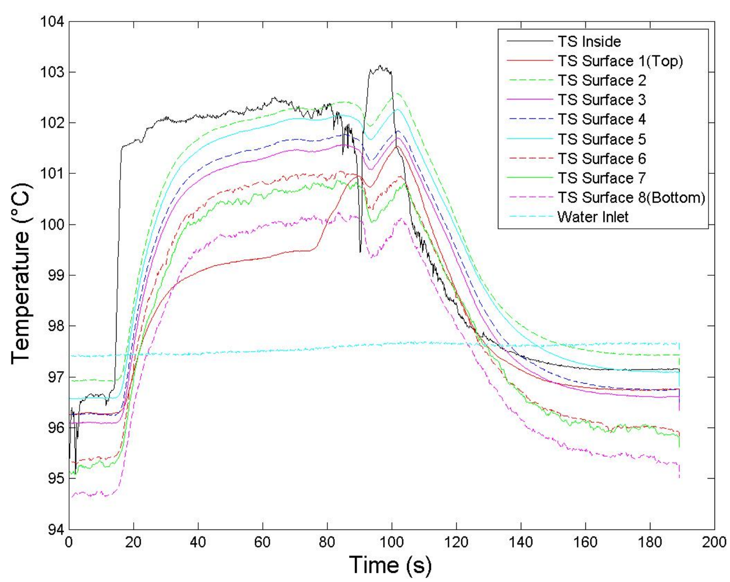

Fig. D.549.: Test section temperatures for test 138.

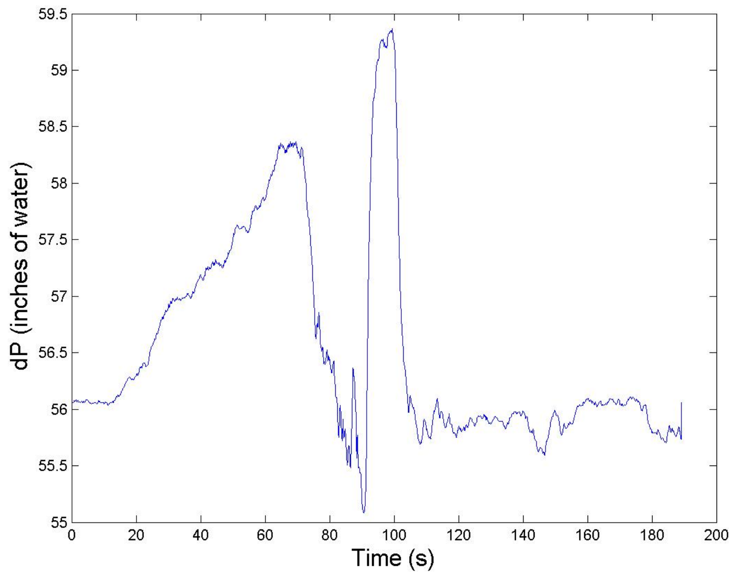

Fig. D.550.: Test section differential pressure for test 138.

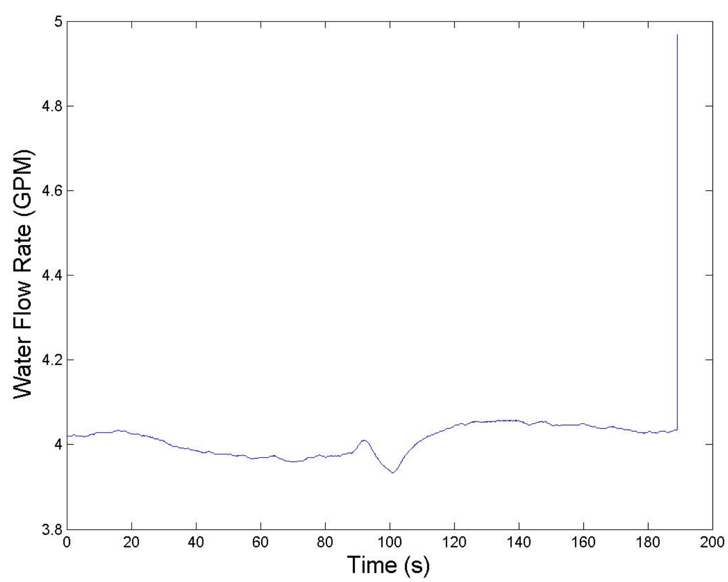

Fig. D.551.: Water flow rate for test 138.

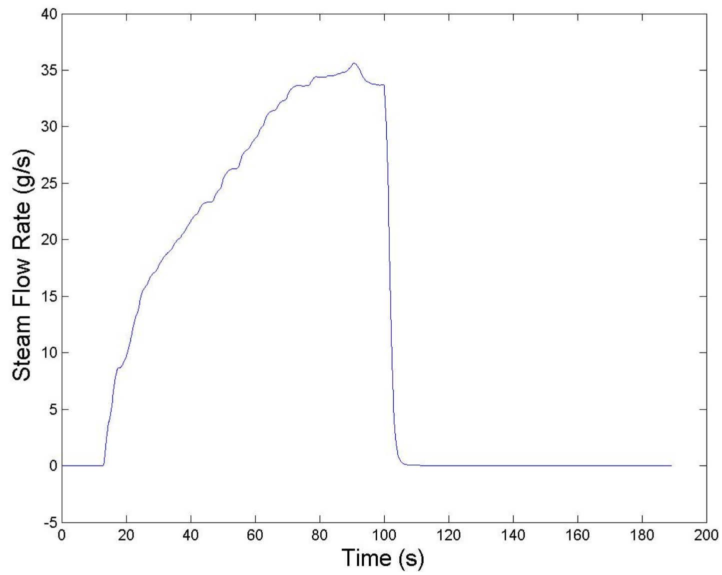

Fig. D.552.: Steam flow rate for test 138.

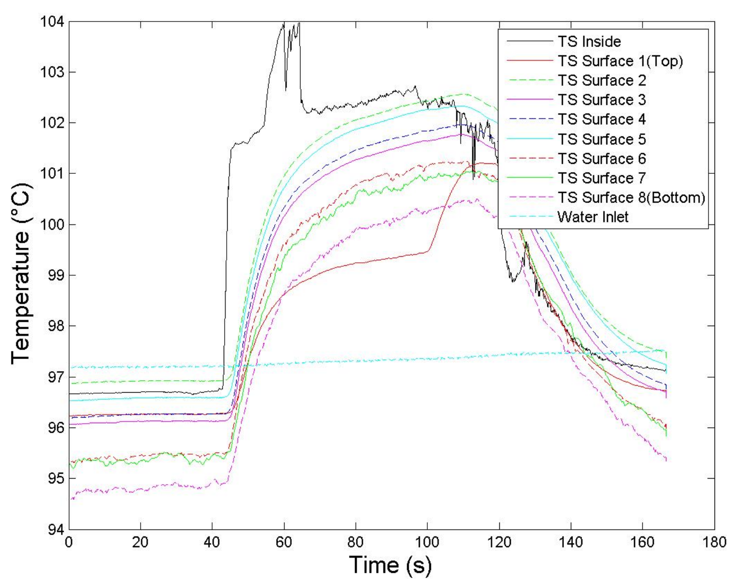

Fig. D.553.: Test section temperatures for test 139.

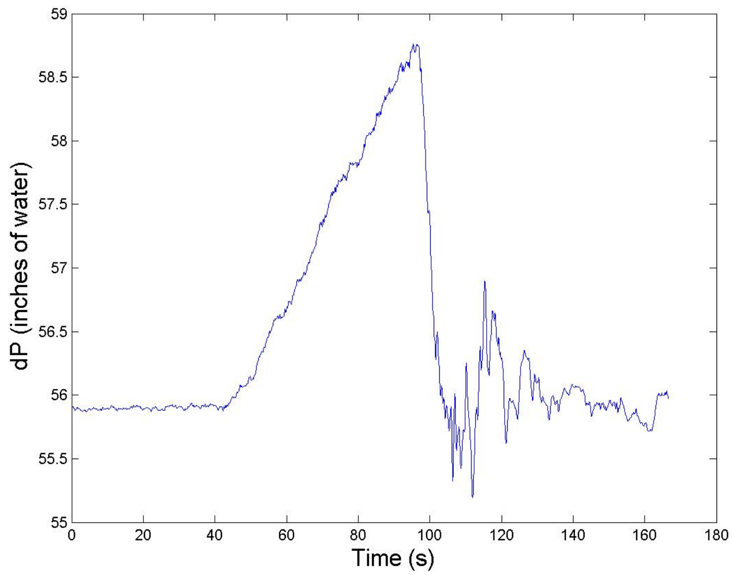

Fig. D.554.: Test section differential pressure for test 139.

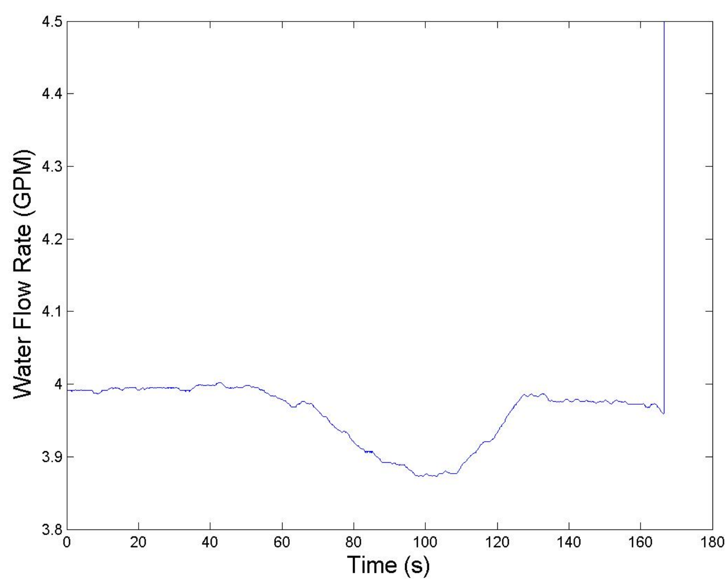

Fig. D.555.: Water flow rate for test 139.

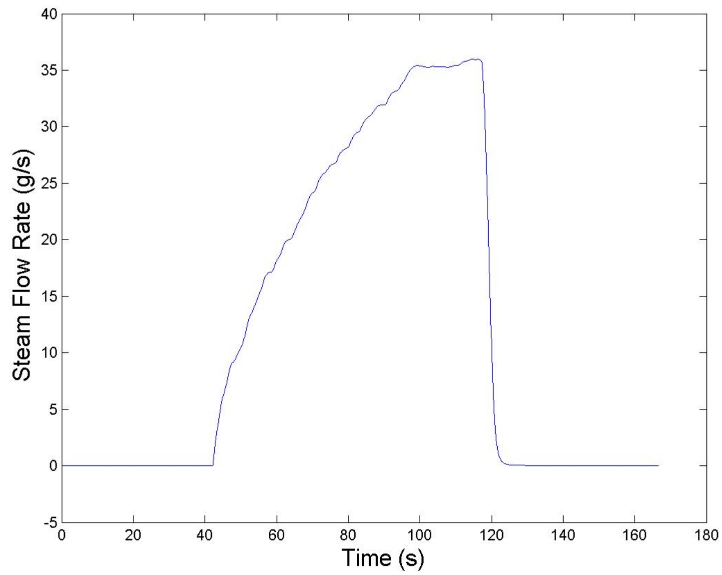

Fig. D.556.: Steam flow rate for test 139.

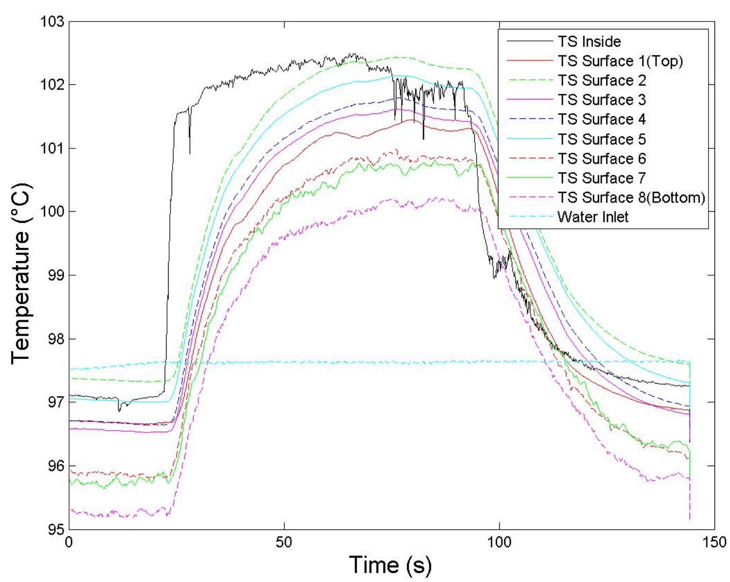

Fig. D.557.: Test section temperatures for test 140.

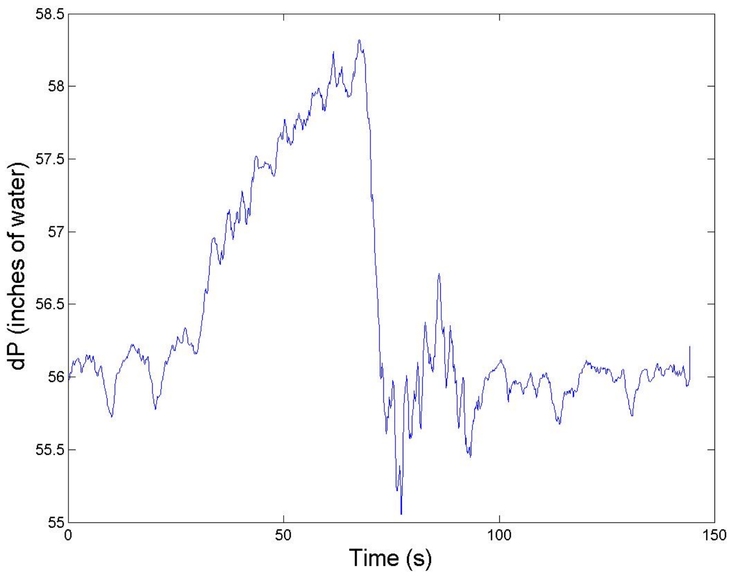

Fig. D.558.: Test section differential pressure for test 140.

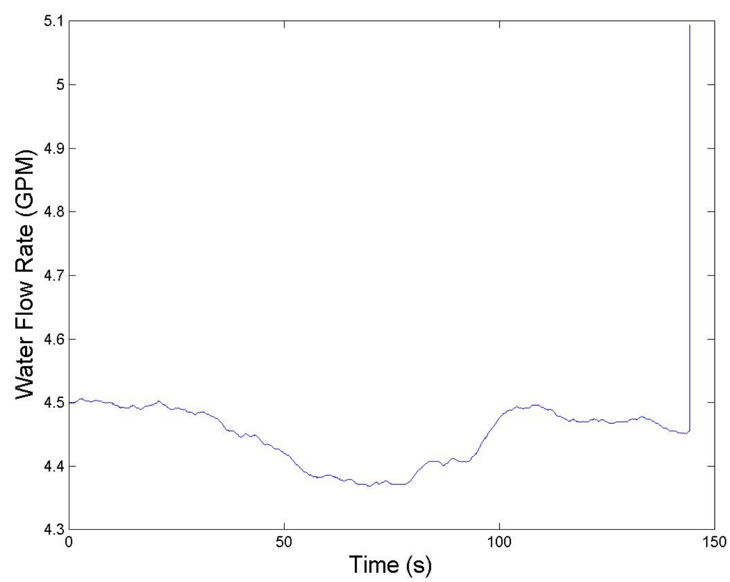

Fig. D.559.: Water flow rate for test 140.

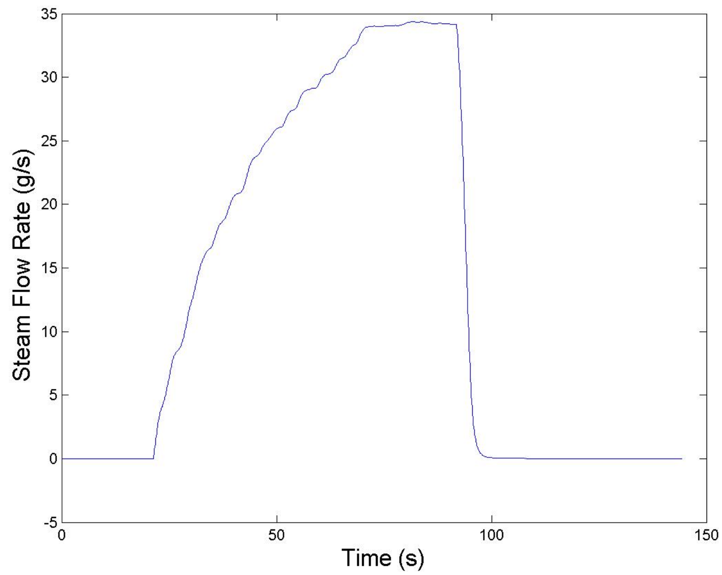

Fig. D.560.: Steam flow rate for test 140.

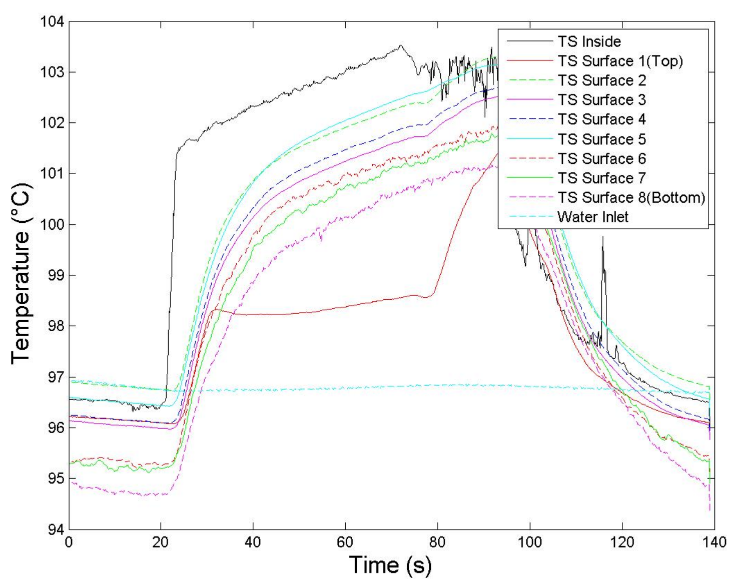

Fig. D.561.: Test section temperatures for test 141.

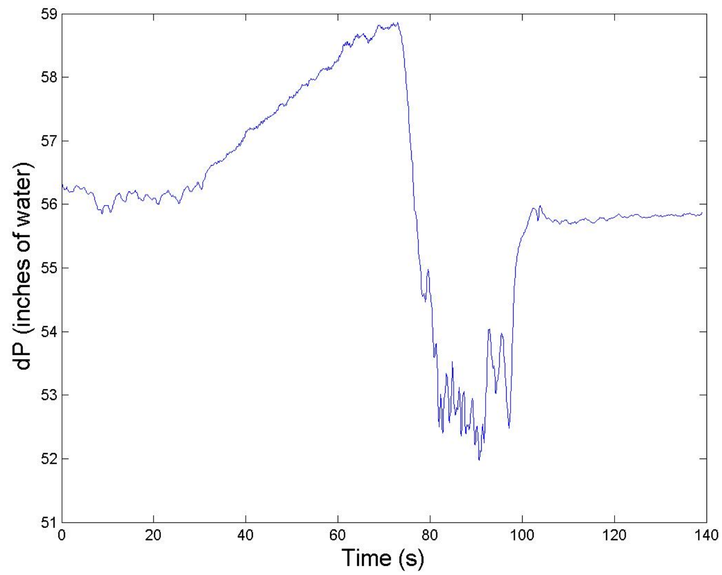

Fig. D.562.: Test section differential pressure for test 141.

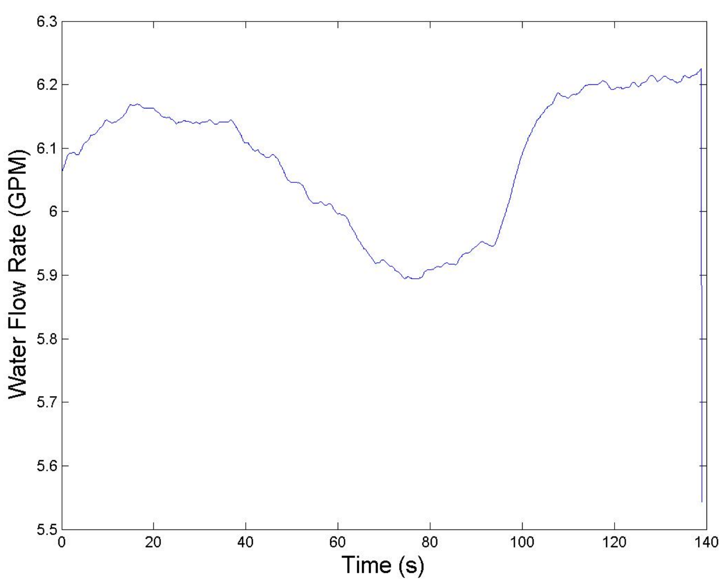

Fig. D.563.: Water flow rate for test 141.

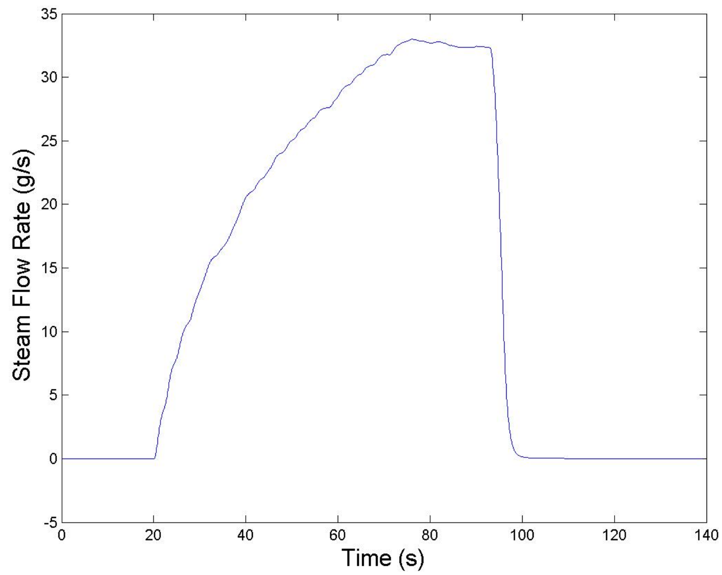

Fig. D.564.: Steam flow rate for test 141.

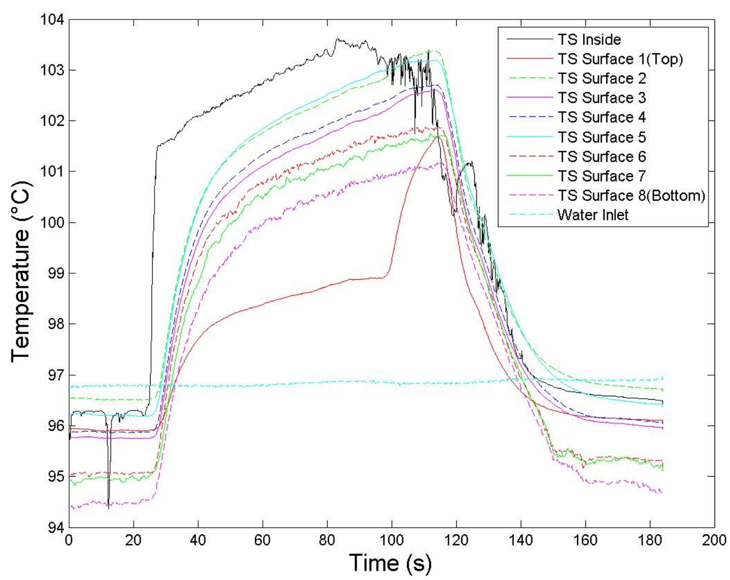

Fig. D.565.: Test section temperatures for test 142.

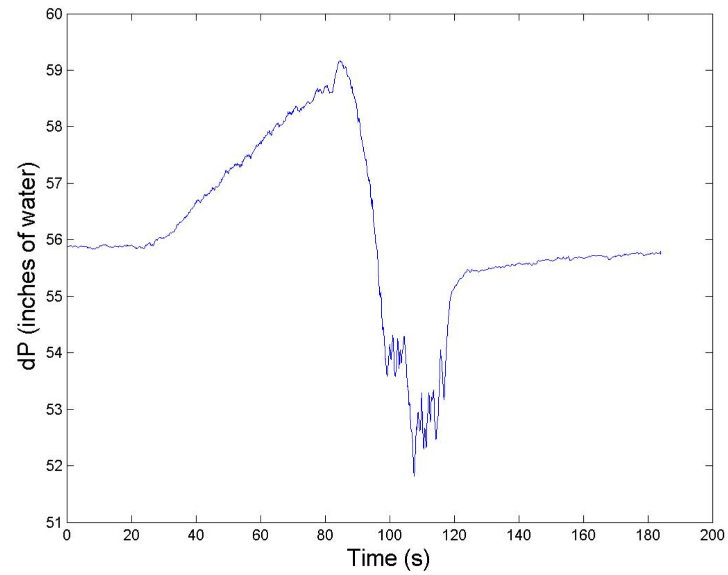

Fig. D.566.: Test section differential pressure for test 142.

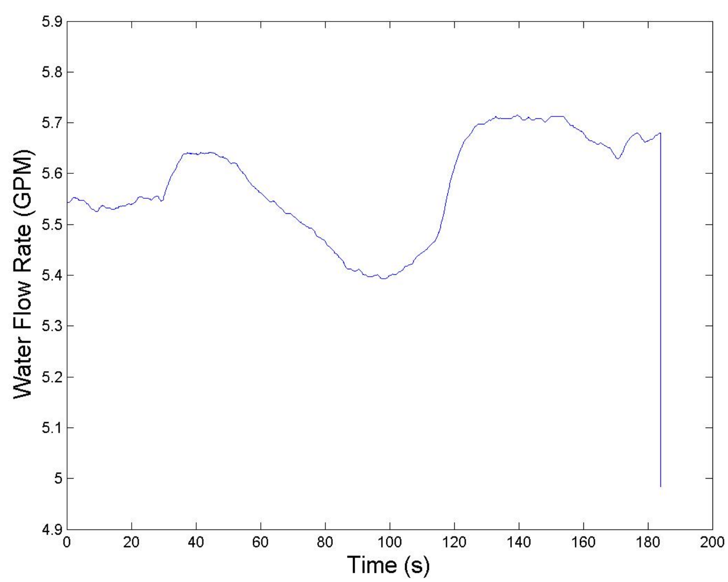

Fig. D.567.: Water flow rate for test 142.

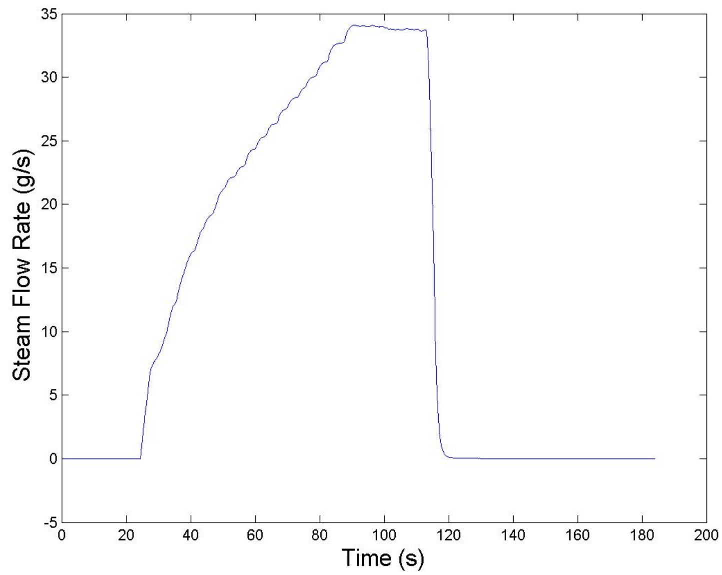

Fig. D.568.: Steam flow rate for test 142.

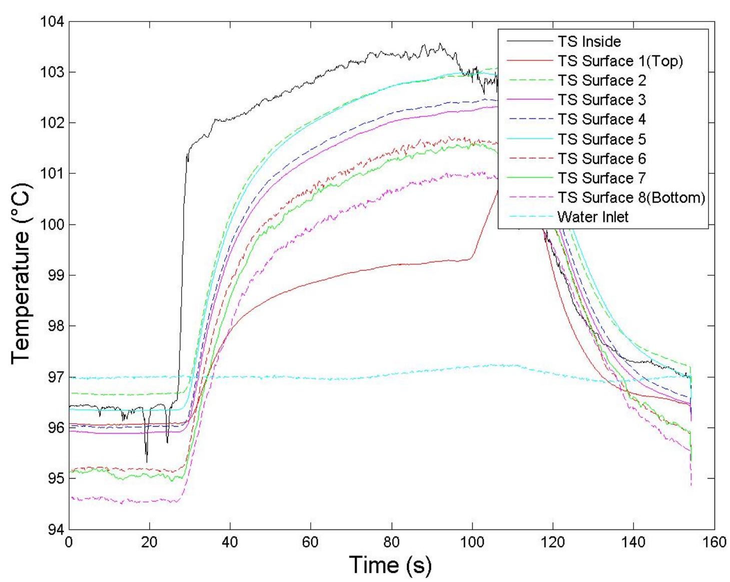

Fig. D.569.: Test section temperatures for test 143.

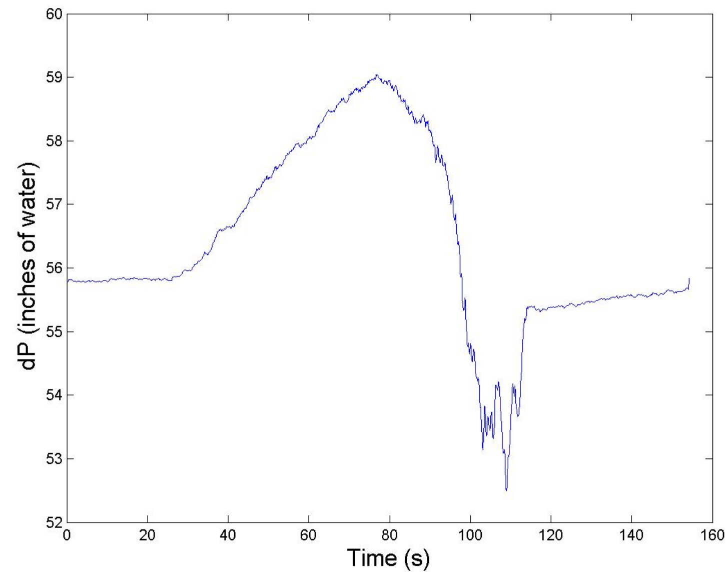

Fig. D.570.: Test section differential pressure for test 143.

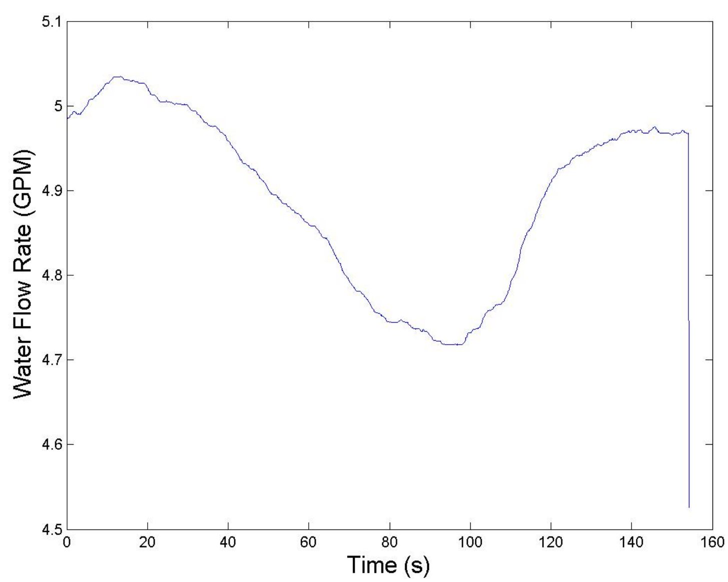

Fig. D.571.: Water flow rate for test 143.

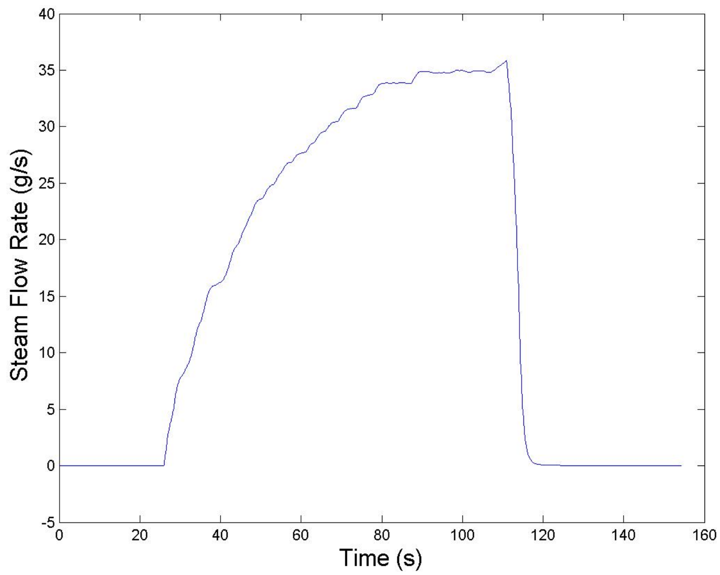

Fig. D.572.: Steam flow rate for test 143.

APPENDIX E

VORTEX FLOW METER CALIBRATION

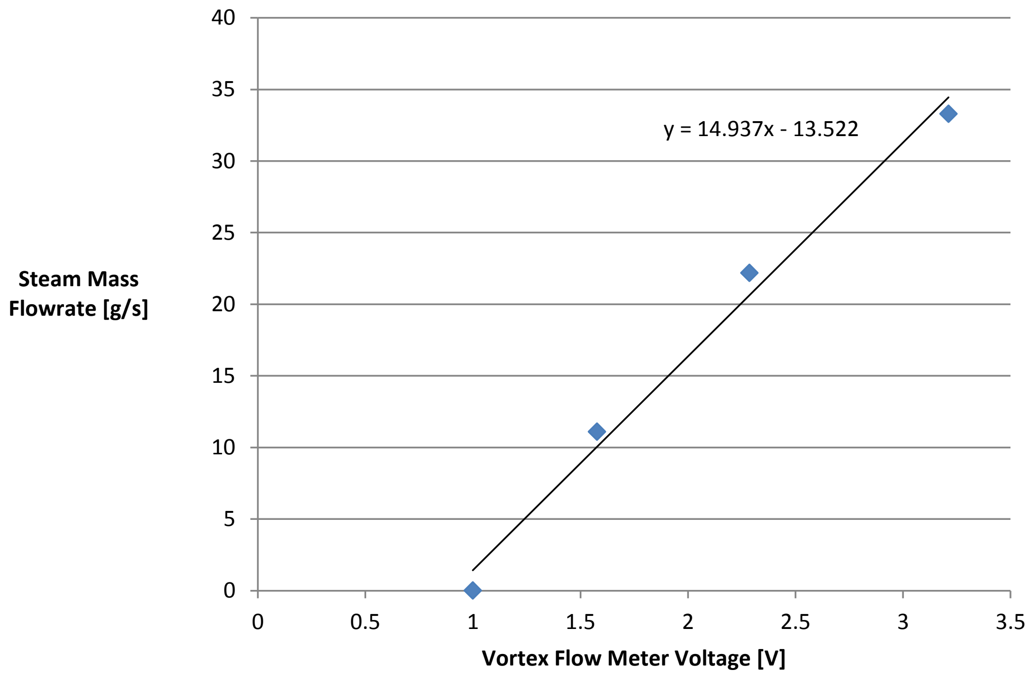

Fig. E.1.: The vortex flow meter calibration curve.

Table E.1: Data from tests used to calibrate the vortex flow meter.

Heater Power [kW]	SG Pressure [psig]	Voltage [V]	Steam Enthalpy [kJ/kg]	Steam Mass Flow Rate [g/s]	Steam Pressure [psia]	Steam Temperature [°C]	Steam Density [kg/m^3]	Steam Velocity [m/s]	Heat Loss [kW]
27	36.26	1.578	2255.12	11.09	14.98	101.73	0.61	13.95	2
52	38.03	2.286	2254.61	22.18	15.08	107.43	0.60	28.18	2
77	38.90	3.212	2253.38	33.28	15.33	118.05	0.59	42.80	2

VITA

Name: Wes Cullum

Address: ATTN: Karen Vierow
Department of Nuclear Engineering
Texas A&M University
129 Zachary Engineering Center, 3133 TAMU
College Station, TX 77843-3133

Email address: weslcullum@gmail.com

Education: B.S., Nuclear Engineering, Texas A&M University, 2010
M.S., Nuclear Engineering, Texas A&M University, 2012